

Expression, Regulation & Evolution of the Plant Immune System

Kumulative Dissertation

zur

Erlangung des Doktorgrades
der Mathematisch-Naturwissenschaftlichen Fakultät
der Heinrich-Heine-Universität Düsseldorf

vorgelegt von

Janina Katharina von Dahlen
aus Aachen

Düsseldorf, August 2023

Aus dem Institut für Populationsgenetik
der Heinrich-Heine-Universität Düsseldorf

Gedruckt mit der Genehmigung der
Mathematisch-Naturwissenschaftlichen Fakultät der
Heinrich-Heine-Universität Düsseldorf

Erstkorrektorin: Prof. Dr. Laura E. Rose
Zweitkorrektorin: Prof. Dr. Nicole Linka

Tag der mündlichen Prüfung: 25.10.2023

Selbstständigkeitserklärung

Hiermit erkläre ich, dass ich die vorliegende Dissertation eigenständig und ohne fremde Hilfe angefertigt habe. Arbeiten Dritter wurden entsprechend zitiert. Diese Dissertation wurde bisher in dieser oder ähnlicher Form noch bei keiner anderen Institution eingereicht. Ich habe bisher keinen erfolglosen Promotionsversuch unternommen.

Düsseldorf, August 2023

.....

(Janina K. von Dahlen)

Statement of authorship

I hereby certify that this dissertation is the result of my own work. No other person's work has been used without due acknowledgement. This dissertation has not been submitted in the same or similar form to other institutions. I have not previously failed a doctoral examination procedure.

Abstract

Plants live in a highly interactive and competitive world with millions of other organisms, some of which can be harmful to them. Disease is the exception however, while resistance to pathogens is most common. Plants owe their resistance to a finely tuned and highly effective immune system. It detects detrimental organisms by recognizing molecules shared by pathogens, such as chitin or flagellin, as well as lineage-specific effectors, proteins or peptides which are secreted by the pathogen to facilitate infection. Pathogens try to avoid triggering the plant's immune reaction by perpetually evolving new infection compounds and mechanisms. To keep up with the adaptive potential of pathogens, the immune system of plants is under strong selection pressure. The plant immune system is a highly dynamic, fine-tuned system. To achieve this fine-tuned dynamic, the plant immune system relies on a tight regulatory system. MicroRNAs (miRs) are one component of resistance gene (*R*-gene) regulation. miRs are small non-coding RNAs that regulate gene expression by triggering mRNA degradation or translational inhibition of gene transcripts – a process also known as RNA silencing. One of these plant immunity-regulating miR-families is the miR482-superfamily which contributes to pathogen resistance by regulating a large family of plant *R*-genes. *R*-genes are responsible for triggering the plant immune system by recognition of pathogenic effectors. Other essential players of the plant immune system are phytohormones, chemical signals which integrate many aspects of plant life such as growth and development, as well as, abiotic stress responses and defense. Key regulatory phytohormones of immunity in angiosperms are jasmonic acid and salicylic acid. These chemical compounds appear to interact with each other in an antagonistic way: Salicylic acid activates programmed cell death, an immune reaction that is conducive to necrotrophs, organisms that feed on dead tissue. However, host cell death is detrimental to biotrophs, which rely on living host tissues. Therefore instead of salicylic acid, jasmonic acid is induced following infection by necrotrophs.

In my Ph.D. thesis, I analyzed the evolution, expression and regulation of different layers of the plant immune system. In the first publication, my co-authors and I verified the regulation of several *R*-genes by the miR482-superfamily and characterized patterns co-regulation of *R*-genes and miR482-superfamily members. Furthermore, we were able to show that the expression levels of both *R*-genes and the miR482-superfamily are shaped by the co-evolution of pathogens with their hosts. In addition to the miR482-superfamily, several other miRs are also down-regulated during pathogen attacks. We therefore conclude that the miR482 family might contribute to higher susceptibility to *Phytophthora infestans* overall. The “miR482 paradox” is based on the observation that some pathogens secrete specific effectors to suppress the RNA silencing machinery of the plant. This releases the suppression of *R*-genes – but also and other genes – by miRs. The suppression of the RNA silencing machinery by the pathogen (and therefore up-regulation of *R*-genes) appears at first glance to be counterproductive

for the pathogen, however the benefit of releasing many other genes from negative regulation may outweigh the negative consequences of activating a subset of *R*-genes. The second publication is based on a large-scale meta-analysis of several hundred *R*-genes of tomatoes and potatoes in the presence, as well as in the absence of infection. Most importantly, we detected a core set of *R*-genes which are expressed at moderate to high levels independent of the infection status of the plant. We conclude that not all *R*-genes show a high cost of expression as assumed previously. A major factor associated with difference in *R*-gene expression was the tissue-type. Furthermore, although we do not detect strong pathogen induced activation of *R*-gene, it is still possible that the encoded protein show pathogen-specific activation. However, the mechanisms by which activated *R*-genes trigger a pathogen-specific immune reaction is still underexplored.

To reconstruct the network of miR-regulation – and specifically the miR482-family/*R*-gene network – we analyzed 28 publicly available degradomes of tomato. Degradomes (also known as PARE-libraries) can verify miR/mRNA interactions by identifying whether miR cleavage sites show an overaccumulation of degraded products. Overall, we identified 996 high-confidence mRNA-interactions for a total 137 miRs, 316 isomeric length variants of these miRs (isomiRs) and 1615 putative phasiRNAs, a special class of secondary miRs produced by cleavage events of miRs. We were able to show that miRs not only produce gene-silencing active isomiRs and phasiRNAs, but they also target the same genes multiple times or target genes which themselves contribute to the regulation of diverse processes such as *R*-genes or transcription factors. Our findings support the “few target” hypothesis of miR interactions, a hypothesis stating that miRs achieve their regulatory power by strongly repressing a small set of genes. However, the alternative “many but weak” hypothesis could not be completely excluded since degradomes do not detect weakly degraded targets or translation inhibition events.

In a fourth publication, we analyzed putative genes coding for phytohormones: Salicylic and jasmonic acid from the water fern *Azolla filiculoides* (*A. filiculoides*). We were able to show that *A. filiculoides* possesses most genes and protein domains to produce and perceive both phytohormones, but is likely to be insensitive towards jasmonic acid. This observation is further supported by recent studies reporting that most basal lineages of plants do not produce jasmonic acid in sufficient amounts, but instead produce dn-OPDA, a precursor of jasmonic acid. Furthermore, our data suggest that salicylic acid might be involved in the communication of the water fern with its nitrogen-fixation cyanobiont as the amount of the cyanobiont increases after long-term salicylic acid treatment. In a final study, we established the putative broad-spectrum biocontrol organism *Phoma eupatorii* to outcompete *Phytophthora infestans* infections on cultivated tomato. Biocontrol organisms are organisms that are

applied to plants to prime the plant for subsequent infections or directly combat pathogens or pests by e.g. hyperparasitism or competition for nutrients. *Phytophthora infestans* in turn is one of the most detrimental pests of cultivated tomatoes and other Solanaceae such as potatoes or chilis. In our study *Phoma eupatorii* was able to inhibit *Phytophthora infestans* *in vitro* on plates and *in vivo* on tomato plants.

In summary, the plant immune system consists of a multilayered, highly interactive system that needs to be tightly controlled in expression, as well as function to constantly co-adapt with the adaptive potential of its pathogens. The evolutionary history of the immune system might help shed light on its potential to protect plants in the future.

Zusammenfassung

Pflanzen konkurrieren mit Millionen anderer Organismen auf eine hochgradig interaktive Weise. Einige dieser Organismen können dabei schädlich für die Pflanze sein. Das Auftreten von Krankheiten ist jedoch die Ausnahme, während üblicherweise Resistenz vorliegt. Ihre Resistenz verdanken Pflanzen ihrem fein abgestimmten und hochwirksamen Immunsystem. Das Immunsystem erkennt schädliche Organismen anhand von konservierten Molekülen wie Chitin oder Flagellin, sowie anhand von pathogenspezifischen Effektoren - Proteine oder Peptide, die von Pathogenen sekretiert werden, um die Infektion zu ermöglichen. Die Auslösung der Immunreaktion der Pflanze versuchen Pathogene zu verhindern, indem sie ständig neue Moleküle und -mechanismen zur Infektion entwickeln. Um mit diesem hohen Anpassungspotenzial von Pathogenen Schritt halten zu können, steht das Immunsystem von Pflanzen unter einem starken Selektionsdruck. Das pflanzliche Immunsystem ist folglich ein hochdynamisches, fein abgestimmtes System. Um diese fein abgestimmte Dynamik zu erreichen, ist das pflanzliche Immunsystem auf Regulation angewiesen. Eine entscheidende Komponente dabei ist die Regulation von Resistenzgenen (*R*-Genen) durch microRNAs (miRs). miRs sind kleine nichtkodierende RNAs, die die Genexpression regulieren, indem sie die Degradation der messengerRNA (mRNA) oder die translationale Hemmung von Gentranskripten auslösen, einen Prozess, der als RNA-Silencing bekannt ist. Die miR482-Superfamilie trägt durch die Regulierung einer großen Familie pflanzlicher *R*-Gene zur Resistenz gegenüber Pathogenen bei. *R*-Gene aktivieren das pflanzliche Immunsystem indem sie pathogene Effektoren detektieren. Weitere wichtige Akteure des pflanzlichen Immunsystems sind Phytohormone, chemische Signalstoffe, die viele physiologischen Prozesse von Pflanzen wie Wachstum und Entwicklung sowie abiotische Stressreaktionen und Immunität koordinieren. Die wichtigsten Phytohormone in Angiospermen in Bezug auf Immunität sind Jasmonsäure und Salicylsäure. Beide chemischen Verbindungen interagieren auf antagonistische Weise: Salicylsäure aktiviert den programmierten Zelltod und führt zur Entstehung von nekrotischen Pflanzengewebe. Diese Immunreaktion begünstigt zwar nekrotrophe Organismen, da sich diese von totem Gewebe ernähren, ist jedoch zugleich schädlich für biotrophe Organismen, welche auf lebendes Wirtsgewebe angewiesen sind. Daher wird bei einer Infektion durch nekrotrophe Organismen anstelle von Salicylsäure Jasmonsäure induziert.

Während meiner Doktorarbeit habe ich die Evolution, Expression und Regulierung verschiedener Ebenen des pflanzlichen Immunsystems studiert. In der ersten Veröffentlichung haben meine Co-Autoren und ich die Regulation mehrerer *R*-Gene durch die miR482-Superfamilie verifiziert und Muster der Co-Regulation von *R*-Genen und Mitgliedern der miR482-Superfamilie identifiziert. Darüber hinaus konnten wir zeigen, dass die Höhe der Expression der *R*-Gene und der miR482-Superfamilie durch die Koevolution von Pathogenen mit ihren Wirten beeinflusst wird. Neben der miR482-Superfamilie

werden auch mehrere andere miRs während der Infektion herunterreguliert. Wir folgern daraus, dass die Regulierung der miR482-Familie zu einer höheren Anfälligkeit gegen das Pathogen *Phytophthora infestans* führt. Dieses „miR482-Paradoxon“ basiert auf der Beobachtung, dass einige Pathogene spezifische Effektoren sekretieren, um das RNA-Silencing der Pflanze zu unterdrücken. Dadurch wird jedoch die Inhibierung von *R*-Genen – ebenso wie weiterer Gene – durch miRs aufgehoben. Die Inhibierung des RNA-Silencings durch Pathogene (und damit die Hochregulierung der *R*-Gene) scheint auf den ersten Blick kontraproduktiv für Pathogene zu sein. Der Vorteil, viele andere Gene von der Inhibierung durch miRs loszulösen, könnte jedoch die negativen Folgen der Expression einiger *R*-Gene überwiegen. Die zweite Veröffentlichung basiert auf einer groß angelegten Metaanalyse zur Expression von mehreren hundert *R*-Genen von Tomaten und Kartoffeln sowohl in Gegenwart als auch in Abwesenheit einer Infektion. Unsere wichtigste Erkenntnis in dieser Publikation ist, dass eine Kerngruppe von *R*-Genen existiert, die unabhängig vom Infektionsstatus der Pflanze in moderaten bis hohen Mengen konstitutiv exprimiert wird. Wir schlussfolgern daher, dass nicht alle *R*-Gene wie bisher angenommen hohe Kosten der Expression verursachen. Der Hauptfaktor im Zusammenhang mit der unterschiedlichen Expression von *R*-Genen ist der Gewebetyp. Des Weiteren konnten wir zwar keine pathogeninduzierte Expression von *R*-Genen nachweisen, es ist aber dennoch möglich, dass die *R*-Proteine eine pathogenspezifische Aktivierung aufzeigen. Wie aktivierte *R*-Gene eine erregerspezifische Immunreaktion auslösen ist jedoch aktuell noch wenig erforscht.

Um das Netzwerk der Regulation durch miRs – und insbesondere das miR482-Familie/*R*-Gen-Netzwerk – zu rekonstruieren, haben wir anschließend 28 öffentlich verfügbare Degradome von Tomaten analysiert. Anhand von Degradome (auch bekannt als PARE-Libraries) ist es möglich miR/mRNA-Wechselwirkungen zu verifizieren und zwar durch den Nachweis einer Überakkumulation von degradierten mRNAs, die exakt an einer miR-Schnittstelle beginnen. Insgesamt konnten wir 996 mRNA-Interaktionen für insgesamt 137 miRs, 316 isomeren Längenvarianten dieser miRs (isomiRs) und 1615 mutmaßlichen phasiRNAs nachweisen. Bei phasiRNAs handelt es sich um eine spezielle Klasse sekundärer miRs, die durch vorangehende Degradierung durch miRs erzeugt werden. Wir konnten zeigen, dass miRs zum Gen-Silencing nicht nur isomiRs sowie phasiRNAs produzieren, sondern auch Gene gleich mehrfach regulieren sowie Gene wie *R*-Gene oder Transkriptionsfaktoren regulieren, die ihrerseits an der Regulierung verschiedener Prozesse beteiligt sind. Unsere Ergebnisse stützen damit die „Few Target“-Hypothese der miR-Interaktionen. Diese besagt, dass miRs ihre Regulierungsstärke durch die starke Unterdrückung einer kleinen Gruppe von Genen erreichen. Die alternative „many, but weak“ Hypothese konnten wir im Rahmen dieser Arbeit jedoch nicht vollständig ausschließen, da Degradomanalysen keine schwach degradierten mRNAs oder Ereignisse translationaler Inhibierung detektieren können.

In unserer vierten Veröffentlichung analysierten wir anschließend Gene des Wasserfarns *Azolla filiculoides* (*A. filiculoides*), die mutmaßlich für die Phytohormone Salicyl- und Jasmonsäure kodieren. Wir konnten zeigen, dass *A. filiculoides* über die meisten Gene und Proteindomänen zur Produktion und Sensitivität beider Phytohormone verfügt, jedoch wahrscheinlich Jasmonsäure nicht wahrnimmt. Diese Beobachtung wird durch neuere Studien gestützt, die zeigen, dass die meisten basalen Pflanzenlinien – zu denen auch Wasserfarne gehören – Jasmonsäure nicht in ausreichenden Mengen produzieren können, sondern stattdessen dn-OPDA, eine Vorstufe der Jasmonsäure, synthetisieren. Darüber hinaus deuten unsere Daten darauf hin, dass Salicylsäure an der Kommunikation des Wasserfarns mit seinem stickstofffixierenden Cyanobionts beteiligt sein könnte, da die Menge des Cyanobionts nach einer Langzeitbehandlung mit Salicylsäure zugenommen hat. In einer finalen Studie haben wir den mutmaßlichen Breitband-Biokontrollorganismus *Phoma eupatorii* etabliert, um in Zukunft Infektionen der kultivierten Tomaten mit dem Pathogen *Phytophthora infestans* zu bekämpfen. Biokontrollorganismen sind Organismen, die auf Pflanzen aufgebracht werden, um die Pflanzen wahlweise auf spätere Infektionen vorzubereiten oder Pathogene direkt zu bekämpfen, indem sie zum Beispiel Hyperparasitismus betreiben oder in Konkurrenz um Nährstoffe mit dem Pathogen stehen. *Phytophthora infestans* wiederum ist eines der schädlichsten Pathogene der kultivierten Tomate sowie anderer Nachtschattengewächse wie Kartoffeln und Chili. In unserer Studie hemmte *Phoma eupatorii* *Phytophthora infestans* *in vitro* auf Platten und *in vivo* auf Tomatenpflanzen.

Zusammenfassend lässt sich sagen, dass das pflanzliche Immunsystem aus einem vielschichtigen, hochgradig interaktiven System besteht, dessen Expression und Funktion streng kontrolliert werden muss, um eine ständige Anpassung an das hohe Entwicklungspotential potentieller Pathogene zu garantieren. Weitere Studien zur evolutionären Geschichte des Immunsystems könnten dabei helfen das Potential des Immunsystems zum Schutz von Pflanzen näher zu charakterisieren.

Table of contents

1.1 Motivation and research aim	11
1.2 Personal bibliography	13
1.3 Outline	15
2.1 The plant immune system	17
2.2 A case study: The interaction of cultivated tomato and its wild relatives with the pathogen <i>Phytophthora infestans</i>	23
2.3 Expression profiling of <i>R</i> -genes	30
2.4 The few- & the many-targets hypotheses of microRNAs.....	34
2.5 About the interaction of phytohormones with the plant immune system.....	40
2.6 Biocontrol as a natural approach to fight back disease	44
2.7 The Yin-and-Yang of plants and pathogens: Uncovering the rapid arms race.....	47
3. Discussion	51
4. Outlook	55
5. References:.....	58
6. Publications	73

1.1 Motivation and research aim

Plants are permanently interacting with millions of microbes. Most of these interactions are neutral or sometimes even beneficial to the plant. However, a plethora of these interactions cause damage. Yet, resistance to pathogens is common, while susceptibility is the exception. The pervasive resistance of plants towards their pathogens relies on their finely tuned immune systems, which aims to prevent the establishment of pathogen infections. Following the arms-race model of Jones and Dangl (2006) plants and their pathogens are permanently challenged by one another. Analyzing this complex co-evolutionary system requires a highly interdisciplinary approach, combining the fields of plant-microbe interactions, molecular biology, ecology, evolutionary genetics and computational biology. The motivation for my Ph.D. was to study the diverse layers of the plant immune system by analyzing the expression of key immunity genes as well as the regulation and evolution of these layers. My work should therefore contribute knowledge to the following questions:

- i) What are the major determinants of the plant immune system and how do they contribute to resistance?
- ii) How does the plant immune system evolve?
- iii) How is the immune system regulated as it constantly needs to react to changing conditions?
How is specificity to pathogens achieved?
- iv) How can we use our current knowledge about the plant immune system to counter infections?

To address these questions, my co-authors and I applied different computational and wet-lab approaches. Beginning with the reconstruction of the interactions of the cultivated tomato and two of its wild relatives with the devastating pathogen *Phytophthora infestans* (*P. infestans*) by time-series experiments, we moved on to large-scale profiling the expression of resistance genes (*R*-genes) in potato and tomato during infection. *R*-genes – powerful activators of immunity – recognize infections by binding to pathogen secreted effectors or monitoring alterations caused by these effectors (Jones and Dangl, 2006). Afterwards, we reconstructed the network of genes (specifically immune-related genes), which are regulated by microRNAs (miRs). miRs are short, non-coding RNAs that degrade or translational inhibit messengerRNAs (mRNAs) by complementary binding (Bartel, 2009). Additionally, we analyzed the potential of the water fern *Azolla filiculoidse* (*A. filiculoides*) to receive and signal the two immune-related phytohormones jasmonic acid and salicylic acid as well as its interaction with its nitrogen-fixing cyanobiont. Finally, we used my experience with the tomato/*P. infestans* time-series experiment to identify potential biocontrol organisms of *P. infestans* on tomato. Biocontrol organisms

are organisms that either directly defeat pests or prime the plant for upcoming infections without causing damage to the hosts. In summary, my experiments showed that the plant immune system is a complex multilayered and highly adaptive system which needs to be tightly controlled to ensure the healthy status of most plants.

1.2 Personal bibliography

This dissertation is written in a cumulative style. It contains five peer-reviewed publications from international journals, as well as two unpublished articles. The five peer-reviewed publications consist of three research papers as well as one review paper and one meeting report. I contributed either as first author or co-author to each publication. The level of contribution to each article is given on the title page of each publication. The articles are sorted by theme rather than in chronological order. The content of the articles (including text figures and tables) has not been changed. The original PDF versions of the publications are provided in the Appendix. Supplementary materials such as figures and tables of each publication are published together with the original journal publications.

de Vries, S., de Vries, J., **von Dahlen, J. K.**, Gould, S. B., Archibald, J. M., Rose, L. E., & Slamovits, C. H. (2018). On plant defense signaling networks and early land plant evolution. *Communicative & Integrative Biology*, *11*(3), 1-14.

de Vries, S., Kukuk, A., **von Dahlen, J. K.**, Schnake, A., Kloesges, T., & Rose, L. E. (2018). Expression profiling across wild and cultivated tomatoes supports the relevance of early miR482/2118 suppression for Phytophthora resistance. *Proceedings of the Royal Society B: Biological Sciences*, *285*(1873), 20172560.

von Dahlen, J. K., Schulz, K., Nicolai, J., Rose, L. E. (in review at *Frontiers in Plant Science*): Global expression patterns of *R*-genes in tomato and potato.

von Dahlen, J. K., Graf, C., Rose, L. E. (unpublished): Large-scale study of miRNA targets and their functions in tomatoes.

de Vries, S., de Vries, J., Teschke, H., **von Dahlen, J. K.**, Rose, L. E., & Gould, S. B. (2018). Jasmonic and salicylic acid response in the fern *Azolla filiculoides* and its cyanobiont. *Plant, Cell & Environment*, *41*(11), 2530-2548.

de Vries, S., **von Dahlen, J. K.**, Schnake, A., Ginschel, S., Schulz, B., & Rose, L. E. (2018). Broad-spectrum inhibition of *Phytophthora infestans* by fungal endophytes. *FEMS Microbiology Ecology*, *94*(4), fiy037.

Frantzeskakis, L., **von Dahlen, J. K.**, Panstruga, R., & Rose, L. E. (2018). Rapid evolution in the tug-of-war between microbes and plants. *New Phytologist*, *219*(1), 12-14.

The following two publications are not part of this thesis. The original PDF versions of the publications are not provided in the Appendix but are online available in form of the original journal publications.

Houwaart, T., Belhaj, S., Tawalbeh, E., Nagels, D., Fröhlich, Y., Finzer, P., ...**von Dahlen, J. K.**, ... & German COVID-19 OMICS Initiative. (2022). Integrated genomic surveillance enables tracing of person-to-person SARS-CoV-2 transmission chains during community transmission and reveals extensive onward transmission of travel-imported infections, Germany, June to July 2021. *Eurosurveillance*, 27(43), 2101089.

Schnake, A., Hartmann, M., Schreiber, S., Malik, J., Brahmman, L., Yildiz, I., **von Dahlen, J. K.**, ... & Zeier, J. (2020). Inducible biosynthesis and immune function of the systemic acquired resistance inducer N-hydroxypipelicolic acid in monocotyledonous and dicotyledonous plants. *Journal of experimental botany*, 71(20), 6444-6459.

The following publication based on my master thesis. It is therefore not included in this thesis. The original PDF version of the publication is not provided in the Appendix but is online available in form of the original journal publication.

de Vries, S., **von Dahlen, J. K.**, Uhlmann, C., Schnake, A., Kloesges, T., & Rose, L. E. (2017). Signatures of selection and host-adapted gene expression of the *Phytophthora infestans* RNA silencing suppressor PSR2. *Molecular plant pathology*, 18(1), 110-124.

1.3 Outline

This dissertation is written in a cumulative style. It contains five peer-reviewed publications from international journals as well as two unpublished articles. The five peer-reviewed publications consist of three research papers as well as one review paper and one meeting report. I have contributed to each publication either as first or joint author. The contribution level of each article is indicated on the title page of each publication. The articles are sorted by topic, not chronologically.

Based on the first publication – the review **“On plant defense signaling networks and early land plant evolution”** – I will introduce the general concept of plant defense and its evolution to the reader. The main aspect of this introduction will be ancient plant-microbe interactions and the evolution of the pattern- as well as the effector-triggered immunities (PTI, ETI; Jones and Dangl, 2006). The upcoming three articles will focus on the interaction of the miR482-superfamily with *R*-genes. First, I will present our data showing that the miR482-superfamily regulates *R*-genes of the nucleotide-binding leucine-rich-repeat class (NBS-LRRs) within the cultivated tomato. We further hypothesize in our paper **“Expression profiling across wild and cultivated tomatoes supports the relevance of early miR482/2118 suppression for *Phytophthora* resistance”** that *P. infestans* mediated RNA silencing suppression is predominantly active in the interaction of the pathogen with the cultivated tomato rather than wild tomatoes. At the same time, the RNA silencing suppressors of *P. infestans* seem to interact with the RNA silencing machine of the plant to disturb the synthesis of miRs and/or to release the suppression of RNA silencing targets by miRs. Inspired by expression profiling of a few *R*-genes using real-time quantitative polymerase chain reaction (qPCR), we became interested in the general patterns of *R*-gene expression across species, time and pathogens. In the next, yet to be published article **“Global expression patterns of *R*-genes in tomato and potato”** we therefore profiled the expression of 940 *R*-genes of tomato and potato in 315 transcriptomes investigating both beneficial and pathogenic interactions. The study indicates that potatoes and tomatoes possess a core of permanently low to moderately expressed *R*-genes. These core *R*-genes might be necessary to detect and classify attacking pathogens at any given time. Furthermore, we noticed that the expression of *R*-genes is influenced by the tissue-type rather than the pathogens. The primary aim of the fourth, yet to be published paper **“Large-scale study of miRNA targets and their functions in tomatoes”** is to reconstruct the whole miR repertoire interacting network (with a focus on the miR482/*R*-gene network). We found out that the few-targets hypothesis (Zhao et al., 2017) describes the reconstructed network the best, meaning that instead of regulating many targets miRs regulate only a few targets in a powerful manner. Since miRs mainly regulate the expression of transcription factors and *R*-genes, which are themselves powerful regulators of expression (Hobert, 2008; Jones and Dangl, 2006), we hypothesize that the contribution of miRs towards transcriptional regulation is considerable.

Coming back to my review paper **“On plant defense signaling networks and early land plant evolution”**, we shed light on the role of phytohormones in the plant immune system. Phytohormones such as ethylene (ET) or jasmonic acid (JA) are small signalling molecules in plants controlling all aspects of life such as growth, stress tolerance and, most importantly for us, defense (Peleg & Blumwald, 2011; Wani et al., 2016; Hartmann & Zeier, 2019). For example, during infection salicylic acid (SA) regulates the production of reactive oxygen species (ROS; Herrera-Vásquez et al., 2015) and is also involved in the activation of the hypersensitive response, both intertwined defense mechanisms of the plant that cause cell death (Ishikawa et al., 2006). In the study **“Jasmonic and salicylic acid response in the fern *Azolla filiculoides* and its cyanobiont”** we reconstructed the JA and SA signaling of the water fern *Azolla filiculoides* (*A. filiculoides*) that belongs to an underrepresented non-angiosperm lineage. By using transcriptomic data, we could show that *A. filiculoides* is theoretically capable of producing and sensing SA and JA. Following that we showed that the fern is responsive to exogenously applied SA. Further we suggest that *Azolla* might interact with its cyanobiont by using phytohormones.

Identifying ways to support the plant immune system during pathogen attack is another aspect of studying plant immunity. In the article **“Broad-spectrum inhibition of *Phytophthora infestans* by fungal endophytes”** I studied four potential biocontrol organisms for their potential to control the devastating pathogen *P. infestans* of the cultivated tomato. Biocontrol organisms among others support the plant during an infection by promoting plant fitness (Hiruma et al., 2016) and/or directly fighting pathogens, for example by competing for nutrients (Lahlali and Hijri, 2010) or secreting antimicrobial compounds (Mousa and Raizada, 2013). Our data proved that *Phoma eupatorii* (*P. eupatorii*) in particular can inhibit *P. infestans* both *in vitro* and *in vivo*. The final article – a meeting report about **“Rapid evolution in the tug-of-war between microbes and plants”** – will give a general overview of the future challenges the plant immune system (and the scientist working in this field) has to tackle. The main focus is the antagonistic co-evolution of both microbes and plants, which forces them to permanently co-adapt to each other.

2.1 The plant immune system

Plants need a finely-tuned, powerful immune system to defeat the constant efforts of pathogens to establish infections. When confronted with an attack the plant has to tighten its screws – namely its immune system – with extreme care and precision to create the best conditions for fighting off the pathogen without wasting resources. This precise tightening of the screws is hampered by constitutively changing environments, diverse pathogenic infection strategies and resource limitations among other factors (McDowell et al., 2005; Krasileva et al., 2011; MacQueen & Bergelson, 2016). A young plant with access to limited resources but highly competitive pressure, for example, can spend less energy in fending off pathogens than older well-established plants. But the plant immune system has to achieve even more: It needs to classify any bypassing microbe as fast as possible based on both its detrimental as well as its advantageous potential. Fending off every kind of interaction will not only prevent the establishment of advantageous interactions such as the colonization by nitrogen-fixing bacteria (Black et al., 2012) but can also stimulate the growth-defense trade-off in a negative way, meaning that plants can either invest in defense or growth but not both at the same time (Tian et al., 2003; Vos et al., 2013; Karasov et al., 2014).

In this chapter, I will give first insights into the highly dynamic system of plant resistance by referring to the most essential parts of my review paper “**On plant defense signaling networks and early land plant evolution**”. More detailed information on the evolution of the plant immune system and early land plant evolution can be found in the review. To classify microbes and counteract infections the plant immune system relies among others on diverse signal-transducing phytohormones (Hartmann & Zeier, 2019), pathogen-recognizing cell-membrane bound receptors and *R*-genes (Jones and Dangl, 2006; Zipfel, 2014) as well as toxic or cell wall reinforcing phenylpropanoids (La Camera et al., 2004). Thereby the defense system itself consists of common defense mechanisms across plant species (e.g. *R*-genes of the nucleotide-binding site leucine-rich repeat (NBS-LRR) class; Shao et al., 2019) as well as of lineage-specific ones (e.g. the synthesis of the antimicrobial and fungicidal glycoalkaloid alpha-tomatine in tomatoes (Gomes et al., 2014)). In addition, it is reasonable to assume that parts of the immune system predate the terrestrialization of plants as ancient basal lineages of land plants as well as the closest extant relatives of land plants, streptophyte algae, already had to and to this day still have to deal with microbes (Wickett et al., 2014; Delaux et al., 2015; Selosse et al., 2015; de Vries & Archibald, 2018). Furthermore, members of the basal land plant lineages and streptophyte algae were shown to own compounds of the modern plant immune system such as receptor-like kinases (LysM-RLKs), phytohormones and NBS-LRRs (Gust et al., 2012; Yue et al., 2012; Gao et al., 2018; Rey & Jacquet, 2018; de Vries & Archibald, 2018). It is therefore thought that plant terrestrialization merely

changed and shaped the kind of microbe-plant interactions that already existed prior. In agreement with this statement liverworts of the genus *Marchantia*, which belong as hornworts to the bryophytes, seed- and flowerless land plants of the basal lineage, were able to establish mutualistic interactions with growth-promoting endophytes (Nelson et al., 2018) as well as with several mycorrhiza-like species (Humphreys et al., 2010). Complementary to *Marchantia*, Kowal et al. (2018) have determined that another liverwort genus called *Cephalozia* was able to establish mutualistic interactions as well.

Similar to most bryophytes the streptophyte algae *Coleochaete pulvinata*, *Chaetosphaeridium globosum* and *Nitella tenuissima* were also shown to interact with nitrogen-fixing microbes (Knack et al., 2015). Fossil records of the symbiosis between streptophyte algae and fungi date back more than 400 million years (Strullu-Derrien et al., 2014). In agreement with these versatile interactions of bryophytes and streptophytes with microbes, molecular data indicates that homologs of symbiosis-associated genes were already present in streptophyte algae and most likely also in the last common ancestor of land plants (Wang et al., 2010; Delaux et al., 2015). Besides such examples of symbiosis, all lineages of land plants and their closest relatives had and will always have to deal with potentially harmful organisms. In agreement with that, a fossil documented that a parasitic fungus colonized *Paleonitella*, a relative of streptophyte algae, more than 400 million years ago (Taylor et al., 1992). It is also known that several LysM-RLKs, phytohormones as well as symbiotic transcription factors carry out dual functions in symbiosis and immunity (Gust et al., 2012; Rey & Jacquet, 2018). Therefore, land plants ranging from bryophytes to gymno- and angiosperms as well as their closest relatives have had and still have to deal with diverse microbes being potentially both beneficial as well as harmful to them.

These examples of early occurring interactions with microbes emphasize the essential function of the immune system to classify microbes. Therefore, the recognition of microbes relies on the PTI as well as the ETI (Jones and Dangl, 2006; Figure 1). To trigger PTI, highly abundant and surface-exposed molecular structures that are common as well as essential for microbes called pathogen-associated molecular patterns (PAMPs) are bound by cell-surface pattern recognition receptors of the plant (PRRs; Medzhitov & Janeway, 1997). Typical PAMPs are the cell wall compound flagellin of fungi (Felix et al., 1999) and the bacterial cold shock protein CSP (Felix & Boller, 2003). By binding, PRRs recognize these PAMPs as belonging to external organisms and therefore trigger the PTI (Jones and Dangl, 2006). Activation of PTI results among others in cell death caused by the hypersensitive response (HR) through the accumulation of ROS (Lloyd et al., 2014), stomata closure (Melotto et al., 2006), or cell wall reinforcements at the site of infection to prevent the establishment of the pathogen within the host (Figure 1). In detail: Cell wall reinforcements are established through callose deposition, lignification

of lignin molecules or formation of papillae, a thickening of the plant cuticle (Smit & Dubery, 1997; Lloyd et al., 2014). Koh et al. (2012) even identified callose depositions within plasmodesmata, microscopic small channels between phloem cells of plants that control phloem flux from source to sink tissue, in citrus leaves as a reaction to infection with *Candidatus Liberibacter asiaticus*.

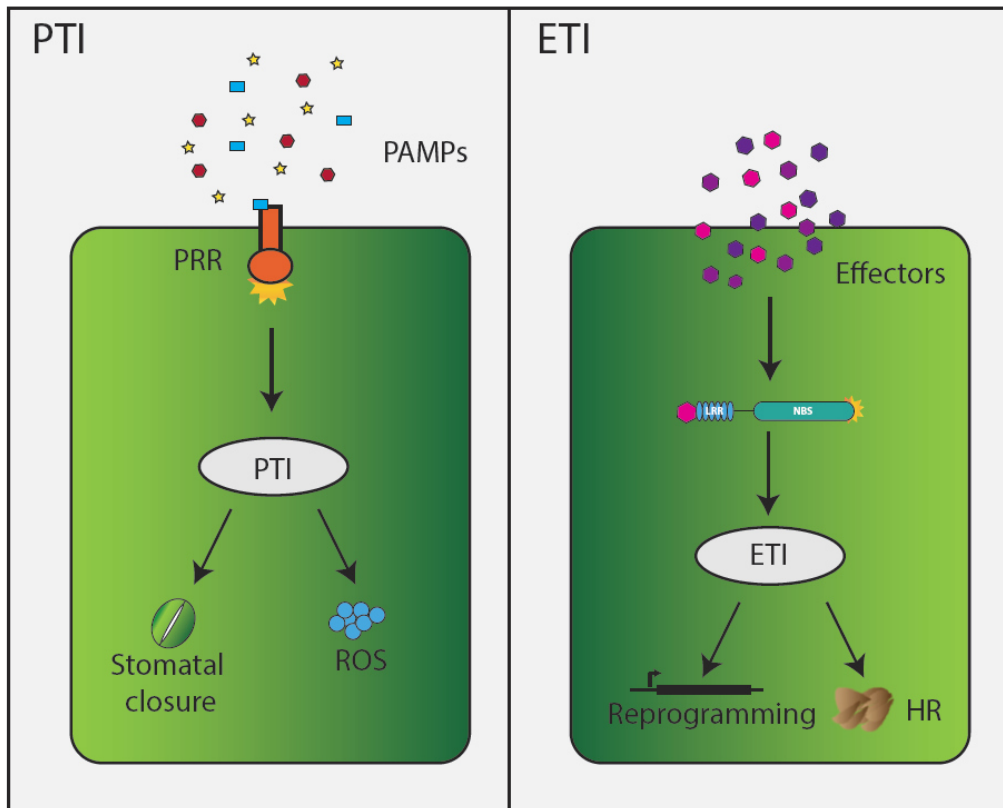


Figure 1: The interplay of PTI and ETI with the plant immune system

Left side: Recognition of PAMPs such as flagellin or chitin by host receptors of the PRR-family leads to the triggering of PTI, an unspecific, but broad counter-reaction of the plant immune system. PTI results among others in the accumulation of ROS or stomatal closure. *Right side:* Virulent pathogens evolved various effectors to suppress PTI. In response to the evolution of pathogenic effectors, plants use R-proteins (such as NBS-LRRs) to recognize effectors. These R-proteins elicit the ETI, a pathogen-specific and more powerful counter-reaction of the plant immune system. ETI results among others in cell death caused by HR and transcriptional reprogramming. The figure is modified from Rovenich et al. (2014) and Pieterse et al. (2009).

The PTI seems to be an ancient layer of the plant immune system as the potential for triggering PTI was already discovered in streptophyte algae as well as in several other early-branching land plants. Streptophyte algae such as *Coleochaete* and *Nitella* for example contain lignin-like compounds which might be used as cell wall reinforcements against the penetration of pathogens (Delwiche et al., 1989; Ligrone et al., 2008; Sørensen et al., 2011). Another streptophyte algae named *Klebsormidium* spp. In turn accumulates callose on its cell wall as a reaction to desiccation stimulus (Herburger & Holzinger, 2015). Matching this scheme, *Marchantia polymorpha*, a liverwort belonging to the early-branching land plants, was shown to deposit callose in its cell wall as well after infection with the oomycete

Phytophthora palmivora (Carella et al., 2018). The mosses *Funaria hygrometrica* and *Physcomitrella patens* (*P. patens*) in turn form papillae at microbial penetration sites to prevent the establishment of infections (Davey et al., 2009; Davey et al., 2010; Overdijk et al., 2016). In addition to papillae formation, *P. patens* reacts to oomycete and fungal infections by accumulating ROS and/or toxic compounds (Oliver et al., 2009). It is also thought by many scientists that to induce such immune reactions, bryophytes as well as streptophyte algae need to sense microbes using pattern-recognition receptors. However, at least *P. patens* is missing an orthologue of the most prominent pattern-recognition receptor FLS2 that is responsible for sensing bacterial flagellin (Boller & Felix, 2009). Yet, *P. patens* is not able to trigger an immune reaction following flagellin-treatment (Bressendorff et al., 2016). Instead, *P. patens* possesses an orthologue of CERK1 which recognizes and reacts to bacterial peptidoglycan as well as fungal chitin (Bressendorff et al., 2016). These results let the authors of Bressendorff et al. (2016) suggest that lineage-specific receptors or evolutionary younger receptors are responsible for recognizing microbes of modern land plants.

Overall, since common molecular structures evolve in a slow manner based on their essential functions for pathogens, PTI represents a durable and irremissible first layer of the plant immune system. As such it prevents non-adapted microbes from establishing an infection (Jones & Dangl, 2006). However, successfully co-adapted microbes can overcome PTI by evolving effectors. Effectors are pathogen-specific molecules and proteins which interfere with the immune system of the plant to establish pathogenic infections (e.g. by suppressing callose deposition at the infection site (Fabro et al., 2011), transcriptional re-programming of the host (Tsuda & Katagiri, 2010) or by secreting protease inhibitors (Song et al., 2009)). Therefore, plants have evolved a second, more specific layer of immunity, the ETI (Figure 1). To induce ETI, plant resistance proteins (R-proteins) either bind directly to the corresponding pathogen-secreted effectors or trigger ETI indirectly by monitoring either effector-modified proteins called guardees or effector-activated proteins which are specialized in detecting infections called decoys (Jones & Dangl, 2006; Kourelis & van der Hoorn, 2018, Figure 2). Once elucidated, ETI induces a cascade of pathogen-specific immune reactions (e.g. activation of HR or ETI-mediated pathogen-specific transcriptional re-programming (Glazebrook, 2005; Tsuda & Katagiri, 2010; Figure 1).

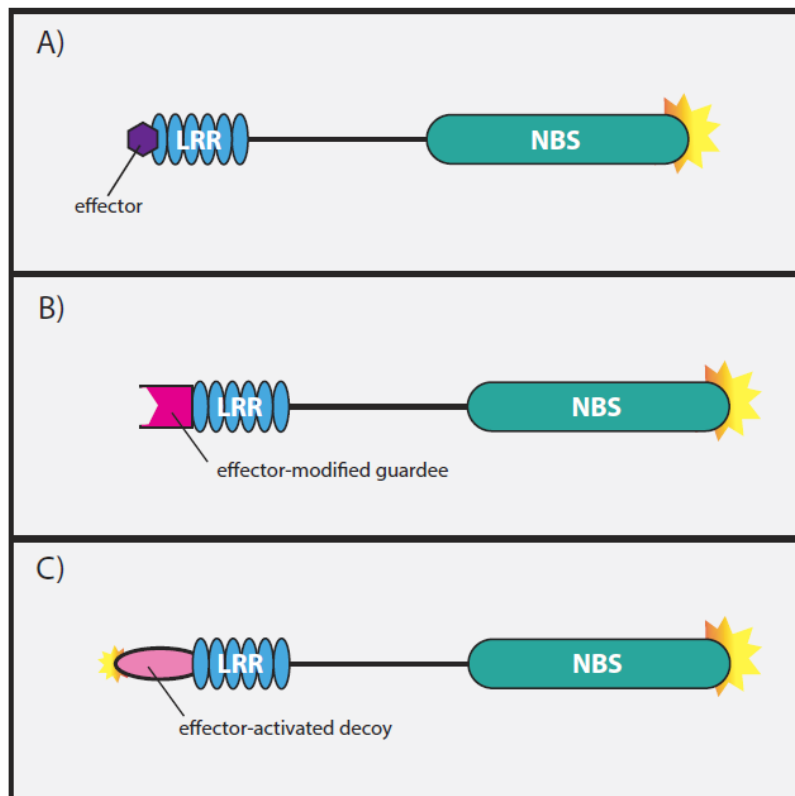


Figure 2: The three ways of NSB-LRR activation by pathogenic effectors

NBS-LRRs, the major class of *R*-genes in plants, consist of the pathogenic infection recognizing LRR-domains (light blue) and a downstream signaling activating NBS-domain (turquoise). NBS-LRRs trigger ETI by either binding directly to corresponding pathogenic effectors (gene-for-gene hypothesis; purple hexagon; A) or activating immunity by monitoring either effector-modified proteins called gardees (pink square; B) or proteins which are specialized to detect infections called decoys (rose oval; C).

Besides a few enzymatic *R*-genes (Gururani et al., 2012), the major class of *R*-genes is formed by the NBS-LRRs (Meyers et al., 2005). Recognition of effectors or modified/activated gardees and decoys of this prominent *R*-gene family is mediated by the LRR-domain while downstream signaling is triggered by the NBS-domain (McHale et al., 2006; Figure 2). Potential NBS-LRRs can be found in gymno- and angiosperms (Yue et al., 2012) as well as in diverse streptophyte algae such as *Coleochaetales* (Yue et al., 2012) and *Klebsormidium nitens* (Gao et al., 2018). A high variance in the number of NBS-LRR genes within species is common ranging from 16 putative NBS-LRRs in the lycophyte *Selaginella moellendorffii* (Gao et al., 2018) to 2042 NBS-LRRs in the wild pepper Chiltepin (Wei et al., 2016). This is caused by the fact that NBS-LRR repertoires are known to be shaped by species-specific reduction as well as expansion processes reflecting the highly dynamic co-adaptation of this gene class with the pathogenic effector repertoires (Zhang et al., 2016).

In summary, compared to the PTI, the ETI (and therefore *R*-genes) is more precisely adapted towards attacking pathogens and is consequently the more powerful layer of the plant immune system. The basis of ETI pre-dates thereby the terrestrialization by plants (Cui et al., 2015). However, even the ETI sometimes fails because pathogens have evolved new repertoires of effectors or new infection strategies to avoid the triggering the plant immune system in the past and will incessantly continue to do so. This permanent circle of co-evolving between pathogens and hosts is well known and is called the molecular arms race or zig-zag-zig model (Jones & Dangl, 2006). For analyzing the expression, regulation and evolution of the plant immune system, this highly dynamic background of the plant immune system always needs to be considered.

2.2 A case study: The interaction of cultivated tomato and its wild relatives with the pathogen *Phytophthora infestans*

Oomycetes belong to the eukaryotic stramenopiles to which also brown algae and diatoms count (Thines, 2018). Although being morphologically alike fungi, oomycetes accumulate among others cellulose instead of chitin in their cell walls, produce two flagellated spores and utilize distant biosynthesis pathways for lysine and sterol than fungi (Thines, 2018). One of the best-known oomycetes is *P. infestans* a devastating pathogen of Solanaceae such as cultivated tomatoes (*Solanum lycopersicum*, *S. lycopersicum*), eggplants, chili or potatoes (*Solanum tuberosum*, *S. tuberosum*; Fry, 2008). Many of these Solanaceae species are of fundamental importance for feeding the world. Potato as the most important non-cereal crop, for example, yielded in 2017 in 487 million tons (Food and Agriculture Organization of the United Nations). Yet, even nowadays *P. infestans* and other deleterious pathogens cause huge harm to these crops by outcompeting their immune systems (Nowicki et al., 2012). *P. infestans* as a hemibiotrophic pathogen is having a pi-parted life cycle (Figure 3). The pathogen first establishes its colonization by feeding on living host tissue while staying asymptomatic to the plant (Glazebrook, 2005). After a few days, *P. infestans* switches to the necrotrophic phase meaning that it starts to kill off the host to feed on dead tissue (Glazebrook, 2005). To establish the biotrophic stage, *P. infestans* spores germinate on the plant surface, form a cell wall penetrating appressorium and enter through this structure the plant. During its biotrophic phase, *P. infestans* spreads within the host by forming between plant cells growing hyphae as well as haustoria, interacting sites of hosts and pathogens where proteins and molecules such as effectors are secreted (Allen & Friend, 1983; de Vries et al., 2017). By switching to the necrotrophic phase, the hyphae start to ramify and spore mature within sporangia to be released for infection of other plant compartments of the same plant or other plants in general (Grenville-Briggs et al., 2005). The necrotrophic phase of *P. infestans* is characterized by water soaking, rotting of fruits or tubers and necrosis of the plant (Grenville-Briggs et al., 2005; de Vries et al., 2017). *P. infestans* can propagate both asexual and sexual (Nowicki et al., 2012). By the asexual propagation rapid spread of the pest is achieved; by sexual propagation of two mating types that co-infect the same host the genetic variation within the species increases. Both life cycles are essential for *P. infestans* to be one step ahead of the plant and its immune system.

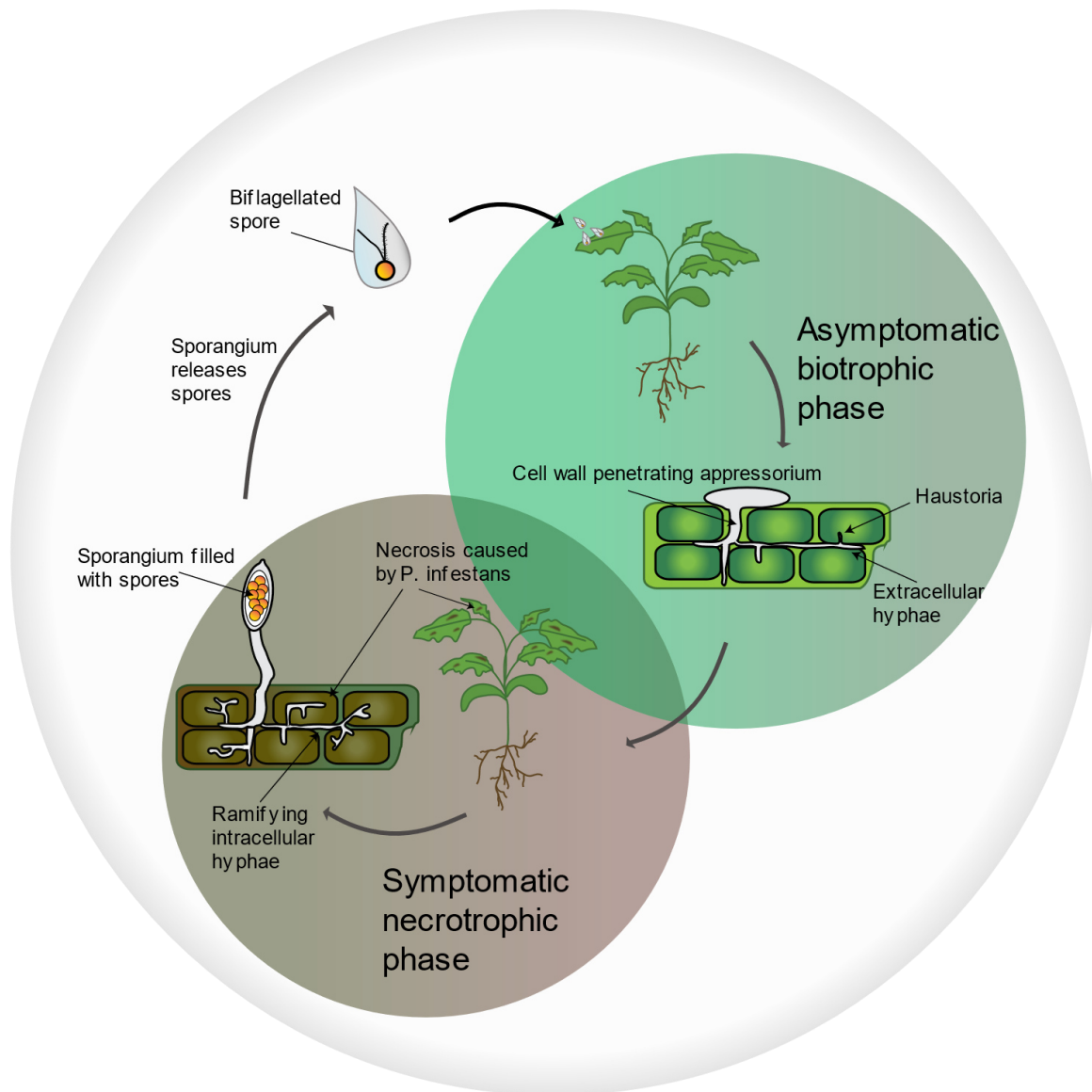


Figure 3: The bi-parted, asexual life cycle of *P. infestans*

When attached to plants biflagellated spores of *P. infestans* form cell walls penetrating appressoria. After entering the plant through appressorium formation, *P. infestans* colonizes the plant by forming extracellular hyphae as well as haustoria. Haustoria are interacting sites of hosts and pathogens (e.g. for the secretion of effectors). During its biotrophic phase the pathogen stays asymptomatic to its host. When entering the necrotrophic phase, the hyphae start to ramify and grow intracellular. The plant becomes furthermore symptomatic as the pathogen starts to kill the host to feed on dead plant tissue. The up-taken nutrition of the host is used by *P. infestans* to form spore containing sporangia. Mature spores are released from sporangia to infect other plant compartments or plants (modified from Bianca Griebel (2019), unpublished Master thesis in the Institute of Population genetics).

Wild relatives of cultivated crops are well-known natural sources of resistance. They have experienced other evolutionary pressure caused by pathogens such as *P. infestans* as their highly breeding affected and often in monocultures growing cultivated relatives (Garry et al., 2005). Therefore, they may have evolved other mechanisms of defense. In agreement with that several studies identified candidate genes for resistance gene cloning into cultivated crops from wild relatives. In case of cultivated tomatoes these are: the black nightshade *Solanum americanum* (Witek et al., 2016), the litchi tomato *Solanum sisymbriifolium* (Namisy et al., 2019), the turkey berry *Solanum torvum* (Namisy et al., 2019), the wild tomato *Solanum habrochaites* (Arafa et al., 2017) as well as diverse nontuber-bearing *Solanum* spp. (Garry et al., 2005).

miRs are short, non-coding RNAs that select messenger RNAs (mRNAs) by complementary binding for degradation or translational inhibition (Bartel, 2009; Figure 4). As non-coding RNAs, miRs belong to the smallRNAs and are part of the RNA silencing machinery in which gene expression is negatively regulated by smallRNAs (Bartel, 2009). miRs are transcribed from miR encoding genes and are further processed by Dicer-like proteins (Dicer) from the longer double-stranded hairpin-structured primary miRNAs (pri-miRNAs) into the shorter likewise hairpin-structured precursor-miRNAs (pre-miRNAs; Bernstein et al., 2001; Figure 4). Finally, Dicer cleaves the short double-stranded miR/miR* complex out of the precursor-miR (Bernstein et al., 2001). Then the complementary and slightly to each other shifted mature miR or miR* are single-stranded loaded into Argonaute proteins which bind guided by the miR or miR* to complementary target-mRNAs (Fagard et al., 2000; Zhang et al., 2011). The binding results either in the degradation or translational inhibition of the targets (Voinnet, 2009). miRs are involved in the regulation of most major plant processes ranging from plant organ development over disease resistance to abiotic stress responses (Rubio-Somoza & Weigel, 2011). The miR156 of *Arabidopsis thaliana*, for example, determines gene doses-dependent the root cell fate by degrading class III homeodomain-leucine zipper transcription factors (Carlsbecker et al., 2010). Another example of a miR/mRNA interaction is the miR-JAW. It controls the development of leaves by controlling expression levels of TCP transcription factors (Palatnik et al., 2003). Furthermore Vaucheret et al. (2004) determined that the expression levels of Argonaute1 itself are regulated by miR168 creating a positive feedback loop within miR-synthesis.

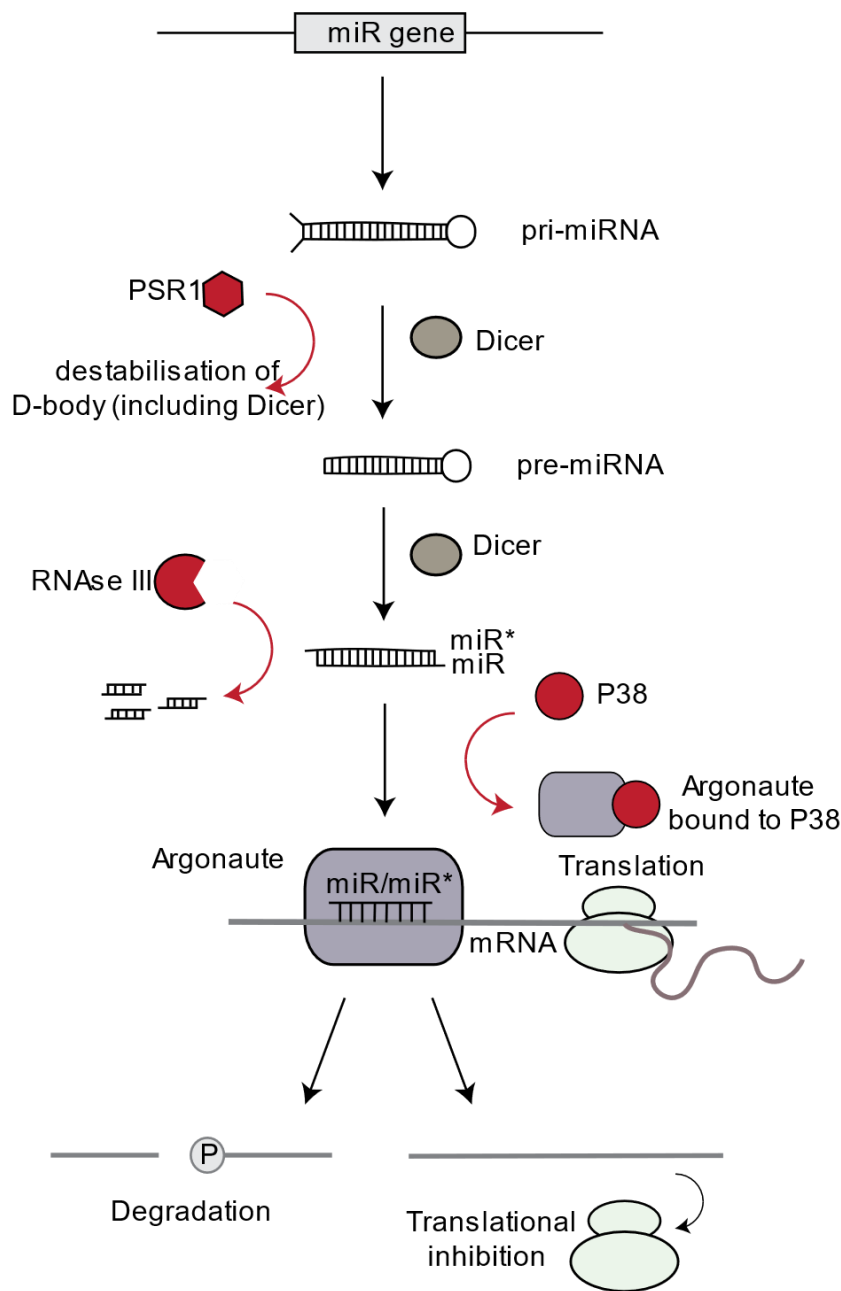


Figure 4: Interaction of pathogenic RNA silencing suppressors with the RNA silencing machinery of the plant
 miRs are transcribed from miR encoding genes and processed by Dicer (grey oval) from hairpin-structured pri-miRNAs into shorter likewise hairpin-structured pre-miRNAs. In the following Dicer cleaves the short double-stranded miR/miR* complex out of the pre-miRNA which is in turn single-stranded loaded into an Argonaute protein (purple round-shaped rectangle). The miR/Argonaute- (or the miR*/Argonaute) complex binds guided by the miR or miR* to reverse-complementary target-mRNAs. The targets become either degraded or translational inhibited. To manipulate the RNA silencing machinery of the plant, virulent pathogens secrete effectors (red-shaped forms). The pathogenic effector PSR1 of *P. infestans* disrupts for example miR synthesis by destabilizing the D-body (and the within the D-body accumulating Dicer). The effector RNase III of the *Sweet potato chlorotic stunt virus* in turn inactivates miRs/miR*s by degradation into extremely short fragments. P38, another effector, inactivates Argonaute by mimicking glycine/tryptophan-containing proteins. The figure was inspired by Pumplin & Voinnet (2013).

R-genes, as an essential part of the plant immune system, rely on tight transcriptional as well as post-transcriptional regulatory systems to avoid misregulations which came along with high fitness costs (for detailed information on fitness costs and alternative regulation of *R*-genes see part 2.3; Li et al., 2015). Post-transcriptional regulation of *R*-genes in dicots is achieved among other factors by miRs such as miR6024 (Wei et al., 2014) and miR482/2118 (Shivaprasad et al., 2012; de Vries et al., 2015) in tomato as well as miR6019 and miR6020 in tobacco (Li et al., 2012). I will focus in the following section on the miR482/*R*-gene interaction as this miR-family is predicted to regulate far the most *R*-genes from *S. lycopersicum* (~20%; de Vries et al., 2015). For comparison: The miR6024 of tomato is known to regulate only *R*-genes of the *I2*-homologue family (Wei et al., 2014). Furthermore, the rise of the miR482/2118-superfamily within the gymnosperms seems to be accompanied by an enlargement of *R*-genes of the NBS-LRR class, emphasizing the important regulative role of this superfamily (Zhang et al., 2016). The miR482/2118-superfamily consists in *S. lycopersicum* of seven members which display unusually high sequence diversity even within closely related species (Shivaprasad et al., 2012; de Vries et al., 2015). De Vries et al. (2015) further determined a high degree of interconnectivity and redundancy in the miR482/*R*-gene network meaning that several miR482-superfamily members are predicted to target the same *R*-genes. They suggest that this high interconnectivity and redundancy make the network more robust toward the adaptive potential of pathogens.

Several pathogenic effectors were shown to suppress the RNA silencing machinery (and hence also the miR biosynthesis) of their hosts (Pumplin & Voinnet, 2013; Figure 4). The *turnip crinkle virus* protein P38, for example, mimics glycine/tryptophan-containing proteins to bind to and thus inactivate Argonaute1 (Azevedo et al., 2010). Another protein, RNA endoribonuclease III (RNase III), of the *Sweet potato chlorotic stunt virus* was shown to inactivate smallRNAs such as miRs by degradation (Cuellar et al., 2009). Qiao et al. (2013) in turn identified the across diverse oomycetes such as *P. infestans* conserved effector *RNA silencing suppressor 2* (*PSR2*). It was recently shown that *PSR2* suppresses the RNA silencing machinery by associating with the dsRNA-binding protein 4 (DRB4) which is known to stabilize Dicer-like 4, a protein responsible for the synthesis of phasi-miRNAs (for more details on phasi-miRNAs: see part 2.4; Hou et al., 2019). The *RNA silencing suppressor 1* (*PSR1*) in turn destabilizes the formation of the dicing-body (D-body) that includes the Dicer protein and by doing so inhibits miR synthesis (Qiao et al., 2015). Vetukuri et al. (2017) identified another putative, in this case *P. infestans*-specific RNA silencing suppressor: Pi14054. All RNA silencing suppressors have in common that they release genes from the suppression of the RNA silencing machinery. However, suppression of the RNA silencing machinery, results in decreased levels of the miR482/2118-superfamily and therefore in

elevated *R*-gene expression levels – a reaction that seem to be contra-productive to pathogens. It has been thought by Shivaprasad et al. (2012) that this miR482/2118-paradox may have evolved as a counter-defense mechanism of the plant to detect pathogens. In detail: Pathogens evolved RNA silencing suppressors first. As a reaction towards them, plants established the miR/*R*-genes interactions to detect the pathogenic RNA silencing suppressors. However transient silencing of *PSR2* was shown to reduce the virulence of *P. infestans* (Qiao et al., 2013). It is therefore also suggested that the suppression of the RNA silencing machinery destroys the regulative balance of the plant and therefore enhances virulence. In detail: Through the *R*-genes are released from their suppression by the miRs, other genes are as well released and might cause problems to the plant to fightback the pathogen.

With the study “**Expression profiling across wild and cultivated tomatoes supports the relevance of early miR482/2118 suppression for *Phytophthora* resistance**” I wanted to address the following questions:

- i) Can we confirm the regulation of *R*-genes by the miR482/2118-superfamily following infection of *P. infestans* on the cultivated tomato?
- ii) How does the co-evolution between *P. infestans* and cultivated as well as wild tomatoes shape the regulation of *R*-genes by the miR482/2118-superfamily?
- iii) How can this help to explain the miR482/2118 paradox?

In the study, we performed sterile infections of the cultivated as well as two wild-type tomatoes with *P. infestans* and investigated i) the infection progress ii) the expression of the miR482/2118-superfamily and iii) 12 *R*-genes at five different time points (6-96 hours post-infection (hpi)). We determined examples of co-regulation between putative targeted *R*-genes and the miR482/2118-superfamily meaning that when miR482/2118-members were downregulated in turn their target-predicted *R*-genes were upregulated and *vice versa*. As not all *R*-genes were co-regulated with their putative regulators of the miR482/2118-superfamily, we suggested other regulative systems to interact with *R*-genes expression (see also sections 2.3 and 2.4). Also, positive co-regulation between miRs and their targets has been shown (Lopez-Gomollon et al., 2012; Laxman et al., 2015; Wen et al., 2016). In addition, we confirmed by 5’RLM-RACE (for detailed information on the method see section 2.4) that *R*-genes of *S. lycopersicum* are indeed cleaved by members of the miR482/2118-superfamily while infection with *P. infestans*. Prior to our study the cleavage of *R*-genes from tomato by a miR482/2118 member was only shown by overexpression within *Nicotiana benthamiana* (Ouyang et al., 2014). In a next step, we suggested that the expression levels of *R*-genes and miR482/2118-

superfamily members are shaped by co-evolution with hosts as several miR482 members of the most susceptible tested plant, the cultivated tomato, were downregulated while infection starting at 24 hpi. The higher susceptibility of *S. lycopersicum* towards *P. infestans* correlated also with the early downregulation of miR482f and miR482a at 6 hpi. Such early time points of infections are often crucial for the plant as an early HR significantly reduces the infection success by pathogens such as *P. infestans* (Vleeshouwers et al., 2000). In addition to the miR482/2118-family members, we were also able to show that several other miRs (miR156a/b/c, miR166a/b, miR168a/b and miR172a/b) are substantially downregulated in *S. lycopersicum* following infection. This indicates that RNA silencing suppression by *P. infestans* seems to be effective in *S. lycopersicum*. In summary, we confirmed the regulation of *R*-genes by the miR482/2118-superfamily following infection of *P. infestans* on the cultivated tomato, found signs of co-regulation between *R*-genes and the miR482-superfamily and detected that the expression of *R*-genes and miR482/2118-superfamily members were shaped by co-evolution with its hosts. Taken together this hints to the fact that the miR482/2118 paradox might contribute to the higher susceptibility of the cultivated tomato towards *P. infestans*.

2.3 Expression profiling of *R*-genes

Possession and expression of *R*-genes are accompanied by high costs for the plant as a trade-off between growth and defense exists (Kempel et al., 2011; Huot et al., 2014). The growth-defense trade-off occurs as resources are restricted either to defense or growth. For example, Tian et al. (2003) and Karasov et al. (2014) determined in their studies that possession of the *R*-genes *RPM1* as well as *RPS5* significantly reduced seed production. Other studies of fitness costs reported that the transient expression of *R*-genes resulted in high costs in term of cell death (Kim et al., 2010; Chae et al., 2014). Because of this trade-off between growth and defense, *R*-gene expression needs to be controlled by several layers (Figure 5). Besides *R*-gene regulation by miRs (Li et al., 2012; Shivaprasad et al., 2012; Wei et al., 2014; de Vries et al., 2015) another mechanism of regulation are transcription factors that bind to upstream elements of genes to enhance or repress their expression (e.g. ethylene-responsive factor (ERF) which controls *R*-gene expression by binding to their GCC box/non-GCC box cis elements (Latchman, 1997; Chakravarthy et al., 2003)). Another mood of *R*-gene regulation is alternative splicing which means the including or excluding of certain exons of genes from final mRNAs (Baralle & Giudice, 2017). Yang et al. (2014) determined, for example, two *R*-gene splice variants called NAT and NRT for the *R*-gene *N* which even show distinct resistance phenotypes.

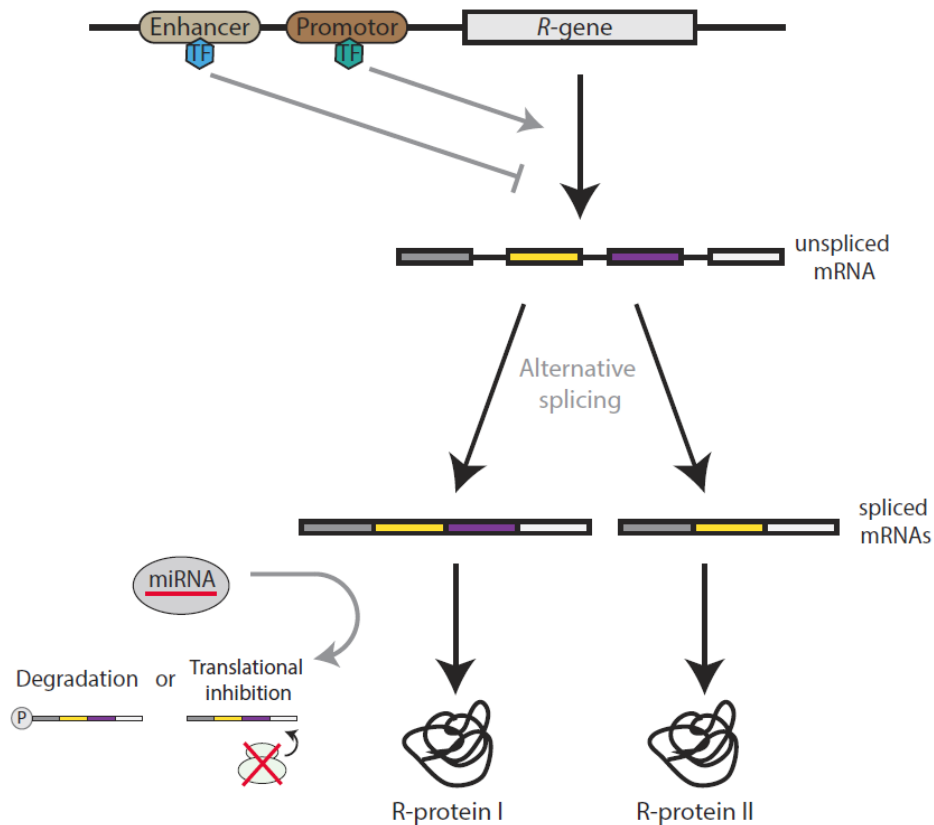


Figure 5: Expression regulation of *R*-genes

The expression of *R*-genes is among others controlled by transcription factors (TF; light blue and turquoise hexagons), alternative splicing events or miRs. TFs bind to upstream laying enhancer (beige box) or promotor (brown box) elements of genes to enhance or repress their expression. Alternative splicing describes the splicing of different splice variants of the mRNA by including or excluding different exons (grey, yellow, purple and white boxes) to produce protein-coding mRNAs. Alternative splicing causes that single genes might code for multiple proteins with distinct functions/phenotypes (e.g. R-protein I and R-protein II). Furthermore, RNA silencing by miRs contributes towards *R*-gene expression regulation by degradation or translational inhibition of mRNAs (e.g. by the miR482-superfamily of tomato or miR6019 and miR6020 from tobacco).

The molecular arms races between hosts and their pathogens force *R*-genes to constantly co-adapt with their corresponding pathogenic effectors to still guarantee recognition of infection. Rose et al. (2004) and Allen et al. (2004) proved for example that the *R*-gene *RPP13* of *Arabidopsis thaliana* and the effector gene *ATR13* of *Hyaloperonospora arabidopsidis* co-adapted as both loci are under balancing. Balancing selection is meaning that multiple alleles of a gene are maintained in genomes. However, most *R*-genes are under purifying selection meaning that deleterious alleles are removed (Gao et al., 2018). But *R*-genes not only need to properly recognize pathogens, they also need to activate pathogen-specific immune responses as particular immune reactions might be effective against certain pathogens but without effect or even infect-supporting on other pathogens (e.g. necrotrophic pathogens might profit from induction of HR as they feed on dead tissue; Gururani et al., 2012). How this specificity of *R*-genes towards pathogens is achieved is however unknown. *Rx* and *Gpa2*, two on sequence levels very similar *R*-genes, detect for example quite different pathogens (Van der Vossen et al., 2000).

With the publication “**Global expression patterns of *R*-genes in tomato and potato**” I address two questions:

- i) How is *R*-gene expression in tomatoes and potatoes shaped by infections?
- ii) How is specificity towards pathogens achieved?

Within the study we analyzed the expression profiles of 940 *R*-genes of tomato and potato across 315 publicly available transcriptomes. We determined that tomato and potato possess a core of continuously expressed *R*-genes which refute the high costs of *R*-gene possession and expression. In agreement with that Burdon and Thrall (2003) emphasized that *R*-genes possess most likely varying fitness costs as otherwise additive and/or multiplicative fitness effects are strongly harmful to the plant. Thus, high fitness costs of single *R*-genes such as *RPM1* (Tian et al., 2003) might be only an exception. It is also worth mentioning that fitness costs are in general hard to calculate as they might be falsified by various background noises (e.g. pleiotropic effects; Brown & Rant, 2013). Moreover, the age – with young plants having only limited resources and high competition levels – and shifting environments were shown to influence the fitness costs of *R*-genes (McDowell et al., 2005; Krasileva et al., 2011; MacQueen & Bergelson, 2016). We assume that the core expressed *R*-genes are permanently turned on as they are needed to permanently monitor and classify plant interacting microbes by their harmful or beneficial potential for the plant. But why is a bunch of permanently activated *R*-genes not enough? Gururani et al. (2012) already stated that *R*-genes most likely expanded as plants need to trigger pathogen-specific signaling cascades to hinder infections. To establish these pathogen-specific signaling cascades, a bunch of different pathogen co-adapted *R*-genes are needed. Additionally, already the three different ways of *R*-gene function (binding of pathogenic effectors (Flor et al., 1971) or monitoring guard cells and decoys (Jones & Dangl, 2006)) underline the need for an enlargement in the *R*-gene repertoires of plants (and therefore also the core *R*-genes).

We further detected that pathogens influence *R*-gene expression only in a minor way. Instead, the tissue type (and the bioproject) are major determinants of *R*-gene expression. In agreement with that tissue-specific expression was also reported for the *R*-genes *CaMi* and *CreZ* by Chen et al. (2007) and Zhai et al. (2008) as well as within transcriptomes of chickpeas (Sharma et al., 2017). Most likely tissue-specific expression of *R*-genes is caused by functional and structural differences between tissues such as higher light intensity and heat stress for leaves than roots. Following these functional and structural differences, the different tissues of plants possess varying challenges for pathogens to establish infections. Driven by the molecular arms race between pathogens and hosts, this tissue-specific expression of *R*-genes might have been even more shaped and strengthened in the past. Consistently

several microbiome studies reveal that tissue-specific colonization of microbes is a common pattern in plants (Jin et al., 2015; Sapp et al., 2018; Maggini et al., 2019).

While tissue-specificity seems to be because of all this a reasonable parameter for explaining *R*-gene expression, the bioproject cannot be counted most likely as reliable. The term bioproject here refers to one laboratory group publishing transcriptomes under their own very specific conditions (e.g. different cultivars, different time points of collecting, different watering schedules). Significance for this factor was presumably achieved as the standardization between experiments was insufficient. For analyzing the true influence of the plant age on *R*-gene expression, one has to minimize, for example, the influence of different pathogens and abiotic stressors on the transcriptomes. Study design and gene expression are therefore indispensably interwoven (Auer & Doerge, 2010; Krzywinski & Altman, 2013; Bi & Liu, 2016). We noticed furthermore that $>¼$ of all tomato *R*-genes are not at all expressed implicating that they represent, for example, inactive fragments or chromosomal silencing or co-evolution with pathogens events. By analyzing the expression patterns of these *R*-genes in wild relatives of the tomato, most of them are still not expressed indicating that they are indeed inactive fragments. However, five *R*-genes – with all of them showing signs of balancing selection which acts against the accumulation of mutations – are expressed in wild relatives of the tomato and are therefore potential candidates for introgression into the cultivated tomato. Summarizing our results, we were able to detect a core of permanently expressed *R*-genes and determined in addition that the expression of *R*-genes is not shaped by their pathogens but instead by the tissue-type. Therefore, we assume that pathogen-specificity is not achieved towards (induction of) *R*-gene expression but by activation of *R*-genes.

2.4 The few- & the many-targets hypotheses of microRNAs

Currently there are two competing hypotheses of miR function existing: The “few-targets” versus the “many targets” hypotheses (Zhao et al., 2017). The “few-targets” hypothesis posits that each miR represses up to ten targets effectively, while the “many-targets” hypothesis assumes that each miR may target hundreds of genes. Evidence for the few-target hypothesis are that i) only a few targets are conserved over time ii) usually targets are weakly repressed by miRs and this leads to negligible fitness effects iii) only a few miR-target interactions influence the phenotype of organisms (Zhao et al., 2017). Evidence for the many-targets hypothesis stems mainly from bioinformatic/genomic analysis which typically uncover up to several hundred putative targets per miR (Enright et al., 2003; John et al., 2004; Fahlgren et al. 2007; Bonnet et al., 2010; Dai et al., 2018). But why should miRs dilute their regulatory power by weakly repressing many targets, instead of targeting a few genes in a powerful way? It was first assumed that the vast majority of putative repressed miR-targets represent noise with no biological relevance (Ecsedi et al., 2015; Pinzón et al., 2017). However further analysis proved that the more nodes a miR/target-network has, the more stable the network becomes, as each additional node might contribute indirectly to the regulation of even more targets (Tay et al., 2014; Chen et al., 2017). In addition, Zhao et al. (2017) assume that if the repression of most miRs is biological noise, the miR-repertoire should have decreased over time. Instead expansions of several miR-families (Tanzer & Stadler, 2004; Marco et al., 2012; Shivaprasad et al., 2012; de Vries et al., 2015) as well as the processing of miRs from both strands of the precursors (further enlarging the regulative network of miRs) were observed (Okamura et al., 2008; Jagadeeswaran et al., 2010; Zhang et al., 2011). Matching the “many-targets” hypothesis the omnigenic model proposes that many complex traits are strongly affected by peripheral genes which have no direct influence on a trait (Boyle et al., 2017). Core genes – genes directly linked to a trait – in turn explain traits to a lesser extent than peripheral genes.

Since miRs play essential roles in a range of spatial and temporal regulatory processes, their abundance and activity need to be tightly controlled. Nucleotide variation within the different regions of the primary miR can affect the expression abundance of miRs and lead to functionally distinct miRs (Liu et al., 2008; Todesco et al., 2012; Wang et al., 2013; Zhu et al., 2013). Additionally, two miRs co-regulate important parts of the miR processing pathway: miR168 regulates the abundance of Argonaute1 (Vaucheret et al., 2004) and miR162 regulates the abundance of Dicer-like1 (Xie et al., 2003). Furthermore, several transcription factors have been shown to influence miR abundance. For example, the SPL transcription factor family promotes the expression abundance of miR172 and miR156 (Wu et al., 2009) and the SLP7 gene activates the expression of miR398 in response to low copper (Yamasaki et al., 2009).

To identify the cleavage of target mRNAs by miRs three methods exist. The fastest and cheapest method uses algorithmic programs such as psRNATarget (Dai et al., 2018) or TAPIR (Bonnet et al., 2010) to predict potential miR-targets in genomes. Both programs rate the likelihood of mRNAs being putative cleaved and/or translational inhibited by miRs by analyzing the complementary similarity between the target-mRNA and the miR, as well as the target site accessibility of the Argonaute/miR-complex. The second method experimentally overexpresses miRs to identify their corresponding downregulated target-mRNAs (Schwab et al., 2005). However, since miRs form complex regulatory networks, direct cleavage of mRNA-targets by miRs is hard to verify using this method. The most accurate verification method up until now relies on the experimental parallel analysis of RNA ends (PARE)-libraries to verify cleaved targets (German et al., 2009; Figure 6). PARE-libraries – also called degradomes or 5'RLM-RACE (see section 2.2) – exploit the fact that a 5' phosphate is left at the miR cleavage site (Figure 5). PARE-libraries are generated by binding of these 5'-phosphates by specific adaptors. Cleaved targets can be verified either by sequencing of single target genes using gene-specific primers or by high-throughput sequencing of entire PARE-libraries. Subsequently the PARE-reads are aligned to their complementary regions in the genome (Figure 6). However, degradation by specific miR cleavage needs to be distinguished from natural mRNA degradation. Therefore, analytical methods are used to evaluate whether an enrichment of degraded products coincides with predicted miR cleavage sites.

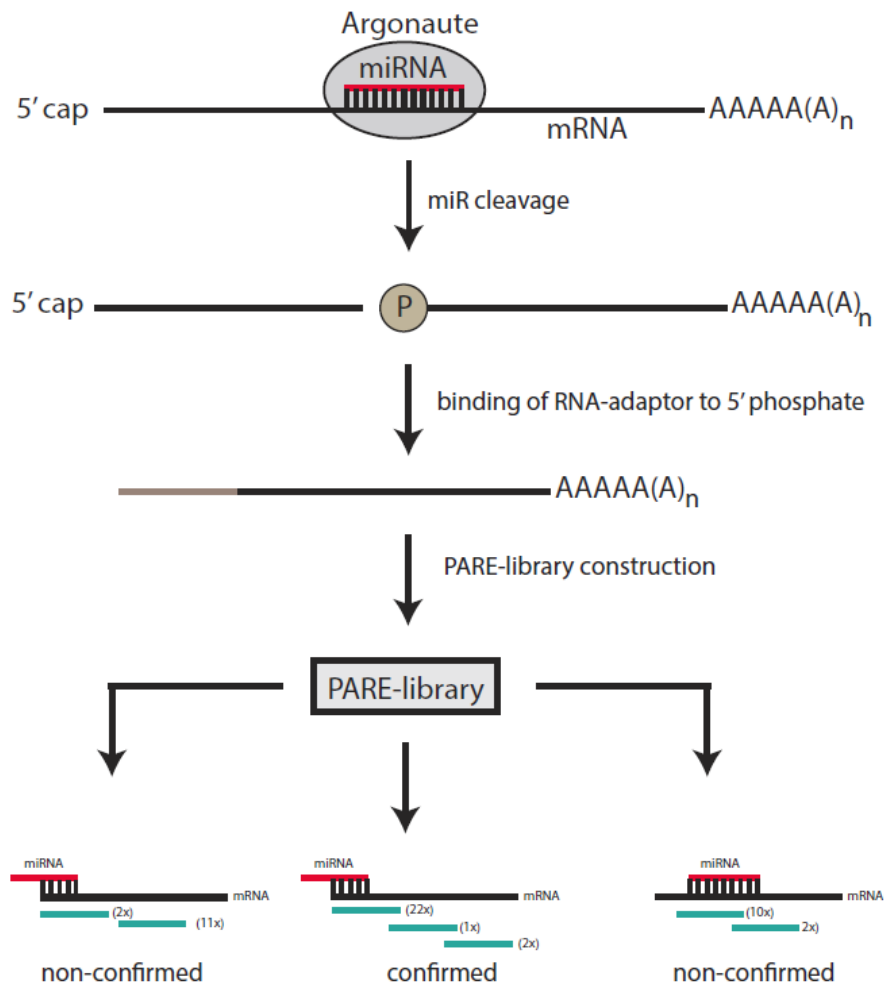


Figure 6: Verification of miR degradation events using PARE-libraries

Cleavage miRs results in 5' phosphates group overhangs at the beginning of each miR-cleavage site. These 5' overhangs are bound to an RNA-adaptor (grey line). PARE-libraries are constructed by reverse transcription, second-strand synthesis, PCR amplification and sequencing of adaptor-bounded mRNA sequences. Valid miR-targets are distinguished from naturally degraded mRNAs by being enriched for reads that start exactly at the cleavage site of miRs (turquoise lines; the number in brackets stands for the number of reads). *Left side*: Non-validated miR-target: the miR-cleavage site is lacking adequate read coverage (non-enriched). *Middle*: Validated miR-target: the read starts at the miR-cleavage site and features adequate read coverage. *Right side*: Non-validated miR-target: no read starts at the miR-cleavage site.

For the previously published paper “**Expression profiling across wild and cultivated tomatoes supports the relevance of early miR482/2118 suppression for *Phytophthora* resistance**” we used gene-specific primers to generate clonal PARE-libraries (see chapter 2.2). However, as this type of analysis is time-consuming and limited to single genes, we sought to reconstruct and verify the miR482/mRNA networks of tomatoes by analyzing high-throughput sequenced degradomes. In addition to miRs, we analyzed the contribution of isomeric forms of miRs (isomiRs) as well as phased secondary small interfering RNAs (phasiRNAs) in the target-network. isomiRs are miRs that are produced from the same loci as miRs but start at different transcription sites (Nielsen et al., 2012). In

contrast, phasiRNAs are triggered by miR cleavage of target-mRNAs and subsequent recruitment of proteins which transform the single-stranded, cleaved mRNAs into double-stranded ones (Fei et al., 2013; Xia et al., 2019). To generate the mature phasiRNAs, Dicer-like proteins process these double-stranded molecules into “in-phase” 21nt or 24nt long pieces. These pieces, the phasiRNAs, are loaded into Argonaute proteins to guide phasiRNA-directed cleavage of additional mRNAs. phasiRNAs are known to enlarge the regulatory target-network of miRs by targeting additional mRNAs and not only the target mRNA that gave birth to them (Fei et al., 2013). They have been shown to play important regulatory roles in resistance (Zhai et al., 2011; Fei et al., 2013; Shivaprasad et al., 2012), putative abiotic stress responses (Sosa-Valencia et al., 2017), developmental processes (Fei et al., 2016) and presumably reproduction (Dukowic-Schulze et al., 2016). Within the paper **“Large-scale study of miRNA targets and their functions in tomatoes”** the following questions were addressed:

- i) How complex are miR/target networks? Do they consist of many or few members?
- ii) What kind of functions do the miR-regulated genes exercise? Do they contribute to a putative amplification of the regulative system?
- iii) How do isomiRs and phasiRNAs influence the network? Do they stabilize it?
- iv) What can we learn about the regulation of the plant immune system by miRs using this approach?

Within the study we used 28 publicly available PARE-libraries of the tomato to identify 996 unique miR/isomiR/phasiRNA/mRNA interactions. Targets are broadly overlapping between miRs and isomiRs but only to a smaller degree between miRs/isomiRs and phasiRNANAs. In addition, with 268 interactions the phasiRNANAs possess the smallest ratio of RNA-silencing active members (7.93% compared to 35.77% for the miRs). We verified most of the interactions within several, independently generated PARE-libraries (e.g. 53.45% of all miR targets have been verified in more than four PARE-libraries). Furthermore, most targets were confirmed independent of the biological treatment applied to the plants (no treatment (mock), abiotic treatment, biotic treatment).

In agreement with several other studies, most of the verified targets encode for transcription factors or participate in immune response reactions (Palatnik et al. 2003, Achard et al. 2004, Jones-Rhoades and Bartel 2004, Zhou et al. 2010, Shivaprasad et al., 2012, de Vries et al., 2015). The transcription factors (and to a minor degree immune response genes) appear targeted by multiple, independent miRs as well as by isomiRs. For example, the transcription factors *Solyc08g066500* and *Solyc12g044410* are targeted by 18 different miRs/isomiRs. The two largest targeting networks were formed mainly by the growth regulating miR396-family and the *R*-gene regulating miR482-family. On average, a

miR/target networks consists of 1.88 ± 1.48 miRNA members and 4.46 ± 5.06 targets. In comparison, a typical isomiRNA network consists of 6.17 ± 5.23 isomiRNAs and 6.00 ± 6.99 targets per network. PhasiRNAs formed smaller networks with 1.94 ± 1.90 phasiRNAs and 1.88 ± 1.48 targets per network.

Our study does not allow us to draw conclusions as to why a target is degraded in one library, but not in another, even if we consider the well-known miR482-network. As originally put forth by Shivaprasad et al. (2012) the miR482-members are expected to be downregulated following pathogen infection, thereby releasing the *R*-genes from their suppression by the miR482-family. Therefore, we expected more cleavage events of *R*-genes in libraries from plants not infected by pathogens. However, this was not the case. Returning to our study on global *R*-gene expression patterns in the tomato, we observed that only a minority of *R*-genes are specifically up-regulated following infection. Rather than inducible resistance, we observed a core of constitutively expressed *R*-genes. Moreover, we validated fewer miR482/*R*-gene interactions than previous bioinformatic prediction-based studies had predicted (de Vries et al., 2015). In terms of discovery of novel miRNA-targeting, this set of PARE-libraries seem to be saturated for identifying new targets, because 75% of the targets could be confirmed by analyzing only 16.53% of all PARE-library reads. By comparing our results from degradome studies to bioinformatically predicted ones, we found Target Finder (Fahlgren et al., 2017) covered 95.81% of the targets identified in our study. However, Target Finder also had an overprediction rate of 2.35, which is consistent with previous studies (Fridrich et al., 2019).

It is important to note that miR expression can be influenced by various factors, such as tissue-type (Korir et al., 2013) and different pathogenic treatments (Feng et al., 2013), raising the possibility that the 28 PARE-libraries we used may not have sufficiently covered all putative miR/mRNA interactions. By including PARE-libraries from underrepresented tissue types, such as flower and fruit, we only observed a slight increase in the total number of miR/mRNA interactions in our study. This raises the question of whether miRs play a less significant role in regulatory systems of gene expression. However, we conducted a final analysis that calculated the ratio of confirmed miR, isomiR, and phasiRNA degraded reads to other types of degraded reads, and the small RNA fraction was only 0.14% of the entire dataset. This indicates that more than 99% of the degraded reads have a different origin than miR, isomiR, or phasiRNA cleavage events. Despite this, we still believe that miRNAs have an important role in gene expression regulation for several reasons. Firstly, miRNAs, isomiRs, and phasimiRs are known to be a fast and highly precise mode of expression regulation (Baulcombe 2004, Axtell et al. 2013). Secondly, miRNAs themselves are tightly controlled by multiple layers of regulation (Xie et al. 2003; Vaucheret et al. 2004; Bak & Mikkelsen 2014; Liu et al. 2008, Todesco et al. 2012, Wang et al. 2013, Zhu et al. 2013). Thirdly, the repertoire of miRNAs is conserved and even expanding in

many species (Tanzer & Stadler 2004, Marco et al. 2012, Shivaprasad et al. 2012). Finally, miRNAs mainly act as regulating hubs at the top of regulatory cascades.

In conclusion, we believe that miRNAs most likely increase their regulatory power through the production of isomiRs and phasiRNAs, targeting genes upstream of regulatory cascades, being mobile, and displaying high specificity towards their targets. Furthermore, our findings support the few target hypothesis (Zhao et al., 2017). However, it is important to consider that the PARE-libraries used in our analysis do not allowed for the detection of translational inhibition and weak repression, which are essential for mRNA regulation (Brodersen et al. 2008, Iwakawa & Tomari, 2013, Yu et al. 2017). Therefore, the suitability of the PARE method for confirming these hypotheses is open to discussion.

2.5 About the interaction of phytohormones with the plant immune system

Another yet not discussed part of the plant immune system in my review paper **“On plant defense signaling networks and early land plant evolution”** is how phytohormones contribute to plant immunity. Phytohormones are endogenous chemical signal molecules controlling all aspects of life such as growth (Iqbal et al., 2017), stress tolerance (Javid et al., 2011) or defense (Shigenaga & Argueso, 2016; Berens et al., 2017). Plant phytohormones accumulate in small concentrations however they can move within plants by for example cytoplasmic streaming within cells, slow diffusion between cells or by the vascular tissue from one plant compartment to another (Kramer, 2004; Lacombe & Achard, 2016). Key-regulatory phytohormones of plant immunity are ET, SA and JA (Shigenaga & Argueso, 2016). Their importance for the plant immune system was for example shown by Penninckx et al. (1998): Mutants that were insensitive to sense ET or JA showed within their study decreased expression levels of pathogenic defense genes and following this reduced immunity levels. ET, SA and JA biosynthesis are adjusted among others by other phytohormones such as auxin (Naseem et al., 2015), abscisic acid (Ton et al., 2009) and brassinosteroids (Yu et al., 2018). The focus of this chapter will be SA and JA (Figure 7). JA-synthesis is triggered in response to herbivore-induced wounding (McConn et al., 1997) as well as by necrotrophic pathogens (Glazebrook, 2005). Its activation causes the transcriptional regulation of JA-responsive genes (Plett et al., 2014; Ranjan et al., 2015) or the production of antimicrobials (Bolouri Moghaddam et al., 2016). SA in turn triggers immunity towards biotrophs by regulating the synthesis of ROS (Herrera-Vásquez et al., 2015), transcriptional regulation of SA-responsive genes (Molinari et al., 2014) or by inducing HR (Ishikawa et al., 2006). SA reacts therefore antagonistically towards JA which means that while programmed cell death induced by SA is a powerful immune reaction towards biotrophs, necrotrophs might profit from it. Therefore, another regulatory system than SA – the triggering of the immune reaction by JA – has to take over to defeat necrotrophic pathogens (Glazebrook, 2005; Figure 7). The JA/SA-antagonism is among others controlled by the interaction of JA with ET (Pré et al., 2008) and transcription factors such as WRKYs which promote (Journot-Catalino et al., 2006) as well as negatively regulate (Mao et al., 2007) JA responses.

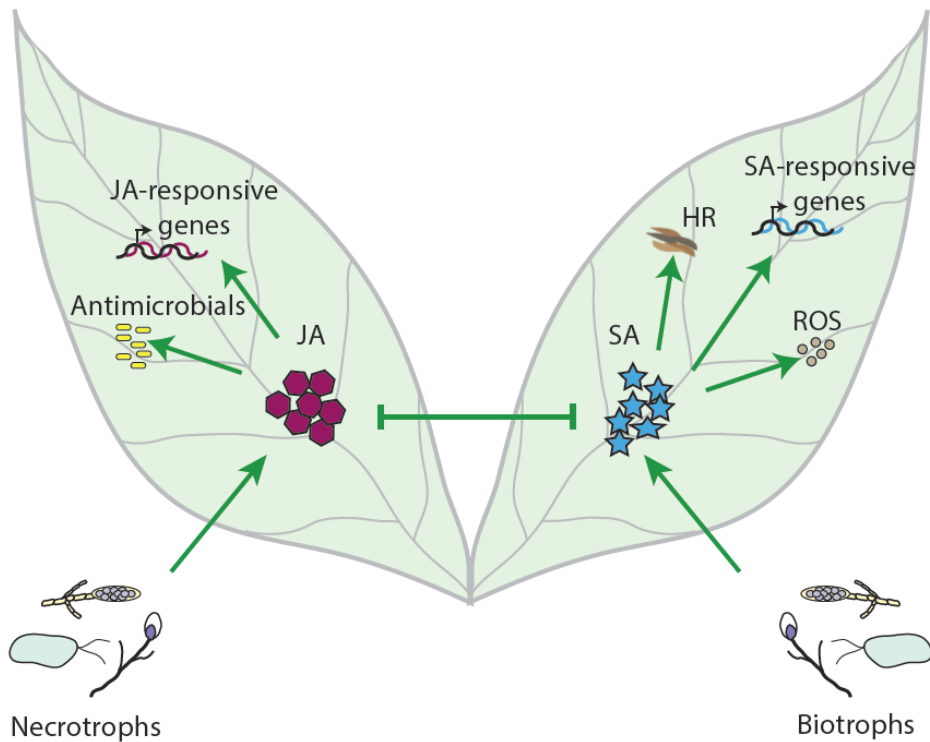


Figure 7: The JA/SA-antagonism

JA-synthesis is triggered in response to necrotrophic pathogens or herbivore-induced wounding. Its accumulation causes among others transcriptional regulation of JA-responsive genes and the production of antimicrobials. SA in turn is induced by biotrophs. It contributes to elevated ROS levels, HR and the transcriptional regulation of SA-responsive genes. JA/SA act antagonistic to each other as necrotrophs might profit from SA-triggered immune reactions as they feed on dead tissue.

It is most likely believed that the interaction of phytohormones with the plant immune system represents an ancient branch of immunity. In agreement with that several studies confirm that genes for the synthesis of diverse phytohormones as well as diverse phytohormones themselves can be already found in various streptophyte algae although not in all of them (Delaux et al., 2012; Hori et al., 2014; Wang et al., 2015; Gachet et al., 2017). The function of the phytohormones within streptophyte algae however still needs to be evaluated (Van de Poel et al., 2016; Mutte et al., 2018). Ethylene was for example suggested to play within streptophyte algae a role in cell wall metabolism, abiotic stress responses and photosynthesis (Van de Poel et al., 2016). The ancient origin of phytohormones and their connection to the immune system is also supported by the accumulation of SA within mosses in response to pathogens or pathogen secreted effectors (Ponce De Leon et al., 2012). Also, JA production within the moss *P. patens* increased towards infections with the oomycetes *Pythium irregulare* and *Pythium debaryanum* although the phytohormone concentration is overall extremely low (Oliver et al., 2009). No such JA increase was however observed for *P. patens* by infection with the fungi *Botrytis cinerea* (Ponce De Leon et al., 2012). The antagonism between JA/SA most likely evolved after the split of gymno- and angiosperms (Arnerup et al., 2013; Kozlowski et al., 1999). This is reasonable to assume as diverse studies suggest that SA and SA-signaling are present in all land plant lineages (Ponce de Leon

et al., 2012; Wang et al., 2015) through studies on liverworts, mosses and lycophytes suggest that JA and JA-signaling emerge first within vascular plants (Stumpe et al., 2010; Yamamoto et al., 2015; Pratiwi et al., 2017). JA-precursors such as OPDA have however been determined to interact with the immune system of early-branching land plants (de León et al., 2015).

The water fern *Azolla filiculoides* (*A. filiculoides*) establishes with the cyanobiont *Nostoc azollae* (*N. azollae*) a nitrogen-fixing symbiosis from which both symbiosis partners profit (Peters & Meeks, 1989). Cyanobionts are cyanobacteria that live within extracellular or intracellular compartments of their hosts (Rai et al., 2000). To successfully establish symbiosis, they need to exchange signals with their hosts and defeat defense triggering. Symbiotic interactions with cyanobionts are common for diverse members of liverworts, hornworts, water ferns as well as gymno- und angiosperms (Rai et al., 2000). The nitrogen-fixing symbiosis of *N. azollae* and *A. filiculoides* is however unique among all land plants as i) *A. filiculoides* is in contrast to most other plant species capable of fixing its whole nitrogen demand solely from the atmosphere with the help of its cyanobionts (Rai et al., 2000) ii) *A. filiculoides* possesses the only documented symbiosis in which the symbiont partner, the cyanobiont, is passed from one generation to the next (Peters & Meeks, 1989; Rai et al., 2000) and iii) the symbiosis of *A. filiculoides* with its cyanobiont is documented back to 66-100 million years ago (Carrapiço, 2006; Collinson et al., 2002). Within the article “**Jasmonic and salicylic acid response in the fern *Azolla filiculoides* and its cyanobiont**” we analyzed the capability of JA/SA sensing and producing in *A. filiculoides* and its unique interaction with its symbiosis partner by addressing the following questions:

- i) Is *A. filiculoides* capable of producing and sensing the phytohormones SA and JA? If so, what kind of implications does this have on the evolution of SA/JA-signaling and antagonism considering that *A. filiculoides* belongs to a non-angiosperm lineage?
- ii) Does *Azolla* interact with its cyanobiont *N. azollae* using phytohormones?

By using *A. filiculoides* transcriptomes in combination with protein domain prediction programs we were able to confirm that *A. filiculoides* possesses most genes as well as protein domains to produce and sense JA and SA. The fern furthermore reacts to exogenous MeSA application (SA mixed with methanol) with well-known stress responses such as root shedding, the disintegration of the fern body and probably cell death (Uheda & Kitoh, 1994). In contrast to MeSA, *A. filiculoides* did not react toward exogenous MeJA-treatment. Two studies by Camloh et al. (1996; 1999) on another fern, *Platyserium bifurcatum*, documented however growth-promoting effects by exogenous JA-application. Furthermore, our real-time quantitative PCR analyses suggest that MeSA induction resulted in *A. filiculoides* in expression patterns which partially overlap with JA-regulated pathways in

angiosperms (Cao et al., 1994; Zimmerli et al., 2004). In summary, the results suggest that *A. filiculoides* either do not sense MeJA or do not produce/use it for growth-promoting or immune triggering. The reason for the lack of sense might be that we detected a low conservation of the JA-Ile binding pocket for *Jasmonate Resistant 1 (JAR1)*, the protein catalyzing the formation of JA to the biologically active jasmonyl-isoleucine (JA-Ile). Newer studies meanwhile suggest that bryophytes and lycophytes do not produce JA in relevant amounts but instead dn-OPDA, a precursor of JA (Monte et al., 2022). Our data agrees with the statement that the JA/SA antagonism evolved after the split of gymno- and angiosperms (Arnerup et al., 2013; Kozłowski et al., 1999).

Our data furthermore suggest that SA might be involved in the communication of *A. filiculoides* with its cyanobiont as the amount of *N. azollae* increases after long-term MeSA treatment. In addition, the expression of *Nitrogen fixation E (NifE)* from *N. azollae* which is crucial for the fixation of nitrogen (Roll et al., 1995) was reduced after MeSA treatment. Besides *N. azollae*, *A. filiculoides* leaf cavities are also inhabited by diverse other bacteria which are by *A. filiculoides* as well vertically passed to the next generation (Dijkhuizen et al., 2018). However, Dijkhuizen et al. (2018) assume that only *N. azollae* can fix nitrogen in a significant manner. To sum up, our results suggested that SA might be involved in the communication of *A. filiculoides* with its cyanobiont while the influence of JA and SA on other microbiome members is still unexplored.

2.6 Biocontrol as a natural approach to fight back disease

The nowadays most common control mechanisms of pests are resistance breeding and agrochemical applications. However both mechanisms come along with several liabilities such as expenditure of time, environmental and user damages or low durability of the protective function (Grünwald et al., 2006; Vleeshouwers et al., 2011; Childers et al., 2015). As an example: the former mentioned plant pathogen *P. infestans* tends to adapt rapidly to resistant plants as well as pesticides as it possesses a high evolutionary potential (Fry, 2008). This high evolutionary potential is i) a consequence of its sexual as well as asexual propagation cycle and ii) its unusually large and highly repetitive genome (Haas et al., 2009). Because of this high evolutionary potential of many pathogens and in turn the low durability of many protective control mechanisms, continual scientific efforts for effective crop protection are needed.

In this part of my Ph.D. thesis, I will therefore introduce biocontrol as a natural approach to fighting back diseases. Biocontrol organisms are organisms that are applied to plants to either directly combat pathogens or pests or to prime plants for upcoming infections (Pal & Gardener, 2006). Another biocontrol approach uses biocontrol agents – substances derived from the biocontrol organism such as metabolites – to outcompete pathogens. Biocontrol organisms combat pathogens for example by inducing the systemic acquired resistance (SAR) of the plant (Pal & Gardener, 2006). SAR is a defense response that primes the whole plant for following infections after a local attack (Klessig et al., 2018). Other mechanisms of biocontrol are hyperparasitism of the pathogen which means the colonization of hosts who are already hosts of other organisms (Kiss, 2003) or competition for essential nutrients (Elad & Chet, 1987).

We used for the article “**Broad-spectrum inhibition of *Phytophthora infestans* by fungal endophytes**” endophytes to inhibit the infection of *P. infestans* on the cultivated tomato *S. lycopersicum*. Endophytes are organisms that grow within plants without causing at the time of sampling visible disease symptoms on them (Schulz & Boyle, 2005; Le Cocq et al., 2016). Members of endophytes belong to prokaryotes as well as eukaryotes and their members are colonists of nearly every plant species (Strobel & Daisy, 2003). They are predestined as biocontrol organisms as several endophytes have been shown to support plant fitness following infection whereas others directly inhibit pathogens (Schulz, 2006; Panke-Buisse et al., 2015; Rolli et al., 2015; Hiruma et al., 2016; Martínez-Medina et al., 2017). Their inhibition potential is often linked to their produced metabolites (Puopolo et al., 2014; Mousa et al., 2016). For example the reddish pigment bikaverin as well as the derivate fusaric acid of the fungi *Fusarium oxysporum* suppress the growth of *P. infestans* *in vitro* and *in vivo* (Son et al., 2008).

Also, volatile compounds – organic or inorganic gasses such as ammonia – of biocontrol organisms such as *Trichoderma* or *Diaporthe spp.* were able to inhibit several pathogens (Dick & Hutchinson 1966; Kottb et al., 2015; Yan et al., 2018). The following questions need to be addressed to successfully establish a biocontrol organism or agent:

- i) Does the biocontrol organism/agent successfully inhibit the pathogen on the host? Is the biocontrol organism/agent limited to single isolates of pathogens or does it include broad-spectrum inhibition?
- ii) Does infection by the biocontrol organism/agent damage the host in the absence of pathogens or reduce the yield?
- iii) Does the biocontrol organism/agent influence consumer safety? Does the biocontrol organism/agent harm other plants or animals next to the application site?

In the following I will discuss some of these questions based on our publication “**Broad-spectrum inhibition of *Phytophthora infestans* by fungal endophytes**”. Within this study we were able to show that the metabolites of four out of twelve tested endophytes have the potential to inhibit the growth of *P. infestans* on media. Next, we tested the potential of these four endophytes (*Phoma eupatorii* (*P. eupatorii*), isolate 9907, *Monosporascus sp.* and *Phialocephala fortinii*) to inhibit a broad range of *P. infestans* strains by co-cultivation of each endophyte and each *P. infestans* strain on media. This experiment proved that all four endophytes have the potential to inhibit the majority of the nine tested *P. infestans* strains. Finally, we co-infected *S. lycopersicum* with both each single endophyte and *P. infestans* and examined *P. infestans* infection success by measuring health parameters of the plant as well as the amount of *P. infestans* within leaves of *S. lycopersicum*. The endophyte with the largest anti-*P. infestans* potential was *P. eupatorii* as it nearly abolished infection by *P. infestans* on *S. lycopersicum*. In agreement with that several other biocontrol active endophytes have been described to defeat *P. infestans* although none of these endophytes was tested for broad-spectrum inhibition (Kim et al., 2007; Miles et al., 2012; Puopolo et al., 2014). Since *P. eupatorii* was pre-selected based on its metabolites being able to inhibit *P. infestans*, we suggest that its metabolites might contribute to its biocontrol potential. As *P. eupatorii* restricted the growth of all *P. infestans* strains on plate, the inhibiting metabolite(s) of *P. eupatorii* may have conserved targets. Another explanation for the broad-spectrum inhibitory potential of *P. eupatorii* might be that the target of the metabolite is specific for *P. infestans*. Both scenarios might limit the potential of *P. infestans* to co-adapt to the direct application of the metabolite(s) or the pre-infection of the plant by *P. eupatorii* as the target may be essential to the pathogen. Another reason why *P. eupatorii* can defeat *P. infestans* infection is that it might trigger plant defense which becomes obvious by the elevated levels of the stress hormone anthocyanin in *S.*

lycopersicum after colonization of *P. eupatorii*. A similar induction of the plant immune system by anthocyanin was among others shown for the endophytes *Serendipita indica* and *Fusarium oxysporum* (Stein et al., 2008; Aimé et al., 2013). Furthermore by testing all four endophytes for their potential to harm the host, the isolate 9907 and *Phialocephala fortinii* kill the host. This might be caused by the fact that the endophytes used in this study neither originated from *S. lycopersicum* nor from another Solanaceae species. Asymptomatic colonization events of endophytes are also known to shift in dependency from several other factors (Schulz & Boyle, 2005; Junker et al., 2012; Busby et al., 2016). This also opens the door to assumptions how *P. eupatorii* reacts to *P. infestans* in more natural conditions and if it is causing harm to close-by growing plants. Also, the mood of inhibition is unknown to us. To sum up, we identified in our study the endophyte *P. eupatorii* as a potential new broad-spectrum biocontrol agent of *P. infestans* as it is limiting *P. infestans* growth successfully *in vitro* and *in vivo* without causing damage to the host.

2.7 The Yin-and-Yang of plants and pathogens: Uncovering the rapid arms race

The immune system is permanently challenged by the adaptive potential of pathogens to avoid triggering the plant immune system and successfully establish infections. Like the Yin-and-Yang symbol, studying the plant immune system without taking the plant pathogens into account will never result in an accurate portrait (Figure 8). The Yin-and-Yang philosophy represents the dualisms of two contrary forces which are permanently interconnected and dependent on each other. For the arms race, this would mean that as pathogens try to escape to trigger the immune system by alteration of e.g. their effector repertoire, plants in turn will favor innovations that guarantee the triggering of the immune system (Jones & Dangl, 2006). With reference to the meeting report **“Rapid evolution in the tug-of-war between microbes and plants”** that based on the NewPhytologist/DFG SPP1819 workshop “Molecular mechanisms underlying the rapid evolution of plant-microbe interactions” from February 2018 in the Netherlands, I will close this thesis about the expression, regulation & evolution of the plant immune system by referring to the Yin-and-Yang dynamic between plants and pathogens. In the upcoming section, I will therefore present diverse examples of antagonistic interactions between plants and pathogens with a focus on adaptive processes. Already during my master’s thesis I looked at the black, pathogenic side of the Yin-and-Yang symbol by studying the pathogenic oomycete *P. infestans* and its effector PSR2 (de Vries et al., 2017). We were with this study able to show that i) the RNA silencing suppressor PSR2 seems to be relevant for establishing infections, ii) the major deterrent of PSR2 evolution seems to be the host range and iii) PSR2 shows partial signs of balancing selection meaning that it is conserved within and between *Phytophthora spp.*. The latter is a rather uncommon pattern of effectors but in this case understandable by the fact that *PSR2* suppresses the RNA silencing machinery of the host (Hou et al., 2019). By starting my Ph.D., I changed sites by focusing on the plant immune system but of course never forgot my beloved pathogenic background.



Figure 8: The Yin-and-Yang model of plant-microbe interactions

The plant immune system is permanently challenged by the adaptive potential of pathogens to successfully establish themselves within the plant (e.g. by alteration or jettison of *Avr*-genes or the birth of new effectors; *right side*). *Avr*-genes refer to pathogenic genes which are detected by the plant and therefore trigger an immune reaction. By outcompeting the plant immune system, plants become sensitive to pathogens. Following the arms race dynamic plants in turn need to evolve new or mutated *R*-gene(s) to catch alternated *Avr*-genes or new effectors of pathogens (*bottom side*). The plant becomes resistant to the pathogen. Meanwhile it is expected that the frequencies of ineffective *R*-genes decrease due to high fitness costs while the frequencies of new, effective *R*-gene(s) increase. Successful pathogens however establish as part of their counter-defense a rapid birth and death-evolution of their effector repertoires (*left side*). Subsequently plants become sensitive to the pathogens and their *R*-gene repertoire ineffective. To catch up with the adaptive potential of pathogens, *R*-genes need to be renewed by e.g. transposons, inversions or duplications (*top side*). Entering the Yin-and-Yang dynamic of successive adaptations and counter-adaptations plants and pathogens need to permanently interact and react to each other. The figure was inspired by Jones and Dangl (2006).

Several studies proved that the arms race between plants and pathogens took place and shaped the evolution of both. The simplest way of adaptation for pathogens would be to mutate their effector genes which were recognized by the plant and trigger immunity (Figure 8). These kinds of plant recognized effectors are called *Avirulence* genes (*Avr*-genes; Jones and Dangl, 2006). Indeed, several studies proved that by single nucleotide polymorphisms (Plissonneau et al., 2017; Zhong et al., 2017), deletions (Hartmann et al., 2017) or insertions of transposable elements (Wu et al., 2015) pathogens achieved susceptibility of their hosts. Also, larger changes within pathogens such as adaptive chromosome length polymorphisms (Rincones et al., 2006), chromosomal rearrangements (de Jonge et al., 2013; Hartmann et al., 2017) or repeat-induced point mutations (Rouxel et al., 2011) were shown to contribute to pathogenicity. In summary, the arms race forces pathogens to give among others rise to a rapid birth and death-evolution of their effector repertoires (Plissonneau et al., 2017). In turn the plants need to catch up with this enormous adaptive potential of pathogens by adjusting their *R*-gene repertoires. In agreement with that several *R*-genes/*R*-gene families are permanently renewed by among others duplication, transposon or inversion events (Wei et al., 2002; Hurni et al., 2013). The powdery mildew *R*-gene loci *Mla* for example has been subjected to functional diversification by positive selection of its NLR domain which means that advantageous mutations are driven to fixation (Seeholzer et al., 2010). Moreover Yang et al. (2013) identified three rapidly evolving *R*-gene families within various grass species of which several family members confer resistance towards rice blast disease. It is thought that frequencies of *R*-genes that lose their potential to recognize pathogens decrease while new, mutated *R*-genes with a favorable phenotype become fixed within populations (Michelmore & Meyers, 1998; Jones and Dangl, 2006).

Another key aspect of the molecular arms races the participants of the workshop referred to is the microbiome of the plant. The plant microbiome represents the totality of organisms that are associated with a plant (Turner et al., 2013). This bunch of associated organisms may have implications on plant health in the form of detrimental pathogens such as *P. infestans* or *Botrytis cinerea* (Weller et al., 2002; Williamson et al., 2007; Fry, 2008; Berendsen et al., 2012) or fitness supporting organisms such as certain plant growth-promoting *Pseudomonas* species (Preston, 2004). Another example of disease suppression by the microbiome of the plant is described by Mendes et al. (2011): They identified Proteobacteria that secrete nonribosomal peptide synthetases for the synthesis of secondary metabolites to suppress disease. To examine the influence of the microbiome on plant immunity, Eric Kemen, a participant of the workshop, created synthetic *A. thaliana* communities and showed by composition changes of these synthetic communities that the epiphytic yeast *Moesziomyces albugensis* suppress the oomycete pathogen *Albugo laibachii* (Eitzen et al., 2020). It is nowadays assumed that plants may even actively recruit certain organisms to protect themselves from pathogens

(Berendsen et al., 2012). Meanwhile Joy Bergelson pointed out during the workshop that the recruiting and structure of the plant microbiome are as well affected by host genotype and local environments (Brachi et al., 2017). In summary, during the workshop diverse examples of the adaptive arms race between plants and pathogens were presented. According to the Yin-and-Yang symbol, analyzing one side of the arms race will result in an inaccurate impression of the highly interactive evolving plant immune system. Therefore, I conclude this part of my thesis by reminding all readers of this important fact.

3. Discussion

The aim of my Ph.D. was to analyze different layers of the plant immune system and relate these layers in their expression, their regulation and their evolution. My work addressed the four main questions from the motivation and research aims section (1.1). In the following section, I will return to these questions and present how my work contributes to our current understanding of the plant immune system.

What are the major determinants of the plant immune system and how do they contribute to resistance?

In addition to several minor determinants, the major determinants of the plant immune system are the PAMP-detecting PRR-receptors (Bigéard et al., 2015), effector recognizing *R*-genes (Jones and Dangl, 2006) and the signal-transducing phytohormones (Shigenaga & Argueso, 2016; Berens et al., 2017). During my Ph.D., I worked on *R*-genes the majority of the time and on phytohormones to a minor degree. I analyzed their expression, their evolution or their regulation. Each of these elements contributes in an individual but powerful and essential manner towards preventing infection of the plant. Also during my Ph.D., I discovered a core set of *R*-genes that are constitutively expressed within potato and tomato. This core is likely needed by the plant to continuously distinguish harmful microbes from beneficial microbes and to trigger situation-specific immune reactions. Furthermore, tissue-specific expression patterns of *R*-genes were identified within this study. Tissue specificity might have evolved because of functional and structural differences between tissues and allows for more specific targeting of pathogens at their specific infection sites.

How does the plant immune system evolve?

Several basic principles of the plant immune system predated the terrestrialization by plants (e.g. as the closest extant relative of land plants, streptophyte algae, always had to and still have to deal with diverse microbes (Wickett et al., 2014; Delaux et al., 2015; Selosse et al., 2015; de Vries & Archibald, 2018)). Streptophyte algae were also shown to accumulate lignin-like compounds (Delwiche et al., 1989; Ligrone et al., 2008; Sørensen et al., 2011) and callose both of which protect the plant from cell wall penetrating pathogens (Herburger & Holzinger, 2015). In addition, NBS-LRRs, the major class of *R*-genes, can be found from streptophyte algae to gymnosperms and angiosperms (Yue et al., 2012). I was able to show during my Ph.D. that the water fern *A. filiculoides* can sense the phytohormone SA, but not JA. Our data are therefore not in conflict with other studies stipulating that the JA/SA antagonisms, an important layer of regulation between JA-sensitive and SA-sensitive immune reactions (Glazebrook, 2005; Ishikawa et al., 2006; Herrera-Vásquez et al., 2015), evolved after the

split of gymnosperms and angiosperms (Arnerup et al., 2013; Kozłowski et al., 1999). Instead of JA, de León et al. (2015) showed that JA-precursors such as OPDA interact with the plant immune system of early-branching land plants such as ferns. The ancient origin of SA signaling was further supported by our observations that SA might be involved in the communication of *A. filiculoides* with its cyanobiont. The symbiosis is assumed to date back to 66-100 million years ago, highlighting the ancient origin of the SA as a signaling molecule (Carrapiço, 2006; Collinson et al., 2002). Furthermore we were able to show that MeSA application triggers typical stress responses of *A. filiculoides* such as root shedding, the disintegration of the fern body and probably cell death (Uheda & Kitoh, 1994). Therefore it seems likely that SA contributes to the resistance of *A. filiculoides*.

Prior to my study on *A. filiculoides*, I analyzed the miR482-paradox. The miR482-paradox describes the fact that several pathogenic effectors are known to suppress the RNA silencing machinery of the host and in doing so, release the suppression of *R*-genes from the miR482-superfamily (Pumplin & Voinnet, 2013). Examples of such RNA silencing suppressing effectors are glycine/tryptophane-containing proteins that bind to Argonaute1 to occupy their miR binding-sites (Azevedo et al., 2010) and proteins that inhibit HEN1, a protein preventing miRs from degrading (Vogler et al., 2007). By secreting RNA silencing suppressors, pathogens actively contribute to the up-regulation of *R*-genes and enhanced plant immunity – a reaction which seems to be at first glance counter-productive to pathogens. However Qiao et al. (2013) determined that transient silencing of an RNA silencing suppressor of *P. infestans* decreased pathogen virulence. The authors conclude that suppression of the RNA silencing machinery enhances virulence by disturbing the general transcriptional programming of the plant. Another explanation for the miR482-paradox put forth by Shivaprasad et al. (2012) is that it evolved as a counter-counter-defense mechanism by pathogens. They believe that RNA silencing suppressors emerged first; the miR482/*R*-gene interaction subsequently evolved to activate immunity in case of an RNA silencing event. Using *S. lycopersicum*, its wild relatives and the pathogen *P. infestans*, as a case study, I was able to show that the expression of *R*-genes and the miR482-superfamily is most likely shaped by co-evolution with the host. Therefore, I assume that miR482/2118 paradox might contribute to the higher susceptibility of the cultivated tomato by *P. infestans*.

How is the immune system regulated as it constantly needs to react to changing conditions? How is specificity to pathogens achieved?

The immune system is constantly adjusted by multiple layers of regulation such as transcription factors (Journot-Catalino et al., 2006; Mao et al., 2007), phytohormones (Ton et al., 2009; Naseem et al., 2015; Yu et al., 2018) or transcriptional reprogramming (Glazebrook, 2005; Tsuda and Katagiri, 2010). As previously highlighted, my data agree with the hypothesis that the JA/SA antagonism, an important layer of regulation between JA-sensitive and SA-sensitive immune reactions, first evolved after the split of gymnosperms and angiosperms (Arnerup et al., 2013; Kozlowski et al., 1999). By analyzing the global expression patterns of *R*-genes, I was able to show that many *R*-genes do not respond in a pathogen-specific manner. I concluded that pathogen-specificity is not achieved by induction of *R*-gene expression, but by activation of R-proteins. How *R*-genes become activated in specific immune reactions is still under discussion. Recently it has been shown that the R-protein ZAR1 triggers an HR by forming a calcium-permeable channel within the plant cell wall through which cell plasma leaks out (Wang et al., 2019; Bi et al., 2021).

In my case study of tomatoes and *P. infestans*, I was able to confirm that several *R*-genes are regulated by members of miR482-superfamily using a 5'RLM-RACE. In addition, we observed patterns of co-regulation in expression of *R*-genes and miR482-members. Both results verify that the miR482-superfamily is an important regulator of *R*-genes and immunity. The importance of the miR482-family as a regulator of *R*-genes is further strengthened by our study on degradomes: Here the miR482-family formed the largest network. On the other hand, by reconstructing the entire miR/target network, no pattern of degradation events (neither by all miRs nor by specifically the miR482 family) could be identified. It is therefore still unknown why a miR (or miR482) acts in one case and not in another one. Instead we were able to show that miRs broaden their regulatory power by giving rise to active RNA-silencing isomiRs and phasiRNAs and regulate the expression of hub genes such as transcription factors and *R*-genes. The importance of miRs is further strengthened by the fact that they are, on one hand, highly conserved across many species, and on the other hand, still diversifying (Tanzer & Stadler 2004, Marco et al. 2012, Shivaprasad et al. 2012). Also the observation that they are highly specific (Baulcombe 2004, Axtell et al. 2013), controlled in their expression by several layers (Liu et al. 2008, Todesco et al. 2012, Wang et al. 2013, Zhu et al. 2013, Bak & Mikkelsen 2014) and are mobile (Gursansky et al., 2011; Carlsbecker et al., 2010) contribute to their importance.

How can we use our knowledge about the plant immune system to counter infections?

Pathogens continue to challenge both cultivated and wild plant species (Dean et al., 2012; Mansfield et al., 2012; Kamoun et al., 2015). By widening our knowledge about the plant immune system, we may better employ existing genetic variation to combat specific pathogens. Wild relatives of cultivated crops can serve as natural immunity resources to improve crop immunity (Dwivedi et al., 2008; Schröder et al., 2015). During my Ph.D., I identified five potential *R*-gene candidates for introgression from wild relatives into the cultivated tomato. All of these genes are not expressed in the cultivated tomato, but stably expressed in most of the wild tomatoes. Their functional importance in wild tomatoes is underscored by the fact that all of them show signs of purifying selection, which acts against the accumulation of mutations. However, their functions in pathogen perception still need to be evaluated.

In another study, I established the potential biocontrol organism *P. eupatorii* to combat *P. infestans* on tomato. Biocontrol organisms either combat pathogens directly or prime plants for subsequent infections (Pal & Gardener, 2006). Known modes of action of biocontrol agents are hyperparasitism of pathogens (Kiss, 2003) or competition for essential nutrients (Elad & Chet, 1987). While, prior studies on the biocontrol of *P. infestans* have been performed (Kim et al., 2007; Miles et al., 2012; Puopolo et al., 2014), none took broad-spectrum inhibition into account, limiting the potential of each biocontrol organism. *P. eupatorii*, on the other hand, successfully restricted the growth of several *P. infestans* strains. The broad-spectrum potential of *P. eupatorii* suggests that the target of this biocontrol organism might be conserved across *P. infestans* strains or highly specific towards *P. infestans*. This might enhance the durability of *P. eupatorii* as a biocontrol agent, since a conserved target of the biocontrol agent may slow the evolution of the pathogen to become resistance.

4. Outlook

Despite impressive progress in the last years, much is still unknown about the plant immune system. Each aspect of the plant immune system – its expression, evolution and regulation – poses different challenges. The reconstruction of the evolutionary history of a trait such as the plant immune system, can be hampered by missing data as well as by real evolutionary events such as horizontal genes transfer, hybridization or genetic recombination between species (Arbuckle et al., 1996; Chan et al., 2017; Huang et al., 2017; Schrepf & Szöllösi, 2020). Fossil records of the immune system (Taylor et al., 1992; Strullu-Derrien et al., 2014) or an ancient DNA record (Soltis & Soltis, 1993; Hofreiter et al., 2001) are often lacking. Instead our primary information about the evolution of the plant immune system based on studying the status of the trait in extant species and evaluating the distribution of the character states across a phylogenetic tree (chapter 2.1).

By enlarging the number of species, especially of the underrepresented basal branches, within phylogenetic studies, higher resolutions will be achieved. Therefore scientists have invested much effort in the sequencing of early branching lineages of plants such as *Anthoceros* hornworts (Li et al., 2020), the moss *Physcomitrella patens* (Lang et al., 2008) or the terrestrial alga *Klebsormidium flaccidum* (Hori et al., 2014). At the same time, shared characters do not necessarily mean that the characters possess the same function. For example, Yu et al. (2012) detected NBS-coding genes within higher-branching streptophyte algae, but whether these genes interact with the algal immune system is still unknown. The same is also true for many phytohormones (Van de Poel et al., 2016; Mutte et al., 2018). Instead of regulating immunity within streptophyte algae, ethylene was shown to interact with cell wall metabolism, abiotic stress or photosynthesis (Van de Poel et al., 2016). Another example is *A. filiculoides* which possesses most genes to produce and sense JA, but seems nonetheless to be insensitive towards MeJA-treatment implying that JA might be engaged in unknown processes (chapter 2.5).

In the case of expression, standardization between studies and sampling is still challenging (Auer & Doerge, 2010; Krzywinski & Altman, 2013; Bi & Liu, 2016). In my case, this meant that it was not possible to trace back the influence of several plant/pathogen factors such as cultivar or age to the expression of *R*-genes (chapter 2.3). To overcome such problems, the study design as well as sample size and replication are of fundamental importance. Furthermore, many genes of transcriptomes are not expressed, which might either represent the true status of the gene or might be caused by insufficient read depth (Tarazona et al., 2011; Haas et al., 2012). Instead of elevating the depth of sequencing, I suggest however using as well large-scale comparison of different transcriptomes to

uncover non-expressed genes (chapter 2.3). In addition to sufficient read depth, sufficient read length is needed to improve transcriptome/genome assemblies and annotations to reliably identify novel transcripts and novel splice variants of genes (Chang et al., 2014; Cho et al., 2014). This is of special interest for gene families such as *R*-genes which consist of many hundreds of modular members (Shao et al., 2019). A different approach to improve transcriptomic studies is the inclusion of external RNA controls to sequencing samples (Jiang et al., 2011). These external RNA controls allow the quantification of sensitivity and accuracy of transcriptomes. As sequencing gets increasingly cheaper and the quality of sequencing increases, future studies will hopefully result in high(er)-quality data.

The reconstruction of gene-regulatory networks is challenging due to the intrinsic interconnectedness of many regulatory networks, since one node might be influenced by several other nodes (de Vries et al., 2015; Banf & Rhee, 2017). Spatial and temporal activation of regulators may also hinder the reconstruction of regulatory networks (Peng & Han, 2018). In chapter 2.2, I analyzed the miR482/*R*-gene network by correlating the expression patterns of these genes. The analysis of co-regulation patterns is often restricted to cases in which both partners of the regulatory network are suspected to interact. Screening large-scale datasets for patterns of co-regulation is more complex because of the vast number of genes/nodes (Banf & Rhee, 2017). However approaches such as the weighted correlation network analysis (WGCNA) have become more and more established in science (Langfelder & Horvath, 2008). To confirm the regulative function of genes, overexpression or silencing of these loci can be used. For example, Hong et al. (2019) verified that several miR482c-predicted targets are downregulated when miR482c is overexpressed. Furthermore, overexpression of miR482c results in greater susceptibility to *P. infestans*. Meanwhile, inactivation of miR482 family-members resulted in lower susceptibility (Canto-Pastor et al., 2019). To verify hundreds or even thousands of miR-targets, German et al. (2009) developed the PARE-analysis method (chapter 2.4). By using this method, we verified 996 unique miR, isomiR and phasiRNA interactions. Since the number of verified targets is smaller than expected based on other studies, the question arose whether the limited number of verified targets was caused by limitations of the method or represents the real miR/target network (Zhao et al., 2017). The importance of regulating biological systems is however beyond doubt. Simple introgressions of the five wild-type *R*-genes (chapter 2.3) into the cultivated tomato for example might be insufficient for triggering immunity as the regulative system might be missing. But good news is on the way: Deep learning methods may help to remove many barriers in reconstructing gene-regulatory networks in the future (Banf & Rhee, 2017).

Beyond field-specific challenges, much effort is needed to combine knowledge across single studies to create a comprehensive, broader picture of the plant immune system. For example, what have the plant immune systems of various plant species in common and which immune reactions are specific to hosts? To shed light on these questions, it is necessary to leave single species analyses behind and enter the field of large-scale studies. Therefore in my upcoming studies, I would like to transfer my *R*-gene analysis pipeline to other species: both model and non-model plants. This will to answer the questions if i) core-expressed *R*-genes are typically for many plant species (or if they are restricted to Solanaceae) and ii) tissue-specific expression of *R*-genes is common or unusual within plants. My further interest is to shed light on how pathogen specificity is achieved, since the overall expression of *R*-gene does not seem to contribute to it. Instead specificity might be achieved by activation of single *R*-genes, as it has been recently shown by crystallization studies. The *R*-gene ZAR1 triggers HR by forming a calcium-permeable pore within the plant cell resulting in leaking of the plant cell contents (Wang et al., 2019; Bi et al., 2021).

5. References:

- Achard, P., Herr, A., Baulcombe, D. C., & Harberd, N. P. (2004). Modulation of floral development by a gibberellin-regulated microRNA. *Development*, 131 (14).
- Aimé, S., Alabouvette, C., Steinberg, C., & Olivain, C. (2013). The endophytic strain *Fusarium oxysporum* Fo47: a good candidate for priming the defense responses in tomato roots. *Molecular plant-microbe interactions*, 26(8), 918-926.
- Allen, R. L., Bittner-Eddy, P. D., Grenville-Briggs, L. J., Meitz, J. C., Rehmany, A. P., Rose, L. E., & Beynon, J. L. (2004). Host-parasite coevolutionary conflict between *Arabidopsis* and downy mildew. *Science*, 306(5703), 1957-1960.
- Allen, F. H., & Friend, J. (1983). Resistance of potato tubers to infection by *Phytophthora infestans*: a structural study of haustorial encasement. *Physiological Plant Pathology*, 22(3), 285-IN4.
- Arafa, R. A., Rakha, M. T., Soliman, N. E. K., Moussa, O. M., Kamel, S. M., & Shirasawa, K. (2017). Rapid identification of candidate genes for resistance to tomato late blight disease using next-generation sequencing technologies. *PLoS one*, 12(12).
- Arbuckle, J. L., Marcoulides, G. A., & Schumacker, R. E. (1996). Full information estimation in the presence of incomplete data. *Advanced structural equation modeling: Issues and techniques*, 243, 277.
- Arnerup, J., Nemesio-Gorriz, M., Lundén, K., Asiegbu, F. O., Stenlid, J., & Elfstrand, M. (2013). The primary module in Norway spruce defence signalling against *H. annosum* s.l. seems to be jasmonate-mediated signalling without antagonism of salicylate-mediated signalling. *Planta*, 237(4), 1037-1045.
- Auer, P. L., & Doerge, R. W. (2010). Statistical design and analysis of RNA sequencing data. *Genetics*, 185(2), 405-416.
- Axtell, M. J. (2013). Classification and comparison of small RNAs from plants. *Annual review of plant biology*, 64, 137-159.
- Azevedo, J., Garcia, D., Pontier, D., Ohnesorge, S., Yu, A., Garcia, S., ... & Voinnet, O. (2010). Argonaute quenching and global changes in Dicer homeostasis caused by a pathogen-encoded GW repeat protein. *Genes & development*, 24(9), 904-915.
- Bak, R. O., & Mikkelsen, J. G. (2014). miRNA sponges: soaking up miRNAs for regulation of gene expression. *Wiley interdisciplinary reviews: RNA*, 5(3), 317-333.
- Banf, M., & Rhee, S. Y. (2017). Computational inference of gene regulatory networks: approaches, limitations and opportunities. *Biochimica et Biophysica Acta (BBA)-Gene Regulatory Mechanisms*, 1860(1), 41-52.
- Baralle, F. E., & Giudice, J. (2017). Alternative splicing as a regulator of development and tissue identity. *Nature Reviews Molecular Cell Biology*, 18(7), 437.
- Bartel, D. P. (2009). MicroRNAs: target recognition and regulatory functions. *Cell*, 136(2), 215-233.
- Baulcombe, D. (2004). RNA silencing in plants. *Nature*, 431(7006), 356-363.
- Berendsen, R. L., Pieterse, C. M., & Bakker, P. A. (2012). The rhizosphere microbiome and plant health. *Trends in plant science*, 17(8), 478-486.
- Berens, M. L., Berry, H. M., Mine, A., Argueso, C. T., & Tsuda, K. (2017). Evolution of hormone signaling networks in plant defense. *Annual Review of Phytopathology*, 55, 401-425.
- Bernstein, E., Caudy, A. A., Hammond, S. M., & Hannon, G. J. (2001). Role for a bidentate ribonuclease in the initiation step of RNA interference. *Nature*, 409(6818), 363-366.
- Bianca Griebel (2019): The inhibitory effect of fungal endophytes on the pathogen *Phytophthora infestans* in *Solanum lycopersicum*. Unpublished master thesis in the Institute of population genetics, Heinrich-Heine Universität Düsseldorf
- Bigeard, J., Colcombet, J., & Hirt, H. (2015). Signaling mechanisms in pattern-triggered immunity (PTI). *Molecular plant*, 8(4), 521-539.

- Bi, R., & Liu, P. (2016). Sample size calculation while controlling false discovery rate for differential expression analysis with RNA-sequencing experiments. *BMC bioinformatics*, *17*(1), 146.
- Bi, G., Su, M., Li, N., Liang, Y. U., Dang, S., Xu, J., ... & Zhou, J. M. (2021). The ZAR1 resistosome is a calcium-permeable channel triggering plant immune signaling. *Cell*, *184*(13), 3528-3541.
- Black, M., Moolhuijzen, P., Chapman, B., Barrero, R., Howieson, J., Hungria, M., & Bellgard, M. (2012). The genetics of symbiotic nitrogen fixation: comparative genomics of 14 rhizobia strains by resolution of protein clusters. *Genes*, *3*(1), 138-166.
- Boller, T., & Felix, G. (2009). A renaissance of elicitors: perception of microbe-associated molecular patterns and danger signals by pattern-recognition receptors. *Annual review of plant biology*, *60*, 379-406.
- Bolouri Moghaddam, M. R., Vilcinskis, A., & Rahnamaeian, M. (2016). Cooperative interaction of antimicrobial peptides with the interrelated immune pathways in plants. *Molecular plant pathology*, *17*(3), 464-471.
- Bonnet, E., He, Y., Billiau, K., & Van de Peer, Y. (2010). TAPIR, a web server for the prediction of plant microRNA targets, including target mimics. *Bioinformatics*, *26*(12), 1566-1568.
- Boyle, E. A., Li, Y. I., & Pritchard, J. K. (2017). An expanded view of complex traits: from polygenic to omnigenic. *Cell*, *169*(7), 1177-1186.
- Brachi, B., Filiault, D., Darne, P., Le Mentec, M., Kerdaffrec, E., Rabanal, F., ... & Novikova, P. (2017). Plant genes influence microbial hubs that shape beneficial leaf communities. *Biorxiv*, 181198.
- Bressendorff, S., Azevedo, R., Kenchappa, C. S., de León, I. P., Olsen, J. V., Rasmussen, M. W., ... & Mundy, J. (2016). An innate immunity pathway in the moss *Physcomitrella patens*. *The Plant Cell*, *28*(6), 1328-1342.
- Brodersen, P., Sakvarelidze-Achard, L., Bruun-Rasmussen, M., Dunoyer, P., Yamamoto, Y. Y., Sieburth, L., & Voinnet, O. (2008). Widespread translational inhibition by plant miRNAs and siRNAs. *Science*, *320*(5880), 1185-1190.
- Brown, J. K. M., & Rant, J. C. (2013). Fitness costs and trade-offs of disease resistance and their consequences for breeding arable crops. *Plant Pathology*, *62*, 83-95.
- Burdon, J. J., & Thrall, P. H. (2003). The fitness costs to plants of resistance to pathogens. *Genome biology*, *4*(9), 227.
- Busby, P. E., Peay, K. G., & Newcombe, G. (2016). Common foliar fungi of *Populus trichocarpa* modify *Melampsora* rust disease severity. *New Phytologist*, *209*(4), 1681-1692.
- Camloh, M., Ravnkar, M., & Zel, J. (1996). Jasmonic acid promotes division of fern protoplasts, elongation of rhizoids and early development of gametophytes. *Physiologia Plantarum*, *97*(4), 659-664.
- Camloh, M., Vilhar, B., Žel, J., & Ravnkar, M. (1999). Jasmonic acid stimulates development of rhizoids and shoots in fern leaf culture. *Journal of plant physiology*, *155*(6), 798-801.
- Canto-Pastor, A., Santos, B. A., Valli, A. A., Summers, W., Schornack, S., & Baulcombe, D. C. (2019). Enhanced resistance to bacterial and oomycete pathogens by short tandem target mimic RNAs in tomato. *Proceedings of the National Academy of Sciences*, *116*(7), 2755-2760.
- Cao, H., Bowling, S. A., Gordon, A. S., & Dong, X. (1994). Characterization of an *Arabidopsis* mutant that is nonresponsive to inducers of systemic acquired resistance. *The Plant Cell*, *6*(11), 1583-1592.
- Carella, P., Gogleva, A., Tomaselli, M., Alfs, C., & Schornack, S. (2018). *Phytophthora palmivora* establishes tissue-specific intracellular infection structures in the earliest divergent land plant lineage. *Proceedings of the National Academy of Sciences*, *115*(16), E3846-E3855.
- Carlsbecker, A., Lee, J. Y., Roberts, C. J., Dettmer, J., Lehesranta, S., Zhou, J., ... & Campilho, A. (2010). Cell signalling by microRNA165/6 directs gene dose-dependent root cell fate. *Nature*, *465*(7296), 316-321.
- Carrapiço, F. (2006). Is the *Azolla-Anabaena* symbiosis a co-evolution case. In *General botany: traditions and perspectives. Book of international conference dedicated to 200th anniversary of the Kazan Botanical School. Part I, Kazan* (pp. 193-195).
- Chae, E., Bomblies, K., Kim, S. T., Karelina, D., Zaidem, M., Ossowski, S., ... & Lechner, S. (2014). Species-wide genetic incompatibility analysis identifies immune genes as hot spots of deleterious epistasis. *Cell*, *159*(6), 1341-1351.

- Chakravarthy, S., Tuori, R. P., D'Ascenzo, M. D., Fobert, P. R., Després, C., & Martin, G. B. (2003). The tomato transcription factor Pti4 regulates defense-related gene expression via GCC box and non-GCC box cis elements. *The Plant Cell*, 15(12), 3033-3050.
- Chan, C. X., Beiko, R. G., & Ragan, M. A. (2017). Scaling up the phylogenetic detection of lateral gene transfer events. In *Bioinformatics* (pp. 421-432). Humana Press, New York, NY.
- Chang, Z., Wang, Z., & Li, G. (2014). The impacts of read length and transcriptome complexity for de novo assembly: a simulation study. *PLoS one*, 9(4).
- Chen, R., Li, H., Zhang, L., Zhang, J., Xiao, J., & Ye, Z. (2007). CaMi, a root-knot nematode resistance gene from hot pepper (*Capsium annuum* L.) confers nematode resistance in tomato. *Plant cell reports*, 26(7), 895-905.
- Chen, Y., Shen, Y., Allesina, S., & Wu, C. I. (2017). From foodwebs to gene regulatory networks (GRNs)-weak repressions by microRNAs confer system stability. *bioRxiv*, 176701.
- Childers, R., Danies, G., Myers, K., Fei, Z., Small, I. M., & Fry, W. E. (2015). Acquired resistance to mefenoxam in sensitive isolates of *Phytophthora infestans*. *Phytopathology*, 105(3), 342-349.
- Cho, H., Davis, J., Li, X., Smith, K. S., Battle, A., & Montgomery, S. B. (2014). High-resolution transcriptome analysis with long-read RNA sequencing. *PLoS one*, 9(9).
- Le Cocq, K., Gurr, S. J., Hirsch, P. R., & Mauchline, T. H. (2017). Exploitation of endophytes for sustainable agricultural intensification. *Molecular plant pathology*, 18(3), 469-473.
- Collinson, M. E. (2002). The ecology of Cainozoic ferns. *Review of Palaeobotany and Palynology*, 119(1-2), 51-68.
- Cuellar, W. J., Kreuze, J. F., Rajamäki, M. L., Cruzado, K. R., Untiveros, M., & Valkonen, J. P. (2009). Elimination of antiviral defense by viral RNase III. *Proceedings of the National Academy of Sciences*, 106(25), 10354-10358.
- Cui, H., Tsuda, K., & Parker, J. E. (2015). Effector-triggered immunity: from pathogen perception to robust defense. *Annual review of plant biology*, 66, 487-511
- Dai, X., Zhuang, Z., & Zhao, P. X. (2018). psRNATarget: a plant small RNA target analysis server (2017 release). *Nucleic acids research*, 46(W1), W49-W54.
- Davey, M. L., Tsuneda, A., & Currah, R. S. (2009). Pathogenesis of bryophyte hosts by the ascomycete *Atradiydymella muscivora*. *American journal of botany*, 96(7), 1274-1280.
- Davey, M. L., Tsuneda, A., & Currah, R. S. (2010). Saprobic and parasitic interactions of *Coniochaeta velutina* with mosses. *Botany*, 88(3), 258-265.
- Dean, R., Van Kan, J. A., Pretorius, Z. A., Hammond-Kosack, K. E., Di Pietro, A., Spanu, P. D., ... & Foster, G. D. (2012). The Top 10 fungal pathogens in molecular plant pathology. *Molecular plant pathology*, 13(4), 414-430.
- Delaux, P. M., Radhakrishnan, G. V., Jayaraman, D., Cheema, J., Malbreil, M., Volkening, J. D., ... & Rothfels, C. J. (2015). Algal ancestor of land plants was preadapted for symbiosis. *Proceedings of the National Academy of Sciences*, 112(43), 13390-13395.
- Delaux, P. M., Xie, X., Timme, R. E., Puech-Pages, V., Dunand, C., Lecompte, E., ... & Séjalon-Delmas, N. (2012). Origin of strigolactones in the green lineage. *New Phytologist*, 195(4), 857-871.
- Delwiche, C. F., Graham, L. E., & Thomson, N. (1989). Lignin-like compounds and sporopollenin in coleochaete, an algal model for land plant ancestry. *Science*, 245(4916), 399-401.
- Dick, C. M., & Hutchinson, S. A. (1966). Biological activity of volatile fungal metabolites. *Nature*, 211(5051), 868-868.
- Dijkhuizen, L. W., Brouwer, P., Bolhuis, H., Reichart, G. J., Koppers, N., Huettel, B., ... & Wong, G. K. S. (2018). Is there foul play in the leaf pocket? The metagenome of floating fern *Azolla* reveals endophytes that do not fix N₂ but may denitrify. *New Phytologist*, 217(1), 453-466.
- Dukowic-Schulze, S., Sundararajan, A., Ramaraj, T., Kianian, S., Pawlowski, W. P., Mudge, J., & Chen, C. (2016). Novel meiotic miRNAs and indications for a role of phasiRNAs in meiosis. *Frontiers in plant science*, 7, 762.
- Dwivedi, S. L., Upadhyaya, H. D., Stalker, H. T., Blair, M. W., Bertoli, D. J., Nielen, S., & Ortiz, R. (2008). Enhancing crop gene pools with beneficial traits using wild relatives. *Plant Breeding Reviews*, 30, 179.

- Ecsedi, M., Rausch, M., & Großhans, H. (2015). The let-7 microRNA directs vulval development through a single target. *Developmental cell*, 32(3), 335-344.
- Eitzen, K., Sengupta, P., Kroll, S., Kemen, E., & Doehlemann, G. (2020). An antagonistic driver of the microbial phyllosphere suppresses infection of *Arabidopsis thaliana* by the oomycete pathogen *Albugo laibachii* via a secreted hydrolase. *bioRxiv*. 2020-04.
- Elad, Y., & Chet, I. (1987). Possible role of competition for nutrients in biocontrol of *Pythium damping-off* by bacteria. *Phytopathology*, 77(2), 190-195.
- Enright, A., John, B., Gaul, U., Tuschl, T., Sander, C., & Marks, D. (2003). MicroRNA targets in *Drosophila*. *Genome biology*, 4, 1-27.
- Fabro, G., Steinbrenner, J., Coates, M., Ishaque, N., Baxter, L., Studholme, D. J., ... & Greenshields, D. (2011). Multiple candidate effectors from the oomycete pathogen *Hyaloperonospora arabidopsidis* suppress host plant immunity. *PLoS pathogens*, 7(11).
- Fagard, M., Boutet, S., Morel, J. B., Bellini, C., & Vaucheret, H. (2000). AGO1, QDE-2, and RDE-1 are related proteins required for post-transcriptional gene silencing in plants, quelling in fungi, and RNA interference in animals. *Proceedings of the National Academy of Sciences*, 97(21), 11650-11654.
- Fahlgren, N., Howell, M. D., Kasschau, K. D., Chapman, E. J., Sullivan, C. M., Cumbie, J. S., ... & Carrington, J. C. (2007). High-throughput sequencing of *Arabidopsis* microRNAs: evidence for frequent birth and death of MIRNA genes. *PLoS one*, 2(2).
- Fei, Q., Xia, R., & Meyers, B. C. (2013). Phased, secondary, small interfering RNAs in posttranscriptional regulatory networks. *The Plant Cell*, 25(7), 2400-2415.
- Fei, Q., Yang, L., Liang, W., Zhang, D., & Meyers, B. C. (2016). Dynamic changes of small RNAs in rice spikelet development reveal specialized reproductive phasiRNA pathways. *Journal of experimental botany*, 67(21), 6037-6049.
- Felix, G., & Boller, T. (2003). Molecular Sensing of Bacteria in Plants the highly conserved RNA-binding motif rnp-1 of bacterial cold shock proteins is recognized as an elicitor signal in tobacco. *Journal of Biological Chemistry*, 278(8), 6201-6208.
- Felix, G., Duran, J. D., Volko, S., & Boller, T. (1999). Plants have a sensitive perception system for the most conserved domain of bacterial flagellin. *The Plant Journal*, 18(3), 265-276.
- Feng, J., Liu, S., Wang, M., Lang, Q., & Jin, C. (2014). Identification of microRNAs and their targets in tomato infected with Cucumber mosaic virus based on deep sequencing. *Planta*, 240, 1335-1352.
- Flor, H. H. (1971). Current status of the gene-for-gene concept. *Annual review of phytopathology*, 9(1), 275-296.
- Frantzeskakis, L., von Dahlen, J. K., Panstruga, R., & Rose, L. E. (2018). Rapid evolution in the tug-of-war between microbes and plants. *New Phytologist*, 219(1), 12-14.
- Fridrich, A., Hazan, Y., & Moran, Y. (2019). Too many false targets for MicroRNAs: challenges and Pitfalls in Prediction of miRNA targets and their gene ontology in model and non-model organisms. *Bioessays*, 41(4), 1800169.
- Fry, W. (2008). *Phytophthora infestans*: the plant (and R gene) destroyer. *Molecular plant pathology*, 9(3), 385-402.
- Gachet, M. S., Schubert, A., Calarco, S., Boccard, J., & Gertsch, J. (2017). Targeted metabolomics shows plasticity in the evolution of signaling lipids and uncovers old and new endocannabinoids in the plant kingdom. *Scientific reports*, 7, 41177.
- Gao, Y., Wang, W., Zhang, T., Gong, Z., Zhao, H., & Han, G. Z. (2018). Out of water: The origin and early diversification of plant R-genes. *Plant physiology*, 177(1), 82-89.
- Garry, G., Forbes, G. A., Salas, A., Santa Cruz, M., Perez, W. G., & Nelson, R. J. (2005). Genetic diversity and host differentiation among isolates of *Phytophthora infestans* from cultivated potato and wild solanaceous hosts in Peru. *Plant Pathology*, 54(6), 740-748

- German, M. A., Luo, S., Schroth, G., Meyers, B. C., & Green, P. J. (2009). Construction of Parallel Analysis of RNA Ends (PARE) libraries for the study of cleaved miRNA targets and the RNA degradome. *Nature protocols*, *4*(3), 356.
- Glazebrook, J. (2005). Contrasting mechanisms of defense against biotrophic and necrotrophic pathogens. *Annu. Rev. Phytopathol.*, *43*, 205-227.
- Gomes, L. H., Duarte, K. M. R., Andrino, F. G., Leal Jr, G. A., Garcia, L. M., Figueira, A., & de Lira, S. P. (2014). Alpha-Tomatoin against Witches' Broom Disease. *American Journal of Plant Sciences*, *2014*.
- Grenville-Briggs, L. J., Avrova, A. O., Bruce, C. R., Williams, A., Whisson, S. C., Birch, P. R., & van West, P. (2005). Elevated amino acid biosynthesis in *Phytophthora infestans* during appressorium formation and potato infection. *Fungal Genetics and Biology*, *42*(3), 244-256.
- Grünwald, N. J., Sturbaum, A. K., Montes, G. R., Serrano, E. G., Lozoya-Saldaña, H., & Fry, W. E. (2006). Selection for fungicide resistance within a growing season in field populations of *Phytophthora infestans* at the center of origin. *Phytopathology*, *96*(12), 1397-1403.
- Gursansky, N. R., Searle, I. R., & Carroll, B. J. (2011). Mobile microRNAs hit the target. *Traffic*, *12*(11), 1475-1482.
- Gururani, M. A., Venkatesh, J., Upadhyaya, C. P., Nookaraju, A., Pandey, S. K., & Park, S. W. (2012). Plant disease resistance genes: current status and future directions. *Physiological and molecular plant pathology*, *78*, 51-65.
- Gust, A. A., Willmann, R., Desaki, Y., Grabherr, H. M., & Nürnberger, T. (2012). Plant LysM proteins: modules mediating symbiosis and immunity. *Trends in plant science*, *17*(8), 495-502.
- Haas, B. J., Chin, M., Nusbaum, C., Birren, B. W., & Livny, J. (2012). How deep is deep enough for RNA-Seq profiling of bacterial transcriptomes?. *BMC genomics*, *13*(1), 734.
- Haas, B. J., Kamoun, S., Zody, M. C., Jiang, R. H., Handsaker, R. E., Cano, L. M., ... & Bozkurt, T. O. (2009). Genome sequence and analysis of the Irish potato famine pathogen *Phytophthora infestans*. *Nature*, *461*(7262), 393-398.
- Hartmann, F. E., Sánchez-Vallet, A., McDonald, B. A., & Croll, D. (2017). A fungal wheat pathogen evolved host specialization by extensive chromosomal rearrangements. *The ISME journal*, *11*(5), 1189-1204.
- Hartmann, M., & Zeier, J. (2019). N-Hydroxy-pipecolic acid and salicylic acid: A metabolic duo for systemic acquired resistance. *Current opinion in plant biology*, *50*, 44-57.
- Herburger, K., & Holzinger, A. (2015). Localization and quantification of callose in the streptophyte green algae *Zygnema* and *Klebsormidium*: correlation with desiccation tolerance. *Plant and Cell Physiology*, *56*(11), 2259-2270.
- Herrera-Vásquez, A., Salinas, P., & Holuigue, L. (2015). Salicylic acid and reactive oxygen species interplay in the transcriptional control of defense genes expression. *Frontiers in plant science*, *6*, 171.
- Hiruma, K., Gerlach, N., Sacristán, S., Nakano, R. T., Hacquard, S., Kracher, B., ... & Schulze-Lefert, P. (2016). Root endophyte *Colletotrichum tofieldiae* confers plant fitness benefits that are phosphate status dependent. *Cell*, *165*(2), 464-474.
- Hobert, O. (2008). Gene regulation by transcription factors and microRNAs. *Science*, *319*(5871), 1785-1786.
- Hofreiter, M., Serre, D., Poinar, H. N., Kuch, M., & Pääbo, S. (2001). Ancient DNA. *Nature Reviews Genetics*, *2*(5), 353-359.
- Hong, Y. H., Meng, J., He, X. L., Zhang, Y. Y., & Luan, Y. S. (2019). Overexpression of MiR482c in Tomato Induces Enhanced Susceptibility to Late Blight. *Cells*, *8*(8), 822.
- Hori, K., Maruyama, F., Fujisawa, T., Togashi, T., Yamamoto, N., Seo, M., ... & Moriyama, T. (2014). *Klebsormidium flaccidum* genome reveals primary factors for plant terrestrial adaptation. *Nature communications*, *5*(1), 1-9.
- Hou, Y., Zhai, Y., Feng, L., Karimi, H. Z., Rutter, B. D., Zeng, L., ... & Ye, W. (2019). A *Phytophthora* effector suppresses trans-kingdom RNAi to promote disease susceptibility. *Cell host & microbe*, *25*(1), 153-165.
- Huang, H., Sukumaran, J., Smith, S. A., & Knowles, L. L. (2017). Cause of gene tree discord? Distinguishing incomplete lineage sorting and lateral gene transfer in phylogenetics. *PeerJ Preprints*, *5*, e3489v1.
- Humphreys, C. P., Franks, P. J., Rees, M., Bidartondo, M. I., Leake, J. R., & Beerling, D. J. (2010). Mutualistic mycorrhiza-like symbiosis in the most ancient group of land plants. *Nature communications*, *1*(1), 1-7.

- Huot, B., Yao, J., Montgomery, B. L., & He, S. Y. (2014). Growth–defense tradeoffs in plants: a balancing act to optimize fitness. *Molecular plant*, *7*(8), 1267-1287.
- Hurni, S., Brunner, S., Buchmann, G., Herren, G., Jordan, T., Krukowski, P., ... & Keller, B. (2013). Rye P m8 and wheat P m3 are orthologous genes and show evolutionary conservation of resistance function against powdery mildew. *The Plant Journal*, *76*(6), 957-969.
- Iqbal, N., Khan, N. A., Ferrante, A., Trivellini, A., Francini, A., & Khan, M. I. R. (2017). Ethylene role in plant growth, development and senescence: interaction with other phytohormones. *Frontiers in plant science*, *8*, 475.
- Ishikawa, A., Kimura, Y., Yasuda, M., Nakashita, H., & Yoshida, S. (2006). Salicylic acid-mediated cell death in the Arabidopsis len3 mutant. *Bioscience, biotechnology, and biochemistry*, *70*(6), 1447-1453.
- Iwakawa, H. O., & Tomari, Y. (2013). Molecular insights into microRNA-mediated translational repression in plants. *Molecular cell*, *52*(4), 591-601.
- Jagadeeswaran, G., Zheng, Y., Sumathipala, N., Jiang, H., Arrese, E. L., Soulages, J. L., ... & Sunkar, R. (2010). Deep sequencing of small RNA libraries reveals dynamic regulation of conserved and novel microRNAs and microRNA-stars during silkworm development. *BMC genomics*, *11*(1), 52.
- Javid, M. G., Sorooshzadeh, A., Moradi, F., Modarres Sanavy, S. A. M., & Allahdadi, I. (2011). The role of phytohormones in alleviating salt stress in crop plants. *Australian Journal of Crop Science*, *5*(6), 726.
- Jiang, L., Schlesinger, F., Davis, C. A., Zhang, Y., Li, R., Salit, M., ... & Oliver, B. (2011). Synthetic spike-in standards for RNA-seq experiments. *Genome research*, *21*(9), 1543-1551.
- Jin, H., Yang, X., Lu, D., Li, C., Yan, Z., Li, X., ... & Qin, B. (2015). Phylogenetic diversity and tissue specificity of fungal endophytes associated with the pharmaceutical plant, *Stellera chamaejasme* L. revealed by a cultivation-independent approach. *Antonie Van Leeuwenhoek*, *108*(4), 835-850.
- John, B., Enright, A. J., Aravin, A., Tuschl, T., Sander, C., & Marks, D. S. (2004). Human microRNA targets. *PLoS biology*, *2*(11), e363.
- Jones, J. D., & Dangl, J. L. (2006). The plant immune system. *Nature*, *444*(7117), 323-329.
- Jones-Rhoades, M. W., & Bartel, D. P. (2004). Computational identification of plant microRNAs and their targets, including a stress-induced miRNA. *Molecular cell*, *14*(6), 787-799.
- de Jonge, R., Bolton, M. D., Kombrink, A., van den Berg, G. C., Yadeta, K. A., & Thomma, B. P. (2013). Extensive chromosomal reshuffling drives evolution of virulence in an asexual pathogen. *Genome research*, *23*(8), 1271-1282.
- Journot-Catalino, N., Somssich, I. E., Roby, D., & Kroj, T. (2006). The transcription factors WRKY11 and WRKY17 act as negative regulators of basal resistance in Arabidopsis thaliana. *The Plant Cell*, *18*(11), 3289-3302.
- Junker, C., Draeger, S., & Schulz, B. (2012). A fine line—endophytes or pathogens in Arabidopsis thaliana. *Fungal Ecology*, *5*(6), 657-662.
- Kamoun, S., Furzer, O., Jones, J. D., Judelson, H. S., Ali, G. S., Dalio, R. J., ... & Cahill, D. (2015). The Top 10 oomycete pathogens in molecular plant pathology. *Molecular plant pathology*, *16*(4), 413-434.
- Karasov, T. L., Kniskern, J. M., Gao, L., DeYoung, B. J., Ding, J., Dubiella, U., ... & Barrett, L. G. (2014). The long-term maintenance of a resistance polymorphism through diffuse interactions. *Nature*, *512*(7515), 436-440.
- Kempel, A., Schädler, M., Chrobock, T., Fischer, M., & van Kleunen, M. (2011). Tradeoffs associated with constitutive and induced plant resistance against herbivory. *Proceedings of the National Academy of Sciences*, *108*(14), 5685-5689.
- Kim, H. Y., Choi, G. J., Lee, H. B., Lee, S. W., Lim, H. K., Jang, K. S., ... & Kim, J. C. (2007). Some fungal endophytes from vegetable crops and their anti-oomycete activities against tomato late blight. *Letters in applied microbiology*, *44*(3), 332-337.
- Kim, S. H., Gao, F., Bhattacharjee, S., Adiasor, J. A., Nam, J. C., & Gassmann, W. (2010). The Arabidopsis resistance-like gene SNC1 is activated by mutations in SRFR1 and contributes to resistance to the bacterial effector AvrRps4. *PLoS pathogens*, *6*(11).
- Kiss, L. (2003). A review of fungal antagonists of powdery mildews and their potential as biocontrol agents. *Pest Management Science: formerly Pesticide Science*, *59*(4), 475-483.

- Klessig, D. F., Choi, H. W., & Dempsey, D. M. A. (2018). Systemic acquired resistance and salicylic acid: past, present, and future. *Molecular plant-microbe interactions*, 31(9), 871-888.
- Knack, J. J., Wilcox, L. W., Delaux, P. M., Ané, J. M., Piotrowski, M. J., Cook, M. E., ... & Graham, L. E. (2015). Microbiomes of streptophyte algae and bryophytes suggest that a functional suite of microbiota fostered plant colonization of land. *International Journal of Plant Sciences*, 176(5), 405-420.
- Koh, E. J., Zhou, L., Williams, D. S., Park, J., Ding, N., Duan, Y. P., & Kang, B. H. (2012). Callose deposition in the phloem plasmodesmata and inhibition of phloem transport in citrus leaves infected with "*Candidatus Liberibacter asiaticus*". *Protoplasma*, 249(3), 687-697.
- Korir, N. K., Li, X., Xin, S., Wang, C., Changnian, S., Kayesh, E., & Fang, J. (2013). Characterization and expression profiling of selected microRNAs in tomato (*Solanum lycopersicon*) 'Jiangshu14'. *Molecular biology reports*, 40(5), 3503-3521.
- Kottb, M., Gigolashvili, T., Großkinsky, D. K., & Piechulla, B. (2015). Trichoderma volatiles effecting Arabidopsis: from inhibition to protection against phytopathogenic fungi. *Frontiers in microbiology*, 6, 995.
- Kourelis, J., & van der Hoorn, R. A. (2018). Defended to the nines: 25 years of resistance gene cloning identifies nine mechanisms for R protein function. *The Plant Cell*, 30(2), 285-299.
- Kowal, J., Pressel, S., Duckett, J. G., Bidartondo, M. I., & Field, K. J. (2018). From rhizoids to roots? Experimental evidence of mutualism between liverworts and ascomycete fungi. *Annals of botany*, 121(2), 221-227.
- Kozłowski, G., Buchala, A., & Métraux, J. P. (1999). Methyl jasmonate protects Norway spruce [*Picea abies* (L.) Karst.] seedlings against *Pythium ultimum* Trow. *Physiological and Molecular Plant Pathology*, 55(1), 53-58.
- Kramer, E. M. (2004). PIN and AUX/LAX proteins: their role in auxin accumulation. *Trends in plant science*, 9(12), 578-582.
- Krasileva, K. V., Zheng, C., Leonelli, L., Goritschnig, S., Dahlbeck, D., & Staskawicz, B. J. (2011). Global analysis of Arabidopsis/downy mildew interactions reveals prevalence of incomplete resistance and rapid evolution of pathogen recognition. *PLoS one*, 6(12).
- Krzywinski, M., & Altman, N. (2013). Points of significance: Power and sample size. *Nature Methods*, 10(12), 1139-1140.
- La Camera, S., Gouzerh, G., Dhondt, S., Hoffmann, L., Fritig, B., Legrand, M., & Heitz, T. (2004). Metabolic reprogramming in plant innate immunity: the contributions of phenylpropanoid and oxylipin pathways. *Immunological reviews*, 198(1), 267-284.
- Lacombe, B., & Achard, P. (2016). Long-distance transport of phytohormones through the plant vascular system. *Current opinion in plant biology*, 34, 1-8.
- Lahlali, R., & Hijri, M. (2010). Screening, identification and evaluation of potential biocontrol fungal endophytes against *Rhizoctonia solani* AG3 on potato plants. *FEMS microbiology letters*, 311(2), 152-159.
- Langfelder, P., & Horvath, S. (2008). WGCNA: an R package for weighted correlation network analysis. *BMC bioinformatics*, 9(1), 1-13.
- Lang, D., Zimmer, A. D., Rensing, S. A., & Reski, R. (2008). Exploring plant biodiversity: the Physcomitrella genome and beyond. *Trends in plant science*, 13(10), 542-549.
- Latchman, D. S. (1997). Transcription factors: an overview. *The international journal of biochemistry & cell biology*, 29(12), 1305-1312.
- Laxman, N., Rubin, C. J., Mallmin, H., Nilsson, O., Pastinen, T., Grundberg, E., & Kindmark, A. (2015). Global miRNA expression and correlation with mRNA levels in primary human bone cells. *Rna*, 21(8), 1433-1443.
- de León, I. P., Hamberg, M., & Castresana, C. (2015). Oxylipins in moss development and defense. *Frontiers in plant science*, 6, 483.
- Ligrone, R., Carafa, A., Duckett, J. G., Renzaglia, K. S., & Ruel, K. (2008). Immunocytochemical detection of lignin-related epitopes in cell walls in bryophytes and the charalean alga *Nitella*. *Plant Systematics and Evolution*, 270(3-4), 257-272.
- Li, X., Kapos, P., & Zhang, Y. (2015). NLRs in plants. *Current opinion in immunology*, 32, 114-121.

- Li, F. W., Nishiyama, T., Waller, M., Frangedakis, E., Keller, J., Li, Z., ... & Cheng, S. (2020). Anthoceros genomes illuminate the origin of land plants and the unique biology of hornworts. *Nature Plants*, 6(3), 259-272.
- Li, F., Pignatta, D., Bendix, C., Brunkard, J. O., Cohn, M. M., Tung, J., ... & Baker, B. (2012). MicroRNA regulation of plant innate immune receptors. *Proceedings of the National Academy of Sciences*, 109(5), 1790-1795.
- Liu, G., Min, H., Yue, S., & Chen, C. Z. (2008). Pre-miRNA loop nucleotides control the distinct activities of mir-181a-1 and mir-181c in early T cell development. *PLoS one*, 3(10).
- Lloyd, S. R., Schoonbeek, H. J., Trick, M., Zipfel, C., & Ridout, C. J. (2014). Methods to study PAMP-triggered immunity in Brassica species. *Molecular Plant-Microbe Interactions*, 27(3), 286-295.
- Lopez-Gomollon, S., Mohorianu, I., Szitty, G., Moulton, V., & Dalmay, T. (2012). Diverse correlation patterns between microRNAs and their targets during tomato fruit development indicates different modes of microRNA actions. *Planta*, 236(6), 1875-1887.
- MacQueen, A., & Bergelson, J. (2016). Modulation of R-gene expression across environments. *Journal of experimental botany*, 67(7), 2093-2105.
- Maggini, V., Mengoni, A., Gallo, E. R., Biffi, S., Fani, R., Firenzuoli, F., & Bogani, P. (2019). Tissue specificity and differential effects on in vitro plant growth of single bacterial endophytes isolated from the roots, leaves and rhizospheric soil of *Echinacea purpurea*. *BMC plant biology*, 19(1), 284.
- Mansfield, J., Genin, S., Magori, S., Citovsky, V., Sriariyanum, M., Ronald, P., ... & Toth, I. A. N. (2012). Top 10 plant pathogenic bacteria in molecular plant pathology. *Molecular plant pathology*, 13(6), 614-629.
- Mao, P., Duan, M., Wei, C., & Li, Y. (2007). WRKY62 transcription factor acts downstream of cytosolic NPR1 and negatively regulates jasmonate-responsive gene expression. *Plant & Cell Physiology*, 48 (6).
- Marco, A., Hooks, K., & Griffiths-Jones, S. (2012). Evolution and function of the extended miR-2 microRNA family. *RNA biology*, 9(3), 242-248.
- Martínez-Medina, A., Fernandez, I., Lok, G. B., Pozo, M. J., Pieterse, C. M., & Van Wees, S. C. (2017). Shifting from priming of salicylic acid-to jasmonic acid-regulated defences by *Trichoderma* protects tomato against the root knot nematode *Meloidogyne incognita*. *New Phytologist*, 213(3), 1363-1377.
- McConn, M., Creelman, R. A., Bell, E., & Mullet, J. E. (1997). Jasmonate is essential for insect defense in *Arabidopsis*. *Proceedings of the National Academy of Sciences*, 94(10), 5473-5477.
- McDowell, J. M., Williams, S. G., Funderburg, N. T., Eulgem, T., & Dangl, J. L. (2005). Genetic analysis of developmentally regulated resistance to downy mildew (*Hyaloperonospora parasitica*) in *Arabidopsis thaliana*. *Molecular Plant-Microbe Interactions*, 18(11), 1226-1234.
- McHale, L., Tan, X., Koehl, P., & Michelmore, R. W. (2006). Plant NBS-LRR proteins: adaptable guards. *Genome biology*, 7(4), 212
- Medzhitov, R., & Janeway Jr, C. A. (1997). Innate immunity: impact on the adaptive immune response. *Current opinion in immunology*, 9(1), 4-9.
- Melotto, M., Underwood, W., Koczan, J., Nomura, K., & He, S. Y. (2006). Plant stomata function in innate immunity against bacterial invasion. *Cell*, 126(5), 969-980.
- Mendes, R., Kruijt, M., De Bruijn, I., Dekkers, E., van der Voort, M., Schneider, J. H., ... & Raaijmakers, J. M. (2011). Deciphering the rhizosphere microbiome for disease-suppressive bacteria. *Science*, 332(6033), 1097-1100.
- Meyers, B. C., Kaushik, S., & Nandety, R. S. (2005). Evolving disease resistance genes. *Current opinion in plant biology*, 8(2), 129-134.
- Michelmore, R. W., & Meyers, B. C. (1998). Clusters of resistance genes in plants evolve by divergent selection and a birth-and-death process. *Genome research*, 8(11), 1113-1130.
- Miles, L. A., Lopera, C. A., González, S., de García, M. C., Franco, A. E., & Restrepo, S. (2012). Exploring the biocontrol potential of fungal endophytes from an Andean Colombian Paramo ecosystem. *BioControl*, 57(5), 697-710.
- Molinari, S., Fanelli, E., & Leonetti, P. (2014). Expression of tomato salicylic acid (SA)-responsive pathogenesis-related genes in Mi-1-mediated and SA-induced resistance to root-knot nematodes. *Molecular plant pathology*, 15(3), 255-264.

- Monte, I., Caballero, J., Zamarreño, A. M., Fernández-Barbero, G., García-Mina, J. M., & Solano, R. (2022). JAZ is essential for ligand specificity of the COI1/JAZ co-receptor. *Proceedings of the National Academy of Sciences*, 119(49), e2212155119.
- Mousa, W. K., & Raizada, M. N. (2013). The diversity of anti-microbial secondary metabolites produced by fungal endophytes: an interdisciplinary perspective. *Frontiers in microbiology*, 4, 65.
- Mousa, W. K., Shearer, C., Limay-Rios, V., Ettinger, C. L., Eisen, J. A., & Raizada, M. N. (2016). Root-hair endophyte stacking in finger millet creates a physicochemical barrier to trap the fungal pathogen *Fusarium graminearum*. *Nature microbiology*, 1(12), 1-12.
- Mutte, S. K., Kato, H., Rothfels, C., Melkonian, M., Wong, G. K. S., & Weijers, D. (2018). Origin and evolution of the nuclear auxin response system. *Elife*, 7, e33399.
- Namisy, A., Chen, J. R., Prohens, J., Metwally, E., Elmahrouk, M., & Rakha, M. (2019). Screening Cultivated Eggplant and Wild Relatives for Resistance to Bacterial Wilt (*Ralstonia solanacearum*). *Agriculture*, 9(7), 157.
- Naseem, M., Kaldorf, M., & Dandekar, T. (2015). The nexus between growth and defence signalling: auxin and cytokinin modulate plant immune response pathways. *Journal of Experimental Botany*, 66(16), 4885-4896.
- Nelson, J. M., Hauser, D. A., Hinson, R., & Shaw, A. J. (2018). A novel experimental system using the liverwort *Marchantia polymorpha* and its fungal endophytes reveals diverse and context-dependent effects. *New Phytologist*, 218(3), 1217-1232.
- Neilsen, C. T., Goodall, G. J., & Bracken, C. P. (2012). IsomiRs—the overlooked repertoire in the dynamic microRNAome. *Trends in genetics*, 28(11), 544-549.
- Nowicki, M., Foolad, M. R., Nowakowska, M., & Kozik, E. U. (2012). Potato and tomato late blight caused by *Phytophthora infestans*: an overview of pathology and resistance breeding. *Plant disease*, 96(1), 4-17.
- Okamura, K., Phillips, M. D., Tyler, D. M., Duan, H., Chou, Y. T., & Lai, E. C. (2008). The regulatory activity of microRNA* species has substantial influence on microRNA and 3' UTR evolution. *Nature structural & molecular biology*, 15(4), 354.
- Oliver, J. P., Castro, A., Gaggero, C., Cascón, T., Schmelz, E. A., Castresana, C., & De León, I. P. (2009). *Pythium* infection activates conserved plant defense responses in mosses. *Planta*, 230(3), 569-579.
- Ouyang, S., Park, G., Atamian, H. S., Han, C. S., Stajich, J. E., Kaloshian, I., & Borkovich, K. A. (2014). MicroRNAs suppress NB domain genes in tomato that confer resistance to *Fusarium oxysporum*. *PLoS pathogens*, 10(10).
- Overdijk, E. J., De Keijzer, J., De Groot, D., Schoina, C., Bouwmeester, K., Ketelaar, T., & Govers, F. (2016). Interaction between the moss *Physcomitrella patens* and *Phytophthora*: a novel pathosystem for live-cell imaging of subcellular defence. *Journal of microscopy*, 263(2), 171-180.
- Palatnik, J. F., Allen, E., Wu, X., Schommer, C., Schwab, R., Carrington, J. C., & Weigel, D. (2003). Control of leaf morphogenesis by microRNAs. *Nature*, 425(6955), 257-263.
- Pal, K. K., & Gardener, B. M. (2006). Biological control of plant pathogens. *The Plant Health Instructor*, 1–25.
- Panke-Buisse, K., Poole, A. C., Goodrich, J. K., Ley, R. E., & Kao-Kniffin, J. (2015). Selection on soil microbiomes reveals reproducible impacts on plant function. *The ISME journal*, 9(4), 980-989.
- Peleg, Z., & Blumwald, E. (2011). Hormone balance and abiotic stress tolerance in crop plants. *Current opinion in plant biology*, 14(3), 290-295.
- Peng, G., & Han, J. D. J. (2018). Regulatory network characterization in development: challenges and opportunities. *F1000Research*, 7.
- Penninckx, I. A., Thomma, B. P., Buchala, A., Métraux, J. P., & Broekaert, W. F. (1998). Concomitant activation of jasmonate and ethylene response pathways is required for induction of a plant defensin gene in *Arabidopsis*. *The Plant Cell*, 10(12), 2103-2113.
- Peters, G. A., & Meeks, J. C. (1989). The *Azolla-Anabaena* symbiosis: basic biology. *Annual review of plant biology*, 40(1), 193-210.
- Pieterse, C. M., Leon-Reyes, A., Van der Ent, S., & Van Wees, S. C. (2009). Networking by small-molecule hormones in plant immunity. *Nature chemical biology*, 5(5), 308-316.

- Pinzón, N., Li, B., Martínez, L., Sergeeva, A., Presumej, J., Apparailly, F., & Seitz, H. (2017). microRNA target prediction programs predict many false positives. *Genome research*, 27(2), 234-245.
- Plett, J. M., Daguerre, Y., Wittulsky, S., Vayssières, A., Deveau, A., Melton, S. J., ... & Martin, F. (2014). Effector MiSSP7 of the mutualistic fungus *Laccaria bicolor* stabilizes the *Populus* JAZ6 protein and represses jasmonic acid (JA) responsive genes. *Proceedings of the National Academy of Sciences*, 111(22), 8299-8304.
- Plissonneau, C., Blaise, F., Ollivier, B., Leflon, M., Carpezat, J., Rouxel, T., & Balesdent, M. H. (2017). Unusual evolutionary mechanisms to escape effector-triggered immunity in the fungal phytopathogen *Leptosphaeria maculans*. *Molecular ecology*, 26(7), 2183-2198.
- Van de Poel, B., Cooper, E. D., Van Der Straeten, D., Chang, C., & Delwiche, C. F. (2016). Transcriptome profiling of the green alga *Spirogyra pratensis* (Charophyta) suggests an ancestral role for ethylene in cell wall metabolism, photosynthesis, and abiotic stress responses. *Plant physiology*, 172(1), 533-545.
- Ponce De Leon, I., Schmelz, E. A., Gaggero, C., Castro, A., Alvarez, A., & Montesano, M. (2012). *Physcomitrella patens* activates reinforcement of the cell wall, programmed cell death and accumulation of evolutionary conserved defence signals, such as salicylic acid and 12-oxo-phytodienoic acid, but not jasmonic acid, upon *Botrytis cinerea* infection. *Molecular plant pathology*, 13(8), 960-974.
- Pratiwi, P., Tanaka, G., Takahashi, T., Xie, X., Yoneyama, K., Matsuura, H., & Takahashi, K. (2017). Identification of jasmonic acid and jasmonoyl-isoleucine, and characterization of AOS, AOC, OPR and JAR1 in the model lycophyte *Selaginella moellendorffii*. *Plant and Cell Physiology*, 58(4), 789-801.
- Pré, M., Atallah, M., Champion, A., De Vos, M., Pieterse, C. M., & Memelink, J. (2008). The AP2/ERF domain transcription factor ORA59 integrates jasmonic acid and ethylene signals in plant defense. *Plant physiology*, 147(3), 1347-1357.
- Preston, G. M. (2004). Plant perceptions of plant growth-promoting *Pseudomonas*. *Philosophical Transactions of the Royal Society of London. Series B: Biological Sciences*, 359(1446), 907-918.
- Pumplin, N., & Voinnet, O. (2013). RNA silencing suppression by plant pathogens: defence, counter-defence and counter-counter-defence. *Nature Reviews Microbiology*, 11(11), 745-760.
- Puopolo, G., Cimmino, A., Palmieri, M. C., Giovannini, O., Evidente, A., & Pertot, I. (2014). *Lysobacter capsici* AZ78 produces cyclo (l-Pro-l-Tyr), a 2, 5-diketopiperazine with toxic activity against sporangia of *P. hytophthora infestans* and *P. lasmopara viticola*. *Journal of applied microbiology*, 117(4), 1168-1180.
- Qiao, Y., Liu, L., Xiong, Q., Flores, C., Wong, J., Shi, J., ... & Ma, W. (2013). Oomycete pathogens encode RNA silencing suppressors. *Nature genetics*, 45(3), 330-333.
- Qiao, Y., Shi, J., Zhai, Y., Hou, Y., & Ma, W. (2015). *Phytophthora* effector targets a novel component of small RNA pathway in plants to promote infection. *Proceedings of the National Academy of Sciences*, 112(18), 5850-5855.
- Rai, A. N., Söderbäck, E., & Bergman, B. (2000). Cyanobacterium-plant symbioses. *New Phytologist*, 147(3), 449-481.
- Ranjan, A., Vadassery, J., Patel, H. K., Pandey, A., Palaparathi, R., Mithöfer, A., & Sonti, R. V. (2015). Upregulation of jasmonate biosynthesis and jasmonate-responsive genes in rice leaves in response to a bacterial pathogen mimic. *Functional & integrative genomics*, 15(3), 363-373.
- Rey, T., & Jacquet, C. (2018). Symbiosis genes for immunity and vice versa. *Current opinion in plant biology*, 44, 64-71.
- Rincones, J., Mazotti, G. D., Griffith, G. W., Pomela, A., Figueira, A., Leal Jr, G. A., ... & Meinhardt, L. W. (2006). Genetic variability and chromosome-length polymorphisms of the witches' broom pathogen *Crinipellis perniciosa* from various plant hosts in South America. *Mycological research*, 110(7), 821-832.
- Rolli, E., Marasco, R., Vigani, G., Ettoumi, B., Mapelli, F., Deangelis, M. L., ... & Pierotti Cei, F. (2015). Improved plant resistance to drought is promoted by the root-associated microbiome as a water stress-dependent trait. *Environmental microbiology*, 17(2), 316-331.
- Roll, J. T., Shah, V. K., Dean, D. R., & Roberts, G. P. (1995). Characteristics of NifNE in *Azotobacter vinelandii* strains Implications for the synthesis of the iron-molybdenum cofactor of dinitrogenase. *Journal of Biological Chemistry*, 270(9), 4432-4437.

- Rose, L. E., Bittner-Eddy, P. D., Langley, C. H., Holub, E. B., Michelmore, R. W., & Beynon, J. L. (2004). The maintenance of extreme amino acid diversity at the disease resistance gene, RPP13, in *Arabidopsis thaliana*. *Genetics*, *166*(3), 1517-1527.
- Rouxel, T., Grandaubert, J., Hane, J. K., Hoede, C., Van de Wouw, A. P., Couloux, A., ... & Cozijnsen, A. J. (2011). Effector diversification within compartments of the *Leptosphaeria maculans* genome affected by Repeat-Induced Point mutations. *Nature communications*, *2*(1), 1-10.
- Rovenich, H., Boshoven, J. C., & Thomma, B. P. (2014). Filamentous pathogen effector functions: of pathogens, hosts and microbiomes. *Current opinion in plant biology*, *20*, 96-103.
- Rubio-Somoza, I., & Weigel, D. (2011). MicroRNA networks and developmental plasticity in plants. *Trends in plant science*, *16*(5), 258-264
- Sapp, M., Ploch, S., Fiore-Donno, A. M., Bonkowski, M., & Rose, L. E. (2018). Protists are an integral part of the *Arabidopsis thaliana* microbiome. *Environmental microbiology*, *20*(1), 30-43.
- Schrempf, D., & Szöllösi, G. (2020). The sources of phylogenetic conflicts. *Phylogenetics in the genomic era*, 3-1.
- Schröder, S., Kortekamp, A., Heene, E., Daumann, J., Valea, I., & Nick, P. (2015). Crop wild relatives as genetic resources—the case of the European wild grape. *Canadian journal of plant science*, *95*(5), 905-912.
- Schulz, B. (2006). Mutualistic interactions with fungal root endophytes. *Microbial root endophytes*, 261-279.
- Schulz, B., & Boyle, C. (2005). The endophytic continuum. *Mycological research*, *109*(6), 661-686.
- Schwab, R., Palatnik, J. F., Riester, M., Schommer, C., Schmid, M., & Weigel, D. (2005). Specific effects of microRNAs on the plant transcriptome. *Developmental cell*, *8*(4), 517-527.
- Seeholzer, S., Tsuchimatsu, T., Jordan, T., Bieri, S., Pajonk, S., Yang, W., ... & Schulze-Lefert, P. (2010). Diversity at the Mla powdery mildew resistance locus from cultivated barley reveals sites of positive selection. *Molecular plant-microbe interactions*, *23*(4), 497-509.
- Selosse, M. A., Strullu-Derrien, C., Martin, F. M., Kamoun, S., & Kenrick, P. (2015). Plants, fungi and oomycetes: a 400-million year affair that shapes the biosphere. *New Phytologist*, *206*(2), 501-506.
- Shao, Z. Q., Xue, J. Y., Wang, Q., Wang, B., & Chen, J. Q. (2019). Revisiting the origin of plant NBS-LRR genes. *Trends in plant science*, *24*(1), 9-12.
- Sharma, R., Rawat, V., & Suresh, C. G. (2017). Genome-wide identification and tissue-specific expression analysis of nucleotide binding site-leucine rich repeat gene family in *Cicer arietinum* (kabuli chickpea). *Genomics data*, *14*, 24-31.
- Shigenaga, A. M., & Argueso, C. T. (2016, August). No hormone to rule them all: Interactions of plant hormones during the responses of plants to pathogens. In *Seminars in Cell & Developmental Biology* (Vol. 56, pp. 174-189). Academic Press.
- Shivaprasad, P. V., Chen, H. M., Patel, K., Bond, D. M., Santos, B. A., & Baulcombe, D. C. (2012). A microRNA superfamily regulates nucleotide binding site-leucine-rich repeats and other mRNAs. *The Plant Cell*, *24*(3), 859-874.
- Smit, F., & Dubery, I. A. (1997). Cell wall reinforcement in cotton hypocotyls in response to a *Verticillium dahliae* elicitor. *Phytochemistry*, *44*(5), 811-815.
- Soltis, P. S., & Soltis, D. E. (1993). Ancient DNA: Prospects and limitations. *New Zealand Journal of Botany*, *31*(3), 203-209.
- Song, J., Win, J., Tian, M., Schornack, S., Kaschani, F., Ilyas, M., ... & Kamoun, S. (2009). Apoplastic effectors secreted by two unrelated eukaryotic plant pathogens target the tomato defense protease Rcr3. *Proceedings of the National Academy of Sciences*, *106*(5), 1654-1659.
- Son, S. W., Kim, H. Y., Choi, G. J., Lim, H. K., Jang, K. S., Lee, S. O., ... & Kim, J. C. (2008). Bikaverin and fusaric acid from *Fusarium oxysporum* show antioomycete activity against *Phytophthora infestans*. *Journal of applied microbiology*, *104*(3), 692-698.
- Sørensen, I., Pettolino, F. A., Bacic, A., Ralph, J., Lu, F., O'Neill, M. A., ... & Willats, W. G. (2011). The charophycean green algae provide insights into the early origins of plant cell walls. *The Plant Journal*, *68*(2), 201-211.

- Sosa-Valencia, G., Palomar, M., Covarrubias, A. A., & Reyes, J. L. (2017). The legume miR1514a modulates a NAC transcription factor transcript to trigger phasiRNA formation in response to drought. *Journal of experimental botany*, *68*(8), 2013-2026.
- Stein, E., Molitor, A., Kogel, K. H., & Waller, F. (2008). Systemic resistance in Arabidopsis conferred by the mycorrhizal fungus Piriformospora indica requires jasmonic acid signaling and the cytoplasmic function of NPR1. *Plant and Cell Physiology*, *49*(11), 1747-1751.
- Strobel, G., & Daisy, B. (2003). Bioprospecting for microbial endophytes and their natural products. *Microbiology and molecular biology reviews*, *67*(4), 491-502.
- Strullu-Derrien, C., Kenrick, P., Pressel, S., Duckett, J. G., Rioult, J. P., & Strullu, D. G. (2014). Fungal associations in H orneophyton ligneri from the R hynie C hert (c. 407 million year old) closely resemble those in extant lower land plants: novel insights into ancestral plant–fungus symbioses. *New Phytologist*, *203*(3), 964-979.
- Stumpe, M., Göbel, C., Faltin, B., Beike, A. K., Hause, B., Himmelsbach, K., ... & Reski, R. (2010). The moss Physcomitrella patens contains cyclopentenones but no jasmonates: mutations in allene oxide cyclase lead to reduced fertility and altered sporophyte morphology. *New Phytologist*, *188*(3), 740-749.
- Tanzer, A., & Stadler, P. F. (2004). Molecular evolution of a microRNA cluster. *Journal of molecular biology*, *339*(2), 327-335.
- Tarazona, S., García-Alcalde, F., Dopazo, J., Ferrer, A., & Conesa, A. (2011). Differential expression in RNA-seq: a matter of depth. *Genome research*, *21*(12), 2213-2223.
- Taylor, T. N., Remy, W., & Hass, H. (1992). Parasitism in a 400-million-year-old green alga. *Nature*, *357*(6378), 493-494.
- Tay, Y., Rinn, J., & Pandolfi, P. P. (2014). The multilayered complexity of ceRNA crosstalk and competition. *Nature*, *505*(7483), 344-352.
- Thines, M. (2018). Oomycetes. *Current Biology*, *28*(15), R812-R813.
- Tian, D., Traw, M. B., Chen, J. Q., Kreitman, M., & Bergelson, J. (2003). Fitness costs of R-gene-mediated resistance in Arabidopsis thaliana. *Nature*, *423*(6935), 74-77.
- Todesco, M., Balasubramanian, S., Cao, J., Ott, F., Sureshkumar, S., Schneeberger, K., ... & Weigel, D. (2012). Natural variation in biogenesis efficiency of individual Arabidopsis thaliana microRNAs. *Current Biology*, *22*(2), 166-170.
- Ton, J., Flors, V., & Mauch-Mani, B. (2009). The multifaceted role of ABA in disease resistance. *Trends in plant science*, *14*(6), 310-317.
- Tsuda, K., & Katagiri, F. (2010). Comparing signaling mechanisms engaged in pattern-triggered and effector-triggered immunity. *Current opinion in plant biology*, *13*(4), 459-465.
- Turner, T. R., James, E. K., & Poole, P. S. (2013). The plant microbiome. *Genome biology*, *14*(6), 209.
- Uheda, E., & Kitoh, S. (1994). Rapid shedding of roots from Azolla filiculoides plants in response to inhibitors of respiration. *Plant and cell physiology*, *35*(1), 37-43.
- Vaucheret, H., Vazquez, F., Crété, P., & Bartel, D. P. (2004). The action of ARGONAUTE1 in the miRNA pathway and its regulation by the miRNA pathway are crucial for plant development. *Genes & development*, *18*(10), 1187-1197.
- Vetukuri, R. R., Whisson, S. C., & Grenville-Briggs, L. J. (2017). Phytophthora infestans effector Pi14054 is a novel candidate suppressor of host silencing mechanisms. *European Journal of Plant Pathology*, *149*(3), 771-777.
- Vleeshouwers, V. G., van Dooijeweert, W., Govers, F., Kamoun, S., & Colon, L. T. (2000). The hypersensitive response is associated with host and nonhost resistance to Phytophthora infestans. *Planta*, *210*(6), 853-864.
- Vleeshouwers, V. G., Raffaele, S., Vossen, J. H., Champouret, N., Oliva, R., Segretin, M. E., ... & Pel, M. A. (2011). Understanding and exploiting late blight resistance in the age of effectors. *Annual review of phytopathology*, *49*, 507-531.
- Vogler, H., Akbergenov, R., Shivaprasad, P. V., Dang, V., Fasler, M., Kwon, M. O., ... & Heinlein, M. (2007). Modification of small RNAs associated with suppression of RNA silencing by tobamovirus replicase protein. *Journal of virology*, *81*(19), 10379-10388.

- Voinnet, O. (2009). Origin, biogenesis, and activity of plant microRNAs. *Cell*, 136(4), 669-687.
- Vos, I. A., Pieterse, C. M., & Van Wees, S. C. (2013). Costs and benefits of hormone-regulated plant defences. *Plant Pathology*, 62, 43-55.
- Van Der Vossen, E. A., Van Der Voort, J. N. R., Kanyuka, K., Bendahmane, A., Sandbrink, H., Baulcombe, D. C., ... & Klein-Lankhorst, R. M. (2000). Homologues of a single resistance-gene cluster in potato confer resistance to distinct pathogens: a virus and a nematode. *The Plant Journal*, 23(5), 567-576.
- de Vries, J., & Archibald, J. M. (2018). Plant evolution: landmarks on the path to terrestrial life. *New Phytologist*, 217(4), 1428-1434.
- de Vries, S., von Dahlen, J. K., Schnake, A., Ginschel, S., Schulz, B., & Rose, L. E. (2018). Broad-spectrum inhibition of *Phytophthora infestans* by fungal endophytes. *FEMS Microbiology Ecology*, 94(4), fiy037.
- de Vries, S., von Dahlen, J. K., Uhlmann, C., Schnake, A., Kloesges, T., & Rose, L. E. (2017). Signatures of selection and host-adapted gene expression of the *Phytophthora infestans* RNA silencing suppressor PSR2. *Molecular plant pathology*, 18(1), 110-124.
- de Vries, S., Kloesges, T., & Rose, L. E. (2015). Evolutionarily dynamic, but robust, targeting of resistance genes by the miR482/2118 gene family in the Solanaceae. *Genome biology and evolution*, 7(12), 3307-3321.
- de Vries, S., Kukuk, A., von Dahlen, J. K., Schnake, A., Kloesges, T., & Rose, L. E. (2018). Expression profiling across wild and cultivated tomatoes supports the relevance of early miR482/2118 suppression for *Phytophthora* resistance. *Proceedings of the Royal Society B: Biological Sciences*, 285(1873), 20172560.
- de Vries, S., de Vries, J., von Dahlen, J. K., Gould, S. B., Archibald, J. M., Rose, L. E., & Slamovits, C. H. (2018). On plant defense signaling networks and early land plant evolution. *Communicative & Integrative Biology*, 11(3), 1-14.
- de Vries, S., de Vries, J., Teschke, H., von Dahlen, J. K., Rose, L. E., & Gould, S. B. (2018). Jasmonic and salicylic acid response in the fern *Azolla filiculoides* and its cyanobiont. *Plant, Cell & Environment*, 41(11), 2530-2548.
- Wang, J., Hu, M., Wang, J., Qi, J., Han, Z., Wang, G., ... & Chai, J. (2019). Reconstitution and structure of a plant NLR resistosome conferring immunity. *Science*, 364(6435), eaav5870
- Wang, C., Liu, Y., Li, S. S., & Han, G. Z. (2015). Insights into the origin and evolution of the plant hormone signaling machinery. *Plant physiology*, 167(3), 872-886.
- Wang, C., Ye, J., Tang, W., Liu, Z., Zhu, C., Wang, M., & Wan, J. (2013). Loop nucleotide polymorphism in a putative miRNA precursor associated with seed length in rice (*Oryza sativa* L.). *International journal of biological sciences*, 9(6), 578.
- Wang, B., Yeun, L. H., Xue, J. Y., Liu, Y., Ané, J. M., & Qiu, Y. L. (2010). Presence of three mycorrhizal genes in the common ancestor of land plants suggests a key role of mycorrhizas in the colonization of land by plants. *New Phytologist*, 186(2), 514-525.
- Wani, S. H., Kumar, V., Shriram, V., & Sah, S. K. (2016). Phytohormones and their metabolic engineering for abiotic stress tolerance in crop plants. *The Crop Journal*, 4(3), 162-176.
- Wei, C., Chen, J., & Kuang, H. (2016). Dramatic number variation of R genes in Solanaceae species accounted for by a few R gene subfamilies. *PLoS One*, 11(2).
- Wei, C., Kuang, H., Li, F., & Chen, J. (2014). The I2 resistance gene homologues in *Solanum* have complex evolutionary patterns and are targeted by miRNAs. *BMC genomics*, 15(1), 743.
- Wei, F., Wing, R. A., & Wise, R. P. (2002). Genome dynamics and evolution of the Mla (powdery mildew) resistance locus in barley. *The Plant Cell*, 14(8), 1903-1917.
- Weller, D. M., Raaijmakers, J. M., Gardener, B. B. M., & Thomashow, L. S. (2002). Microbial populations responsible for specific soil suppressiveness to plant pathogens. *Annual review of phytopathology*, 40(1), 309-348.
- Wen, M., Xie, M., He, L., Wang, Y., Shi, S., & Tang, T. (2016). Expression variations of miRNAs and mRNAs in rice (*Oryza sativa*). *Genome biology and evolution*, 8(11), 3529-3544.

- Wickett, N. J., Mirarab, S., Nguyen, N., Warnow, T., Carpenter, E., Matasci, N., ... & Ruhfel, B. R. (2014). Phylotranscriptomic analysis of the origin and early diversification of land plants. *Proceedings of the National Academy of Sciences*, *111*(45), E4859-E4868.
- Williamson, B., Tudzynski, B., Tudzynski, P., & Van Kan, J. A. (2007). Botrytis cinerea: the cause of grey mould disease. *Molecular plant pathology*, *8*(5), 561-580.
- Witek, K., Jupe, F., Witek, A. I., Baker, D., Clark, M. D., & Jones, J. D. (2016). Accelerated cloning of a potato late blight-resistance gene using RenSeq and SMRT sequencing. *Nature Biotechnology*, *34*(6), 656.
- Wu, J., Kou, Y., Bao, J., Li, Y., Tang, M., Zhu, X., ... & Song, M. Y. (2015). Comparative genomics identifies the Magnaporthe oryzae avirulence effector AvrPiz-t that triggers Piz-t-mediated blast resistance in rice. *New Phytologist*, *206*(4), 1463-1475.
- Wu, G., Park, M. Y., Conway, S. R., Wang, J. W., Weigel, D., & Poethig, R. S. (2009). The sequential action of miR156 and miR172 regulates developmental timing in Arabidopsis. *Cell*, *138*(4), 750-759.
- Xia, R., Chen, C., Pokhrel, S., Ma, W., Huang, K., Patel, P., ... & Meyers, B. C. (2019). 24-nt reproductive phasiRNAs are broadly present in angiosperms. *Nature communications*, *10*(1), 1-8.
- Xie, Z., Kasschau, K. D., & Carrington, J. C. (2003). Negative feedback regulation of Dicer-Like1 in Arabidopsis by microRNA-guided mRNA degradation. *Current Biology*, *13*(9), 784-789.
- Yamamoto, Y., Ohshika, J., Takahashi, T., Ishizaki, K., Kohchi, T., Matusuura, H., & Takahashi, K. (2015). Functional analysis of allene oxide cyclase, MpAOC, in the liverwort Marchantia polymorpha. *Phytochemistry*, *116*, 48-56.
- Yamasaki, H., Hayashi, M., Fukazawa, M., Kobayashi, Y., & Shikanai, T. (2009). SQUAMOSA promoter binding protein-like7 is a central regulator for copper homeostasis in Arabidopsis. *The Plant Cell*, *21*(1), 347-361.
- Yang, S., Li, J., Zhang, X., Zhang, Q., Huang, J., Chen, J. Q., ... & Tian, D. (2013). Rapidly evolving R genes in diverse grass species confer resistance to rice blast disease. *Proceedings of the National Academy of Sciences*, *110*(46), 18572-18577.
- Yang, S., Tang, F., & Zhu, H. (2014). Alternative splicing in plant immunity. *International journal of molecular sciences*, *15*(6), 10424-10445.
- Yan, D. H., Song, X., Li, H., Luo, T., Dou, G., & Strobel, G. (2018). Antifungal activities of volatile secondary metabolites of four Diaporthe strains isolated from Catharanthus roseus. *Journal of Fungi*, *4*(2), 65.
- Yue, J. X., Meyers, B. C., Chen, J. Q., Tian, D., & Yang, S. (2012). Tracing the origin and evolutionary history of plant nucleotide-binding site-leucine-rich repeat (NBS-LRR) genes. *New Phytologist*, *193*(4), 1049-1063.
- Yu, Y., Jia, T., & Chen, X. (2017). The 'how' and 'where' of plant micro RNA s. *New Phytologist*, *216*(4), 1002-1017.
- Yu, M. H., Zhao, Z. Z., & He, J. X. (2018). Brassinosteroid signaling in plant-microbe interactions. *International journal of molecular sciences*, *19*(12), 4091.
- Zhai, J., Jeong, D. H., De Paoli, E., Park, S., Rosen, B. D., Li, Y., ... & Meyers, B. C. (2011). MicroRNAs as master regulators of the plant NB-LRR defense gene family via the production of phased, trans-acting siRNAs. *Genes & development*, *25*(23), 2540-2553.
- Zhai, X. G., Zhao, T., Liu, Y. H., Long, H., Deng, G. B., Pan, Z. F., & Yu, M. Q. (2008). Characterization and expression profiling of a novel cereal cyst nematode resistance gene analog in wheat. *Molecular biology*, *42*(6), 960-965.
- Zhang, Y., Xia, R., Kuang, H., & Meyers, B. C. (2016). The diversification of plant NBS-LRR defense genes directs the evolution of microRNAs that target them. *Molecular biology and evolution*, *33*(10), 2692-2705.
- Zhang, X., Zhao, H., Gao, S., Wang, W. C., Katiyar-Agarwal, S., Huang, H. D., ... & Jin, H. (2011). Arabidopsis Argonaute 2 regulates innate immunity via miRNA393*-mediated silencing of a Golgi-localized SNARE gene, MEMB12. *Molecular cell*, *42*(3), 356-366.
- Zhao, Y., Shen, X., Tang, T., & Wu, C. I. (2017). Weak regulation of many targets is cumulatively powerful—an evolutionary perspective on microRNA functionality. *Molecular Biology and Evolution*, *34*(12), 3041-3046.
- Zhong, Z., Marcel, T. C., Hartmann, F. E., Ma, X., Plissonneau, C., Zala, M., ... & Amselem, J. (2017). A small secreted protein in Zymoseptoria tritici is responsible for avirulence on wheat cultivars carrying the Stb6 resistance gene. *New Phytologist*, *214*(2), 619-631.






- Zhou, L., Liu, Y., Liu, Z., Kong, D., Duan, M., & Luo, L. (2010). Genome-wide identification and analysis of drought-responsive microRNAs in *Oryza sativa*. *Journal of experimental botany*, *61*(15), 4157-4168.
- Zhu, H., Zhou, Y., Castillo-González, C., Lu, A., Ge, C., Zhao, Y. T., ... & Zhang, X. (2013). Bidirectional processing of pri-miRNAs with branched terminal loops by Arabidopsis Dicer-like1. *Nature structural & molecular biology*, *20*(9), 1106.
- Zimmerli, L., Stein, M., Lipka, V., Schulze-Lefert, P., & Somerville, S. (2004). Host and non-host pathogens elicit different jasmonate/ethylene responses in Arabidopsis. *The Plant Journal*, *40*(5), 633-646.
- Zipfel, C. (2014). Plant pattern-recognition receptors. *Trends in immunology*, *35*(7), 345-351.

Publication I

On plant defense signaling networks and early land plant evolution

Status	Published
Journal	<i>Communicative & integrative biology</i>
Citation	de Vries, S., de Vries, J., von Dahlen, J. K. , Gould, S. B., Archibald, J. M., Rose, L. E., & Slamovits, C. H. (2018). On plant defense signaling networks and early land plant evolution. <i>Communicative & integrative biology</i> , 11(3), 1-14
Own contribution	Contributed to the writing of the manuscript (Review)

On plant defense signaling networks and early land plant evolution

Sophie de Vries ^{*a}, Jan de Vries ^{*a}, Janina K. von Dahlen^{b,c}, Sven B. Gould ^d, John M. Archibald ^a,
Laura E. Rose^{b,c,e}, and Claudio H. Slamovits ^a

^aDepartment of Biochemistry and Molecular Biology, Dalhousie University, Halifax, Canada; ^bInstitute of Population Genetics, Heinrich-Heine University Duesseldorf, Duesseldorf, Germany; ^ciGRAD-Plant Graduate School, Heinrich-Heine University Duesseldorf, Duesseldorf, Germany; ^dInstitute of Molecular Evolution, Heinrich-Heine University Duesseldorf, Duesseldorf, Germany; ^eCeplas, Cluster of Excellence in Plant Sciences, Heinrich-Heine University Duesseldorf, Duesseldorf, Germany

ABSTRACT

All land plants must cope with phytopathogens. Algae face pathogens, too, and it is reasonable to assume that some of the strategies for dealing with pathogens evolved prior to the origin of embryophytes – plant terrestrialization simply changed the nature of the plant-pathogen interactions. Here we highlight that many potential components of the angiosperm defense toolkit are i) found in streptophyte algae and non-flowering embryophytes and ii) might be used in non-flowering plant defense as inferred from published experimental data. Nonetheless, the common signaling networks governing these defense responses appear to have become more intricate during embryophyte evolution. This includes the evolution of the antagonistic signaling pathways of jasmonic and salicylic acid, multiple independent expansions of resistance genes, and the evolution of resistance gene-regulating microRNAs. Future comparative studies will illuminate which modules of the streptophyte defense signaling network constitute the core and which constitute lineage- and/or environment-specific (peripheral) signaling circuits.

ARTICLE HISTORY

Received 1 April 2018
Accepted 28 May 2018

KEYWORDS

Plant evolution; molecular plant-microbe interaction; charophytes; streptophyte algae; plant defense; phytopathology

Introduction

Macroscopic algae and plants are bathed in micro-organisms. Whatever their natural habitat, they are forced to interact with their microbial companions in some manner. Such interactions are diverse in nature. For example, various algae are known to depend on vitamin B₁₂ provided by bacteria in their environment [1]. Another famous example is the “regulation” of algal blooms of the haptophyte *Emiliania huxleyi* by bacteria [2]. Interactions with microbes – both positive and negative – are thus part of every photosynthetic eukaryote’s life. This article will focus on the evolution of the framework that underlies molecular phytopathology in modern-day plants and algae. We review what is known about the recurrent evolution of plant defense signaling networks across streptophyte evolution (Figure 1). In so doing, we span the trajectory from streptophyte algae (the closest extant relatives to land plants [3-5]), mosses, gymnosperms, and angiosperms. Since most data have been gathered for angiosperms, we will use them primarily for comparative purposes.

Evolutionary phytopathology: The nuts-and-bolts of plant-microbe interactions

Common themes in the evolution of plant defense signaling networks become apparent when diverse species from different lineages are compared. Across angiosperm lineages, plant defense signaling is based on core sets of phytohormones (*e.g.*, jasmonic acid; JA) and proteins (*e.g.*, receptors that sense microbial proteins, such as Flagellin sensitive 2; FLS2). Genetic diversity is further shaped by co-evolution driven by arms race dynamics between plants and microbes – affecting, for example, both resistance genes [6,7] and the factors that regulate them, *e.g.* miRNAs [8,9]. Studying these factors in an evolutionary context has been summarized as the “coming of age” for the study of evolutionary molecular plant-microbe interactions (coined EvoMPMI) by Upson and colleagues [10]. Upson and colleagues [10] emphasized the need for evolutionarily informed studies that focus on a broad scale covering entire land plant diversity as well as on fine-scale variation within or between closely related species.

While the vast body of literature on how land plants deal with phytopathogens is focused primarily on

CONTACT Sophie de Vries  sophie.devries@dal.ca  Department of Biochemistry and Molecular Biology, Dalhousie University, Halifax, NS B3H 4R2, Canada

*These authors contributed equally to this work.

© 2018 The Author(s). Published by Informa UK Limited, trading as Taylor & Francis Group.

This is an Open Access article distributed under the terms of the Creative Commons Attribution-NonCommercial License (<http://creativecommons.org/licenses/by-nc/4.0/>), which permits unrestricted non-commercial use, distribution, and reproduction in any medium, provided the original work is properly cited.

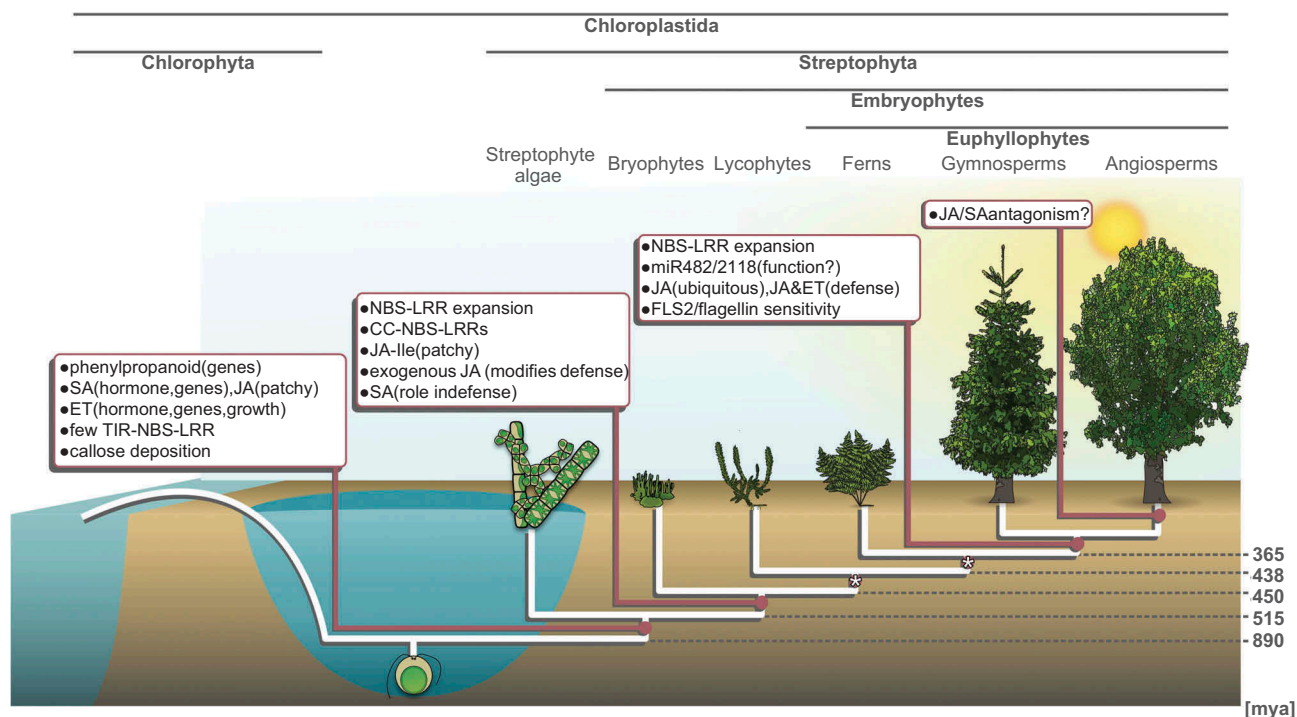


Figure 1. Key phytopathogen interaction factors across the trajectory of streptophyte evolution. Schematic cladogram (white lines) of the Chloroplastida depicts the deep split of the green lineage into Chlorophyta and Streptophyta about 900 million years ago (divergence times based on Morris et al. [45]). The Streptophyta encompass the paraphyletic streptophyte algae and the monophyletic land plants (Embryophyta). Land plants are likely >500 million years old and consist of the non-vascular bryophytes and the ~430 million year old clade of vascular plants, encompassing lycophytes and euphylllophytes. The euphylllophytes are the clade of ferns, gymnosperms and angiosperms (the latter two are the seed plants). Boxes highlight when – along this trajectory – signaling factors in plant defense are thought to have evolved; brackets further specify the type of data and/or functional significance of a given factor. The asterisks indicate nodes for which data are limited. JA, jasmonic acid; JA-Ile, jasmonic acid-isoleucine; SA, salicylic acid; ET, ethylene; NBS-LRR, nucleotide binding site-leucine-rich repeat; TIR-NBS-LRR, Toll-interleukin 1 receptor-nucleotide binding site-leucine-rich repeat; CC-NBS-LRR, coiled coil-nucleotide binding site-leucine-rich repeat; FLS2, FLAGELLIN SENSITIVE2.

angiosperms, research on gymnosperms and bryophytes is catching up [11–14] – yet, as highlighted by Upson et al. [10], ferns and lycophytes have yet to follow suit. Further, at the present time, little is known about the interactions between streptophyte algae and their phytopathogens. As outlined above, understanding commonalities in streptophyte algae and non-flowering plants is important to pinpoint how the defense signaling networks of plants arose. Because of the dynamics in plant-pathogen interactions, however, a plethora of different strategies in plant defense have come about.

Therefore, plant defense mechanisms are composed of common defense strategies as well as lineage-specific ones. A straightforward example of a lineage-specific defense strategy in gymnosperms is the flow of resin in wounded conifers, which depends upon resin ducts. Some resin ducts are formed during plant growth and flooded with resin in response to stress, while other resin ducts are only induced upon infection and wounding through the action of phytohormones [15–17]. By exploring the commonalities and differences, we will highlight both the evolutionary trajectories and

underlying principles of land plant signaling upon phytopathogen attack – including the potential for this signaling in streptophyte algae. We will first consider an example from basal-branching embryophytes and their interactions with substrate-dwelling fungi.

Fungal symbioses exemplify ancient plant-microbe interactions

Symbioses with Glomeromycota-like fungi are hypothesized to have occurred during an early phase of land plant terrestrialization and to have contributed significantly to the global colonization of land [[5,18–20], see also [21]]. Motivated not least by these observations, there is a growing body of literature on bryophyte–fungus interactions.

Various fungal interactions have been observed in liverworts. For example, a recent study by Nelson and colleagues [22] describes several growth-promoting endophytes associated with the liverwort *Marchantia polymorpha*, providing fertile ground for future Evo-MPMI research (see [23]). Other *Marchantia* species

were shown to engage in mutualistic interactions with Glomeromycota [24,25]. And other liverwort genera, such as *Cephalozia bicuspidata* [26], have also been shown to engage in mutualistic interactions with mycorrhizal fungi.

Several bryophytes form mycorrhizae by interacting with fungi [24,27,28], but the picture for bryophytes as a whole is patchy [29]. While many liverworts (outlined above) and hornworts [30,31] exhibit interactions with mycorrhizal fungi, mosses generally do not form mycorrhizae [32,33]; for a recent and comprehensive overview see [29]. That mosses do not form mycorrhizae is further corroborated by Wang and colleagues [34], who showed that moss arbuscular mycorrhizal symbiosis genes show high sequence divergence as compared to their homologous counterparts in all other land plants. Yet, in light of the recently supported monophyly of the bryophytes [35], the phenomenon that mosses do not form mycorrhizae likely represents a case of secondary loss [29]. On balance, symbiosis with arbuscular mycorrhizal fungi appears to be an ancestral feature of all land plants [36]. Indeed, molecular data presented by Wang et al. [34] indicate that genes associated with interactions with mycorrhizal fungi were likely present in the last common ancestor of land plants, which was corroborated by Delaux et al. [18]. But what about the algal progenitors of land plants?

Ancient land plant-microbe interactions and evidence from molecular data in streptophyte algae

Streptophyte algae are known to associate with various kinds of microorganisms. Knack and colleagues [37] performed a metagenomic study of aquatic streptophyte alga- and liverwort-associated microbes, including epiphytic microorganisms (e.g. those growing in the mucilage of streptophyte algae) as well as those colonizing the tissue. Their analyses of three higher-branching streptophyte algae (*Coleochaete pulvinata*, *Chaetosphaeridium globosum* and *Nitella tenuissima*) identified potentially beneficial microbes, for example nitrogen-fixing or cobalamin-producing bacteria, but also potentially harmful ones, such as bacteria associated with cellulose degradation [37]. Interestingly, Knack and colleagues [37] also detected some fungi in metagenomic data, an observation that warrants further investigation. Among the streptophyte algae investigated, the detected signals included sequences stemming from fungi belonging to the Cryptomycota and Chytridiomycota [37]. For the investigated liverwort *Conocephalum conicum* an association with glomalean fungi was demonstrated [37].

As mentioned earlier, Glomeromycota-like fungi feature in discussions revolving around the beneficial symbioses that the earliest land plants engaged in [19,20]. Delaux et al. [18] found that streptophyte algae have most of the genes that land plants put to use during symbiosis signaling. These authors also performed functional complementation experiments in which the capacity to engage in symbiosis with arbuscular mycorrhizal fungi was rescued by heterologously expressing streptophyte algal *CCaMK* in *Medicago ccamk* mutants (which are deficient in interacting with mycorrhizal fungi). This underscores the functional conservation of symbiosis signaling across long evolutionary timescales.

The fossil record also provides insight into streptophyte-fungal symbioses. 400-plus million-year-old *Horneophyton* land plant fossils have been shown to harbor glomeromycotean- and mucoromycotean-resembling structures [38]. Together with the aforementioned molecular data, this information makes a strong case for the idea that the interaction with mycorrhizal fungi is ancient. The genes underlying these beneficial interactions likely predate the origin of the terrestrial flora.

Microorganisms are not only beneficial to plants and algae – they can exploit their hosts as (facultative) phytopathogens [39]. For example, several bacterial and fungal genera or species complexes include mutualistic, pathogenic and endophytic species [39]. Such microbe-host relationships can in fact switch between neutral, beneficial and detrimental in response to, for example, environmental factors [40,41]. It is noteworthy that some of the components necessary for a successful arbuscular mycorrhizal symbiosis, and which are present in streptophyte algae or bryophytes, can also be used for defense signaling [42]. For example, mutations in several symbiosis-associated LysM-RLKs (Lysin Motif Receptor-like Kinases) have been reported to impair defense signaling [42]. In contrast, in the case of *Arabidopsis thaliana*, which does not engage in symbioses with arbuscular mycorrhizal fungi, the oomycete pathogen *Hyaloperonospora arabidopsidis* seems to require components of the arbuscular mycorrhizal symbiosis-associated molecular machinery to successfully complete its life cycle [43]. Hence, “symbiosis genes” might not only tell a tale of ancient mutualism, but also ancient interactions with phytopathogens.

The terrestrial habitat was teeming with microbes before the dawn of land plants [reviewed by [44]]. Hence, during terrestrialization >500 million years ago [see [45] for the latest dating] one can imagine that the earliest land plants would have encountered a very different set of microbes than those in the freshwater environments from which they were emerging.

Yet, a fluent passage scenario seems equally reasonable if one considers, e.g., a freshwater environment (microbe load A) that routinely dried out (microbe load B). It should further be noted that microbe load A and B may also have overlapped given that, for example, many oomycetes and fungi grow equally well in liquid or on solid medium in the laboratory – it goes without saying that this is a mere proxy for what might happen in nature and will require further studies. No matter the scenario, fossils have interesting stories to tell in this case, too.

Taylor et al. [46] reported the existence of a parasitic fungus in a likely more than 400-million-year-old fossil of *Paleonitella*, which appears to be related to extant charophyceae streptophyte algae (such as *Nitella*). But the algal progenitors of land plants would have encountered (terrestrial and/or non-terrestrial) microbes even before this time. Berbee and colleagues [47] recently argued that the occurrence of pectinases (enzymes used for the degradation of pectin in plant cell walls) in even the earliest-diverging fungi [see [48]] argues for the antiquity of the fungal ability to exploit plant material. How so? Pectin is a cell wall component characteristic of land plants and streptophyte algae (reviewed in [49]). Berbee et al. [47] argue that since pectinase-harboring fungal lineages are older than the land plant clade, these fungi used their pectinases for the degradation of streptophyte algal cell walls. This is corroborated by the fact that i) phytoplankton are readily attacked by chytrid fungi [50] and ii) chytrid fungi have been found associated with streptophyte algal microbiomes [37].

In summary, land plants and their closest relatives are, and always have been, associated with both symbiotic and pathogenic microorganisms – their interactions with microbes are truly ancient. Because it is important for hosts to be able to distinguish between a pathogen or a symbiont – and to react accordingly – defense signaling mechanisms must presumably also be present in the algae that are most closely related to land plants. The question that remains is: how similar are these mechanisms in plants and algae? The answer will shed light on the plant-microbe interaction tool kit that was present in the earliest land plants.

PTI and ETI in non-flowering land plants and maybe streptophyte algae

Most of what we know about the plant immune system derives from studying angiosperms. The pathogen recognition system is based upon two components: pattern triggered immunity (PTI) and effector triggered immunity (ETI) [6]. The latter is more specific towards the infecting pathogen because plant resistance genes

(*R* genes) recognize effector proteins secreted by, and specific to, a certain pathogen [51]. PTI causes, for example, stomata closure and cell wall reinforcements at the site of pathogen attack (e.g., through callose deposition, formation of papillae [deposits consisting of callose, phenolic compounds and polysaccharides], and lignification) [52–55]. PTI can also result in cell death caused by the release of reactive oxygen species (ROS) [56]. Additionally, ROS production and thus the initiation of the hypersensitive response (HR) is a classical hallmark of *R* gene-based immunity [51].

Not surprisingly, the potential for PTI can be found in early-branching land plant lineages as well as streptophyte algae (for a comprehensive discussion of genetic potential in streptophyte algae, see [5]). Streptophyte algae such as *Coleochaete* and *Nitella* have been found to contain lignin-like components [49,57–59], potentially used for cell wall reinforcement during pathogen attack. Moreover, the basal-branching streptophyte algae *Klebsormidium* spp. deposit callose in response to abiotic (desiccation) stress [60]. It is further noteworthy that even though Herburger and Holzinger [60] found that *Zygnema* spp. did not deposit callose in response to desiccation stress, callose was nonetheless present in these species. In the moss *Physcomitrella patens*, papillae formation is readily observed close to unsuccessful infection attempts by different *Phytophthora* pathogens [61]. Oomycete and fungal pathogens also induce ROS [62,63] and inoculations with oomycetes resulted in the accumulation of toxic phenolic compounds in *P. patens* [61,62]. Similarly, other mosses, including *Funaria hygrometrica*, also form papillae around fungal penetration sites to prohibit their entry [64,65]. Callose deposition was also observed in the interaction between the liverwort *M. polymorpha* and the oomycete *Phytophthora palmivora* [66].

PTI responses require receptors. One of the best-explored PTI-associated pattern recognition receptors (PRRs) in angiosperms is FLS2. FLS2 recognizes the microbe-associated molecular pattern (MAMP) flg22, a peptide component of the bacterial flagellin [56,67]. Orthologs of FLS2 were not found in the moss *P. patens* [68], although a homolog with appreciable sequence conservation was found [69]. Yet, *P. patens* is flg22-insensitive [70]. Likewise, the receptor for the bacterial translation elongation factor Tu (Ef-Tu), EFR [71,72], seems to be missing outside of the Brassicaceae [68,71] and Ef-Tu does not induce a PTI-like response in *P. patens* [70]. However, the moss does recognize bacteria and mounts a defense response accordingly [73]. This suggests that either more ancient or lineage-specific receptors are used in *P. patens* to recognize bacteria, and that FLS2 and EFR are more recent acquisitions. Indeed, in support of the

presence of a more ancient type of receptor in mosses, *P. patens* is known to respond to bacterial peptidoglycan, which is recognized by the ortholog of the *A. thaliana* receptor CERK1 [70]. Moreover, CERK1 of *P. patens* recognizes chitin from fungi and triggers downstream signaling responses [70]. This might hint that CERK1 was present and functioning in peptidoglycan recognition in the last common ancestor of land plants – but this needs further clarification by investigating CERK1 function across a broader diversity of land plants. In contrast to *P. patens*, protoplasts of the conifer *Pinus thunbergii* produce ROS in response to flagellin treatment [74] and FLS2 is hypothesized to be present in gymnosperms [75]. This suggests that a diversification of PTI-associated PRRs occurred during the evolution of land plants, perhaps associated with the refinement of MAMP-triggered responses.

Components of the heterotrimeric G-protein complex, a signaling switch that consists of an α -, β - and several γ -subunits [76], are involved in land plant defense responses (e.g. [77]); the role of β - and γ -subunits in defense is also implicated to be mediated by FLS2, EF-Tu and CERK1 in *A. thaliana* [78]. Homologs of all three subunits are present in land plants and streptophyte algae [79,80]. Moreover, in the interaction of *P. abies* with the fungal pathogens *Heterobasidion annosum*, *Heterobasidion parviporum* and the saprotroph *Phlebiopsis gigantea*, genes for several subunits of the heterotrimeric G-protein complex were shown to be up-regulated [81]. It was further suggested that this response may be triggered by conserved molecular patterns of the fungi [81], hence possibly associated with PTI. Whether heterotrimeric G-proteins also play a role in defense responses of earlier-diverging land plants and streptophyte algae remains to be investigated.

ETI requires the presence of R proteins to detect pathogen secreted effector proteins either through direct binding or by monitoring whether other host proteins are altered by the actions of effectors [51]; such alterations can include changes in protein conformation and/or phosphorylation status [82,83]. Once R proteins detect an effector protein of a pathogen, they induce pathogen-specific immune responses [84–86]. Nucleotide-binding site leucine-rich repeats (NBS-LRRs) are one of the major classes of R proteins [87]. They are combined with various N-terminal domains, for example the coiled-coil (CC-NBS-LRR) or Toll-interleukin 1 receptor domain (TIR-NBS-LRR) [87].

Potential NBS-LRR-encoding genes have been found from streptophyte algae to angiosperms, but there is pronounced variation in the number of NBS-LRR genes

present in any given genome. Conifers have undergone a dramatic expansion of their suite of NBS-LRR genes: while 69 putative NBS-LRR genes are predicted for *P. patens* and 16 for the lycophyte *Selaginella moellendorffii*, *P. abies* and *Pinus taeda* have been predicted to possess 562 and 677 putative NBS-LRR genes, respectively [88,89]. It is noteworthy that gymnosperms tend to have large genomes (often more than 10 Gbp in size [90]), which could suggest that the expansion of NBS-LRRs in plants is related to genome size of the respective plant. Yet, the large genomes of gymnosperms appear to be the result of an expansion of intron size because of repeated insertion of transposable elements and the total number of genes is in fact similar to that observed in *A. thaliana* [90]. Additionally, numbers of NBS-LRRs reported in Zhang et al. [88] seem to not necessarily be related to genome size. For example *Medicago truncatula* has “only” a 370 Mbp genome [91], but a similar number of NBS-LRRs as *P. abies* [88]. Likewise, the monocot *Triticum aestivum* has a 17 Gbp genome, similar in size to some gymnosperms [92], but has roughly double the number of NBS-LRRs than *P. abies* [88].

Species-specific expansions and reductions of NBS-LRRs have been observed throughout the Embryophyta [88] – including lineages with differentially expanded NBS-LRR subsets. For example, TIR-NBS-LRR-encoding genes are absent from the grasses (Poaceae; [e.g. [88]]). NBS-LRR genes also appear to be encoded in the genome of streptophyte algae, but whether they are required for streptophyte algal immunity is currently not known. Yue et al. [69] found three NBS-encoding sequences within the Coleochaetales (higher-branching streptophyte algae), two with sequence similarity to TIR-NBS-LRRs from angiosperms. Furthermore, Urbach and Ausubel ([93; see supplementary appendix) reported the detection of two TIR-NBS-LRR genes in the genome of the early-branching streptophyte alga *Klebsormidium nitens* (whose whole genome sequence was reported by [94]). In agreement with this, Gao and colleagues [89] reported three TIR-NBS-LRRs in *K. nitens* as well as one NBS-LRR with an additional N-terminal domain (*non-TIR-NBS-LRRs*). Several *non-TIR-NBS-LRRs* were found in transcriptomes of six streptophyte algae [89]. Yet, CC-NBS-LRRs (a class of non-TIR-NBS-LRRs) have thus far only been found among land plants, including the moss *P. patens* [88]. It hence appears that one of the most prominent NBS-LRR combinations – the CC-NBS-LRRs – evolved on land.

Given that the recognition of effector proteins by NBS-LRRs results in the initiation of plant cell death, tight regulatory control is essential. Indeed, these proteins are regulated in many ways, including multiple posttranslational mechanisms, such as ubiquitination

and oligomerization with different partners [95]. At the level of expression, they can be regulated by transcriptional as well as post-transcriptional means [95]. The latter is mediated by microRNAs (miRNAs) in angiosperms [96-99]. Several *NBS-LRR*-targeting miRNA families exist, but due to the broad distribution of the miR482/2118 family, this family has received more attention than others.

Members of the miR482/2118 family show low sequence conservation even between closely related species [8]. The family first emerged in gymnosperms [96,100], which seems to coincide with an expansion of *NBS-LRRs* during this time period [88]. The coniferous plant *P. abies* has one of the largest expansions of miR482/2118 [8,100] and the genes likely originated through inverted duplication of *NBS-LRR* genes [100]. miR482/2118 is a direct regulator of resistance to a diverse range of pathogens in dicots [9,98,101-103]. In monocots miR482/2118 is expressed in reproductive tissue and may function in its development [104]. Given the expression patterns of miR482/2118 in *P. abies*, with some members of this family solely expressed in reproductive organs [100], a broader function in the regulation of both reproductive organ development and disease resistance seems to be the more ancient mechanism.

Evolution of phytohormone defense networks

The plant immune system and phytohormone signaling are interwoven [105]. While almost all major phytohormones have been linked to plant immunity at some level [106], jasmonic acid (JA), salicylic acid (SA) and ethylene (ET) are key regulators [105]. In angiosperms, SA and JA act primarily antagonistically [107]. SA triggers immunity towards biotrophic pathogens, i.e., those requiring a living host [107]. SA regulates ROS levels by induction as well as scavenging [108]. Furthermore, SA is involved in the induction of HR, resulting in plant cell death [109]. On the other hand, JA is produced in response to herbivores, which induce wounding [110]. In concert with ET, JA also regulates responses towards several necrotrophic pathogens, i.e. those pathogens that actively induce host cell death [107].

It is likely that defense networks similar to those in land plants exist in streptophyte algae. A series of recent studies have revealed the presence of homologs of plant hormone biosynthesis and signaling pathway genes and/or the presence of various phytohormones in streptophyte algae [e.g. [94,111-114]]; yet we are only beginning to understand the function of these phytohormones in streptophyte algae [115-117]. All three

canonical plant defense phytohormones, JA, SA and ET, have been detected in at least some species of streptophyte algae [94,112,115,118]. They also have been explored with regard to pathogen defense in non-flowering land plants. SA has been measured in mosses and gymnosperms – indeed, as in angiosperms, SA has been shown to accumulate in response to elicitors or pathogen attack [63,119,120], supporting its function in defense across land plant diversity.

In streptophyte algae, Ju et al. [112] detected Isochorismate Synthase 1 (ICS1) homologs; ICS1 catalyzes the first step in SA biosynthesis. Furthermore, an ortholog of phenylalanine ammonia lyase (PAL), the enzyme catalyzing the first step in the phenylpropanoid (PP) pathway, was detected in the genome of *K. nitens* [121]. The PP pathway is also a source for SA biosynthesis [122]. Moreover, potential homologs for the SA receptor Nonexpressor of PR genes 1 (NPR1) [123], were reported for all land plants [113] and the putative *NPR1* homolog of *P. patens* can partially complement defense signaling-associated phenotypes of the *Arabidopsis npr1* mutant [124]. As for ET, recent studies showed that streptophyte algae produce, sense and respond to ET [112,115], but these studies did not dissect the role of ET as a hormone involved in defense.

The existence and distribution of JA in early-diverging land plants and streptophyte algae is complex. The canonical pathway genes for JA biosynthesis (13-LOX, 13-Lipoxygenase; AOS, 13-Allene Oxide Synthase; AOC, Allene Oxide Cyclase, OPR3, OPDA Reductase 3 and JAR1, Jasmonate Resistant 1) are present in all land plant lineages [125], and some of its components were also detected in several streptophyte algae [94,112,125]. However, actual (mainly mass spectrometry-based) measurements of JA levels are suggestive of a patchier distribution among land plants and streptophyte algae. For example, while JA is reported to be produced in small quantities in the streptophyte algae *K. nitens* [94] and *Chara australis* [118], Hackenberg and Pandey [126] did not detect JA in *Chara braunii*. Furthermore, Gachet et al. [127] did not detect JA in *Chara vulgaris* and *Klebsormidium elegans*, while Koeduka et al. [128] found only minimal levels of JA in *Klebsormidium flaccidum*. Thus, within the genera *Chara* and *Klebsormidium*, the detection of JA is variable.

Like in *K. flaccidum* (a streptophyte alga) only non-existent or only minimal amounts of JA and its active derivative JA-Ile were detected for *M. polymorpha* (a liverwort) [128,129]. Furthermore, tissue wounding did not increase their amounts [128]. In bryophytes, like in streptophyte algae, JA seems to be produced in a species-specific manner [127,130]. However, JA appears to

be absent from the model moss *P. patens* [131]. Yet, when the moss *P. patens* was infected with two species of *Pythium*, an increase in the production of endogenous JA was detected over time and compared to control plants [62] – although the levels of JA were minimal both before and after infection. In contrast, exposure to the fungal pathogen *Botrytis cinerea* did not result in an increase in JA, but instead an increase in SA and the JA-precursor 12-oxo-phytodienoic acid (OPDA [63]); OPDA also increased after wounding in *M. polymorpha* [129]. These patterns suggest that in bryophytes the function of JA in defense may in fact be conferred by OPDA. Indeed, the signaling pathway of JA in angiosperms is fully functional in *M. polymorpha* [132]. Yet, in contrast to *Arabidopsis*, a derivative of OPDA, 2,3-dinor-OPDA (dn-OPDA), is the functional ligand of the JA receptor ortholog in *M. polymorpha*, Coronatine insensitive 1 (COI1) [132].

Unlike *P. patens*, the model lycophyte *S. moellendorffii* produces JA and is able to sense the phytohormone [133]. However, other lycophytes including another species from the genus *Selaginella* did not produce measurable levels of JA [127], supporting the notion of a high species-specificity in JA biosynthesis. Similarly, some species of ferns show pronounced JA responses, while others do not [134–136]; likewise, the production of JA was shown to be species-specific in ferns [127]. This distribution of JA biosynthesis becomes less patchy in gymnosperms and angiosperms, as shown in the dataset by Gachet and colleagues [127], where only one species in each of these two lineages was identified that did not produce a detectable amount of JA.

How do non-flowering land plants mount their defense responses? In *P. patens*, infection by oomycete and fungal pathogens leads to up-regulation of the usual suspects of angiosperm defense signaling: *PAL*, *Dirigent (DIR)*, *Chalcone synthase (CHS)* and *Pathogen related (PR)* genes, as well as genes involved in JA and JA-precursor biosynthesis, such as *LOX*, *AOS* and *OPR* [62,63,137]. This is, however, not surprising, since infections with *B. cinerea* or two *Pythium* pathogens lead to OPDA production [62,63]. In the spruce *P. abies*, the pathogens *H. parviporum* and *H. annosum* induce the expression of, among other genes, the JA biosynthesis and signaling genes *LOX* and *Jasmonate Zim Domain (JAZ)*, as well as genes for the biosynthesis of ET (*ACO*, *1-aminocyclopropane-1-carboxylic acid [ACC]-oxidase*; *ACS*, *ACC-synthase*), and *PAL*, *DIR2/32* and *PR1* [138–140]. JA and ET act in concert to induce defense responses against necrotrophic pathogens in angiosperms [107]. Hence, the activation of both JA and ET biosynthesis genes in response to

necrotrophic fungal pathogens in *P. abies* suggests a similar interaction between the two phytohormones. In agreement with this, in the two conifers *Pseudotsuga menziesii* and *Sequoiadendron giganteum* the application of MeJA and wounding induce ET biosynthesis, as measured by the activation of *ACO* [16]. In that study, ET was (at least partially) required for the plants' defense responses induced by MeJA and wounding [16]. This suggests that both mosses and gymnosperms not only induce similar defense pathways during infection with necrotrophic pathogens, but also that non-flowering land plants produce immune reactions similar to those observed in angiosperms.

Despite the apparent similarities in immune responses in non-flowering land plants and angiosperms, some differences have been discovered. As mentioned earlier, in the moss *P. patens*, the necrotrophic pathogen *B. cinerea* induced SA production in addition to the biosynthesis of the JA-precursor OPDA [63]. In agreement with this, expression of moss *PpPAL* is induced by SA, JA, MeJA, and OPDA [62,63], suggesting that exogenous JA and SA at least partially activate similar pathways. Indeed, Thaler et al. [141] and Han [125] suggested that the JA/SA-antagonism arose at the earliest in seed plants. Along these lines, it was hypothesized that in the fern *Azolla* some JA-orchestrated signaling responses may be initiated via SA instead of JA because MeSA application induced the expression of *Plant Defensin 1.4 (AfPDF1.4)* [136]; in *Arabidopsis*, *PDFs* are JA-responsive [142]. These results, together with the data from mosses, speak in favor of a reduced antagonism – or perhaps complete lack thereof – between JA and SA in mosses and ferns. In contrast to the hypothesis of Thaler et al. [141], a lack of a canonical antagonism between JA and SA was also suggested for *P. abies* [143]. Both MeJA and MeSA induce marker genes of SA signaling (*PR1* and *Late up-regulated in response to Hyaloperonospora parasitica 1 [LURP1]*) [143]. These genes are also up-regulated in response to the fungal pathogen *H. parviporum*, and upon inhibition of JA signaling, *PR1* expression is significantly reduced after fungal attack [143]. Furthermore, Kozłowski et al. [119] showed that exogenous MeJA can increase SA levels in *P. abies*. In *Ginkgo biloba* an elicitor from *Phytophthora boehmeriae* causes an increase in both endogenous JA and SA [120]. Moreover, both JA and SA were required to produce a defense-associated metabolite in response to the elicitor treatment in *G. biloba* [120]. Yet this study also found that artificially reduced SA led to an increase in JA levels, complementing the loss of SA-derived production of the defense metabolite. This

points to some negative regulatory effects of SA on JA, although the downstream signaling pathways of both hormones do not seem to be antagonistic.

Overall, it seems that JA synthesis was either lost or highly reduced several times throughout the evolution of land plants. Therefore, the requirement for JA in defense responses may be lineage specific. JA precursors, on the other hand, such as OPDA and other oxylipins, are involved in immune signaling in early-branching land plants [144]. As the production of JA became more consistent in gymnosperms and angiosperms, and levels of JA increased compared to earlier-branching lineages, its use in defense signaling was cemented. Long before that, however, at the base of the vascular plants, COI1 acquired a mutation leading to a broader binding pocket, which enabled binding to JA-Ile, the active JA-derivative [132]. After the establishment of JA as another regulator of defense responses, JA and SA signaling evolved into a highly specific antagonistic network.

There are, however, many complexities with regard to the antagonism of JA and SA in *A. thaliana* [145]. Liu et al. [145] showed that SA promotes the synthesis of JA and the activation of its signaling during ETI. However, a recent study by Betsuyaku et al. [146] showed that SA and JA act antagonistically during ETI on a narrow spatial scale. So far, spatial information on JA responses in non-flowering plants is only available for conifers, where MeJA treatment results in cell type-specific PAL activation [17]. Moreover, cell type-specific transcriptomes of *Picea glauca* showed strong cell-specific modulation of gene expression by MeJA treatment, including PP pathway-associated genes, such as *PAL* [147]. Nevertheless, these studies did not dissect the JA/SA antagonism on spatial scales. Moreover, we cannot exclude the possibility that JA/SA antagonism (or in organisms lacking JA, dn-OPDA/SA antagonism) is lineage-specific in non-angiosperms. However, for the time being, the evidence points to the evolution of JA/SA antagonism with regard to the regulation of defense responses after the split of gymnosperms and angiosperms.

Phenylpropanoids and their derivatives in streptophyte defense responses

Many of the defense- and JA/SA-regulated genes described above encode enzymes in the PP pathway or those downstream of it. PPs and PP-derived compounds, such as lignins, lignans, flavonoids and stilbenes, are defense metabolites, because they i) can be toxic for pathogens and/or ii) reinforce cell wall structures, thereby reducing the possibility of penetration by pathogens [122,148]. *PAL* encodes

the first enzyme in the PP pathway [122]. It shows a strong responsiveness to pathogens or exogenously applied JA in gymnosperms and JA and SA in mosses [62,63,73,143,149,150]. Therefore, it is not surprising that the defense response of *P. patens* following the inoculation with oomycete and fungal pathogens includes the production of phenolic compounds [61-63]. Cell wall reinforcements in *P. patens* by lignification after *B. cinerea* infection was also suggested because of the enhanced expression of the *Dirigent-like* gene, *PpDIR* [63]; DIR and DIR-like enzymes function both in lignan and lignin formation [151]. Moreover, in a study focused on gene expression of nearly all enzymes required for lignin production in *P. abies*, Koutaniemi and colleagues [138] found that *PAL* and at least one representative of the nine tested gene families were up-regulated in response to *H. annosum* – a pathogen inducing JA biosynthesis and signaling genes in its host [139]. This points to enhanced lignification as a pathogen defense response in conifers. Indeed, enhanced lignification in cell walls was observed for conifer species from the Cupressaceae and Podocarpaceae after MeJA application [17]. Furthermore, in conifers from different families, the application of MeJA increased the amount of PAL in polyphenolic and ray parenchyma cells [17]. These cell types also accumulated phenolic compounds after the treatment with MeJA in several of the species tested [17].

While it was previously thought that the PP pathway was limited to land plants, de Vries and colleagues [121] showed that streptophyte algae likely possess genes (orthologous to their respective, well-characterized land plant counterparts) for the production of PPs and lignins. As discussed above, a PAL-encoding orthologous gene was detected in the genome of *K. nitens* [121], suggesting that this early-branching streptophyte alga is capable of producing PPs. This is in agreement with the aforementioned detection of lignin-like compounds in streptophyte algae [see 49, 57, 58, 59], which are also derived from the PP pathway. While this suggests that both mechanisms are ancient, we do not know whether PPs and their derivatives are used by streptophyte algae for pathogen and parasite defense.

The expression of flavonoid-associated genes is also triggered by pathogens: Pinaceae up-regulate genes from the flavonoid biosynthesis pathway during infection [149,152]. The expression of flavonoid biosynthesis genes was also correlated with an increase in the flavonoid (+)-catechin in *P. abies* 15 days after infection with *H. annosum* [149]. However, in this study, the increase was genotype dependent, with more susceptible genotypes showing no increase or less of the flavonoid. In *P. patens* flavonoids seem to also play a role in defense responses, as bacterial elicitors as well as oomycete and fungal pathogens induce *CHS* [61,62,73]. Furthermore, other genes of

the flavonoid biosynthesis pathway are induced by bacterial elicitors [153]. In streptophyte algae, several homologs, but few orthologs of the genes required for flavonoid biosynthesis were detected [121]. That being said, Goiris et al. [154] reported the presence of flavonoids in algae from various lineages, including chlorophytes. A 1969 study by Markham and Porter [155] reported on the presence of flavonoids in the charophyceae *Nitella*, highlighting the need to further investigate streptophyte algae with regard to the presence of these metabolites. It is noteworthy that Van de Poel and colleagues [115] found ET-dependent regulation of a homolog of *TRANSPARENT TESTA 8 (TT8)* in the Zygnematophyceae *Spirogyra pratensis*; TT8 is a known regulator of flavonoid biosynthesis [156]. A TT8 ortholog is also present in the dataset for the Coleochaetophyceae *Coleochaete scutata* [114], where it is induced by high light stress.

Conclusion

Angiosperms have evolved complex and fine-tuned regulatory networks to mount their defense responses against microbial pathogens. Many molecular components of these networks can be found in the closest relatives of land plants, the streptophyte algae. We are, however, just beginning to understand whether these pathways are required for streptophyte algal defense responses – and hence likely to have served this purpose in the ancestor of land plants – or whether other pathways are more important in these lineages. We know that non-flowering land plants induce many of these pathways for defense against bacteria, fungi and oomycetes. Defense responses in non-flowering land plants utilize different regulatory modes than do angiosperms, as exemplified by the lack of the JA/SA antagonism in non-flowering land plants (Figure 1). Moreover, regulatory circuits have become seemingly more elaborate throughout land plant evolution, with the expansion of PTI-associated PRRs and NBS-LRRs and the occurrence of NBS-LRR-regulating miRNAs (Figure 1). In conclusion, it seems that many defense pathways of angiosperms existed in the last common land plant ancestor. The same pathways have, however, been reinvented and interwoven during subsequent land plant evolution, resulting in highly intertwined, specific and complex regulatory networks for plant defense.

Acknowledgments

SdV thanks the Killam Trusts for the Izaak Walton Killam Postdoctoral Fellowship. JdV (Research Fellowship, VR132/1-1),

JKvD and LER (Research Training Group, GRK1525) thank the German Research Foundation (*Deutsche Forschungsgemeinschaft*, DFG) for funding. CHS acknowledges funding by NSERC (Discovery grant RGPIN/05754-2015).

Disclosure statement

No potential conflict of interest was reported by the authors.

Funding

This work was supported by the Canadian Network for Research and Innovation in Machining Technology, Natural Sciences and Engineering Research Council of Canada [Discovery grant RGPIN/05754-2015]; Deutsche Forschungsgemeinschaft [VR 132/1-1]; Deutsche Forschungsgemeinschaft [Research Training Group GRK1525]; Killam Trusts [Izaak Walton Killam Postdoctoral Fellowship].

ORCID

Sophie de Vries  <http://orcid.org/0000-0002-5267-8935>
 Jan de Vries  <http://orcid.org/0000-0003-3507-5195>
 Sven B. Gould  <http://orcid.org/0000-0002-2038-8474>
 John M. Archibald  <http://orcid.org/0000-0001-7255-780X>
 Claudio H. Slamovits  <http://orcid.org/0000-0003-3050-1474>

References

- [1] Croft MT, Lawrence AD, Raux-Deery E, et al. Algae acquire vitamin B₁₂ through a symbiotic relationship with bacteria. *Nature*. 2005;438:90–93.
- [2] Segev E, Wyche TP, Kim KH, et al. Dynamic metabolic exchange governs a marine algal-bacterial interaction. *Elife*. 2016;18:5.
- [3] Wickett NJ, Mirarab S, Nguyen N, et al. Phylotranscriptomic analysis of the origin and early diversification of land plants. *Proc Natl Acad Sci USA*. 2014;111:E4859–E4868.
- [4] Delwiche CF, Cooper ED. The evolutionary origin of a terrestrial flora. *Curr Biol*. 2015;25:R899–R910.
- [5] de Vries J, Archibald JM. Plant evolution: Landmarks on the path to terrestrial life. *New Phytol*. 2018;217:1428–1434.
- [6] Jones JDG, Dangl JL. The plant immune system. *Nature*. 2006;444:323–329.
- [7] Stukenbrock EH, McDonald BA. Population genetics of fungal and oomycete effectors involved in gene-for-gene interactions. *Mol Plant Microbe In*. 2009;22:371–380.
- [8] de Vries S, Kloesges T, Rose LE. Evolutionarily dynamic, but robust, targeting of resistance genes by the miR482/2118 gene family in the Solanaceae. *Genome Biol Evol*. 2015;7:3307–3321.
- [9] de Vries S, Kukuk A, von Dahlen JK, et al. Expression profiling across wild and cultivated tomatoes supports the relevance of early miR482/2118 suppression for *Phytophthora* resistance. *Proc R Soc B*. 2018;285:20172560.

- [10] Upson JL, Zess EK, Bialas A, et al. The coming of age of EvoMPMI: evolutionary molecular plant–microbe interactions across multiple timescales. *Curr Opin Plant Biol.* 2018;44:108–116.
- [11] Kovalchuk A, Keriö S, Oghenekaro AO, et al. Antimicrobial defenses and resistance in forest trees: Challenges and perspectives in a genomic era. *Annu Rev Phytopathol.* 2013;51:221–244.
- [12] Parent GJ, Raheison E, Sena J, et al. Chapter two – Forest Tree Genomics: Review of Progress. In: Plomion C, Adam-Blondon A-Feditors. *Land Plants – Trees: Advances in Botanical Research.* London (UK), Oxford (UK), Waltham (MA), San Diego (CA): Academic Press; 2015. p. 39–92.
- [13] Ponce De León I, Montesano M. Adaptation mechanisms of moss defenses to microbes. *Front Plant Sci.* 2017;8:366.
- [14] Carella P, Schornack S. Manipulation of bryophyte hosts by pathogenic and symbiotic microbes. *Plant Cell Physiol.* 2018;59:651–660.
- [15] Nagy NE, Franceschi VR, Solheim H, et al. Wound-induced traumatic resin duct development in stems of Norway spruce (Pinaceae): Anatomy and cytochemical traits. *Am J Bot.* 2000;87:302–313.
- [16] Hudgins JW, Franceschi VR. Methyl jasmonate-induced ethylene production is responsible for conifer phloem defense responses and reprogramming of stem cambial zone for traumatic resin duct formation. *Plant Physiol.* 2004;135:2134–2149.
- [17] Hudgins JW, Christiansen E, Franceschi VR. Induction of anatomically based defense responses in stems of diverse conifers by methyl jasmonate: a phylogenetic perspective. *Tree Physiol.* 2004;24:251–264.
- [18] Delaux PM, Radhakrishnan GV, Jayaraman D, et al. Algal ancestor of land plants was preadapted for symbiosis. *Proc Natl Acad Sci USA.* 2015;112:13390–13395.
- [19] Field KJ, Pressel S, Duckat JG, et al. Symbiotic options for the conquest of land. *Trends Ecol Evol.* 2015;30:477–486.
- [20] Selosse MA, Strullu-Derrien C, Martin FM, et al. Plants, fungi and oomycetes: a 400-million year affair that shapes the biosphere. *New Phytol.* 2015;206:501–506.
- [21] Edwards D, Kenrick P. The early evolution of land plants, from fossils to genomics: a commentary on Lang (1937) ‘On the plant-remains from the Downtonian of England and Wales’. *Phil Trans R Soc B.* 2015;370:20140343.
- [22] Nelson JM, Hauser DA, Hinson R, et al. A novel experimental system using the liverwort *Marchantia polymorpha* and its fungal endophytes reveals diverse and context-dependent effects. *New Phytol.* 2018. DOI:10.1111/nph.15012.
- [23] Rich M, Delaux P-M. Taking the step: from Evo-Devo to plant–microbe interaction evolution with the liverwort *Marchantia*. *New Phytol.* 2018;218:882–884.
- [24] Humphreys CP, Franks PJ, Rees M, et al. Mutualistic mycorrhiza-like symbiosis in the most ancient group of land plants. *Nat Commun.* 2010;1:103.
- [25] Field KJ, Cameron DD, Leake JR, et al. Contrasting arbuscular mycorrhizal responses of vascular and non-vascular plants to a simulated Paleozoic CO₂ decline. *Nat Commun.* 2012;3:835.
- [26] Kowal J, Pressel S, Duckett JG, et al. From rhizoid to roots? Experimental evidence of mutualism between liverworts and ascomycete fungi. *Ann Bot.* 2018;121:221–227.
- [27] Zhang Y, Guo LD. Arbuscular mycorrhizal structure and fungi associated with mosses. *Mycorrhiza.* 2007;17:319–325.
- [28] Field KJ, Rimington WR, Bidartondo MI, et al. First evidence of mutualism between ancient plant lineages (Haplomitriopsida liverworts) and Mucoromycotina fungi and its response to simulated Palaeozoic changes in atmospheric CO₂. *New Phytol.* 2015;205:743–756.
- [29] Field KJ, Pressel S. Unity in diversity: structural and functional insights into the ancient partnerships between plants and fungi. *New Phytol.* 2018. DOI:10.1111/nph.15158
- [30] Schüßler A. *Glomus claroideum* forms an arbuscular mycorrhiza-like symbiosis with the hornwort *Anthoceros punctatus*. *Mycorrhiza.* 2000;10:15–21.
- [31] Desirò A, Duckett JG, Pressel S, et al. Fungal symbioses in hornworts: a chequered history. *Proc R Soc B.* 2013;280:20130207.
- [32] Wang B, Qiu YL. Phylogenetic distribution and evolution of mycorrhizas in land plants. *Mycorrhiza.* 2006;16:299–363.
- [33] Pressel S, Bidartondo MI, Ligrone R, et al. Fungal symbioses in bryophytes: new insights in the Twenty First Century. *Phytotaxa.* 2010;9:238–253.
- [34] Wang B, Yeun LH, Xue J-Y, et al. Presence of three mycorrhizal genes in the common ancestor of land plants suggests a key role of mycorrhizas in the colonization of land by plants. *New Phytol.* 2010;186:514–525.
- [35] Puttick MN, Morris JL, William TA, et al. The inter-relationships of land plants and the nature of the ancestral embryophyte. *Curr Biol.* 2018;28:733–745.
- [36] Bonfante P, Selosse M-A. A glimpse into the past of land plants and of their mycorrhizal affairs: from fossils to evo-devo. *New Phytol.* 2010;186:267–270.
- [37] Knack JJ, Wilcox LW, Delaux P-M, et al. Microbiomes of streptophyte algae and bryophytes suggest that a functional suite of microbiota fostered plant colonization of land. *Int J Plant Sci.* 2015;176:405–420.
- [38] Strullu-Derrien C, Kenrick P, Pressel S, et al. Fungal associations in *Horneophyton ligneri* from the Rhynie Chert (c. 407 million year old) closely resemble those in extant lower land plants: novel insights into ancestral plant–fungus symbioses. *New Phytol.* 2014;203:964–979.
- [39] Brader G, Compant S, Vescio K, et al. Ecology and genomic insights into plant-pathogenic and plant-nonpathogenic endophytes. *Annu Rev Phytopathol.* 2017;55:61–83.
- [40] Schulz B, Boyle C. The endophytic continuum. *Mycol Res.* 2005;109:661–686.
- [41] Junker C, Draeger S, Schulz B. A fine line — edophytes or pathogens in *Arabidopsis thaliana*. *Fungal Ecol.* 2012;5:657–662.
- [42] Rey T, Jacquet C. Symbiosis genes for immunity and vice versa. *Curr Opin Plant Biol.* 2018;44:64–71.
- [43] Ried MK, Banhara A, Binder A, et al. Symbiosis-related genes sustain the development of a downy mildew pathogen on *Arabidopsis thaliana*. *bioRxiv.* 2018. DOI:10.1101/286872.
- [44] Wellman CH, Strother PK. The terrestrial biota prior to the origin of land plants (embryophytes): a review of the evidence. *Paleontology.* 2015;58:601–627.

- [45] Morris JL, Puttick MN, Clark JW, et al. The timescale of early land plant evolution. *Proc Natl Acad Sci USA*. [2018](#);115:E2274– E2283.
- [46] Taylor TN, Remy W, Hass H. Parasitism in a 400-million-year-old green alga. *Nature*. [1992](#);357:493–494.
- [47] Berbee ML, James TY, Strulle-Derrien C. Early diverging fungi: diversity and impact at the dawn of terrestrial life. *Ann Rev Microbiol*. [2017](#);71:41–60.
- [48] Spatafora JW, Chang Y, Benny GL, et al. A phylum-level phylogenetic classification of zygomycete fungi based on genome-scale data. *Mycologia*. [2016](#);108:1028–1046.
- [49] Sørensen I, Pettolino FA, Bacic A, et al. The charophycean green algae provide insights into the early origins of plant cell walls. *Plant J*. [2011](#);68:201–211.
- [50] Rasconi S, Niquil N, Sime-Ngando T. Phytoplankton chytridiomycosis: community structure and infectivity of fungal parasites in aquatic ecosystems. *Environ Microbiol*. [2012](#);14:2151–2170.
- [51] Cui H, Tsuda K, Parker JE. Effector-triggered immunity: from pathogen perception to robust defense. *Annu Rev Plant Biol*. [2015](#);66:487–511.
- [52] Melotto M, Underwood W, Koczan J, et al. Plant stomata function in innate immunity against bacterial invasion. *Cell*. [2006](#);126:969–980.
- [53] Underwood W. The plant cell wall: a dynamic barrier against pathogen invasion. *Front Plant Sci*. [2012](#);3:85.
- [54] Lloyd SR, Schoonbeek H-J, Trick M, et al. Methods to studies PAMP-triggered immunity in *Brassica* species. *Mol Plant Microbe Int*. [2014](#);27:286–295.
- [55] Mott GA, Guttman DS, Desveaux D. The study of pattern-triggered immunity in *Arabidopsis*. *Can J Plant Pathol*. [2017](#);39:275–281.
- [56] Felix G, Duran JD, Volko S, et al. Plants have a sensitive perception system for the most conserved domain of bacterial flagellin. *Plant J*. [1999](#);18:265–276.
- [57] Delwiche CF, Graham LE, Thomson N. Lignin-like compounds and sporopollenin in *Coleochaete*, an algal model for land plant ancestry. *Science*. [1989](#);245:399–401.
- [58] Kroken SB, Graham LE, Cook ME. Occurrence and evolutionary significance of resistant cell walls in charophytes and bryophytes. *Am J Bot*. [1996](#);83:1241–1254.
- [59] Ligrone R, Carafa A, Duckett JG, et al. Immunocytochemical detection of lignin-related epitopes in cell walls in bryophytes and the charalean alga *Nitella*. *Plant Syst Evol*. [2008](#);270:257–272.
- [60] Herburger K, Holzinger A. Localization and quantification of callose in the streptophyte green algae *Zygnema* and *Klebsormidium*: correlation with desiccation tolerance. *Plant Cell Physiol*. [2015](#);56:2259–2270.
- [61] Overdijk EJR, de Keijzer J, de Groot D, et al. Interaction between the moss *Physcomitrella patens* and *Phytophthora*: a novel pathosystem for live-cell imaging of subcellular defence. *J Microsc*. [2016](#);263:171–180.
- [62] Oliver JP, Castro A, Gaggero C, et al. *Pythium* infection activates conserved plant defense responses in mosses. *Planta*. [2009](#);230:569–579.
- [63] Ponce de León I, Schmelz EA, Gaggero C, et al. *Physcomitrella patens* activates reinforcement of the cell wall, programmed cell death and accumulation of evolutionary conserved defence signals, such as salicylic acid and 12-oxo-phytodienoic acid, but not jasmonic acid, upon *Botrytis cinerea* infection. *Mol Plant Pathol*. [2012](#);13:960–974.
- [64] Davey ML, Tsuneda A, Currah RS. Pathogenesis of bryophyte hosts by the ascomycete *Atracidium muscivora*. *Am J Bot*. [2009](#);96:1274–1280.
- [65] Davey ML, Tsuneda A, Currah RS. Saprobic and parasitic interactions of *Coniochaeta velutina* with mosses. *Botany*. [2010](#);88:258–265.
- [66] Carella P, Gogleva A, Tomaselli M, et al. *Phytophthora palmivora* establishes tissue-specific intracellular infection structures in the earliest divergent land plant lineage. *Proc Natl Acad Sci USA*. [2018](#);115:E3846– E3845.
- [67] Gómez-Gómez L, Boller T. FLS2: an LRR receptor-like kinase involved in the perception of the bacterial elicitor flagellin in *Arabidopsis*. *Mol Cell*. [2000](#);5:1003–1011.
- [68] Boller T, Felix GA. Renaissance of elicitors: Perception of microbe-associated molecular patterns and danger signals by pattern-recognition receptors. *Annu Rev Plant Biol*. [2009](#);60:379–406.
- [69] Yue J-X, Meyers BC, Chen J-Q, et al. Tracing the origin and evolutionary history of plant nucleotide-binding site-leucine-rich repeat (*NBS-LRR*) genes. *New Phytol*. [2012](#);193:1049–1063.
- [70] Bressendorf S, Azevedo R, Kenchappa CS, et al. An innate immunity pathway in the moss *Physcomitrella patens*. *Plant Cell*. [2016](#);28:1328–1342.
- [71] Kunze G, Zipfel C, Robatzek S, et al. The N terminus of bacterial Elongation factor Tu elicits innate immunity in *Arabidopsis* plants. *Plant Cell*. [2004](#);16:3496–3507.
- [72] Zipfel C, Kunze G, Chinchilla D, et al. Perception of the bacterial PAMP EF-Tu by the receptor EFR restricts *Agrobacterium*-mediated transformation. *Cell*. [2006](#);125:749–760.
- [73] Ponce de León I, Oliver JP, Castro A, et al. *Erwinia carotovora* elicitors and *Botrytis cinerea* activate defense responses in *Physcomitrella patens*. *BMC Plant Biol*. [2007](#);7:52.
- [74] Xu Z, Yu J, Cui L, et al. Effects of *Pseudomonas fluorescens* flagellin on physiological and biochemical characteristics in the suspension cells of *Pinus thunbergii*. *Eur J Plant Pathol*. [2013](#);136:729–736.
- [75] Albert M, Jehle AK, Lipschis M, et al. Regulation of cell behaviour by plant receptor kinases: Pattern recognition receptors as prototypical models. *Eur J Cell Biol*. [2010](#);89:200–207.
- [76] Urano D, Jones AM. Heterotrimeric G protein-coupled signaling in plants. *Annu Rev Plant Biol*. [2014](#);65:365–384.
- [77] Delgado-Cerezo M, Sánchez-Rodríguez C, Escudero V, et al. *Arabidopsis* heterotrimeric G-protein regulates cell wall defense and resistance to necrotrophic fungi. *Mol Plant*. [2012](#);5:98–114.
- [78] Liu J, Ding P, Sun T, et al. Heterotrimeric G proteins serve as a converging point in plant defense signaling activated by multiple Receptor-like Kinases. *Plant Physiol*. [2013](#);161:2146–2158.
- [79] Hackenberg D, Sakayama H, Nishiyama T, et al. Characterization of the heterotrimeric G-protein complex and its regulator from the green alga *Chara braunii* expands the evolutionary breadth of plant G-protein signaling. *Plant Physiol*. [2013](#);163:1510–1517.

- [80] Urano D, Chen J-G, Botello JR, et al. Heterotrimeric G protein signalling in the plant kingdom. *Open Biol.* **2013**;3:120186.
- [81] de Vries S, Nemesio-Gorriz M, Blair PB, et al. Heterotrimeric G-protein in *Picea abies* and their regulation in response to *Heterobasidion annosum s.l.* infection. *BMC Plant Biol.* **2015**;15:287.
- [82] Chung E-H, El-Kasmi F, Loehr A, et al. A plant phosphoswitch platform repeatedly targeted by type III effector proteins regulates the output of both tiers of plant immunity receptors. *Cell Host Microbe.* **2014**;16:484–494.
- [83] Li M, Ma X, Chiang Y-H, et al. Proline isomerization of the immune receptor-interacting protein RIN4 by a cyclophilin inhibits effector-triggered immunity in *Arabidopsis*. *Cell Host Microbe.* **2014**;16:473–483.
- [84] Rehmany AP, Gordon A, Rose LE. Differential recognition of highly divergent downy mildew avirulence gene alleles by RPP1 genes from two *Arabidopsis* lines. *Plant Cell.* **2005**;17:1839–1850.
- [85] Allen RL, Meitz JC, Baumber RE, et al. Natural variation reveals key amino acids for recognition specificity between downy mildew effector and an *Arabidopsis* resistance gene. *Mol Plant Pathol.* **2008**;9:511–523.
- [86] Krasileva KV, Dahlbeck D, Staskawicz BJ. Activation of an *Arabidopsis* resistance protein is specified by the *in planta* association of its leucine-rich repeat domain with the cognate oomycete effector. *Plant Cell.* **2010**;22:2444–2458.
- [87] Meyers BC, Kaushik S, Nandety RS. Evolving disease resistance genes. *Curr Opin Plant Biol.* **2005**;8:129–134.
- [88] Zhang Y, Xia R, Kuang H, et al. The diversification of plant NBS-LRR defense genes directs the evolution of microRNAs that target them. *Mol Biol Evol.* **2016**;33:2692–2705.
- [89] Gao Y, Wang W, Zhang T, et al. Out of water: The origin and early diversification of plant R-genes. *Plant Phys.* **2018**;177:82–89.
- [90] Nystedt B, Street NR, Wetterbom A, et al. The Norway spruce genome sequence and conifer genome evolution. *Nature.* **2013**;497:579–584.
- [91] Young ND, Debelle F, Oldroyd GE, et al. The *Medicago* genome provides insight into the evolution of rhizobial symbioses. *Nature.* **2011**;480:520–524.
- [92] International Wheat Genome Sequencing Consortium. A chromosome-based draft sequence of the hexaploid bread wheat (*Triticum aestivum*) genome. *Science.* **2014**;345:1251788.
- [93] Urbach JM, Ausubel FM. The NBS-LRR architectures of plant R-proteins and metazoan NLRs evolved in independent events. *Proc Natl Acad Sci USA.* **2017**;114:1063–1068.
- [94] Hori K, Maruyama F, Fujisawa T, et al. *Klebsormidium flaccidum* genome reveals primary factors for plant terrestrial adaptation. *Nat Commun.* **2014**;5:3978.
- [95] Li X, Kapos P, Zhang Y. NLRs in plants. *Curr Opin Immunol.* **2015**;32:114–121.
- [96] Zhai J, Jeong D-H, De Paoli E, et al. MicroRNAs as master regulators of the plant NB-LRR defense gene family via the production of phased, *trans*-acting siRNAs. *Genes Dev.* **2011**;25:2540–2553.
- [97] Li F, Pignatta D, Bendix C, et al. MicroRNA regulation of plant innate immune receptors. *Proc Natl Acad Sci USA.* **2012**;109:1790–1795.
- [98] Shivaprasad PV, Chen HM, Patel K, et al. A microRNA superfamily regulates nucleotide binding site-leucine rich repeats and other mRNAs. *Plant Cell.* **2012**;24:859–874.
- [99] Fei Q, Xia R, Meyers BC. Phased, secondary, small interfering RNAs in posttranscriptional regulatory networks. *Plant Cell.* **2013**;25:2400–2415.
- [100] Xia R, Xu J, Arikiti S, et al. Extensive families of miRNAs and PHAS loci in Norway spruce demonstrate the origins of complex phasiRNA networks in seed plants. *Mol Biol Evol.* **2015**;32:2905–2918.
- [101] Boccara M, Sarazin A, Thiébeault O, et al. The *Arabidopsis* miR472-RDR6 silencing pathway modulates PAMP- and effector-triggered immunity through the post-transcriptional control of disease resistance genes. *PLoS Pathog.* **2014**;10:e1003883.
- [102] Ouyang S, Park G, Atamian HS, et al. MicroRNAs suppress NB domain genes in tomato that confer resistance to *Fusarium oxysporum*. *PLoS Pathog.* **2014**;10:e1004464.
- [103] Ji H-M, Zhao M, Gao Y, et al. FRG3, a target of slmiR482e-3p, provides resistance against the fungal pathogen *Fusarium oxysporum* in tomato. *Front Plant Sci.* **2018**;9:26.
- [104] Zhai J, Zhang H, Arikiti S, et al. Spatiotemporally dynamic, cell-type-dependent premeiotic and meiotic phasiRNAs in maize anthers. *Proc Natl Acad Sci USA.* **2015**;112:3146–3151.
- [105] Shigenaga AM, Argueso CT. No hormone to rule them all: Interactions of plant hormones during the responses of plants to pathogens. *Semin Cell Dev Biol.* **2016**;56:174–189.
- [106] Berens ML, Berry HM, Mine A, et al. Evolution of hormone signaling networks in plant defense. *Annu Rev Phytopathol.* **2017**;55:401–425.
- [107] Glazebrook J. Contrasting mechanisms of defense against biotrophic and necrotrophic pathogens. *Annu Rev Phytopathol.* **2005**;43:205–227.
- [108] Herrera-Vásquez A, Salinas P, Holuigue L. Salicylic acid and reactive oxygen species interplay in the transcriptional control of defense genes expression. *Front Plant Sci.* **2015**;6:171.
- [109] Ishikawa A, Kimura Y, Yasuda M, et al. Salicylic acid-mediated cell death in the *Arabidopsis len3* mutant. *Biosci Biotechnol Biochem.* **2006**;70:1447–1453.
- [110] McConn M, Creelman RA, Bell E, et al. Jasmonate is essential for insect defense in *Arabidopsis*. *Proc Natl Acad Sci USA.* **1997**;94:5473–5477.
- [111] Delaux P-M, Xie X, Timme RE, et al. Origin of strigolactones in the green lineage. *New Phytol.* **2012**;195:857–871.
- [112] Ju C, Van De Poel B, Cooper ED, et al. Conservation of ethylene as a plant hormone over 450 million years of evolution. *Nat Plants.* **2015**;1:14004.
- [113] Wang C, Liu Y, Li -S-S, et al. Insights into the origin and evolution of the plant hormone signaling machinery. *Plant Physiol.* **2015**;167:872–886.
- [114] de Vries J, Curtis BA, Gould SB, et al. Embryophyte stress signaling evolved in the algal progenitors of land plants. *Proc Natl Acad Sci USA.* **2018**;115:E3471–E3480.
- [115] Van de Poel B, Cooper ED, Van Der Straeten D, et al. Transcriptome profiling of the green alga *Spirogyra pratensis* (Charophyta) suggests an ancestral role for ethylene in cell wall metabolism, photosynthesis, and abiotic stress responses. *Plant Physiol.* **2016**;172:533–545.

- [116] Ohtaka K, Hori K, Kanno Y, et al. Primitive auxin response without TIR1 and Aux/IAA in the charophyte alga *Klebsormidium nitens*. *Plant Physiol.* **2017**;174:1621–1632.
- [117] Mutte S, Kato H, Rothfels C, et al. Origin and evolution of the nuclear auxin response system. *eLife.* **2018**;7:e33399.
- [118] Beilby MJ, Turi CE, Baker TC, et al. Circadian changes in endogenous concentrations of indole-3-acetic acid, melatonin, serotonin, abscisic acid and jasmonic acid in Characeae (*Chara australis* Brown). *Plant Signal Behav.* **2015**;10:e1082697.
- [119] Kozłowski G, Métraux J-P. Infection of Norway spruce (*Picea abies* (L.) Karst.) seedlings with *Pythium irregularre* Buism. and *Pythium ultimum* Trow.: histological and biochemical responses. *Eur J Plant Pathol.* **1998**;104:225–234.
- [120] Xu M, Dong J, Wang H, et al. Complementary action of jasmonic acid on salicylic acid in mediating fungal elicitor-induced flavonol glycoside accumulation of *Ginkgo biloba* cells. *Plant Cell Environ.* **2009**;32:960–967.
- [121] de Vries J, de Vries S, Slamovits CH, et al. How embryophytic is the biosynthesis of phenylpropanoids and their derivatives in streptophyte algae. *Plant Cell Physiol.* **2017**;58:934–945.
- [122] Dixon RA, Achnine L, Kota P, et al. The phenylpropanoid pathway and plant defence – genomics perspective. *Mol Plant Pathol.* **2002**;3:371–390.
- [123] Wu Y, Zhang D, Chu JY, et al. The *Arabidopsis* NPR1 protein is a receptor for the plant defense hormone salicylic acid. *Cell Rep.* **2012**;1:639–647.
- [124] Peng Y, Sun T, Zhang Y. Perception of salicylic acid in *Physcomitrella patens*. *Front Plant Sci.* **2017**;8:2145.
- [125] Han G-Z. Evolution of jasmonate biosynthesis and signaling mechanisms. *J Exp Bot.* **2017**;68:1323–1331.
- [126] Hackenberg D, Pandey S. Heterotrimeric G-proteins in green algae. *Plant Signal Behav.* **2014**;9:e28457.
- [127] Gachet MS, Schubert A, Calarco S, et al. Targeted metabolomics shows plasticity in the evolution of signaling lipids and uncovers old and new endocannabinoids in the plant kingdom. *Sci Rep.* **2017**;7:41177.
- [128] Koeduka T, Ishizaki K, Mugo Mwenda M, et al. Biochemical characterization of allene oxide synthases from the liverwort *Marchantia polymorpha* and green microalgae *Klebsormidium flaccidum* provides insight into the evolutionary divergence of the plant CYP74 family. *Planta.* **2015**;242:1175–1186.
- [129] Yamamoto Y, Ohshika J, Takahashi T, et al. Functional analysis of allene oxide cyclase, MpAOC, in the liverwort *Marchantia polymorpha*. *Phytochemistry.* **2015**;116:48–56.
- [130] Závěská Drábková L, Dobrev PI, Motyka V. Phytohormone profiling across the bryophytes. *PLoS One.* **2015**;10:e0125411.
- [131] Stumpe M, Göbel C, Faltin B, et al. The moss *Physcomitrella patens* contains cyclopentenones but no jasmonates: mutations in allene oxide cyclase lead to reduced fertility and altered sporophyte morphology. *New Phytol.* **2010**;188:740–749.
- [132] Monte I, Ishida S, Zamarreño AM, et al. Ligand-receptor co-evolution shaped the jasmonate pathway in land plants. *Nat Chem Biol.* **2018**;14:480–488.
- [133] Pratiwi P, Tanaka G, Takahashi T, et al. Identification of jasmonic acid and jasmonoyl-isoleucine, and characterization of AOS, AOC, OPR and JAR1 in the model lycophyte *Selaginella moellendorffii*. *Plant Cell Physiol.* **2017**;58:789–801.
- [134] Camloh M, Ravinkar M, Žel J. Jasmonic acid promotes division of fern protoplasts, elongation of rhizoids and early development of gametophytes. *Physiol Plantarum.* **1996**;97:659–664.
- [135] Camloh M, Vilhar B, Žel J, et al. Jasmonic acid stimulates development of rhizoids and shoots in fern leaf culture. *J Plant Physiol.* **1999**;155:798–801.
- [136] de Vries S, de Vries J, Teschke H, et al. Jasmonic and salicylic acid response in the fern *Azolla filiculoides* and its cyanobiont. *Plant Cell Environ.* **2018**. DOI:10.1111/pce.13131.
- [137] Castro A, Vidal S, Ponce De León I. Moss pathogenesis-related-10 protein enhances resistance to *Pythium irregulare* in *Physcomitrella patens* and *Arabidopsis thaliana*. *Front Plant Sci.* **2016**;7:580.
- [138] Koutaniemi S, Warinowski T, Kärkönen A, et al. Expression profiling of the lignin biosynthetic pathway in Norway spruce using EST sequencing and real-time RT-PCR. *Plant Mol Biol.* **2007**;65:311–328.
- [139] Arnerup J, Lind M, Olson Å, et al. The pathogenic white-rot fungus *Heterobasidion parviporum* triggers non-specific defence response in the bark of Norway spruce. *Tree Physiol.* **2011**;31:1262–1272.
- [140] Oliva J, Rommel S, Fossdal CG, et al. Transcriptional responses of Norway spruce (*Picea abies*) inner sapwood against *Heterobasidion parviporum*. *Tree Physiol.* **2015**;35:1007–1015.
- [141] Thaler JS, Humphrey PT, Whiteman NK. Evolution of jasmonate and salicylate signal crosstalk. *Trends Plant Sci.* **2012**;17:260–270.
- [142] Zimmerli L, Stein M, Lipka V, et al. Host and non-host pathogens elicit different jasmonate/ethylene responses in *Arabidopsis*. *Plant J.* **2004**;40:633–646.
- [143] Arnerup J, Nemesio-Gorrioz M, Lunden K, et al. The primary module in Norway spruce defence signaling against *H. annosum s.l.* seems to be jasmonate-mediated signalling without antagonism of salicylate-mediated signalling. *Planta.* **2013**;237:1037–1045.
- [144] Ponce De León I, Hamberg M, Castresana C. Oxylipins in moss development and defense. *Front Plant Sci.* **2015**;6:483.
- [145] Liu L, Sonbol F-M, Huot B, et al. Salicylic acid receptors activate jasmonic acid signaling through a non-canonical pathway to promote effector-triggered immunity. *Nat Commun.* **2016**;7:13099.
- [146] Betsuyaku S, Katou S, Takebayashi Y, et al. Salicylic acid and jasmonic acid pathways are activated in spatially different domains around the infection site during effector-triggered immunity in *Arabidopsis thaliana*. *Plant Cell Physiol.* **2018**;59:8–16.
- [147] Celedon JM, Yuen MMS, Chiang A, et al. Cell-type- and tissue-specific transcriptomes of the white spruce (*Picea glauca*) bark unmask fine-scale spatial patterns of constitutive and induced conifer defense. *Plant J.* **2017**;92:710–726.
- [148] Miedes E, Vanholme R, Boerjan W, et al. The role of the secondary cell wall in plant resistance to pathogens. *Front Plant Sci.* **2014**;5:358.

- [149] Danielsson M, Lunden K, Elfstrand M, et al. Chemical and transcriptional responses of Norway spruce genotypes with different susceptibility to *Heterobasidion* spp. infection. *BMC Plant Biol.* **2011**;11:154.
- [150] Deflorio G, Horgan G, Woodward S, et al. Gene expression profiles, phenolics and lignin of Sikta spruce bark and sapwood before and after wounding and inoculation with *Heterobasidion annosum*. *Physiol Mol Plant P.* **2011**;75:180–187.
- [151] Paniagua C, Bilkova A, Jackson P, et al. Dirigent proteins in plants: modulating cell wall metabolism during abiotic and biotic stress exposure. *J Exp Bot.* **2017**;68:3287–3301.
- [152] Adomas A, Heller G, Li G, et al. Transcript profiling of a conifer pathosystem: response of *Pinus sylvestris* root tissue to pathogen (*Heterobasidion annosum*) invasion. *Tree Physiol.* **2007**;27:1441–1458.
- [153] Ponce de León I, Montesano M. Activation of defense mechanisms against pathogens in mosses and flowering plants. *Int J Mol Sci.* **2013**;14:3178–3200.
- [154] Goiris K, Muylaert K, Voorspoels S, et al. Detection of flavonoids in microalgae from different evolutionary lineages. *J Phycol.* **2014**;50:483–492.
- [155] Markham KR, Poster LJ. Flavonoids in the green algae (Chlorophyta). *Phytochemistry.* **1969**;8:1777–1781.
- [156] Nesi N, Debeaujon I, Jond C, et al. The *TT8* gene encodes a basic helix-loop-helix domain protein required for expression of *DFR* and *BAN* genes in *Arabidopsis* siliques. *Plant Cell.* **2000**;12:1863–1878.

Publication II

Expression profiling across wild and cultivated tomatoes supports the relevance of early miR482/2118 suppression for *Phytophthora* resistance

Status	Published
Journal	<i>Proceedings of the Royal Society B: Biological Sciences</i>
Citation	de Vries, S., Kukuk, A., von Dahlen, J. K. , Schnake, A., Kloesges, T., & Rose, L. E. (2018). Expression profiling across wild and cultivated tomatoes supports the relevance of early miR482/2118 suppression for <i>Phytophthora</i> resistance. <i>Proceedings of the Royal Society B: Biological Sciences</i> , 285(1873), 20172560.
Own contribution	Generated and analyzed the miRNA expression data; contributed to the evaluation of the infection assays; contributed to interpretation and writing of the manuscript

Research



Cite this article: de Vries S, Kukuk A, von Dahlen JK, Schnake A, Kloesges T, Rose LE. 2018 Expression profiling across wild and cultivated tomatoes supports the relevance of early miR482/2118 suppression for *Phytophthora* resistance. *Proc. R. Soc. B* **285**: 20172560.
<http://dx.doi.org/10.1098/rspb.2017.2560>

Received: 16 November 2017

Accepted: 1 February 2018

Subject Category:

Evolution

Subject Areas:

evolution, plant science, microbiology

Keywords:

Solanum, miRNA signalling, evolution, plant immunity

Authors for correspondence:

Sophie de Vries

e-mail: sophie.devries@dal.ca

Laura E. Rose

e-mail: laura.rose@hhu.de

Electronic supplementary material is available online at <https://dx.doi.org/10.6084/m9.figshare.c.4002592>.

Expression profiling across wild and cultivated tomatoes supports the relevance of early miR482/2118 suppression for *Phytophthora* resistance

Sophie de Vries^{1,2}, Andreas Kukuk², Janina K. von Dahlen^{2,3}, Anika Schnake², Thorsten Kloesges² and Laura E. Rose^{2,3,4}

¹Department of Biochemistry and Molecular Biology, Dalhousie University, Halifax, Canada NS B3H 4R2

²Institute of Population Genetics, ³iGRAD-Plant Graduate School, and ⁴Ceplas, Cluster of Excellence in Plant Sciences, Heinrich-Heine University Duesseldorf, Universitaetsstr. 1, 40225 Duesseldorf, Germany

SdV, 0000-0002-5267-8935

Plants possess a battery of specific pathogen resistance (*R*-genes). Precise *R*-gene regulation is important in the presence and absence of a pathogen. Recently, a microRNA family, miR482/2118, was shown to regulate the expression of a major class of *R*-genes, nucleotide-binding site leucine-rich repeats (*NBS-LRRs*). Furthermore, RNA silencing suppressor proteins, secreted by pathogens, prevent the accumulation of miR482/2118, leading to an upregulation of *R*-genes. Despite this transcriptional release of *R*-genes, RNA silencing suppressors positively contribute to the virulence of some pathogens. To investigate this paradox, we analysed how the regulation of *NBS-LRRs* by miR482/2118 has been shaped by the coevolution between *Phytophthora infestans* and cultivated and wild tomatoes. We used degradome analyses and qRT-PCR to evaluate and quantify the co-expression of miR482/2118 and their *NBS-LRR* targets. Our data show that miR482/2118-mediated targeting contributes to the regulation of *NBS-LRRs* in *Solanum lycopersicum*. Based on miR482/2118 expression profiling in two additional tomato species—with different coevolutionary histories with *P. infestans*—we hypothesize that pathogen-mediated RNA silencing suppression is most effective in the interaction between *S. lycopersicum* and *P. infestans*. Furthermore, an upregulation of miR482/2118 early in the infection may increase susceptibility to *P. infestans*.

1. Introduction

Resistance proteins (*R*-proteins) are fundamentally important in plant pathogen interactions. They recognize pathogen molecules, called effectors, which are secreted by pathogens to hijack plant immune responses [1,2]. Upon recognition, *R*-proteins trigger a pathogen-specific immune response [3,4]. Such immune responses include the hypersensitive response (HR), resulting in the release of reactive oxygen species, and can ultimately lead to cell death.

Misregulation of *R*-genes carries high fitness costs. Over-expression of *R*-genes in the absence of a pathogen can severely decrease fitness [5,6]. By contrast, insufficient *R*-gene expression during pathogen attack can allow for pathogen infection [7]. While several regulatory mechanisms are at play for different *R*-genes and *R*-proteins [8,9], negative regulation via small RNAs was proposed to globally buffer *R*-gene expression to avoid misregulation [10].

One example of negative regulation of *R*-genes, specifically of nucleotide-binding site leucine-rich repeats (*NBS-LRRs*), is suppression by the microRNA (miRNA) family miR482/2118 [11–13]. Targeting of miR482/2118 leads either

to the degradation of *NBS-LRR* mRNA or to an inhibition of the translation of the corresponding mRNAs [14]. The family is one of the most labile miRNA families, displaying low sequence conservation, even between closely related species, despite its widespread presence in the plant kingdom [11,13,15]. Its diversity is in part a consequence of the amino acid variability of its target sequence [16].

A major pathogen of cultivated tomato (*Solanum lycopersicum*) is *Phytophthora infestans*. However, *P. infestans* not only infects crops but also their wild relatives [17–22]. Populations of wild tomato species, given that they are not subjected to breeding, have experienced different evolutionary histories with *P. infestans* compared to the cultivated tomato. In fact, wild tomatoes harbour *R*-genes that effectively contribute to the resistance to this pathogen [19,23].

Phytophthora infestans's vast effector repertoire is likely the result of a constant adaptation to its diverse hosts [24]. Among *P. infestans*'s effectors, two were recently identified, which suppress the host's RNA silencing machinery [25–26]. Suppression of the plant RNA silencing pathways would release miRNA targets, including *NBS-LRRs*, from their miRNA-mediated suppression. Therefore, it has been hypothesized that the regulation of *R*-genes by miR482/2118 may have evolved into a pathogen detection mechanism, i.e. a counter-defence mechanism by which pathogen-mediated RNA silencing suppression activates the plant immune system [13]. This is at odds with the observed positive influence on pathogen virulence by these effectors [25] and suggests a complex network of *NBS-LRR* regulation during the infection of plants by their pathogens.

In this study, we analysed how coevolution of tomatoes and their pathogen *P. infestans* has shaped miRNA-mediated *NBS-LRR* regulation and how this regulatory network contributes to resistance in tomato. We first identified miR482/2118 targets associated with *P. infestans* defence in *S. lycopersicum*. Next, we studied the expression of *Sl*miR482/2118 and a set of 12 *NBS-LRRs* in *S. lycopersicum* during infection by *P. infestans*. Although the expression of *NBS-LRRs* is undoubtedly regulated by multiple mechanisms in addition to negative regulation via miRNAs, we observe examples of strong co-regulation between members of miR482/2118 and their targets. Combining comparative expression analyses of members of the miR482/2118 family in three closely related tomato species (*S. lycopersicum*, *Solanum pimpinellifolium* and *Solanum arcanum*) and analyses of host resistance led to two observations: (i) the least resistant tomato, *S. lycopersicum*, showed downregulation of several miRNAs from 24 to 96 hours post-inoculation (hpi) relative to the mock control, while its more resistant wild relatives did not and (ii) downregulation of miR482a and miR482f during early time-points of infection (6 hpi) correlated with resistance to *P. infestans*. Based on these observations, we hypothesize that global pathogen-mediated RNA silencing suppression is more effective in cultivated tomato than in its wild relatives.

2. Material and methods

(a) Plant material and *Phytophthora infestans* inoculation

Seeds of *S. arcanum* were surface sterilized using approximately 5% NaOCl (30 s), washed 3 × 3 min in sterile H₂O, plated on 1.2% H₂O

agar and incubated in dark for 3 days (16 h/8 h with 18°C/15°C). Afterwards, the seeds were transferred to a 16 L (166 ± 17 μmol quanta m⁻² s⁻¹): 8 D regime. Nine days post sterilization (dps), seedlings were transferred to 0.5% Murashige & Skoog medium [27] with 1% sucrose.

The isolate, IPO-C, of *P. infestans* was grown on rye-sucrose-agar plates (with 100 μg ml⁻¹ ampicillin, 10 μg ml⁻¹ amphotericin B and 20 μg ml⁻¹ vancomycin; [28]) at 18°C in the dark. Zoospores were isolated and leaflets of *S. arcanum* were inoculated at 28 dps as described in de Vries *et al.* [29]. Three biological replicates (three to four seedlings each) were sampled per treatment and time-point (0 hpi, 6 hpi, 24 hpi, 48 hpi, 72 hpi and 96 hpi).

(b) RNA extraction, mRNA purification and cDNA synthesis

Total RNA of *S. arcanum* was isolated using the Universal RNA/miRNA Purification Kit (Roboklon, Berlin, Germany). RNA from *S. lycopersicum* and *S. pimpinellifolium* was used from de Vries *et al.* [29]. mRNA was purified using the Dynabeads mRNA Purification Kit (Thermo Scientific, Massachusetts, USA).

cDNA libraries for mature miR482/2118 expression analyses were created using miScript Plant RT Kit (Qiagen, Hilden, Germany) using 250 ng total RNA and diluted 1 : 10 with nuclease-free H₂O. cDNA libraries for all other expression analyses were created with the RevertAid First Strand cDNA Synthesis Kit (Thermo Fisher Scientific, Vilnius, Lithuania) using 1000 ng total RNA and random hexamer primers and libraries were diluted 1 : 1 with nuclease-free H₂O.

cDNA libraries for the modified 5'RNA ligase-mediated rapid amplification of cDNA ends (5'RLM-RACE) were created using the GeneRacer Kit (Invitrogen, California, USA) using 50–100 ng mRNA from infections (24 and 48 hpi) and mock (48 hpi). To identify miRNA cleavage sites, the protocol was modified to omit the enzymatic digest of the cap and proceed directly to the ligation of the 5' GeneRacer RNA oligo adapter. The SuperScript III RT Module (Invitrogen, California, USA) with the GeneRacer Oligo dT Primer was used for reverse transcription.

(c) 5'RLM-RACE

Amplification of 5'RLM-RACE products was performed (1 × High Fidelity PCR buffer, 0.6 μM GeneRacer 5' primer, 0.2 μM of the gene specific primer (electronic supplementary material, table S1), 200 μM dNTPs, 1 mM MgSO₄, 3% DMSO and 0.5U Platinum *Taq* DNA Polymerase High Fidelity) followed by a nested PCR, using 1 μl of the PCR product in a 50 μl reaction (1 × High Fidelity PCR buffer, 0.2 μM GeneRacer 5' nested primer, 0.2 μM of the nested gene specific primer (electronic supplementary material, table S1), 200 μM dNTPs, 1 mM MgSO₄ and 0.5U Platinum *Taq* DNA Polymerase High Fidelity).

PCR products were amplified with a Phusion High-Fidelity DNA Polymerase (New England Biolabs, Massachusetts, USA) and cloned using a Zero Blunt TOPO PCR Cloning Kit (Invitrogen, California, USA).

(d) Confirmation of infection and infection progress

To confirm successful infection and study the disease progression, leaflets of *S. arcanum* seedlings were analysed microscopically. The relative necrotic area and pathogen structures were determined according to [29]. Statistical differences in necrotic area over time and between mock and infections were estimated using a Kruskal–Wallis test [30] with a Tukey and Kramer *post hoc* test, using a Tukey distance approximation [31]. For comparisons of the relative necrotic area between

species, normal distribution of the data was evaluated using a Shapiro–Wilk test [32] and then tested for significant differences using a Mann–Whitney *U* test [33] in R v. 3.2.1. To determine the abundance and life cycle progression of *P. infestans* at the molecular level, expression of three biotrophic, two necrotrophic and one biomass marker gene were analysed according to [29].

(e) Identification of miR482/2118 family members

Members of miR482/2118 from *S. lycopersicum* and *S. pimpinellifolium* have been previously identified in de Vries *et al.* [15]. Members of miR482/2118 from *S. arcanum* were identified via a BLASTn against the *S. arcanum* genome using miR482/2118 precursor sequences of *S. lycopersicum* as query. The best hits in *S. arcanum* were aligned to the *SlmiR482/2118* precursor sequences and the mature miR482/2118 sequences were determined. Folding of *S. arcanum* miR482/2118 precursors into hairpins was predicted using RNAfold [34] (electronic supplementary material, figure S1).

(f) Selection of *R*-genes

We chose *R*-genes that were (i) predicted to be targeted by one or more members of miR482/2118 and (ii) associated with resistance to *P. infestans*. The 52 potential miR482/2118 target genes [15] were used as queries for a BLASTn-search against the NCBI nr/nt database limited to *S. lycopersicum*. The best functional annotated BLAST hit (e.g. excluding hits to entire chromosomes) was recorded. Hits with an e-value of 0, query coverage greater than 90% and an identity greater than 85% to an *R*-gene associated with resistance against *P. infestans* in *S. lycopersicum* or the resistance gene analogues (RGA) complex were determined as likely to be associated with resistance to *P. infestans*.

(g) qRT-PCR

qRT-PCR was performed using the miScript SYBR Green PCR (Qiagen, Hilden, Germany). miR482/2118 forward primers were designed based on the mature miR482/2118 sequences. miR482/2118 primer specificity was tested by creating a qRT-PCR product for each primer. These qRT-PCR products were purified, and each primer was tested with each qRT-PCR product to determine if and at what annealing temperatures the primers would bind to other miR482/2118 paralogues. For all miR482/2118 primers a binding-specific annealing temperature was determined (electronic supplementary material, table S1). The only exceptions were the primers for *SlmiR482h* and *SpmiR482h*, which annealed to miR482h as well as miR482 at all annealing temperatures. *SamiR482h* was specific because of its slightly different mature miRNA sequence (electronic supplementary material, table S1). As a control, the expression of mature *SlmiR156a/b/c*, *SlmiR166a/b*, *SlmiR168a/b* and *SlmiR172a/b* was determined. miR390a was used as a reference due to its constant expression across treatments and time-points according to BESTKEEPER v.1 [35].

Expression of *NBS-LRRs* in *S. lycopersicum* was determined using the SsoAdvanced Universal SYBR Green Supermix (electronic supplementary material, table S1; Bio-Rad, California, USA). As reference genes, we used *SAND* [15], *TIP41* [15] and *Translation Initiation Factor 3 subunit H (TIF3H)*; [29]).

Relative abundance and progression of *P. infestans* were measured using *Histone2a (PiH2a)*. Expression of *PiH2a* at time-points 24 to 96 hpi was set relative to its expression at 24 hpi. The data were normalized with the plant reference genes (*SAND*, *TIP41* and *TIF3H*).

Relative expression was calculated according to [36]. Data were tested for normality using a Shapiro–Wilk test [32] and equal variance using R v. 3.2.1. Comparisons between infections and mock control were tested using either a two-sample *t*-test or a Welch two-sample *t*-test for normally distributed data or a Mann–Whitney *U*-test [33] for non-normally distributed data.

3. Results and discussion

(a) One-third of potential nucleotide-binding site leucine-rich repeats targets have high identity to *Phytophthora infestans*-associated resistance genes

We screened for *NBS-LRRs* that are potential targets of miR482/2118 and classified as *R*-genes for *P. infestans* (electronic supplementary material, table S2). Of the 52 predicted *NBS-LRR* targets [15], we identified 20 which were annotated as a *P. infestans*-associated *R*-gene or the RGA complex, members of which are associated with resistance to the pathogen [37–38]. Of these 20, 17 matched a *P. infestans*-associated *R*-gene with an e-value of 0, a query coverage of greater than 90% and an identity of greater than 85% (electronic supplementary material, table S2). Therefore, approximately 33% of the predicted direct *NBS-LRR* targets of miR482/2118 are associated with resistance to *P. infestans*.

(b) Nucleotide-binding site leucine-rich repeats are targeted by miR482/2118 in *Solanum lycopersicum* during infection by *Phytophthora infestans* infection

Previous studies have used 5'RLM-RACE to test whether the expression of *NBS-LRRs* is regulated by members of the miR482/2118 gene family [13–14]. Targeting by *SlmiR482f* of *Solyc08g075630.2.1* and *Solyc08g076000.2.1*, which are associated with *P. infestans* defence responses (electronic supplementary material, table S2), was only shown in overexpression lines of *Nicotiana benthamiana* [14]. To test whether these *NBS-LRRs* are targeted by miR482/2118 in *S. lycopersicum*, we created 5'RLM-RACE libraries from *S. lycopersicum* infected with the pathogen and mock-treated (figure 1). In addition, we tested *Solyc02g036270.2.1*, because it is a functional miR482/2118 target [13] that is not associated with *P. infestans* resistance (figure 1; electronic supplementary material, table S2).

A cleavage site is determined by an enrichment of a specific degradation product in the 5'RLM-RACE library. This is established by cloning the degradation products of the gene of interest from the library and analysing how often a specific degradation product was cloned. If the gene of interest has a miRNA cleavage site, the majority of the clones should contain a product cut at the predicted cleavage site. All three tested genes revealed a cleavage site in the region complementary to the miR482/2118 sequences. Moreover, these cleavage products were observed in both mock-treated and *P. infestans* infected leaflets of *S. lycopersicum*. Based on clone analyses of the 5'RLM-RACE library of *Solyc02g036270.2.1*, 15 out of 18 clones were cleaved between nucleotide positions 11 and 12 of the miRNA binding site (figure 1a). For *Solyc08g075630.2.1*, all clones (24/24) were cleaved between nucleotide positions 12 and 13 of the miRNA binding site (figure 1b). For *Solyc08g076000.2.1*, 13/17 clones had a cleavage site between nucleotide positions 12 and 13 of the miRNA binding region (figure 1c). Some alternative cleavage products were observed for *Solyc02g036270.2.1* and *Solyc08g076000.2.1* (figure 1). This is in agreement with Ouyang *et al.* [14], who also observed an alternative cleavage site for *Solyc08g076000.2.1*. In summary, we demonstrate that targeting of *NBS-LRRs* by miR482/2118 is effective in pathogen-challenged and unchallenged plants.

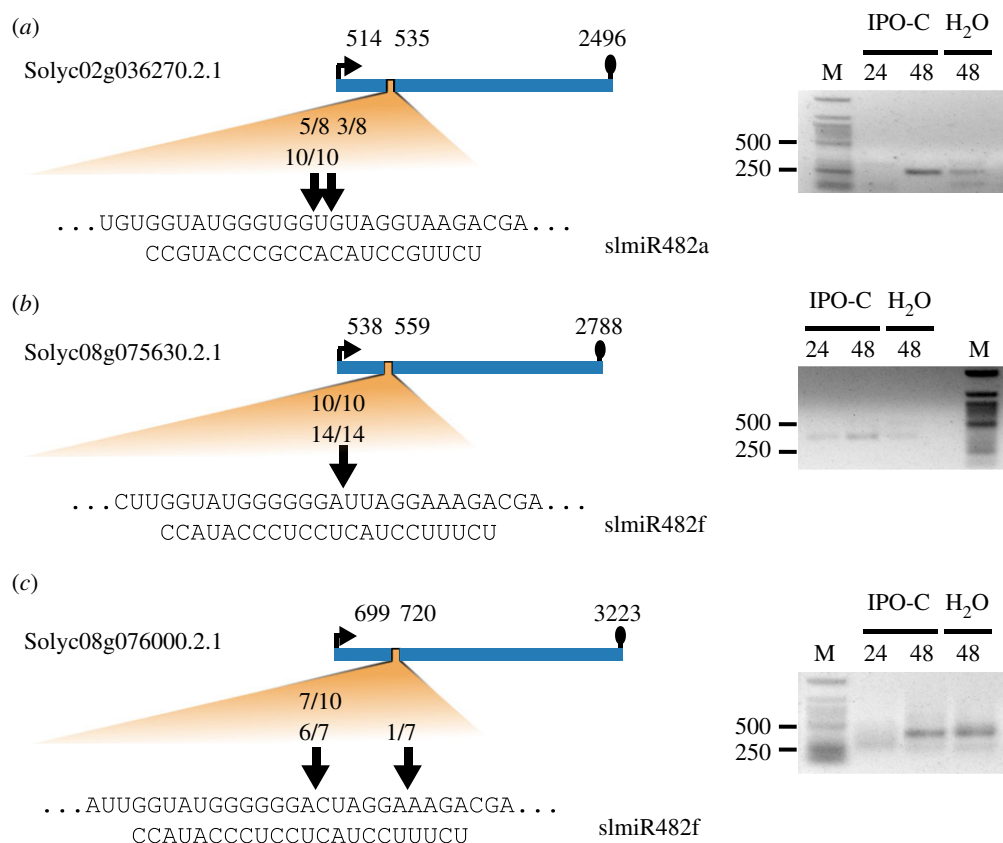


Figure 1. Targeting of *NBS-LRRs* by miR482/2118 family members in *S. lycopersicum*. *In vitro* confirmation of *NBS-LRR* targeting by SlmiR482/2118 using 5'RLM-RACE for *Solyc02g036270.2.1* targeted by SlmiR482a (a), *Solyc08g075630.2.1* targeted by SlmiR482f (b) and *Solyc08g076000.2.1* targeted by SlmiR482f (c). A schematic of the target gene (blue) is on the left. The predicted binding site (P-loop, orange) and its sequence is shown below. The arrows indicate the validated degradation sites. The number of clones supporting the site and the total number of clones sequenced are given above the arrows. Upper numbers indicate clones from the mock controls and lower numbers indicate those from infections. The corresponding PCR products of the 5'RLM-RACE are shown on the right.

(c) Co-regulation of members of miR482/2118 and their nucleotide-binding site leucine-rich repeats targets is time-dependent

Given that a third of the miR482/2118 potential targets in *S. lycopersicum* are associated with disease resistance to *P. infestans* in *S. lycopersicum*, we chose a subset of 11 *NBS-LRRs* associated with *P. infestans* resistance and *Solyc02g036270.2.1* (as a positive control for cleavage, but a negative control in terms of *P. infestans* resistance) to study the co-regulation of *NBS-LRRs* and miR482/2118 in this interaction. We quantified the expression of the seven members of miR482/2118 and 12 *NBS-LRRs* in infected and uninfected plants across five time-points (6 to 96 hpi) (figures 2a and 3).

To identify to what degree the miRNAs show similar expression patterns in response to infection, we compared the expression of the individual miRNAs and recorded how often two miRNAs showed the same expression pattern in parallel at a given time-point, to see whether both show (i) significant upregulation, (ii) significant downregulation or (iii) no differential regulation between infection versus mock. Overall, all SlmiR482/2118 miRNAs show similar dynamics in expression, with the same expression pattern of two miRNAs for 3.1 ± 0.9 time-points, on average (figure 2a).

By contrast, two *NBS-LRRs* show, on average, the same expression pattern at 2.0 ± 1.3 time-points (figure 3). This is a significantly lower co-regulation compared to that observed for miR482/2118 (p -value = 0.0002). Such differences in co-regulation suggest that despite active targeting by

miR482/2118 in *S. lycopersicum*, *NBS-LRRs* are likely to be regulated by other mechanisms in addition to the regulation by miR482/2118.

Next, we evaluated how often pairs of miR482/2118 and *NBS-LRRs* are co-regulated and what type of co-regulation they are subjected to (i.e. negative co-regulation, positive co-regulation or no differential regulation of both miRNA and target). In total (over all time-points), we evaluated 95 miR482/2118–*NBS-LRR* combinations (electronic supplementary material, figure S2). In 45 pairs, the *NBS-LRRs* are predicted to be post-transcriptionally regulated, while 50 are predicted to be translationally regulated (electronic supplementary material, table S2). If a target is post-transcriptionally regulated, one would predict a negative co-regulation of target and miRNA. This means that if the miRNA is significantly upregulated, the target should be significantly downregulated and vice versa. Nevertheless, positive correlations between miRNA and target mRNA levels have been reported [39–41]. Additionally, positive co-regulation has been observed for miRNAs [39] that suppress their targets translationally [42], suggesting that translational repression can lead to positive co-regulation. If the miRNA is not differentially regulated between infection versus mock treatment, the target should not be either.

We observed that the direction of co-regulation is not static for every miR482/2118–*NBS-LRR* combination but can shift between time-points. Such rapid shifts in co-regulation may result from switches between translational and post-transcriptional suppression. For example, *Solyc08g076000.2.1* shows an alternating pattern of co-regulation with SlmiR482f

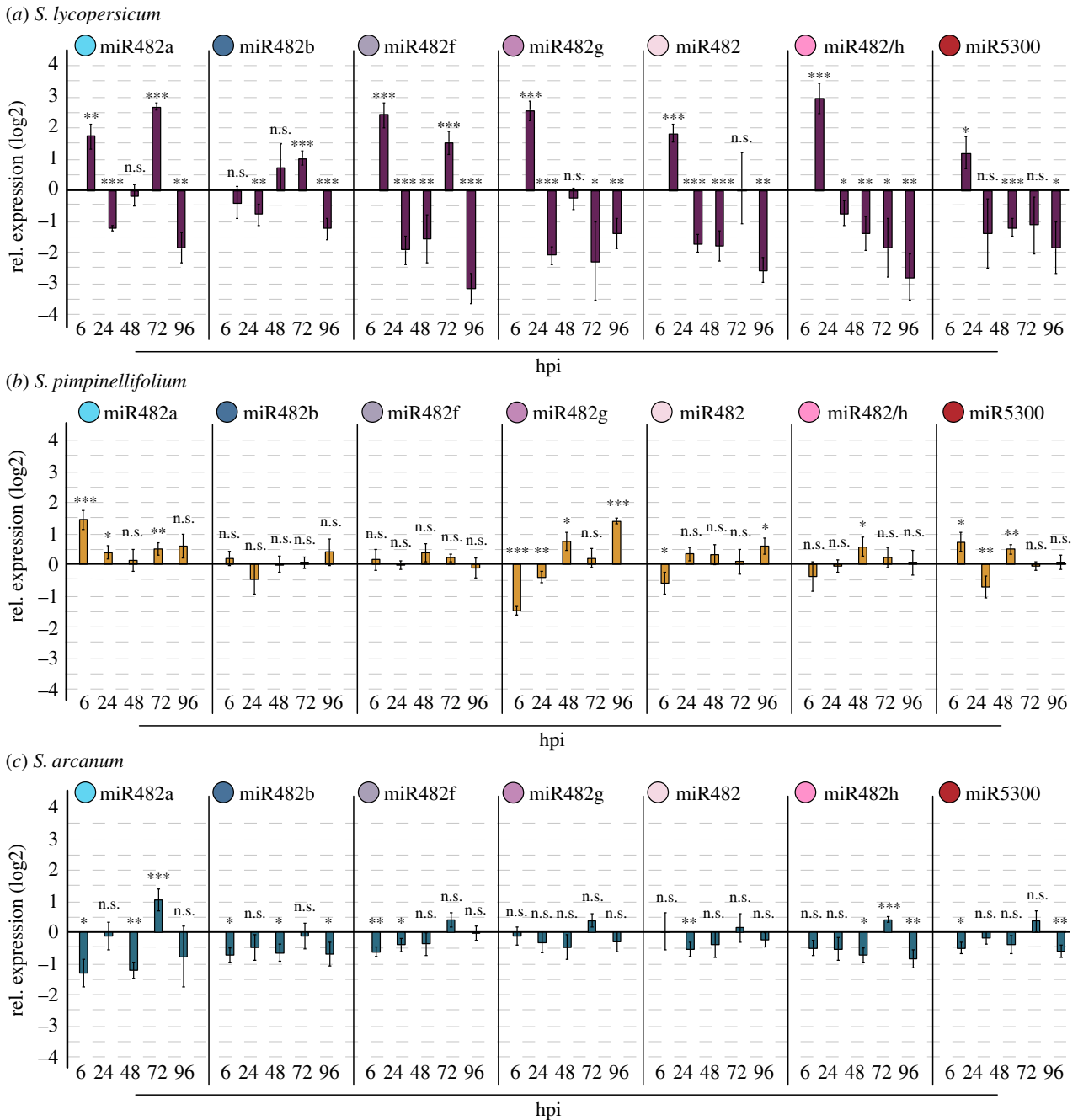


Figure 2. Expression of miR482/2118 family members in *S. lycopersicum*, *S. pimpinellifolium* and *S. arcanum*. Relative expression (\log_2) in infected compared with mock-control plants of *S. lycopersicum* (a), *S. pimpinellifolium* (b) and *S. arcanum* (c) of the seven miR482/2118 family members at 6, 24, 48, 72 and 96 hpi relative to mock control. The bars represent the average relative expression of the mature miRNAs and the error bars indicate the standard error of the mean (SEM). Significant differences of the relative expression of the miRNA in infected versus mock-treated plants at a specific time-point are indicated by * (p -value < 0.05), ** (p -value < 0.01), *** (p -value < 0.001) and ns (not significant).

(figure 3; electronic supplementary material, S2) and is regulated by both modes [14], despite its prediction to be regulated translationally (electronic supplementary material, table S2).

We determined at which time-points co-regulation was most prevalent, suggesting a potential influence of miR482/2118 on *NBS-LRR*-regulation. The greatest co-regulation occurred at 48 hpi with 10/12 *NBS-LRRs* showing co-regulation with at least one of their respective *SlmiR482/2118* members (electronic supplementary material, figure S2). High co-regulation was also detected at 6 and 72 hpi for 9/12 *NBS-LRRs*. All three time-points are biologically interesting: 6 hpi is a crucial time-point for infection success, as early HR significantly contributes to resistance against *P. infestans* [20].

Between 48 and 72 hpi, *P. infestans* switches from a biotrophic (i.e. requiring nutrients from a living host) to a necrotrophic phase (i.e. inducing host cell death) [29].

(d) *Solanum arcanum* is less susceptible to *Phytophthora infestans* than its two relatives

We found that co-regulation of miR482/2118 with their targets was time-dependent, and more prevalent at time-points critical for infection success and transitions in the pathogen's life cycle. To place this in context with resistance, we compared the response of three tomato species, *S. lycopersicum*, *S. pimpinellifolium* and *S. arcanum*, to *P. infestans*. These host species differ in their evolutionary and ecological histories.

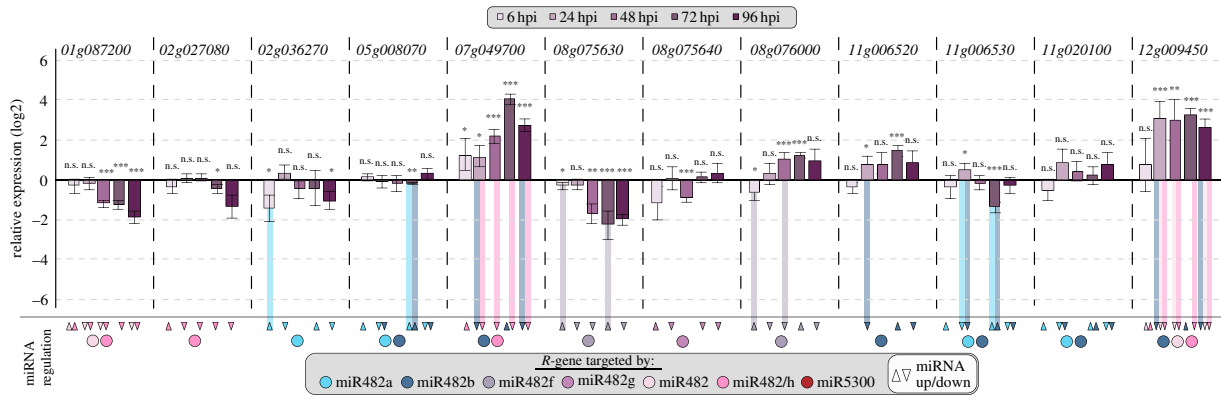


Figure 3. Expression and co-regulation of *S*/miR482/2118 and their *NBS-LRR* targets. Relative expression (\log_2) of potential *NBS-LRR* targets of miR482/2118 in infected compared with mock-control plants of *S. lycopersicum*. Bars show the mean expression and error bars indicate the SEM. Statistical differences in relative expression in infected versus mock-treated plants at a specific time-point are indicated by * (p -value < 0.05), ** (p -value < 0.01), *** (p -value < 0.001) and ns (not significant). Filled circles below each gene corresponds to the miRNA(s) predicted to target each *NBS-LRR*. Arrow heads indicate significant up or down-regulation of the members of *S*/miR482/2118 at a given time-point: upward arrow heads indicate significant upregulation and downward arrow heads indicate significant downregulation of the miRNA. The arrow heads are coloured according to their respective miRNA. Vertical lines between miRNA arrow heads and the relative expression of the *NBS-LRR* highlight significant negative co-regulation between members of the *S*/miR482/2118 family and their targets at a specific time-point.

S. lycopersicum has long been subjected to artificial selection. Furthermore, high-density monocultures of crop species can allow for higher pathogen loads and potentially higher pathogen diversity in the cultivated species [43].

Solanum pimpinellifolium and *S. arcanum* have partially overlapping ranges: *S. pimpinellifolium*'s habitat spans from Central Ecuador to Chile, while *S. arcanum* occurs in Northern Peru [44]. Furthermore, their habitats overlap with that of *P. infestans* [45–47], allowing for exposure to and coevolution with the pathogen. Indeed, *R*-genes associated with resistance to *P. infestans* have been isolated from *S. pimpinellifolium* [23,48]. In addition, *S. pimpinellifolium* is facultative self-compatible and *S. arcanum* is predominantly self-incompatible [44]. Mating system differences can influence the evolutionary history of the hosts and their adaptation potential. We therefore hypothesize that the different hosts will show variation in their resistance to *P. infestans* because they experienced different evolutionary histories.

In our previous study [29], we evaluated the relationship between pathogen abundance, the presence of pathogen infection structures and disease symptoms in *S. lycopersicum* and *S. pimpinellifolium*. Here, we describe our new results on *S. arcanum* and compare these with the results from *S. lycopersicum* and *S. pimpinellifolium*. The relative necrotic area of *S. arcanum* increased significantly at 48 hpi (figure 4c; electronic supplementary material, S3a). Although the variance of relative necrotic area was higher in 72 and 96 hpi compared with 48 hpi, the relative necrotic area did not increase significantly beyond 48 hpi (electronic supplementary material, figure S3a). The abundance of *P. infestans* increased significantly from 24 to 48 hpi, and from 48 to 72 hpi (electronic supplementary material, figure S3b). The lack of correlation between relative necrotic area and *P. infestans* abundance at 72 hpi may stem from a delayed transition to the necrotrophic phase. For *S. pimpinellifolium* and *S. lycopersicum* we pinpointed the transition from biotrophy to necrotrophy to a time between 48 and 72 hpi [29]. For *S. arcanum*, we observed haustoria from 24 hpi onwards, and developing and mature sporangia at 72 and 96 hpi (electronic supplementary material, figure S3c). In

agreement with this, most marker genes for biotrophy are expressed throughout the infection, but the sporulation marker *Cdc14* was only expressed from 72 hpi onwards (electronic supplementary material, figure S3d,e), suggesting that the transition to necrotrophy occurred between 48, 72 hpi. However, the number of all infection structures was lower in *S. arcanum* compared with the other two species (figure 4e). As less virulent isolates of *P. infestans* also show a reduction in haustoria compared with more virulent isolates [49], this suggests that *P. infestans* is less infective and has a delayed life cycle transition on *S. arcanum*.

Across all species, sporangia develop the earliest (48 hpi) in *S. lycopersicum* (figure 4e). The relative necrotic area 72 and 96 hpi is also the highest in *S. lycopersicum* (figure 4a–d). Taken together, this suggests that, although all species are susceptible to *P. infestans*, they are so by a variable degree: *S. lycopersicum* is likely the most susceptible, followed by *S. pimpinellifolium* and finally *S. arcanum*, which is the least susceptible of all three species.

(e) MiR482a and miR482f are candidate miRNAs for defence responses against *Phytophthora infestans*

We evaluated the miRNA expression between the tomatoes in relation to their resistance phenotype. Compared with *S. lycopersicum*, expression between pairs of miRNAs was significantly less correlated in the wild tomatoes: in *S. pimpinellifolium* pairs of miR482/2118 members showed the same expression pattern at 2.2 ± 1.2 time-points (p -value = 0.012; figure 2b) and in *S. arcanum* at 2.2 ± 0.9 time-points (p -value = 0.005; figure 2c). Lower co-regulation suggests additional gene-specific regulatory mechanisms in the wild tomatoes. By contrast, the cultivated tomato appears to have a more global co-regulation of miR482/2118 expression. These differences in co-regulation between wild and cultivated tomatoes could result from (i) differences in the evolutionary history of these plants (i.e. artificial versus natural selection) that brought about a more streamlined regulation of expression of miR482/2118 in *S. lycopersicum* or (ii) greater sensitivity to pathogen manipulation of host RNA silencing in *S. lycopersicum*, for

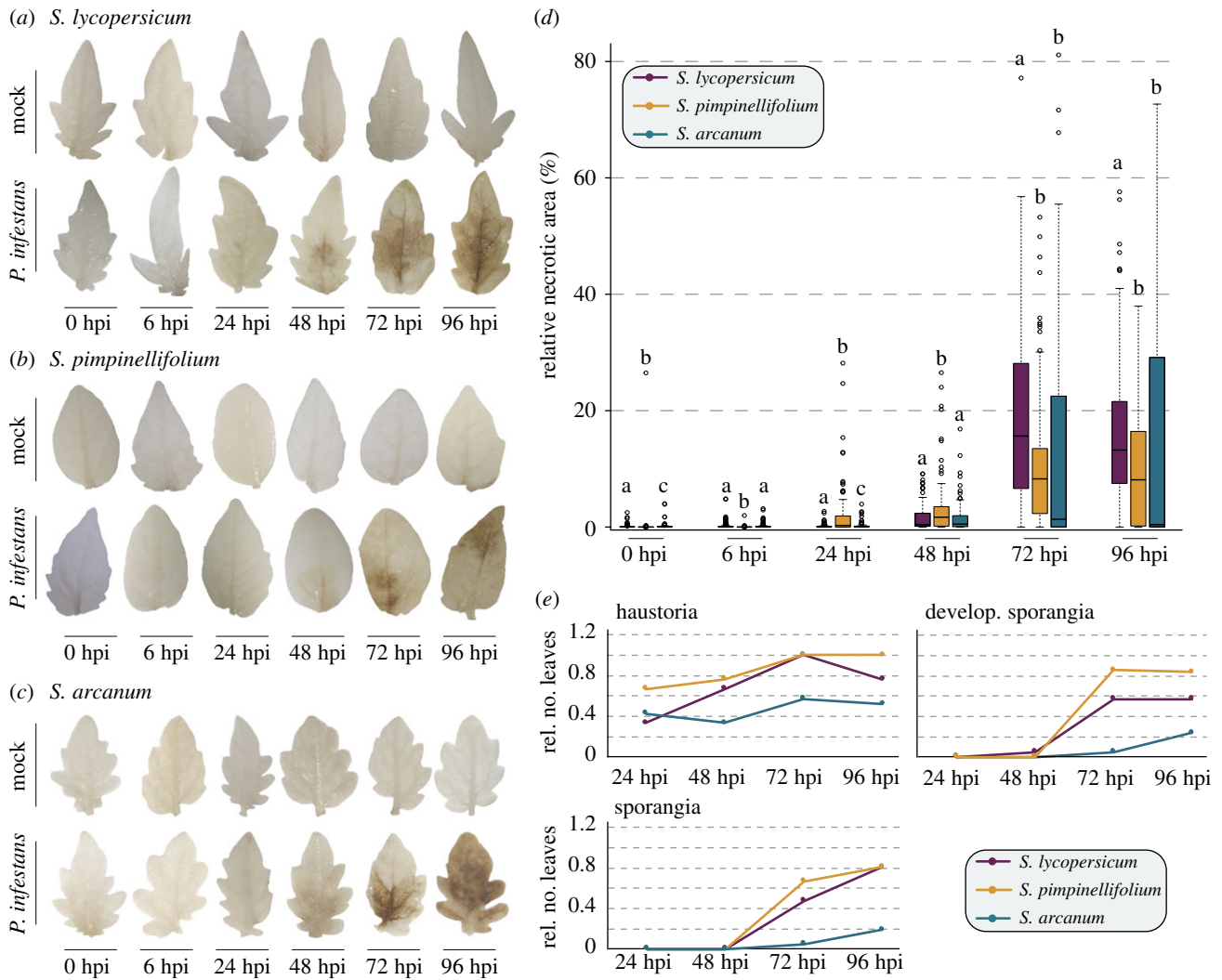


Figure 4. Infection progress in *S. arcanum* in comparison to *S. lycopersicum* and *S. pimpinellifolium*. Necrotic area on the leaflets of *S. lycopersicum* (a), *S. pimpinellifolium* (b) and *S. arcanum* (c) for mock-treated (upper row) and infected (lower row) leaflets. Comparison of the relative necrotic area during *P. infestans* infection in *S. arcanum* (blue), *S. pimpinellifolium* (yellow) and *S. lycopersicum* (purple) (d). Statistical differences in relative necrotic area for the three species were calculated per time-point and are indicated by different letters above the boxes. The *p*-value cut-off was 0.05. Comparison of the number of haustoria, developing and mature sporangia of *P. infestans* after infection of *S. arcanum* (blue), *S. pimpinellifolium* (yellow) and *S. lycopersicum* (purple) (e). All data for *S. pimpinellifolium* and *S. lycopersicum* were published previously in de Vries *et al.* [29].

example, due to pathogen-secreted RNA silencing suppressors. The latter is of interest because two RNA silencing suppressors have been previously described in *P. infestans* [26,50]. Additionally, we observed a substantial downregulation of additional miRNAs in *S. lycopersicum* that do not target *NBS-LRRs* (*SlmiR156a/b/c*, *SlmiR166a/b*, *SlmiR168a/b* and *SlmiR172a/b*) in *S. lycopersicum* from 24 hpi onwards (electronic supplementary material, figure S4). Of these four, only *SlmiR172a/b* is implicated to function in *P. infestans* resistance, albeit by a different mechanism [51].

Next, we examined the relationship between the expression of miR482/2118 miRNAs and the life cycle of *P. infestans*. We focused on 6, 48 and 72 hpi, because they are critical time-points during infection by *P. infestans* and they correspond to the time frame when the greatest co-regulation between pairs of *SlmiR482/2118* and their targets is detected (figure 3; electronic supplementary material, S2). We observed that six of the seven miRNAs were upregulated at 6 hpi (figures 2a and 3), which should result in enhanced suppression of their *NBS-LRR* targets. This was indeed true for three of the *NBS-LRR* targets screened: *Solyc02g036270.2.1*, *Solyc08g075630.2.1* and *Solyc08g076000.2.1*. The gene *Solyc02g036270.2.1* served

as a reference *NBS-LRR*, because it was so far not reported to be associated with resistance to *P. infestans*.

We compared the expression patterns of *SlmiR482/2118* with those in the close relatives of *S. lycopersicum*. In *S. pimpinellifolium*, only two *SpmiR482/2118* members were significantly upregulated at 6 hpi (figure 2b). In *S. arcanum*, none of the seven *SamiR482/2118* members were upregulated at this time-point (figure 2c). Moreover, four out of seven *SamiR482/2118* were significantly downregulated at 6 hpi in *S. arcanum* (figure 2c), which was the most resistant tomato species. All of these members of miR482/2118 have targets associated with *P. infestans* defence in *S. lycopersicum* (electronic supplementary material, table S2). In fact, the *R*-gene targets of *SlmiR482a* and *SlmiR482f* were significantly downregulated at 6 hpi in *S. lycopersicum* (figure 3). Therefore, the downregulation of *SamiR482a* and *SamiR482f* upon infection in *S. arcanum* might be related to the enhanced resistance observed in this species. This downregulation of *SamiR482/2118* in *S. arcanum* in the presence of the pathogen could allow for an earlier response to the pathogen, because the predicted *NBS-LRR* targets would not be repressed during the first 6 h, as they are in *S. lycopersicum*. Taken together, these results point to miR482a

and miR482f as potential regulators of *P. infestans*-associated defence responses.

Given the substantial co-regulation of miRNAs and their targets at 48 and 72 hpi, we evaluated the association of miR482/2118 expression with the life cycle progression of *P. infestans* on its hosts. In the biotrophic phase (prior to 72 hpi), *P. infestans* requires a living host. High R-protein activity during this time frame could lead to earlier pathogen perception and activation of HR/cell death, which in turn would limit pathogen spread [20]. In the necrotrophic phase, *P. infestans* induces host cell death [52–53]. High R-protein activity at this time-point may not be beneficial to the host, but instead benefit the pathogen. An effective plant resistance response during the necrotrophic phase may include the suppression of cell death-inducing proteins, such as R-proteins, perhaps through an upregulation of miR482/2118. By contrast, if pathogen-mediated RNA silencing suppression were effective at these later time-points, one would expect a downregulation of miRNAs, including miR482/2118.

At 48 hpi, four *SlmiR482/2118* (*SlmiR482f*, *SlmiR482*, *SlmiR482/h* and *SlmiR5300*) were downregulated specifically in infected plants (figure 2a). While this does not exclude a plant-mediated downregulation of miR482/2118, the downregulation of the non-NBS-LRR regulating miRNAs (electronic supplementary material, figure S4), indicates that pathogen-mediated RNA silencing suppression may play a role here. In agreement with this, a *P. infestans* RNA silencing suppressor, potentially involved in silencing the miRNA-mediated silencing pathway, has its highest expression in the main biotrophic phase [26]. In *S. arcanum*, three *SamiR482/2118* members (*SamiR482a*, *SamiR482b* and *SamiR482h*) were downregulated during the infection compared to the control (figure 2c). By contrast, none were downregulated in *S. pimpinellifolium* (figure 2b).

After the transition to necrotrophy at 72 hpi, the following miRNAs were upregulated: *SlmiR482a*, *SlmiR482b* and *SlmiR482f* in *S. lycopersicum*, *SamiR482a*, *SamiR482h* and *SamiR5300* in *S. arcanum* and *SpmiR482a* in *S. pimpinellifolium* (figure 2). None of the control *SlmiRNAs* were significantly upregulated (electronic supplementary material, figure S4), suggesting a miRNA-specific plant response at this time-point. miR482a is upregulated at 72 hpi in the infections across all three species, despite the small lag in *S. arcanum* for the transition from biotrophy to necrotrophy. This would suggest that

upregulation of miR482a is a consistent phenotype associated with a plant defence response during the necrotrophic phase of *P. infestans*. This is further supported by the negative co-regulation of *SlmiR482a* and its target *Solyc11g06530.1.1* at this time-point (figure 3; electronic supplementary material, S2).

4. Conclusion

In this study, we investigated the expression of miR482/2118 during the infection of *P. infestans* on three different tomato species. We found that co-regulation of mature *SlmiR482/2118* and their targets in cultivated tomato was highest during the initial phase of infection and during the life cycle transition of *P. infestans* from biotrophy to necrotrophy. Across-species comparisons of the gene expression of mature miR482/2118 and of the strength of resistance led to two main conclusions: (i) Co-evolution of *P. infestans* and *S. lycopersicum* may have resulted in a more efficient pathogen-mediated RNA silencing suppression compared with its more resistant sister species; and (ii) miR482a and miR482f could be identified as candidate miRNAs for mediating the resistance response of tomatoes to *P. infestans*.

Data accessibility. The precursor sequences of the *SamiR482/2118* family, have been identified in the draft genome from *S. arcanum* based on a BLASTn approach. The sequence data are made available in the electronic supplementary material.

Authors' contributions. S.d.V. and L.E.R. designed the study and drafted the manuscript. A.K. and T.K. contributed the bioinformatics analyses. S.d.V., A.K., J.K.v.D. and A.S. generated the molecular laboratory data. S.d.V., A.K. and J.K.v.D. analysed the data. All authors read and approved the manuscript.

Competing interests. We have no competing interests.

Funding. This work was funded by the Deutsche Forschungsgemeinschaft (DFG) (Ro 2491/6-1 and Research Training Group GRK1525). S.d.V. acknowledges a Killam Postdoctoral Fellowship.

Acknowledgements. We thank Francine Govers and Klaas Bouwmeester (Wageningen University, Wageningen, the Netherlands) for the *P. infestans* isolate IPO-C, Predrag Marinovski (Heinrich-Heine University Duesseldorf, Germany) for technical support and Jan de Vries (Dalhousie University, CA) for support with figure 3 during the revision process. Seeds of *S. arcanum* LA2157 were obtained from the Tomato Genetics Resource Center (TGRC) (tgrc.ucdavis.edu).

References

- Whisson SC *et al.* 2007 A translocation signal for delivery of oomycete effector proteins into host plant cells. *Nature* **450**, 115–118. (doi:10.1038/nature06203)
- Fabro G *et al.* 2011 Multiple candidate effectors from the oomycete pathogen *Hyaloperonospora arabidopsidis* suppress host plant immunity. *PLoS Pathog.* **7**, e1002348. (doi:10.1371/journal.ppat.1002348)
- Allen RL, Bittner-Eddy PD, Grenville-Briggs LJ, Meitz JC, Rose LE, Beynon JL. 2004 Host–parasite coevolutionary conflict between *Arabidopsis* and downy mildew. *Science* **306**, 1957–1960. (doi:10.1126/science.1104022)
- Krasileva KV, Dahlbeck D, Staskawicz BJ. 2010 Activation of an *Arabidopsis* resistance protein is specified by the *in planta* association of its leucine-rich repeat domain with the cognate oomycete effector. *Plant Cell* **22**, 2444–2458. (doi:10.1105/tpc.110.075358)
- Stokes TL, Kunkel BN, Richards EJ. 2002 Epigenetic variation in *Arabidopsis* disease resistance. *Gene Dev.* **16**, 171–182. (doi:10.1101/gad.952102)
- Li Y, Yang S, Yang H, Hua J. 2007 The TIR-NB-LRR gene *SN1* is regulated at the transcript level by multiple factors. *Mol. Plant Microbe Interact.* **20**, 1449–1456. (doi:10.1094/MPMI-20-11-1449)
- Holt BF, Belkhadier Y, Dangel JL. 2005 Antagonistic control of disease resistance protein stability in the plant immune system. *Science* **309**, 929–932. (doi:10.1126/science.1109977)
- Li X, Kapos P, Zhang Y. 2015 NLRs in plants. *Curr. Opin. Immunol.* **32**, 114–121. (doi:10.1016/j.coi.2015.01.014)
- Lai Y, Eulgem T. In press. Transcript-level expression control of plant NLR genes. *Mol. Plant Pathol.* (doi:10.1111/mpp.12607)
- Fei Q, Xia R, Meyers BC. 2013 Phased, secondary, small interfering RNAs in posttranscriptional regulatory networks. *Plant Cell* **25**, 2400–2415. (doi:10.1105/tpc.113.114652)
- Zhai J *et al.* 2011 MicroRNAs as master regulators of the plant NB-LRR defense gene family via the production of phased, *trans*-acting siRNAs.

- Gene. Dev.* **25**, 2540–2553. (doi:10.1101/gad.177527.111)
12. Li F, Pignatta D, Brunkard JO, Cohn MM, Tung J, Sun H, Kumar P, Baker B. 2012 MicroRNA regulation of plant innate immune receptors. *Proc. Natl Acad. Sci. USA* **109**, 1790–1795. (doi:10.1073/pnas.1118282109)
 13. Shivaprasad PV, Chen HM, Patel K, Bond DM, Santos BA, Baulcombe DC. 2012 A microRNA superfamily regulates nucleotide binding site-leucine-rich repeats and other mRNAs. *Plant Cell* **24**, 859–874. (doi:10.1105/tpc.111.095380)
 14. Ouyang S, Park G, Atamian HS, Han CS, Stajich JE, Kaloshian I, Borkovich KA. 2014 MicroRNAs suppress NB domain genes in tomato that confer resistance to *Fusarium oxysporum*. *PLoS Pathog.* **10**, e1004464. (doi:10.1371/journal.ppat.1004464)
 15. de Vries S, Kloesges T, Rose LE. 2015 Evolutionarily dynamic, but robust, targeting of resistance genes by the miR482/2118 gene family in the Solanaceae. *Genome Biol. Evol.* **7**, 3307–3321. (doi:10.1093/gbe/evv225)
 16. Zhang Y, Xia R, Kuang H, Meyers BC. 2016 The diversification of plant *NBS-LRR* defense genes directs the evolution of microRNAs that target them. *Mol. Biol. Evol.* **33**, 2692–2705. (doi:10.1093/molbev/msw154)
 17. Garry G, Forbes GA, Salas A, Santa Cruz M, Perez WG, Nelson RJ. 2005 Genetic diversity and host differentiation among isolates of *Phytophthora infestans* from cultivated potato and wild solanaceous hosts in Peru. *Plant Pathol.* **54**, 740–748. (doi:10.1111/j.1365-3059.2005.01250.x)
 18. Smart CD, Tanksley SD, Mayton H, Fry W. 2007 Resistance to *Phytophthora infestans* in *Lycopersicon pennellii*. *Plant Dis.* **91**, 1045–1049. (doi:10.1094/PDIS-91-8-1045)
 19. Li J *et al.* 2011 Identification and mapping of quantitative resistance to late blight (*Phytophthora infestans*) in *Solanum habrochaites* LA1777. *Euphytica* **179**, 427–438. (doi:10.1007/s10681-010-0340-7)
 20. Vleeshouwers VGAA, van Dooiuweert W, Govers F, Kamoun S, Colon LT. 2000 The hypersensitive response is associated with host and nonhost resistance to *Phytophthora infestans*. *Planta* **210**, 853–864. (doi:10.1007/s004250050690)
 21. Fooland MR, Sullenberger MT, Ashrafi H. 2015 Detached-leaflet evaluation of tomato germplasm for late blight resistance and its correspondence to field and greenhouse screenings. *Plant Dis.* **99**, 718–722. (doi:10.1094/PDIS-08-14-0794-RE)
 22. Michalska AM, Sobkowiak S, Flis B, Zimnoch-Guzowska E. 2016 Virulence and aggressiveness of *Phytophthora infestans* isolates collected in Poland from potato and tomato plants identified no strong specificity. *Eur. J. Plant Pathol.* **144**, 325–336. (doi:10.1007/s10658-015-0769-6)
 23. Zhang C *et al.* 2014 The *Ph-3* gene from *Solanum pimpinellifolium* encodes CC-NBS-LRR protein conferring resistance to *Phytophthora infestans*. *Theor. Appl. Genet.* **127**, 1353–1364. (doi:10.1007/s00122-014-2303-1)
 24. Haas BJ *et al.* 2009 Genome sequence and analysis of the Irish potato famine pathogen *Phytophthora infestans*. *Nature* **461**, 393–398. (doi:10.1038/nature08358)
 25. Xiong Q, Ye W, Choi D, Wong J, Qiao Y, Tao K, Wang Y, Ma W. 2014 *Phytophthora* suppressor of RNA silencing 2 is a conserved RxLR effector that promotes infection in soybean and *Arabidopsis thaliana*. *Mol. Plant Microbe Interact.* **27**, 1379–1389. (doi:10.1094/MPMI-06-14-0190-R)
 26. Vetukuri RR, Whisson SC, Grenville-Briggs LJ. 2017 *Phytophthora infestans* effector Pi4054 is a novel candidate suppressor of host silencing mechanisms. *Eur. J. Plant Pathol.* **149**, 771–777. (doi:10.1007/s10658-017-1222-9)
 27. Murashige T, Skoog F. 1962 A revised medium for rapid growth and bio assays with tobacco tissue cultures. *Physiol. Plant.* **15**, 473–497. (doi:10.1111/j.1399-3054.1962.tb08052.x)
 28. Caten CE, Jinks JL. 1968 Spontaneous variability of single isolates of *Phytophthora infestans*. I. Cultural variation. *Can. J. Bot.* **46**, 329–348. (doi:10.1139/b68-055)
 29. de Vries S, von Dahlen JK, Uhlmann C, Schnake A, Kloesges T, Rose LE. 2017 Signatures of selection and host-adapted gene expression of the *Phytophthora infestans* RNA silencing suppressor PSR2. *Mol. Plant Pathol.* **18**, 110–124. (doi:10.1111/mpp.12465)
 30. Kruskal WH, Wallis WA. 1952 Use of ranks in one-criterion variance analysis. *J. Am. Stat. Assoc.* **47**, 583–621. (doi:10.2307/2280779)
 31. Sachs L. 1997 *Angewandte statistik*, pp. 395–397, 662–664. Berlin, Germany: Springer.
 32. Shapiro SS, Wilk MB. 1965 An analysis of variance test for normality (complete samples). *Biometrika* **52**, 591–611. (doi:10.2307/2333709)
 33. Mann HB, Whitney DR. 1947 On a test of whether one of two random variables is stochastically larger than the other. *Ann. Math. Stat.* **18**, 50–60. (doi:10.1214/aoms/1177730491)
 34. Gruber AR, Lorenz R, Bernhart SH, Neuböck R, Hofacker IL. 2008 The Vienna RNA Websuite. *Nucleic Acids Res.* **36**, W70–W74. (doi:10.1093/nar/gkn188)
 35. Pfaffl MW, Tichopad A, Prgomet C, Neuvians TP. 2004 Determination of stable housekeeping genes, differentially regulated target genes and sample integrity: BestKeeper—Excel-based tool using pair-wise correlations. *Biotechnol. Lett.* **26**, 509–515. (doi:10.1023/B:BILE.0000019559.84305.47)
 36. Pfaffl MW. 2001 A new mathematical model for relative quantification in real-time RT-PCR. *Nucleic Acids Res.* **29**, e45. (doi:10.1093/nar/29.9.e45)
 37. Song J *et al.* 2003 Gene *RB* cloned from *Solanum bulbocastanum* confers broad spectrum resistance to potato late blight. *Proc. Natl Acad. Sci. USA* **100**, 9128–9133. (doi:10.1073/pnas.1533501100)
 38. Zhang C *et al.* 2013 Fine mapping of the *Ph-3* gene conferring resistance to late blight (*Phytophthora infestans*) in tomato. *Theor. Appl. Genet.* **126**, 2643–2653. (doi:10.1007/s00122-013-2162-1)
 39. Lopez-Gomollon S, Mohorianu I, Szittyá G, Moulton V, Dalmay T. 2012 Diverse correlation patterns between microRNAs and their targets during tomato fruit development indicates different modes of microRNA actions. *Planta* **236**, 1875–1887. (doi:10.1007/s00425-012-1734-7)
 40. Laxman N, Rubin C-J, Mallmin H, Nilsson O, Pastinen T, Grundberg E, Kindmark A. 2015 Global miRNA expression and correlation with mRNA levels in primary human bone cells. *RNA* **21**, 1433–1443. (doi:10.1261/ma.049148.114)
 41. Wen M, Xie M, Wang Y, Shi S, Tang T. 2016 Expression variations of miRNAs and mRNAs in rice (*Oryza sativa*). *Genome Biol. Evol.* **8**, 3529–3544. (doi:10.1093/gbe/evw252)
 42. Aukerman MJ, Sakai H. 2003 Regulation of flowering time and floral organ identity by a microRNA and its *APETALA2*-like target genes. *Plant Cell* **15**, 2730–2741. (doi:10.1105/tpc.016238)
 43. McDonald BA, Stukenbrock EH. 2016 Rapid emergence of pathogens in agro-ecosystems: global threats to agricultural sustainability and food security. *Phil. Trans. R. Soc. B* **371**, 20160026. (doi:10.1098/rstb.2016.0026)
 44. Moyle LC. 2008 Ecological and evolutionary genomics in the wild tomatoes (*Solanum* sect. *Lycopersicon*). *Evolution* **62**, 2995–3013. (doi:10.1111/j.1558-5646.2008.00487.x)
 45. Tooley PW, Therrien CD, Ritch DL. 1989 Mating type, race composition, nuclear DNA content, and isozyme analysis of Peruvian isolates of *Phytophthora infestans*. *Phytopathology* **79**, 478–481. (doi:10.1094/Phyto-79-478)
 46. Forbes GA, Escobar XC, Ayala CC, Revelo J, Ordoñez ME, Fry BA, Doucett K, Fry WE. 1997 Population genetic structure of *Phytophthora infestans* in Ecuador. *Phytopathology* **87**, 375–380. (doi:10.1094/PHYTO.1997.87.4.375)
 47. Acuña I, Sagredo B, Gutiérrez M, Sandoval C, Fahrenkrog A, Secor G, Rivera V, Mancilla S. 2012 Characterization of *Phytophthora infestans* population in Chile. In *Proceedings of the thirteenth EuroBlight workshop, St Petersburg, Russia* (ed. HTAM Schepers), pp. 145–150. Wageningen, the Netherlands: DLO Foundation.
 48. Moreau P, Thoquet P, Olivier J, Laterrot H, Girmsley N. 1998 Genetic mapping of *Ph-2*, a single locus controlling partial resistance to *Phytophthora infestans* in tomato. *Mol. Plant Microbe Interact.* **11**, 259–269. (doi:10.1094/MPMI.1998.11.4.259)
 49. Schoina C, Bouwmeester K, Govers F. 2017 Infection of a tomato cell culture by *Phytophthora infestans*; a versatile tool to study *Phytophthora*–host interactions. *Plant Methods* **13**, 88. (doi:10.1186/s13007-017-0240-0)
 50. Qiao Y *et al.* 2013 Oomycete pathogens encode RNA silencing suppressors. *Nat. Genet.* **45**, 330–333. (doi:10.1038/ng.2525)

51. Luan Y, Cui J, Li J, Jiang N, Liu P, Meng J. 2017 Effective enhancement of resistance to *Phytophthora infestans* by overexpression of miR172a and b in *Solanum lycopersicum*. *Planta* **247**, 127–138. Early Access Online Version. (doi:10.1007/s00425-017-2773-x)
52. Kanneganti TD, Huitema E, Cakir C, Kamoun S. 2006 Synergistic interactions of the plant cell death pathways induced by *Phytophthora infestans* Nep1-like protein PiNPP1.1 and INF1 elicitor. *Mol. Plant Microbe Interact.* **19**, 854–863. (doi:10.1094/MPMI-19-0854)
53. Kelley BS, Lee SJ, Damasceno CM, Chakravarthy S, Kim BD, Martin GB, Rose JK. 2010 A secreted effector protein (SNE1) from *Phytophthora infestans* is broadly acting suppressor of programmed cell death. *Plant J.* **62**, 357–366. (doi:10.1111/j.1365-3113.2010.04160.x)

Publication III

Global expression patterns of *R*-genes in tomato and potato

Status	In Review
Journal	Frontiers in Plant Science
Citation	von Dahlen, J. K., Schulz, K., Nicolai, J., Rose, L. E. (in review <i>Frontiers in Plant Science</i>): Global expression patterns of <i>R</i> -genes in tomato and potato.
Own contribution	Designed together with L.E.R. the study; co-designed the bioinformatic pipelines; analyzed and interpreted the data; drafted the initial manuscript

Global expression patterns of *R*-genes in tomato and potato

Janina K. von Dahlen^{1,2}, Kerstin Schulz^{1,3}, Jessica Nicolai¹ and Laura E. Rose^{1,3*}

*corresponding author: laura.rose@hhu.de

1 Institute of Population Genetics, Heinrich-Heine University Duesseldorf, Universitaetsstr. 1, 40225 Duesseldorf, Germany

2 iGRAD-Plant Graduate School, Heinrich-Heine University Duesseldorf, Duesseldorf, Germany

3 Ceplas, Cluster of Excellence in Plant Sciences, Heinrich-Heine University Duesseldorf, Duesseldorf, Germany.

Keywords: resistance genes, immune system, plant-pathogen interactions, Solanaceae, NBS-LRRs, NRCs, gene regulation

Abstract

- As key-players of plant immunity, the proteins encoded by resistance genes (*R*-genes) recognize pathogens and initiate pathogen-specific defense responses. The expression of some *R*-genes carry fitness costs and therefore inducible immune responses are likely advantageous. To what degree inducible resistance driven by *R*-genes is triggered by pathogen infection is currently an open question.
- In this study we analyzed the expression of 940 *R*-genes of tomato and potato across 315 transcriptome libraries to investigate how interspecific interactions with microbes influence *R*-gene expression in plants.
- We found that most *R*-genes are expressed at a low level. A small subset of *R*-genes had moderate to high levels of expression and were expressed across many independent libraries, irrespective of infection status. These *R*-genes include members of the class of genes called NRCs (NLR required for cell death). Approximately 10% of all *R*-genes were differentially expressed during infection and this included both up- and down-regulation. One factor associated with the large differences in *R*-gene expression was host tissue, reflecting a considerable degree of tissue-specific transcriptional regulation of this class of genes.
- These results call into question the widespread view that *R*-gene expression is induced upon pathogen attack. Instead, a small core set of *R*-genes is constitutively expressed, imparting upon the plant a ready-to-detect and defend status.

Introduction

Plants are constantly in contact with an array of microbes; some of which may harm the plant, some of which may benefit the plant. A challenge for every species at the outset of an encounter with a potential pathogen is to initiate an appropriate, coordinated cellular and organismal-level response. The plant immune system works to restrict the pathogen's ability to damage the host. Key-players of plant immunity are resistance genes (*R*-genes; reviewed in Jones & Dangl, 2006). Their protein products, R-proteins, recognize secreted pathogen-specific effectors, which may encode proteins, peptides or other molecules. These molecules interfere with the host's physiology, including the immune system. In some cases, pathogen molecules manipulate host gene expression or inactivate host secreted proteolytic enzymes (Allen et al., 2004; Song et al., 2009; Fabro et al., 2011). *R*-gene mediated recognition can involve direct recognition through the binding of a pathogen effector by a corresponding R-protein or via indirect recognition by monitoring effector-altered endogenous plant proteins (Jones & Dangl, 2006; Kourelis & van der Hoorn, 2018). R-proteins are the activators of a powerful, pathogen-specific immune response, which often includes transcriptional re-

51 programming (Glazebrook, 2005; Tsuda & Katagiri, 2010). Recently it has been shown that
52 ZAR1, encoded by an *R*-gene, is the basis of a structure called the resistosome and is directly
53 involved in initiating the hypersensitive resistance response (Wang et al., 2019a). When
54 activated, ZAR1 forms a pore within the cell wall that causes the cell to leak and leads to cell
55 death. Given the diversity of the potential antagonistic interspecific encounters, it is clear that
56 the range of recognition specificities and the ability to orchestrate appropriate downstream
57 responses cannot be achieved by a limited number of host defense proteins. Not surprisingly,
58 *R*-genes in plants are encoded by large multi-gene families (Jupe et al., 2013; Andolfo et al.,
59 2014; Gao et al., 2018; Lee & Chae, 2020). The largest class of *R*-genes is the NBS-LRR class,
60 which stands for Nucleotide Binding Sites (NBS) and Leucine Rich Repeats (LRRs; Jones &
61 Dangl, 2006). The recognition of effectors is typically mediated by the LRR-domain, while the
62 NBS-domain functions as a molecular switch, activating downstream components that initiate
63 plant defense (McHale et al., 2006). Other classes of *R*-genes encode enzymatic proteins and
64 lack NBS/LRR domains (e.g. *Hm1*, *Pto*, *Rpg1*; reviewed in Gururani et al., 2012).

65

66 A tight regulatory system controls the expression of *R*-genes (Stokes et al., 2002; Li et al., 2007;
67 Holt et al., 2005; Huot et al., 2014). One layer of regulation is mediated by transcription factors
68 which alter gene expression by binding to upstream elements of genes (reviewed in Latchman,
69 1997). Transcription factors can enhance or repress the expression of *R*-genes (e.g. ethylene-
70 responsive factor ERF; Chakravarthy et al., 2003). Another mode of gene regulation is RNA
71 silencing, a sequence-specific system that uses small non-coding RNAs (sRNAs) to repress gene
72 expression (reviewed in Baulcombe, 2004). These sRNAs are guided via sequence-
73 complementarity to target mRNAs which, together with Argonaute proteins, degrade or
74 inhibit translation of mRNA transcripts (Baulcombe, 2004). One example of such sRNA-
75 mediated gene suppression of *R*-genes is the microRNA (miRNA) superfamily miR482/2118
76 (Shivaprasad et al., 2012; de Vries et al., 2015; de Vries et al., 2018). Another mode of
77 transcriptional regulation is mediated through alternative splicing. In the context of *R*-genes,
78 it has been shown that different splice variants of the same *R*-gene can lead to the expression
79 of distinct R-proteins which underlie different resistance phenotypes (e.g. splicing variants
80 NAT and NRT of the resistance gene *N*; Yang et al., 2014).

81

82 The Solanaceae plant family harbors many economically important crops including potato,
83 tomato, eggplant, pepper and tobacco. As a chief non-cereal crop, potato cultivation yielded
84 487 million tons in 2017. Due to the economic significance of species in this plant family, a
85 large body of data is available regarding the genetic basis of pathogen resistance. This includes
86 well-described resistance gene repertoires and large-scale transcriptome studies of these
87 species from a range of tissues, time points, cultivars and pathogen treatments. In this study,
88 we analyzed the expression profiles of 940 *R*-genes from tomato and potato using 315
89 transcriptomes with and without pathogen treatment.

90

91 We determined that the majority of *R*-genes in tomato and potato are constitutively
92 expressed at a low level, irrespective of infection status. Based on our analyses, we could
93 define a core set of *R*-genes which are expressed in greater than 90% of all libraries in each
94 species. For tomato, the core set comprises 7.7% of the *R*-genes; in potato 16.6% of the *R*-
95 genes belong to the core set. Members of the core are well known *R*-genes such as *EDS1* and
96 *Pto* as well as NRC2, NRC3 and NRC4, powerful activators of immunity. Analysis of similarity
97 (ANOSIM) based on relative gene expression showed that the two main factors that explain
98 variation in *R*-gene expression are tissue type and “BioProject”. A BioProject is defined by NCBI

99 as a collection of biological data related to a single initiative, originating from a single
100 organization or from a consortium. Infection status and infection time were not associated
101 with significant differences in *R*-gene expression. In an independent analysis based on
102 differential gene expression of paired libraries, we determined that 11.9% of *R*-genes in
103 tomato and 8.6% in potato are differentially expressed in the presence of a microbe
104 treatment. In potato, the same proportion of genes are up-regulated or down-regulated, while
105 in tomato a larger proportion is up-regulated following treatment with microbes. The factors
106 BioProject, tissue type or distinction between treatment with beneficial or pathogenic
107 microbes were not associated with differential gene expression. These results indicate that
108 plants express a core set of *R*-genes, ensuring that they are in a permanent ready-to-defend
109 status. We find little evidence that this class of genes responds with large-scale transcriptional
110 reprogramming following exposure to pathogenic microbes.

111

112 **Material and Methods**

113 **Data set**

114 A total of 315 transcriptome datasets of tomato (Zouari et al., 2014; Du et al., 2015; Barad et
115 al., 2017; Sarkar et al., 2017; Sugimura & Saito, 2017; Xue et al., 2017; Yang et al., 2017; Zheng
116 et al., 2017; Chen et al., 2018; Shukla et al., 2018; Fawke et al., 2019; Pesti et al., 2019; Wang
117 et al., 2019b) and potato (Goyer et al., 2015; Zuluaga et al., 2015; Dees et al., 2016; Gao &
118 Bradeen, 2016; Kochetov et al., 2017; Levy et al., 2017; Li et al., 2017; Lysøe et al., 2017; Hao
119 et al., 2018; Kumar et al., 2018) were obtained from the Sequence Read Archive (Fig. S1).
120 These studies included treatments with potentially beneficial organisms (arbuscular
121 mycorrhizal fungi (AMF) and biocontrol agents) as well as detrimental organisms (pathogenic
122 bacteria, nematodes, fungi, viruses, viroids, insects and oomycetes). Only studies with at least
123 one mock treatment were included. The collected tissues included roots, stems, leaves, fruits
124 and tubers. The time points of sampling after infection range from 0 days post-infection (dpi)
125 up to 42 dpi or until the end of the host's life cycle (Fig. S1). Approximately 20% of all tomato
126 and potato cultivars were denoted as resistant to the applied pathogens.

127

128 ***R*-gene data set**

129 The lists of the *R*-gene repertoires of *S. lycopersicum* and *S. tuberosum* were retrieved from
130 Jupe et al. (2013). *R*-genes were classified as "full-length" NBS-LRRs if they contained both NBS
131 and LRR domains as identified using InterPro (Mitchell et al., 2019). A slightly modified pipeline
132 as described by Jupe et al. (2013) was used to verify their novel *R*-genes (Fig. S2). These novel
133 *R*-genes were designated by the authors as *R gene discovery consortium (RDC)* genes. Using
134 AUGUSTUS (version 3.3.1), a gene-prediction tool developed by Stanke et al. (2008), we
135 analyzed these *RDC* genes for coding regions and searched for NBS and LRR domains using
136 InterPro. *RDCs* were classified as true *R*-genes if they possessed a coding region and an NBS-
137 LRR domain. Otherwise they were excluded from further analysis. In cases in which multiple
138 splice variants were identified, the longest splice variant was analyzed. The well-established
139 *R*-genes *Pto* (Martin et al., 1993) and *EDS1* (Hu et al., 2005) from tomato were included in the
140 dataset. In total, the expression patterns of 359 *R*-genes of tomato and 581 *R*-genes of potato
141 were analyzed.

142

143 **Identification of physical clusters of *R*-genes**

144 *R*-genes were classified as belonging to a cluster when more than one *R*-gene was located in
145 a region of 200 kilobases (kb) on a chromosome (van de Weyer et al., 2019). Since Jupe et al.
146 (2013) performed their analysis on an earlier release of the tomato genome assembly (ITAG2.4

147 release, Tomato Genome Consortium, 2012), the positions of all tomato *R*-genes had to be re-
148 defined (Table S1). Positions of *RDCs* were verified using Blastn v2.6.0 (Altschul et al., 1990;
149 Camacho et al., 2009) against the tomato (ITAG4.0; Hosmani et al., 2019) and potato genomes
150 (PGSC_DM_v4.03; Potato Genome Sequencing Consortium, 2011; Table S1). All *R*-genes
151 without defined chromosomal positions (39 genes in tomato) were classified as *R*-genes with
152 unknown clustering.

153

154 **miRNA targeting prediction**

155 To predict potential regulation of *R*-genes by the miR482-superfamily (de Vries et al., 2015),
156 we used psRNATarget (release 2017; Dai et al., 2018). We used the coding sequence (CDS) of
157 our *R*-genes as the target library. To ensure a low rate of false-positives, the maximum
158 expectation was set to ≤ 3 , since higher expectation values represent less likely mRNA/miRNA
159 interactions. We evaluated the likelihood of an *R*-gene being targeted by the miR482
160 superfamily and whether the *R*-gene encoded a full length NBS-LRR and or belonged to a *R*-
161 gene cluster using a chi-square test (Greenwood & Nikulin, 1996).

162

163 **Calculation of transcript abundances using Kallisto**

164 The program Kallisto (v.0.46.0) was used to estimate the relative expression of genes in
165 tomato and potato (Bray et al., 2016). As a first step, the raw sequence reads were compared
166 to the transcript sequences. This step in Kallisto is designated as the pseudoalignment step.
167 To improve the quality of the pseudoalignment, low-quality reads and adapters were removed
168 from the transcriptomes using Trimmomatic (Bolger et al., 2014; Fig. S2). Subsequent quality
169 controls were performed using FastQC (Andrews, 2010). As Kallisto requires information on
170 fragment length for single-end sequenced transcriptomes, the fragment length denoted by
171 the authors was used. If this information was not available, the recommended fragment
172 length of the reported RNA isolation kit was used. The standard deviation was set to ± 17.5 bp.
173 Kallisto indices (used for generating the pseudoalignments) were based on the tomato
174 ITAG4.0 and the potato PGSC_DM_v4.03 genome releases. *R*-genes missing from the current
175 genome releases were manually added to the list of transcripts (indices in Kallisto). Transcript
176 abundance was calculated as transcripts per million (TPM; Wagner et al., 2012). We chose to
177 use TPM since it normalizes the transcript abundance for gene length and sequencing depth,
178 making TPM values comparable across experiments. Genes for which the TPM values were
179 less than 1 were treated as "off" and for these genes, TPM was set to zero.

180

181 **Comparison of gene expression across gene sets**

182 To compare the mean relative expression between *R*-genes (*R*-gene set size for tomato = 359
183 and for potato = 581) and non-*R*-genes (the rest of genome) we generated 100 replicate
184 datasets for each transcriptome by sampling the TPM values of 359 random genes from
185 tomato and 581 random genes from potato. The average TPM of all expressed genes was
186 calculated for each replicate dataset. To compare expression values, four reference genes
187 were used: ubiquitin (*Solyc09g018730.4.1*), actin4 (*Solyc04g011500.3.1*), an importin subunit
188 (*PGSC0003DMG400007289*) and elongation factor-1 (*PGSC0003DMG400023270*). TPM values
189 were tested for normality using the Anderson-Darling (> 5000 data points; Thode, 2002) or
190 Shapiro test (< 5000 data points; Shapiro & Wilk, 1965) and for equal variances using the test
191 from Kendall (1938). Significant differences in expression were identified using a Mann-
192 Whitney-U test (Mann & Whitney, 1947) for non-normally distributed data or a two-sample t-
193 test for normally distributed data.

194

195 We visualized *R*-gene expression using heatmaps created in R (v. 3.6.1). Genes were classified
196 as off (if TPM < 1) or on (if TPM ≥ 1). In the heatmaps, libraries were clustered by similarity in
197 patterns of expression between libraries and *R*-genes were sorted by the number of libraries
198 expressing the corresponding gene. Correlations between 1) the total number of expressed *R*-
199 genes and the total number of expressed genes, 2) the total number of expressed genes and
200 the number of pseudo-aligned reads, as well as 3) the number of libraries in which an *R*-gene
201 was expressed and the average level of expression of each *R*-gene were performed using a
202 Spearman's rank correlation test (Hollander et al., 2013).

203
204 To investigate the extent to which expression patterns of *R*-genes were similar to wild close
205 relatives of tomatoes, we evaluated additional transcriptomes of four wild tomato species: *S.*
206 *peruvianum*, *S. chilense*, *S. ochranthum*, and *S. lycopersicoides* (Beddows et al., 2017). A subset
207 of *R*-genes was further analyzed for their patterns of sequence variation within and between
208 these wild species. Standard population genetic parameters including intraspecific variation
209 (π) and interspecific divergence (K) were estimated using DNaSP v. 5.10 (Librado & Rozas,
210 2009).

211 212 **Multivariate analysis of expression differences**

213 To identify the factors associated with differences in expression of *R*-genes across
214 transcriptomes, we performed an ANOSIM in Primer 7.0.13 (PRIMER-e; Fig. S2). ANOSIM is a
215 non-parametric statistical test similar to ANOVA. The starting point of the analysis is a pairwise
216 dissimilarity matrix. In our case, the dissimilarity matrix was computed as follows: First the
217 TPM values for each gene within each transcriptome were LOG (x+1) transformed. On the
218 basis of these transformed TPM values, the dissimilarity in gene expression patterns between
219 transcriptomes were calculated based on Euclidean distances. Ranking was applied to the
220 distance matrix. The two libraries from potato (SRR6511453 and ERR791944) with
221 exceptionally low expression of the entire *R*-gene repertoire were excluded in these analyses.

222
223 To determine if gene expression is more similar within groups than between groups (for
224 example when groups are defined by infection status or tissue type) the R test statistic value
225 was calculated. The R values can range from -1 to 1, with larger values corresponding to
226 greater differences between groups. Statistical significance is calculated through permutation
227 of the group labels and recalculation of the R value for each replicate. In our case, 999
228 permutations were generated. The following factors were evaluated: BioProject, tissue type,
229 type of treatment, specific treatment organism, life cycle of the organism, type/kingdom of
230 the organism, susceptible vs. resistant cultivar, relative read depth, paired- or single-end
231 sequencing and days post infection. The ANOSIM analysis was also applied to the differential
232 gene expression data (see below).

233 234 **Differential expression analysis**

235 Differentially expressed genes between microbe treatments and mock treatments were
236 identified using Sleuth (Pimentel et al., 2017; Fig. S2). The p-values were adjusted using the
237 Benjamini-Hochberg correction (FDR ≤ 0.05; Benjamini & Hochberg, 1995). Since Sleuth relies
238 on replicates within treatments, BioProjects without replicates were removed from this part
239 of analysis. Fold changes in the libraries were tested for normality, equal variances and
240 significant differences between i) *R*-genes and all genes, ii) proportion of up- versus down-
241 regulation and iii) average absolute fold changes.

242

243 Results

244 Large scale analysis of expression patterns of *R*-genes

245 In total we analyzed 7.78×10^9 raw reads from 315 transcriptomes of tomato and potato of
 246 which 5.58×10^9 could be uniquely assigned to a transcript from tomato/potato (average
 247 proportion of assigned reads: 77.3% for tomato and 66.8% for potato; Fig. S3). Both mock-
 248 inoculated plants as well as plants inoculated with pathogenic and beneficial organisms were
 249 investigated. In total, 359 *R*-genes from tomato and 581 from potato were examined for their
 250 expression levels and fold changes. In tomato, 62.1% of all *R*-genes possessed NBS- and an
 251 LRR-domains and in potato 89.2% did (Fig. S4, Table S1). A large majority of the *R*-genes of
 252 both species formed physical clusters meaning that two or more *R*-genes were found in a span
 253 of 200kb along the chromosome (62.6% in tomato; 83.1% in potato).

254
 255 Since the miR482-superfamily is a known regulator of NBS-LRR expression (Shivaprasad et al.,
 256 2012; de Vries et al., 2015; de Vries et al., 2018), we evaluated the targeting probability by
 257 members of the miR482 gene family for each *R*-gene. In tomato 17.6% of all *R*-genes were
 258 predicted to be targeted by the miR482-superfamily, while in potato 28.6% were predicted to
 259 be targeted (Fig. S4, Table S1). It has previously been shown that miR482-members regulate
 260 *R*-genes by reverse-complementary binding to the mRNA region encoding NBS-domains
 261 (Shivaprasad et al., 2012). Full length *R*-genes were more likely to be predicted to be regulated
 262 by the miR482-superfamily compared to partial length NBS-LRR genes ($\chi^2_{\text{tomato}} = 21.32$, p-
 263 value < 0.001 ; $\chi^2_{\text{potato}} = 14.69$, p-value < 0.001 ; Fig. S4; Table S2).

265 Most *R*-genes show consistently low expression, both in the presence and absence of 266 pathogens

267 Proteins encoded by *R*-genes act as key regulators of plant immunity by recognizing plant
 268 pathogens and activating the plant immune response. However, the existence of growth-
 269 defense trade-offs implies that the constitutive expression of *R*-genes in the absence of
 270 pathogens might be costly (reviewed in Brown & Rant, 2013; Vos et al., 2013). In this
 271 comparative study, a large proportion of the *R*-gene repertoire in tomato ($67.6\% \pm 13.8\%$) is
 272 not expressed in a given library (or is below the threshold of detection) whether or not the
 273 plant was treated with an interacting organism (Fig. 1a). In contrast, a lower proportion (only
 274 $\sim 46\%$) of the non-*R*-genes are "off" or below the threshold of detection (Fig. 1a). For potato,
 275 the proportion of the *R*-gene repertoire that is not expressed is 49.3% ($\pm 11.7\%$); this is nearly
 276 equal to the proportion of genes that are not expressed in the rest of the genome (Fig. 1b).

277
 278 In both species, the average TPM of *R*-genes per library is significantly lower than the average
 279 TPM of an equal number of randomly selected genes per library (p-value < 0.001 ; Fig. 1c, S5).
 280 Of the *R*-genes that are expressed, most are expressed at very low levels within each library
 281 (between 1 and 10 TPM). Approximately one quarter of *R*-genes in tomato ($25.9\% \pm 8.4\%$) and
 282 44.0% ($\pm 9.8\%$) of *R*-genes in potato are expressed at this level. Less than 1% of the *R*-genes
 283 fall into the medium ($50 \leq \text{TPM} < 200$) or high ($200 \leq \text{TPM} < 1000$) expression classes, a scant
 284 proportion for these two expression classes compared to non-*R*-genes (Fig. 1a and 1b).

285
 286 The distribution of the expression classes for *R*-genes varies greatly across libraries (Fig. S6).
 287 For example, 88.3% of *R*-genes are not expressed in library SRR7073605, while in library
 288 SRR442353, 47.0% are not expressed (Fig. S6). Although the relative transcript abundance of
 289 a few *R*-genes can be high, the average TPM of the top 10% (or even the top 5%) is still well
 290 below the average TPM across all other genes in the genome for a given library (Fig 1c; S5; p-

291 value_{tomato} <0.001; p-value_{potato} <0.001). Taken together, most *R*-genes are typically expressed
 292 at low to extremely low levels across libraries.

293
 294 In our study, the overall distribution of expression classes of *R*-genes is similar between plants
 295 treated with interaction partners versus untreated controls (Fig. 1a-b, S6). However,
 296 conditioning on only the expressed *R*-genes in each individual library, the average expression
 297 level (measured as TPM) of these expressed *R*-genes is significantly higher in tomato plants
 298 treated with microbes compared to mock treated controls (p-value <0.05; Fig. 1c). This effect
 299 was specific for treatment with pathogenic organisms: We observed that the average TPM-
 300 values for expressed *R*-genes (TPM >1) was higher in tomato plants exposed to pathogenic
 301 organisms compared to plants exposed to beneficial microbes (p-value <0.001; Fig. S7a). In
 302 contrast, in potato no difference in the average expression of *R*-genes between treated and
 303 untreated plants, nor between the types of treatments (pathogenic versus beneficial) could
 304 be detected (p-value >0.05; Fig. S5; p-value = 0.58; Fig. S7b).

305
 306 **Some *R*-genes are consistently expressed across libraries**

307 We observed that some *R*-genes were expressed (TPM ≥1) under both challenged and
 308 unchallenged conditions. Therefore, the question arose if these *R*-genes represent a "core set"
 309 of expressed *R*-genes across all libraries. Approximately 7.7% of all *R*-genes in tomato are
 310 expressed in > 90% of all analyzed libraries (Fig. 2a). In potato, 16.6% of all *R*-genes were
 311 expressed in >90% of all libraries (Fig. S8a). Among these expressed "core" *R*-genes in tomato
 312 are *EDS1*, *Pto*, *NRC2*, *NRC3* and *NRC4*. Wu et al. (2017) identified these NRCs as part of a
 313 complex network in Solanaceae in which the NRCs (*Solyc10g047320*, *Solyc05g009630*,
 314 *Solyc04g007070*) interact with NBS-LRR sensors to activate resistance.

315
 316 We evaluated whether this set of expressed "core" *R*-genes shared other characteristics. We
 317 found that the mean TPM-value of an *R*-gene within a library was positively correlated with
 318 expression breadth as defined as the number of libraries in which it was expressed (correlation
 319 factor $\rho_{\text{tomato}} = 0.39$, p-value <0.000, $\rho_{\text{potato}} = 0.47$, p-value < 0.000, Fig. S9a, b). Therefore,
 320 this set of expressed "core" *R*-genes has both higher relative expression within a library and
 321 broader expression across libraries than non-core *R*-genes.

322
 323 The total number of *R*-genes expressed per library varied from 27 to 191 in tomato, with a
 324 mean proportion of ~30 % of *R*-genes expressed in a given library (Table S3; Fig. S10a). For
 325 potato, the number of *R*-genes expressed per library ranged from 1 to 421 *R*-genes, with a
 326 mean proportion of 50.8% of the *R*-genes expressed in a given library (Table S4; Fig. S10b). We
 327 also evaluated whether the proportion of expressed *R*-genes correlated with the total number
 328 of expressed genes in a given library. In both potato and tomato, libraries in which a larger
 329 number of genes were expressed also had a higher proportion of expressed *R*-genes ($\rho_{\text{tomato}} = 0.84$,
 330 $\rho_{\text{potato}} = 0.71$, p-value <0.000; Fig S9c, d). We investigated how the distribution of the
 331 proportion of *R*-genes expressed correlated with the proportion of assigned reads (as a proxy
 332 for sequencing quality). Overall, we detected a weak positive correlation between both factors
 333 ($\rho_{\text{tomato}} = 0.39$, $\rho_{\text{potato}} = 0.42$, p-value <0.001; S9e, f).

334
 335 **Factors associated with variation in *R*-gene expression across libraries are BioProject and
 336 tissue type**

337 We applied an ANOSIM method to evaluate which factors were associated with variation in *R*-
 338 gene expression across the libraries (Table 1; Table S5; Table S6). In the ANOSIM analysis,

339 higher R-values indicate a larger influence of a factor on the patterns of gene expression. The
340 factor with the highest R-value for *R*-genes was BioProject ($R\text{-value}_{\text{tomato}} = 0.876$, $p\text{-value}$
341 <0.001 ; $R\text{-value}_{\text{potato}} = 0.928$, $p\text{-value} <0.001$, Table 1). Differentiation by BioProject is also
342 apparent in the principal component analysis (PCA, Fig. 2b, c, Fig. S8b, c). Libraries clustering
343 closer together in the PCA indicate those with more similar expression patterns. In this study,
344 the factor BioProject corresponds to the set of libraries submitted by a single lab group. In
345 total, 13 BioProjects for tomato were studied and 12 BioProjects for potato. The number of
346 libraries submitted as part of a BioProject ranged from as low as two and up to 36. In some
347 cases, BioProjects sampled only a single tissue type; other BioProjects sampled multiple tissue
348 types. Most BioProjects focused only on a single potato or tomato cultivar. Individual
349 BioProjects typically included one main treatment organism, except for a handful which
350 studied two or more organisms. Due to the diversity of projects in terms of plant genotypes,
351 type of microbial challenge and time of sampling and since the sampling was not based on a
352 nested design, the large effect of the BioProject is not unexpected. However, the value of such
353 a meta-analysis is that robust and consistent patterns of gene expression that do emerge from
354 this study, in the face of a large amount of experimental variation across labs, are likely to be
355 highly reliable because a wide range of sampling conditions were included (different lab
356 conditions, different cultivars, different time of sampling, different treatments, etc.).
357 Furthermore, this type of analysis can be used to identify key experiments that are missing
358 (such as tissue type, time of sampling, cultivar, or pathogen) that if included could provide the
359 necessary cross-lab validation of patterns.

360
361 Despite a large effect of BioProject, gene expression was also strongly affected by tissue type
362 ($R\text{-value}_{\text{tomato}} = 0.527$, $R\text{-value}_{\text{potato}} = 0.758$, $p\text{-value} <0.001$) and days post infection ($R\text{-}$
363 $\text{value}_{\text{tomato}} = 0.408$, $R\text{-value}_{\text{potato}} = 0.522$, $p\text{-value} <0.001$; Table 1; Fig. 2d, e; Fig. S8d, e). All
364 other evaluated factors (type of treatment, life cycle of the organism, susceptible vs. resistant
365 cultivars, specific treatment organism, type/kingdom of the organism) were characterized by
366 lower R-values (Table 1). Library dependent parameters such as relative read depth ($R\text{-}$
367 $\text{value}_{\text{tomato/potato}} = 0.297/0.119$, $p\text{-value}_{\text{max}} <0.001$) and paired- or single-end sequencing ($R\text{-}$
368 $\text{value}_{\text{tomato/potato}} = 0.358/0.218$, $p\text{-value}_{\text{max}} <0.001$) were also characterized by low R-values
369 (Table 1). Furthermore, the rank order of the factors according to R-values did not differ
370 depending upon the classification of *R*-genes into the following categories: full-length versus
371 partial, miR482-targeted versus not targeted or clustered versus not clustered (Table S7). The
372 ANOSIM analyses of all coding genes did not deviate significantly from the analyses of the *R*-
373 genes alone (Table 1; Fig. 2c, e; Fig. S8c, e).

374
375 In a sub-analysis, we performed ANOSIM on the mock-treated libraries only. For the mock-
376 treated libraries, the BioProject ($R\text{-value}_{\text{tomato/potato}} = 0.911/0.936$, $p\text{-value}_{\text{max}} <0.001$) and the
377 tissue type ($R\text{-value}_{\text{tomato/potato}} = 0.561/0.789$, $p\text{-value}_{\text{max}} <0.001$) remain the two dominant
378 factors associated with differences in *R*-gene expression (Table S8; Fig. S11). In a separate sub-
379 analysis of organism-treated libraries only, the R-values for multiple factors increased
380 compared to the ANOSIM analyses of all libraries together (Table S8, Fig. S12). For example,
381 the R-values for the factor "specific organism" was $R=0.264$ in tomato and $R=0.104$ in potato
382 when all available libraries were included. The R-value for this factor increased to $R=0.889$ in
383 tomato and $R=0.85$ potato when only microbe treated libraries were analyzed. This was also
384 true for the related factors "life cycle of the organism" and "type of organism".

385
386

387 **Similar expression patterns extend to closely related wild species**

388 In tomato, 27.5% of the *R*-gene repertoire is not expressed in any library (Fig. 2a). Even under
 389 this wide range of experimental conditions and treatments, these *R*-genes seem to be "off".
 390 In a previous study, we evaluated the transcriptomes of 38 individuals of wild close relatives
 391 of cultivated tomato, namely *S. chilense*, *S. peruvianum*, *S. ochranthum*, and *S. lycopersicoides*
 392 (Beddows et al. 2017). Using this dataset, we evaluated whether any of these *R*-genes that are
 393 "off" in cultivated tomato are "on" in the wild genotypes. Expression was detected for ~35%
 394 of these genes, although the expression was restricted to a few libraries (Fig. S13, Table S9).
 395 Five *R*-genes which were "off" in the studies of cultivated tomatoes (*Solyc01g102920*,
 396 *Solyc01g102930*, *Solyc06g065150*, *Solyc10g079020* and *Solyc12g038890*) were expressed in
 397 >30% of all libraries from the wild species, although their overall relative expression was still
 398 low (\emptyset 1.8-6.6 TPM).

399
 400 For these five *R*-genes which are "off" in all libraries from cultivated tomatoes, but "on" in a
 401 subset of wild genotypes, we evaluated whether these genes showed the genetic signatures
 402 of evolutionary constraint within the population sample from our earlier study (Beddows et
 403 al, 2017). A signature consistent evolutionary constraint (or purifying selection) may indicate
 404 that these *R*-genes are still functionally intact in wild tomato species and could be exploited
 405 for crop improvement in the cultivated tomato. The low π_a/π_s ratios within species and K_a/K_s
 406 ratios between species indicated that purifying selection is the dominant force acting on these
 407 five *R*-genes in wild tomatoes (Table S10).

408 409 **Differential regulation of *R*-genes in the presence of pathogens**

410 We evaluated the differential regulation of *R*-genes in the presence and absence of biotic
 411 treatments (Table S11, S12). This included 26 datasets in tomato and 29 datasets in potato.
 412 On average, 11.9% of *R*-genes were differentially expressed in the presence of pathogens in
 413 tomato and 8.6% in potato (Fig. 3a, S14a). Of these significantly differentially expressed genes
 414 in tomato, a larger proportion were up-regulated (72.5%) compared to down-regulated
 415 (27.5%; p-value <0.05; Fig. 3b). In potato, the proportion of up- versus down-regulated genes
 416 was not statistically different (up = 54.1%, down = 45.9%, p-value >0.05, Fig. S14b). In tomato,
 417 the proportion of genes differentially up- or down-regulated was not statistically different
 418 between the class of *R*-genes and the rest of the genes in the genome (p-value >0.05; Fig. 3b).
 419 In potato the proportion of down-regulated genes is lower for the class *R*-genes compared to
 420 the rest of the genes in the genome (p-value <0.05; Fig. S14b). Of the differentially expressed
 421 genes, the mean of the absolute fold change did not differ between the class of *R*-genes and
 422 the rest of the genes in the genome (Fig. 3c, S14c). However, the mean of the absolute fold
 423 change for differentially up-regulated *R*-genes is significantly larger than the fold change of
 424 differentially down-regulated *R*-genes in tomato (Fig. 3c).

425
 426 The patterns of differential expression of *R*-genes are shared across datasets (Fig. 3a, Fig.
 427 S14a). However, in contrast to the previous ANOSIM analysis based on expression investment
 428 in *R*-genes (as captured by TPM values), variation in differential gene expression is not
 429 associated with the same factors such as BioProject or tissue type (Fig. S15, Table S13, S14,
 430 S15). Likewise, the assignment of *R*-gene type in terms of full-length versus partial, miR482-
 431 targeted versus not targeted or clustered versus not clustered did not correlate with the
 432 likelihood of differential regulation (Table S13). It is known that about 20% of *R*-genes in
 433 tomato are targeted by the miR482-superfamily (de Vries et al., 2015). In the presence of
 434 pathogens, microRNA processing is down-regulated (Shivaprasad et al., 2012; de Vries et al.,

2018). This should lead to a release of the suppression and consequently up-regulation of *R*-genes targeted by miR482 members in pathogen-infected plants. We tested whether *R*-genes predicted to be regulated by miR482 were over-represented in the class of up-regulated *R*-genes in the presence of pathogens. This was not the case. The *R*-genes predicted to be targeted by miR482 were neither enriched nor depleted in the set of differentially regulated *R*-genes (p -value > 0.05; Table S16).

We evaluated the level of shared differential regulation between plants treated with pathogens versus treated with putatively beneficial microbes. In tomato, only three *R*-genes were differentially regulated in the presence of beneficial microbes, two of which were also differentially down-regulated in pathogen treated plants (Fig. S16). In potato, a larger number of genes were differentially regulated in the presence of beneficial microbes and a large proportion of these overlapped with the genes that are differentially expressed in pathogen treated plants (Fig. S16). Only a single *R*-gene (*PGSC0003DMT400014280*) was differentially up-regulated in plants treated with beneficial microbes and was not differentially expressed in plants treated with pathogens. For the set of *R*-genes that are exclusively up- or down-regulated in pathogen treatments, most are limited to specific pathogen treatments, showing a high degree of pathogen specificity.

Discussion

A long-standing objective in genetics and evolutionary biology is to understand which factors affect gene expression. Expression of *R*-genes is of particular interest for plant biologists due to the relevance of this class of genes in crop protection and to understand host-pathogen dynamics in both natural and agricultural settings. Taking a meta-analysis approach, we evaluated the amplitude of expression variation across *R*-genes in tomato and potato and the underlying factors associated with expression differences. By focusing on transcriptome studies that involved treatments with known pathogenic or beneficial organisms, we could specifically address the question whether *R*-genes were modulated by treatment with these organisms. We discovered that pathogen-treated plants showed only relatively modest differences in *R*-gene expression, despite the long-standing belief that pathogen induced resistance would be most effective at restricting pathogen growth, while avoiding high fitness costs in the absence of pathogens.

Fitness costs of *R*-genes have been thoroughly investigated in a handful of cases. In *A. thaliana*, for example, Tian et al. (2003) and Karasov et al. (2014) determined that the presence of the *R*-genes *RPM1* and *RPS5* in the absence of pathogen infection reduced seed production by ~10%. Furthermore, transient expression of several *R*-genes can induce a hypersensitive response (HR) resulting in cell death, which is costly in the absence of pathogen infection (Kim et al., 2010; Chae et al., 2014). Hence specific induction of defenses only when the pathogen is present should be beneficial. In our study, we did not see a strong induction of *R*-genes in the presence of pathogens. On the contrary, we detected a core of constitutively expressed *R*-genes in tomato and potato. Although these genes were expressed at low levels, their expression was mainly insensitive to different treatments and showed no specific up-regulation in the presence of pathogen treatment.

Does this indicate that the possession and expression of *R*-genes are less costly than expected? Burdon & Thrall (2003) surmised that it is unlikely that all *R*-genes possess the same high fitness costs since the additive or multiplicative effects would be prohibitive. Therefore, the

483 high fitness costs documented for single *R*-genes such as *Rpm-1* (Tian et al., 2003) are most
484 likely the exception and not the rule. However, it should be noted that fitness costs are
485 inherently difficult to estimate, in part because costs are not constant over time and under all
486 conditions. Fitness costs can be influenced by many factors such as environmental conditions,
487 plant age, genetic background and pleiotropic effects – the effect of a single gene on multiple
488 traits (McDowell et al., 2005; Krasileva et al., 2011; MacQueen & Bergelson, 2016). For
489 example, while young plants likely face high competition for resources and are strongly
490 constrained in defense allocation, older plants, having already established themselves, may
491 have more resources to allocate to defense. It is likely that growth-defense tradeoffs may be
492 stronger during certain timepoints of a plant's life history. Therefore, the costs and benefits
493 of expressing *R*-genes are likely to be strongly dependent on specific environmental
494 circumstances and depend upon pre-existing growth-defense tradeoffs. Taken together, our
495 discovery of a core of constitutively expressed *R*-genes indicates that the expression and
496 possession of at least some *R*-genes might be less costly than anticipated or that their benefits
497 greatly outweigh their costs.

498
499 What is the function of this core of constitutively expressed *R*-genes? Brown and Rant (2013)
500 speculate that the constitutive expression of *R*-genes might be stimulated by exposure to the
501 natural microbial communities, since some *R*-genes were only induced by pathogens under
502 non-sterile conditions, but not induced in aseptic (but pathogen-treated) plants. Constitutively
503 expressed *R*-genes likely serve as a constant monitor of the plants intimate cellular
504 environment, contributing to the plant's ability to distinguish friend and foe. Plants failing to
505 perceive and distinguish between beneficial or pathogenic organisms may either permit
506 colonization by pathogenic organisms or overreact to non-pathogenic organisms with a
507 defense response. How plants discriminate between organisms is only partially understood.
508 However, it is becoming clearer that *R*-genes may play a role in this discrimination. For
509 example, Yang et al. (2010) showed that the species-specific activation of *R*-genes is essential
510 for establishing symbiosis between soybeans and nitrogen-fixing bacteria. Another hypothesis
511 is that this constitutive core serves a dedicated function, such as a constituent of the plant
512 resistosome (Wang et al., 2019a). Such genes would be expressed, but these encoded proteins
513 lie in wait in a repressed state until other host molecules, dedicated to pathogen detection,
514 activate these proteins.

515
516 The class of core, constitutively expressed *R*-genes constitutes a relatively small proportion of
517 all putative *R*-genes in these genomes. However, it seems plausible that a range of functional
518 diversity would be advantageous to discriminate between the large diversity of microbes a
519 plant encounters across its lifetime. While some *R*-proteins are known to possess dual
520 recognition of completely different pathogens (*Mi-1* gene in tomatoes for example), it has
521 been hypothesized that these *R*-proteins might incur higher fitness costs compared to ones
522 specific to a more limited set of pathogen molecules (Gururani et al., 2012; Brown & Rant,
523 2013). Therefore, an expansion of a constitutive *R*-gene repertoire with distinct recognition
524 functions may be advantageous. This would allow the plant to mount an optimal
525 pathogen/species specific response. For example, activation of HR might be effective to
526 restrict the growth of biotrophic pathogens which require living host tissue; however
527 necrotrophic pathogens may actually benefit from the activation of HR since they feed on
528 dead tissue. Likewise, defense against pathogenic fungi can be achieved through the
529 activation of chitinases, but chitinases would be ineffective against organisms lacking chitin in
530 their cell walls. Furthermore, the diverse repertoire of core *R*-genes might reflect differences

531 in how plants perceive potential invaders. Some *R*-proteins detect infections by direct binding
532 of pathogenic effectors (consistent with the gene-for-gene hypothesis; Flor, 1971); other *R*-
533 proteins monitor host proteins that are modified by pathogens (reviewed in Jones & Dangl,
534 2006). To cover these different functions, a diverse group of specialized *R*-genes is needed.

535

536 While some *R*-genes are constitutively expressed, others showed variable expression across
537 libraries. Only a small proportion of this variation in expression was affected by treatment
538 with pathogenic organisms. Instead, this cross-sectional study revealed that many *R*-genes
539 showed tissue-specific expression. This mirrors prior studies in other species reporting tissue-
540 specificity of *R*-genes including a transcriptome study in chickpeas (Sharma et al., 2017) as well
541 as for individual *R*-genes. For example, *CreZ*, an *R*-gene in wheat is only expressed in the root
542 while the *R*-gene, *CaMi*, in peppers is expressed in flowers, leaves and roots but not in fruits
543 (Chen et al., 2007; Zhai et al., 2008). Tissue-specific expression of *R*-genes might be related to
544 underlying differences of the structures and functions of these tissues and their regulatory
545 networks. Obviously, leaves are exposed to wider fluctuations in temperature and light than
546 roots. Furthermore, leaves and roots differ fundamentally in their main functions:
547 photosynthesis and respiration for leaves versus storage and transport for roots. However,
548 tissue specific *R*-gene expression may also be driven by adaptation to the tissue-associated
549 microbiome (and by extension to specialized pathogens). Since microbes display a high degree
550 of tissue-specificity, evolution may have favored the selection for defenses to be deployed
551 where the encounter likely takes place (Jin et al., 2015; Sapp et al., 2018; Maggini et al., 2019).

552

553 About 20% of the *R*-genes in tomato and potato are predicted to be targeted by the miR482-
554 family (de Vries et al., 2015). This subset of *R*-genes would be predicted to be released from
555 miR482 suppression during pathogen treatment and consequently be up-regulated
556 (Shivaprasad et al., 2012). However, we did not detect a significant up-regulation of these
557 predicted *R*-gene targets in the presence of pathogens. One explanation for this might be that
558 not all pathogens downregulate the microRNA processing machinery. Furthermore, the failure
559 to detect a pathogen-specific change in regulation in the subset of *R*-genes predicted to be
560 targeted by the miR482 family may be linked to the low relative expression of *R*-genes on
561 average compared to other genes in the genome. Detecting relative expression differences of
562 genes with a low average expression is more difficult, compared to genes which show a larger
563 amplitude of expression. Furthermore, repression of *R*-genes by miR482 is not exclusively
564 restricted to uninoculated plants (de Vries et al., 2018). Using 5' RACE, we detected the
565 degradation products of three *R*-genes (*Solyc02g036270*, *Solyc08g075630*, *Solyc08g076000*)
566 both in the presence and absence of pathogen treatment. This points to a more general role
567 of miR482 in gene regulation, independent of pathogen treatment. Therefore, although
568 modulation of *R*-gene expression by members of the miR482 is known to take place in nature,
569 regulation by this microRNA family is only one of many factors that likely influencing *R*-gene
570 expression.

571

572 Our meta-analysis included a handful of experiments conducted in parallel on susceptible and
573 resistant cultivars inoculated with the same pathogen. This made it possible to test whether
574 the expression profiles of resistant and susceptible cultivars differed in a unified manner
575 following pathogen treatment. Although it might be predicted that expression profiles should
576 differ between resistant and susceptible cultivars, we did not detect any consistent
577 differences in the *R*-gene responses between resistant and susceptible cultivars. This may be
578 due to the fact that only a small proportion of genes (or even small differences in gene

579 expression) may be sufficient to confer isolate-specific resistance and that these differences,
580 when present, are not shared across different resistant cultivars. This means that resistant
581 lines do not express a shared resistance syndrome dictated by a uniform transcriptional re-
582 programming following pathogen infection.

583

584 One of the strengths as well as a limitation of our study is the fact that such a large diversity
585 of cultivars, pathogen strains and sampling methods (for example, timepoint or tissue type)
586 were analyzed. On the one hand, this means that consistent signals or patterns in the data are
587 reproducible across a wide range of environments and genotypes. For example, we discovered
588 that a subset of *R*-genes appears to be more or less constitutive and another subset appear to
589 be "off". With a large number of datasets created under lab-specific settings and using
590 different host genotypes and pathogens, these consistent patterns can be viewed as robust,
591 despite the "noisiness" of the data. On the other hand, this diversity in datasets poses a
592 problem, because each experiment was designed with slightly different aims in mind (different
593 host genetic backgrounds, different pathogen species, different tissues sampled, different
594 sampling times, etc.). This made it difficult to unambiguously attribute observed expression
595 differences to the ultimate underlying cause. We observed that BioProject itself accounts for
596 a large amount of the variation in expression. However, BioProjects often differ jointly in a
597 number of factors including cultivar and the pathogen used. Therefore, when we detect clear
598 expression differences, it is not obvious which factor has the greatest influence. This is one
599 motivation for full-factorial designs, which are currently not available for this combination of
600 species. Using such a meta-analysis however, one can quickly reveal which key experiments
601 are missing and which new experiments could, in conjunction with older work, begin to
602 approach a full-factorial design. Nevertheless, this meta-analysis has uncovered a large core
603 of constitutively expressed *R*-genes and a robust signal of tissue-specific expression of *R*-
604 genes.

605

606 **Acknowledgements**

607 We thank the members at the Institute of Population Genetics for their assistance in this work.
608 We especially thank Thorsten Kloesges for his assistance with the data processing and
609 technical support. This work was supported by the Deutsche Forschungsgemeinschaft Grant:
610 Ro 2491/6-1, GRK 1525, and EXC-2048/1 – project ID 390686111.

611

612

613

614

615

616

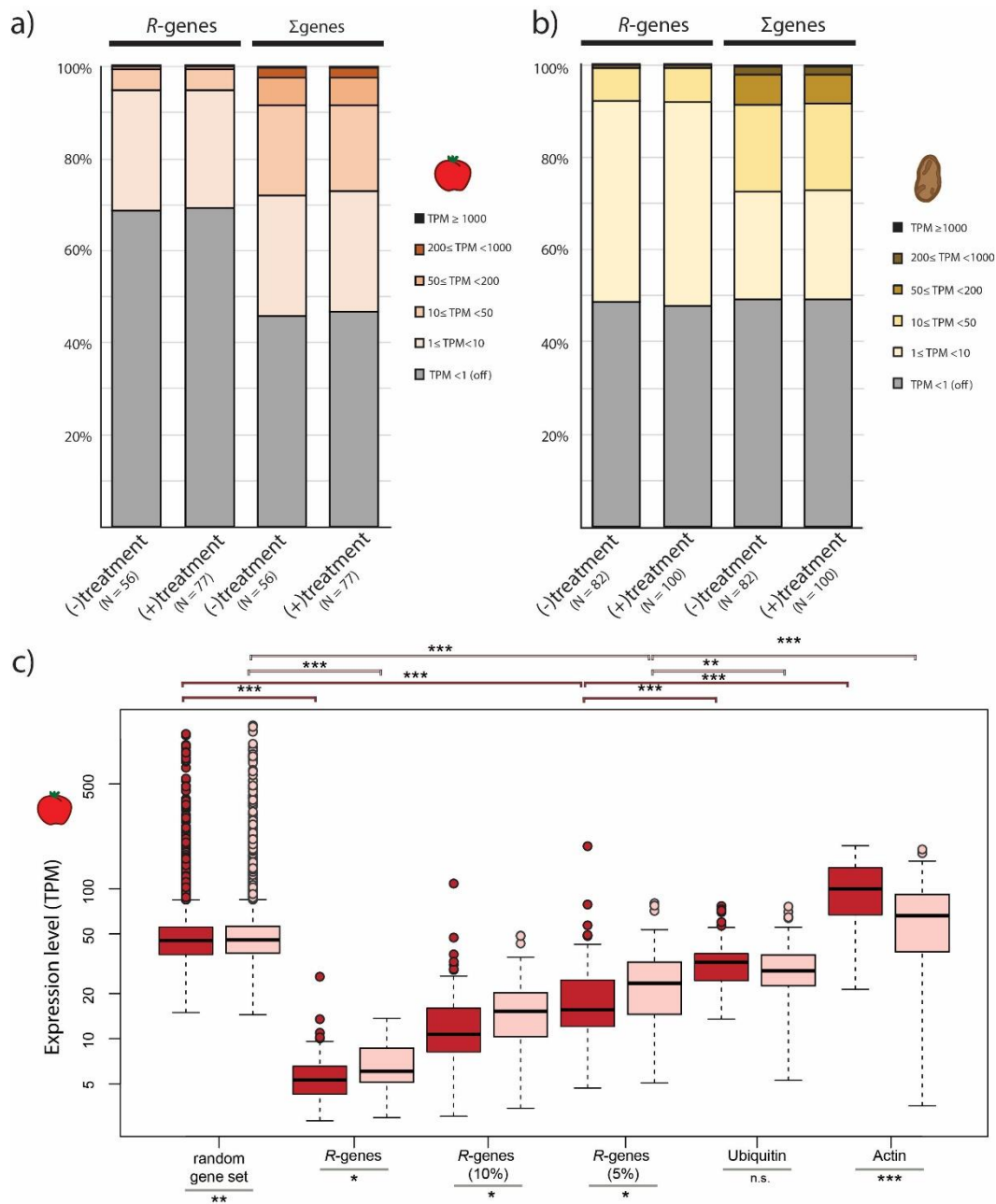
617

618

619

620

621

622 **Figures & Tables**

623

624 **Figure 1: Comparison of relative gene expression in tomato and potato**625 Relative expression of *R*-genes compared to the rest of the genes in the genome for a) tomato and b) potato.

626 Each gene was assigned to 1 of 6 expression categories based on TPM. c) Mean TPM for gene sets in libraries

627 from mock-treated plants (dark red) and plants treated with organisms (light red). Random gene subsets were

628 created by sampling 359 genes randomly (matching the number of *R*-genes in tomato) from each tomato library

629 and calculating the mean TPM of these 359 genes across each library. Overall 100 random gene sets (containing

630 different sets of 359 genes) per library were created and the average TPM across the 100 replicates is displayed

631 in the box plot format. The distribution of gene expression (TPM values) for the top 10% and 5% of the set of *R*-

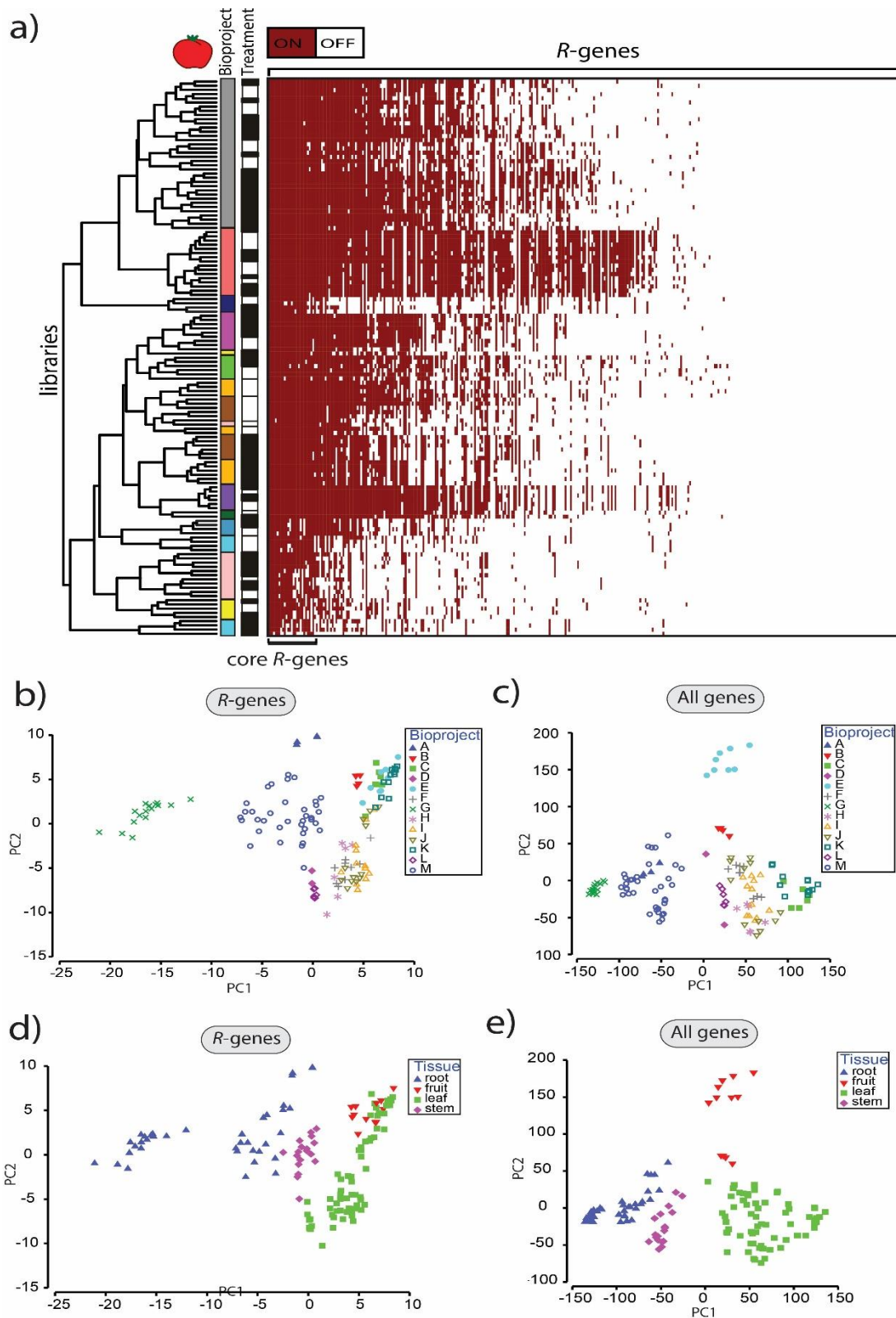
632 genes in each library are displayed as well as the mean TPM for two reference genes (ubiquitin and actin). The

633 midline of each box is the median, boxes extend from the 25th to the 75th percentile, and the dots are outliers.

634 Pairwise differences were computed using either a Mann-Whitney-U test for non-normally distributed data or a

635 two-sample t-test for normally distributed data: n.s. = not significantly different; * p-value < 0.05; ** p-value

636 < 0.01; *** p-value < 0.001.



637

638 **Figure 2: Patterns of *R*-gene expression in tomato**

639 a) Heatmap of *R*-gene expression (359 genes) from tomato (133 libraries). Genes were classified as off/white (if
 640 TPM < 1) and on/red (if TPM ≥ 1). Libraries were clustered by similarity in patterns of expression between libraries.
 641 *R*-genes were sorted by the number of libraries expressing the corresponding *R*-gene from highest (left) to lowest
 642 (right). Assignments to individual bioprojects are indicated by different colors in the first vertical column next to
 643 the dendrogram. The treatment status of the libraries with mock-treated (white) or treated with an organism
 644 (black) is displayed in the 2nd vertical column next to the dendrogram. b-e) Principal component analysis of gene
 645 expression of *R*-genes (b, d) and all genes (c, e). Samples are labeled by the bioproject (b, c) or by the tissue type
 646 (d, e). Clustered groups indicate higher levels of similarity in gene expression.

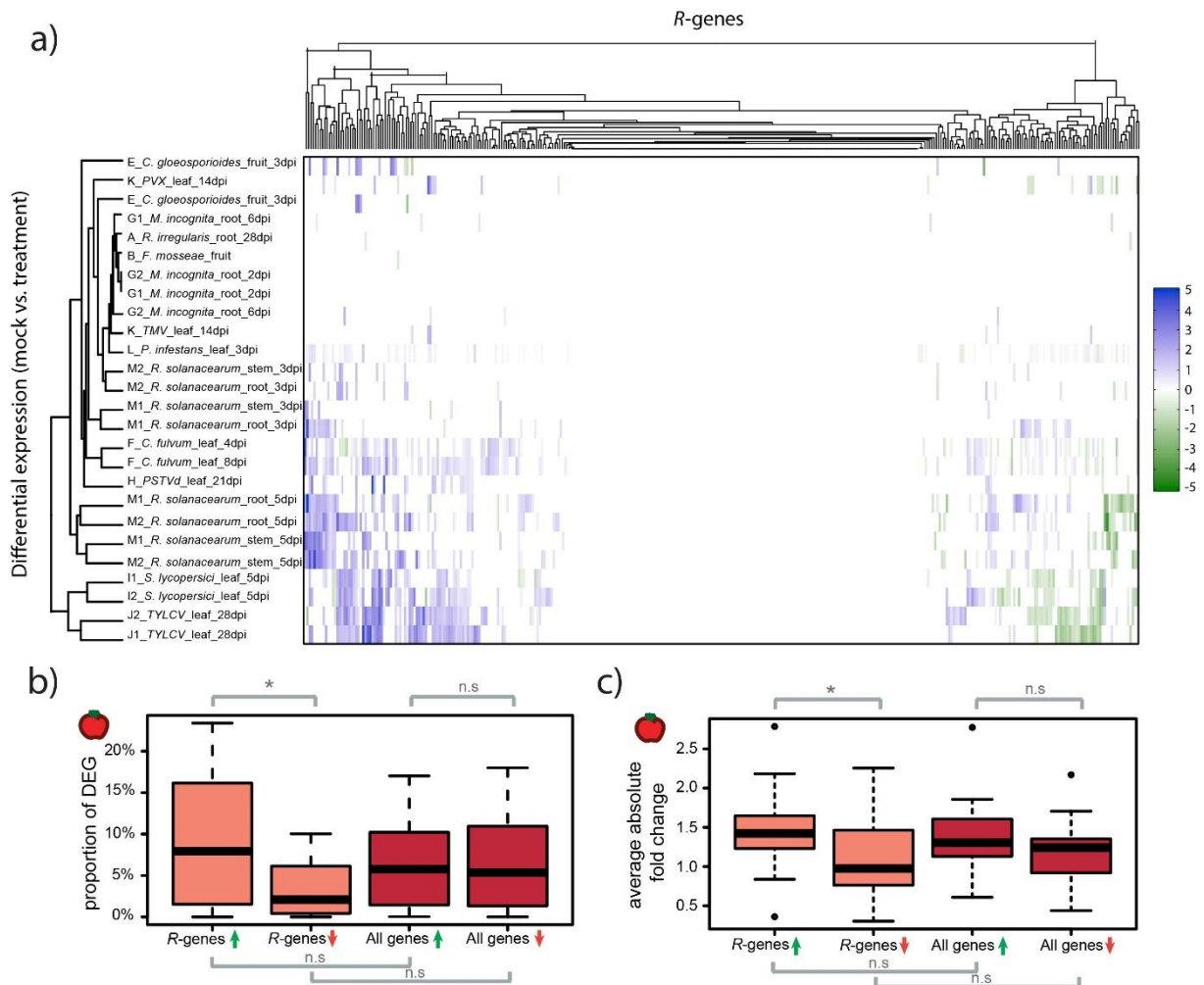


Figure 3: Differential expression of R-genes in tomato plants treated with organisms

a) Differential R-gene expression following treatment with organisms. Up-regulated genes are displayed in blue, down-regulated in green – darker colors represent larger fold changes between mock- and organism-treated libraries. Libraries and R-genes were clustered by similarity. b) Proportions of genes per library which show differential regulation following treatment by an organism. Up-regulation (green arrow); down-regulation (red arrow). c) The average absolute fold changes of up-regulated (green arrow) and down-regulated (red arrow) R-genes and for all genes per library. The midline of each box is the median, boxes extend from the 25th to the 75th percentile, and the dots are outliers. Pairwise differences were evaluated using either a Mann-Whitney-U test for non-normally distributed data or a two-sample t-test for normally distributed data. n.s. = not significantly different; * p-value < 0.05.

647
648
649
650
651
652
653
654
655
656
657
658
659
660
661
662
663
664
665
666
667

668 **Table 1: ANOSIM analysis of (R-)gene expression**

669 R- and p-values for R-genes and all genes from tomato and potato. R-values based on Euclidean distance based
 670 pairwise dissimilarity matrix. p-values ≤5% represent significant R-values. * In addition to assignment of cultivars
 671 to either resistant or susceptible, a third category (beneficial) was used for libraries treated with a beneficial
 672 organism. ** Roots and tubers of *S. tuberosum* were classified as the same tissue-type.

Organism	Factor	All genes		R-genes	
		R-value	p-value	R-value	p-value
Tomato	Bioproject (A through M)	0.959	0.1%	0.867	0.1%
	Tissue type (roots, fruit, leaf, stem)	0.689	0.1%	0.527	0.1%
	Paired- or single-end sequencing	0.495	0.1%	0.358	0.1%
	Days post infection (0 days till end of life cycle of the plant)	0.361	0.1%	0.408	0.1%
	Relative read depth (5 categories from low to high)	0.312	0.1%	0.297	0.1%
	Specific treatment organism (14 types)	0.203	0.1%	0.264	0.1%
	Life cycle of the organism (5 types)	0.152	0.1%	0.189	0.2%
	Type/Kingdom of the organism (6 kingdoms)	0.14	0.1%	0.242	0.1%
	Susceptible vs resistant cultivar*	0.103	0.1%	0.079	0.7%
	Type of treatment (3 treatments)	0.068	0.2%	0.05	2.7%
Potato	Bioproject (A through L)	0.92	0.1%	0.928	0.1%
	Tissue type (tuber, root, leaf)	0.766	0.1%	0.758	0.1%
	Tissue type II** (root, leaf)	0.697	0.1%	0.751	0.1%
	Days post infection (0 to 42 days)	0.538	0.1%	0.522	0.1%
	Paired- or single-end sequencing	0.245	0.1%	0.218	0.1%
	Type/Kingdom of the organism (6 kingdoms)	0.125	0.1%	0.141	0.1%
	Relative read depth (5 categories from low to high)	0.107	0.1%	0.119	0.1%
	Specific treatment organism (11 types)	0.087	0.5%	0.104	0.1%
	Life cycle of the organism (4 types)	0.069	2.5%	0.083	0.2%
	Susceptible vs resistant cultivar*	0.048	0.6%	0.021	9.5%
	Type of treatment (3 treatments)	0.004	34.8%	-0.022	97.6%

673

674

675

676

677

678

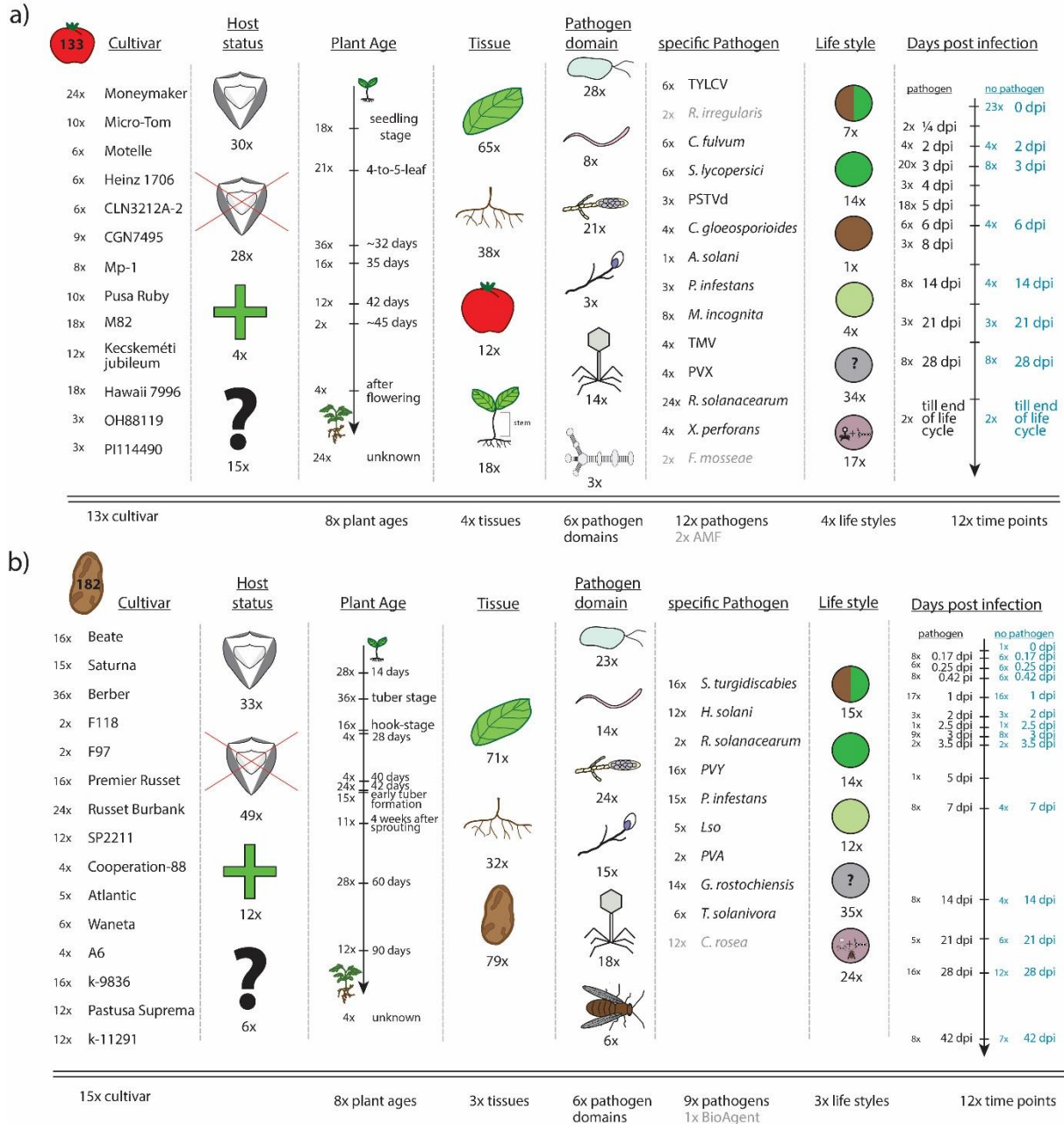
679

680

681

682

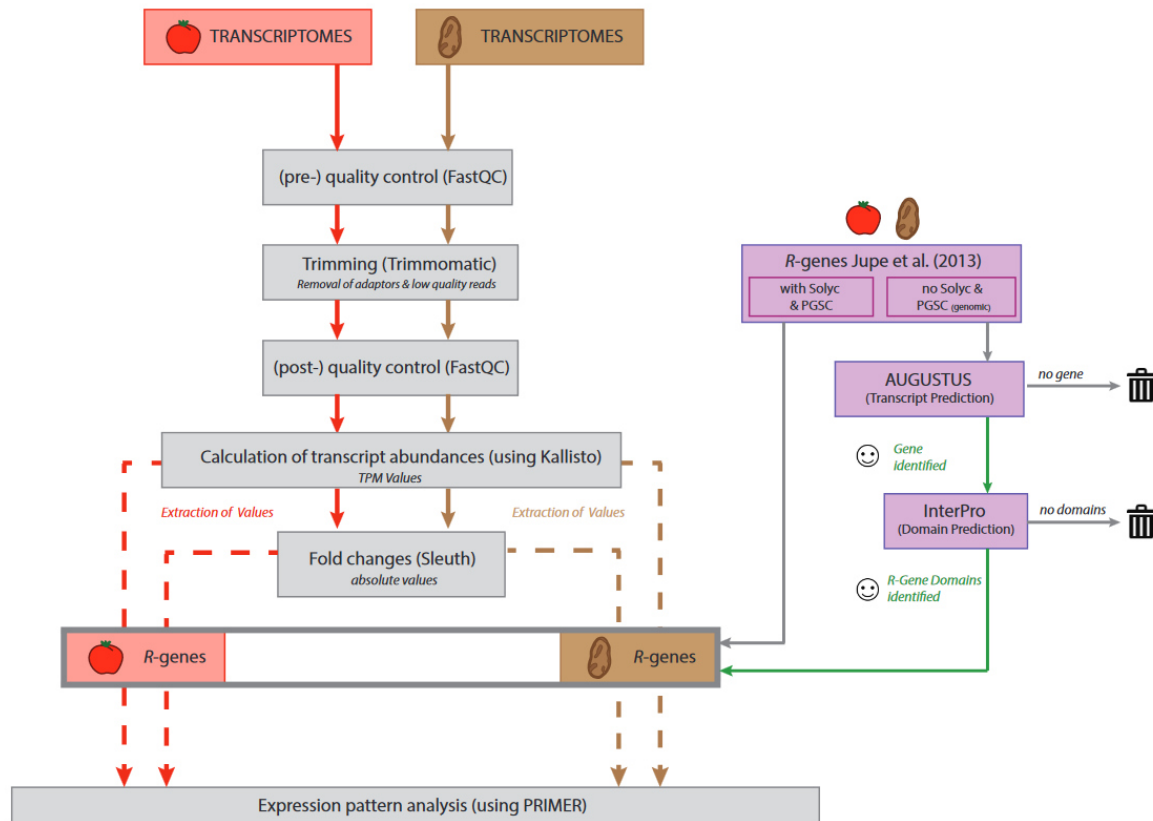
683 Supplemental figures:



684

685 **Figure S1: Composition of data set**

686 This study is based on 315 transcriptomes (133 from tomato (a), 182 from potato (b)) and includes seven plant
 687 pathogen domains (bacteria, fungi, oomycetes, nematodes, viroids, viruses, insects). The pathogens include
 688 common pests of tomato and potato as well as mycorrhizal forming organisms and potential biocontrol agents
 689 (green cross/grey text). The pathogens belong to biotrophic (green circle), necrotrophic (brown circle),
 690 hemibiotrophic (green-brown circle) as well as unknown (grey circle) or none categorical (pink circle) pathogens.
 691 We included transcriptomes from root, fruit, stem and leaves of resistant (shield) as well as susceptible cultivars
 692 (crossed-out shield) that were generated at 12 different time points (0 dpi until the end of the life cycle of the
 693 plant). Cultivars ranged from 13 (a) to 15 (b) per host.
 694



695

696

Figure S2: Workflow

697

Raw sequences of 315 transcriptomes were downloaded from NCBI, pre-quality controlled using FastQC,

698 trimmed (removal of adaptor & low-quality reads) using Trimmomatic and afterwards post-quality controlled

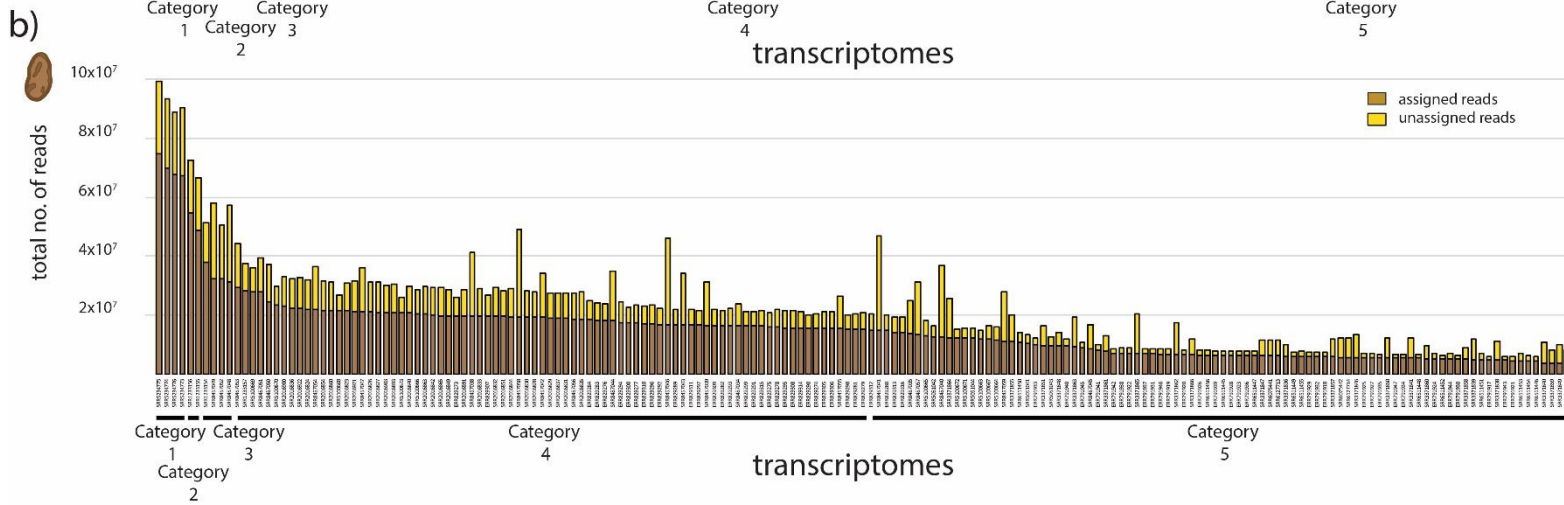
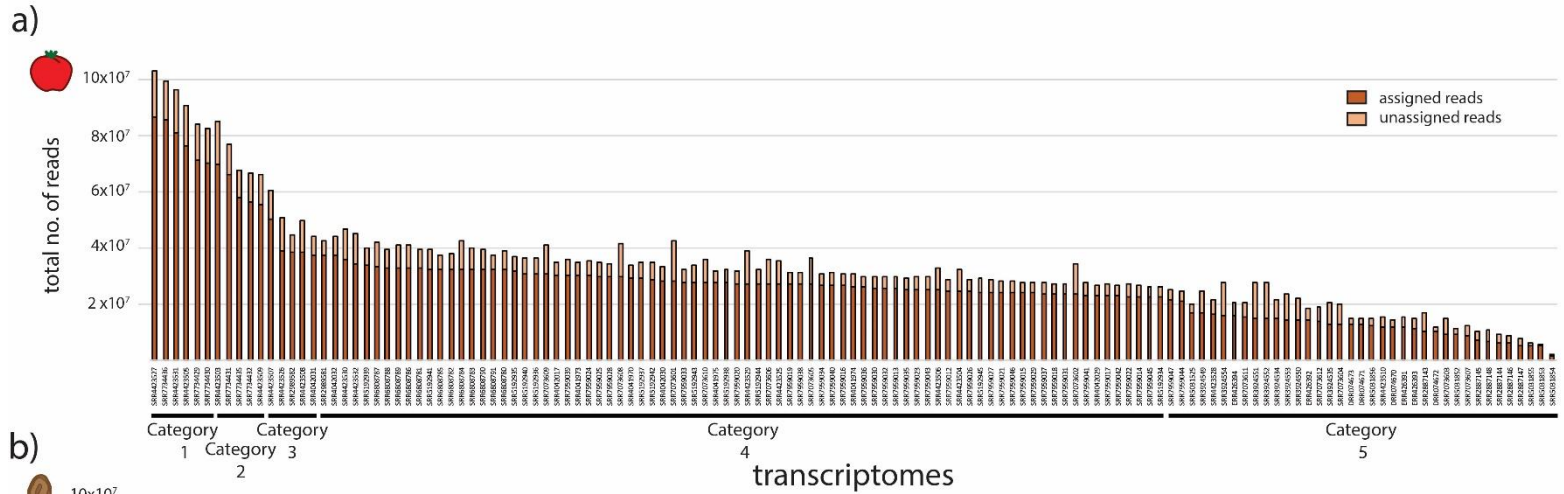
699 using FastQC. Transcript abundances and fold changes were calculated using Kallisto and Sleuth. The multivariate

700 analysis is based on Primer 7.0.13. The *R*-gene repertoire was taken from Jupe et al. (2013). For genes with no

701 Solyc- or PGSC number (genomic *R*-genes), transcripts were predicted using AUGUSTUS 3.3.1. Putative *R*-genes

702 with verified transcripts were evaluated for the presence of NBS and LRR domains using InterPro.

703



704

705

Figure S3: Read library size and pseudoaligned depth

706

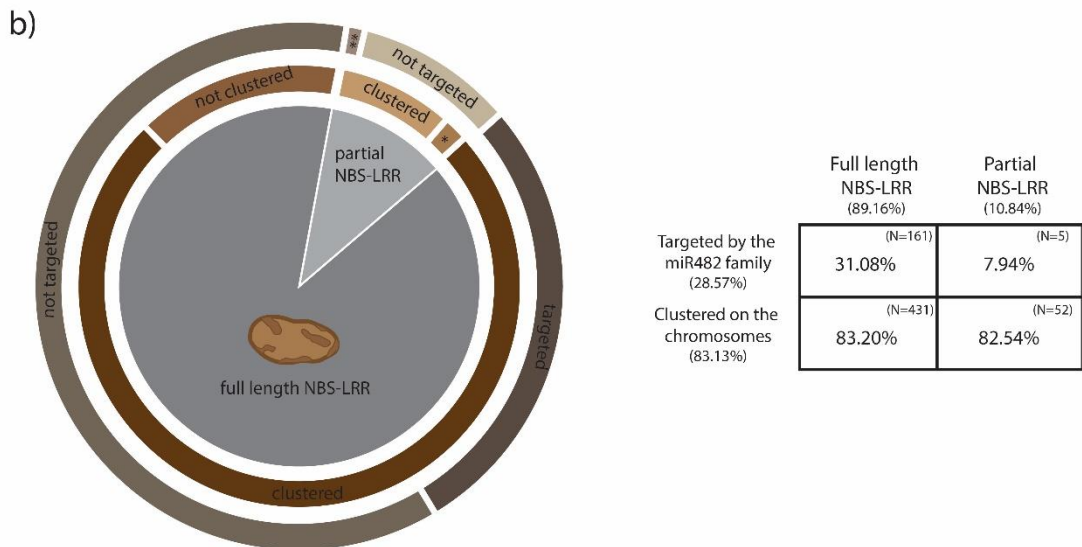
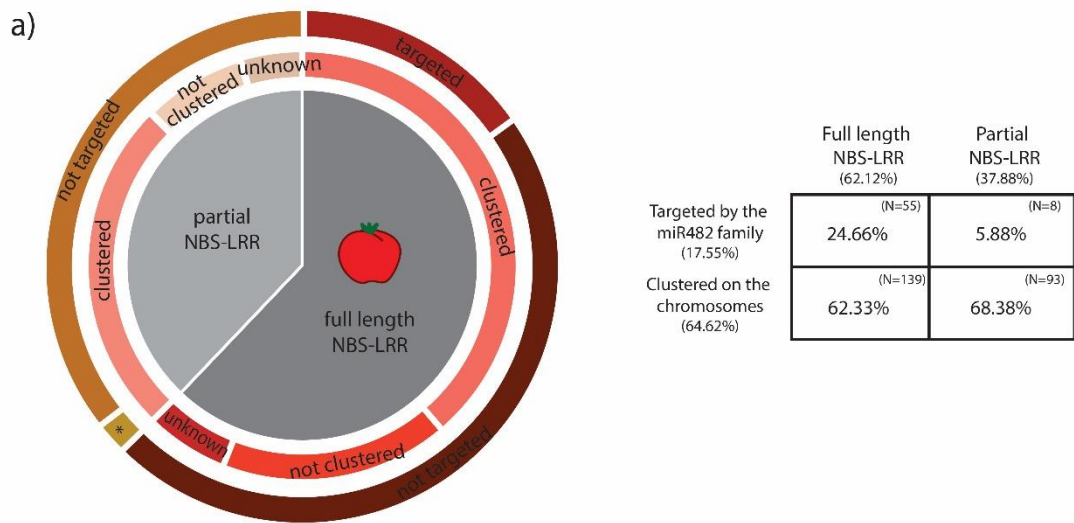
The relative proportions of the assigned reads (dark colored) to unassigned (light colored) reads per library. The libraries were assigned to five categories based on the number of assigned reads, relative to the library with the highest number of assigned reads. Category 1 contained libraries with the highest number of reads (libraries having between 80% up to 100% of the library with the most assigned reads). Category 2 contained libraries from 60% and up to 80%. Category 3 from 40% and up to 60%. Category 4 from 20% and up to 40% and Category 5 from 0% up to 20%.

707

708

709

710

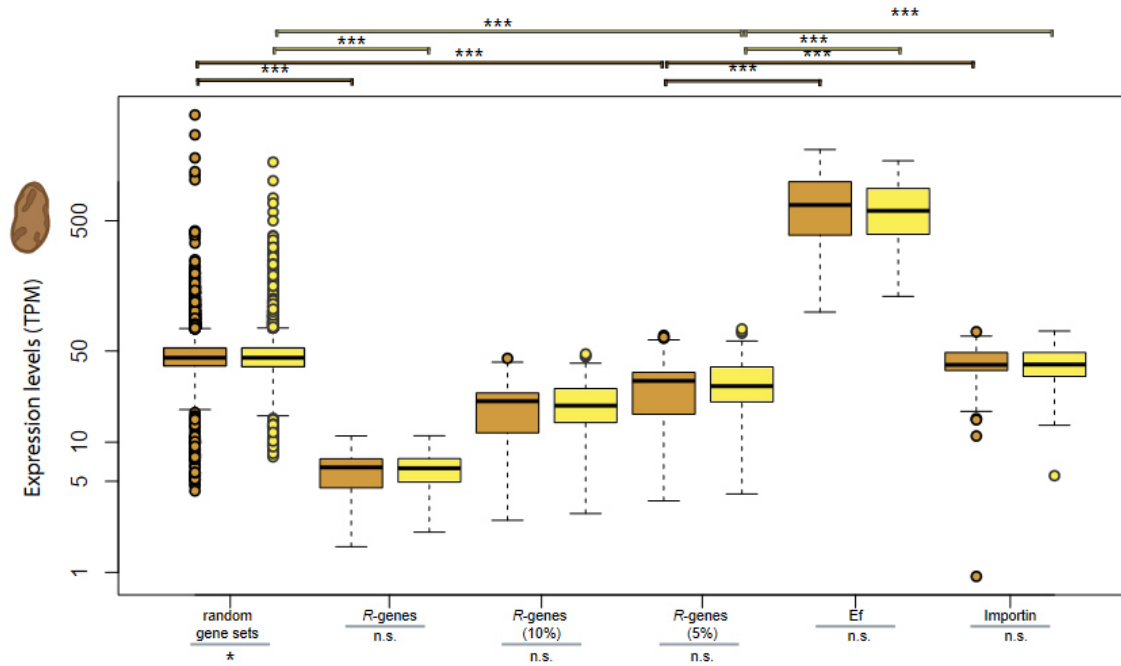


711

712

713 **Figure S4: Characterization of R-genes from tomato and potato**

714 R-genes from a) tomato and b) potato were classified being full length NBS-LRR (containing both domains) or
 715 partial (containing one or none of these domains), potentially clustered or not or potentially targeted by the
 716 miR482-superfamily or not. R-genes without known genomic positions were classified as unknown in their
 717 clustering status. Associations between classifications are given in the tables on the right. N stands for the
 718 number of genes each class includes. * not clustered, ** potentially targeted by miR482-superfamily.



719

720

Figure S5: Comparison of relative gene expression of *R*-genes in potato

721

Mean TPM for gene sets in libraries from mock-treated plants (brown) and plants treated with organisms

722

(yellow). Random gene subsets were created by sampling randomly 581 genes (matching the number of *R*-genes

723

in potato) from each potato library and calculating the mean TPM of these 581 genes across each library. 100

724

random gene sets (containing different sets of 581 genes) per library were created and the average TPM of the

725

100 replicates of each library are displayed in the box plot format. The distribution of gene expression (TPM

726

values) for the top 10% and 5% of the set of *R*-genes in each library are displayed as well as the mean TPM for

727

two reference genes (elongation factor-1(Ef) and an importin subunit). The midline of each box is the median,

728

boxes extend from the 25th to the 75th percentile, and the dots are outliers. Pairwise differences were computed

729

using either a Mann-Whitney-U test for non-normally distributed data or a two-sample t-test for normally

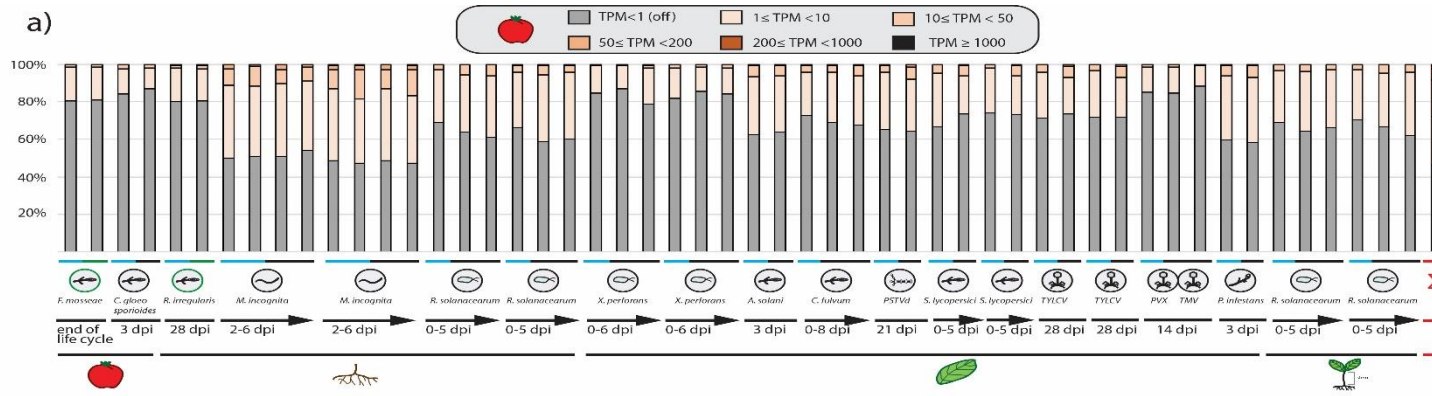
730

distributed data: n.s. = not significantly different; * p-value <0.05; ** p-value <0.01; *** p-value <0.001.

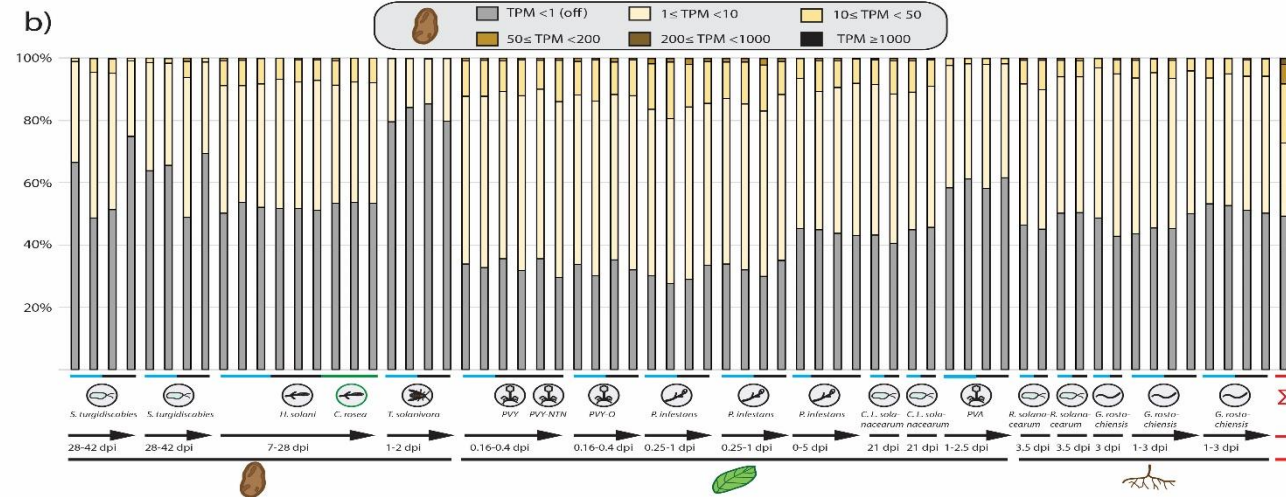
731

732

733



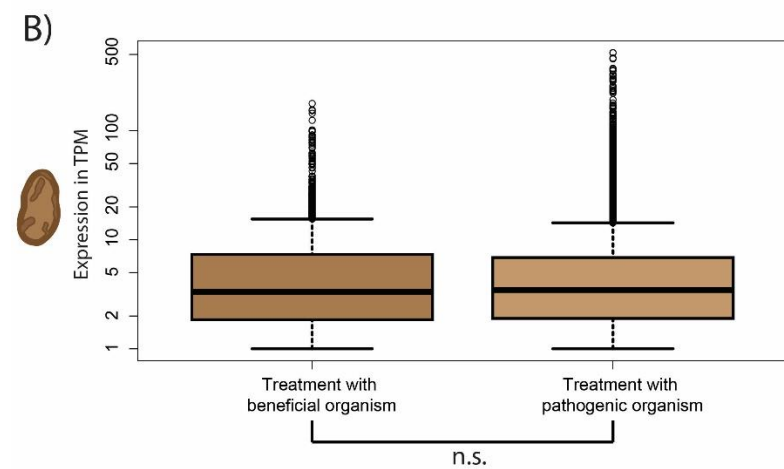
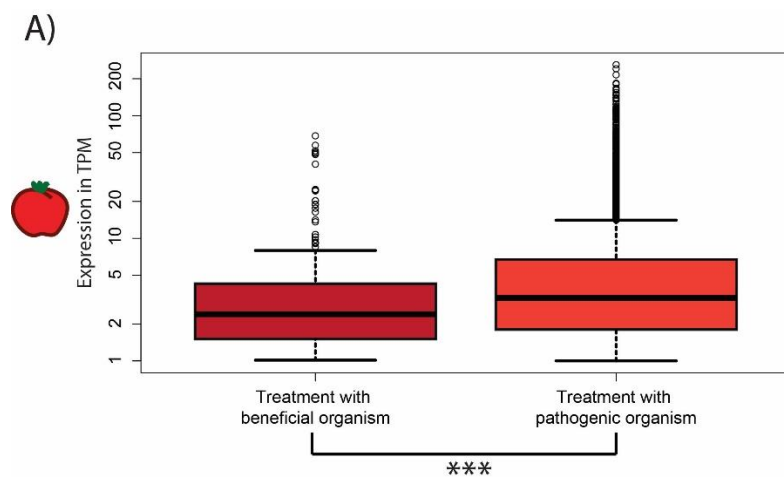
734



735 **Figure S6: Distribution of expression classes of R-genes from tomato and potato**

736 Relative expression of R-genes from a) tomato and b) potato. TPM values were calculated for each gene, in each library. The TPM values for each R-gene are averaged across
 737 biological/technical replicates and then assigned to 1 of 6 categories, from lowest to highest expression. Each vertical bar summarizes the distribution of expression categories
 738 of R-genes in a set of replicates. The far-right column shows the overall patterns of relative gene expression across the entire genome. As for the R-genes, first the TPM values
 739 are calculated for each gene, in each library. Then the TPM values for a single gene are averaged across libraries and then each gene is assigned to an expression category. The
 740 tissue type and kind/kingdom of the organism are indicated by symbols along the x-axis. Mock treatments are underlined in blue; microbial treatments in black. Treatments with
 741 mycorrhizal fungi and potential biocontrol agents are highlighted with green circles.

742



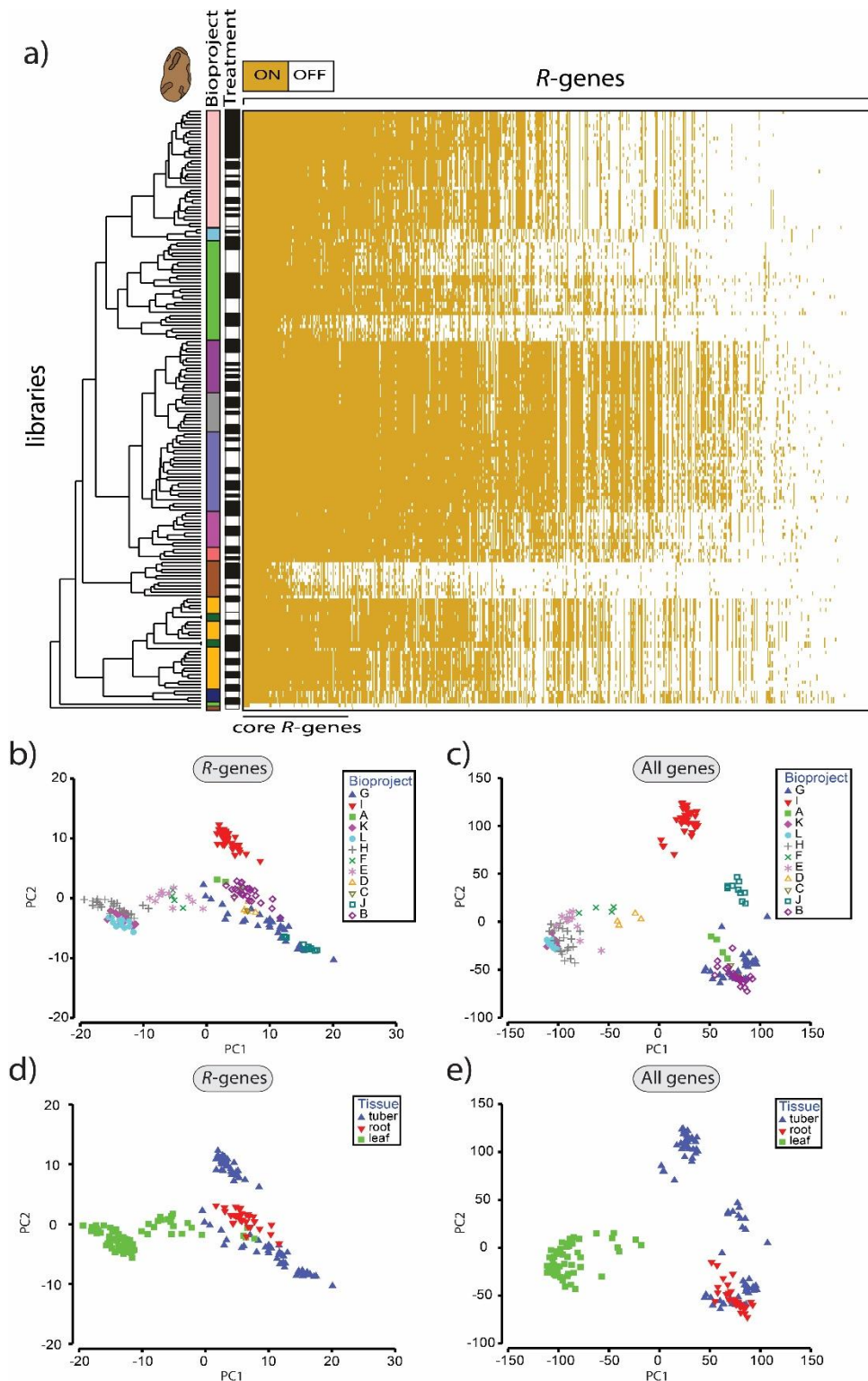
743

744 **Figure S7: Comparison of *R*-gene expression between pathogenic and beneficial treatments**

745 Boxplots of the TPM values for each expressed *R*-gene in each library in a) tomato and b) potato separated by

746 treatment with pathogenic or beneficial organisms. The middle line in the box represents the median, the boxes

747 extend from the 25th to the 75th percentile, and dots outliers. n.s. no significant differences; *** p -value < 0.001.

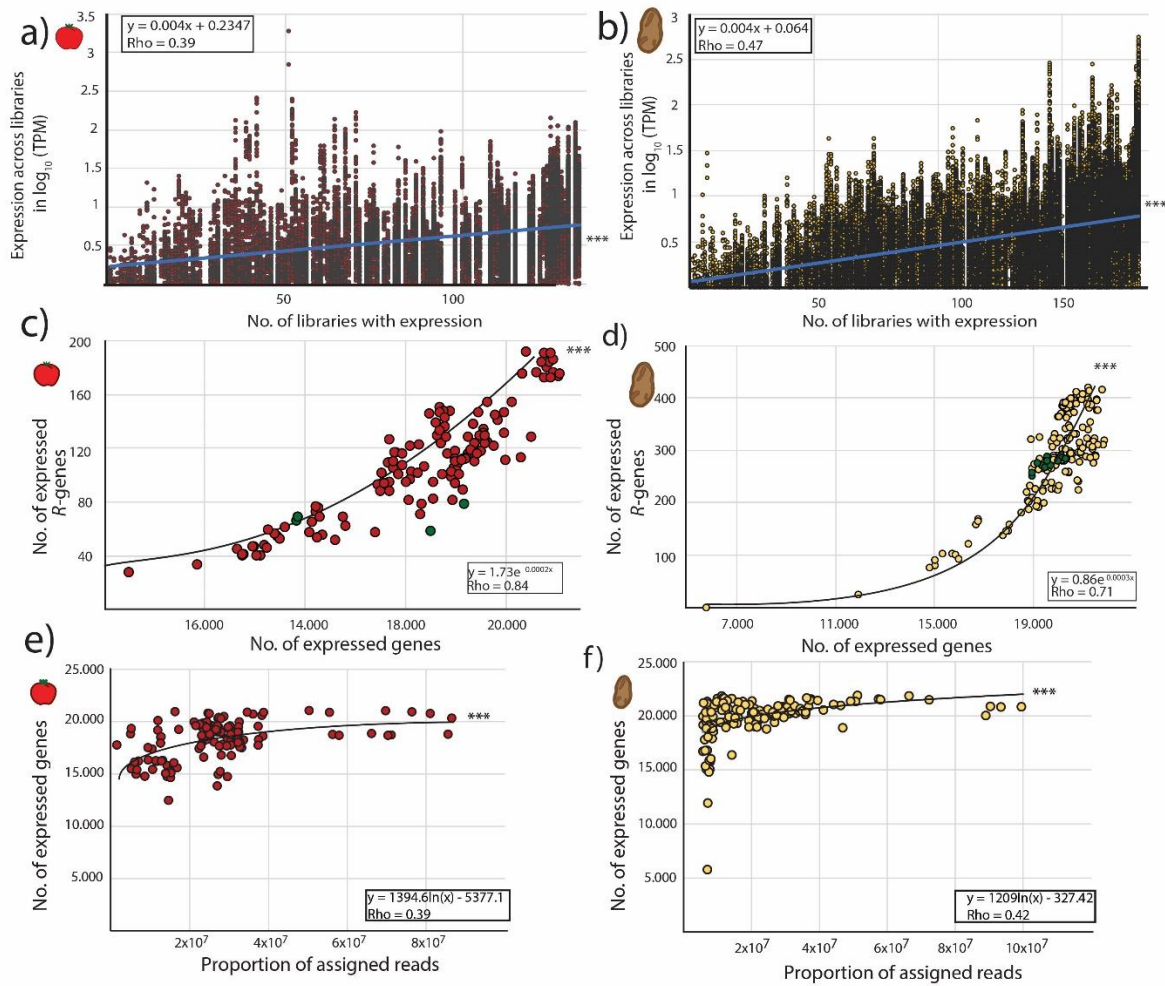


748
749
750
751
752
753
754
755
756
757
758
759

Figure S8: Patterns of *R*-gene expression in potato

a) Heatmap of *R*-gene expression (581 genes) from potato (182 libraries). Genes were classified as off/white (if TPM < 1) and on/red (if TPM ≥ 1). Libraries were clustered by similarity in patterns of expression between libraries. *R*-genes were sorted by the number of libraries expressing the corresponding *R*-gene from highest (left) to lowest (right). Assignments to individual bioprojects are indicated by different colors in the first vertical column next to the dendrogram. The treatment status of the libraries with mock (white) or treated with an organism (black) is displayed in the 2nd vertical column next to the dendrogram. b-e) Principal component analysis of gene expression of *R*-genes (b, d) and all genes (c, e). Samples are labeled by the bioproject (b, c) or by the tissue type (d, e). Clustered groups indicate higher levels of similarity in gene expression.

760



761

762 **Figure S9: Correlation between R-gene expression and transcriptome parameters**

763 TPM values of R-genes plotted against the breadth of expression across transcriptomes of a) tomato and b)

764 potato. Correlation of the total number of R-genes expressed per transcriptome in c) tomato and d) potato with

765 the total number of genes expressed per transcriptome. Turquoise dots represent transcriptomes which were

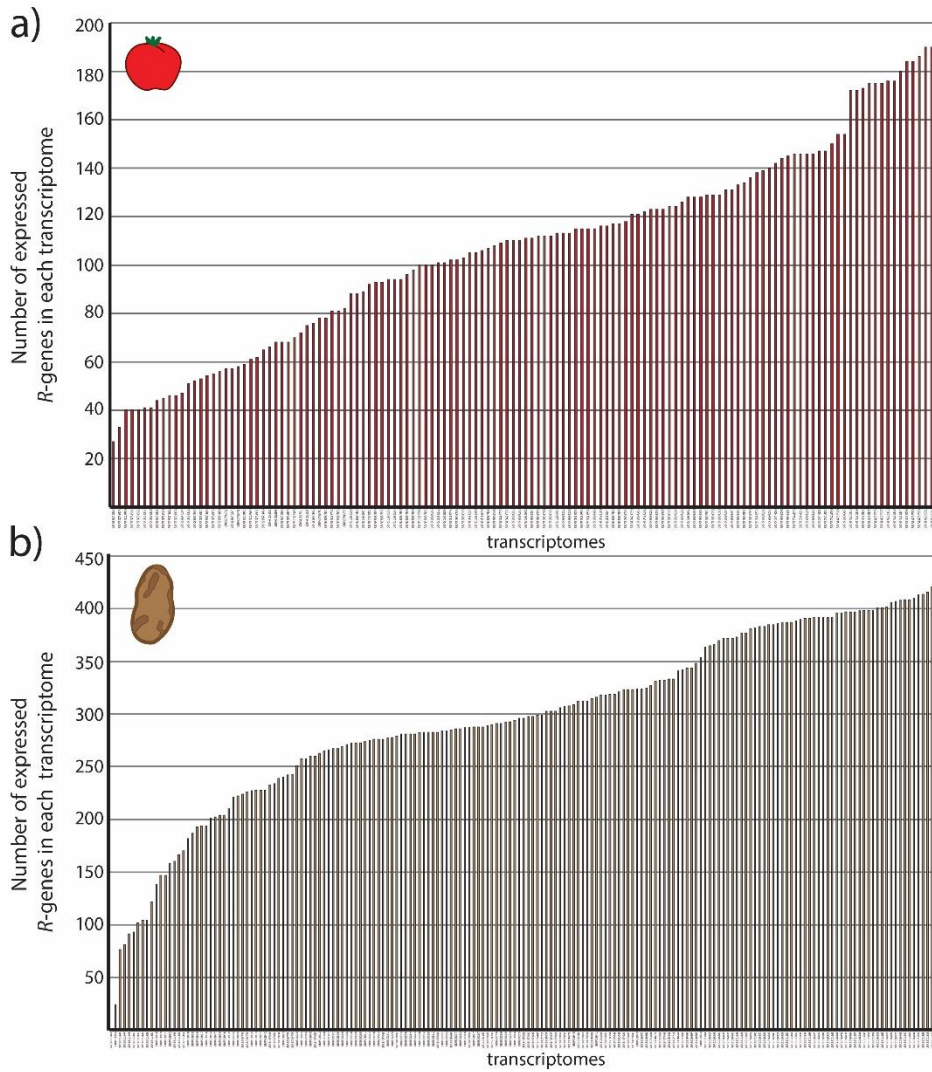
766 treated with beneficial organisms. e, f) Correlation of the total number of genes expressed per transcriptome

767 with the number of pseudoaligned reads per transcriptome in e) tomato and f) potato. Rho values represent the

768 strength of correlation between factors (with larger rho-values representing a stronger correlation). *** p-value

769 <0.001.

770

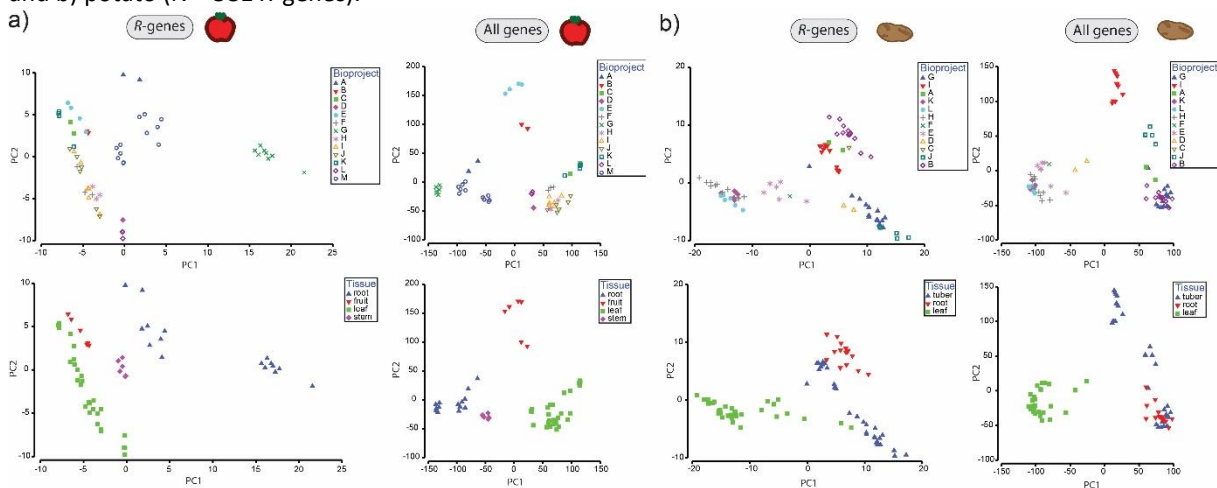


771

772 **Figure S10: Number of expressed *R*-genes in each transcriptome**

773 Distribution of the number of expressed *R*-genes in each transcriptome for a) tomato (N = 359 *R*-genes in total)

774 and b) potato (N = 581 *R*-genes).



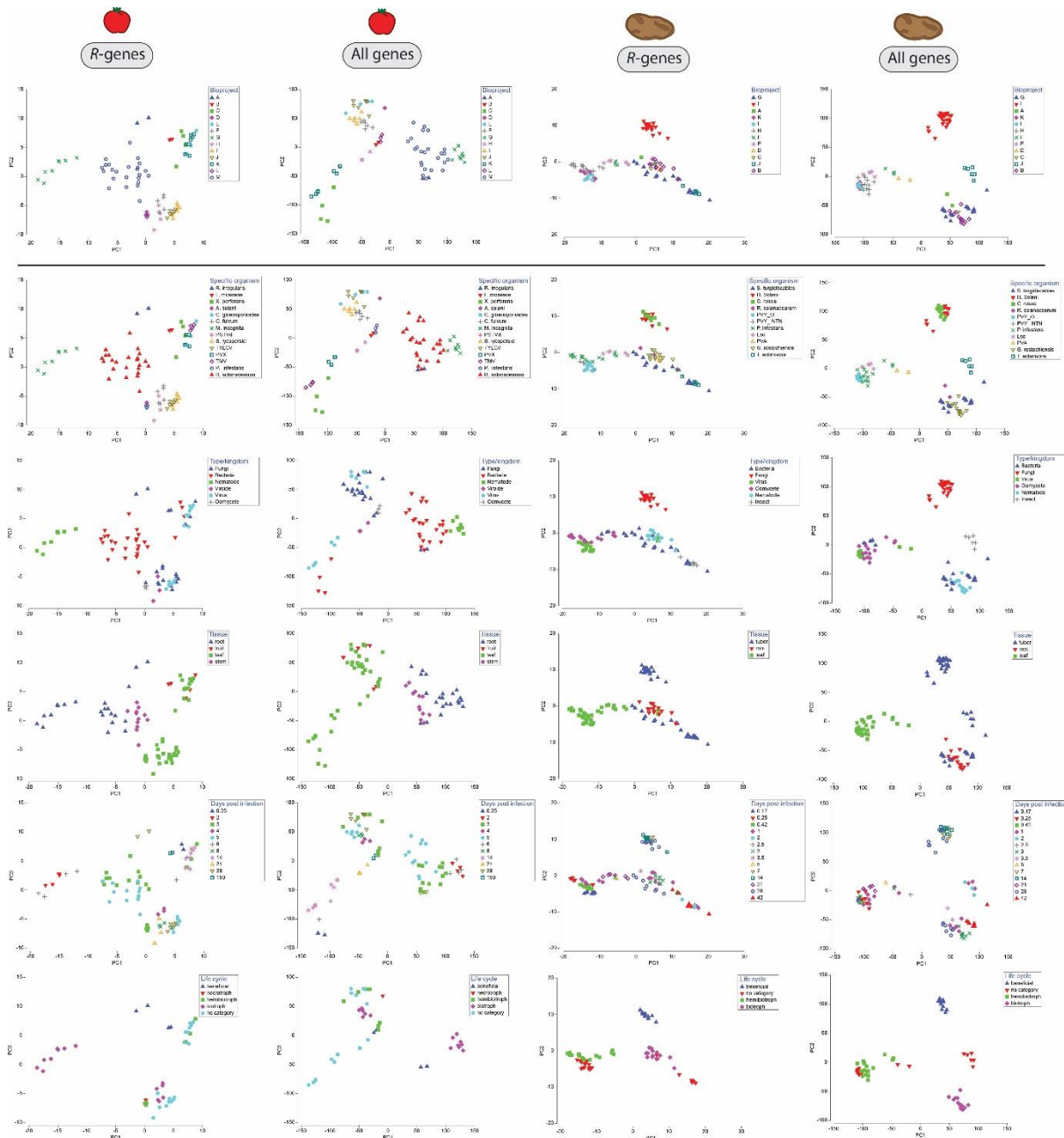
775

776 **Figure S11: PCA plots on mock-treated plants**

777 Principal component plots based on expression of *R*-genes and all genes for a) tomato and b) potato. Each color

778 represents a different bioproject or tissue type. Clustered groups indicate higher levels of similarity in gene

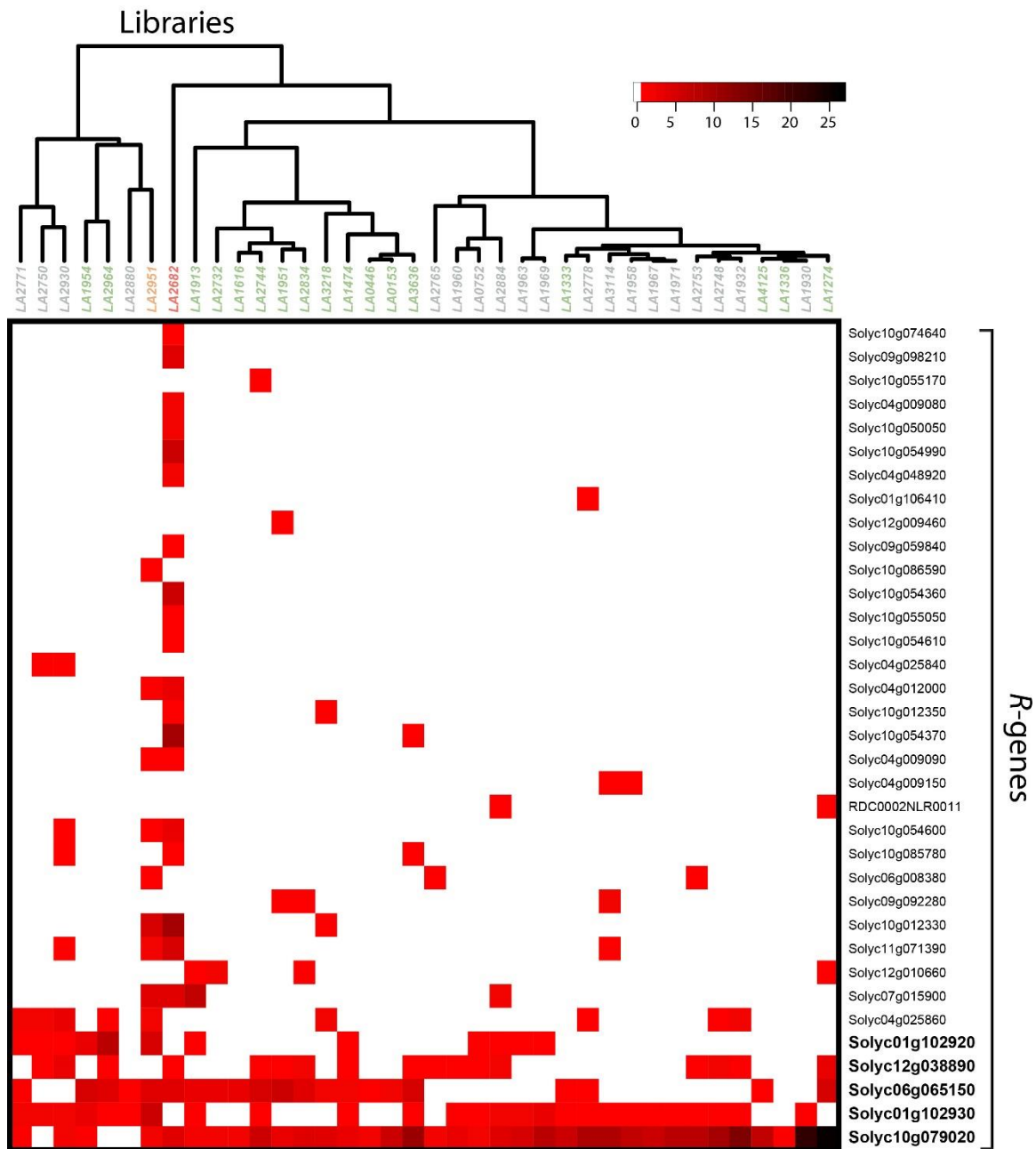
779 expression.



780

781 **Figure S12: PCA plots based on treatment**

782 Principal component analysis plots based on expression of *R*-genes and all genes for tomato (left panel) and
 783 potato (right panel). Each PCA plot displays one ANOSIM factor: bioproject, life cycle of the organism,
 784 type/kingdom of the organism, days post infection, tissue type or specific treatment organism. Clustered groups
 785 indicate higher levels of similarity in gene expression.

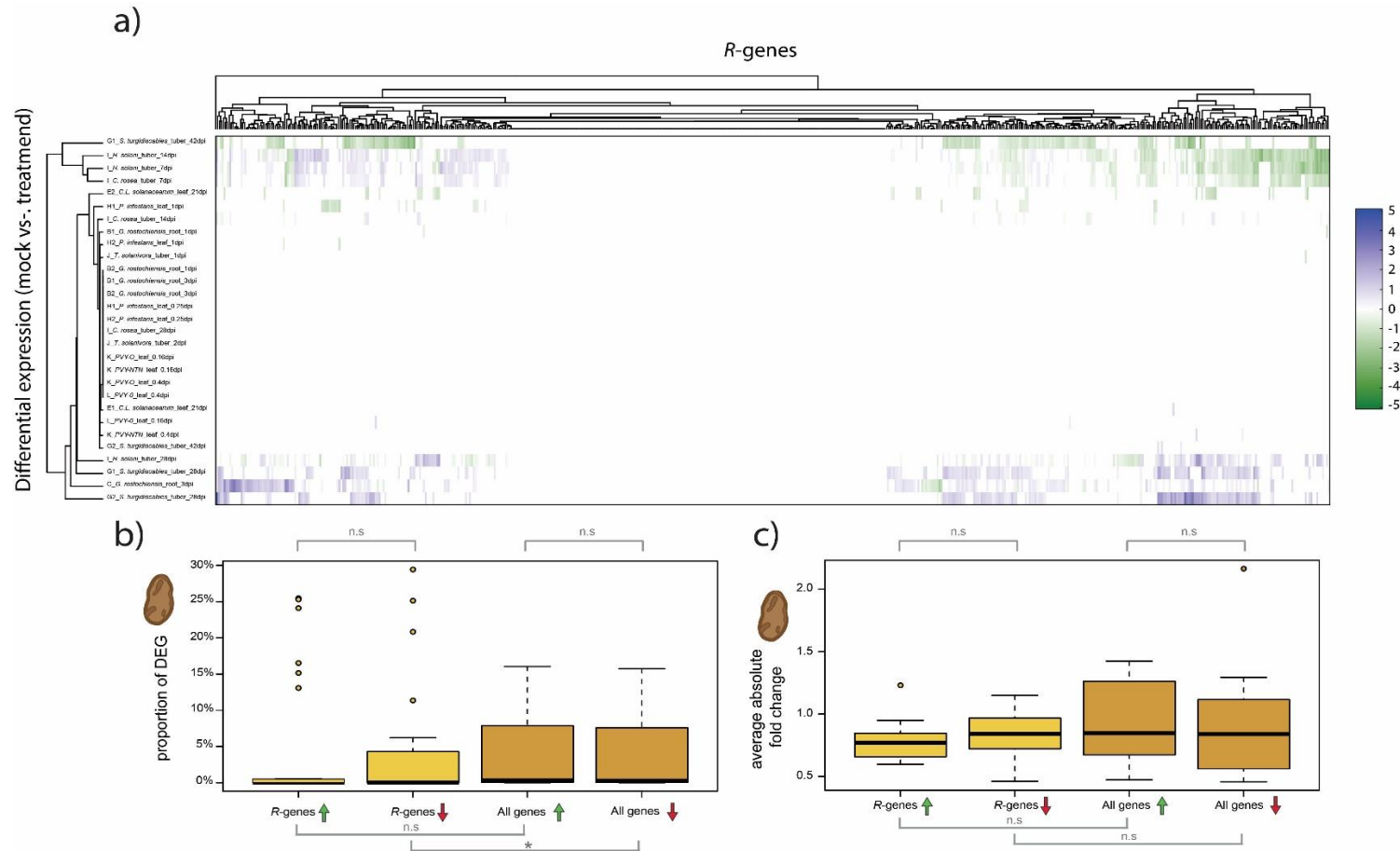


786

787 **Figure S13: Heatmap of R-gene expression in wild tomatoes**

788 Heatmap of the 35 non-expressed R-genes in the cultivated tomato across 38 transcriptomes of wild relatives.
 789 Expression ranges from no expression (TPM <1; white color) to 28 TPM (black). Transcriptomes (x-axis) were
 790 clustered in a dendrogram by expression similarity while R-genes (y-axis) were sorted by the number of libraries
 791 with expression. *S. chilense* (grey), *S. lycopersicoides* (orange), *S. ochranthum* (red), *S. peruvianum* (green). The
 792 five R-genes which were expressed in greater than >30% of all transcriptomes are highlighted in bold.

793



794

795 **Figure S14: Differential expression of R-genes in potato plants treated with organisms**

796

797

798

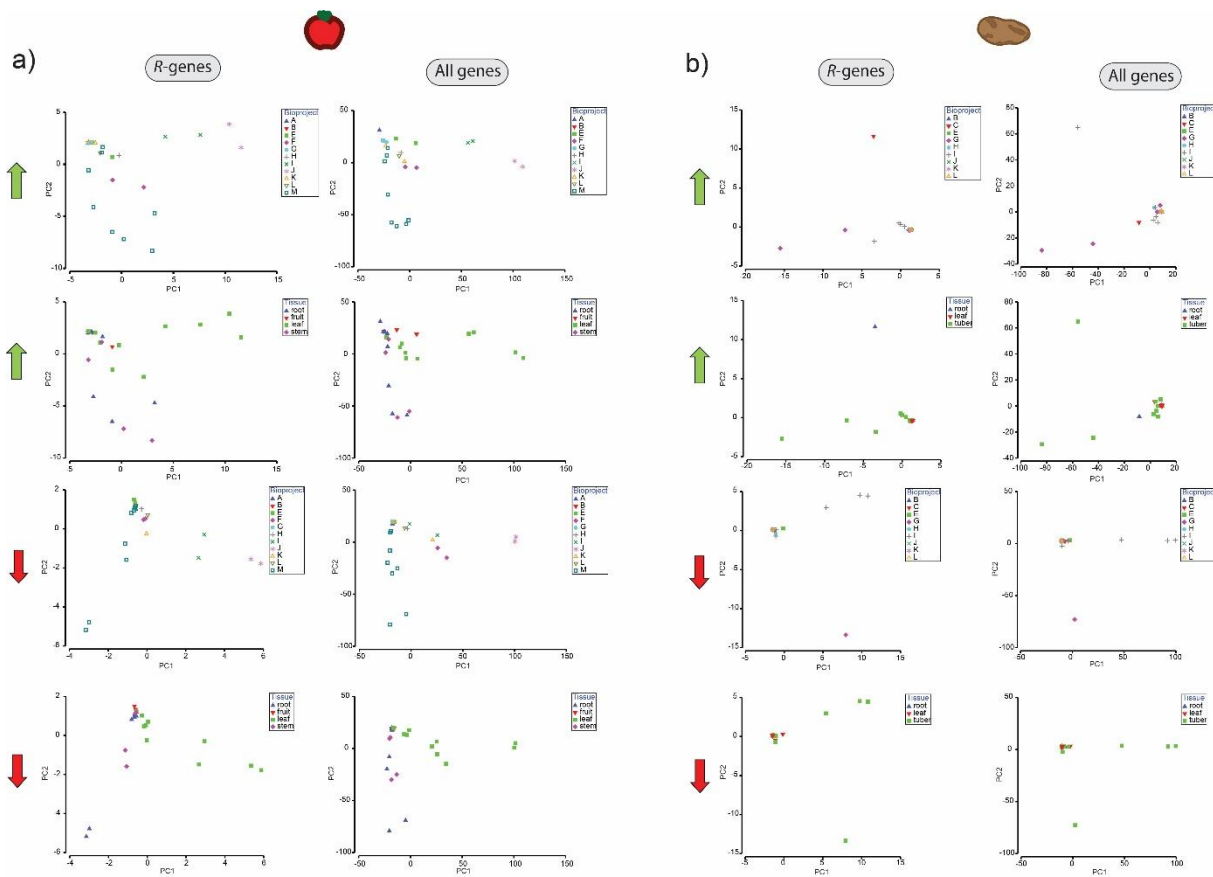
799

800

801

a) Differential R-gene expression following treatment with organisms. Up-regulated genes are displayed in blue, down-regulated in green – darker colors represent larger fold changes between mock- and organism-treated libraries. Libraries and R-genes were clustered by similarity. b) Proportions of genes per library which show differential regulation following treatment by an organism. Up-regulation (green arrow); downregulation (red arrow). c) The averaged absolute fold changes of upregulated (green arrow) and downregulated (red arrow) R-genes and for all genes per library. The midline of each box is the median, boxes extend from the 25th to the 75th percentile, and the dots are outliers. Pairwise differences were evaluated using either a Mann-Whitney-U test for non-normally distributed data or a two-sample t-test for normally distributed data. n.s. = not significantly different; * p-value <0.05.

802

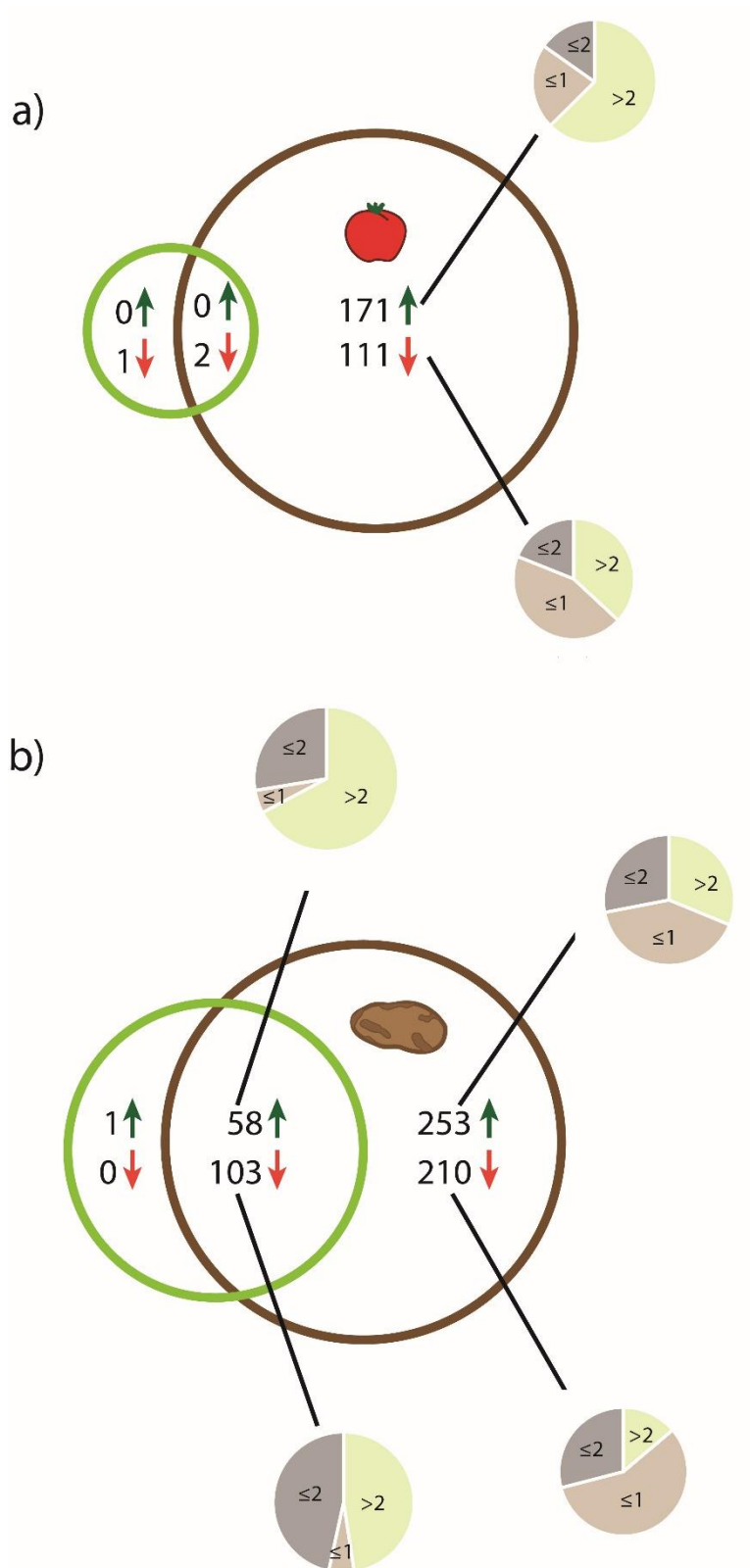


803

804 **Figure S15: PCA plots on differentially expressed *R*-genes**

805 Principal component plots based on expression of *R*-genes and all genes using the first and the second principal
 806 components for tomato (A) and potato (B). Each color represents a different tissue type or bioproject. Clustered
 807 groups indicate higher levels of similarity in gene expression. Data were analyzed separately for up-regulated
 808 (green arrows) or down-regulated genes (red arrows).

809



810

811 **Figure S16: Comparison of fold changes of *R*-genes between treatments with pathogenic or beneficial**
 812 **organisms**

813 The number of differentially expressed *R*-genes in (a) tomato and (b) potato when treated with pathogenic
 814 (brown circle) or beneficial organisms (green circle). Green arrows indicate the number of upregulated *R*-genes;
 815 red arrows the number of downregulated *R*-genes. Small circles indicate the proportion of libraries in which the
 816 *R*-genes are differentially expressed (≤ 1 library (beige); ≤ 2 libraries (grey); > 2 libraries (green)).

817

818 **Supplementary Tables:**819 **Table S1: Characteristics of *R*-genes from potato and tomato**

820 *R*-genes from tomato and potato were classified as being full length NBS-LRRs (containing both domains) or
 821 partial NBS-LRRs (containing one or none of these domains), potentially clustered or not or potentially targeted
 822 by the miR482-superfamily or not. The target probability of the miR482-superfamily was determined using
 823 psRNATarget (maximum expectation ≤ 3). *R*-genes were classified as clustered when two or more *R*-genes were
 824 located within 200 kilobases (kb) (ITAG4.0; PGSC_DM_v4.03). Due to the large dimensions the table is available
 825 online.

826
 827 **Table S2: Chi-square analysis to examine association between NBS-LRR structure, clustering and potential**
 828 **targeting by the miR482-superfamily**

	Characteristics	Chi square	degree of freedom	p-value
Tomato	Full length NBS-LRR ~ Clustered	2.72	1	0.0986
	Full length NBS-LRR ~ Targeted	21.32	1	0.0000
	Clustered ~ Targeted	0.07	1	0.7830
Potato	Full length NBS-LRR ~ Clustered	0.22	1	0.6382
	Full length NBS-LRR ~ Targeted	14.69	1	0.0001
	Clustered ~ Targeted	0.77	1	0.3809

829

830 **Table S3: Expression values of genes in tomatoes**

831 TPM values <1 TPM were set to 0 TPM. Bioprojects are highlighted by different colors. Due to the large
 832 dimensions the table is available online.

833

834 **Table S4: Expression values of genes in potatoes**

835 TPM values <1 TPM were set to 0 TPM. Bioprojects are highlighted by different colors. Due to the large
 836 dimensions the table is available online.

837

838 **Table S5: Metadata of tomato transcriptomes for the ANOSIM analysis**

839 Cells were left blank within the metadata table when no information was available. For life cycle classification of
 840 the organism: organisms are marked with an x if no division of the life cycle exists (viruses, viroid's). The relative
 841 read depth is an assessment of library size. The libraries were assigned to five categories based on the number
 842 of assigned reads, relative to the library with the highest number of assigned reads. Category 1 contained libraries
 843 with the highest number of reads (libraries having between 80% up to 100% of the library with the most assigned
 844 reads). Category 2 = libraries from 60% and up to 80%. Category 3 from 40% and up to 60%. Category 4 from 20%
 845 and up to 40% and category 5 from 0% up to 20%. Due to the large dimensions the table is available online.

846

847 **Table S6: Metadata of potato transcriptomes for the ANOSIM analysis**

848 Cells were left blank within the metadata table when no information was available. For life cycle classification of
 849 the organism: organisms are marked with an x if no division of the life cycle exists (viruses, viroid's). The relative
 850 read depth is an assessment of library size. The libraries were assigned to five categories based on the number
 851 of assigned reads, relative to the library with the highest number of assigned reads. Category 1 contained libraries
 852 with the highest number of reads (libraries having between 80% up to 100% of the library with the most assigned
 853 reads). Category 2 = libraries from 60% and up to 80%. Category 3 from 40% and up to 60%. Category 4 from 20%
 854 and up to 40% and category 5 from 0% up to 20%. For tissue type* roots and tubers were categorized as the
 855 same tissue-type based on their characteristics. Due to the large dimensions the table is available online.

856

857

858

859
860
861**Table S7: ANOSIM analysis of NBS-LRR structure, clustering and potential targeting by the miR482-superfamily**

R- and p-values for tomato and potato. For tissue type* roots and tubers were classified as the same tissue-type based on their characteristics.

Species	Factor	Clustered <i>R</i> -genes		Not clustered <i>R</i> -genes		miR482-targeted <i>R</i> -genes		Not miR482-targeted <i>R</i> -genes		Full length <i>R</i> -genes		Partial <i>R</i> -genes	
		R-value	p-value	R-value	p-value	R-value	p-value	R-value	p-value	R-value	p-value	R-value	p-value
Tomato	Bioproject	0.84	0.1%	0.848	0.1%	0.78	0.1%	0.867	0.1%	0.829	0.1%	0.863	0.1%
	Tissue type	0.547	0.1%	0.449	0.1%	0.313	0.1%	0.562	0.1%	0.452	0.1%	0.642	0.1%
	Days post infection	0.402	0.1%	0.393	0.1%	0.393	0.1%	0.405	0.1%	0.416	0.1%	0.357	0.1%
	Paired or Single-end sequencing	0.356	0.1%	0.372	0.1%	0.235	0.1%	0.373	0.1%	0.314	0.1%	0.37	0.1%
	Relative read depth	0.276	0.1%	0.336	0.1%	0.31	0.1%	0.286	0.1%	0.282	0.1%	0.301	0.1%
	Specific treatment organism	0.261	0.1%	0.267	0.1%	0.23	0.1%	0.263	0.1%	0.245	0.1%	0.279	0.1%
	Type/Kingdom of the organism	0.241	0.1%	0.234	0.1%	0.236	0.1%	0.237	0.1%	0.242	0.1%	0.231	0.1%
	Life cycle of the organism	0.183	0.3%	0.229	0.1%	0.171	0.3%	0.189	0.1%	0.173	0.1%	0.21	0.1%
	Susceptible vs resistant cultivar	0.071	0.5%	0.107	0.1%	0.084	0.3%	0.077	0.2%	0.071	1.1%	0.091	0.2%
	Type of treatment	0.042	3.8%	0.071	0.3%	0.046	2.7%	0.05	1.5%	0.043	3.7%	0.061	0.6%
Potato	Bioproject	0.932	0.1%	0.9	0.1%	0.919	0.1%	0.928	0.1%	0.918	0.1%	0.964	0.1%
	Tissue type	0.768	0.1%	0.685	0.1%	0.698	0.1%	0.779	0.1%	0.761	0.1%	0.689	0.1%
	Tissue type*	0.768	0.1%	0.605	0.1%	0.709	0.1%	0.761	0.1%	0.745	0.1%	0.722	0.1%
	Days post infection	0.525	0.1%	0.495	0.1%	0.523	0.1%	0.519	0.1%	0.518	0.1%	0.521	0.1%
	Paired or Single-end sequencing	0.228	0.1%	0.123	0.1%	0.208	0.1%	0.219	0.1%	0.215	0.1%	0.209	0.1%
	Type/Kingdom of the organism	0.145	0.1%	0.125	0.1%	0.115	0.1%	0.154	0.1%	0.14	0.1%	0.153	0.1%
	Relative read depth	0.112	0.1%	0.156	0.1%	0.133	0.1%	0.111	0.1%	0.117	0.1%	0.136	0.1%

Specific treatment organism	0.109	0.1%	0.08	1%	0.075	1,00%	0.118	0.1%	0.102	0.2%	0.126	0.1%
Life cycle of the organism	0.085	0.1%	0.062	3,00%	0.066	0.8%	0.09	0.1%	0.085	0.1%	0.072	0.8%
Susceptible vs resistant cultivar	0.018	11.2%	0.036	2.8%	0.025	4.5%	0.02	10.8%	0.023	8.9%	0.023	9.8%
Type of treatment	-0.025	99.2%	-0.011	77.3%	-0.022	97.7%	-0.022	96.8%	-0.02	97.1%	-0.031	99.4%

863 **Table S8: ANOSIM analysis of all genes, R-genes and full-length R-genes separated by treatment**
 864 R- and p-values for tomato and potato separated by organism-treated and mock-treated transcriptomes. For
 865 tissue type* roots and tubers were categorized as the same tissue-type based on their characteristics.
 866
 867

Species	Treatment	Factor	All genes		R-genes		Full R-genes	
			R-value	p-value	R-value	p-value	R-value	p-value
Tomato	Mock-treated	Bioproject	0.997	0.1%	0.911	0.1%	0.897	0.1%
		Tissue type	0.844	0.1%	0.561	0.1%	0.512	0.1%
		Paired- or single-end sequencing	0.435	0.1%	0.322	0.1%	0.277	0.3%
		Relative read depth	0.292	0.1%	0.226	0.2%	0.208	0.5%
		Susceptible vs resistant cultivar	-0.009	48.1%	0.021	20.7%	0.028	15.2%
Potato	Mock-treated	Bioproject	0.931	0.1%	0.936	0.1%	0.929	0.1%
		Tissue type	0.803	0.1%	0.789	0.1%	0.792	0.1%
		Tissue type *	0.752	0.1%	0.805	0.1%	0.801	0.1%
		Susceptible vs resistant cultivar	0.026	11.4%	0.052	3.6%	0.051	4.6%
		Paired- or single-end sequencing	0.22	0.1%	0.165	0.1%	0.161	0.1%
		Relative read depth	0.107	0.4%	0.121	0.2%	0.121	0.5%
Tomato	Organism treated	Bioproject	0.966	0.1%	0.902	0.1%	0.872	0.1%
		Specific treatment organism	0.965	0.1%	0.889	0.1%	0.858	0.1%
		Tissue type	0.591	0.1%	0.53	0.1%	0.452	0.1%
		Paired- or single-end sequencing	0.587	0.1%	0.441	0.1%	0.407	0.1%
		Life cycle of the organism	0.497	0.1%	0.37	0.1%	0.336	0.1%
		Type/Kingdom of the organism	0.443	0.1%	0.582	0.1%	0.61	0.1%
		Days post infection	0.412	0.1%	0.413	0.1%	0.428	0.1%
		Relative read depth	0.323	0.1%	0.359	0.1%	0.357	0.1%
		Pathogenic vs beneficial organisms	0.299	3.1%	0.18	9.5%	0.108	20.9%
		Susceptible vs resistant cultivar	0.092	1.3%	0.086	1.5%	0.084	2.9%
Potato	Organism treated	Bioproject	0.921	0.1%	0.92	0.1%	0.91	0.1%
		Specific treatment organism	0.88	0.1%	0.85	0.1%	0.841	0.1%
		Type/Kingdom of the organism	0.755	0.1%	0.736	0.1%	0.736	0.1%
		Tissue type	0.727	0.1%	0.712	0.1%	0.716	0.1%
		Tissue type*	0.645	0.1%	0.693	0.1%	0.686	0.1%
		Life cycle of the organism	0.583	0.1%	0.533	0.1%	0.529	0.1%
		Days post infection	0.538	0.1%	0.537	0.1%	0.536	0.1%
		Paired- or single-end sequencing	0.26	0.1%	0.249	0.1%	0.246	0.1%

	Relative read depth	0.101	0.2%	0.101	0.1%	0.097	0.1%
	Susceptible vs resistant cultivar	0.092	0.2%	0.021	19.5%	0.029	13.2%
	Pathogenic vs beneficial organisms	0.07	12.4%	-0.07	88.2%	-0.055	83.8%

868

869

870 **Table S9: Expression values of *R*-genes in wild tomatoes**

871 Displayed are the expression values of all *R*-genes within wild tomatoes which are expressed in none of the
872 cultivated tomato transcriptomes (n=99 *R*-genes). TPM values <1 TPM were set to 0 TPM. Species are highlighted
873 by different colors. Due to the large dimensions the table is available online.

874

875 **Table S10: Pi(a)/Pi(s)- and Ka/Ks-ratio for *S. chilense* and *S. peruvianum***876 Alleles with greater than 30% or 50% undetermined SNPs (Ns) were excluded from the analyses. *Solyc12g038890* was removed from analysis due to low number of complete
877 alleles in *S. chilense* and *S. peruvianum*.

Species	Gene-ID	Percent of unknown positions (N's)	Number of analysed sequences	Total number of codons	Number of codons analysed	Pi(s)	Pi(a)	Pi(a)/Pi(s) ratio	Number of synonymous substitutions (intraspecific)	Number of nonsynonymous substitutions (intraspecific)	Ks	Ka	Ka/Ks ratio
<i>S. chilense</i>	<i>Solyc01g102920</i>	<30%	9	353	192	0,0161	0,0043	0,266	4	6	0,0395	0,0129	0,32
<i>S. chilense</i>	<i>Solyc01g102920</i>	<50%	15	353	40	0	0,003	-	0	2	0,0395	0,0106	0,262
<i>S. peruvianum</i>	<i>Solyc01g102920</i>	<30%	13	353	311	0,0249	0,0064	0,252	12	13	0,0401	0,0116	0,283
<i>S. peruvianum</i>	<i>Solyc01g102920</i>	<50%	15	353	205	0,0224	0,0064	0,282	8	9	0,0343	0,0139	0,402
<i>S. chilense</i>	<i>Solyc01g102930</i>	<30%	21	353	176	0,0077	0,0002	0,031	5	1	0,0217	0,0074	0,338
<i>S. chilense</i>	<i>Solyc01g102930</i>	<50%	27	353	79	0,0028	0,0012	0,433	2	2	0,0198	0,0116	0,581
<i>S. peruvianum</i>	<i>Solyc01g102930</i>	<30%	15	353	178	0,0205	0,0015	0,073	9	2	0,0289	0,001	0,035
<i>S. peruvianum</i>	<i>Solyc01g102930</i>	<50%	19	353	85	0,0216	0	0	5	0	0,0414	0	0
<i>S. chilense</i>	<i>Solyc06g065150</i>	<50%	5	313	127	0,0075	0,0068	0,907	1	4	0,0283	0,0137	0,479
<i>S. peruvianum</i>	<i>Solyc06g065150</i>	<30%	23	313	189	0,0218	0,0095	0,434	12	17	0,0279	0,0058	0,205
<i>S. peruvianum</i>	<i>Solyc06g065150</i>	<50%	37	313	160	0,0189	0,0069	0,363	12	14	0,0244	0,0041	0,164
<i>S. chilense</i>	<i>Solyc10g079020</i>	<30%	27	133	103	0,0137	0,0246	1,808	5	31	0,0095	0,0159	1,678
<i>S. peruvianum</i>	<i>Solyc10g079020</i>	<30%	27	133	40	0,0289	0,0147	0,503	5	8	0,0158	0,0083	0,519
<i>S. peruvianum</i>	<i>Solyc10g079020</i>	<50%	21	133	81	0,0243	0,0209	0,857	7	20	0,0136	0,012	0,885

878

879 Table S11: Differential expression of genes in tomato

880 Only genes for which the FDR was ≤ 0.05 of the fold change were considered to be differentially expressed. Genes
881 for which the FDR was > 0.05 were treated as being equally expressed across treatments. Differential expression
882 data sets belonging to the same bioproject are highlighted in the same color. Due to the large dimensions the
883 table is available online.

884

885 Table S12: Differential expression of genes in potato

886 Only genes for which the FDR was ≤ 0.05 of the fold change were considered to be differentially expressed. Genes
887 for which the FDR was > 0.05 were treated as being equally expressed across treatments. Differential expression
888 data sets belonging to the same bioproject are highlighted in the same color. Due to the large dimensions the
889 table is available online.

890

891 Table S13: Metadata of differential expression data sets of tomato

892 For organisms marked with an x, life history type is not assigned (viruses, viroids, insects). The factor susceptible
893 vs resistant cultivar is separated into two columns: The column with an * excludes treatments with arbuscular
894 mycorrhizal fungi. Due to the large dimensions the table is available online.

895

896 Table S14: Metadata of differential expression data sets of potato

897 For organisms marked with an x, life history type is not assigned (viruses, viroids, insects). The factor susceptible
898 vs resistant cultivar is separated into two columns: The column with an * excludes treatments with arbuscular
899 mycorrhizal fungi. The factor tissue type was evaluated in two ways. For tissue type**, roots and tubers were
900 categorized as the same tissue type. Due to the large dimensions the table is available online.

901

902 **Table S15: ANOSIM analysis of differentially expressed (*R*-)genes during infection**

903 Genes were identified as either up-regulated or down-regulated following infection compared to mock treated plants. The effect of different factors in explaining the variation
 904 in differential expression was tested using ANOSIM. The factor susceptible vs. resistant cultivar was evaluated in two ways. Susceptible vs. resistant cultivar* does not include
 905 beneficial organism. The factor tissue type was evaluated in two ways. For tissue type**, roots and tubers were categorized as the same tissue type.
 906

Species	Regulation	Factor	All genes		<i>R</i> -genes		Clustered <i>R</i> -genes		Not clustered <i>R</i> -genes		miR482-targeted <i>R</i> -genes		Not miR482-targeted <i>R</i> -genes		Full length <i>R</i> -genes		Partial <i>R</i> -genes	
			R-value	p-value	R-value	p-value	R-value	p-value	R-value	p-value	R-value	p-value	R-value	p-value	R-value	p-value	R-value	p-value
Tomato	Up-regulated genes	Bioproject	0.423	0.6%	0.238	8.9%	0.23	8.9%	0.25	6.8%	0.363	1.8%	0.218	12.2%	0.252	6.8%	0.198	11.2%
		Specific treatment organism	0.419	1.6%	0.219	12.8%	0.212	14.3%	0.231	8.1%	0.353	3%	0.199	13.1%	0.233	10.4%	0.176	14.4%
		Days post infection	0.183	9.5%	0.132	16.8%	0.183	9.3%	0.014	43.4%	0.129	18.4%	0.125	16.8%	0.164	11.1%	0.048	31.8%
		Type/Kingdom of organism	0.134	7.8%	0.085	17%	0.095	16%	0.079	18.9%	0.136	7.9%	0.08	19.3%	0.124	8.9%	0.02	35.5%
		Life cycle of the organism	0.213	5.7%	0.062	26.8%	0.055	27.7%	0.077	22.8%	0.135	14%	0.016	38.6%	0.041	33.9%	0.045	30.9%
		Tissue type	0.049	24.4%	0.053	25.4%	0.048	26.7%	0.074	20%	0.092	14.6%	0.04	27.9%	0.059	22%	0.039	29%
		Susceptible vs. resistant cultivar	-0.04	76%	-0.043	79.2%	-0.044	83.4%	0.004	37.6%	-0.034	68%	-0.047	84.2%	-0.045	78.9%	-0.044	80%
		Susceptible vs. resistant cultivar *	-0.009	51.9%	-0.118	94.9%	-0.116	95.9%	-0.077	77.8%	-0.106	92.5%	-0.121	95.7%	-0.117	94.8%	-0.119	95.9%
		Pathogenic vs beneficial organism	0.076	36%	-0.361	98.2%	-0.348	98.2%	-0.34	97.8%	-0.323	97.5%	-0.354	97.8%	-0.347	97.5%	-0.356	98.5%

907
 908
 909
 910
 911
 912
 913
 914
 915

916

Tomato	Down-regulated genes	Bioproject	0.14	19.8%	0.06	37.5%	-0.029	54.1%	0.186	14,00%	0.103	29.1%	-0.002	46.1%	0.107	27.8%	-0.049	59.1%
		Specific treatment organism	0.142	21,00%	0.057	34.7%	-0.04	58.4%	0.194	15.2%	0.103	25.5%	-0.008	50,00%	0.106	26,00%	-0.054	61.1%
		Days post infection	0.111	20.5%	0.044	34.1%	0.046	36.8%	0.016	43.2%	0.152	12.8%	0.01	44.6%	0.026	40.2%	0.03	39.5%
		Life cycle of the organism	0.014	37.1%	0.024	39.2%	-0.043	61.5%	0.088	22.5%	-0.014	49.4%	0.005	45,00%	0.038	33.6%	-0.023	54,00%
		Tissue type	0.003	44.5%	0.002	44.6%	-0.02	54.3%	0.025	35.4%	-0.011	51.2%	-0.009	52.2%	-0.003	48.2%	0.041	31.2%
		Type/Kingdom of organism	0.096	17.5%	-0.017	54.2%	-0.056	70.7%	0.012	41.7%	0	44.6%	-0.049	67.2%	0.008	42.5%	-0.129	93.3%
		Susceptible vs. resistant cultivar	-0.015	56.2%	-0.048	94.4%	-0.043	92,00%	-0.044	90,00%	-0.022	66%	-0.057	97.2%	-0.034	81.7%	-0.032	82.1%
		Susceptible vs. resistant cultivar *	-0.106	93.2%	-0.128	98.1%	-0.124	96.9%	-0.124	98.4%	-0.094	88.3%	-0.141	99.2%	-0.12	97.4%	-0.108	92.8%
		Pathogenic vs beneficial organism	-0.361	94.2%	-0.335	89.8%	-0.288	80.6%	-0.353	100,00%	-0.224	72.3%	-0.358	92,00%	-0.338	92.3%	-0.282	80.3%

917

Potato	Up-regulated genes	Days post infection	0.11	13.9%	0.161	5.1%	0.134	7.3%	0.131	8.7%	0.136	9%	0.155	6.7%	0.15	7.6%	0.076	21%
		Specific treatment organism	0.076	16.6%	0.108	7.3%	0.084	12.9%	0.077	14.5%	0.059	18.5%	0.105	9%	0.099	10.1%	0.025	34.4%
		Tissue type	0.093	9.1%	0.092	8.9%	0.067	14.5%	0.082	10.6%	0.104	6%	0.086	10.7%	0.077	11.2%	0.078	10.1%
		Life cycle of the organism	0.267	1.8%	0.088	17.6%	0.088	18.6%	0.03	30.5%	0.164	4.2%	0.087	17.7%	0.087	18.6%	0.085	21.8%
		Bioproject	0.03	31.9%	0.085	17.2%	0.059	23.7%	0.07	20.4%	0.039	29.4%	0.076	17.8%	0.077	17.1%	0.021	39.8%
		Pathogenic vs beneficial organism	-0.046	51.7%	0.07	37.7%	0.076	36%	-0.082	59.3%	0.1	32.4%	0.067	35.2%	0.07	35.1%	-0.02	53.3%
		Type/Kingdom of organism	0.022	33.4%	0.005	44.2%	-0.004	50.5%	-0.015	57.1%	0.01	39.8%	-0.003	48.5%	-0.001	48%	-0.019	58.4%
		Tissue type **	-0.049	83.5%	-0.047	81.4%	-0.053	87.2%	-0.047	81.1%	-0.044	79.7%	-0.046	81.2%	-0.05	85.5%	-0.06	94.5%
		Susceptible vs. resistant cultivar	-0.087	76.7%	-0.082	73.9%	-0.091	75.2%	-0.101	79%	-0.045	61.2%	-0.085	76%	-0.089	74.2%	-0.072	72%
		Susceptible vs. resistant cultivar *	-0.069	75.5%	-0.093	88.5%	-0.095	90.4%	-0.073	81.4%	-0.072	82.5%	-0.091	89%	-0.093	92.1%	-0.071	78.1%

918

Potato	Down-regulated genes	Life cycle of the organism	0.184	6.5%	0.238	2.9%	0.285	0.9%	0.168	6%	0.258	0.3%	0.24	2%	0.238	2.4%	0.205	1.7%
		Pathogenic vs beneficial organism	0.041	42.8%	0.153	25.2%	0.158	24.4%	0.109	30.2%	0.152	27.3%	0.151	21.1%	0.151	23.2%	0.165	18.8%
		Days post infection	0.156	5.9%	0.13	10.6%	0.126	10.6%	0.119	12.4%	0.149	7.3%	0.123	10.1%	0.123	10.6%	0.168	
		Specific treatment organism	0.103	8.8%	0.096	9.9%	0.078	15.4%	0.108	7.7%	0.082	13.9%	0.098	9.3%	0.09	11.7%	0.105	7.5%
		Type/Kingdom of organism	0.032	24.9%	0.047	16.1%	0.03	24.3%	0.044	18.8%	0.035	23.9%	0.047	19.3%	0.046	20.4%	0.023	32.7%
		Susceptible vs. resistant cultivar	-0.029	54.3%	0.021	37%	0.024	36.1%	-0.008	49.5%	0.013	39.7%	0.017	39%	0.025	37.4%	0	45.3%
		Susceptible vs. resistant cultivar *	-0.014	48.8%	0.019	36.2%	0.028	31.1%	-0.007	43.7%	0.013	38%	0.018	34.9%	0.026	31.9%	-0.016	49.1%
		Tissue type	0.05	18.9%	-0.01	51.1%	-0.013	52.7%	-0.013	52.9%	-0.02	57.8%	-0.006	49.7%	-0.01	50.5%	0	45.2%
		Bioproject	0.007	42.9%	-0.036	64.8%	-0.05	68.4%	-0.021	58.5%	-0.017	54.7%	-0.039	66.4%	-0.04	63.4%	-0.034	61.6%
		Tissue type **	-0.057	90.8%	-0.057	92.2%	-0.057	91.5%	-0.061	95.2%	-0.053	88.4%	-0.058	91.5%	-0.058	91.1%	-0.062	96.3%

920 **Table S16: Chi-square analysis to examine the association of R-genes of being potentially regulated by the**
 921 **miR482-superfamily and being differently expressed while expression**

922 The category up-/down-regulated applies to genes that are differentially regulated, but not always in the same
 923 direction.
 924

	Classes	Potential targeted	Not targeted	Chi square	Degree of freedom	p-value
Tomato	Up-regulated R-genes	15	81	0.99	3	0.8035
	Down-regulated R-genes	8	30			
	Not differentially regulated	29	121			
	Up-/down-regulated R-genes	12	63			
Potato	Up-regulated R-genes	22	48	1.91	3	0.5916
	Down-regulated R-genes	20	52			
	Not differentially regulated	50	148			
	Up-/down-regulated R-genes	74	167			

925

926 References

927 Allen, R. L., Bittner-Eddy, P. D., Grenville-Briggs, L. J., Meitz, J. C., Rehmany, A. P., Rose, L. E., & Beynon, J. L.
 928 (2004). Host-parasite coevolutionary conflict between Arabidopsis and downy mildew. *Science*, 306(5703), 1957-
 929 1960.

930 Altschul, S. F., Gish, W., Miller, W., Myers, E. W., & Lipman, D. J. (1990). Basic local alignment search tool. *Journal*
 931 *of molecular biology*, 215(3), 403-410.
 932

933 Andolfo, G., Sanseverino, W., Aversano, R., Frusciante, L., & Ercolano, M. R. (2014). Genome-wide identification
 934 and analysis of candidate genes for disease resistance in tomato. *Molecular breeding*, 33(1), 227-233.
 935

936 Andrews S. (2010). FastQC: a quality control tool for high throughput sequence data. Available online at:
 937 <http://www.bioinformatics.babraham.ac.uk/projects/fastqc>
 938

939 Barad, S., Sela, N., Dubey, A. K., Kumar, D., Luria, N., Ment, D., ... & Prusky, D. (2017). Differential gene expression
 940 in tomato fruit and *Colletotrichum gloeosporioides* during colonization of the RNAi-SIPH tomato line with
 941 reduced fruit acidity and higher pH. *BMC genomics*, 18(1), 579.
 942

943 Baulcombe, D. (2004). RNA silencing in plants. *Nature*, 431(7006), 356-363.
 944

945 Beddows, I., Reddy, A., Kloesges, T., & Rose, L. E. (2017). Population genomics in wild tomatoes—the interplay
 946 of divergence and admixture. *Genome biology and evolution*, 9(11), 3023-3038.
 947

948 Benjamini, Y., & Hochberg, Y. (1995). Controlling the false discovery rate: a practical and powerful approach to
 949 multiple testing. *Journal of the Royal statistical society: series B (Methodological)*, 57(1), 289-300.
 950

951 Bolger, A. M., Lohse, M., & Usadel, B. (2014). Trimmomatic: a flexible trimmer for Illumina sequence data.
 952 *Bioinformatics*, 30(15), 2114-2120.
 953

954 Bray, N. L., Pimentel, H., Melsted, P., & Pachter, L. (2016). Near-optimal probabilistic RNA-seq quantification.
 955 *Nature biotechnology*, 34(5), 525.
 956

957 Brown, J. K. M., & Rant, J. C. (2013). Fitness costs and trade-offs of disease resistance and their consequences for
 958 breeding arable crops. *Plant Pathology*, 62, 83-95.
 959

960 Burdon, J. J., & Thrall, P. H. (2003). The fitness costs to plants of resistance to pathogens. *Genome biology*, 4(9),
 961 227.
 962

- 963 Camacho, C., Coulouris, G., Avagyan, V., Ma, N., Papadopoulos, J., Bealer, K., & Madden, T. L. (2009). BLAST+:
964 architecture and applications. *BMC bioinformatics*, *10*(1), 1-9.
965
- 966 Chae, E., Bomblies, K., Kim, S. T., Karelina, D., Zaidem, M., Ossowski, S., ... & Lechner, S. (2014). Species-wide
967 genetic incompatibility analysis identifies immune genes as hot spots of deleterious epistasis. *Cell*, *159*(6), 1341-
968 1351.
969
- 970 Chakravarthy, S., Tuori, R. P., D'Ascenzo, M. D., Fobert, P. R., Després, C., & Martin, G. B. (2003). The tomato
971 transcription factor Pti4 regulates defense-related gene expression via GCC box and non-GCC box cis elements.
972 *The Plant Cell*, *15*(12), 3033-3050.
973
- 974 Chen, R., Li, H., Zhang, L., Zhang, J., Xiao, J., & Ye, Z. (2007). CaMi, a root-knot nematode resistance gene from
975 hot pepper (*Capsium annuum* L.) confers nematode resistance in tomato. *Plant cell reports*, *26*(7), 895-905.
976 Chen, Q., Xu, X., Jiang, J., & Li, J. (2018). *Transcriptome resequencing analysis of the responses of Ty-5-Mediated*
977 *resistance to TYLCV via in resistant vs. susceptible tomato cultivars* (No. e26578v1). PeerJ Preprints.
978
- 979 Dai, X., Zhuang, Z., & Zhao, P. X. (2018). psRNATarget: a plant small RNA target analysis server (2017 release).
980 *Nucleic acids research*, *46*(W1), W49-W54.
981
- 982 Dees, M. W., Lysøe, E., Alsheikh, M., Davik, J., & Brurberg, M. B. (2016). Resistance to *Streptomyces turgidiscabies*
983 in potato involves an early and sustained transcriptional reprogramming at initial stages of tuber
984 formation. *Molecular plant pathology*, *17*(5), 703-713.
985
- 986 Du, H., Wang, Y., Yang, J., & Yang, W. (2015). Comparative transcriptome analysis of resistant and susceptible
987 tomato lines in response to infection by *Xanthomonas perforans* race T3. *Frontiers in plant science*, *6*, 1173.
988
- 989 Fabro, G., Steinbrenner, J., Coates, M., Ishaque, N., Baxter, L., Studholme, D. J., ... & Jones, J. D. (2011). Multiple
990 candidate effectors from the oomycete pathogen *Hyaloperonospora arabidopsidis* suppress host plant immunity.
991 *PLoS pathogens*, *7*(11), e1002348.
992
- 993 Fawke, S., Torode, T. A., Gogleva, A., Fich, E. A., Sørensen, I., Yunusov, T., ... & Schornack, S. (2019). Glycerol-3-
994 phosphate acyltransferase 6 controls filamentous pathogen interactions and cell wall properties of the tomato
995 and *Nicotiana benthamiana* leaf epidermis. *New Phytologist*, *223*(3), 1547-1559.
996
- 997 Flor, H. H. (1971). Current status of the gene-for-gene concept. *Annual review of phytopathology*, *9*(1), 275-296.
998
- 999 Gao, L., & Bradeen, J. M. (2016). Contrasting potato foliage and tuber defense mechanisms against the late blight
1000 pathogen *Phytophthora infestans*. *PloS one*, *11*(7).
1001
- 1002 Gao, Y., Wang, W., Zhang, T., Gong, Z., Zhao, H., & Han, G. Z. (2018). Out of water: The origin and early
1003 diversification of plant R-genes. *Plant physiology*, *177*(1), 82-89.
1004
- 1005 Glazebrook, J. (2005). Contrasting mechanisms of defense against biotrophic and necrotrophic pathogens.
1006 *Annual review of phytopathology*, *43*, 205.
1007
- 1008 Goyer, A., Hamlin, L., Crosslin, J. M., Buchanan, A., & Chang, J. H. (2015). RNA-Seq analysis of resistant and
1009 susceptible potato varieties during the early stages of potato virus Y infection. *BMC genomics*, *16*(1), 472.
1010
- 1011 Greenwood, P. E., & Nikulin, M. S. (1996). *A guide to chi-squared testing* (Vol. 280). John Wiley & Sons.
1012
- 1013 Gururani, M. A., Venkatesh, J., Upadhyaya, C. P., Nookaraju, A., Pandey, S. K., & Park, S. W. (2012). Plant disease
1014 resistance genes: current status and future directions. *Physiological and molecular plant pathology*, *78*, 51-65.
1015
- 1016 Hao, D., Yang, J., Long, W., Yi, J., VanderZaag, P., & Li, C. (2018). Multiple R genes and phenolic compounds
1017 synthesis involved in the durable resistance to *Phytophthora infestans* in potato cv. Cooperation 88. *Agri Gene*,
1018 *8*, 28-36.
1019

- 1020 Hollander, M., Wolfe, D. A., & Chicken, E. (2013). *Nonparametric statistical methods* (Vol. 751). John Wiley &
1021 Sons.
- 1022
- 1023 Holt III, B. F., Belkhadir, Y., & Dangl, J. L. (2005). Antagonistic control of disease resistance protein stability in the
1024 plant immune system. *Science*, *309*(5736), 929-932.
- 1025
- 1026 Hosmani, P. S., Flores-Gonzalez, M., van de Geest, H., Maumus, F., Bakker, L. V., Schijlen, E., ... & Saha, S. (2019).
1027 An improved de novo assembly and annotation of the tomato reference genome using single-molecule
1028 sequencing, Hi-C proximity ligation and optical maps. *BioRxiv*, 767764.
- 1029
- 1030 Hu, G., DeHart, A. K., Li, Y., Ustach, C., Handley, V., Navarre, R., ... & Baker, B. (2005). EDS1 in tomato is required
1031 for resistance mediated by TIR-class R genes and the receptor-like R gene Ve. *The Plant Journal*, *42*(3), 376-391.
- 1032
- 1033 Huot, B., Yao, J., Montgomery, B. L., & He, S. Y. (2014). Growth–defense tradeoffs in plants: a balancing act to
1034 optimize fitness. *Molecular plant*, *7*(8), 1267-1287.
- 1035
- 1036 Jin, H., Yang, X., Lu, D., Li, C., Yan, Z., Li, X., ... & Qin, B. (2015). Phylogenetic diversity and tissue specificity of fungal
1037 endophytes associated with the pharmaceutical plant, *Stellera chamaejasme* L. revealed by a cultivation-
1038 independent approach. *Antonie Van Leeuwenhoek*, *108*(4), 835-850.
- 1039
- 1040 Jones, J. D., & Dangl, J. L. (2006). The plant immune system. *Nature*, *444*(7117), 323-329.
- 1041
- 1042 Jupe, F., Witek, K., Verweij, W., Śliwka, J., Pritchard, L., Etherington, G. J., ... & Jones, J. D. (2013). Resistance gene
1043 enrichment sequencing (R en S eq) enables reannotation of the NB-LRR gene family from sequenced plant
1044 genomes and rapid mapping of resistance loci in segregating populations. *The Plant Journal*, *76*(3), 530-544.
- 1045
- 1046 Karasov, T. L., Kniskern, J. M., Gao, L., DeYoung, B. J., Ding, J., Dubiella, U., ... & Barrett, L. G. (2014). The long-
1047 term maintenance of a resistance polymorphism through diffuse interactions. *Nature*, *512*(7515), 436-440.
- 1048
- 1049 Kendall, M. G. (1938). A new measure of rank correlation. *Biometrika*, *30*(1/2), 81-93.
- 1050
- 1051 Kim, S. H., Gao, F., Bhattacharjee, S., Adiasor, J. A., Nam, J. C., & Gassmann, W. (2010). The Arabidopsis resistance-
1052 like gene SNC1 is activated by mutations in SRFR1 and contributes to resistance to the bacterial effector AvrRps4.
1053 *PLoS pathogens*, *6*(11).
- 1054
- 1055 Kochetov, A. V., Glagoleva, A. Y., Strygina, K. V., Khlestkina, E. K., Gerasimova, S. V., Ibragimova, S. M., ... &
1056 Antonova, O. Y. (2017). Differential expression of NBS-LRR-encoding genes in the root transcriptomes of two
1057 *Solanum phureja* genotypes with contrasting resistance to *Globodera rostochiensis*. *BMC plant biology*, *17*(2),
1058 251.
- 1059
- 1060 Kourelis, J., & van der Hoorn, R. A. (2018). Defended to the nines: 25 years of resistance gene cloning identifies
1061 nine mechanisms for R protein function. *The Plant Cell*, *30*(2), 285-299.
- 1062
- 1063 Krasileva, K. V., Zheng, C., Leonelli, L., Goritschnig, S., Dahlbeck, D., & Staskawicz, B. J. (2011). Global analysis of
1064 Arabidopsis/downy mildew interactions reveals prevalence of incomplete resistance and rapid evolution of
1065 pathogen recognition. *PLoS one*, *6*(12).
- 1066
- 1067 Kumar, P., Garrido, E., Zhao, K., Zheng, Y., Alseekh, S., Vargas-Ortiz, E., ... & Jander, G. (2018). Teciá solanivora
1068 infestation increases tuber starch accumulation in Pastusa Suprema potatoes. *Journal of integrative plant
1069 biology*, *60*(11), 1083-1096.
- 1070
- 1071 Latchman, D. S. (1997). Transcription factors: an overview. *The international journal of biochemistry & cell
1072 biology*, *29*(12), 1305-1312.
- 1073
- 1074 Lee, R. R., & Chae, E. (2020). Variation patterns of NLR clusters in Arabidopsis thaliana genomes. *Plant
1075 Communications*, *1*(4), 100089.
- 1076

- 1077 Levy, J. G., Mendoza, A., Miller, J. C., Tamborindeguy, C., & Pierson, E. A. (2017). Global gene expression in two
1078 potato cultivars in response to 'Candidatus Liberibacter solanacearum' infection. *BMC genomics*, *18*(1), 960.
1079
- 1080 Librado, P., & Rozas, J. (2009). DnaSP v5: a software for comprehensive analysis of DNA polymorphism data.
1081 *Bioinformatics*, *25*(11), 1451-1452.
1082
- 1083 Li, Y., Hu, X., Chen, J., Wang, W., Xiong, X., & He, C. (2017). Integrated mRNA and microRNA transcriptome analysis
1084 reveals miRNA regulation in response to PVA in potato. *Scientific reports*, *7*(1), 1-16.
1085
- 1086 Li, Y., Yang, S., Yang, H., & Hua, J. (2007). The TIR-NB-LRR gene SNC1 is regulated at the transcript level by multiple
1087 factors. *Molecular plant-microbe interactions*, *20*(11), 1449-1456.
1088
- 1089 Lysøe, E., Dees, M. W., & Brurberg, M. B. (2017). A three-way transcriptomic interaction study of a biocontrol
1090 agent (*Clonostachys rosea*), a fungal pathogen (*Helminthosporium solani*), and a potato host (*Solanum*
1091 *tuberosum*). *Molecular Plant-Microbe Interactions*, *30*(8), 646-655.
1092
- 1093 MacQueen, A., & Bergelson, J. (2016). Modulation of R-gene expression across environments. *Journal of*
1094 *experimental botany*, *67*(7), 2093-2105.
1095
- 1096 Maggini, V., Mengoni, A., Gallo, E. R., Biffi, S., Fani, R., Firenzuoli, F., & Bogani, P. (2019). Tissue specificity and
1097 differential effects on in vitro plant growth of single bacterial endophytes isolated from the roots, leaves and
1098 rhizospheric soil of *Echinacea purpurea*. *BMC plant biology*, *19*(1), 284.
1099
- 1100 Mann, H. B., & Whitney, D. R. (1947). On a test of whether one of two random variables is stochastically larger
1101 than the other. *The annals of mathematical statistics*, 50-60.
1102
- 1103 Martin, G. B., Brommonschenkel, S. H., Chunwongse, J., Frary, A., Ganai, M. W., Spivey, R., ... & Tanksley, S. D.
1104 (1993). Map-based cloning of a protein kinase gene conferring disease resistance in tomato. *Science*, *262*(5138),
1105 1432-1436.
1106
- 1107 McDowell, J. M., Williams, S. G., Funderburg, N. T., Eulgem, T., & Dangl, J. L. (2005). Genetic analysis of
1108 developmentally regulated resistance to downy mildew (*Hyaloperonospora parasitica*) in *Arabidopsis thaliana*.
1109 *Molecular Plant-Microbe Interactions*, *18*(11), 1226-1234.
1110
- 1111 McHale, L., Tan, X., Koehl, P., & Michelmore, R. W. (2006). Plant NBS-LRR proteins: adaptable guards. *Genome*
1112 *biology*, *7*(4), 212
1113
- 1114 Mitchell, A. L., Attwood, T. K., Babbitt, P. C., Blum, M., Bork, P., Bridge, A., ... & Finn, R. D. (2019). InterPro in
1115 2019: improving coverage, classification and access to protein sequence annotations. *Nucleic acids research*,
1116 *47*(D1), D351-D360.
1117
- 1118 Pesti, R., Kontra, L., Paul, K., Vass, I., Csorba, T., Havelda, Z., & Várallyay, É. (2019). Differential gene expression
1119 and physiological changes during acute or persistent plant virus interactions may contribute to viral symptom
1120 differences. *PLoS one*, *14*(5).
1121
- 1122 Pimentel, H., Bray, N. L., Puente, S., Melsted, P., & Pachter, L. (2017). Differential analysis of RNA-seq
1123 incorporating quantification uncertainty. *Nature methods*, *14*(7), 687.
1124
- 1125 Potato Genome Sequencing Consortium (2011). Genome sequence and analysis of the tuber crop potato. *Nature*,
1126 *475*.
1127
- 1128 Qiao, Y., Liu, L., Xiong, Q., Flores, C., Wong, J., Shi, J., ... & Ma, W. (2013). Oomycete pathogens encode RNA
1129 silencing suppressors. *Nature genetics*, *45*(3), 330-333.
1130
- 1131 Sarkar, D., Maji, R. K., Dey, S., Sarkar, A., Ghosh, Z., & Kundu, P. (2017). Integrated miRNA and mRNA expression
1132 profiling reveals the response regulators of a susceptible tomato cultivar to early blight disease. *DNA*
1133 *Research*, *24*(3), 235-250.
1134

- 1135 Sapp, M., Ploch, S., Fiore-Donno, A. M., Bonkowski, M., & Rose, L. E. (2018). Protists are an integral part of the
1136 *Arabidopsis thaliana* microbiome. *Environmental microbiology*, 20(1), 30-43.
1137
- 1138 Shapiro, S. S., & Wilk, M. B. (1965). An analysis of variance test for normality (complete samples). *Biometrika*,
1139 52(3/4), 591-611.
1140
- 1141 Sharma, R., Rawat, V., & Suresh, C. G. (2017). Genome-wide identification and tissue-specific expression analysis
1142 of nucleotide binding site-leucine rich repeat gene family in *Cicer arietinum* (kabuli chickpea). *Genomics data*,
1143 14, 24-31.
1144
- 1145 Shivaprasad, P. V., Chen, H. M., Patel, K., Bond, D. M., Santos, B. A., & Baulcombe, D. C. (2012). A microRNA
1146 superfamily regulates nucleotide binding site-leucine-rich repeats and other mRNAs. *The Plant Cell*, 24(3), 859-
1147 874.
1148
- 1149 Shukla, N., Yadav, R., Kaur, P., Rasmussen, S., Goel, S., Agarwal, M., ... & Kumar, A. (2018). Transcriptome analysis
1150 of root-knot nematode (*Meloidogyne incognita*)-infected tomato (*Solanum lycopersicum*) roots reveals complex
1151 gene expression profiles and metabolic networks of both host and nematode during susceptible and resistance
1152 responses. *Molecular plant pathology*, 19(3), 615-633.
1153
- 1154 Song, F., Zhang, H., Zhang, S. Q., Bouarab, K., Brisson, N., & Daayf, F. (2009). Mitogen-activated protein kinase
1155 cascades in plant defence responses. *Molecular plant-microbe interactions*, 36, 58.
1156
- 1157 Stanke, M., Diekhans, M., Baertsch, R., & Haussler, D. (2008). Using native and syntenically mapped cDNA
1158 alignments to improve de novo gene finding. *Bioinformatics*, 24(5), 637-644.
1159
- 1160 Stokes, T. L., Kunkel, B. N., & Richards, E. J. (2002). Epigenetic variation in *Arabidopsis* disease resistance. *Genes*
1161 *& development*, 16(2), 171-182.
1162
- 1163 Sugimura, Y., & Saito, K. (2017). Comparative transcriptome analysis between *Solanum lycopersicum* L. and *Lotus*
1164 *japonicus* L. during arbuscular mycorrhizal development. *Soil Science and Plant Nutrition*, 63(2), 127-136.
1165
- 1166 Thode, H. C. (2002). *Testing for normality* (Vol. 164). CRC press.
1167
- 1168 Tian, D., Traw, M. B., Chen, J. Q., Kreitman, M., & Bergelson, J. (2003). Fitness costs of R-gene-mediated resistance
1169 in *Arabidopsis thaliana*. *Nature*, 423(6935), 74-77.
1170
- 1171 Tomato Genome Consortium. (2012). The tomato genome sequence provides insights into fleshy fruit evolution.
1172 *Nature*, 485(7400), 635.
1173
- 1174 Tsuda, K., & Katagiri, F. (2010). Comparing signaling mechanisms engaged in pattern-triggered and effector-
1175 triggered immunity. *Current opinion in plant biology*, 13(4), 459-465.
1176
- 1177 Van de Weyer, A. L., Monteiro, F., Furzer, O. J., Nishimura, M. T., Cevik, V., Witek, K., ... & Bemm, F. (2019). A
1178 species-wide inventory of NLR genes and alleles in *Arabidopsis thaliana*. *Cell*, 178(5), 1260-1272.
1179
- 1180 Vos, I. A., Pieterse, C. M., & Van Wees, S. C. (2013). Costs and benefits of hormone-regulated plant defences.
1181 *Plant Pathology*, 62, 43-55.
1182
- 1183 de Vries, S., von Dahlen, J. K., Uhlmann, C., Schnake, A., Kloesges, T., & Rose, L. E. (2017). Signatures of selection
1184 and host-adapted gene expression of the *Phytophthora infestans* RNA silencing suppressor PSR2. *Molecular plant*
1185 *pathology*, 18(1), 110-124.
1186
- 1187 de Vries, S., Kloesges, T., & Rose, L. E. (2015). Evolutionarily dynamic, but robust, targeting of resistance genes
1188 by the miR482/2118 gene family in the Solanaceae. *Genome biology and evolution*, 7(12), 3307-3321.
1189
- 1190 de Vries, S., Kukuk, A., von Dahlen, J. K., Schnake, A., Kloesges, T., & Rose, L. E. (2018). Expression profiling across
1191 wild and cultivated tomatoes supports the relevance of early miR482/2118 suppression for *Phytophthora*
1192 resistance. *Proceedings of the Royal Society B: Biological Sciences*, 285(1873), 20172560.

- 1193
1194 Wagner, G. P., Kin, K., & Lynch, V. J. (2012). Measurement of mRNA abundance using RNA-seq data: RPKM
1195 measure is inconsistent among samples. *Theory in biosciences*, *131*(4), 281-285.
1196
- 1197 Wang, J., Hu, M., Wang, J., Qi, J., Han, Z., Wang, G., ... & Chai, J. (2019a). Reconstitution and structure of a plant
1198 NLR resistosome conferring immunity. *Science*, *364*(6435), eaav5870.
1199
- 1200 Wang, G., Kong, J., Cui, D., Zhao, H., Niu, Y., Xu, M., ... & Wang, W. (2019b). Resistance against *Ralstonia*
1201 *solanacearum* in tomato depends on the methionine cycle and the γ -aminobutyric acid metabolic pathway. *The*
1202 *Plant Journal*, *97*(6), 1032-1047.
1203
- 1204 Wu, C. H., Abd-El-Haliem, A., Bozkurt, T. O., Belhaj, K., Terauchi, R., Vossen, J. H., & Kamoun, S. (2017). NLR
1205 network mediates immunity to diverse plant pathogens. *Proceedings of the National Academy of Sciences*,
1206 *114*(30), 8113-8118.
1207
- 1208 Xue, D. Q., Chen, X. L., Zhang, H., Chai, X. F., Jiang, J. B., Xu, X. Y., & Li, J. F. (2017). Transcriptome analysis of the
1209 Cf-12-mediated resistance response to *Cladosporium fulvum* in tomato. *Frontiers in plant science*, *7*, 2012.
1210
- 1211 Yang, S., Tang, F., Gao, M., Krishnan, H. B., & Zhu, H. (2010). R gene-controlled host specificity in the legume-
1212 rhizobia symbiosis. *Proceedings of the National Academy of Sciences*, *107*(43), 18735-18740.
1213
- 1214 Yang, S., Tang, F., & Zhu, H. (2014). Alternative splicing in plant immunity. *International journal of molecular*
1215 *sciences*, *15*(6), 10424-10445.
1216
- 1217 Yang, H., Zhao, T., Jiang, J., Chen, X., Zhang, H., Liu, G., ... & Li, J. (2017). Transcriptome analysis of the Sm-
1218 mediated hypersensitive response to *Stemphylium lycopersici* in tomato. *Frontiers in plant science*, *8*, 1257.
1219
- 1220 Zhai, X. G., Zhao, T., Liu, Y. H., Long, H., Deng, G. B., Pan, Z. F., & Yu, M. Q. (2008). Characterization and expression
1221 profiling of a novel cereal cyst nematode resistance gene analog in wheat. *Molecular biology*, *42*(6), 960-965.
1222
- 1223 Zheng, Y., Wang, Y., Ding, B., & Fei, Z. (2017). Comprehensive transcriptome analyses reveal that potato spindle
1224 tuber viroid triggers genome-wide changes in alternative splicing, inducible trans-acting activity of phased
1225 secondary small interfering RNAs, and immune responses. *Journal of virology*, *91*(11), e00247-17.
1226
- 1227 Zouari, I., Salvioli, A., Chialva, M., Novero, M., Miozzi, L., Tenore, G. C., ... & Bonfante, P. (2014). From root to
1228 fruit: RNA-Seq analysis shows that arbuscular mycorrhizal symbiosis may affect tomato fruit metabolism. *Bmc*
1229 *Genomics*, *15*(1), 221.
1230
- 1231 Zuluaga, A. P., Solé, M., Lu, H., Góngora-Castillo, E., Vaillancourt, B., Coll, N., ... & Valls, M. (2015). Transcriptome
1232 responses to *Ralstonia solanacearum* infection in the roots of the wild potato *Solanum commersonii*. *BMC*
1233 *genomics*, *16*(1), 246.

Publication IV

Large-scale study of miRNA targets and their functions in tomatoes

Status **Not published; manuscript written**

Journal

Citation **von Dahlen, J. K., Graf, C., Rose, L. E. R. (unpublished): Large-scale study of miRNA targets and their functions in tomatoes.**

Own contribution Designed together with L.E.R. the study; designed together with C.G. the bioinformatic pipelines; run together with C.G. the analysis and interpreted the data; drafted together with C.G. the initial manuscript

Large-scale study of miRNA targets and their functions in tomatoes

Janina K. von Dahlen^{1,2}, Corbinian Graf¹ and Laura E. Rose^{1,3*}

*corresponding author: laura.rose@hhu.de

1 Institute of Population Genetics, Heinrich-Heine University Duesseldorf, Universitaetsstr. 1, 40225 Duesseldorf, Germany

2 iGRAD-Plant Graduate School, Heinrich-Heine University Duesseldorf, Duesseldorf, Germany

3 Ceplas, Cluster of Excellence in Plant Sciences, Heinrich-Heine University Duesseldorf, Duesseldorf, Germany.

Abstract

MicroRNAs (miRNAs) are 21-24nt long non-coding RNAs that are involved in gene regulation by conducting gene silencing. miRNAs have been shown to regulate many different processes in plants such as defence or development. Whether they achieve this by strongly repressing a small set of genes (few target hypothesis) or by repressing a large set of genes in a weakly manner (many target hypothesis) is currently a point of debate. Using PAREsnip2 we analysed 28 publicly available PARE-libraries of the tomato for the targets of 137 miRNAs, 316 isomeric variants of miRNAs (isomiRNAs) and 1615 putative phased secondary siRNAs (phasiRNAs). In total we could verify 287 high confidence targets of which most were either transcription factors or participate in immune response reactions. Moreover, miRNAs and isomiRNAs showed a preference on targeting genes with the same biological function. PhasiRNAs in turn formed smaller, mostly PHAS loci dominated networks. miRNAs likely increase their regulatory power by repressing genes upstream of regulatory cascades. Other ways to boost their regulatory power are multiple targeting of mRNAs by members of the same miRNA/isomiRNA family as well as phasiRNAs. At the same time, isomiRNAs and phasiRNAs broaden the regulatory networks by enlarging the network towards several new targets. Taken together, our results support the “few target” hypothesis. However, as the PARE method most likely cannot verify weak repression (and translational inhibition at all), we see ourselves unable to exclude the many target hypothesis.

Key words

microRNAs, expression repression, PARE-libraries, *Solanum lycopersicum*, degradome, expression regulation, isomeric microRNAs, phasiRNAs

1. Introduction

MicroRNAs (miRNA) are short (usually 21 to 24 nucleotide (nt) long) noncoding RNA molecules that regulate genes in both animals and plants by RNA silencing (Axtell et al. 2013). miRNA coding genes are transcribed into hairpin structure forming primary miRNAs (pri-miRNA) that are processed by Dicer-like (DCL) proteins into the shorter, likewise hairpin-structure forming pre-miRNAs (Rogers and Chen 2013). DCL then cleaves the hairpin further, generating a double stranded duplex consisting of the miRNA and its reverse complementary miRNA*. Afterwards, either the miRNA or the miRNA* are loaded single-stranded into a cleavage protein called Argonaut (AGO). This AGO/miRNA (or AGO/miRNA*) complex, called the RNA induced silencing (RISC) complex, aligns itself and is guided by the bound miRNA or miRNA* to reverse complementary coding mRNAs, the so-called targets. After binding, AGO induces either the cleavage of the mRNA at the center of the alignment or inhibits the translation of the mRNA, likely through blocking the ribosomes from accessing parts of the mRNA (Brodersen et al. 2008, Axtell et al. 2013, Li et al. 2013).

The processes miRNAs regulate are both numerous and essential for the development and health of plants. They include developmental processes (Achard et al. 2004, Curaba et al. 2012, Gu et al. 2013), abiotic stress responses (Zhou et al. 2010, Jeong et al. 2011), defense responses (Zhai et al. 2011, Shivaprasad et al. 2012) as well as several cell functions such as transport (Han et al. 2013). miRNAs achieve many of these regulatory functions by targeting a large array of transcription factor families including MYB, SQUAMOSA or Growth-regulating factors (GRFs, Palatnik et al. 2003, Achard et al. 2004, Jones-Rhoades and Bartel 2004, Carlsbecker et al. 2010, Zhou et al. 2010, Curaba et al. 2012, Sun et al. 2015). For example, the miR165/166 family is known to regulate transcription factors that regulate cell differentiation in the endodermis and stele periphery thereby establishing root cell fate (Carlsbecker et al. 2010). Another example of miRNA regulatory power boosting is the miR482/2118 superfamily, which regulates plant immunity by targeting resistance genes (*R*-genes) of the nucleotide-binding site and leucine-rich repeats class (NBS-LRRs, Shivaprasad et al. 2012, de Vries et al. 2015). The vast array of different regulatory functions for miRNAs is also reflected by their enormous repertoire size. miRBase, the largest database for miRNAs, records for example 428 mature miRNAs for *Arabidopsis thaliana* (*A. thaliana*) and as many as 756 mature miRNAs for the clover species *Medicago truncatula* (Kozomara et al. 2019).

Other sorts of miRNAs which conduct gene silencing are the so-called isomeric variants of miRNAs (isomiRNA) as well as phased secondary siRNAs (phasiRNA). The so called templated isomiRNAs are the results of imprecise or alternative cleavages of miRNA-precursors by DCL (Neilsen et al. 2012). Thus, they differ at their start and termini from the canonical miRNA. Non-templated isomiRNAs in turn are the result of posttranscriptional additions of one or more nucleotides to the isomiRNA sequence, creating the rise of an isomiRNA that no longer matches the canonical gene. While the kind of their biosynthesis and their comparative low expression may make isomiRNAs look like a by-product of miRNA biosynthesis, isomiRNAs were shown to indeed perform RNA silencing. For example, miR-10a-5p isoforms of humans and miRNov627 isoforms of the bean (*Phaseolus vulgaris*) have been shown to regulate many targets of their canonical miRNAs as well as new targets (Cloonan et al. 2011, Formey et al. 2015). Furthermore, isomiRNAs were shown to be differentially expressed during different developmental processes as well as infection (Colaiacovo et al. 2012, Ehya et al. 2013). Therefore, it has been proposed by Ahmed et al. (2014) that isomiRNAs strengthen the regulatory power of their canonical miRNAs through sharing their targets.

PhasiRNAs are a class of secondary miRNAs which are the result of miRNA-triggered DCL activity (Fei et al. 2013, Zheng et al. 2015, Xia et al., 2019). After the cleavage by a miRNA, single-stranded phasiRNA-producing mRNAs are synthesised by RNA-dependent RNA polymerases into double-stranded RNA strands (dsRNA, Fei et al. 2013). The dsRNA is then successively cleaved by DCL into 21 or 24 nucleotide long phased siRNAs which can be subsequently loaded into an AGO and perform RNA silencing (Fei et al. 2013). The regions phasiRNAs arise from are called PHAS loci. In plants PHAS loci do not necessarily encode for proteins. The most prominent non-coding PHAS loci are the TAS-loci (Allen et al. 2005, Yoshikawa et al. 2005, Talmor-Neiman et al. 2006, Rajagopalan et al. 2006). One of the most studied TAS loci is for example the TAS3 family, which is generated by miR390 and targets auxin response factors (Allen et al. 2005). PhasiRNAs are known to regulate pentatricopeptide repeat carrying proteins (Howell et al. 2007, Xia et al. 2013), transcription factors of the MYB family (Rajagopalan et al. 2006, Xia et al. 2012) and NBS-LRRs (Zhai et al. 2011, Shivaprasad et al. 2012). In detail: the miR482/2118 superfamily uses a vast network of secondary miRNAs to

relieve evolutionary pressure from *R*-genes by suppressing the evolution of malicious mutations on the *R*-genes, reducing the cost of having multiple gene copies and therefore allowing for the differentiation of more *R*-genes (Shivaprasad et al. 2012).

There are three common ways to identify putative miRNA targets: i) prediction-based programs such as psRNATarget (Dai et al. 2018) or TargetFinder (Allen et al. 2005, Fahlgren et al. 2007), ii) overexpression studies of miRNAs (Schwab et al., 2005) or iii) parallel analysis of RNA ends (PARE, German et al. 2009). The prediction-based methods rely on reverse complementary to miRNAs to identify and score regions in the genomic DNA. The scoring algorithms differ from program to program, for example, taking mismatches as well as gaps between miRNAs and mRNAs, the minimum free energy needed to unpair mRNAs at their target site or the accessibility of mRNAs for the RISC complex into account (Fahlgren et al. 2007, Ding et al. 2012, Dai et al. 2018). Another target identification approach uses the overexpression of miRNAs to identify their corresponding downregulated targets (Schwab et al. 2005). However, as miRNAs together with their mRNA targets form complex networks with diverse interaction partners, direct cleavage of mRNA targets by miRNAs is difficult to verify using this method. PARE-libraries confirm miRNA/mRNA interactions by employing RNA ligase-mediated 5' amplification of cDNA ends (5'RLM-RACE, Scotto-Lavino et al. 2006). The 5'RLM-RACE captures miRNA-degraded mRNAs by their phosphorylation status: Naturally- as well as miRNA-degraded mRNAs possess at their 5' end a phosphate after the degradation. Using 5'phosphate specific adaptors, degraded mRNAs can either be analyzed by amplification and cloning of single genes or by high-throughput sequencing of whole PARE-libraries (also called degradomes). miRNA targets are verified by the overaccumulation of degraded reads that start exactly at a potential cleavage site of a miRNA (German et al. 2009).

While some plants like *A. thaliana* have been studied extensively regarding their potential miRNA-targets and functions (Pegler et al. 2019, Tiwari et al. 2020), other plants of great research interest such as tomato have not yet been studied to such a great extent. In this paper we therefore performed a large-scale identification of miRNA, isomiRNA and phasiRNA degraded mRNAs in tomato using the PARE approach. Overall, we identified within 28 PARE-libraries 116 miRNA-, 144 isomiRNA- and 150 phasiRNA-targets, leading to a total of 287 individual targets, most often across multiple PARE-libraries verified. We could confirm by using a simulation, that the number of verifiable miRNA targets was saturated meaning that adding further PARE-libraries to our study would have resulted in only a minimal increase of verified targets. Additionally, we observed that miRNAs and isomiRNAs mainly targeted genes that encode for transcription factors and defense, while phasiRNAs mainly target mRNAs that encode for defense and essential cell functions. The importance of the regulation of transcription factor and defense genes by miRNAs was further underscored by the observation that many of these transcripts were targeted by multiple members of the same miRNA family. In general, miRNAs and isomiRNAs formed family-specific networks with targets restricted to one function of category such as transcription factors or defense. PhasiRNAs typically formed smaller and as well mostly family related networks. Despite our results overall being in support of the few target hypothesis, we were unable to reject its counterpart, the many target hypothesis, as weak repression as well as translational repression cannot be verified using the PARE method.

2. Material and Methods

2.1. miRNA & PARE library datasets

PARE-libraries were retrieved from the NCBI Sequence Read Archive (supplemental table 1, Lopez-Gomollon et al. 2012, Karlova et al. 2013, Cao et al. 2014, Feng et al. 2014, Zhou et al. 2016, Bai et al. 2016, Adkar-Purushothama et al. 2017, Zheng et al. 2017, Chiumenti et al. 2018, Olivier and Bragard 2018). This study included 28 PARE-libraries; 23 from the cultivated tomato *Solanum lycopersicum* (*S. lycopersicum*), three from its wild sister species *Solanum pimpinellifolium* (*S. pimpinellifolium*) and two from *Solanum habrochaites* (*S. habrochaites*.) Complete or partial adapters were identified by using FastQC (Andrews 2010) and removed using Cutadapt (Martin 2011). Reads shorter than 20 nucleotides were filtered out and remaining reads were cut to a standard size of 20nt. The standard size of 20nt was chosen because in several PARE-libraries the read quality decreased after about 20nts, making sequencing errors more likely and possibly reducing the number of verifiable targets.

The 137 miRNAs of *S. lycopersicum* were obtained from miRBase (Kozomara et al. 2019), the 316 templated isomiRNAs from the Plant IsomiR Atlas (Yang et al. 2019) and the 1615 21nt long phasiRNAs from Zheng et al. (2015; supplemental table 2). In total we scanned 28 PARE-libraries for the cleavage sites of 2069 miRNAs, isomiRNAs and phasiRNAs.

2.2. Target verification and analysis of target function

miRNAs, isomiRNAs and phasiRNAs targets were verified using the PAREsnip2 tool from the SmallRNA Workbench with default parameters (Stocks et al. 2018, Thody et al. 2018). PAREsnip2 aligns the PARE-libraries and the repertoires of miRNAs, isomiRNAs and phasiRNAs to the *S. lycopersicum* cDNA reference genome (ITAG3.2, Fernandez-Pozo et al. 2015). The program verifies targets as miRNA-degraded when they start at the exact cleavage site of a miRNA, isomiRNA or phasiRNA. PAREsnip2 differentiates between five categories of miRNA/target interactions, with category 0 meaning that the highest read count for the entire target occurred at the miRNA cleavage site and category 4 meaning that only one single read aligned to the cleavage site (Thody et al. 2018). Such category 4 cleavage events might be caused by noise. To decrease the false-discovery rate we therefore excluded target sites with less than ten reads and category 4 from our study. In a sub-analysis however, such category 4 interactions as well as interactions with less than ten reads in general were included again to verify weak-degraded targets. Verified targets that are targeted by more than one miRNA, isomiRNA or phasiRNA were in the following analysis not counted multiple times if not stated otherwise. We tested for significant differences in the number of verified targets between PARE-libraries with pathogenic, abiotic/biotic and without treatments by performing a Mann-Whitney-U (Mann and Whitney, 1947) test for non-normally distributed data or a two-sample t-test for normally distributed data.

Functions of verified targets were determined through comparison with the Sol Genomics Network annotations (Fernandez-Pozo et al. 2015) and a literature search. While we used the ITAG3.2 release of the tomato reference genome for the PARE analysis, we used the meanwhile published annotation of the ITAG4.0 release for describing the gene functions of our targets (Fernandez-Pozo et al. 2015). We assigned the targets to the following ten functional categories: transcription factors, growth regulation, defense related, metabolic processes, transport, miRNA biosynthesis, photosynthesis, cell function, unknown and outdated annotations. The category growth regulation contains genes that were annotated as

part of the growth-regulation factor family (GRF). Defense related targets were either part of the pathogen recognition system or part of the defense response of the plant. Metabolic processes included all chemical reactions transforming a substrate into a new substrate (with the exception of energy/ATP transfer). Transport encompassed both transport into and out of the cell as well as transport of components within the cell. miRNA biosynthesis contained genes necessary for the maturation as well as functional activation of miRNAs. Photosynthesis related genes included genes taking part in the photosynthetic electron transfer. Energy/ATP transfers as well as protein modifications fell into the category cell function together with any other gene which is needed to maintain a cell. Genes with no annotated functions were classified as unknown. Targets which were no longer supported under the newest genome release SL4.0 were grouped into outdated annotations.

To test for significant differences in the distribution of target functions in the mock vs pathogen derived PARE-libraries, we performed Chi-square tests (Greenwood and Nikulin, 1996). Chi-square tests were as well used to test if the function of miRNAs, isomiRNAs and phasiRNAs targets significantly differ. To compare the PARE-method with bioinformatic prediction pipelines, we used psRNATarget with a maximum expectation of ≤ 3.0 as well as TargetFinder with default parameters; both analyses based on the *S. lycopersicum* cDNA v3.2 release. Whenever multiple predictions for the same miRNA/mRNA interaction occurred, only the interaction with the lowest maximum expectation was taken (with a lower expectation representing a higher likelihood of mRNAs being potentially targeted). To assess whether miRNAs prefer to target high or low expressed mRNAs at a higher frequency, expression values of over 34,000 genes derived from 133 transcriptomes of tomato were taken from von Dahlen et al. (unpublished). The expression values (transcripts per million, TPM) per gene were averaged across all 133 transcriptomes and binned in nine expression classes (off = 0-1, extremely low = 1-25, low = 25-100, medium-low = 100-250, medium = 250-500, medium-high = 500-750, high = 750-1000, very high ≥ 1000). To test for targeting preferences of miRNAs on expression height, the proportion of verified targets in each bin was plotted against the total number of genes in each bin.

2.3. Target saturation curve & correlation analysis

To check whether the comparatively low number of targets was caused by an insufficient number of PARE-libraries, a target saturation curve was generated by pooling all 28 PARE-libraries and using an in-house script to create ten datasets containing each 100×10^6 out of 372×10^6 randomly chosen reads (no duplicates allowed). The miRNA targets of these ten datasets were identified using PAREsnip2, starting with the first 2×10^6 unique reads of each dataset and continuously adding the next 2×10^6 unique reads until the complete size of 100×10^6 reads was analyzed for their targets. A size of 2×10^6 per sub-dataset was chosen as this size equals the number of reads of the smallest PARE library used in this study. Additionally, we tested for correlation between the PARE library size and the number of identified targets as well as between the number of mapped reads and identified targets, using Spearman's rank correlations (Hollander et al. 2013).

2.4. Data visualization

The targeting networks based on information from the temporary.align file created by PAREsnip2. The networks were created using Cytoscape (Shannon et al. 2003). miRNAs, isomiRNAs and phasiRNAs were grouped into families according to their miRBase/isomiR Atlas annotations or their PHAS loci described by Zheng et al. (2015).

3. Results

3.1. PARE-libraries generated high confident targets

We performed a large-scale identification and analysis of mRNAs regulated by miRNA, isomiRNA and phasiRNA and their functions in tomato. To identify such high confident mRNAs, we employed PAREsnip2 on 28 publicly available PARE-libraries (supplemental table 1). Cleavage sites with a PAREsnip2 category higher than three or less than ten reads were discarded from the study, yielding in 116 high confident targets from in total 137 investigated miRNAs (supplemental table 3). High confidence targets are characterized by a high number of reads starting exactly at the predicted cleavage site of a miRNA in relation to the total reads aligned to this target (supplemental figure 1A). In contrast, low confidence targets of for example category 4 are characterized by only one read aligned to the putative cleavage site of the miRNA (supplemental figure 1B).

3.2 The yield of verified targets depends on sequencing quality

We noticed that the two PARE-libraries SRR5179088 and SRR5179089 with the highest number of reads yielded very few verified miRNA targets (1 and 6 respectively). Two of the smallest PARE-libraries (SRR2071657 and SRR4420593) in turn yielded a medium number of verified targets (26 and 43 respectively, figure 1A). We therefore performed a Spearman's rank correlation, confirming that the number of verified targets is indeed not correlated with the PARE library size represented by the reads per library (p-value = 0.0589, rho = 0.3023, figure 1B). Yet, the PARE-libraries still contained reads that were, for example because of their low complexity or low sequencing quality, not suitable for analysis by PAREsnip2. Indeed, by correlating the number of mapped reads with the number of verified targets per PARE library, the Spearman's rank correlation confirmed a moderately, positive correlation between both factors (p-value = 0.0062, rho = 0.4657, figure 1C). The correlation becomes even stronger when the two outliers SRR5179088 and SRR5179089 were removed from analysis (supplemental figure 2). This overall indicates that the number of identifiable targets within PARE-libraries does not depend on the sequencing depth but on the sequencing quality.

We furthermore noticed that several targets have been confirmed by more than one PARE library (curve of verified cumulative unique targets, figure 1A). Indeed, 81.03% of all targets could be verified in more than one PARE library; 53.45% of all targets in more than four PARE-libraries (figure 1D). As the average number of PARE-libraries per bioproject in our study is 2.8, this would mean that at least half of our targets were identified independent of their bioproject and its experimental procedure. In contrast only 22 targets (18.97%) were verified in a single PARE library. These results overall suggest that adding more bioprojects to our study would increase the number of verified targets only slightly. Furthermore, these results indicate that the verified targets are of high confidence as the majority of them have been verified in more than one PARE library and even between different bioprojects.

Since the expression of many genes and therefore their regulatory mechanisms change in response to stress such as pathogens, (biotic stress, Moy et al. 2004, Agudelo-Romero et al. 2008, Guo et al. 2011, Fan et al. 2017) or temperature, drought or salinity, (abiotic stress, Xiong et al. 2002, Wahid 2007, Li et al., 2011), we overlapped the verified targets of biotic (12x PARE-libraries), abiotic (3x PARE-libraries) and untreated (mock, 13x PARE-libraries) PARE-libraries. This confirmed that the majority of targets (75.86%) were not treatment specific degraded (figure 1E). In agreement with that we could not observe a significant difference in the average number of unique targets between mock, abiotic/biotic and pathogenic treated

plants (supplemental figure 3). In summary, any global significant changes in miRNA targeting were not discovered between treated and untreated plants.

Next, we noticed that PARE-libraries collected from different tissues seemed not to add many unique targets to the cumulation curve (figure 1A, blue line, supplemental table 1). This suggests that most targets can be verified independent of the tissue-type. As a verification for this hypothesis, we analyzed the overlap of targets between the most common tissue type leaves (21x PARE-libraries) and all other tissue-types (7x PARE-libraries, supplemental figure 4). Only five targets (4.31% of all targets) were unique to tissues other than leaf (e.g. fruits, upper part of plant). However, 41 targets (35.34% of all targets) were unique to leaves. If these differences are caused by the unequal sampling size or the different tissues, could not be determined in this study.

3.3. The PARE-libraries are saturated and confirm less verified targets than bioinformatical approaches

To test if expanding the number of PARE-libraries yields in an increase in verified targets, we generated a target saturation curve by pooling all 28 PARE-libraries and using an in-house script to create ten datasets each containing 100×10^6 randomly chosen unique reads out of the 372×10^6 pooled reads of all PARE-libraries (mapped and unmapped reads; figure 2A). Subsequently, all ten pooled datasets were divided into 50 subsets each containing 2×10^6 reads. Each subset was then analyzed with PAREsnip2 and the number of unique targets cumulative plotted against the size of the ten datasets (figure 2A). This approach yielded in a logarithmical saturation curve proving that the number of PARE-libraries – after a certain cut-off – has only a small positive effect on the total number of verified miRNA targets. Half of the 116 targets of this study were for example identified using 16.3×10^6 reads (or 4.38% of all 372×10^6 reads); 75% of the targets by analyzing 61.5×10^6 (or 16.53%) reads. To verify according to the logarithmic function all 116 miRNAs targets, one would need to analyze approximately 232.4×10^6 reads (or 62.47% of all reads). However, an increase of less than one miRNA target over 2×10^6 reads would already be reached by analyzing about 44×10^6 reads (or 11.83% of all reads). These results overall indicate that enlarging the number of PARE-libraries will most likely increase the number of verified targets in this study only by a few.

Another reason for the low number of identified targets could be that other forms of miRNAs such as isomiRNAs and phasiRNAs play a larger role in gene silencing than previously thought. We added therefore 316 isomiRNAs to our study allowing us to identify in total 144 targets. However, only 35 (or 24.31%) of these isomiRNAs targets were not as well targeted by miRNAs (figure 2B). To boost our target yield further, we included 1615 phasiRNAs from Zheng et al. (2015) into the study. The phasiRNAs resulted in 150 targets out of which 136 were previously not validated by miRNAs and isomiRNAs bringing us to in total 287 verified targets for this study (figure 2B). While the phasiRNAs in numbers verified the most targets, they possessed the smallest ratio of a miRNA group with a target with 7.93% compared to 35.77% for miRNAs and 46.52% for isomiRNAs (figure 2C). This indicates that most phasiRNAs do not participate in gene silencing. By comparing the number of phasiRNAs with targets with the PHAS loci frames, we observed that the PHAS loci frames one to nine possessed overall more phasiRNAs with at least one target than the loci frames ten and higher (supplemental figure 5A). However, in proportion to the total number of phasiRNAs each PHAS loci generated, we did not notice such overaccumulation anymore (supplemental figure 5B). In summary while

miRNAs and isomiRNAs were very similar in their targeting patterns, phasiRNAs might represent a different mode of gene silencing.

In a next step, we used psRNATarget as well as TargetFinder to compare our targets with the bioinformatical predicted ones. TargetFinder predicted for the 137 miRNAs a total of 891 potential miRNA/mRNA interactions with an expectation cut-off of four or lower (with a lower expectation rate representing more confident interactions, supplemental table 4). These 891 potential miRNA/mRNA interactions covered 95.81% of the 191 interactions verified by PAREsnip2. This meant that TargetFinder predicted 4.87 more interactions than we could verify. While a stricter cut-off of three would lower the overprediction rate to 2.35, it would also remove 30.37% of all verified interactions. In contrast, psRNATarget reported 1599 potential cleavage based miRNA/mRNA interactions with an expectation of ≤ 3 (supplemental table 4). These 1599 predictions covered 91.10% of all verified interactions translating into an overprediction rate of 9.19. In summary, while both programs came with a tradeoff of either a greater number of verifiable targets not being predicted or an increased overprediction rate, we determined that the tradeoff is the smallest in TargetFinder at an expectation rate of four.

3.4. miRNAs and isomiRNAs mainly regulate transcription factors and defense related mRNAs

Previous studies have shown that miRNAs regulate diverse processes such as developmental and stress responses (Achard et al. 2004, Zhai et al. 2011, Zhou et al. 2010, Jeong et al. 2011, Curaba et al. 2012, Shivaprasad et al. 2012, Gu et al. 2013). To evaluate the functions of our targets, we assigned all targets into one out of the ten following functional categories: transcription factor, growth regulation, defense related, metabolic process, transport, miRNA biosynthesis, cell function, unknown and outdated annotation. Nearly two-thirds of all miRNA targets assigned to the category's transcription factors (37.93%) and defense related genes (25.86%, figure 3A). The other categories contribute in the following descending order towards miRNA regulation: growth regulation (8.62%), cell function and unknown (each 6.90%), miRNA biosynthesis (5.17%), transport (3.45%), metabolic processes (2.59%), outdated annotations (1.72%) and photosynthesis (0.86%). The large overlap in targets between miRNAs and isomiRNAs (figure 2B) is also noticeable in the fact that isomiRNAs comparable to miRNAs target mainly transcription factors (33.33%) and defense related genes (27.78%, figure 3B). Indeed, we did not observe significant differences in the distribution of the functional categories between miRNA and isomiRNA targets (p-value = 0.7245; supplemental table 5). On the contrary phasiRNAs regulate mainly genes which interact with cell function (26.67%) as well as plant defense (24.67%) followed by metabolic processes and genes with an unknown classification (18.00% and 14.00% respectively, figure 3C). Transcription factors in turn account for only 6% of all phasiRNA targets. In accordance we observed a significant difference in the distribution of the functional categories between phasiRNA and miRNA/isomiRNA targets (p-value <0.00001, supplemental table 5).

To adapt to shifting environmental circumstances such as drought, heat or pathogens, plants constantly adapt the expression of their genes and miRNAs (Moy et al. 2004, Agudelo-Romero et al. 2008, Yang et al. 2019, Feng et al. 2014, Cao et al. 2014). Taking this into account we investigated whether miRNA mediated degradations reflect adaptations to shifting environmental circumstances. However, we did not observe any significant difference in the distribution of functional categories between mock treated and abiotic/biotic treated plants

for the miRNA, isomiRNA and phasiRNA targets (p-value = 0.9907, p-value = 0.9795 and p-value = 0.1666 respectively (supplemental table 6)).

3.5. Particularly transcriptions factors are multiple targeted by miRNAs and isomiRNAs

Several miRNA targets are known to be multiple times targeted by members of the same miRNA family (Palatnik et al. 2007, de Vries et al. 2015). Indeed, 82.12% of the iso-miRNA targets (combined miRNA and isomiRNA targets) of this study were targeted by more than one iso-miRNA (figure 3D). However, the distribution of functional categories was for these multiple targeted genes not significantly different to all targets (p-value 0.9027; supplemental table 7). Out of all iso-miRNA targets 46.36% are regulated by even five or more iso-miRNAs (figure 3D). This group of ≥ 5 iso-miRNAs targets was significantly enriched for transcription factors and growth regulating genes (p-value = 0.0046, figure 3D, supplemental table 7). Yet 10.60% of all iso-miRNA targets were regulated by ten or more iso-miRNAs with the transcription factors *Solyc08g066500* and *Solyc12g044410* being targeted by 18 different iso-miRNAs. Nearly all of these highly multiple times targeted genes (≥ 10 iso-miRNAs) were transcriptions factors, with six belonging to the Squamosa promoter binding protein family, five belonging to the Class III homeodomain-leucine zipper family and two members of the *Solanum lycopersicum* TCP family. The only by ≥ 10 iso-miRNAs targeted non-transcription factor gene was the defense gene *Solyc05g008070*.

In contrast to iso-miRNAs, only 12.67% of phasiRNA targets are regulated by more than one phasiRNA (supplemental figure 6). Most of these multiple phasiRNA targeted genes were defense related genes (52.63%). The two to the highest rate targeted genes were the two defense related genes *Solyc10g051050* and *Solyc11g069990* with five respectively seven phasiRNAs targeting them. In summary while phasiRNA targets are overwhelmingly regulated by a single phasiRNA, iso-miRNA targets were mainly regulated by multiple iso-miRNAs and encode most often for transcription factors.

3.6. miRNAs and isomiRNAs form divers via multiple targeting connected miRNA family networks

With the target functions and their distribution analysed, we next reconstructed the miRNA/target network. The 28 miRNA families form 26 miRNA/target networks with an average (avg.) of 1.88 ± 1.48 miRNA members and 4.46 ± 5.06 targets per network (figure 4A). Although most networks were formed by individual miRNA families, the miR482 and miR6024 targeting networks were interconnected through the defense gene *Solyc05g008070* with robust targeting bounds on both sides of the networks (verified both in eight independent PARE-libraries, figure 4B). Another inter-miRNA family connected network is the miR159 and miR319 network. Both families are connected with a high confidence by *gamyb-like1* (*Solyc01g009070*; verified in five PARE-libraries on each miRNA family side) and *gamyb-like 2* (*Solyc06g073640*; verified in ten PARE-libraries on each miRNA family side, figure 4B). Furthermore, of the 13 networks containing ≥ 3 targets, all focused on one functional category meaning that at least 60% of all targets in a network had the same functional category. Even when elevated to 90%, more than two-third of all networks still displayed a categorical focus (69.23%). These results overall indicate that miRNAs form robust, mostly miRNA family-based networks which consist most often of targets of a certain functional category.

The two largest family networks were the miR482 and miR396 family networks with each consisting of 15 targets (figure 4B). The miR482 network is clearly enriched for defense related targets (80% of all targeted genes) while the miR396 family mainly targeted growth regulating genes (60% of all targeted genes). In comparison, 73.33% of all targets in the miR396 network were targeted by more than one family member compared to only 26.67% in the miR482 network. Both networks displayed moreover at first glance a high target-confidence, with the targets being verified on average in 4.68 ± 4.86 (miR482) and 7.15 ± 6.43 (miR396) PARE-libraries respectively. At second glance the miR482 network is clearly enriched for verification within a single bioproject (SRS472306, SRS472307, SRS472308 and SRS472309, supplemental table 3). Meanwhile two targets in the miR482 network (*Solyc02g036270*, *Solyc06g005410*) were verified in >50% of all PARE-libraries, with *Solyc02g036270* being the highest degree targeted gene of the whole study with verification in 21 PARE-libraries. There are controversy studies existing about *R*-genes being induced upon infection (as their expression is cost-intensive) or being constantly expressed no matter the infection status (Tian et al. 2003, Karasov et al. 2014, Gu et al. 2005 vs. Brown & Rant 2013, von Dahlen et al. unpublished). Within this study degradation events by the miR482-superfamily, a master regulator of *R*-genes (Shivaprasad et al. 2012, de Vries et al. 2015), could be verified in untreated as well as treated libraries to an approximately equal level (supplemental table 3).

In comparison to miRNAs, the 26 isomiRNA families form 24 isomiRNA/target networks with an avg. of 6.17 ± 5.23 isomiRNA and 6.00 ± 6.99 targets per network (supplemental figure 7). This indicates that while isomiRNA networks obtain compared to miRNA networks on average more miRNA members (1.88 ± 1.48 to 6.17 ± 5.23) they obtain an only slightly higher level of targets per family member (4.46 ± 5.06 to 6.00 ± 6.99). Not surprisingly, more isomiRNA than miRNA targets were targeted by more than one miRNA (75.69% vs. 42.24%). While for isomiRNAs of the families miR395, miR399, miR5303 and miR827 no targets could be verified, we were able to verify targets for their miRNAs (supplemental table 3). In turn iso-miR5302 (eight targets) and iso-miR9472 (one target) were represented in the isomiRNA but not the miRNA networks. Similar to the miRNAs, 81.25% of all isomiRNA targets from networks with ≥ 3 targets focused on one categorical function. At the elevated threshold, meaning that 90% of all targets in a family network had to share the same functional category, still 50.00% of the networks retained a focus for one categorical function. The two largest isomiRNA networks were again miR482 and miR396 with 22 and 19 targets respectively (figure 4C). However, this time the proportion of genes targeted by more than one isomiRNA was closer between miR482 and miR396, than for the miRNA families (84.21% and 68.18% respectively). This strong increase for the rate of multiple targeting could also be observed for example for miR6024 and miR6027 (91.67% and 77.78% respectively). Overall, isomiRNA networks were larger than miRNA networks by having more isomiRNA family members and targets and are to a higher degree interconnected due to the elevated level of multiple targeting.

The phasiRNA networks in turn possesses a nearly 1:1 ratio of phasiRNA family to network members (75 families (here referring to phasiRNAs sharing the same PHAS locus); 66 networks, supplemental figure 8). In accordance, phasiRNA networks contained compared to miRNAs a similar number of phasiRNAs/miRNAs per network (1.94 ± 1.90 to 1.88 ± 1.48 respectively), but approximately half as much targets per network (2.27 ± 2.27 to 4.46 ± 5.06 respectively, supplemental figure 8). Of all 128 phasiRNAs with a verified target, 75.78% targeted only a single gene. Consequently, the number of networks with ≥ 3 targets was compared to the miRNA (50.00%) and isomiRNA (60.00%) networks with 22.73% much lower.

Furthermore, of these networks with ≥ 3 targets fewer focused on one functional category (40.00%) compared to miRNA and isomiRNA networks (100.00% and 81.25% respectively). At the elevated threshold of 90% only two networks still show a functional focus. Of all 29 networks with at least two phasiRNAs, only three consist of phasiRNAs from more than one PHAS locus. The network with the most phasiRNAs from different PHAS loci is the one formed by SL2.40ch07_C, SL2.40ch11_B and SL2.40ch11_A. These results overall indicate that phasiRNAs form smaller networks with fewer members and fewer targets than miRNAs or isomiRNAs. In addition, the phasiRNA networks share rarely a functional category and seldomly form interconnected family member (PHAS loci) networks.

3.7. Low confident targets enlarge the miRNA network only to a relatively small level

As the miRNAs formed a smaller network than expected in this study, we questioned if low confident targets meaning targets that are only supported by a few or even a single degraded read will enlarge the miRNA network to a relevant level. Some authors state that such weak regulated targets are just noise (Soto-Suárez et al. 2017, Zhao et al. 2017). Other authors emphasise that weakly degraded targets might contribute to the regulatory power of miRNAs (Chen et al. 2017). To identify such weakly degraded targets of miRNAs, we re-analysis the degradomes by including category 4 targets as well as targets which were confirmed with less than 10 reads to our study. Across all 28 libraries we were able to identify 269 low-confident miRNA-mRNA interactions (compared to 191 high confident miRNA/mRNA interactions, supplemental table 8). However, most of these interactions (63.20%) have been already verified with a high confident level. In addition, only 26 of the remaining low confident miRNA/target interactions were in more than three degradomes confirmed, making most of the remaining interactions more likely to represent noise. Overall, low confident targets enlarge therefore the miRNA network to a relatively small level.

3.8. The degree of iso-miRNA/phasiRNA targeting is independent of its target's expression levels

Chen et al. (2017) observed in humans, that to a higher degree expressed genes generally harbour fewer miRNA target sites than weakly expressed genes. In addition, following the many target hypothesis the avoidance of high expressed genes increases the suppression rate of low to moderately expressed genes by less competition for RISC complex loading (Chen et al. 2017). To test this hypothesis, we averaged the expression values of >34,000 genes from 133 transcriptomes (von Dahlen et al. unpublished), divided them into eight expression categories (from off to very high) and determined the proportion of targets to non-targets in each category (supplemental figure 9). Expression categories have in average $0.39 \pm 0.31\%$ (iso-miRNA) to $0.77 \pm 1.05\%$ (phasiRNA) of their genes regulated by smallRNAs. The category with the highest ration of smallRNA regulated genes is the 750-1000 TPM category of phasiRNAs. Four categories included no targeted genes: 500-750 TPM and 750-1000 TPM for iso-miRNAs; 500-750 TPM and ≥ 100 TPM for phasiRNAs. All in all, this suggests that iso-miRNAs/phasiRNAs target their genes within *S. lycopersicum* independent of their expression status.

3.9. miRNA, isomiRNA and phasiRNA cleavages cause <1% of all degradation events

miRNAs have been shown to regulate diverse processes in plants such as immunity (Zhai et al. 2011, Shivaprasad et al. 2012, de Vries et al. 2015) or development (Achard et al. 2004, Curaba et al. 2012, Gu et al. 2013). This raises the question to which level miRNAs, isomiRNAs and phasiRNAs contribute to gene expression regulation within the plant. By sorting all mapped

reads of the degradomes towards having a miRNA, isomiRNA or phasiRNA cleavage event origin or not, we determined that across all degradomes 0.14% of all mapped reads were caused by a miRNA, isomiRNA or phasiRNA cleavage event. Consequently, the vast majority of degraded reads has an origin beyond miRNA, isomiRNA or phasiRNA cleaving and therefore might either represent other forms of expression regulation or mRNA senescence.

4. Discussion

miRNA guided gene silencing has been shown to regulate diverse processes in plants such as development (Achard et al. 2004, Curaba et al. 2012, Gu et al. 2013), abiotic stress responses (Zhou et al. 2010, Jeong et al. 2011) or immunity (Zhai et al. 2011, Shivaprasad et al. 2012, de Vries et al. 2015). Over the last years, PARE-libraries have been established as an efficient tool to verify direct cleavage of miRNAs using a combination of experimental and bioinformatical approaches (German et al. 2008, Li et al. 2011, Lopez-Gomollon et al. 2012, Xia et al. 2012, Candar-Cakir et al. 2016). Using the program PAREsnip2 we analysed 28 public available PARE-libraries for the targets of miRNAs, isomiRNAs and phasiRNAs from *S. lycopersicum*. We were able to verify 116 high confident targets for 49 miRNAs. This number is comparatively lower than for other studies which include only one bioproject and therefore a lower number of PARE-libraries (Pantaleo et al. 2010, Li et al. 2010). As causal, we suggest our stringent cut-off criteria (discarding targets of category 4 and with less than 10 reads). Indeed, a study using similar cut-offs as us confirmed a comparable number of targets (Karlova et al. 2013). In fact, the authors of PAREsnip2 (Thody et al. 2018) advise to put more weight on high abundance of reads and validation of miRNA/mRNA interactions in multiple PARE-libraries than on miRNA/mRNA interactions with low read abundance or single PARE library verification. This advice may become even more important when analysing plants other than *A. thaliana* as the settings of PAREsnip2 are fitted towards this Brassicaceae (Thody et al. 2018). As the vast majority of our miRNA/mRNA interactions could be verified in several, independent of each other created PARE-libraries and are having a high read abundance, our miRNA/mRNA interactions are most likely of high confident.

To reconstruct miRNA regulatory networks, different methods have been employed within plants. The fastest and easiest method to identify potential miRNA regulated mRNAs are prediction-based programs such as psRNATarget (Dai et al. 2018), TAPIR (Bonnet et al. 2010) or TargetFinder (Allen et al. 2005, Fahlgren et al. 2007). However, as Fridrich et al. (2019) noted even the best prediction programs seem to generally overpredict the number of miRNA/mRNA interactions, while never predicting all verified miRNA/mRNA interactions. A phenomenon we could as well observe in our own study as psRNATarget overpredicted the miRNA/mRNA interactions at a rate of 9.19 and TargetFinder at a rate of 4.87. Meanwhile, psRNATarget predicted 91.10% of all interactions verified by PAREsnip2, while TargetFinder predicted 95.81%. However how vastly prediction programs really overpredict (or not) miRNA/mRNA interactions is even with our study hard to assess, as PARE-libraries often based on a limited number of tissues, time points and external stimuli (Adkar-Purushothama et al. 2017, Zheng et al. 2017, Chiumenti et al. 2018, Olivier and Bragard 2018). Likewise, while we used PARE-libraries from different plant organs, close related species, sampling points and biotic as well as abiotic treated plants, some tissues and conditions were still underrepresented and/or missing in our study such as flowers, roots, seeds or drought and salt stress. However at least for the by us analysed PARE-libraries from fruit and flowers, the number of targets unique to them compared to the PARE-libraries sampled from leaves was comparatively low. This suggest that only a few new targets could be additionally verified by

enriching the study by such underrepresented tissues. Likewise, most miRNA targets of pathogenic treated plants could by us also be verified in untreated plants. In agreement with that, our PARE-libraries were saturated in their power to predict miRNA/mRNA interactions. For example, 50% of all miRNA targets of our study could already be verified with about 4.38% of the total reads analysed in this study. To verify further targets, a logarithmically increase of reads would be needed. Or in other words: Most miRNA targets can be verified with a relatively small number of PARE-libraries/PARE reads, while to verify further targets a significant increase in effort would be needed. Overall, our results displayed for prediction programmes a discrepancy between the overprediction and covering of true miRNA/mRNA interactions. Due to its better performance, we recommend to use TargetFinder with an expectation category cut-off of 4 when studying miRNAs within tomato.

The discovery of a limited number of miRNA/mRNA interactions hints furthermore directly to the two contrary hypotheses of miRNA targeting: The few and the many target hypotheses. The many target hypothesis asserts that each miRNA/ miRNA family has based on genome-wide revers-complementary target searches >100 targets (Zhao et al. 2017). The few target hypothesis in turn argues that the vast majority of those predicted miRNA targets are just noise, since miRNAs seem to repress only a few of their targets strong enough to cause phenotypic changes (Soto-Suárez et al. 2017, Zhao et al. 2017). Our results agree with the latter theory. However, one has to question, whether PARE is the right method to verify for example weaker degradation interactions as the PARE scoring based on the proportion of miRNA cleavage associated reads to total degraded reads of a gene. By using within this study a less stringent cut-off, low confident targets increased the miRNA/target network by the factor of 1.41x. However, 63.20% of these low confident interactions reflect only the high confident interactions. This overlap between stringent to less stringent targets may indicate that a variance within the rate of degradation within each PARE library exists. Indeed, several publications proved, as already mentioned, that for example miRNA expression can be altered by pathogens (Feng et al. 2014) or tissue-types (Korir et al. 2013) within *S. lycopersicum*. Following these different miRNA expression levels, degradation levels might be as well shifted between conditions. In addition, targets and as such also weak regulated targets become more likely as in more libraries they are degraded (Thody et al. 2018). By including this approach of multiple library verification to our low confident target analysis the number of new miRNA/target interactions increased only by 26. Thus, the vast majority of the weak regulated degradation events are less likely to take place. To ultimately verify miRNA interactions, pull down methods have to be employed. This method uses biotin tagged miRNA and streptavidin-agarose beads to purify and isolate miRNA/mRNA complexes from cell lysate (Ørom et al. 2008). Overall, our results are in accordance with the few target hypothesis. However, we also acknowledge that the PARE method is not optimized to truly verify weak degradation events, which are central to the many target hypothesis. In combination, with the fact that PARE is unable to detect translational inhibition, we see ourselves unable to exclude either hypotheses of miRNA targeting. Matching the “many-targets” hypothesis the omnigenic model proposes that many complex traits are strongly affected by peripheral genes which have no direct influence on a trait (Boyle et al., 2017). Core genes – genes directly linked to a trait – in turn explain traits to a lesser extent than peripheral genes.

Proponents of the many targets hypothesis have further argued that weakly repressed targets are no noise because they potentially stabilise the gene regulatory network (GRN) through the cumulation of broad but weak repression of targets (Chen et al. 2017). The theory underlines that miRNAs influence GRN by targeting many factors that sit at or near the top of gene regulatory cascades, where even a small change in expression can lead to significant changes further downstream. Chen et al. (2017) concluded that hence transcription factors are preferred targets of miRNAs. Indeed, both literature (Palatnik et al. 2003, Achard et al. 2004, Jones-Rhoades and Bartel 2004, Carlsbecker et al. 2010, Zhou et al. 2010, Curaba et al. 2012, Gu et al. 2013) and our results proofed that transcription factors are the most targeted functional class of miRNAs/ miRNA families, bursting the regulatory power of miRNAs. Next to transcription factors, defense-related genes such as *R*-genes form the second largest group of miRNA targets in our study. As such they most likely play as well a part in the stabilisation of the GRN as *R*-genes elucidate gene regulatory cascades in response to pathogens. Furthermore, *R*-genes and transcription factors are multiple times targeted by different miRNA family members. De Vries et al (2015) theorised that this kind of multiple targeting reduces the fitness costs plants suffer from miss-expressed *R*-genes, as well as lowering the evolutionary constraint on *R*-genes allowing them for a greater diversification. However, one has to consider that we could verify fewer interactions than predicted by de Vries et al. (2015) with their bioinformatical approach.

Our results furthermore show that isomiRNAs, isomeric variants of known miRNAs, boost the robustness of miRNAs, by targeting most often the same targets as their canonical miRNAs, applying a further layer of multiple targeting to the networks. Besides that, isomiRNAs are having their own targets that further broadens the network. Especially the isomiRNAs of the miR482 family boosted the network robustness as nearly all targets were targeted by more than one iso-miRNA. A similar increase of multiple targeting by isomiRNAs could be seen for other defense gene targeting miRNAs like miR6024 and miR6027. Similar observations to the ones above led Ahmed et al. (2014) to the theory that isomiRNAs help miRNAs to facilitate gene silencing as they share their targets. Therefore, isomiRNAs reduce suppression on unintended targets as these unintended targets compete with the main targets of canonical miRNAs for degradation by binding of the RISC complex. Indeed, only a small fraction of new targets was added to our study by including isomiRNAs. We therefore propose that isomiRNAs play a vital role in the stabilisation and enlargement of miRNA networks through multiple targeting of miRNA targeted genes as well as targeting of new, miRNA non-targeted genes.

Another way to enhance the broad regulatory effects of miRNAs are phasiRNAs. phasiRNAs can be generated after a miRNA mediated cleavage event when the cleaved mRNA is processed into 21 or 24 nt long miRNAs that themselves can facilitate gene silencing. phasiRNAs regulate either the same or other targets than their parental miRNAs, which lead to entire new regulatory cascades within the miRNA regulatory network (Chen et al. 2007, Howell et al. 2007). Thus, miRNAs regulate, next to their direct targets, through phasiRNAs several more mRNAs, broadening not only their network capacity but also increasing their stabilizing effects. phasiRNA producing mRNAs are known to encode more likely for *R*-genes, making it more likely that because of sequence similarity phasiRNAs will as well target *R*-genes (Zhai et al. 2011). Indeed, most of our phasiRNAs originated from *R*-genes, though their targets were more divers than their origin miRNA ones indicating that the miRNA cascade influences indirectly processes like the metabolism, transport and other processes crucial for the function of the cell. While phasiRNAs have been as well shown to target transcription factors

(Allen et al. 2005, Zheng et al. 2015), in our study they were underrepresented as targets of phasiRNAs. This, however, is likely due to the underrepresentation of transcription factor coding PHAS loci in the study of Zheng et al. (2015) which we used as phasiRNA input for PAREsnip2.

The likelihood of phasiRNA interactions is further strengthened by the fact that >20% of the verified PHAS loci were produced from miRNA cleavage event which were verified within this study. The majority of this PHAS loci were targeted by the plant immunity regulators miR482 and miR6024 family (Shivaprasad et al. 2012, Chiumenti et al. 2018). The known PHAS loci *Solyc06g005410* (Li et al. 2012, Canto-Pastor et al. 2019) for example was in this study the second most verified target gene within the miR482 network. At the same time, 20% is a relatively small amount of PHAS loci with a verified miRNA cleavage event origin. This raises the question when those other phasiRNAs were triggered. While up to 39 phasiRNAs are generated from a single PHAS locus, our results proof that only a few, in most cases even a single member of each loci facilitate gene silencing. Xia et al (2017) argued nevertheless that phasiRNAs are most likely essential for gene regulation as otherwise genes like the TAS loci families would not have been conserved across multiple plant families.

Another yet not mentioned method how miRNAs, isomiRNAs and phasiRNAs broaden their regulatory power is their mobility. As mobile expression regulators they can move either from cell-to-cell or systemically between plant compartments (Chitwood et al. 2009, Schwab et al. 2009, Pagliarani and Gambino, 2019). An example of a mobile miRNA was reported by Carlsbecker et al. (2010) who determined that miR165/166 generated in the endodermis are transported to the plant vascular cylinder. In another study by Tsikou et al. (2018) miR2111 was shown to be translocated from shoot to root to establish rhizobial symbiosis. Hence iso-miRNAs as well as phasiRNAs are not limited to their location of expression. Instead they can regulate gene expression on a more global level. At the same time their mobility might also be one reason why we observed many degradation events independent of the tissue type.

In addition to cleaving the target-mRNA, translational inhibition by miRNAs was shown to be essential for expression regulation of genes (Brodersen et al. 2008, Iwakawa & Tomari, 2013, Yu et al. 2017) for example in response to abiotic stress responses (Reis et al. 2015) or temperature and developmental stages (von Born et al. 2018). Studies employing PARE however miss the extent of miRNAs regulating these responses as translational inhibition does not include the cleavage of the mRNA. The factor that determined the mode of miRNA action – either cleaving or translational inhibition – is so far unknown. Yet, sequence complementary is not the driving force as the same mRNAs can undergo translational inhibition as well as cleaving by the same miRNA (Iwakawa & Tomari, 2013).

The fact that only 0.14% of all mappable degraded reads within the degradomes have a miRNA, isomiRNA or phasiRNA cleavage origin, raises in turn the question how important miRNA mediated regulation of gene expression for plants is. As the vast majority of degraded reads represent other forms of expression regulation as well as natural occurring senescence, one might erroneously conclude that miRNAs and its relatives might represent a less important branch of mRNA regulation. However, one has to consider that miRNA mediated regulation is a fast acting and highly specific form of expression regulation (Baulcombe 2004, Axtell et al. 2013). As such it allows for precise regulation of even single mRNAs. Its importance becomes even more apparent when considering the fact that miRNAs themselves are highly

regulated in their abundance and activity. Their expression is for example controlled by miRNA sponges (Bak & Mikkelsen 2014), nucleotide variations within the primary miRNAs (Liu et al. 2008, Todesco et al. 2012, Zhu et al. 2013) or transcription factors (Wu et al. 2009). Additionally, the expression abundance of miRNAs is influenced by negative feedback loops as for example miR168 regulates the expression abundance of Argonaute1 (Vaucheret et al. 2004) and miR162 in turn the abundance of Dicer like1 (Xie et al. 2003). Also the fact that the miRNA-repertoire did not decline over time (Zhao et al. 2017) but instead expands (Tanzer & Stadler 2004, Marco et al. 2012, Shivaprasad et al. 2012) and that both processed strands of miRNA synthesis (the mature miRNA and its miRNA*) can be potentially regulative active (Okamura et al. 2008, Jagadeeswaran et al. 2010, Zhang et al. 2011) show how important miRNAs are for plants.

At the same time our study does not allow us to draw conclusions for the reason why in some libraries a target is degraded while it isn't in others. Even in the case of the highly analyzed miR482 superfamily no consistent pattern of miRNA regulation became obvious: While Shivaprasad et al. (2012) pointed out that *R*-genes are induced upon infection – and consequently released from miRNA482 degradation – a new study by us proofed that many *R*-genes are consistently at a low level expressed across 133 transcriptomes (von Dahlen et al. unpublished). In case of an inducible system, one would expect *R*-genes to be degraded in absence of pathogens. However, we did not see such a pattern in this study. One reason for the absence of such pattern might however be that for the verification of a target both – the mRNA as well as the miRNA – need to be expressed. At the same time most degradation events might be time-sensitive meaning that *R*-genes might be for example only an extremely short period after infection non-degraded.

In conclusion, by combining 28 PARE-libraries from different studies we were able to explore the miRNA/mRNA interactions in tomato to a so far unprecedented degree. We confirmed 116 miRNA, 144 isomiRNA and 150 phasiRNA high confidence targets. Our results therefore support the few target theory meaning that miRNAs regulate only a handful of genes in a meaningful manner. However, we cannot exclude its counterpart – the many but weak – theory, as the limitations of the PARE method most likely did not allow us to assess weak (and translationally inhibited) miRNA/target interactions. Furthermore, our results point to miRNAs achieving a burst in their regulatory effect by targeting mainly transcription factors, *R*-genes and other genes upstream of regulatory cascades. Further boosting is achieved through robust multiple targeting of genes and enlargement of target networks through isomiRNAs and phasiRNAs.

Figure and Tables:

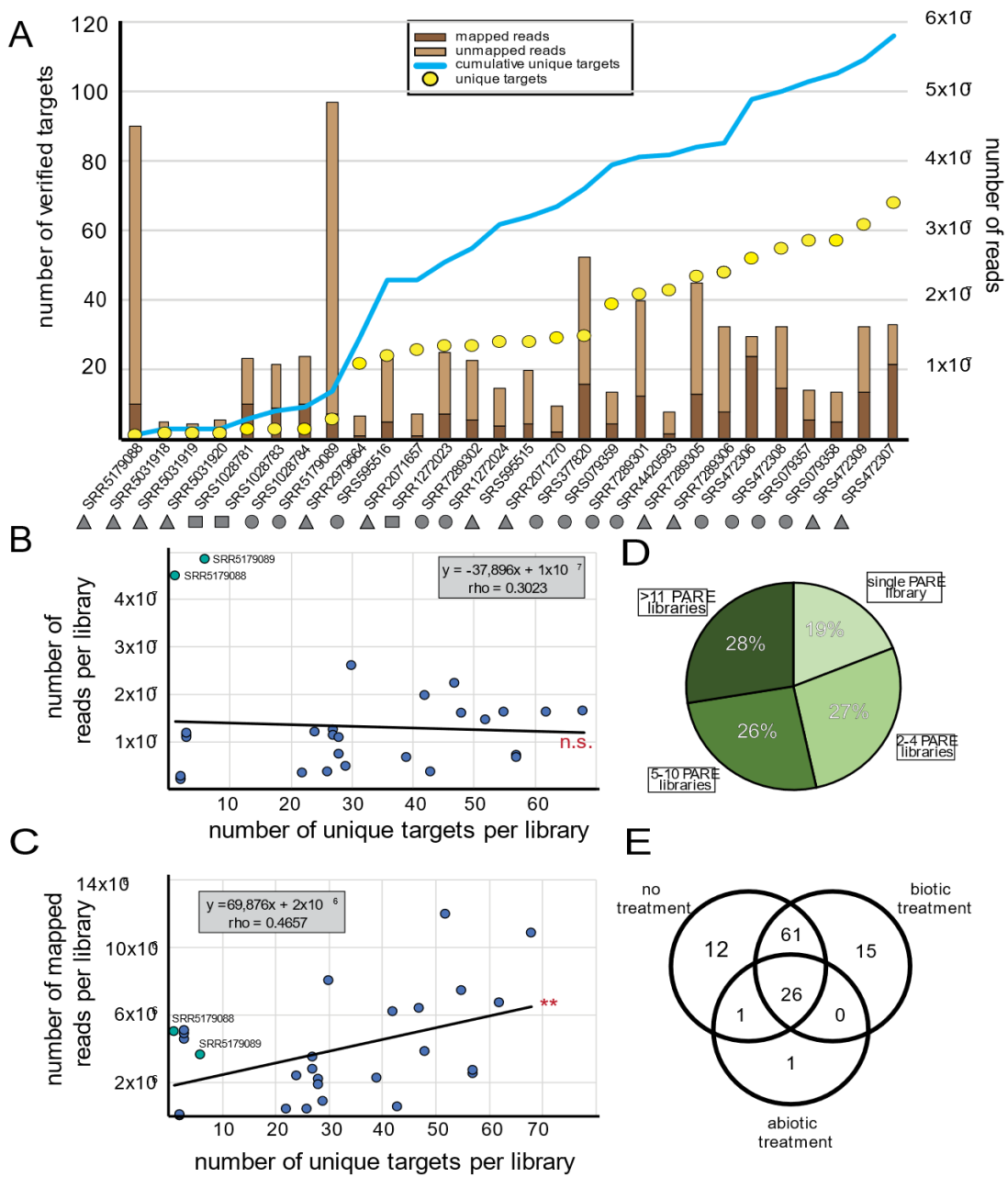


Figure 1: Quality (dependency) of the PARE library verified targets

(A) For each of the 28 PARE libraries the number of total reads (light brown) and mapped reads (dark brown, y-axis on the right) is indicated by a staggered bar graph. The number of unique miRNA targets per PARE library is represented by a yellow dot (left y-axis). The PARE libraries were sorted from left to right by the number of unique miRNA targets in ascending order. The kind of treatment of each PARE library is indicated next to its name (mock [circle], biotic [triangle] or abiotic treatment [square]). The orange line reflects the cumulation of the total number of unique targets across all PARE libraries. (B-C) Spearman rank correlation between the number of verified targets (x-axis) for each PARE library against the number of reads (B) or against the number of mapped reads (C) (y-axis) in each PARE library (blue dots). The turquoise dots highlight the two outlier PARE libraries. Correlation values: $\rho = 0.3023$ (B), $\rho = 0.4657$ (C). p-value < 0.01 (**), not significant (n.s.). (D) Overlap of miRNA targets between PARE libraries. One PARE library (light green), between 2 and 4 PARE libraries (medium light green), between 5 and 10 PARE libraries (medium dark green), more than 11 PARE libraries (dark green). N = 116 unique targets. (E) Venn diagram displaying the overlap of miRNA targets between PARE libraries with different treatments (mock (N = 13), biotic (N = 12), abiotic treatment (N = 3)).

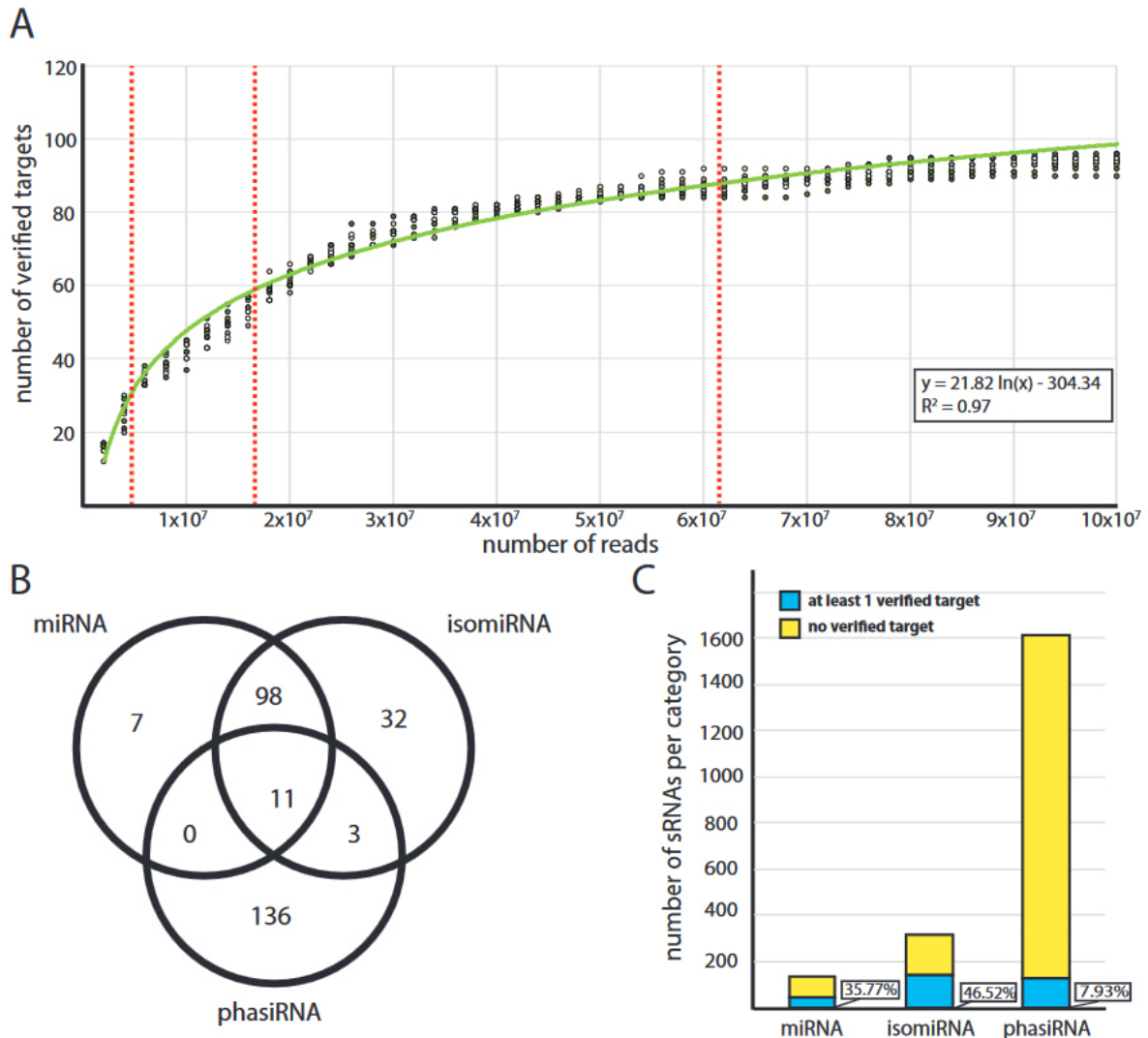


Figure 2: Target yield in dependency of the number of reads analyzed and among miRNAs, isomiRNAs and phasiRNAs
(A) Simulation of the number of miRNA targets in dependency of the number of reads analyzed. Each color stands for one out of ten datasets containing 100×10^6 unique, randomly selected reads from the 28 PARE libraries. The graph is plotted cumulative meaning that for each addition of 2×10^6 reads only previous unverified miRNA targets were added. The green line represents the logarithmic function fitted to the data; the R^2 quantifies the goodness of fit towards the logarithmic function. The dashed red lines represent the library sizes in which 25%, 50% or 75% of all targets could be verified. **(B)** Overlap of targets between miRNAs, isomiRNAs and phasiRNAs. **(C)** Staggered bargraph of the total number of miRNAs, isomiRNAs and phasiRNAs with at least one target (light blue) or no such target (yellow). The numbers next to the bargraphs are representing the fractions of miRNAs, isomiRNAs or phasiRNAs with targets compared to all miRNAs, isomiRNAs or phasiRNAs.

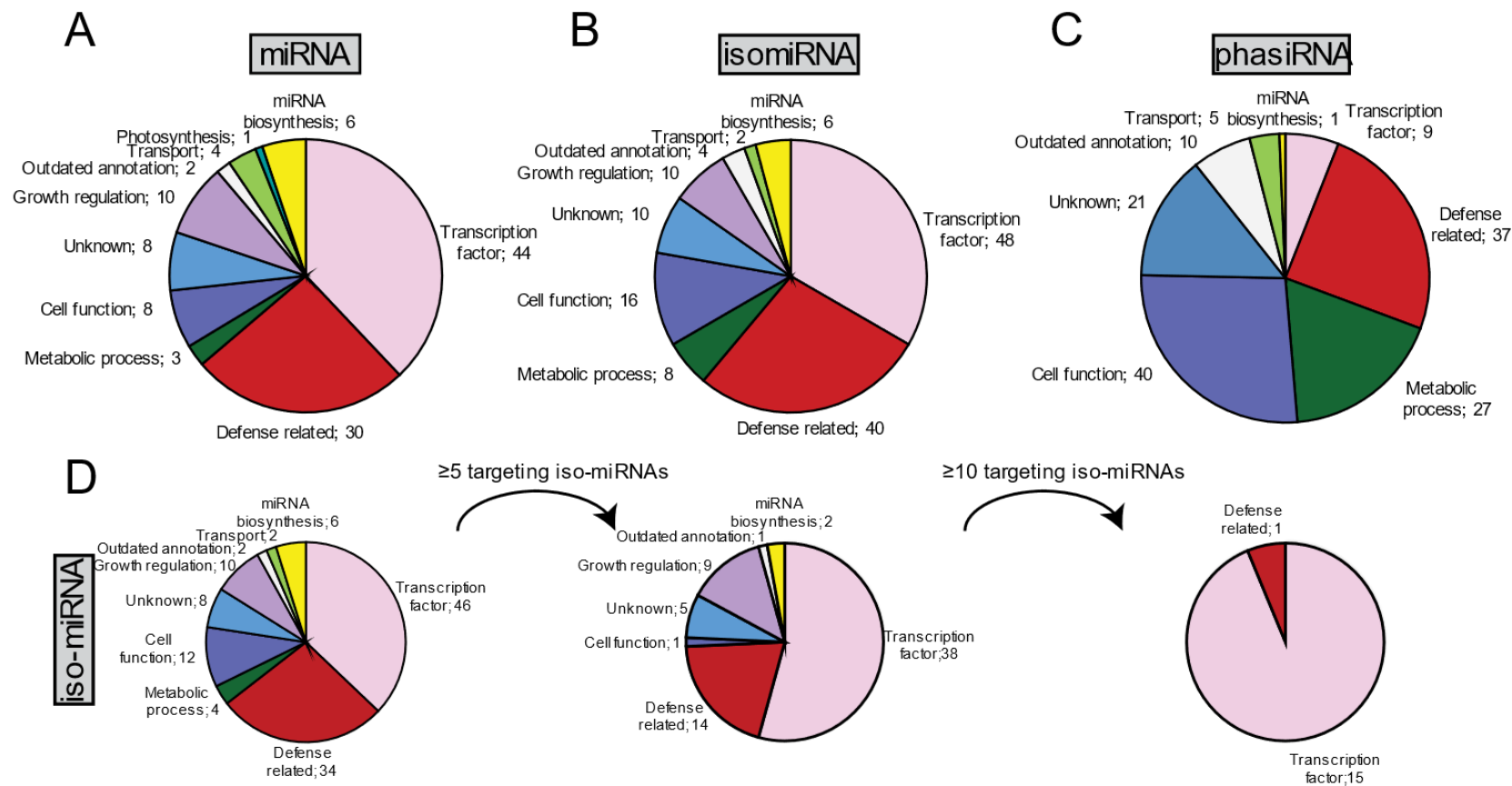


Figure 3: Function of miRNA, isomiRNA and phasiRNA targeted genes

(A-C) Distribution of all miRNA (A), isomiRNA (B) and phasiRNA (C) targets into one of the following ten gene function categories: Transcription factor (pink), Defense related (red), Metabolic process (dark green), Cell function (dark blue), Unknown (light blue), Growth regulation (purple), Outdated annotation (white), Transport (light green), Photosynthesis (turquoise) and miRNA Biosynthesis (yellow). The number of unique targets in each category can be found next to its name. (D) Distribution by gene function of all iso-miRNA (miRNAs and isomiRNAs combined) targets that were regulated by more than one (left circle), five or more (middle circle) and ten or more (right circle) iso-miRNAs

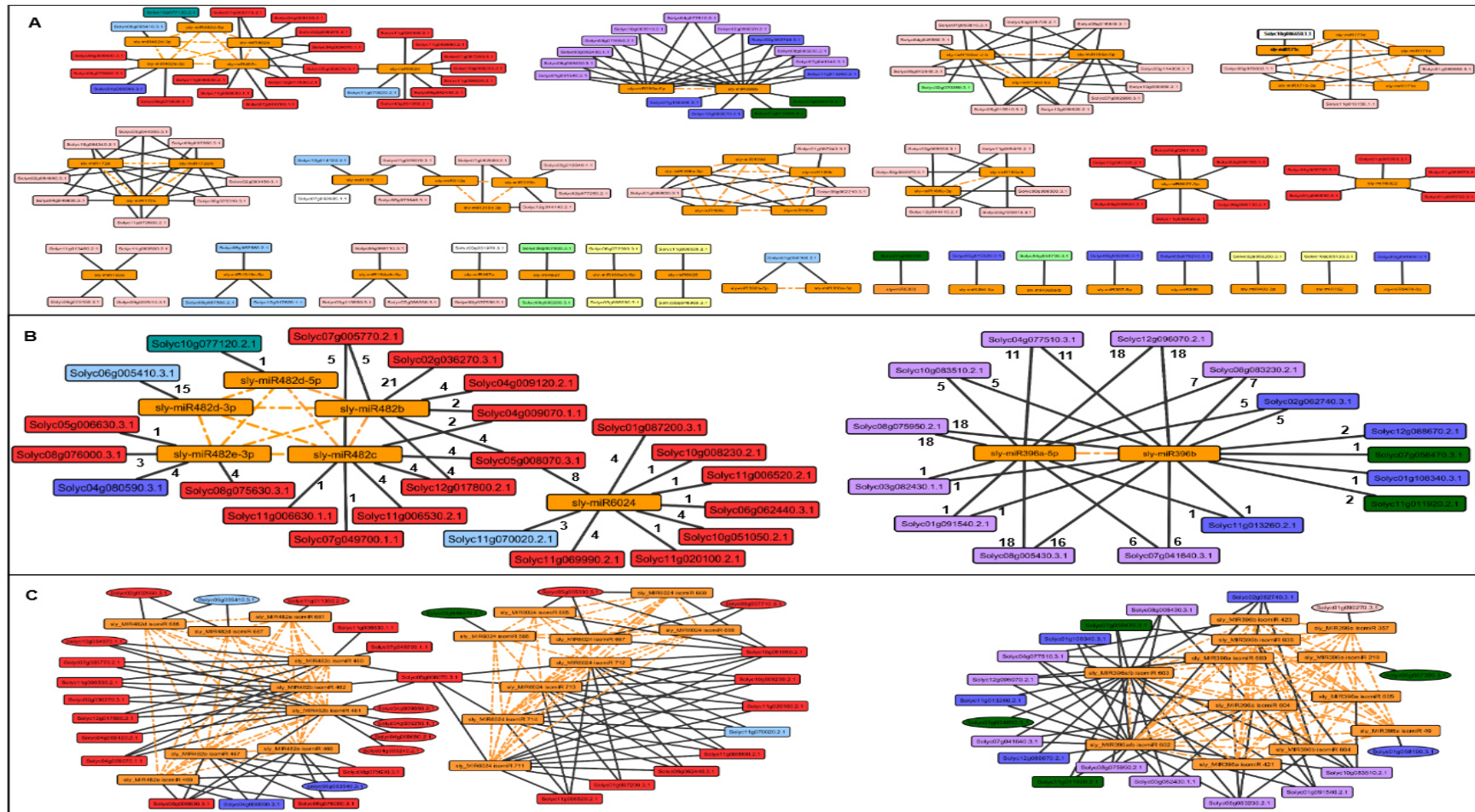
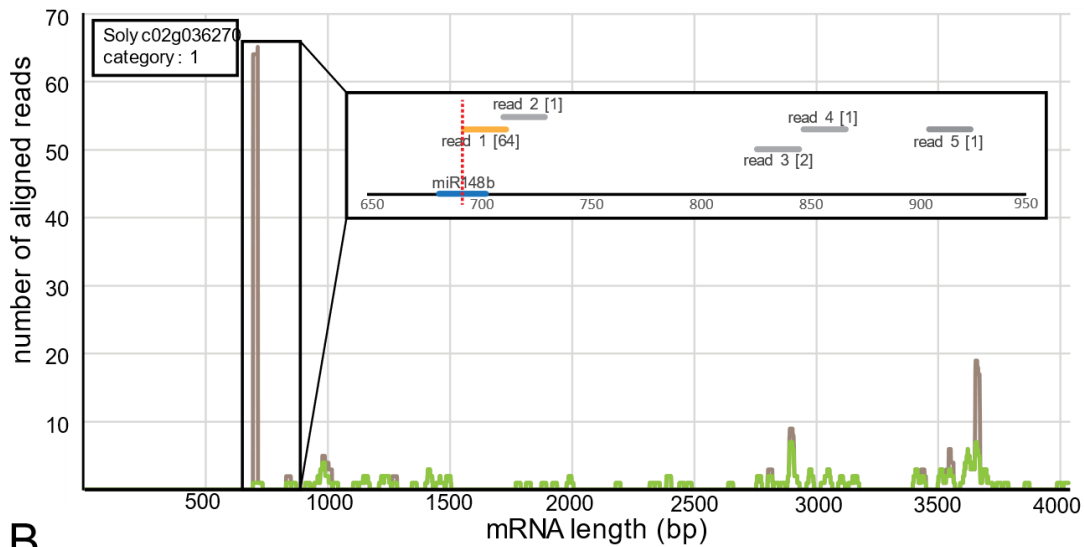


Figure 4: (iso)-miRNA/mRNA interaction networks

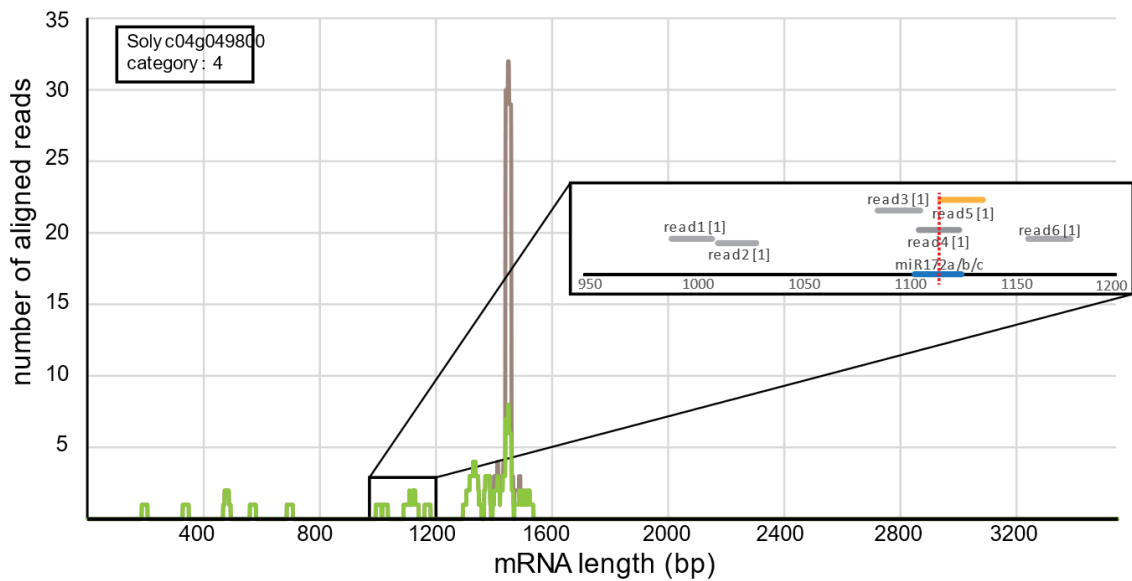
(A) Members of the same miRNA family are connected with a dotted orange line, while targets are connected with their regulating miRNAs through a black line. Targets are coloured in accordance with their function (red = defense related, pink = transcription factor, dark blue = cell function, light blue = Unknown, turquoise = photosynthesis, purple = growth regulation, dark green = metabolic process, light green = transport, yellow = miRNA biosynthesis, white = outdated annotation). **(B)** Close-up of the two largest miRNA/mRNA networks, miR482 (left) and miR396 (right). The numbers next to the edges represent the number of PARE libraries in which the miRNA/mRNA cleavage events were verified. **(C)** Close-up of the two largest isomiRNA networks, miR482 (left) and miR396 (right). Targets surrounded by a square are targets of miRNAs as well as isomiRNAs; oval-shaped targets are specific to isomiRNAs.

Supplemental figure and tables:

A

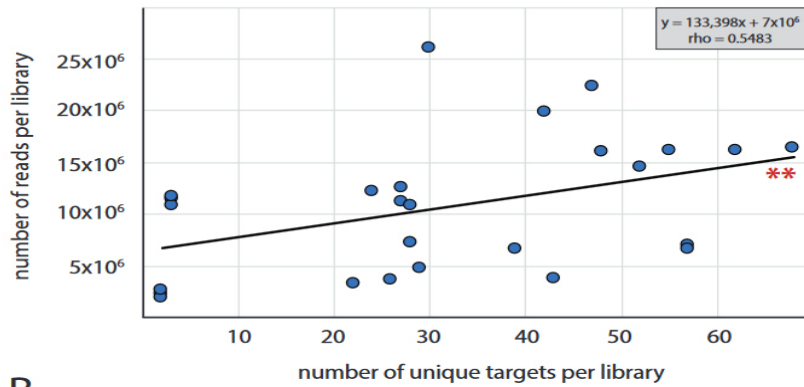
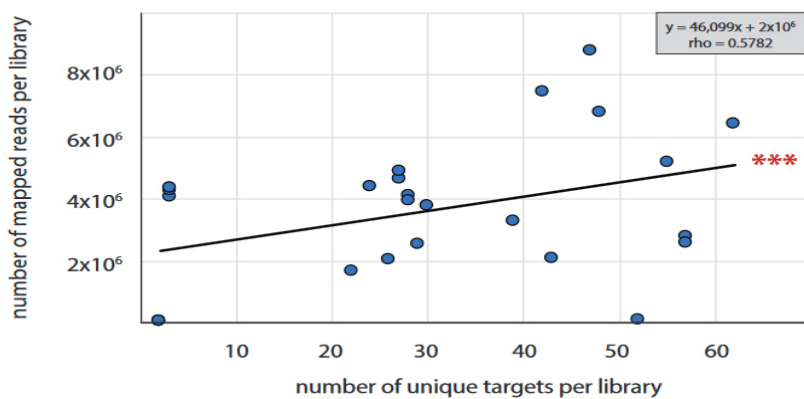


B



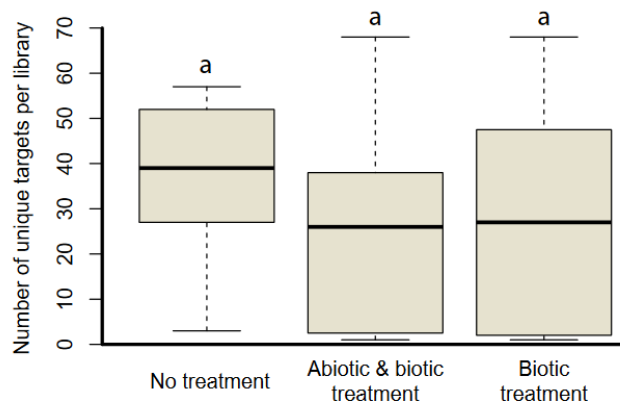
Supplemental Figure 1: Examples of high and low confidence miRNA targets

Unique reads (green) and total reads (brown) from the PARE library SRR2071657 were aligned to the genes Solyc02g036270.3.1 **(A)** and Solyc04g049800.3.1 **(B)**. Peak heights indicate the aligned read abundance. Unique reads are having a unique sequence, not shared with any other read. The boxes contain a zoom into the alignments at the miR482b **(A)** and miR172a/b/c **(B)**-binding regions (both shown in blue) and their flanking areas. All PARE library reads aligned to this region are indicated and numbered consecutively; the abundance of each read within the PARE library is displayed in brackets next to the read name. The cleavage site of the miRNA is marked by a dotted red line and the towards the cleavage site aligned read in orange. **(A)** Shows a high confidence target [read1, category 0] meaning that the highest read abundance for the whole gene accumulates at the cleavage site of miR148b. **(B)** Shows a low confidence target [read 5, category 4], meaning that only one read is located to the cleavage site of miRNA172a/b/c.

A**B**

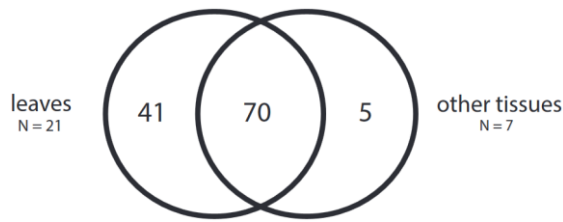
Supplemental Figure 2: Correlation of the number of verified targets to the number of (mapped) reads without outlier PARE libraries

Spearman rank correlation without the two outliers PARE libraries SRR5179088 and SRR5179089. Number of verified targets (x-axis) for each PARE library against the number of reads (A) or against the number of mapped reads (B) (y-axis) in each PARE library (blue dots). The correlation between the two factors is visualized by an exponential equation (black line; formula). Rho = 0.5453 (A); Rho = 0.5782 (B). p-value < 0.01 (**); p-value < 0.001 (***)



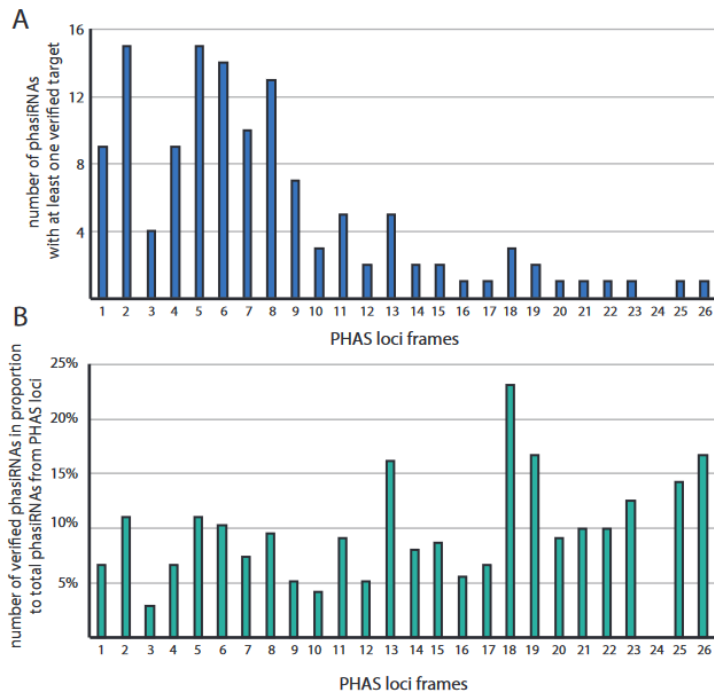
Supplemental Figure 3: Distribution of the number of unique targets verified in each PARE library sorted by treatment

The PARE libraries were sorted into three groups: no treatment (mock; left), abiotic and biotic treatment (middle) or pathogenic treatment (right). The middle line in the box represents the median, the boxes the upper and lower 50% quartile and the dotted lines the standard deviation. Significant differences between the groups are indicated by different letters above the boxplots.



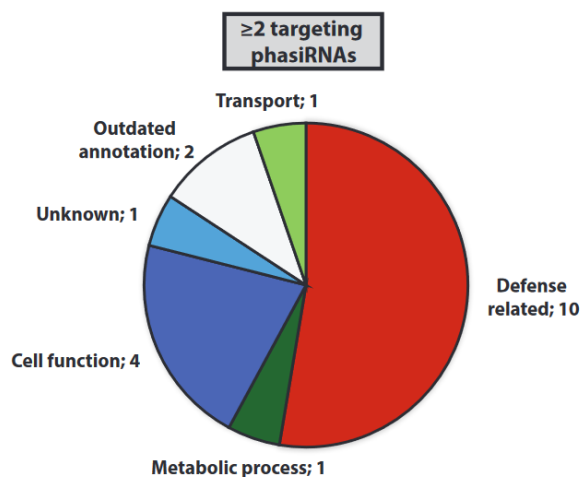
Supplemental Figure 4: Overlap of targets between tissues

Venn diagram displaying the overlap of miRNA/mRNA interactions between PARE libraries derived from leaf tissue (N = 21) and tissues other than leaf (N = 7), pooled together due to their individually low number.



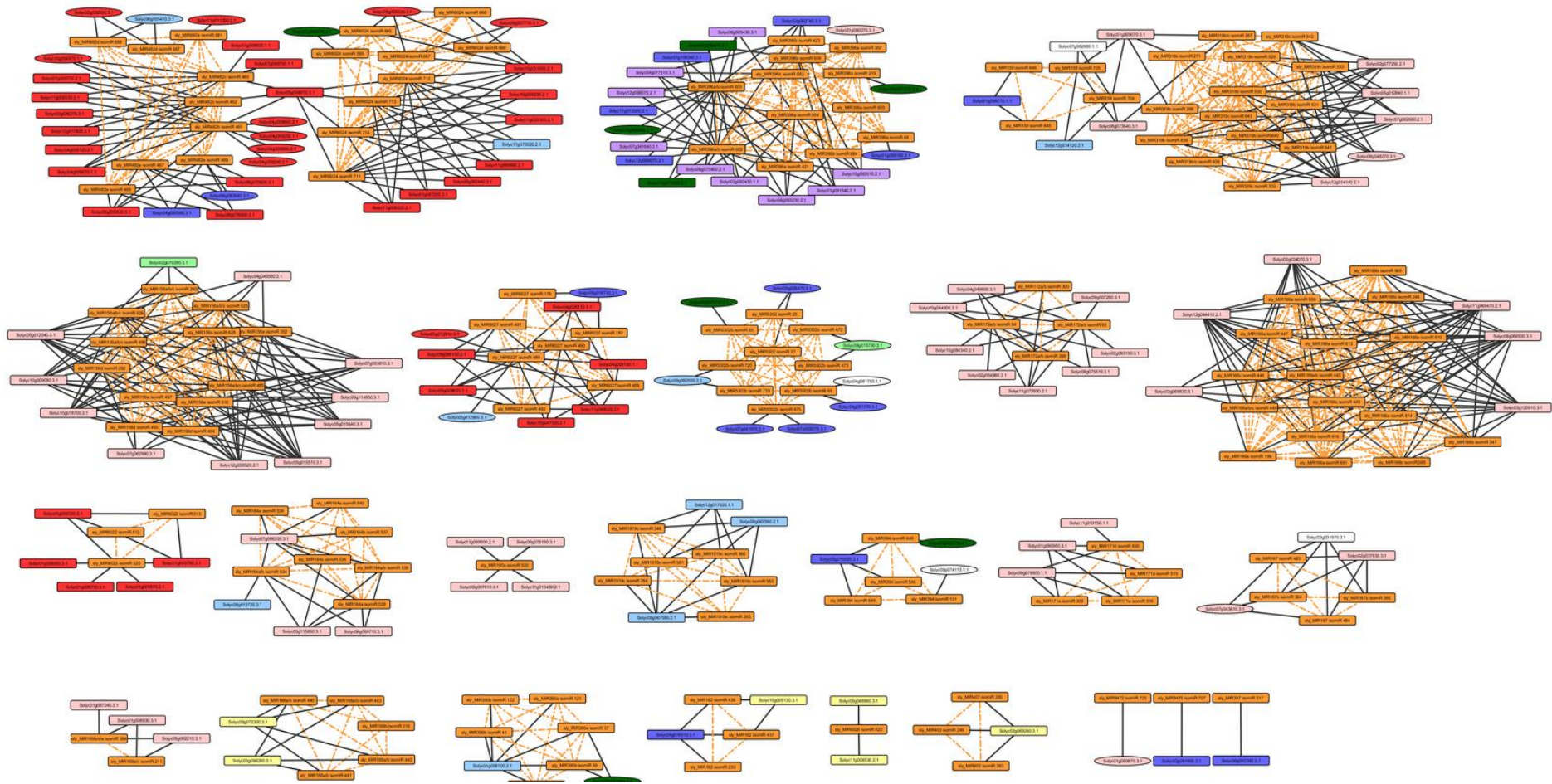
Supplemental Figure 5: Distribution of phasiRNAs with targets for each PHAS locus frame

(A) Number of phasiRNAs with at least one verified target in each PHAS locus frame. (B) Number of phasiRNAs with targets in proportion to the total number of phasiRNAs from each PHAS locus frame. The PHAS locus frames from 27 to 40 are not displayed as they do not have a single verified target.



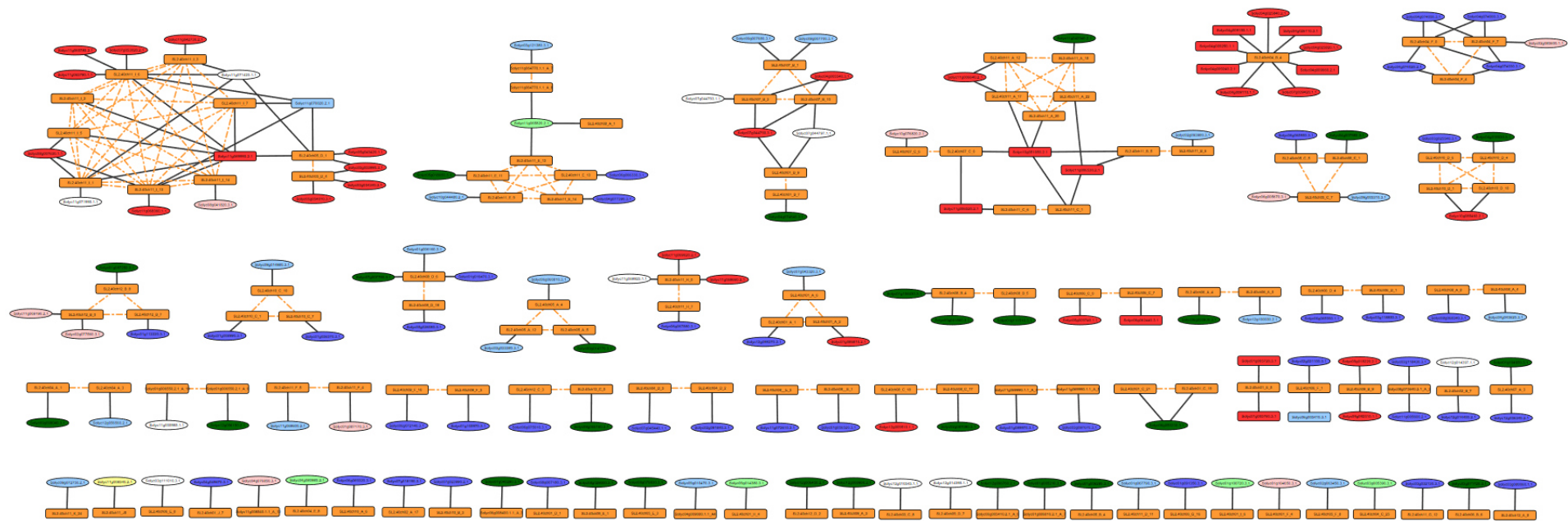
Supplemental Figure 6: Function of phasiRNA targets that are targeted by more than one phasiRNA

Categories in order: Defense related (red), Metabolic process (dark green), Cell function (dark blue), Unknown (blue), Outdated annotation (white), Transport (light green).



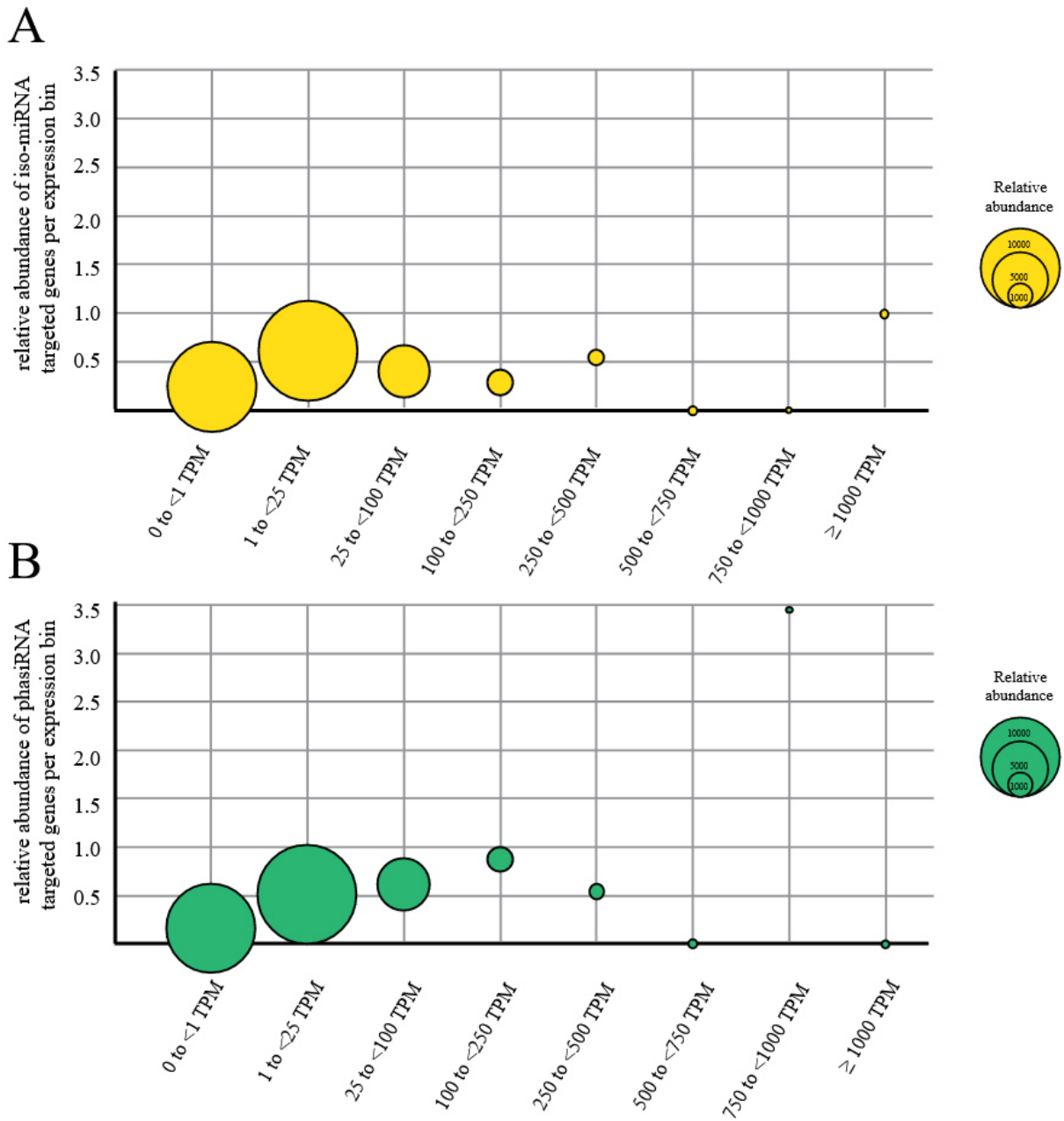
Supplemental Figure 7: isomiRNA/mRNA interaction networks

Members of the same isomiRNA family are connected with a dotted orange line, while targets are connected with their verified isomiRNAs through a black line. The targets are coloured in accordance with their function (red = defense related, pink = transcription factor, dark blue = cell function, light blue = unknown, turquoise = photosynthesis, purple = growth regulation, dark green = metabolic process, light green = transport, yellow = miRNA biosynthesis, white = outdated annotation). Targets surrounded by a square are as well targets of miRNAs; oval-shaped targets are specific to isomiRNAs.



Supplemental Figure 8: phasiRNA/mRNA interaction networks

Members of the same phasiRNA family (with family here meaning all phasiRNAs generated from the same PHAS locus) are connected with a dotted orange line, while targets are connected with their verified phasiRNAs through a black line. Targets are coloured in accordance with their function (red = defense related, pink = transcription factor, dark blue = cell function, light blue = unknown, turquoise = photosynthesis, purple = growth regulation, dark green = metabolic process, light green = transport, yellow = miRNA biosynthesis, white = outdated annotation). Targets surrounded by a square are as well targets of miRNAs/isomiRNAs; oval-shaped targets are specific to phasiRNAs.



Supplemental Figure 9: Expression height of iso-miRNAs and phasiRNA targets in proportion to non-targets

(A-B) The targets of iso-miRNAs (combination of miRNAs and isomiRNAs) **(A)** and phasiRNAs **(B)** as well as non-targeted genes of tomato were sorted into eight expression bins (x-axis). The size of the circles is relative to the total number of genes in each bin (legend on the right). The height of each circle corresponds to the relative abundance of iso-miRNA/phasiRNA targeted genes to non-targeted genes in each bin (y-axis).

Supplemental Table 1: Overview of the PARE libraries

Overview of the PARE libraries used in this study. Given are the SRA number, the species (and cultivar), the tissue-type used, the kind of treatment, the number of reads in each library and the number of mapped reads

SRA No.	Species	Tissue	Treatment	Library reads	Mapped Reads
SRR1272023	<i>S. habrochaites</i> LA1777	leaves	chilling treatment, 4°C/4°C*	12.497.283	3.513.150
SRR1272024	<i>S. habrochaites</i> LA1777	leaves	no treatment, 25°C/20°C*	7.348.176	1.859.038
SRR2071270	<i>S. lycopersicum</i> Rutgers	leaves	Potato Spindle Tuber Viroid-I	4.808.901	895.160
SRR2071657	<i>S. lycopersicum</i> Rutgers	leaves	Potato Spindle Tuber Viroid-RG1	3.666.860	426.147
SRR2979664	<i>S. lycopersicum</i> Rutgers	leaves	Potato Spindle Tuber Viroid-M	3.353.693	433.076
SRR4420593	<i>S. lycopersicum</i> Rutgers	leaves	MOCK	3.785.269	600.973
SRR5031918	<i>S. lycopersicum</i> Heinz 1706	leaves	Potato Spindle Tuber Viroid	2.402.302	67.478
SRR5031919	<i>S. lycopersicum</i> Heinz 1706	leaves	Potato Spindle Tuber Viroid	2.047.684	59.989
SRR5031920	<i>S. lycopersicum</i> Heinz 1706	leaves	Potato Spindle Tuber Viroid	2.751.056	90.431
SRR5179088	<i>S. lycopersicum</i> v. Moneymaker	leaves	Tomato Leaf Curl Sardinia Virus	44.921.818	4.994.497
SRR5179089	<i>S. lycopersicum</i> v. Moneymaker	leaves	MOCK	48.559.330	3.621.352
SRR7289301	<i>S. lycopersicum</i> v. Heinz 1706	top 5 cm of the plant (leaves, stem, petioles, and apex)	MOCK	19.882.048	6.174.968
SRR7289302	<i>S. lycopersicum</i> v. Heinz 1706	top 5 cm of the plant (leaves, stem, petioles and apex)	MOCK	11.326.629	2.820.075
SRR7289305	<i>S. lycopersicum</i> cv. Heinz 1706	top 5 cm of the plant (leaves, stem, petioles and apex)	<i>Citrus exocortis viroid</i>	22.449.833	6.377.433
SRR7289306	<i>S. lycopersicum</i> cv. Heinz 1706	top 5 cm of the plant (leaves, stem, petioles and apex)	<i>Citrus exocortis viroid</i>	16.098.592	3.824.853
SRS079357	<i>S. lycopersicum</i> cv. Micro-Tom	leaves	untreated	7.111.228	2.749.667
SRS079358	<i>S. lycopersicum</i> cv. Micro-Tom	flower	untreated	6.667.847	2.507.683

SRS079359	<i>S. lycopersicum</i> cv. Micro-Tom	green fruit	untreated	6.667.458	2.285.149
SRS1028781	<i>S. pimpinellifolium</i> LA2093	leaves	elevated temperature: 40/40 °C*	11.457.253	4.886.263
SRS1028783	<i>S. pimpinellifolium</i> LA2093	leaves	moderate elevated temperature: 33/33 °C*	10.842.033	4.530.685
SRS1028784	<i>S. pimpinellifolium</i> LA2093	leaves	control temperature: 26/18 °C*	11.759.208	5.071.156
SRS377820	<i>S. lycopersicum</i> variety Ailsa Craig	fruit	untreated	26.131.544	8.015.002
SRS472306	<i>S. lycopersicum</i> cv. Moneymaker (Ty-1 gene; less susceptible)	leaves	MOCK	14.647.802	11.965.977
SRS472307	<i>S. lycopersicum</i> cv. Moneymaker (Ty-1 gene; less susceptible)	leaves	Tomato Yellow Leaf Curl Virus (infectious clones of pBinPLUS-SH2-1.4A)	16.420.359	10.836.918
SRS472308	<i>S. lycopersicum</i> FL505 (TYLCV susceptible strain)	leaves	MOCK	16.248.068	7.434.495
SRS472309	<i>S. lycopersicum</i> FL505 (TYLCV susceptible strain)	leaves	Tomato Yellow Leaf Curl Virus (infectious clones of pBinPLUS-SH2-1.4A)	16.255.591	6.737.118
SRS595515	<i>S. lycopersicum</i> cv. Micro-Tom	leaves	Cucumber mosaic virus strain Fny	9.808.528	2.217.112
SRS595516	<i>S. lycopersicum</i> cv. Micro-Tom	leaves	MOCK	12.204.159	2.426.769

*day/night temperature

Supplemental Table 2: smallRNA sequences (miRNA, isomiRNA, phasiRNA)

The miRNAs are received from miRBase (Kozomara et al. 2019), the isomiRNAs from the Plant IsomiR Atlas (Yang et al. 2019). The phasiRNA ID is abbreviated from the paper Zheng et al. (2015). Due to the large dimensions the table is available online.

Supplemental Table 3: Verified targets of miRNAs, isomiRNAs and phasiRNAs using the PARE method

Due to the large dimensions the table is available online.

Supplemental Table 3: Results of psRNATarget and TargetFinder

psRNATarget and TargetFinder were run with an expectation value cut-off of 3.0 and 4 respectively. When two hits for the same miRNA/mRNA interaction occurred, only the lower/more likely expectation hit was kept. Additionally, miRNA/mRNA interactions predicted to execute translational inhibition were removed. The psRNATarget/Target Finder predicted interactions that were also verified using PAREsnip2 were displayed (yes/no). Due to the large dimensions the table is available online.

Supplemental Table 5: Chi-square test for the distribution of gene functions between miRNAs, isomiRNAs and phasiRNAs

	miRNA ~ isomiRNA	miRNA ~ phasiRNA	isomiRNA ~ phasiRNA
Degree of freedom	9	9	8
Chi-square value	6.1534	87.3018	68.6390
p-value	0.7245	<0.00001	<0.00001

Supplemental Table 6: Chi-square test for the distribution of gene functions between non-treated and treated PARE libraries for miRNA, isomiRNA and phasiRNA targets

The treatments included abiotic and biotic treated plants.

	miRNA (mocks vs. treatment)	isomiRNA (mocks vs. treatment)	phasiRNA (mocks vs. treatment)
Degree of freedom	9	8	7
Chi-square value	2.0486	3.5118	10.4092
p-value	0.9907	0.9795	0.1666

Supplemental Table 7: Chi-square test results for gene function distribution between different levels of multiple targeting for iso-miRNAs

	genes targeted by ≥ 2 iso-miRNAs vs all targets	genes targeted by ≥ 5 iso-miRNAs vs all targets	genes targeted by ≥ 10 iso-miRNAs vs all targets
Degree of freedom	9	9	9
Chi-square value	4.1291	22.3162	23.8128
p-value	0.9027	0.0079	0.0046

Supplemental Table 7: miRNA/mRNA interactions with less than 10 reads or category 4

Due to the large dimensions the table is available online.

Supplemental Table 8: Chi-square test results for gene function distribution between different levels of multiple targeting for iso-miRNA and phasiRNA targets

	genes targeted by ≥ 2 iso-miRNAs	genes targeted by ≥ 5 iso-miRNAs	genes targeted by ≥ 10 iso-miRNAs
Degree of freedom	9	9	9
Chi-square value	7.4961	23.7986	24.0330
p-value	0.5856	0.0046	0.0042

References:

Achard, P., Herr, A., Baulcombe, D. C., & Harberd, N. P. (2004). Modulation of floral development by a gibberellin-regulated microRNA. *Development*, 131(14), 3357–3365.

Adkar-Purushothama, C. R., Iyer, P. S., & Perreault, J. P. (2017). Potato spindle tuber viroid infection triggers degradation of chloride channel protein CLC-b-like and Ribosomal protein S3a-like mRNAs in tomato plants. *Scientific Reports*, 7(1), 8341.

Agudelo-Romero, P., Carbonell, P., De La Iglesia, F., Carrera, J., Rodrigo, G., Jaramillo, A., ... & Elena, S. F. (2008). Changes in the gene expression profile of *Arabidopsis thaliana* after infection with Tobacco etch virus. *Virology journal*, 5(1), 1-11.

Ahmed, F., Senthil-Kumar, M., Lee, S., Dai, X., Mysore, K. S., & Zhao, P. X. (2014). Comprehensive analysis of small RNA-seq data reveals that combination of miRNA with its isomiRs increase the accuracy of target prediction in *Arabidopsis thaliana*. *RNA biology*, 11(11), 1414-1429.

- Allen, E., Xie, Z., Gustafson, A. M., & Carrington, J. C. (2005). microRNA-directed phasing during trans-acting siRNA biogenesis in plants. *Cell*, *121*(2), 207-221.
- Andrews S. (2010). FastQC: a quality control tool for high throughput sequence data. Available online at: <http://www.bioinformatics.babraham.ac.uk/projects/fastqc>
- Axtell, M. J. (2013). Classification and comparison of small RNAs from plants. *Annual review of plant biology*, *64*, 137-159.
- Miao, B. A. I., Yang, G. S., Chen, W. T., Lin, R. M., Jian, L. I. N. G., Mai, Z. C., & Xie, B. Y. (2016). Characterization and function of Tomato yellow leaf curl virus-derived small RNAs generated in tolerant and susceptible tomato varieties. *Journal of integrative agriculture*, *15*(8), 1785-1797.
- Bak, R. O., & Mikkelsen, J. G. (2014). miRNA sponges: soaking up miRNAs for regulation of gene expression. *Wiley interdisciplinary reviews: RNA*, *5*(3), 317-333.
- Baulcombe, D. (2004). RNA silencing in plants. *Nature*, *431*(7006), 356-363.
- Bonnet, E., He, Y., Billiau, K., & Van de Peer, Y. (2010). TAPIR, a web server for the prediction of plant microRNA targets, including target mimics. *Bioinformatics*, *26*(12), 1566-1568.
- von Born, P., Bernardo-Faura, M., & Rubio-Somoza, I. (2018). An artificial miRNA system reveals that relative contribution of translational inhibition to miRNA-mediated regulation depends on environmental and developmental factors in *Arabidopsis thaliana*. *PLoS one*, *13*(2), e0192984.
- Boyle, E. A., Li, Y. I., & Pritchard, J. K. (2017). An expanded view of complex traits: from polygenic to omnigenic. *Cell*, *169*(7), 1177-1186.
- Brodersen, P., Sakvarelidze-Achard, L., Bruun-Rasmussen, M., Dunoyer, P., Yamamoto, Y. Y., Sieburth, L., & Voinnet, O. (2008). Widespread translational inhibition by plant miRNAs and siRNAs. *Science*, *320*(5880), 1185-1190.
- Brown, J. K. M., & Rant, J. C. (2013). Fitness costs and trade-offs of disease resistance and their consequences for breeding arable crops. *Plant Pathology*, *62*, 83-95.
- Candar-Cakir, B., Arican, E., & Zhang, B. (2016). Small RNA and degradome deep sequencing reveals drought-and tissue-specific micrornas and their important roles in drought-sensitive and drought-tolerant tomato genotypes. *Plant biotechnology journal*, *14*(8), 1727-1746.
- Canto-Pastor, A., Santos, B. A., Valli, A. A., Summers, W., Schornack, S., & Baulcombe, D. C. (2019). Enhanced resistance to bacterial and oomycete pathogens by short tandem target mimic RNAs in tomato. *Proceedings of the National Academy of Sciences*, *116*(7), 2755-2760.
- Cao, X., Wu, Z., Jiang, F., Zhou, R., & Yang, Z. (2014). Identification of chilling stress-responsive tomato microRNAs and their target genes by high-throughput sequencing and degradome analysis. *BMC genomics*, *15*(1), 1-16.
- Carlsbecker, A., Lee, J. Y., Roberts, C. J., Dettmer, J., Lehesranta, S., Zhou, J., ... & Benfey, P. N. (2010). Cell signalling by microRNA165/6 directs gene dose-dependent root cell fate. *Nature*, *465*(7296), 316-321.
- Chen, H. M., Li, Y. H., & Wu, S. H. (2007). Bioinformatic prediction and experimental validation of a microRNA-directed tandem trans-acting siRNA cascade in *Arabidopsis*. *Proceedings of the National Academy of Sciences*, *104*(9), 3318-3323.
- Chen, Y., Shen, Y., Allesina, S., & Wu, C. I. (2017). From foodwebs to gene regulatory networks (GRNs)—weak repressions by microRNAs confer system stability. *bioRxiv*, 176701.
- Chitwood, D. H., Nogueira, F. T., Howell, M. D., Montgomery, T. A., Carrington, J. C., & Timmermans, M. C. (2009). Pattern formation via small RNA mobility. *Genes & development*, *23*(5), 549-554.
- Chiumenti, M., Catacchio, C. R., Miozzi, L., Pirovano, W., Ventura, M., & Pantaleo, V. (2018). A short indel-lacking-resistance gene triggers silencing of the photosynthetic machinery components through TYLCSV-associated endogenous siRNAs in tomato. *Frontiers in Plant Science*, *9*, 1470.
- Cloonan, N., Wani, S., Xu, Q., Gu, J., Lea, K., Heater, S., ... & Grimmond, S. M. (2011). MicroRNAs and their isomiRs function cooperatively to target common biological pathways. *Genome biology*, *12*(12), 1-20.

- Colaiacono, M., Bernardo, L., Centomani, I., Crosatti, C., Giusti, L., Orrù, L., ... & Faccioli, P. (2012). A survey of microRNA length variants contributing to miRNome complexity in peach (*Prunus persica* L.). *Frontiers in Plant Science*, *3*, 165.
- Curaba, J., Spriggs, A., Taylor, J., Li, Z., & Helliwell, C. (2012). miRNA regulation in the early development of barley seed. *BMC plant biology*, *12*, 1-16.
- Dai, X., Zhuang, Z., & Zhao, P. X. (2018). psRNATarget: a plant small RNA target analysis server (2017 release). *Nucleic acids research*, *46*(W1), W49-W54.
- Ding, J., Zhou, S., & Guan, J. (2012). Finding microRNA targets in plants: current status and perspectives. *Genomics, proteomics & bioinformatics*, *10*(5), 264-275.
- Ehya, F., Monavarfeshani, A., Mohseni Fard, E., Karimi Farsad, L., Khayam Nekouei, M., Mardi, M., & Salekdeh, G. H. (2013). Phytoplasma-responsive microRNAs modulate hormonal, nutritional, and stress signalling pathways in Mexican lime trees. *PLoS one*, *8*(6), e66372.
- Fahlgren, N., Howell, M. D., Kasschau, K. D., Chapman, E. J., Sullivan, C. M., Cumbie, J. S., ... & Carrington, J. C. (2007). High-throughput sequencing of Arabidopsis microRNAs: evidence for frequent birth and death of MIRNA genes. *PLoS one*, *2*(2), e219.
- Fan, G., Cao, Y., Deng, M., Zhai, X., Zhao, Z., Niu, S., & Ren, Y. (2017). Identification and dynamic expression profiling of microRNAs and target genes of *Paulownia tomentosa* in response to *Paulownia witches' broom* disease. *Acta Physiologiae Plantarum*, *39*, 1-9.
- Fei, Q., Xia, R., & Meyers, B. C. (2013). Phased, secondary, small interfering RNAs in posttranscriptional regulatory networks. *The Plant Cell*, *25*(7), 2400-2415.
- Feng, J., Liu, S., Wang, M., Lang, Q., & Jin, C. (2014). Identification of microRNAs and their targets in tomato infected with Cucumber mosaic virus based on deep sequencing. *Planta*, *240*, 1335-1352.
- Fernandez-Pozo, N., Menda, N., Edwards, J. D., Saha, S., Teclé, I. Y., Strickler, S. R., ... & Mueller, L. A. (2015). The Sol Genomics Network (SGN)—from genotype to phenotype to breeding. *Nucleic acids research*, *43*(D1), D1036-D1041.
- Formey, D., Iñiguez, L. P., Peláez, P., Li, Y. F., Sunkar, R., Sánchez, F., ... & Hernández, G. (2015). Genome-wide identification of the *Phaseolus vulgaris* sRNAome using small RNA and degradome sequencing. *BMC genomics*, *16*(1), 1-17.
- Fridrich, A., Hazan, Y., & Moran, Y. (2019). Too many false targets for MicroRNAs: challenges and Pitfalls in Prediction of miRNA targets and their gene ontology in model and non-model organisms. *Bioessays*, *41*(4), 1800169.
- German, M. A., Pillay, M., Jeong, D. H., Hetawal, A., Luo, S., Janardhanan, P., ... & Green, P. J. (2008). Global identification of microRNA–target RNA pairs by parallel analysis of RNA ends. *Nature biotechnology*, *26*(8), 941-946.
- German, M. A., Luo, S., Schroth, G., Meyers, B. C., & Green, P. J. (2009). Construction of Parallel Analysis of RNA Ends (PARE) libraries for the study of cleaved miRNA targets and the RNA degradome. *Nature protocols*, *4*(3), 356-362.
- Gu, Y., Liu, Y., Zhang, J., Liu, H., Hu, Y., Du, H., ... & Huang, Y. (2013). Identification and characterization of microRNAs in the developing maize endosperm. *Genomics*, *102*(5-6), 472-478.
- Guo, N., Ye, W. W., Wu, X. L., Shen, D. Y., Wang, Y. C., Xing, H., & Dou, D. L. (2011). Microarray profiling reveals microRNAs involving soybean resistance to *Phytophthora sojae*. *Genome*, *54*(11), 954-958.
- Gu, K., Yang, B., Tian, D., Wu, L., Wang, D., Sreekala, C., ... & Yin, Z. (2005). R gene expression induced by a type-III effector triggers disease resistance in rice. *Nature*, *435*(7045), 1122-1125.
- Greenwood, P. E., & Nikulin, M. S. (1996). A guide to chi-squared testing. *Wiley Series in Probability and Statistics*. Vol. 280
- Han, J., Kong, M. L., Xie, H., Sun, Q. P., Nan, Z. J., Zhang, Q. Z., & Pan, J. B. (2013). Identification of miRNAs and their targets in wheat (*Triticum aestivum* L.) by EST analysis. *Genetic and Molecular Research*, *12*(3), 805.
- Hollander, M., Wolfe, D. A., & Chicken, E. (2013). Nonparametric statistical methods. *Wiley Series in Probability and Statistics*. Vol. 751, 3rd edition

- Howell, M. D., Fahlgren, N., Chapman, E. J., Cumbie, J. S., Sullivan, C. M., Givan, S. A., ... & Carrington, J. C. (2007). Genome-wide analysis of the RNA-DEPENDENT RNA POLYMERASE6/DICER-LIKE4 pathway in Arabidopsis reveals dependency on miRNA-and tasiRNA-directed targeting. *The Plant Cell*, *19*(3), 926-942.
- Iwakawa, H. O., & Tomari, Y. (2013). Molecular insights into microRNA-mediated translational repression in plants. *Molecular cell*, *52*(4), 591-601.
- Jagadeeswaran, G., Zheng, Y., Sumathipala, N., Jiang, H., Arrese, E. L., Soulages, J. L., ... & Sunkar, R. (2010). Deep sequencing of small RNA libraries reveals dynamic regulation of conserved and novel microRNAs and microRNA-stars during silkworm development. *BMC genomics*, *11*(1), 52.
- Jeong, D. H., Park, S., Zhai, J., Gurazada, S. G. R., De Paoli, E., Meyers, B. C., & Green, P. J. (2011). Massive analysis of rice small RNAs: mechanistic implications of regulated microRNAs and variants for differential target RNA cleavage. *The Plant Cell*, *23*(12), 4185-4207.
- Jones-Rhoades, M. W., & Bartel, D. P. (2004). Computational identification of plant microRNAs and their targets, including a stress-induced miRNA. *Molecular cell*, *14*(6), 787-799.
- Karasov, T. L., Kniskern, J. M., Gao, L., DeYoung, B. J., Ding, J., Dubiella, U., ... & Barrett, L. G. (2014). The long-term maintenance of a resistance polymorphism through diffuse interactions. *Nature*, *512*(7515), 436-440.
- Karlova, R., van Haarst, J. C., Maliepaard, C., van de Geest, H., Bovy, A. G., Lammers, M., ... & de Maagd, R. A. (2013). Identification of microRNA targets in tomato fruit development using high-throughput sequencing and degradome analysis. *Journal of experimental botany*, *64*(7), 1863-1878.
- Korir, N. K., Li, X., Xin, S., Wang, C., Changnian, S., Kayesh, E., & Fang, J. (2013). Characterization and expression profiling of selected microRNAs in tomato (*Solanum lycopersicon*) 'Jiangshu14'. *Molecular biology reports*, *40*(5), 3503-3521.
- Kozomara, A., Birgaoanu, M., & Griffiths-Jones, S. (2019). miRBase: from microRNA sequences to function. *Nucleic acids research*, *47*(D1), D155-D162.
- Li, B., Qin, Y., Duan, H., Yin, W., & Xia, X. (2011). Genome-wide characterization of new and drought stress responsive microRNAs in *Populus euphratica*. *Journal of experimental botany*, *62*(11), 3765-3779.
- Li, F., Orban, R., & Baker, B. (2012). SoMART: a web server for plant miRNA, tasiRNA and target gene analysis. *The Plant Journal*, *70*(5), 891-901.
- Li, S., Liu, L., Zhuang, X., Yu, Y., Liu, X., Cui, X., ... & Chen, X. (2013). MicroRNAs inhibit the translation of target mRNAs on the endoplasmic reticulum in Arabidopsis. *Cell*, *153*(3), 562-574.
- Li, Y. F., Zheng, Y., Addo-Quaye, C., Zhang, L., Saini, A., Jagadeeswaran, G., ... & Sunkar, R. (2010). Transcriptome-wide identification of microRNA targets in rice. *The Plant Journal*, *62*(5), 742-759.
- Liu, G., Min, H., Yue, S., & Chen, C. Z. (2008). Pre-miRNA loop nucleotides control the distinct activities of mir-181a-1 and mir-181c in early T cell development. *PloS one*, *3*(10).
- Lopez-Gomollon, S., Mohorianu, I., Szitty, G., Moulton, V., & Dalmay, T. (2012). Diverse correlation patterns between microRNAs and their targets during tomato fruit development indicates different modes of microRNA actions. *Planta*, *236*, 1875-1887.
- Mann, H. B., & Whitney, D. R. (1947). On a test of whether one of two random variables is stochastically larger than the other. *The annals of mathematical statistics*, 50-60.
- Marco, A., Hooks, K., & Griffiths-Jones, S. (2012). Evolution and function of the extended miR-2 microRNA family. *RNA biology*, *9*(3), 242-248.
- Martin, M. (2011). Cutadapt removes adapter sequences from high-throughput sequencing reads. *EMBnet. journal*, *17*(1), 10-12.
- Moy, P., Qutob, D., Chapman, B. P., Atkinson, I., & Gijzen, M. (2004). Patterns of gene expression upon infection of soybean plants by *Phytophthora sojae*. *Molecular Plant-Microbe Interactions*, *17*(10), 1051-1062.

- Neilsen, C. T., Goodall, G. J., & Bracken, C. P. (2012). IsomiRs—the overlooked repertoire in the dynamic microRNAome. *Trends in genetics*, *28*(11), 544-549.
- Okamura, K., Phillips, M. D., Tyler, D. M., Duan, H., Chou, Y. T., & Lai, E. C. (2008). The regulatory activity of microRNA* species has substantial influence on microRNA and 3' UTR evolution. *Nature structural & molecular biology*, *15*(4), 354.
- Olivier, T., & Bragard, C. (2018). Innate immunity activation and RNAi interplay in citrus exocortis viroid—Tomato pathosystem. *Viruses*, *10*(11), 587.
- Ørom, U. A., Nielsen, F. C., & Lund, A. H. (2008). MicroRNA-10a binds the 5' UTR of ribosomal protein mRNAs and enhances their translation. *Molecular cell*, *30*(4), 460-471.
- Pagliarani, C., & Gambino, G. (2019). Small RNA Mobility: Spread of RNA Silencing Effectors and its Effect on Developmental Processes and Stress Adaptation in Plants. *International Journal of Molecular Sciences*, *20*(17), 4306.
- Palatnik, J. F., Allen, E., Wu, X., Schommer, C., Schwab, R., Carrington, J. C., & Weigel, D. (2003). Control of leaf morphogenesis by microRNAs. *Nature*, *425*(6955), 257-263.
- Palatnik, J. F., Wollmann, H., Schommer, C., Schwab, R., Boisbouvier, J., Rodriguez, R., ... & Weigel, D. (2007). Sequence and expression differences underlie functional specialization of Arabidopsis microRNAs miR159 and miR319. *Developmental cell*, *13*(1), 115-125.
- Pantaleo, V., Szittyá, G., Moxon, S., Miozzi, L., Moulton, V., Dalmay, T., & Burgyan, J. (2010). Identification of grapevine microRNAs and their targets using high-throughput sequencing and degradome analysis. *The Plant Journal*, *62*(6), 960-976.
- Pegler, J. L., Oultram, J. M., Grof, C. P., & Eamens, A. L. (2019). Profiling the abiotic stress responsive microRNA landscape of Arabidopsis thaliana. *Plants*, *8*(3), 58.
- Rajagopalan, R., Vaucheret, H., Trejo, J., & Bartel, D. P. (2006). A diverse and evolutionarily fluid set of microRNAs in Arabidopsis thaliana. *Genes & development*, *20*(24), 3407-3425.
- Reis, R. S., Hart-Smith, G., Eamens, A. L., Wilkins, M. R., & Waterhouse, P. M. (2015). MicroRNA regulatory mechanisms play different roles in Arabidopsis. *Journal of Proteome Research*, *14*(11), 4743-4751.
- Rogers, K., & Chen, X. (2013). Biogenesis, turnover, and mode of action of plant microRNAs. *The Plant Cell*, *25*(7), 2383-2399.
- Schwab, R., Maizel, A., Ruiz-Ferrer, V., Garcia, D., Bayer, M., Crespi, M., ... & Martienssen, R. A. (2009). Endogenous TasiRNAs mediate non-cell autonomous effects on gene regulation in Arabidopsis thaliana. *PLoS one*, *4*(6), e5980.
- Schwab, R., Palatnik, J. F., Riester, M., Schommer, C., Schmid, M., & Weigel, D. (2005). Specific effects of microRNAs on the plant transcriptome. *Developmental cell*, *8*(4), 517-527.
- Scotto-Lavino, E., Du, G., & Frohman, M. A. (2006). 5' end cDNA amplification using classic RACE. *Nature protocols*, *1*(6), 2555-2562.
- Shannon, P., Markiel, A., Ozier, O., Baliga, N. S., Wang, J. T., Ramage, D., ... & Ideker, T. (2003). Cytoscape: a software environment for integrated models of biomolecular interaction networks. *Genome research*, *13*(11), 2498-2504.
- Shivaprasad, P. V., Chen, H. M., Patel, K., Bond, D. M., Santos, B. A., & Baulcombe, D. C. (2012). A microRNA superfamily regulates nucleotide binding site–leucine-rich repeats and other mRNAs. *The Plant Cell*, *24*(3), 859-874.
- Soto-Suárez, M., Baldrich, P., Weigel, D., Rubio-Somoza, I., & San Segundo, B. (2017). The Arabidopsis miR396 mediates pathogen-associated molecular pattern-triggered immune responses against fungal pathogens. *Scientific reports*, *7*(1), 44898.
- Stocks, M. B., Mohorianu, I., Beckers, M., Paicu, C., Moxon, S., Thody, J., ... & Moulton, V. (2018). The UEA sRNA Workbench (version 4.4): a comprehensive suite of tools for analyzing miRNAs and sRNAs. *Bioinformatics*, *34*(19), 3382-3384.
- Sun, G. (2012). MicroRNAs and their diverse functions in plants. *Plant molecular biology*, *80*, 17-36.
- Talmor-Neiman, M., Stav, R., Klipcan, L., Buxdorf, K., Baulcombe, D. C., & Arazi, T. (2006). Identification of trans-acting siRNAs in moss and an RNA-dependent RNA polymerase required for their biogenesis. *The Plant Journal*, *48*(4), 511-521.

- Tanzer, A., & Stadler, P. F. (2004). Molecular evolution of a microRNA cluster. *Journal of molecular biology*, 339(2), 327-335.
- Thody, J., Folkes, L., Medina-Calzada, Z., Xu, P., Dalmay, T., & Moulton, V. (2018). PAREsnip2: a tool for high-throughput prediction of small RNA targets from degradome sequencing data using configurable targeting rules. *Nucleic acids research*, 46(17), 8730-8739.
- Tian, D., Traw, M. B., Chen, J. Q., Kreitman, M., & Bergelson, J. (2003). Fitness costs of R-gene-mediated resistance in *Arabidopsis thaliana*. *Nature*, 423(6935), 74-77.
- Tiwari, B., Habermann, K., Arif, M. A., Weil, H. L., Garcia-Molina, A., Kleine, T., ... & Frank, W. (2020). Identification of small RNAs during cold acclimation in *Arabidopsis thaliana*. *BMC Plant Biology*, 20(1), 1-25.
- Todesco, M., Balasubramanian, S., Cao, J., Ott, F., Sureshkumar, S., Schneeberger, K., ... & Weigel, D. (2012). Natural variation in biogenesis efficiency of individual *Arabidopsis thaliana* microRNAs. *Current Biology*, 22(2), 166-170.
- Tsikou, D., Yan, Z., Holt, D. B., Abel, N. B., Reid, D. E., Madsen, L. H., ... & Markmann, K. (2018). Systemic control of legume susceptibility to rhizobial infection by a mobile microRNA. *Science*, 362(6411), 233-236.
- Vaucheret, H., Vazquez, F., Cr  t  , P., & Bartel, D. P. (2004). The action of ARGONAUTE1 in the miRNA pathway and its regulation by the miRNA pathway are crucial for plant development. *Genes & development*, 18(10), 1187-1197.
- de Vries, S., Kloesges, T., & Rose, L. E. (2015). Evolutionarily dynamic, but robust, targeting of resistance genes by the miR482/2118 gene family in the Solanaceae. *Genome Biology and Evolution*, 7(12), 3307-3321.
- Wahid, A. (2007). Physiological implications of metabolite biosynthesis for net assimilation and heat-stress tolerance of sugarcane (*Saccharum officinarum*) sprouts. *Journal of plant Research*, 120, 219-228.
- Wu, G., Park, M. Y., Conway, S. R., Wang, J. W., Weigel, D., & Poethig, R. S. (2009). The sequential action of miR156 and miR172 regulates developmental timing in *Arabidopsis*. *Cell*, 138(4), 750-759.
- Xia, R., Chen, C., Pokhrel, S., Ma, W., Huang, K., Patel, P., ... & Meyers, B. C. (2019). 24-nt reproductive phasiRNAs are broadly present in angiosperms. *Nature communications*, 10(1), 627.
- Xia, R., Meyers, B. C., Liu, Z., Beers, E. P., Ye, S., & Liu, Z. (2013). MicroRNA superfamilies descended from miR390 and their roles in secondary small interfering RNA biogenesis in eudicots. *The Plant Cell*, 25(5), 1555-1572.
- Xia, R., Xu, J., & Meyers, B. C. (2017). The emergence, evolution, and diversification of the miR390-TAS3-ARF pathway in land plants. *The Plant Cell*, 29(6), 1232-1247.
- Xia, R., Zhu, H., An, Y. Q., Beers, E. P., & Liu, Z. (2012). Apple miRNAs and tasiRNAs with novel regulatory networks. *Genome biology*, 13(6), 1-18.
- Xie, Z., Kasschau, K. D., & Carrington, J. C. (2003). Negative feedback regulation of Dicer-Like1 in *Arabidopsis* by microRNA-guided mRNA degradation. *Current Biology*, 13(9), 784-789.
- Xiong, L., Lee, H., Ishitani, M., & Zhu, J. K. (2002). Regulation of osmotic stress-responsive gene expression by the *los6/aba1* locus in *Arabidopsis*. *Journal of Biological Chemistry*, 277(10), 8588-8596.
- Yang, K., Wen, X., Mudunuri, S. B., & Sablok, G. (2019). Plant IsomiR atlas: large scale detection, profiling, and target repertoire of IsomiRs in plants. *Frontiers in plant science*, 9, 1881.
- Yoshikawa, M., Peragine, A., Park, M. Y., & Poethig, R. S. (2005). A pathway for the biogenesis of trans-acting siRNAs in *Arabidopsis*. *Genes & development*, 19(18), 2164-2175.
- Yu, Y., Jia, T., & Chen, X. (2017). The 'how' and 'where' of plant micro RNA s. *New Phytologist*, 216(4), 1002-1017.
- Zhai, J., Jeong, D. H., De Paoli, E., Park, S., Rosen, B. D., Li, Y., ... & Meyers, B. C. (2011). MicroRNAs as master regulators of the plant NB-LRR defense gene family via the production of phased, trans-acting siRNAs. *Genes & development*, 25(23), 2540-2553.

Zhang, X., Zhao, H., Gao, S., Wang, W. C., Katiyar-Agarwal, S., Huang, H. D., ... & Jin, H. (2011). Arabidopsis Argonaute 2 regulates innate immunity via miRNA393*-mediated silencing of a Golgi-localized SNARE gene, MEMB12. *Molecular cell*, 42(3), 356-366.

Zhao, Y., Shen, X., Tang, T., & Wu, C. I. (2017). Weak regulation of many targets is cumulatively powerful—an evolutionary perspective on microRNA functionality. *Molecular biology and evolution*, 34(12), 3041-3046.

Zheng, Y., Wang, Y., Ding, B., & Fei, Z. (2017). Comprehensive transcriptome analyses reveal that potato spindle tuber viroid triggers genome-wide changes in alternative splicing, inducible trans-acting activity of phased secondary small interfering RNAs, and immune responses. *Journal of Virology*, 91(11), 10-1128.

Zheng, Y., Wang, Y., Wu, J., Ding, B., & Fei, Z. (2015). A dynamic evolutionary and functional landscape of plant phased small interfering RNAs. *BMC biology*, 13(1), 1-15.

Zhou, L., Liu, Y., Liu, Z., Kong, D., Duan, M., & Luo, L. (2010). Genome-wide identification and analysis of drought-responsive microRNAs in *Oryza sativa*. *Journal of experimental botany*, 61(15), 4157-4168.

Zhou, R., Wang, Q., Jiang, F., Cao, X., Sun, M., Liu, M., & Wu, Z. (2016). Identification of miRNAs and their targets in wild tomato at moderately and acutely elevated temperatures by high-throughput sequencing and degradome analysis. *Scientific Reports*, 6(1), 33777.

Zhu, H., Zhou, Y., Castillo-González, C., Lu, A., Ge, C., Zhao, Y. T., ... & Zhang, X. (2013). Bidirectional processing of pri-miRNAs with branched terminal loops by Arabidopsis Dicer-like1. *Nature structural & molecular biology*, 20(9), 1106.

Jasmonic and salicylic acid response in the fern
Azolla filiculoides and its cyanobiont

Status	Published
Journal	Plant, cell & environment
Citation	de Vries, S., de Vries, J., Teschke, H., von Dahlen, J. K. , Rose, L. E., & Gould, S. B. (2018). Jasmonic and salicylic acid response in the fern <i>Azolla filiculoides</i> and its cyanobiont. <i>Plant, cell & environment</i> , 41(11), 2530-2548.
Own contribution	Generated most of the expression data for JA and SA-associated genes of <i>Azolla</i> ; contributed to microscopy of Cyanobiont abundance/fluorescence; contributed to writing of the manuscript

Jasmonic and salicylic acid response in the fern *Azolla filiculoides* and its cyanobiont

Sophie de Vries^{1,2*}  | Jan de Vries^{1,3*}  | Hendrik Teschke³ | Janina K. von Dahlen² | Laura E. Rose^{2,4} | Sven B. Gould³

¹Department of Biochemistry and Molecular Biology, Dalhousie University, 5850 College Street, Halifax, Nova Scotia B3H 4R2, Canada

²Institute of Population Genetics, Heinrich-Heine University Duesseldorf, Universitaetsstrasse 1, 40225, Duesseldorf, Germany

³Institute of Molecular Evolution, Heinrich-Heine University Duesseldorf, Universitaetsstrasse 1, 40225, Duesseldorf, Germany

⁴Ceplas, Cluster of Excellence in Plant Sciences, Heinrich-Heine University Duesseldorf, Universitaetsstr. 1, 40225, Duesseldorf, Germany

Correspondence

S. de Vries, Department of Biochemistry and Molecular Biology, Dalhousie University, 5850 College Street, Halifax, Nova Scotia B3H 4R2, Canada.

Email: sophie.devries@dal.ca

S. B. Gould, Institute of Molecular Evolution, Heinrich-Heine University Duesseldorf, Universitaetsstrasse 1, 40225 Duesseldorf, Germany.

Email: gould@hhu.de

Funding information

Killam Trusts; Heinrich Heine University; German Research Foundation (DFG), Grant/Award Number: VR 132/1-1

Abstract

Plants sense and respond to microbes utilizing a multilayered signalling cascade. In seed plants, the phytohormones jasmonic and salicylic acid (JA and SA) are key denominators of how plants respond to certain microbes. Their interplay is especially well-known for tipping the scales in plants' strategies of dealing with phytopathogens. In non-angiosperm lineages, the interplay is less well understood, but current data indicate that it is intertwined to a lesser extent and the canonical JA/SA antagonism appears to be absent. Here, we used the water fern *Azolla filiculoides* to gain insights into the fern's JA/SA signalling and the molecular communication with its unique nitrogen fixing cyanobiont *Nostoc azollae*, which the fern inherits both during sexual and vegetative reproduction. By mining large-scale sequencing data, we demonstrate that *Azolla* has most of the genetic repertoire to produce and sense JA and SA. Using qRT-PCR on the identified biosynthesis and signalling marker genes, we show that *Azolla* is responsive to exogenously applied SA. Furthermore, exogenous SA application influenced the abundance and gene expression of *Azolla*'s cyanobiont. Our data provide a framework for JA/SA signalling in ferns and suggest that SA might be involved in *Azolla*'s communication with its vertically inherited cyanobiont.

KEYWORDS

ferns, nitrogen fixation, phytohormones, symbiosis, plant evolution

1 | INTRODUCTION

Plants interact with various kinds of microbes on a regular basis. These microbes range from beneficial symbionts to harmful phytopathogens. For angiosperms, many studies have provided detailed insights into the molecular mechanisms of sensing microbes, defending themselves against them, and establishing symbiotic interactions (Berens, Berry, Mine, Argueso, & Tsuda, 2017; Zipfel & Oldroyd, 2017). In contrast, studies on gymnosperms, ferns, lycophytes, and mosses are scarcer and limited to very few species. The algal relatives of land plants, the streptophyte algae (de Vries,

Stanton, Archibald, & Gould, 2016; Delwiche & Cooper, 2015), possess the genetic potential for interacting with beneficial microbiota (Delaux et al., 2015; Knack et al., 2015) and for producing phenolic defence metabolites (de Vries, de Vries, Slamovits, Rose, & Archibald, 2017). One can therefore conclude that even prior to the conquest of land, streptophytes had intricate microbe-elicited signalling mechanisms. That would mean that streptophyte-microbe signalling mechanisms have been evolving for more than 500 million years (cf. Parfrey, Lahr, Knoll, & Katz, 2011), presumably resulting in a yet-to-be explored lineage-specificity. Nonetheless, there are common themes in the underlying pathways. Two of these common factors in plant-microbe interaction, potentially present already in basal-branching streptophyte algae, are jasmonic and salicylic acid

*Sophie de Vries and Jan de Vries contributed equally to this work.

(JA and SA; Pieterse, Van der Does, Zamioudis, Leon-Reyes, & Van Wees, 2012, cf. Hori et al., 2014).

The biosynthesis of JA and SA occurs (at least partially) in the plastid (Figure 1; Garcion et al., 2008; Serrano et al., 2013; Strawn et al., 2007; Vick & Zimmerman, 1987; Ziegler et al., 2000). JA is synthesized from galactolipids, which are converted to α -linolenic acid (Nilsson, Fahlberg, Ellerström, & Andersson, 2012; Wasternack & Hause, 2013; Figure 1). The 13-Lipoxygenase (13-LOX) converts this fatty acid into 13(S)-hydroperoxyoctadecatrienoic acid (13(S)-HPOT; Bannenberg, Martínez, Hamberg, & Castresana, 2009; Howe & Schillmiller, 2002; Siedow, 1991). The conversion of 13(S)-HPOT to the allene oxide (9Z,15Z)-(13S)-12,13-epoxyoctadeca-9,11,15-trienoic acid (12,13-EOT) by 13-Allene Oxide Synthase (AOS) is considered the first committed step in JA biosynthesis (D. -S. Lee, Nioche, Hamberg, & Raman, 2008; Simpson & Gardner, 1995; W. -C. Song, Baertschi, Boeglin, Harrist, & Brasch, 1993; W. -C. Song & Brash, 1991). 12,13-EOT is further processed into cyclic *cis*-(+)-12-oxo-phytodienic acid ((9S,13S)-OPDA) by the enzyme Allene Oxide Cyclase (AOC; Zimmerman & Feng, 1978, Hamberg & Fahlstadius, 1990, Simpson & Gardner, 1995, Ziegler, Hamberg, Miersch, & Parthier, 1997). (9S,13S)-OPDA is then translocated from the plastid into the peroxisome, where OPDA Reductase 3 (OPR3) converts it into 3-oxo-2-(*cis*-2'-pentenyl)cyclopentane-1-

octanoic acid (OPC8:0; Schaller, Biesgen, Müssig, Altmann, & Weiler, 2000, Stintzi & Browse, 2000). This product is then subjected to several steps of β -oxidation, ultimately converting it into the first JA-derivative, (+)-7-*iso*-JA (Cruz Castillo, Martínez, Buchala, Métraux, & Léon, 2004; C. Li et al., 2005; Vick & Zimmerman, 1984). Subsequent isomerization converts this first JA-derivative into (-)-JA (Wasternack & Parthier, 1997). (-)-JA spontaneously epimerizes to (+)-JA and is conjugated with isoleucine to the active JA-derivative JA-Ile by the jasmonic acid-amido synthetase Jasmonate Resistant 1 (JAR1) in the cytoplasm (Fonseca et al., 2009; Staswick & Tiryaki, 2004; Staswick, Tiryaki, & Rowe, 2002; Suza & Staswick, 2008).

SA is synthesized from chorismate via Isochorismate Synthase 1 (ICS1; Wildermuth, Dewdney, Wu, & Ausubel, 2001). Hereby, chorismate is converted into isochorismate via ICS1 and isochorismate is further converted into SA. Alternatively, SA can also be synthesized from phenylalanine, which is first converted into cinnamate by the phenylalanine ammonia lyase and further processed into SA (Coquoz, Buchala, & Métraux, 1998; Huang et al., 2010; Meuwly, Mölders, Buchala, & Métraux, 1995; Pallas, Paiva, Lamb, & Dixon, 1996). The acyl acid amido synthetase GH3.12 (also known as PBS3) and Enhanced Pseudomonas Susceptibility 1 (EPS1) further contribute to SA biosynthesis (Jagadeeswaran et al., 2007; M. W. Lee, Lu, Jung, & Greenberg, 2007; Nobuta et al., 2007; Z. Zheng, Qualley, Fan, Dudareva, & Chen, 2009). Once SA is synthesized, it is hypothesized to be exported from the chloroplast by the transporter protein Enhanced Disease Susceptibility 5 (EDS5; Nawrath, Heck, Parinshawong, & Métraux, 2002; Serrano et al., 2013).

JA and SA have been detected in the basal-branching streptophyte alga *Klebsormidium nitens* (Hori et al., 2014). One would, hence, predict that both hormones arose early in streptophyte evolution and are ubiquitous among all land plants; in reality, it is more involved. The model moss *Physcomitrella patens* was found to produce OPDA, but to lack both JA (Stumpe et al., 2010) and the recently described jasmonate *cis*-(+)-OPDA-Ile (Floková et al., 2016). The same seems to apply to the liverwort *Marchantia polymorpha* (Yamamoto et al., 2015). On the other hand, some bryophytes synthesize JA, although the levels of JA seem lineage-specific (Záveská Drábková, Dobrev, & Motyka, 2015). Very recently, the lycophyte *Selaginella moellendorffii* was found to contain OPDA, JA, and JA-Ile, all of which were inducible by wounding (Pratiwi et al., 2017). In contrast to the findings with regard to JA, Ponce de León et al. (2012) found that the moss *P. patens* produces SA. The authors further found that SA was induced upon infecting the moss with the pathogen *Botrytis cinerea*. However, our knowledge on the presence and function of SA in basal branching vascular plants (i.e., lycophytes and ferns) remains scarce.

The role of JA and SA is well-established in pathogen defence (Glazebrook, 2005; Pieterse et al., 2012; Robert-Seilaniantz, Grant, & Jones, 2011). JA/SA's function in symbiotic interaction—though repeatedly implied—is, however, less clear (Foo, Ross, Jones, & Reid, 2013; Gutjahr, Siegler, Haga, Lion, & Paszkowski, 2015). As a defence mechanism, enhanced SA biosynthesis and SA-associated defence gene expression are hallmarks of the plants' response to biotrophic and hemibiotrophic pathogens (Glazebrook, 2005; McDowell & Dangl, 2000), both of which are pathogen types that start their life cycle

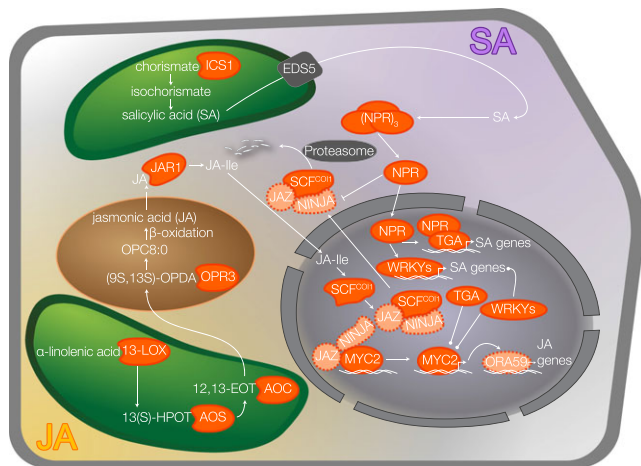


FIGURE 1 Presence/absence of JA and SA biosynthesis, perception and signalling genes. Biosynthesis and signalling of the two phytohormones JA and SA based on the current data retrieved from studies on angiosperms. Intermediate products in the biosynthesis towards JA and SA are provided. Genes present in *A. filiculoides* are highlighted in orange; absent genes are in grey. Genes with ambiguous results are shown in light orange and a dotted outline. Chloroplasts are shown in green, a peroxisome is shown in brown, and the nucleus is shown in grey. Abbreviations: 13-LOX = 13-Lipoxygenase; 13(S)-HPOT = 13(S)-hydroperoxyoctadecatrienoic acid; AOS = 13-Allene Oxide Synthase; 12,13-EOT = (9Z,15Z)-(13S)-12,13-epoxyoctadeca-9,11,15-trienoic acid; AOC = Allene Oxide Cyclase; (9S,13S)-OPDA = *cis*-(+)-12-oxo-phytodienic acid; OPR3 = OPDA Reductase 3; OPC8:0 = 3-oxo-2-(*cis*-2'-pentenyl)cyclopentane-1-octanoic acid; JAR1 = Jasmonate Resistant 1; JA-Ile = Jasmonoyl-L-isoleucine; ICS1 = Isochorismate Synthase 1; EDS5 = Enhanced Disease Susceptibility 5; NPR = Non-expressor of Pathogenesis-Related genes; SCF = Skp, Cullin, F-box containing complex; COI1 = F-box protein Coronatine Insensitive 1; JAZ = Jasmonate Zim Domain; NINJA = Novel Interactor of JAZ; TGA, WRKYs, MYC2 and ORA59 = TFs

dependent on a living host. JA-dependent defence pathways, in contrast, are up-regulated in response to wounding, insects, and necrotrophic pathogens (pathogens living of dead and degrading host tissue; McDowell & Dangel, 2000; Glazebrook, 2005). In case of the latter, an interaction with ethylene (ET) signalling is required (Glazebrook, 2005; Lorenzo, Piqueras, Sánchez-Serrano, & Solano, 2003). Given that SA and JA aid in defending the plant against such different pathogens, it is not surprising that studies on the model plant *Arabidopsis thaliana* revealed an antagonistic mechanism of interaction between the two phytohormones (Niki, Mitsuhara, Seo, Ohtsubo, & Ohashi, 1998; Peña-Cortés, Albrecht, Prat, Weiler, & Willmitzer, 1993; Spoel et al., 2003; Van der Does et al., 2013).

The presence of the JA-Ile conjugate triggers the association of Jasmonate Zim Domain (JAZ) with the F-box protein Coronatine Insensitive 1 (COI1), leading to the ubiquitination and subsequent degradation of JAZ proteins (Chini et al., 2007; Thines et al., 2007; Xie, Feys, James, Nieto-Rostro, & Turner, 1998). JAZ and Novel Interactor of JAZ (NINJA) together facilitated a repression on the transcription factor (TF) MYC2 (Chini et al., 2007; Pauwels et al., 2010), which controls the expression of JA-responsive genes such as *Plant Defensin 1.2* (*PDF1.2*; Lorenzo, Chico, Sánchez-Serrano, & Solano, 2004). Hence, the COI1-mediated degradation of the JAZ-NINJA repressor system allows activation of the transcription of JA signalling. The Ethylene Response Factor 1 (ERF1) positively regulates JA and ET signalling. Expression of *ERF1* and *ORA59* is enhanced by ET responsive TFs of the Ethylene Insensitive 3 (EIN3) family, EIN3 and EIN1, (Zhu et al., 2011). *ERF1* and *ORA59* both enhance expression of *PDF1.2* (Lorenzo et al., 2003; Penninckx, Thomma, Buchala, Métraux, & Broekaert, 1998; Pré et al., 2008), indicating the positive interaction between JA and ET signalling.

The exact perception mechanism of SA is less understood. It was shown that the three Non-expressor of Pathogenesis-Related genes (NPR) homologs NPR1, 3, and 4 all can bind SA (Fu et al., 2012; Y. Wu et al., 2012), although Fu et al. (2012) showed that at least NPR3 and 4 had different affinities towards SA. NPR1 is indicated to undergo a biochemical change after SA perception (Y. Wu et al., 2012). It translocates into the nucleus (Després, DeLong, Glaze, Liu, & Fobert, 2000; Kinkema, Fan, & Dong, 2000) where it interacts with TFs such as TGACG motif-binding factors (TGAs) (Després et al., 2000; Y. Zhang, Fan, Kinkema, Li, & Dong, 1999), which in turn induce WRKY TFs (D. Wang, Amornsiripanitch, & Dong, 2006). Both TGAs and WRKYs regulate the transcription of SA-responsive genes, such as *Pathogenesis Related gene 1* (*PR1*, Kim, Lai, Fan, & Chen, 2008; Kinkema et al., 2000; Y. Zhang et al., 1999; Zhou et al., 2000,). Additionally, WRKYs and TGAs play a crucial role in the JA/SA antagonism. For example, TGA TFs regulate the expression of both the JA-responsive *PDF1.2* and the SA-responsive *PR1* genes (Ndamukong et al., 2007; Zander, La Camera, Lamotte, Métraux, & Gatz, 2010; Y. Zhang, Tessaro, Lassner, & Li, 2003). Similarly, *WRKY70* and *WRKY62* are induced by SA and negatively regulate JA (Kim et al., 2008; Li, Brader, & Plava, 2004; Mao, Duan, Wei, & Li, 2007). Other WRKYs promote JA responses (Journot-Catalino, Somssich, Roby, & Kroj, 2006). Furthermore, SA is able to reduce the accumulation of the JA-responsive TF *ORA59* (Van der Does et al., 2013). Although these data have only been analysed in a few model species, evidence for an antagonism

goes as far back as *Gingko* (Thaler, Humphrey, & Whiteman, 2012; Xu, Dong, Wang, & Huang, 2009). The gymnosperm *Picea abies* seems to lack the antagonistic function of SA and JA (Arnerup et al., 2013; Kozłowski, Buchala, & Métraux, 1999). Ancestral character state reconstruction places the origin of the JA/SA antagonism at the base of angiosperms or before the angiosperm/gymnosperm split (Thaler et al., 2012). But, as Thaler et al. (2012) highlight, these inferences are hampered by the absence of data from a diversity of plants. This is especially true for non-seed plants.

Azolla filiculoides is on the brink of becoming a model system for fern biology. It is fast growing (Wagner, 1997), has been the subject of multiple transcriptomic studies (Brouwer et al., 2014; Brouwer et al., 2017; de Vries, Fischer, et al., 2016), and is one of the few ferns whose genome is under investigation (F. -W. Li & Pryer, 2014; Sessa et al., 2014; Sessa & Der, 2016). What is more, *Azolla* engages in a (among the entirety of land plants) unique nitrogen fixing symbiosis with a cyanobiont that we will henceforth refer to as *Nostoc azollae*. The cyanobiont's taxonomic classification is, however, still debated as morphological, physiological, and molecular characters show affinities to different cyanobacterial genera within the family Nostocaceae (summarized in Pereira & Vasconcelos, 2014). Hence, the cyanobiont that we here refer to as *N. azollae* is, among others, also referred to as *Anabaena azollae* and *Trichormus azollae* (see, Pereira & Vasconcelos, 2014; Rajaniemi et al., 2005). This cyanobiont resides within *Azolla*'s leaf cavities and is both vertically (sexually) and horizontally (vegetatively) transmitted (Becking, 1987; Peters & Meeks, 1989; Rai, Soderback, & Bergman, 2000). These circumstances make *Azolla* a twofold interesting candidate for studying fern-microbe interaction.

Here, we screened *Azolla filiculoides* RNAseq data for JA and SA biosynthesis genes and associated signalling toolkits. We find that *Azolla* possesses most of the genetic toolkit necessary for synthesizing and perceiving JA and SA. Gene expression analysis shows that *Azolla* responds to exogenously applied SA, but not JA. These data also indicate that canonical JA defence responses may partially be regulated by SA in *Azolla*. Moreover, SA application altered cyanobacterial abundance and gene expression. These data impact current views on the JA/SA signalling evolution and how *Azolla* communicates with its nitrogen-fixing partner.

2 | MATERIAL AND METHODS

2.1 | Identification of JA and SA genes and phylogenetic analyses

We searched *A. filiculoides* sporophyte and root transcriptome data sets (Brouwer et al., 2014; de Vries, Fischer, et al., 2016) for genes encoding JA and SA biosynthesis and signalling proteins (e-value cut-off 10^{-5}) based on their hits against *A. thaliana* proteins (selected via literature and The Arabidopsis Information Resource [Huala et al., 2001]).

Next, we generated a data set from the proteins encoded by the genomes of *Klebsormidium nitens* (Hori et al., 2014), *P. patens* (Rensing et al., 2008), *S. moellendorffii* (Banks et al., 2011), and *P. abies* (Nystedt et al., 2013). To identify orthologs, we conducted a reciprocal BLASTp

search of the best hit using *A. thaliana* JA and SA biosynthesis and signalling protein sequences as query (e-value cut-off $\leq 10^{-5}$, in both directions). To expand the data set, we included homologous hits from the reciprocal BLAST result in our phylogenies.

We created phylogenies for each gene family including the sequences identified in our initial searches, additional members of these and closely related gene families from *A. thaliana*, and, if appropriate, representatives from animals and prokaryotes. In case of the EIN3/EIL1 analyses, we also included other EIN proteins, despite them having different functions. Alignments were generated using G-INS-I in MAFFT v.7.305b (Katoh, Misawa, Kuma, & Miyata, 2002; Katoh & Standley, 2013) and incomplete sequences were removed. Exceptions were the AOC, EIN3-family, WRKY, and ORA59/ERF alignments. For AOC and WRKY, all sequences that covered the conserved regions were included. The AOC alignment was further restricted to include only the conserved regions. For the EIN3-family alignment, a potentially partial *S. moellendorffii* sequence was included to represent the lycophyte ortholog. For ORA59/ERF, all partial *Azolla* sequences were included. New alignments were created using either the G-INS-I (alignments LOX, JAR, NINJA, NPR, MYC, and Jasmonate-associated MYC2-like [JAM], TGA, and EIN3-family) or L-INS-I (alignments AOS, AOC, OPR, PDF, COI1 and WRKY) option in MAFFT v. 7.305b. Maximum-likelihood (ML)-phylogenies with 500 bootstrap replicates were created using iQTree v1.4.4 (Nguyen, Schmidt, von Haeseler, & Minh, 2015; LG + G model) and MEGA7 (Kumar, Stecher, & Tamura, 2016; best model prediction via MEGA7, 95% partial deletion cut-off).

2.2 | Phytohormone treatments

A. filiculoides was grown under semi-sterile conditions. We first transferred greenhouse plants to vessels (120 mm × 104 mm, PTcon™-11 W, PhytoTechnology Laboratories) filled with sterile tap water, incubated them for a week at 24 °C, and then transferred them into new vessels (77 mm × 77 mm × 97 mm, Magenta™ vessels GA-7, Sigma Aldrich) with sterile International Rice Research Institute (IRRI) medium (Watanabe, Roger, Ladha, & Van Hove, 1992; prepared with tap water and no trace element solution for comparability to de Vries, Fischer, et al., 2016). Treatments were applied after 12 days of acclimation to the medium condition. Cultures were regularly split and transferred to new vessels and fresh medium. We treated the plants with 10% MeSA (SA mixed with MeOH; Arnerup et al., 2013), 10% MeJA (JA mixed with MeOH; Arnerup et al., 2013); controls included an MeOH solvent control (all mixtures were applied with 75 µl/1 l air) and an untreated control. Treatments with volatiles (MeSA, MeJA, and MeOH) were replenished after each sampling and cross-contamination of MeSA, MeJA, or MeOH was prohibited by using a separate desiccator per treatment. Because of the fast growth of *A. filiculoides*, we removed the young leaf tissue from the tips to ensure that we only sampled tissue that was exposed to the treatments during the entire time. Samples were taken at 0 hr post-treatment (hpt), 24, 48, 72, and 96 hpt. All roots were removed during the sampling. Images were taken using a Canon EOS 70D. In total, three biological replicates per time point and treatment were sampled.

2.3 | Microscopy

Cyanobiont abundance/fluorescence was assessed using a Nikon SMZ18 dissection microscope with a DS-Ri1 camera and a TRITC fluorescence filter (EX535/50, BS575, EM590LP). We analyzed 10 plant bodies per time point, treatment, and replicate. Image analysis was performed using ImageJ2 (Schindelin, Rueden, Hiner, & Eliceiri, 2015). MeSA and MeJA treatment data were normalized against MeOH, and we tested for significant differences in fluorescence over time via a Kruskal-Wallis test (Kruskal & Wallis, 1952) combined with a Tukey and Kramer post hoc test, which uses a Tukey distance approximation (Sachs, 1997) using R v.3.2.1.

2.4 | DNA and RNA extraction and cDNA synthesis

DNA and RNA were extracted from the 24 and 72 hpt samples. The DNA extraction was carried out according to Edwards, Johnstone, and Thompson (1991) from tissue that was directly ground within the extraction buffer. DNA was diluted to 10 ng/µl. RNA was extracted using the Spectrum™ Plant Total RNA Kit (Sigma Aldrich) and treated with DNase I (Thermo Scientific). RNA quality was assessed using a formamide gel (5:6 RNA:deionized formamide, 5 min at 65 °C, 5 min on ice). Total RNA (300 ng) was used in the RevertAid First Strand cDNA Synthesis Kit (Thermo Fisher Scientific).

2.5 | Expression of *Azolla* JA and SA-associated genes and *N. azollae* nitrogen fixation genes

The expression of *AfAOS*, *AfPR5*, *AfJAZ3*, *AfNPR1*, and *AfPDF1.4* was determined via a quantitative reverse transcription PCR (qRT-PCR). We used the Takyon™ Rox SYBR® 2X MasterMix dTTP blue (Eurogentec) in a 20 µl reaction with 2 µl template for all genes except *AfAOS*, for which 1 µl template input was used. All reactions were run on a StepOnePlus Real-Time PCR System (Applied Biosystems; initial denaturation, 95 °C for 3 min; 40 cycles of 15 s denaturation at 95 °C followed by 1 min combined annealing and elongation at a primer specific temperature [Table S1]). A melting curve was added after each run. Relative expression was calculated according to Pfaffl (2001). Based on steady expression, we picked *Elongation factor 1α-AfELF1α*, *Tubulin α2 chain-AfTUA2*, *Cyclin D1-AfCYCD1* as reference genes. For expression analysis of the cyanobionts' *Nif* genes *NaNifE* and *NaNifH*, *NaRnpB* and *NaRPS4* served as reference genes. All data were tested for normality using a Shapiro-Wilk test (Shapiro & Wilk, 1965) and equal variance and accordingly either a Mann-Whitney *U* (Mann & Whitney, 1947), two-sample *t* test or a Welch two-sample *t* test was performed in R v.3.2.1.

2.6 | Relative abundance of *Azolla*'s cyanobiont *Nostoc azollae* in the fern cavities

We quantified the relative abundance of the *N. azollae* DNA using the loci *Nitrogen fixation E (NaNifE)*, *RNase P RNA (NaRnpB)*, *Ribosomal protein L25 (NaRPL25)*, and *Ribosomal protein S4 (NaRPS4)* as well as the *A. filiculoides* DNA loci *Calmodulin 5 (AfCam5)* and *AfElf1α* using quantitative PCR (qPCR). Relative abundance of *N. azollae* DNA was calculated according to Pfaffl (2001) using the *A. filiculoides* DNA loci

as reference and aforementioned statistics were performed. The qPCRs were performed using SsoAdvanced™ Universal SYBR® Green Supermix (BioRad) in a CFX Connect™ Real-Time System (BioRad). All qPCRs were run with the following settings: initial denaturation at 95 °C for 3 min, followed by 40 cycles of a denaturation step at 95 °C for 10 s and an annealing at 60 °C (Table S1) for 30 s. A melting curve was added after each run.

3 | RESULTS

3.1 | *Azolla filiculoides* possesses a repertoire of JA and SA biosynthesis and signalling genes

JA and SA are among the best-studied phytohormonal signals in plant-microbe interactions (Glazebrook, 2005). We surveyed to what degree *A. filiculoides* is theoretically able to synthesize these two phytohormones and respond to their presence, by screening the transcriptomes of roots and complete sporophytes of the fern (Brouwer et al., 2014; de Vries, Fischer, et al., 2016).

The *Azolla* transcriptomes included 38 LOX, nine AOS, nine AOC, 15 OPR, and eight JAR1 like sequences (Figure 1, Table S2), hence possessing candidate sequences coding for enzymes of the entire JA biosynthesis pathway. SA biosynthesis in plants can take place via isochorismate or cinnamate (Coquoz et al., 1998; Huang et al., 2010; Meuwly et al., 1995; Pallas et al., 1996; Wildermuth et al., 2001). We chose to focus on the isochorismate pathway, which in *Arabidopsis* requires the enzymes ICS1 and ICS2, PBS3, and EPS1 (Jagadeeswaran et al., 2007; M. W. Lee et al., 2007; Nobuta et al., 2007; Wildermuth et al., 2001; Z. Zheng, Qualley, et al., 2009). We, however, found only three candidate sequences encoding ICS1-like sequences (Figure 1, Table S2) and no candidates for ICS2, PBS3, or EPS1 (Table S2). The SA exporter EDS5 (Nawrath et al., 2002; Serrano et al., 2013) was absent in both transcriptome data sets (Figure 1).

JA signalling is orchestrated by the signalling repressor JAZ, its interaction factor NINJA, and the F-box protein COI1 (Chini et al., 2007; Pauwels et al., 2010; Thines et al., 2007; Xie et al., 1998). We found 20 JAZ, one NINJA, and 11 COI1 candidate sequences (Figure 1, Table S2). Downstream of JAZ, NINJA, and COI1 are MYC2, 3, and 4, as well as JAM1, 2, 3, and 4. In the *Azolla* transcriptomes, we found 14 MYC2, three MYC3, and two MYC4 candidate sequences, as well as two JAM candidates (JAM1 and JAM4); additionally, we detected one PDF1.4 candidate (Table S2).

When plants respond to necrotrophic pathogens, JA and ET signalling act in concert (Glazebrook, 2005; Lorenzo et al., 2003). This is regulated by ERF1, EIN3 and EIL1, MYC2, and ORA59 (Lorenzo et al., 2003; Pré et al., 2008; S. Song et al., 2014; Zhu et al., 2011). We found two ERF1a (AT4G17500.1) candidate sequences, eight candidates for EIL1, and one ORA59 candidate sequence (Table S2).

SA signalling is perceived and transduced via NPR proteins. Screening the transcriptomes, we detected five NPR sequences, one NPR1, two NPR3, and three NPR4 sequences. Downstream the NPR proteins activate SA signalling and the JA/SA antagonism via WRKY and TGA TFs. Here, we found 13 candidate sequences encoding for

selected WRKYs (that have been associated with JA and SA signalling) and 28 sequences corresponding to TGA TFs (Figure 1, Table S2). SA leads to the transcription of *PR1* and sometimes other *PRs*, such as *PR5* (Cao, Bowling, Gordon, & Dong, 1994; Uknes et al., 1992). In *Malus hupehensis*, these *PR* genes were responsive to not only SA but also MeJA (J. Zhang et al., 2010). Here, we found candidate sequences for each *PR1* (one), *PR3* (four), and *PR5* (one; Table S2). Taken together, the combination of the two transcriptomes allowed the identification of representatives of most of the essential gene families involved in the biosynthesis of JA and SA and their downstream signalling (Figure 1).

3.2 | Phylogenetics identifies a potentially functional JA/SA biosynthesis pathway in *Azolla*

To support our findings and gain a better resolution of the gene families we identified, we created phylogenies with the sequences of *A. filiculoides*, related sequences from the streptophyte alga *K. nitens*, the moss *P. patens*, the lycophyte *S. moellendorffii*, the gymnosperm *P. abies*, and the angiosperm *A. thaliana*, and included related subfamilies of the respective enzymes. The sequences of *P. patens*, *S. moellendorffii*, and *P. abies* were identified based on a BLASTp approach with the sequence of *A. thaliana* as query.

LOX synthesizes the precursor for JA biosynthesis. Of the two plant LOX protein subfamilies, 9-LOX and 13-LOX, only the latter synthesizes the JA precursor 13(S)-HPOT (Bannenberg et al., 2009). Of the seven full-length sequences of *A. filiculoides*, three clustered with a weak support (bootstrap value of 64) with three of the four representatives of the 13-LOX clade in *A. thaliana*, AtLOX3, 4, and 6 (Figure 2a). This shows that *A. filiculoides* possesses representatives of 13-LOX and could potentially produce 13(S)-HPOT.

AOS is the first enzyme in the JA biosynthesis pathway. AOS is a CYP P450 enzyme in the subfamily CYP74 (W. -C. Song & Brash, 1991); in plants, the enzymes Hydroperoxidylase (HPL) and Divinylethersynthase also belong to this protein subfamily; however, in *Arabidopsis*, only HPL is present. We created an ML-phylogeny including the *A. thaliana* AOS and HPL sequences, the full-length sequences of *A. filiculoides* and the other model plants, as well as a representative CYP74 sequence from the animal kingdom (Figure 2b). All three *A. filiculoides* sequences clustered with AtAOS and AtHPL, but the resolution within the clade was too low to draw any sound conclusions. We therefore analyzed the domain and modelled the 3D-structure of the potential AfAOS AfzIRT00652 via CD-search and I-TASSER. Additionally, we analyzed the active site for conserved residues between all three *Azolla* AOS sequences, the previously characterized SmAOS2 (Pratiwi et al., 2017) and the AtAOS sequence. CD-search showed that the potential AfAOS sequence encodes an AOS domain similar to that of *A. thaliana* (Figure 3) and I-TASSER recovered an AOS of *Parthenium argentatum* (3DAN) as the best structural analogue hit (TM-score 0.860; cf. Li, Chang, Pan, Fu, & Wang, 2008) and AtAOS (3DSI, TM-score 0.854; cf. D. -S. Lee et al., 2008) as the second best structural model for the potential AfAOS sequence. I-TASSER furthermore predicted a protoporphyrin IX binding site (c-score 0.74, corroborating AOS's heme binding) for AfAOS and as best Cscore^{EC} (0.439) the EC number 4.2.1.92, which corresponds to

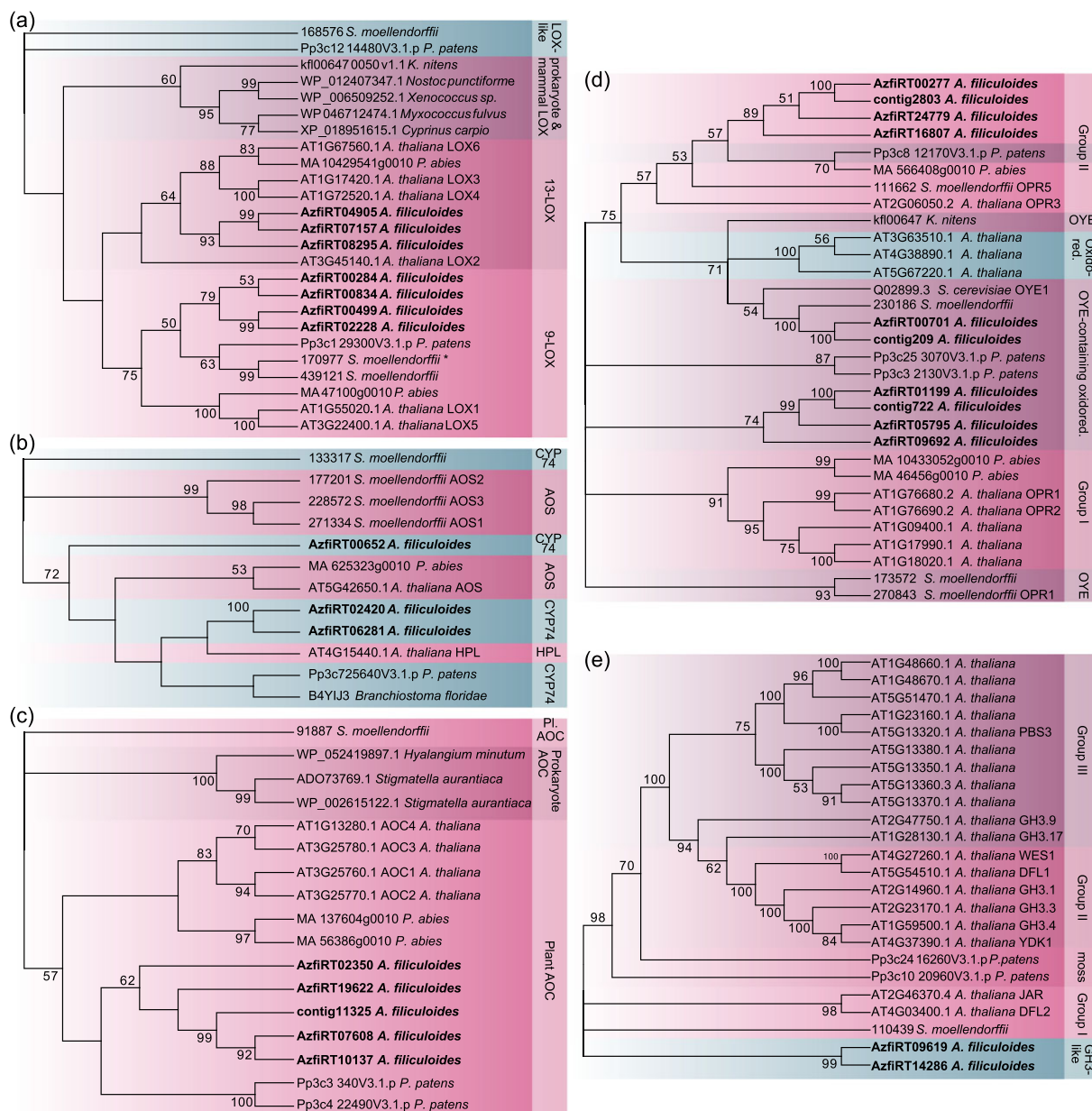


FIGURE 2 Phylogenetic analyses of enzymes involved in JA biosynthesis. ML-phylogenies of the five enzymes involved in JA biosynthesis, 13-LOX protein family (a), AOS (b), AOC (c), OPR3 (d), and JAR1 (e). All phylogenies have been computed using the LG + G model. Only the consensus tree is shown. Bootstrap values <50 are not shown. All *A. filiculoides* sequences are shown in bold. Closely related protein (sub)families or groups within a protein family were included in each phylogeny. Clusters of a specific (sub)family or group within a protein family are highlighted by pink and purple backgrounds. Blue backgrounds indicate that the sequences could not be sorted to a specific cluster. Cluster specifications are given on the right of each phylogeny. * indicates sequences of *P. patens*, *S. moellendorffii*, and *P. abies* that have been retrieved as homologs, not orthologs in the reciprocal BLAST search, yet were still included in the phylogeny [Colour figure can be viewed at wileyonlinelibrary.com]

AOS. The active site was most conserved for AzfiRT00652 compared to the other two *Azolla* sequences. When AzfiRT00652 was then compared with *SmAOS2* and *AtAOS*, we found that seven of the 10 active site residues were conserved between AzfiRT00652 and *AtAOS* (active sites according to Lee et al. [2008]). Two of the remaining three residues were the same as in *SmAOS2*, and only T389 (position according to *AtAOS*) was a proline in all *Azolla* sequences and a glutamine in *SmAOS2*.

The next step in JA biosynthesis is conducted by AOC. In addition to the plant AOC sequences, we also included bacterial AOC sequences. Due to the divergence of the bacterial to plant sequences,

we built the phylogeny only on the conserved region present in all sequences. All sequences that covered this part were included in the analyses, independent of whether or not a full-length sequence was present. All sequences of *A. filiculoides* clustered with the AOC sequences of *A. thaliana*, but formed their own clade within that cluster (Figure 2c). In *P. patens*, AOC utilizes the allene oxide 11,12-EETE instead of 12,13-EOT, resulting in no production of JA (Stumpe et al., 2010). Because the two *P. patens* sequences in our data set cluster with the *Azolla* clade (albeit not supported), we also analyzed the four potential AfAOC sequences from the root transcriptome for the presence of the functional residues of *AtAOC2* and compared the data

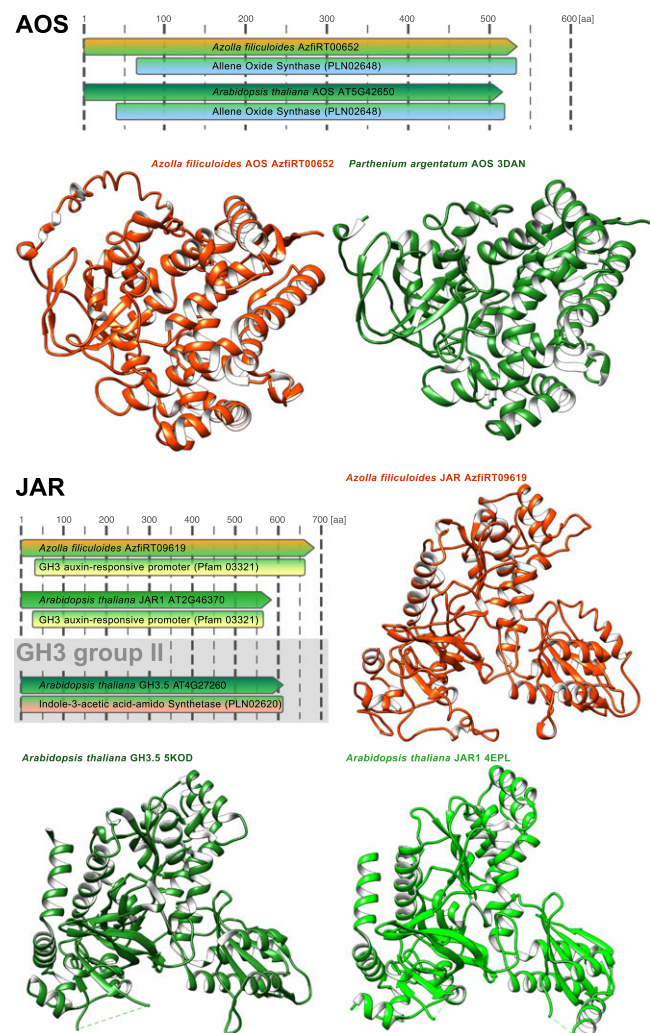


FIGURE 3 Comparative analyses on the AOS and JAR1 protein structure. Domain structures of the *AfAOS* candidate sequence (AzfiRT00652) in orange in comparison to the *AtAOS* protein sequence (AT5G42650) in green (top). Proteins are drawn to scale. The domain present in the sequence as identified by CD-search are shown below each protein. 3D-structures for *AfAOS* as predicted by I-TASSER (orange, AOS bottom left) and its closest structural hit, the AOS protein of *Parthenium argentatum* (green, AOS bottom right) are given below the CD-search results. Domain structure comparison of the *AfJAR1* candidate sequence (AzfiRT09619, orange), the *AtJAR1* sequence (AT2G46370, light green), and a representative of the closely related GH3 Group II, *AtGH3.5* (AT4G27260, dark green [bottom]). The protein sequences are drawn to scale, and the domains as predicted by CD search are given below. The 3D structure of *AfJAR1* (orange, JAR top right) was predicted using I-TASSER, its closest structural hit was *AtGH3.5* (dark green, JAR bottom left). For comparison, also its third best structural hit *AtJAR1* (light green, JAR bottom right) is shown [Colour figure can be viewed at wileyonlinelibrary.com]

with the previously characterized functional *SmAOC*. *AtAOC2* has five residues that bind water, which is important for the epoxide reaction catalyzed by AOC (E88, N90, S96, P97, and N118; all positions are given according to *AtAOC2* with a target peptide; Hofmann, Zerbe, & Schaller, 2006). All these residues were conserved in *AtAOC1–4*, all analyzed *Azolla* sequences and *SmAOC*. The same is true for the residues involved in stabilizing the reaction and constraining the

binding site for specific substrates (V110, F116, C136, Y170, Hofmann et al., 2006). Position F150, important for substrate binding and space constraint (Hofmann et al., 2006), was changed to tyrosine in the *Azolla* and *Selaginella* sequences. Only one residue in the binding pocket, F108, was different in *AtAOC3* and 4 (leucine), *Azolla* (glycine or alanine), and *Selaginella* (asparagine). In summary, 10 out of the 11 functional residues analysed were identical either to the *AtAOCs* or to the functional *SmAOC*.

The last enzyme in the JA biosynthesis is OPR3. *AtOPR3* is characterized by its 12-oxophytodienoate reductase and its ICL KPHMT superfamily domain, whereas the other two OPRs (*AtOPR1* and *AtOPR2*) possess a domain called Old Yellow Enzyme. Overall, our phylogenetic analysis recreated the separation of OPR Group I (represented by *AtOPR1* and 2) and OPR Group II (represented by *AtOPR3*), previously reported (Al-Momany & Abu-Romman, 2016). The related FMN-linked oxidoreductase superfamily proteins split in two groups clustering with either OPR Group I or II (Figure 2d). Six *Azolla* sequences clustered with the group containing *AtOPR3* (bootstrap value 75), four of those clustered more closely with OPR3, albeit with low support (bootstrap value 57). A CD-search analysis showed that the four *Azolla* sequences that clustered with OPR3, possessed the ICL KPHMT superfamily domain. The functional *S. moellendorffii* sequence *SmOPR5* also contained the ICL KPHMT superfamily domain.

The likely active form of JA is its amino acid conjugate JA-Ile (Staswick & Tiryaki, 2004; Fonseca et al., 2009). After JA is exported into the cytoplasm JAR, a GH3 protein, conjugates isoleucine to JA (Staswick et al., 2002; Staswick & Tiryaki, 2004; Suza & Staswick, 2008). Here, we created a phylogeny for *JAR1* (Figure 2e) and resolved all three main groups of GH3 enzymes. Yet the *Azolla* sequences clustered outside of the GH3 cluster. I-TASSER analyses with AzfiRT09619 showed that the best structural hit was *AtGH3.5* (5KOD, C-score 0.845; cf. Westfall et al., 2016), but the third best was *AtJAR1* (4EPL, C-score 0.736; cf. Westfall et al., 2012). Looking closer, we observed strong similarities between all three of them (Figure 3), suggesting that they are indeed GH3-like sequences. CD-search helped distinguishing the *AtJAR1* sequence and AzfiRT09619 from *AtGH3.5*, as both *AtJAR1* and the *Azolla* sequence bear a GH3 auxin responsive promoter domain, whereas *AtGH3.5* has an Indole-3-acetic acid-amido synthetase domain (Figure 3). To obtain more information on whether the *Azolla* sequences could function as a JAR enzyme, we analyzed the JAR binding pocket conservation (Westfall et al., 2012) between *AtJAR1*, *SmJAR*, and the *Azolla* candidates. *SmJAR* has five of nine residues conserved with *AtJAR1*, the same is true for AzfiRT09619, whereas for AzfiRT14286, only three of nine residues were found to be conserved with *AtJAR1*. Unlike for AOS and AOC, residues not conserved between the fern and *Arabidopsis* were also not conserved between *Selaginella* and *Azolla*, suggesting an overall low conservation of the JA-Ile binding pocket.

We only found sequences for the first enzyme in the SA biosynthesis. ICS1 converts chorismate to isochorismate. We found three potential ICS1 sequences, albeit all cover only a small portion of the protein, rendering a phylogeny impossible. However, the 81-amino acid protein sequence of *Azolla* contig_36119 possesses a

chorismate binding enzyme domain, which includes the catalytic region, spanning 72 amino acids of ICS1.

3.3 | Phylogenetics of *Azolla* JA/SA signalling

JA-Ile, the most active derivative of JA, triggers the degradation of the JAZ repressor by the F-box protein COI1 (Thines et al., 2007). This leads to a release of the repression on MYC2 facilitated by JAZ and NINJA (Chini et al., 2007; Pauwels et al., 2010). JAZ is part of the TIFY domain TF family, although the JAZ proteins themselves have no direct DNA interacting motifs (Chini et al., 2007). We included the 13 *A. thaliana* members of the JAZ protein subfamily, the *A. filiculoides* JAZ candidate sequences, the JAZ homologs in the other model species, as well as representatives of *A. thaliana* TIFY domain TFs in the phylogenetic analysis. The JAZ sequences are rather diverse, resulting in an unresolved phylogeny and impeding any further conclusions on the presence of JAZ in *A. filiculoides* (Figure 4a). The JAZ interactor NINJA is part of the ABI5-binding protein family (AFP, Pauwels et al., 2010). We included representatives of AtAFP1–4 in the phylogenetic analysis to better determine the placement of the AfNINJA candidate sequence (Figure 4b). Except for the PaNINJA ortholog, the potential orthologs from *P. patens* and *S. moellendorffii*, as well as the *A. filiculoides* sequence lie outside of the NINJA and AtAFP cluster. COI1 is an F-box protein, related to the F-box protein TIR1 involved in auxin signalling (Xie et al., 1998). Both AfCOI1 candidates cluster with AtCOI1 (bootstrap support value 63, Figure 4c) suggesting that *A. filiculoides* possesses a COI1 ortholog.

Key regulators of JA signalling are the TFs MYC2, 3 and 4 and JAM1, 2, 3 and 4, (Fernández-Calvo et al., 2011; Lorenzo et al., 2004; Sasaki-Sekimoto et al., 2013; S. Song et al., 2013). They regulate several JA-dependent defence responses, including the production of the defensin family PDF1 and others (Lorenzo et al., 2004; Sasaki-Sekimoto et al., 2013). MYC and JAM TFs belong to the TF superfamily of basic-Helix-Loop-Helix DNA binding proteins, more precisely subfamily III (Pires & Dolan, 2010; Sasaki-Sekimoto et al., 2013). Our phylogenetic analysis recovered the basic-Helix-Loop-Helix subfamily III groups (Pires & Dolan, 2010). Two *A. filiculoides*' MYC2 candidate sequences cluster with the subgroup containing AtMYC2, 3, and 4 and JAM4 (Figure 4d). In case of the JA responsive gene family PDF1, we found one full-length sequence from *A. filiculoides* as a candidate for a PDF1.4 ortholog. Additionally, we included the second defensin family present in *A. thaliana* (Thomma, Cammue, & Thevissen, 2002), PDF2, in our analysis. Although the PDF2 cluster was well supported, and includes sequences from *P. abies*, the PDF1 subfamily could not be resolved (Figure 4e). Still, our AfPDF1.4 candidate ortholog clustered with the AtPDF1.4 sequence, suggesting that *A. filiculoides* possesses the downstream JA responsive gene.

Integrated JA and ET signalling is required for establishing a response towards necrotrophic pathogens (Glazebrook, 2005). We surveyed the *Azolla* data sets for ERF1, EIN3, and ORA59 sequences. We only detected full-length sequences for EIN3 candidates in the *A. filiculoides* data sets. All three *A. filiculoides* sequences cluster within the EIN3-family and more specifically with the subgroup of AtEIN3 and AtEIL1 (bootstrap support value of 72, Figure 4f). ERF1 and ORA59 belong to the AP2/ERF proteins. A CD-search with all three *Azolla*

candidates showed that, as for AtORA59 and AtERF1a and b, the *Azolla* candidates possess the AP2/ERF DNA-binding domain, indicating that they are indeed an AP2/ERF protein. Phylogenetic analysis of the AP2/ERF TF family placed the AfORA59 and the two AfERF1a candidate sequences within the B3 group (Caarls et al., 2017; Sakuma et al., 2002) of AP2/ERF TFs containing AtORA59, AtERF1a and b (bootstrap value 94; Figure 4f).

SA is perceived via NPR proteins (Fu et al., 2012; Y. Wu et al., 2012). The NPR1 monomer is additionally a co-activator of SA signalling, fulfilling both a role in perception as a component of an oligomer and signal transduction and activation as a monomer (Fu et al., 2012; Mou, Fan, & Dong, 2003; Y. Wu et al., 2012). Here, we analyzed whether *A. filiculoides* has the potential to perceive, transduce, and activate SA signalling by analyzing the phylogenetic placement of NPR candidate sequences of the fern (Figure 5a). NPR contains a Broad-Complex, Tramtrack, and Bric a brac domain and POxvirus and Zinc finger domain (BTB/POZ) as well as an ankyrin repeat domain (Cao, Glazebrook, Clarke, Volko, & Dong, 1997; Liu, Holub, Alonso, Ecker, & Fobert, 2005). We included *A. thaliana* representatives from related BTB domain containing subfamilies (Vierstra, 2009) in the ML-phylogeny to estimate the placement of the *A. filiculoides* NPR candidates. In total, we found three full-length candidate sequences in the *Azolla* transcriptomes, all of which group with *A. thaliana* NPR sequences NPR1, 3 and 4 (Figure 5a). This cluster also contains one NPR representative for *P. abies*, *S. moellendorffii*, and *P. patens*.

SA and JA signalling is integrated by WRKY and TGA TFs (Bakshi & Oelmüller, 2014; Ndamukong et al., 2007; Pandey & Somssich, 2009; Zander et al., 2010; Y. Zhang et al., 2003). The WRKY TF family consists of several 100 members in *A. thaliana* and is divided into three main subgroups (Q. Wang et al., 2011). For the phylogenetic analysis, we selected WRKYs reported to function in JA and SA signalling (Chen et al., 2013; Gao, Venugopal, Navarre, & Kachroo, 2011; Higashi et al., 2008; Journot-Catalino et al., 2006; Kloth et al., 2016; J. Li et al., 2004; Mao et al., 2007): subgroup Ib (WRKY75), IIb (WRKY11, 17 and 22), III (WRKY41, 62 and 70), and WRKY50 and 51 (Q. Wang et al., 2011). In addition, we included closely related members (subgroup Ia, Ib, and IIa; Q. Wang et al., 2011), orthologs for the JA/SA associated WRKYs in *P. abies*, *S. moellendorffii*, and *P. patens* and the candidates for the JA/SA associated WRKYs from *A. filiculoides* into the analysis (Figure 5b). The phylogeny recovered Groups Ia and b (bootstrap value 62), IIa (bootstrap value 96), and III (bootstrap value 97). Only Group IIb is not monophyletic. From the seven *Azolla* candidate sequences, four associated with specific groups of WRKYs at varying levels of support: One of these four *Azolla* candidates clustered with the selected Group III WRKY members (bootstrap support value of 97), all of which are associated with JA/SA signalling. One clustered with WRKY Group I (bootstrap value 62) and the two others cluster with WRKY50 and 51, which cluster with Group Ia and b, (bootstrap value 55), and are associated with the JA/SA antagonism. The TGA TFs are bZIP TFs, belonging to the bZIP group D (Jakoby et al., 2002). Within the bZIP phylogeny, we recovered all bZIP groups except group D (containing the TGAs) with high support, although the relationships between the groups remained unresolved (Figure 5c; Jakoby et al., 2002). The *Azolla* candidate sequences formed their own cluster. However, studying the alignment of the bZIP TFs, we discovered a conservation between all *Azolla* candidate and AtTGA

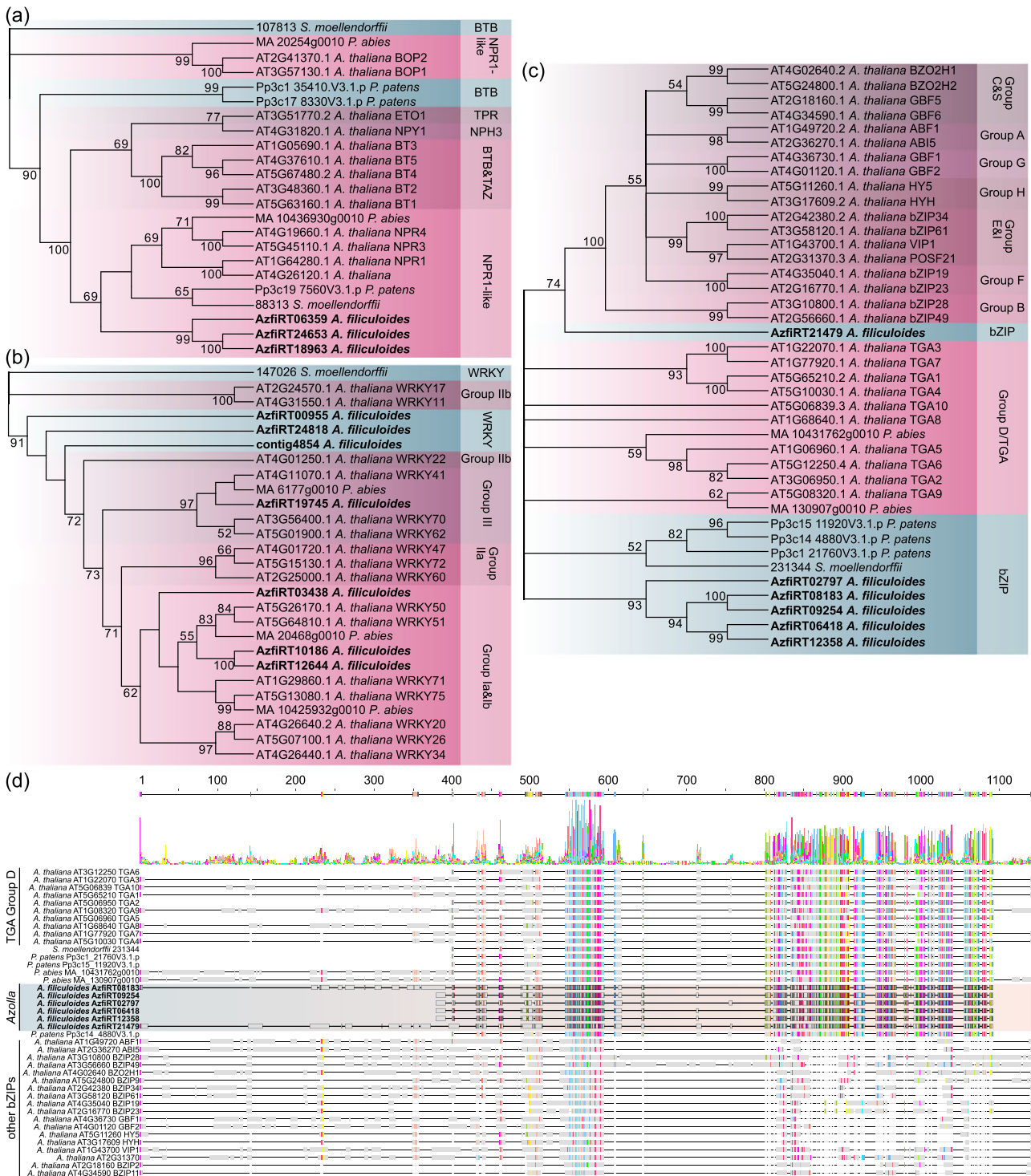


FIGURE 5 Analyses of the SA signalling pathway. Consensus ML-phylogenies of NPR (a), selected JA and SA responsive WRKY TFs (b), and TGA TFs (c). Phylogenies of NPR and WRKY were computed based on the LG + G model, whereas the TGA phylogeny was computed based on the LG + G + I model. Representatives of *A. thaliana* for proteins from closely related groups within each TF family were included in each phylogeny. Clusters of each of these groups are highlighted by a pink or purple background, whereas a blue background indicates clusters of non-specific groups. Group specifications are given on the right of each phylogeny. *A. filiculoides* sequences are shown in bold. Bootstrap values <50 are not shown. Depiction of the 1,141 amino acid long protein alignment of TGA and other bZIP TFs (d) for comparison of the *AfTGA* candidates with the *AtTGA* sequences. The alignment includes 40 sequences, including the six *AfTGA* candidates (highlighted). On the left the position of the *AtTGA*, *Azolla* and other bZIP sequences are indicated. Blocks in the alignment indicate conserved regions, whereas colours indicate conserved residues (one colour per amino acid). The frequency of the particular residues is given on top of the alignment [Colour figure can be viewed at [wileyonlinelibrary.com](https://onlinelibrary.wiley.com/doi/10.1111/pce.13131)]

SA activates *PR* expression, but all *PR* sequences found here encoded only partial protein sequences. We therefore performed a

comparative CD-search with each of the *PR* sequences and compared the domain structure to the one of the corresponding homolog in

A. thaliana. AtPR1 contains a SCP PR1-like domain, which we did not detect for the AfPR1 candidate sequence. AtPR3 contains a chitin-binding 1 domain, which co-occurs with the glycosyl hydrolases family 19 domain (which is a chitin class I domain). Three of the four potential *Azolla* homologs revealed a domain hit using CD-search. Two of these (AzfiRT30013 and azolla_contig_4123) were predicted to contain a chitin-binding 1 domain. However, none was predicted to have a glycosyl hydrolase family 19 domain, but rather, all three were predicted to contain a lysozyme-like superfamily domain. AtPR5 contains a glycoside hydrolase family 64 and thaumatin-like protein domain. This domain was also recovered for the AfPR5 candidate sequence.

3.4 | *Azolla filiculoides* responds to MeSA but not MeJA

A. filiculoides possesses most of the essential repertoire of the JA and SA signalling pathway, suggesting that it may be able to sense the two phytohormones. To test JA and SA perception and action in *Azolla*, we treated whole *Azolla* plants in IRR1 medium with MeJA and MeSA and analyzed them at 24 hpt and 72 hpt. MeSA treatment led to the strongest change in phenotype (Figure 6). After 24 hpt of exposure to MeSA, in three out of three culture vessels (each having been

inoculated with 10 *Azolla* plants), the fern bodies disintegrated into many smaller pieces and lost most of their roots; by 72 hpt with MeSA, all roots were shed and only small stumps remained (Figure 6). In contrast, neither the MeOH (solvent control) nor the MeJA treatment induced such a strong phenotype. These results suggest that *A. filiculoides* can recognize and respond to MeSA.

To support these observations and to analyse whether MeSA treatment elicits specific molecular responses in *A. filiculoides*, we studied the expression of five JA and SA-associated genes (*AfAOS*, *AfJAZ*, *AfPR5*, *AfNPR1*, and *AfPDF1.4*) after MeJA and MeSA treatments (Figure 6). MeJA did not change expression of any of the genes, except *AfPR5*, which was slightly (1.2-fold) but significantly increased at 24 hpt ($p < .05$). In contrast, MeSA treatment led to a significant 2.1- to 3.5-fold down-regulation of *AfAOS* and *AfPR5* at 24 and 72 hpt ($p < .001$). Additionally, MeSA treatment induced a 4.9-fold up-regulation of the defensin *AfPDF1.4* after 72 hpt. *AfJAZ3* and *AfNPR1* did not show significant regulation in any of the treatments. This is, however, not surprising, because the activity of both is regulated post-translationally. In summary, our data provide evidence for viable SA perception (and putative associated defence signalling) in *A. filiculoides*.

3.5 | MeSA slightly increases the amount of the cyanobiont and decreases expression of *NifE*

The regulation of plant defence mechanisms not only alters the success of pathogen infections but could impact the communication between host and symbiont. We set out to test if the defence-related phytohormones JA and SA can impact the stable symbiosis of *A. filiculoides* with its cyanobiont, *N. azollae*. We evaluated the amount of the cyanobiont after MeJA, MeSA, MeOH treatment and untreated control by measuring the autofluorescence of the cyanobacterium in the leaf cavities. We observed a significant change of autofluorescence of the cyanobacterium over time (Table S3, Figure 7a,b). After an initial drop of autofluorescence at 24 hpt in all treatments and control, MeSA led to an increase in autofluorescence each day. In contrast, MeJA and MeOH treatment and the untreated control showed a reduction of autofluorescence at 24, 48, 72, and 96 hpt compared to 0 hpt. To clearly evaluate the effect of MeSA and MeJA, we therefore normalized the autofluorescence of the cyanobiont in MeSA and MeJA treatments with the autofluorescence observed in the MeOH treatment (Figure 7c). We found that treatment with MeSA led to an increase in relative autofluorescence over all time points from 0 to 96 hpt (except from 24 hpt to 48 hpt, Table S3, Figure 7c). MeJA showed no effect on the cyanobacterial autofluorescence, when subsequent days are compared (Table S3, Figure 7c). However, autofluorescence was significantly reduced in the MeJA treatment at 72 hpt and 96 hpt compared to 0 hpt and 24 hpt.

To corroborate our observations based on cyanobacterial autofluorescence, we quantified the abundance of *N. azollae* in each treatment. We estimated the cyanobacterial abundance from extracted DNA using qPCR based on four cyanobacterial loci (*NaNifE*, *NaNifH*, *NaRPL25*, and *NaRPS4*) and normalized those with two loci from the fern (*AfCam5* and *AfElf1a*, Figure 7d). In the MeJA treatment, only

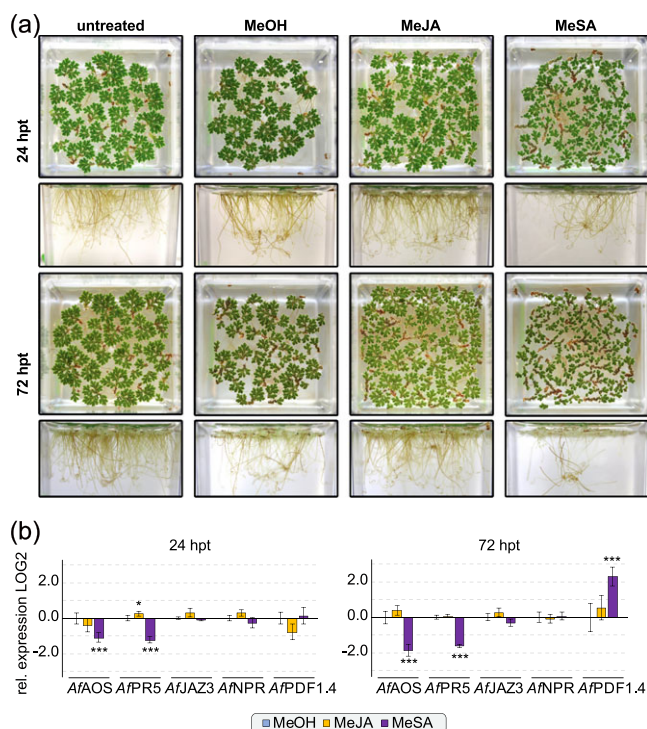


FIGURE 6 *Azolla* response to exogenous MeJA and MeSA application. (a) Phenotypic response of the *Azolla* sporophyte and roots 24 and 72 hr post-treatment (hpt) in untreated conditions in comparison to exogenous treatment with MeOH (solvent control), MeJA and MeSA. (b) Relative expression of JA and SA biosynthesis and signalling genes (*AfAOS*, *AfPR5*, *AfJAZ3*, *AfNPR1*, and *AfPDF1.4*) at 24 and 72 hpt after exogenous treatment of MeOH (blue), MeJA (yellow), and MeSA (purple) in comparison to MeOH and normalized with the reference genes *AfELF1 α* , *AfTUA2*, and *AfCYCD1* in LOG2 values. Significant changes are indicated by * for $p < .05$, ** for $p < .01$, and *** for $p < .001$ [Colour figure can be viewed at wileyonlinelibrary.com]

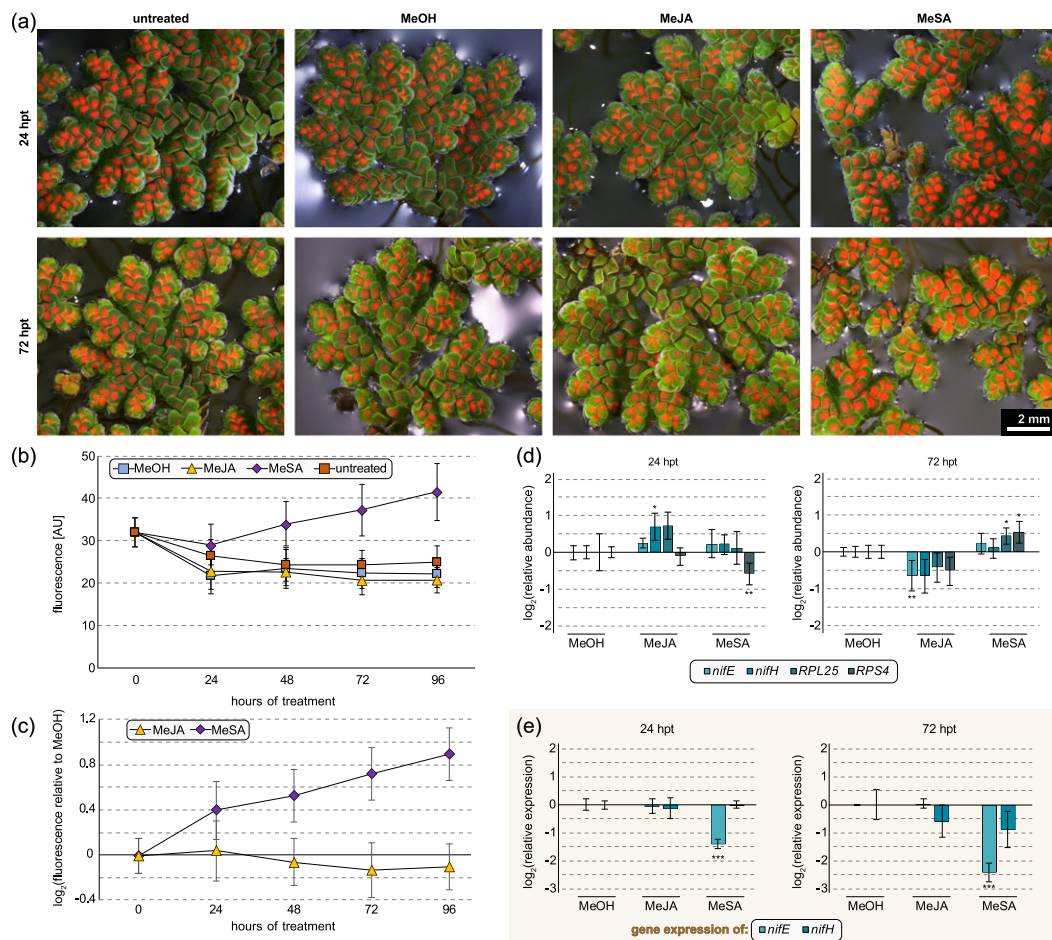


FIGURE 7 Cyanobiont response to exogenous treatment of MeJA and MeSA. (a) Pictures of *Azolla* 24 and 72 hr post-treatment (hpt) in untreated, MeOH treated (solvent control), and MeJA and MeSA treated samples. False colouring (red) indicates the autofluorescence of the cyanobiont. (b) The progression of the cyanobiont's fluorescence over time from 0 to 96 hpt in arbitrary units (AU) for untreated, MeOH, MeJA, and MeSA treated samples ($n = 90$ leaflets per time point and treatment). (c) Relative change in the autofluorescence of the cyanobiont after MeJA and MeSA treatment in comparison to the MeOH treatment over a time course of 96 hr. (d) Relative abundance of the cyanobiont relative to fern tissue at 24 and 72 hpt. Relative abundance was measured using a qPCR with DNA samples and is based on the presence of *NaNifE*, *NaNifH*, *NaRPL25*, and *NaRPS4* relative to the presence of the ferns genes *AfCam5* and *AfELF1a*. The treatments MeOH, MeJA, and MeSA have been set relative to MeOH. (e) Relative expression of *Nif* genes (*NaNifE* and *NaNifH*) after MeOH, MeJA, and MeSA treatment relative to MeOH treatment 24 and 72 hpt. The expression is given in LOG₂ values. Reference genes were *NarnpB* and *NaRPS4*. Significant differences in relative abundance of the cyanobiont and relative expression of the *Nif* genes is indicated by * for $p < .05$, ** for $p < .01$, and *** for $p < .001$ [Colour figure can be viewed at wileyonlinelibrary.com]

one of the four loci (*NifH*) was significantly increased after 24 hpt, and one of four was significantly decreased (*NifE*) after 72 hpt compared to 0 hpt (Figure 7d). This is roughly in agreement with the normalized autofluorescence data for the MeJA treatment that also showed a slight increase at 24 hpt and a decrease at 72 hpt compared to 0 hpt. Yet in the normalized autofluorescent data, only the reduction observed at 72 hpt was significant. In the MeSA treatment, one of four loci showed a reduction after 24 hpt and two of four loci showed a significant increase at 72 hpt (Figure 7d). The latter agrees with the normalized autofluorescence data.

To test whether any of the two phytohormones can potentially impact nitrogen fixation of *N. azollae* in *A. filiculoides*, we also tested expression of *NaNifE* and *NaNifH* after MeJA and MeSA treatment (Figure 7e). MeJA treatment did not affect the expression of the two genes. In contrast, MeSA treatment resulted in a down-regulation of the expression of *NaNifE*. This indicates that altered SA levels can

potentially influence the nitrogen fixation of *N. azollae* and, as a consequence, the physiology that underpins their symbiosis.

4 | DISCUSSION

4.1 | *Azolla* encodes the genes associated with producing and perceiving JA/SA

Here, we analyzed the genetic toolkit for JA and SA biosynthesis and signalling of *Azolla*. Although SA and its signalling is implicated to be present in all land plant lineages (Ponce de León et al., 2012; C. Wang, Liu, Li, & Han, 2015), studies on the liverwort *M. polymorpha*, the moss *P. patens*, and the lycophyte *S. moellendorffii* suggest that JA first originated in vascular plants (Pratiwi et al., 2017; Stumpe et al., 2010; Yamamoto et al., 2015). It is noteworthy, though, that Závěská

Drábková et al. (2015) found JA in some bryophytes. In agreement with JA and SA having originated before the appearance of ferns, our phylogenies and additional analyses of domain and 3D protein structures as well as conservation of the active sites support that *Azolla* possesses most of what is needed to produce and sense the two phytohormones.

Absence of some genes may stem from low expression and may be detected in the genome that is underway (F. -W. Li & Pryer, 2014; Sessa et al., 2014; Sessa & Der, 2016). Indeed, even though we did not detect two of three enzymes of the SA biosynthesis pathway, we detected ICS1 and observed root shedding and disintegration of the fern body upon MeSA application. Because root shedding is a well-known stress response of *Azolla* (Uheda & Kitoh, 1994), it suggests that SA is a functional stress hormone in the water fern. It is noteworthy that brownish-coloured tissue forms at the base of the fern bodies, suggesting a cell death reaction. This is in agreement with SA triggering defence responses such as the hypersensitive response, which leads to an enhanced cell death (Brodersen, Malinovsky, Hétamy, Newman, & Mundy, 2005; Greenberg, Silverman, & Liang, 2000).

In contrast to the strong response seen towards MeSA, we did not observe a strong phenotype towards MeJA. This is in contrast to other studies on the fern *Platyserium bifurcatum*, where Camloh, Ravnikar, and Žel (1996) and Camloh, Vilhar, Žel, and Ravnikar (1999) reported growth-promoting effects on rhizoids and observed promotion of shoot development after exogenous application of jasmonates. The moss *P. patens*, which does not produce JA, does only show a weak response towards exogenously applied MeJA (Ponce de León et al., 2012). Together, these studies suggest that MeJA is either not perceived by *A. filiculoides* or that JA is not produced and used as a phytohormone in this particular fern. These two possibilities are further supported by the lack of significant transcriptional reprogramming by MeJA of the tested genes.

In angiosperms, JA-Ile is the active conjugate of JA (Staswick & Tiryaki, 2004). Nevertheless, exogenous treatment with MeJA can rescue phenotypes of JA biosynthesis mutants (Park et al., 2002; Vijayan, Shockey, Lévesque, Cook, & Browse, 1998). The JAR1 mutant *jar1-1* is, however, moderately insensitive to MeJA application (Staswick et al., 2002). This suggests that JA can be recognized by JAR1 and conjugated, after the methyl-group is removed from MeJA by the Methyl jasmonate esterase (J. Wu, Wang, & Baldwin, 2008). If *Azolla* does indeed not perceive MeJA, this may be due to the *AfJAR1* candidate being unable to convert it into a JA-Ile derivative in sufficient amounts. This is further supported by the low conservation of the JA-Ile binding pocket. Additionally, the only significant regulation induced by MeJA is the enhanced expression of the *AfPFR5* gene, further hinting at insufficient MeJA conversion. Functional analyses of *AfJAR1* and JA measurements in *Azolla* will, however, be necessary to test whether this is the case.

The JA/SA antagonism was shown to have originated after the split of gymnosperms and angiosperms (Arnerup et al., 2013; Kozłowski et al., 1999). Our phenotypic and qRT-PCR data support this not only because MeJA had almost no effect on either of them but also because SA induced expression patterns that were opposite to what is known in angiosperms. As one would predict, MeSA treatment led to down-regulation of the JA biosynthesis gene *AfAOS*. However, based on angiosperm data, one could have expected an up-regulation of

the SA-responsive *AfPFR5* (Cao et al., 1994; Uknes et al., 1992), which showed an opposite regulatory pattern in *A. filiculoides*. *PDF1.4* is sometimes up-regulated in response to MeJA (Zimmerli, Stein, Lipka, Schulze-Lefert, & Somerville, 2004), but in other experiments did not show a strong response towards SA or JA, albeit being up-regulated in response to a virus infection (Manacorda et al., 2013). In *A. filiculoides* *PDF1.4* was up-regulated after MeSA treatment but not in response to MeJA treatment. This suggests that MeSA induced signalling in *A. filiculoides* partially overlaps with pathways regulated by JA in angiosperms.

4.2 | SA might be involved in the *Azolla*-cyanobiont communication

In addition to emerging as a novel system for evo-devo studies (cf. Chang, Bowman, & Meyerowitz, 2016; de Vries, Fischer, et al., 2016; F. -W. Li & Pryer, 2014; Sessa et al., 2014), *Azolla* is best-known for its unique symbiosis (Carrapiço, 2010; Rai et al., 2000; Ran et al., 2010). Symbiotic nitrogen fixation has been the focus of many studies revolving around *Azolla* and its cyanobiont (Adams et al., 2013; Brouwer et al., 2017; Meeks, 2009; Meeks, Steinberg, Enderlin, Joseph, & Peters, 1987; Ray, Peters, Toia Jr., & Mayne, 1978). The integration of the cyanobiont into the biology of *Azolla* has progressed to a level beyond that observed for any other known (land) plant-cyanobacterium symbiosis (Rai et al., 2000), as the cyanobionts are passed on vertically to the next fern generation (Becking, 1987, Peters & Meeks, 1989, W. Zheng, Bergman, et al., 2009). Despite well-described observations of, for example, hormogonia attraction to a specific location in the sporocarp, the indusium chamber (W. Zheng, Bergman, et al., 2009), little is known about the molecular mechanisms underlying the *Azolla*-cyanobiont communication. Since, JA and SA are canonical hormones involved in the interaction with microbiota, they are strong candidates for being involved in the *Azolla*-*Nostoc* interaction.

Our observations suggest that SA might play a role in the communication of *Azolla* and its cyanobiont. Not only did the amount of cyanobacteria increase significantly after long-term MeSA treatment, it also reduced the expression of *NaNifE*. *NifE*'s gene product is crucial for the MoFe cofactor biosynthesis of the nitrogenase (Dean, Bolin, & Zheng, 1993; Roll, Shah, Dean, & Roberts, 1995), therefore directly impacting nitrogen fixation. This may also play a vital role in case *Azolla* has to combat pathogens—some pathogens use their hosts as a source for fixed nitrogen (Horst et al., 2010; Mur, Simpson, Kumari, Gupta, & Gupta, 2016). Hence, SA may alter the cyanobionts nitrogen fixation to directly or indirectly reduce available fixed nitrogen for pathogens. In addition, fixed nitrogen and its derivatives are actively regulating JA and SA signalling (Lindermayr, Sell, Müller, Leister, & Durner, 2010; Mur et al., 2016; Tada et al., 2008).

Along these lines, it is important to highlight that the leaf cavity is inhabited by other bacteria in addition to *N. azollae* (Carrapiço, 2017; Dijkhuizen et al., 2017; W. Zheng, Bergman, et al., 2009). These bacteria are also directly or indirectly vertically transferred to the next generation of their *Azolla* host plant by accumulation in the indusium chamber (W. Zheng, Bergman, et al., 2009). Together, they form an *Azolla* species-specific community (Dijkhuizen et al., 2017), suggesting a tight interaction between them and *Azolla*. However, although some

members of this community are described as possibly nitrogen fixing (Lindblad, Bergman, & Nierzwicki-Bauer, 1991), others were suggested to be potential denitrifiers (Dijkhuizen et al., 2017). It should be noted further that although Dijkhuizen et al. (2017) found, among others, Rhizobiales in *Azolla's* leaf cavity microbiome, they did not contribute to the nitrogen fixation; indeed, their data suggests that *N. azollae* is the only prokaryote in the community that fixes nitrogen in a significant manner. Both nitrogen fixation and denitrification by the other members of the leaf cavity microbiome warrant further exploration.

Azolla's leaf cavity harbours more than just the cyanobiont. It harbours an entire microbiome, which likely shows dynamic responses towards alterations in its environment and community structure. Hence, JA and SA-mediated signalling might not only affect the cyanobiont population but the entire leaf cavity community with which the cyanobionts share their habitat. However, based on the data at hand, we cannot provide any conclusions on whether SA may actively regulate any such tri/multi-partite interactions or whether the cyanobiont shows a microbiome-independent response towards SA. Nevertheless, chemical communication between *Azolla* and its leaf cavity-inhabiting microbial community through simple hairs of the host has been previously suggested (Carrapiço & Tavares, 1989; Pereira & Carrapiço, 2007). Moreover, *Azolla* spp. produce phenylpropanoids, anthocyanins, and alkaloids, some of which were detected in the simple hairs (Ishikura, 1982; Pereira & Carrapiço, 2007). The production of these compounds is tightly associated with JA and SA signalling in gymnosperms and angiosperms (Arnerup et al., 2013; Cho et al., 2008; Dong, Wan, & Liang, 2010; Franceschi & Grimes, 1991; Kang et al., 2004; Kauss, Theisinger-Hinkerl, Mindermann, & Conrath, 1992; Misra, Maiti, Chanotiya, Shanker, & Ghosh, 2014; Shan, Zhang, Peng, Wang, & Xie, 2009; Sudha & Ravishankar, 2003). It is therefore conceivable that, during their (co-)evolution of 66–100 million years (Carrapiço, 2006; Collinson 2002), SA might have been co-opted as a signalling factor between *N. azollae* and its host

ACKNOWLEDGMENTS

We gratefully acknowledge funding by the German Research Foundation (DFG) to J. dV (VR 132/1-1), the SFF of the Heinrich Heine University to S. B. G, and the Killam Trusts to S. dV (Izaak Walton Killam Postdoctoral Fellowship). We thank the Centre for Comparative Genomics and Evolutionary Bioinformatics, Dalhousie University, for providing access to their computational resources. We also thank Ulla Rasmussen, Birgitta Bergman, and John Larsson (Department of Ecology, Environment and Plant Sciences, Stockholm University) for providing the *Azolla filiculoides* plants and Predrag Marinovski and Maria Handrich from Heinrich-Heine University Duesseldorf for technical assistance.

ORCID

Sophie de Vries  <http://orcid.org/0000-0002-5267-8935>

Jan de Vries  <http://orcid.org/0000-0003-3507-5195>

REFERENCES

- Adams, D. G., Bergman, B., Nierzwicki-Bauer, S. A., Duggan, P. S., Rai, A. N., & Schüßler, A. (2013). Cyanobacterial-plant symbioses. In E. Rosenberg, E. F. DeLong, S. Lory, E. Stackebrandt, & F. Thompson (Eds.), *The prokaryotes* (pp. 359–400). Berlin Heidelberg: Springer.
- Al-Momany, B., & Abu-Romman, S. (2016). Homologs of old yellow enzyme in plants. *Australian Journal of Crop Science*, 10, 584–590.
- Arnerup, J., Nemesio-Gorriz, M., Lundén, K., Asiegbu, F. O., Stenlid, J., & Elfstrand, M. (2013). The primary module in Norway spruce defence signalling against *H. annosum* s.l. seems to be jasmonate-mediated signalling without antagonism of salicylate-mediated signalling. *Planta*, 237, 1037–1045.
- Bakshi, M., & Oelmüller, R. (2014). WRKY transcription factors: Jack of many trades in plants. *Plant Signaling and Behavior*, 9, e27700.
- Banks, J. A., Nishiyama, T., Hasebe, M., Bowman, J. L., Gribskov, M., dePamphilis, C., ... Grigoriev, I. V. (2011). The *Selaginella* genome identifies genetic changes associated with the evolution of vascular plants. *Science*, 332, 960–963.
- Bannenberg, G., Martínez, M., Hamberg, M., & Castresana, C. (2009). Diversity of the enzymatic activity in the lipoxygenase gene family of *Arabidopsis thaliana*. *Lipids*, 44, 85–95.
- Becking, J. H. (1987). Endophyte transmission and activity in the *Anabaena-Azolla* association. *Plant and Soil*, 100, 183–212.
- Berens, M. L., Berry, H. M., Mine, A., Argueso, C. T., & Tsuda, K. (2017). Evolution of hormone signaling networks in plant defense. *Annual Review of Phytopathology*, 55, 18.1–18.25.
- Brodersen, P., Malinovsky, F. G., Hétamy, K., Newman, M.-A., & Mundy, J. (2005). The role of salicylic acid in the induction of cell death in *Arabidopsis acd11*. *Plant Physiology*, 138, 1037–1045.
- Brouwer, P., Bräutigam, A., Buijss, V. A., Tazelaar, A. O. E., van der Werf, A., Schlüter, U., ... Schlupepmann, H. (2017). Metabolic adaptation, a specialized leaf organ structure and vascular responses to diurnal N₂ fixation by *Nostoc azollae* sustain the astonishing productivity of *Azolla* ferns without nitrogen fertilizer. *Frontiers in Plant Science*, 8, 442.
- Brouwer, P., Bräutigam, A., Külahoglu, C., Tazelaar, A. O., Kurz, S., Nierop, K. G. J., ... Schlupepmann, H. (2014). *Azolla* domestication towards a biobased economy. *New Phytologist*, 202, 1069–1082.
- Caarls, L., Van der Does, D., Hickman, R., Jansen, W., Van Verk, M. C., Proietti, S., ... Van Wees, S. C. M. (2017). Assessing the role of ETHYLENE RESPONSE FACTOR transcriptional repressors in salicylic acid-mediated suppression of jasmonic acid-responsive genes. *Plant and Cell Physiology*, 58, 266–278.
- Camloh, M., Ravnikar, M., & Žel, J. (1996). Jasmonic acid promotes division of fern protoplasts, elongation of rhizoids and early development of gametophytes. *Physiologia Plantarum*, 97, 659–664.
- Camloh, M., Vilhar, B., Žel, J., & Ravnikar, M. (1999). Jasmonic acid stimulates development of rhizoids and shoots in fern leaf culture. *Journal of Plant Physiology*, 155, 798–801.
- Cao, H., Bowling, S. A., Gordon, A. S., & Dong, X. (1994). Characterization of an *Arabidopsis* mutant that is nonresponsive to inducers of systemic acquired resistance. *The Plant Cell*, 6, 1583–1592.
- Cao, H., Glazebrook, J., Clarke, J. D., Volko, S., & Dong, X. (1997). The *Arabidopsis NPR1* gene that controls systemic acquired resistance encodes a novel protein containing Ankyrin repeats. *Cell*, 88, 57–63.
- Carrapiço, F. (2006). Is the *Azolla-Anabaena* symbiosis a co-evolution case? In J. Seckbach, & M. Gruber (Eds.), *General botany: Traditions and perspectives* (pp. 193–195). Kazan: Kazan University.
- Carrapiço, F. (2010). *Azolla* as a superorganism. Its implication in symbiotic studies. In J. Seckbach, & M. Grube (Eds.), *Symbioses and stress: Joint ventures in biology, cellular origin, life in extreme habitats and astrobiology* 17 (pp. 225–241). Dordrecht: Springer.
- Carrapiço, F. (2017). The *Azolla-Anabaena*-Bacteria association: A case of symbiotic abduction? In M. Grube, J. Seckbach, & L. Muggia (Eds.), *Algal and cyanobacteria symbioses* (pp. 329–345). London: World Scientific Publishing Europe Ltd.
- Carrapiço, F., & Tavares, R. (1989). New data on the *Azolla-Anabaena* symbiosis. II. Cytochemical and immunocytochemical aspects. In F. A.

- Skinner, R. M. Boddey, & I. Frederik (Eds.), *Nitrogen fixation with non-legumes* (pp. 89–94). Dordrecht: Kluwer Academic.
- Chang, C., Bowman, J. L., & Meyerowitz, E. M. (2016). Field guide to plant model systems. *Cell*, *167*, 325–339.
- Chen, X., Liu, J., Lin, G., Wang, A., Wang, Z., & Lu, G. (2013). Overexpression of *AtWRKY28* and *AtWRKY75* in *Arabidopsis* enhances resistance to oxalic acid and *Sclerotinia sclerotiorum*. *Plant Cell Reports*, *32*, 1589–1599.
- Chini, A., Fonseca, S., Fernández, G., Adie, B., Chico, J. M., Lorenzo, O., ... Solano, R. (2007). The JAZ family of repressors is the missing link in jasmonate signalling. *Nature*, *448*, 666–671.
- Cho, H.-Y., Son, S. Y., Rhee, H. S., Yoon, S. Y., Lee-Parsons, C. W., & Park, J. M. (2008). Synergistic effects of sequential treatment with methyl jasmonate, salicylic acid and yeast extract on benzophenanthridine alkaloid accumulation and protein expression in *Eschscholtzia californica* suspension cultures. *Journal of Biotechnology*, *135*, 117–122.
- Collinson, M. E. (2002). The ecology of Cainozoic ferns. *Review of Paleobotany & Palynology*, *119*, 51–68.
- Coquoz, J.-L., Buchala, A., & Métraux, J.-P. (1998). The biosynthesis of salicylic acid in potato plants. *Plant Physiology*, *117*, 1095–1101.
- Cruz Castillo, M., Martínez, C., Buchala, A., Métraux, J.-P., & León, J. (2004). Gene-specific involvement of β -oxidation in wound-activated responses in *Arabidopsis*. *Plant Physiology*, *135*, 85–94.
- de Vries, J., de Vries, S., Slamovits, C. H., Rose, L. E., & Archibald, J. M. (2017). How embryophytic is the biosynthesis of phenylpropanoids and their derivatives in streptophyte algae? *Plant and Cell Physiology*, *58*, 934–945.
- de Vries, J., Fischer, A. M., Roettger, M., Rommel, S., Schluempmann, H., Bräutigam, A., ... Gould, S. B. (2016). Cytokinin-induced promotion of root meristem size in the fern *Azolla* supports a shoot-like origin of euphyllophyte roots. *New Phytologist*, *209*, 705–720.
- de Vries, J., Stanton, A., Archibald, J. M., & Gould, S. B. (2016). Streptophyte terrestrialization in light of plastid evolution. *Trends in Plant Sciences*, *21*, 467–476.
- Dean, D. R., Bolin, J. T., & Zheng, L. (1993). Nitrogenase metalloclusters: Structures, organization, and synthesis. *Journal of Bacteriology*, *175*, 6737–6744.
- Delaux, P.-M., Radhakrishnan, G. V., Jayaraman, D., Cheema, J., Malbreil, M., Volkening, J. D., ... Ané, J. M. (2015). Algal ancestor of land plants was preadapted for symbiosis. *Proceedings of the National Academy of Sciences USA*, *112*, 13390–13395.
- Delwiche, C. F., & Cooper, E. D. (2015). The evolutionary origin of a terrestrial flora. *Current Biology*, *25*, R899–R910.
- Després, C., DeLong, C., Glaze, S., Liu, E., & Fobert, P. R. (2000). The *Arabidopsis* NPR1/NIM1 protein enhances the DNA binding activity of a subgroup of the TGA family of bZIP transcription factors. *The Plant Cell*, *12*, 279–290.
- Dijkhuizen, L. W., Brouwer, P., Bolhuis, H., Reichart, G.-J., Koppers, N., Huettel, B., ... Schluempmann, H. (2017). Is there foul play in the leaf pocket? The metagenome of floating fern *Azolla* reveals endophytes that do not fix N_2 but may denitrify. *New Phytologist*, in press doi: <https://doi.org/10.1111/nph.14843>
- Dong, J., Wan, G., & Liang, Z. (2010). Accumulation of salicylic acid-induced phenolic compounds and raised activities of secondary metabolic and antioxidative enzymes in *Salvia miltiorrhiza* cell culture. *Journal of Biotechnology*, *148*, 99–104.
- Edwards, K., Johnstone, C., & Thompson, C. (1991). A simple and rapid method for the preparation of plant genomic DNA for PCR analysis. *Nucleic Acids Research*, *19*, 1349.
- Fernández-Calvo, P., Chini, A., Fernández-Barbero, G., Chico, J.-M., Gimenez-Ibanez, S., Geerinck, J., ... Solano, R. (2011). The *Arabidopsis* bHLH transcription factors MYC3 and MYC4 are targets of JAZ repressors and act additively in the activation of jasmonate responses. *The Plant Cell*, *23*, 701–715.
- Floková, K., Feussner, K., Herfurth, C., Miersch, O., Mik, V., Tarkowská, D., ... Novák, O. (2016). A previously undescribed jasmonate compound in flowering *Arabidopsis thaliana* – The identification of *cis*(+)-OPDA-Ile. *Phytochemistry*, *122*, 230–237.
- Fonseca, S., Chini, A., Hamberg, M., Adie, B., Porzel, A., Kramell, R., ... Solano, R. (2009). (+)-7-*iso*-Jasmonoyl-L-isoleucine is the endogenous bioactive jasmonate. *Nature Chemical Biology*, *5*, 344–350.
- Foo, E., Ross, J. J., Jones, W. T., & Reid, J. B. (2013). Plant hormones in arbuscular mycorrhizal symbioses: An emerging role for gibberellins. *Annals of Botany*, *111*, 769–779.
- Franceschi, V. R., & Grimes, H. D. (1991). Induction of soybean vegetative storage proteins and anthocyanins by low-level atmospheric methyl jasmonate. *Proceedings of the National Academy of Sciences USA*, *88*, 6745–6749.
- Fu, Z. Q., Yan, S., Saleh, A., Wang, W., Ruble, J., Oka, N., ... Dong, X. (2012). NPR3 and NPR4 are receptors for the immune signal salicylic acid in plants. *Nature*, *486*, 228–232.
- Gao, Q.-M., Venugopal, S., Navarre, D., & Kachroo, A. (2011). Low oleic acid-derived repression of jasmonic acid-inducible defense responses requires the WRKY50 and WRKY51 proteins. *Plant Physiology*, *155*, 464–476.
- Garcion, C., Lohmann, A., Lamodièrre, E., Catinot, J., Buchala, A., Doermann, P., & Métraux, J.-P. (2008). Characterization and biological function of the ISOCHORISMATE SYNTHASE2 gene of *Arabidopsis*. *Plant Physiology*, *147*, 1279–1287.
- Glazebrook, J. (2005). Contrasting mechanisms of defense against biotrophic and necrotrophic pathogens. *Annual Reviews of Phytopathology*, *43*, 205–227.
- Greenberg, J. T., Silverman, F. P., & Liang, H. (2000). Uncoupling salicylic acid-dependent cell death and defense-related responses from disease resistance in the *Arabidopsis* mutant *acd5*. *Genetics*, *156*, 341–350.
- Gutjahr, C., Siegler, H., Haga, K., Iion, M., & Paszkowski, U. (2015). Full establishment of arbuscular mycorrhizal symbiosis in rice occurs independently of enzymatic jasmonate biosynthesis. *PLoS One*, *10*, e0123422.
- Hamberg, M., & Fahlstadius, P. (1990). Allene oxide cyclase: A new enzyme in plant lipid metabolism. *Archives of Biochemistry and Biophysics*, *276*, 518–526.
- Higashi, K., Ishiga, Y., Inagaki, Y., Toyoda, K., Shiraishi, T., & Ichinose, Y. (2008). Modulation of defense signal transduction by flagellin-induced WRKY41 transcription factor in *Arabidopsis thaliana*. *Molecular Genetics and Genomics*, *279*, 303–312.
- Hofmann, E., Zerbe, P., & Schaller, F. (2006). The crystal structure of *Arabidopsis thaliana* Allene oxide cyclase: Insights into the oxylipin cyclization reaction. *The Plant Cell*, *18*, 3201–3217.
- Hori, K., Maruyama, F., Fujisawa, T., Togashi, T., Yamamoto, N., Seo, M., ... Ohta, H. (2014). *Klebsormidium flaccidum* genome reveals primary factors for plant terrestrial adaptation. *Nature Communications*, *5*, 3978.
- Horst, R. J., Doehlemann, G., Wahl, R., Hofmann, J., Schmiedl, A., Kahmann, R., ... Voll, L. M. (2010). *Ustilago maydis* infection strongly alters organic nitrogen allocation in maize and stimulates productivity of systemic source leaves. *Plant Physiology*, *152*, 293–308.
- Howe, G. A., & Schilmiller, A. L. (2002). Oxylipin metabolism in response to stress. *Current Opinion in Plant Biology*, *5*, 230–236.
- Huala, E., Dickerman, A., Garcia-Hernandez, M., Weems, D., Reiser, L., LaFond, F., ... Rhee, S. Y. (2001). The *Arabidopsis* Information Resource (TAIR): A comprehensive database and web-based information retrieval, analysis, and visualization system for a model plant. *Nucleic Acids Research*, *29*, 102–105.
- Huang, J., Gu, M., Lai, Z., Fan, B., Shi, K., Zhou, Y.-H., ... Chen, Z. (2010). Functional analysis of the *Arabidopsis* PAL gene family in plant growth, development, and response to environmental stress. *Plant Physiology*, *153*, 1526–1538.
- Ishikura, N. (1982). 3-Desoxyanthocyanin and other phenolics in the water fern *Azolla*. *The Botanical Magazine*, *95*, 303–308.

- Jagadeeswaran, G., Raina, S., Acharya, B. R., Maqbool, S. B., Mosher, S. L., Appel, H. M., ... Raina, R. (2007). Arabidopsis GH3-LIKE DEFENSE GENE 1 is required for accumulation of salicylic acid, activation of defense responses and resistance to *Pseudomonas syringae*. *The Plant Journal*, 51, 234–246.
- Jakoby, M., Weisshaar, B., Dröge-Laser, W., Vicent-Carbajosa, J., Tiedemann, J., Kroj, T., & Parcy, F. (2002). bZIP transcription factors in Arabidopsis. *Trends in Plant Sciences*, 7, 106–111.
- Journot-Catalino, N., Somssich, I. E., Roby, D., & Kroj, T. (2006). The transcription factors WRKY11 and WRKY17 act as negative regulators of basal resistance in *Arabidopsis thaliana*. *The Plant Cell*, 18, 3289–3302.
- Kang, S.-M., Jung, H.-J., Kang, Y.-M., Yun, D.-J., Bahk, J.-D., Yang, J.-k., & Choi, M.-S. (2004). Effects of methyl jasmonate and salicylic acid on the production of tropane alkaloids and the expression of PMT and H6H in adventitious root cultures of *Scopolia parviflora*. *Plant Science*, 166, 745–751.
- Katoh, K., Misawa, K., Kuma, K.-i., & Miyata, T. (2002). MAFFT: A novel method for rapid multiple sequence alignment based on fast Fourier transform. *Nucleic Acids Research*, 30, 3059–3066.
- Katoh, K., & Standley, D. M. (2013). MAFFT multiple sequence alignment software version 7: Improvements in performance and usability. *Molecular Biology and Evolution*, 30, 772–780.
- Kauss, H., Theisinger-Hinkler, E., Mindermann, R., & Conrath, U. (1992). Dichloroisonicotinic and salicylic acid, inducers of systemic acquired resistance, enhance fungal elicitor responses in parsley cells. *The Plant Journal*, 2, 655–660.
- Kim, K.-C., Lai, Z., Fan, B., & Chen, Z. (2008). Arabidopsis WRKY38 and WRKY62 transcription factors interact with histone deacetylase 19 in basal defense. *The Plant Cell*, 20, 2357–2371.
- Kinkema, M., Fan, W., & Dong, X. (2000). Nuclear localization of NPR1 is required for activation of PR gene expression. *The Plant Cell*, 12, 2339–2350.
- Kloth, K. J., Wieggers, G. L., Busscher-Lange, J., van Haarst, J. C., Kruijer, W., Bouwmeester, H. J., ... Jongsma, M. A. (2016). AtWRKY22 promotes susceptibility to aphids and modulates salicylic acid and jasmonic acid signalling. *Journal of Experimental Botany*, 67, 3383–3396.
- Knack, J. J., Wilcox, L. W., Delaux, P. M., Ané, J.-M., Piotrowski, M. J., Cook, M. E., ... Graham, L. E. (2015). Microbiomes of streptophyte algae and bryophytes suggest that a functional suite of microbiota fostered plant colonization of land. *International Journal of Plant Sciences*, 176, 405–420.
- Kozłowski, G., Buchala, A., & Métraux, J.-P. (1999). Methyl jasmonate protects Norway spruce [*Picea abies* (L.) Karst.] seedlings against *Pythium ultimum* Trow. *Physiological and Molecular Plant Pathology*, 55, 53–58.
- Kruskal, W. H., & Wallis, W. A. (1952). Use of ranks in one-criterion variance analysis. *Journal of the American Statistical Association*, 47, 583–621.
- Kumar, S., Stecher, G., & Tamura, K. (2016). MEGA7: Molecular evolutionary genetics analysis version 7.0 for bigger datasets. *Molecular Biology and Evolution*, 33, 1870–1874.
- Lee, D.-S., Nioche, P., Hamberg, M., & Raman, C. S. (2008). Structural insights into the evolutionary paths of oxylipin biosynthetic enzymes. *Nature*, 455, 363–368.
- Lee, M. W., Lu, H., Jung, H. W., & Greenberg, J. T. (2007). A key role for the Arabidopsis WIN3 protein in disease resistance triggered by *Pseudomonas syringae* that secrete AvrRpt2. *Molecular Plant-Microbe Interaction*, 20, 1192–1200.
- Li, C., Schillmiller, A. L., Liu, G., Lee, G. I., Jayanty, S., Sageman, C., ... Howe, G. A. (2005). Role of β -oxidation in jasmonate biosynthesis and systemic wound signaling in tomato. *The Plant Cell*, 17, 971–986.
- Li, F.-W., & Pryer, K. M. (2014). Crowdfunding the *Azolla* fern genome project: A grassroots approach. *GigaScience*, 3, 16.
- Li, J., Brader, G., & Plava, E. T. (2004). The WRKY70 transcription factor: A node of convergence for jasmonate-mediated and salicylate-mediated signals in plant defense. *The Plant Cell*, 16, 319–331.
- Li, L., Chang, Z., Pan, Z., Fu, Z. Q., & Wang, X. (2008). Modes of heme binding and substrate access for cytochrome P450 CYP74A revealed by crystal structures of allene oxide synthase. *Proceedings of the National Academy of Sciences USA*, 105, 13883–13888.
- Lindblad, P., Bergman, B., & Nierzwicki-Bauer, S. A. (1991). Immunocytochemical localization of nitrogenase in bacteria symbiotically associated with *Azolla* spp. *Applied and Environmental Microbiology*, 57, 3637–3640.
- Lindermayr, C., Sell, S., Müller, B., Leister, D., & Durner, J. (2010). Redox regulation of the NPR1-TGA1 system of *Arabidopsis thaliana* by nitric oxide. *The Plant Cell*, 22, 2894–2907.
- Liu, G., Holub, E. B., Alonso, J. M., Ecker, J. R., & Fobert, P. R. (2005). An Arabidopsis NPR1-like gene, NPR4, is required for disease resistance. *The Plant Journal*, 41, 304–318.
- Lorenzo, O., Chico, J. M., Sánchez-Serrano, J. J., & Solano, R. (2004). JASMONATE-INSENSITIVE1 encodes a MYC transcription factor essential to discriminate between different jasmonate-regulated defense responses in Arabidopsis. *The Plant Cell*, 16, 1938–1950.
- Lorenzo, O., Piqueras, R., Sánchez-Serrano, J. J., & Solano, R. (2003). ETHYLENE RESPONSE FACTOR1 integrates signals from ethylene and jasmonate pathways in plant defense. *The Plant Cell*, 15, 165–178.
- Manacorda, C. A., Mansilla, C., Debat, H. J., Zavallo, D., Sánchez, F., Ponz, F., & Asurmendi, S. (2013). Salicylic acid determines differential senescence produced by two *Turnip mosaic virus* strains involving reactive oxygen species and early transcriptomic changes. *Molecular Plant Microbe Interactions*, 26, 1486–1498.
- Mann, H. B., & Whitney, D. R. (1947). On a test of whether one of two random variables is stochastically larger than the other. *The Annals of Mathematical Statistics*, 18, 50–60.
- Mao, P., Duan, M., Wei, C., & Li, Y. (2007). WRKY62 transcription factor acts downstream of cytosolic NPR1 and negatively regulates jasmonate-responsive gene expression. *Plant and Cell Physiology*, 48, 833–842.
- McDowell, J. M., & Dangl, J. L. (2000). Signal transduction in the plant immune response. *Trends in Biochemical Sciences*, 25, 79–82.
- Meeks, J. C. (2009). Physiological adaptations in nitrogen-fixing Nostoc-plant symbiotic associations. In K. Pawłowski (Ed.), *Prokaryotic symbionts in plants* (pp. 181–205). Berlin Heidelberg: Springer.
- Meeks, J. C., Steinberg, N. A., Enderlin, C. S., Joseph, C. M., & Peters, G. D. (1987). *Azolla-Anabaena* relationship: XIII. Fixation of [13 N] N_2 . *Plant Physiology*, 84, 883–886.
- Meuwly, P., Mölders, W., Buchala, A., & Métraux, J.-P. (1995). Local and systemic biosynthesis of salicylic acid in infected cucumber plants. *Plant Physiology*, 109, 1107–1114.
- Misra, R. C., Maiti, P., Chanotiya, C. S., Shanker, K., & Ghosh, S. (2014). Methyl jasmonate-elicited transcriptional responses and pentacyclic triterpene biosynthesis in sweet basil. *Plant Physiology*, 164, 1028–1044.
- Mou, Z., Fan, W., & Dong, X. (2003). Inducers of plant systemic acquired resistance regulate NPR1 function through redox changes. *Cell*, 113, 935–944.
- Mur, L. A. J., Simpson, C., Kumari, A., Gupta, A. K., & Gupta, K. J. (2016). Moving nitrogen to the centre of plant defence against pathogens. *Annals of Botany*, 119, 703–709.
- Nawrath, C., Heck, S., Parinshawong, N., & Métraux, J.-P. (2002). EDS5, an essential component of salicylic acid-dependent signaling for disease resistance in Arabidopsis, is a member of the MATE transporter family. *The Plant Cell*, 14, 275–286.
- Ndamukong I., Al Abdallat A., Thurow C., Fode B., Zander M., Weigel R. & Gatz C. (2007) SA-inducible Arabidopsis glutaredoxin interacts with TGA factors and suppresses JA-responsive PDF1.2 transcription.
- Nguyen, L.-T., Schmidt, H. A., von Haeseler, A., & Minh, B. Q. (2015). IQ-TREE: A fast and effective stochastic algorithm for estimating maximum likelihood phylogenies. *Molecular Biology and Evolution*, 32, 268–274.

- Niki, T., Mitsuhara, I., Seo, S., Ohtsubo, N., & Ohashi, Y. (1998). Antagonistic effect of salicylic acid and jasmonic acid on the expression of pathogenesis-related (PR) protein genes in wounded mature tobacco leaves. *Plant and Cell Physiology*, 39, 500–507.
- Nilsson, A. K., Fahlberg, P., Ellerström, M., & Andersson, M. X. (2012). Oxo-phytodienoic acid (OPDA) is formed on fatty acids esterified to galactolipids after tissue disruption in *Arabidopsis thaliana*. *FEBS Letters*, 586, 2483–2487.
- Nobuta, K., Okrent, R. A., Stoutemyer, M., Rodibaugh, N., Kempema, L., Wildermuth, M. C., & Innes, R. W. (2007). The GH3 acyl adenylase family member PBS3 regulates salicylic acid-dependent defense responses in *Arabidopsis*. *Plant Physiology*, 144, 1144–1156.
- Nystedt, B., Street, N. R., Wetterbom, A., Zuccolo, A., Lin, Y. C., Scofield, D. G., ... Jansson, S. (2013). The Norway spruce genome sequence and conifer genome evolution. *Nature*, 497, 579–584.
- Pallas, J. A., Paiva, N. L., Lamb, C., & Dixon, R. A. (1996). Tobacco plants epigenetically suppressed in phenylalanine ammonia-lyase expression do not develop systemic acquired resistance in response to infection by tobacco mosaic virus. *The Plant Journal*, 10, 281–293.
- Pandey, S. P., & Somssich, I. E. (2009). The role of WRKY transcription factors in plant immunity. *Plant Physiology*, 150, 1648–1655.
- Parfrey, L. W., Lahr, D. J. G., Knoll, A. H., & Katz, L. A. (2011). Estimating the timing of early eukaryotic diversification with multigene molecular clocks. *Proceedings of the National Academy of Sciences USA*, 108, 13624–13629.
- Park, J.-H., Halitschke, R., Kim, H. B., Baldwin, I. T., Feldmann, K. A., & Feyereisen, R. (2002). A knock-out mutation in allene oxide synthase results in male sterility and defective wound signal transduction in *Arabidopsis* due to a block in jasmonic acid biosynthesis. *The Plant Journal*, 31, 1–12.
- Pauwels, L., Fernández Barbero, G., Geerinck, J., Tilleman, S., Grunewald, W., Cuéllar Pérez, A., ... Goossens, A. (2010). NINJA connects the co-repressor TOPLESS to jasmonate signalling. *Nature*, 464, 788–791.
- Peña-Cortés, H., Albrecht, T., Prat, S., Weiler, E. W., & Willmitzer, L. (1993). Aspirin prevents wound-induced gene expression in tomato leaves by blocking jasmonic acid biosynthesis. *Planta*, 191, 123–128.
- Penninckx, I. A. M. A., Thomma, B. P. H. J., Buchala, A., Métraux, J.-P., & Broekaert, W. F. (1998). Concomitant activation of jasmonate and ethylene response pathways is required for induction of a plant defensin gene in *Arabidopsis*. *The Plant Cell*, 10, 2103–2113.
- Pereira, A. L., & Carrapiço, F. (2007). Histochemistry of simple hairs from the foliar cavities of *Azolla filiculoides*. *Plant Biosystems*, 141, 323–328.
- Pereira, A. L., & Vasconcelos, V. (2014). Classification and phylogeny of the cyanobiont *Anabaena azollae* Strasburger: An answered question? *International Journal of Systematic and Evolutionary Microbiology*, 64, 1830–1840.
- Peters, G. A., & Meeks, J. C. (1989). The *Azolla-Anabaena* symbiosis: Basic biology. *Annual Review of Plant Physiology and Plant Molecular Biology*, 40, 193–210.
- Pfaffl, M. W. (2001). A new mathematical model for relative quantification in real-time RT-PCR. *Nucleic Acids Research*, 29, e45.
- Pieterse, C. M. J., Van der Does, D., Zamioudis, C., Leon-Reyes, A., & Van Wees, S. C. M. (2012). Hormonal modulation of plant immunity. *Annual Review of Cell and Developmental Biology*, 28, 489–521.
- Pires, N., & Dolan, L. (2010). Origin and diversification of Basic-Helix-Loop-Helix proteins in plants. *Molecular Biology and Evolution*, 27, 862–874.
- Ponce de León, I., Schmelz, E. A., Gaggero, C., Castro, A., Álvarez, A., & Montesano, M. (2012). *Physcomitrella patens* activates reinforcement of the cell wall, programmed cell death and accumulation of evolutionary conserved defence signals, such as salicylic acid and 12-oxo-phytodienoic acid, but not jasmonic acid, upon *Botrytis cinerea* infection. *Molecular Plant Pathology*, 13, 960–974.
- Pratiwi, P., Tanaka, G., Takahashi, T., Xie, X., Yoneyama, K., Matsuura, H., & Takahashi, K. (2017). Identification of jasmonic acid and jasmonoyl-isoleucine, and characterization of AOS, AOC, OPR and JAR1 in the model lycophyte *Selaginella moellendorffii*. *Plant and Cell Physiology*, 58, 789–801.
- Pré, M., Atallah, M., Champion, A., De Vos, M., Pieterse, C. M. J., & Memelink, J. (2008). The AP2/ERF domain transcription factor ORA59 integrates jasmonic acid and ethylene signals in plant defense. *Plant Physiology*, 147, 1347–1357.
- Rai, A. N., Soderback, E., & Bergman, B. (2000). Cyanobacterium-plant symbioses. *New Phytologist*, 147, 449–481.
- Rajaniemi, P., Hrouzek, P., Kastovská, K., Willame, R., Rantala, A., Hoffmann, L., ... Sivonen, K. (2005). Phylogenetic and morphological evaluation of the genera *Anabaena*, *Aphanizomenon*, *Trichormus* and *Nostoc* (Nostocales, Cyanobacteria). *International Journal of Systematic and Evolutionary Microbiology*, 55, 11–26.
- Ran, L., Larsson, J., Vigil-Stenman, T., Nylander, J. A. A., Ininbergs, K., Zheng, W.-W., ... Bergman, B. (2010). Genome erosion in a nitrogen-fixing vertically transmitted endosymbiotic multicellular cyanobacterium. *PLoS One*, 5, e11486.
- Ray, T. B., Peters, G. A., Toia, R. E. Jr., & Mayne, B. C. (1978). *Azolla-Anabaena* relationship. VII. Distribution of ammonia-assimilating enzymes, protein and chlorophyll between host and symbiont. *Plant Physiology*, 62, 463–467.
- Rensing, S. A., Lang, D., Zimmer, A. D., Terry, A., Salamov, A., Shapiro, H., ... Boore, J. L. (2008). The *Physcomitrella* genome reveals evolutionary insights into the conquest of land by plants. *Science*, 319, 64–69.
- Robert-Seilaniantz, A., Grant, M., & Jones, J. D. G. (2011). Hormone crosstalk in plant disease and defense: More than just JASMONATE-SALICYLATE antagonism. *Annual Review of Phytopathology*, 49, 317–343.
- Roll, J. T., Shah, V. K., Dean, D. R., & Roberts, G. P. (1995). Characteristics of NIFNE in *Azotobacter vinelandii* strains. Implications for the synthesis of the iron-molybdenum cofactor of dinitrogenase. *Journal of Biological Chemistry*, 270, 4432–4437.
- Sachs, L. (1997). In L. Sachs (Ed.), *Angewandte statistik* (pp. 395–397 & 662–664). Berlin: Springer.
- Sakuma, Y., Liu, Q., Dubouzet, J. G., Abe, H., Shinozaki, K., & Yamaguchi-Shinozaki, K. (2002). DNA-binding specificity of the ERF/AP2 domain of *Arabidopsis* DREBs, transcription factors involved in dehydration- and cold inducible gene expression. *Biochemical and Biophysical Research Communications*, 290, 998–1009.
- Sasaki-Sekimoto, Y., Jikumaru, Y., Obayashi, T., Saito, H., Masuda, S., Kamiya, Y., ... Shirasu, K. (2013). Basic helix-loop-helix transcription factors JASMONATE-ASSOCIATED MYC2-LIKE1 (JAM1), JAM2 and JAM3 are negative regulators of jasmonate responses in *Arabidopsis*. *Plant Physiology*, 163, 291–304.
- Schaller, F., Biesgen, C., Müssig, C., Altmann, T., & Weiler, E. W. (2000). 12-Oxophytodienoate reductase 3 (OPR3) is the isoenzyme involved in jasmonate biosynthesis. *Planta*, 210, 979–984.
- Schindelin, J., Rueden, C. T., Hiner, M. C., & Eliceiri, K. W. (2015). The ImageJ ecosystem: An open platform for biomedical image analysis. *Molecular Reproduction & Development*, 82, 518–529.
- Serrano, M., Wang, B., Aryal, B., Garcion, C., Abou-Mansour, E., Heck, S., ... Métraux, J.-P. (2013). Export of salicylic acid from the chloroplast requires the multidrug and toxin extrusion-like transporter ED55. *Plant Physiology*, 162, 1815–1821.
- Sessa, E. B., Banks, J. A., Barker, M. S., Der, J. P., Duffy, A. M., Graham, S. W., ... Wolf, P. G. (2014). Between two fern genomes. *GigaScience*, 3, 15.
- Sessa, E. B., & Der, J. P. (2016). Evolutionary genomics of ferns and lycophytes. *Advances in Botanical Research*, 78, 215–254.
- Shan, X., Zhang, Y., Peng, W., Wang, Z., & Xie, D. (2009). Molecular mechanisms for jasmonate-induction of anthocyanin accumulation in *Arabidopsis*. *Journal of Experimental Botany*, 60, 3849–3860.
- Shapiro, S. S., & Wilk, M. B. (1965). An analysis of variance test for normality (complete samples). *Biometrika*, 52, 591–611.
- Siedow, J. N. (1991). Plant lipoxygenase: Structure and function. *Annual Reviews of Plant Physiology*, 42, 145–188.

- Simpson, T. D., & Gardner, H. W. (1995). Allene oxide synthase and allene oxide cyclase, enzymes of the jasmonic acid pathway, localized in *Glycine max* tissue. *Plant Physiology*, 108, 199–202.
- Song, S., Huang, H., Gao, H., Wang, J., Wu, D., Liu, X., ... Xie, D. (2014). Interaction between MYC2 and ETHYLENE INSENSITIVE 3 modulates antagonism between jasmonate and ethylene signaling in *Arabidopsis*. *The Plant Cell*, 26, 263–279.
- Song, S., Qi, T., Fan, M., Zhang, X., Gao, H., Huang, H., ... Xie, D. (2013). The bHLH subgroup IIIId factors negatively regulate jasmonate-mediated plant defense and development. *PLoS Genetics*, 9, e1003653.
- Song, W.-C., Baertschi, S. W., Boeglin, W. E., Harrist, T. M., & Brasch, A. R. (1993). Formation of epoxyalcohols by a purified allene oxide synthase. *The Journal of Biological Chemistry*, 268, 6293–6298.
- Song, W.-C., & Brash, A. R. (1991). Purification of an allene oxide synthase and identification of the enzyme as a cytochrome P-450. *Science*, 253, 781–784.
- Spoel, S. H., Koornneef, A., Claessens, S. M. C., Korzelius, J. P., Van Pelt, J. A., Mueller, M. J., ... Pieterse, C. M. J. (2003). NPR1 modulates cross-talk between salicylate- and jasmonate-dependent defense pathways through a novel function in the cytosol. *The Plant Cell*, 15, 760–770.
- Staswick, P. E., & Tiryaki, I. (2004). The oxylipin signal jasmonic acid is activated by an enzyme that conjugates it to isoleucine in *Arabidopsis*. *The Plant Cell*, 16, 2117–2127.
- Staswick, P. E., Tiryaki, I., & Rowe, M. L. (2002). Jasmonate response locus JAR1 and several related *Arabidopsis* genes encode enzymes of the firefly luciferase superfamily that show activity on jasmonic, salicylic and indole-3-acetic acids in an assay for adenylation. *The Plant Cell*, 14, 1405–1415.
- Stintzi, A., & Browse, J. (2000). The *Arabidopsis* male-sterile mutant, *opr3*, lacks the 12-oxophytodienoic acid reductase required for jasmonate synthesis. *Proceedings of the National Academy of Sciences USA*, 97, 10625–10630.
- Strawn, M. A., Marr, S. K., Inoue, K., Inada, N., Zubieta, C., & Wildermuth, C. (2007). *Arabidopsis* isochorismate synthase functional in pathogen-induced salicylate biosynthesis exhibits properties consistent with a role in diverse stress responses. *Journal of Biological Chemistry*, 282, 5919–5933.
- Stumpe, M., Göbel, C., Faltin, B., Beike, A. K., Hause, B., Himmelsbach, K., ... Feussner, I. (2010). The moss *Physcomitrella patens* contains cyclopentenones but no jasmonates: Mutations in allene oxide cyclase lead to reduced fertility and altered sporophyte morphology. *New Phytologist*, 188, 740–749.
- Sudha, G., & Ravishankar, G. A. (2003). Elicitation of anthocyanin production in callus cultures of *Daucus carota* and the involvement of methyl jasmonate and salicylic acid. *Acta Physiologia Plantarum*, 25, 249–256.
- Suza, W. P., & Staswick, P. E. (2008). The role of JAR1 in jasmonoyl-L-isoleucine production during *Arabidopsis* wound response. *Planta*, 221, 1221–1232.
- Tada, Y., Spoel, S. H., Pajeroska-Mukhtar, K., Mou, Z., Song, J., Wang, C., ... Dong, X. (2008). Plant immunity requires conformational charges of NPR1 via S-nitrosylation and thioredoxins. *Science*, 321, 952–956.
- Thaler, J. S., Humphrey, P. T., & Whiteman, N. K. (2012). Evolution of jasmonate and salicylate signal crosstalk. *Trends in Plant Sciences*, 17, 260–270.
- Thines, B., Katsir, L., Melotto, M., Niu, Y., Mandaokar, A., Liu, G., ... Browse, J. (2007). JAZ repressor proteins are targets of the SCF^{COI1} complex during jasmonate signaling. *Nature*, 448, 661–665.
- Thomma, B. P. H. J., Cammue, B. P. A., & Thevissen, K. (2002). Plant defensins. *Planta*, 216, 193–202.
- Uheda, E., & Kitoh, S. (1994). Rapid shedding of roots from *Azolla filiculoides* plants in response to inhibitors of respiration. *Plant and Cell Physiology*, 35, 37–34.
- Uknes, S., Mauch-Mani, B., Moyer, M., Potter, S., Williams, S., Dincher, S., ... Ryals, J. (1992). Acquired resistance in *Arabidopsis*. *The Plant Cell*, 4, 645–656.
- Van der Does, D., Leon-Reyes, A., Koornneef, A., Van Verk, M. C., Roderburg, N., Pauwels, L., ... Pieterse, C. M. J. (2013). Salicylic acid suppresses jasmonic acid signaling downstream of SCF^{COI1}-JAZ by targeting GCC promoter motifs via transcription factor ORA59. *The Plant Cell*, 25, 744–761.
- Vick, B. A., & Zimmerman, D. C. (1984). Biosynthesis of jasmonic acid by several plant species. *Plant Physiology*, 75, 458–461.
- Vick, B. A., & Zimmerman, D. C. (1987). Pathways of fatty acid hydroperoxide metabolism in spinach leaf chloroplasts. *Plant Physiology*, 85, 1073–1078.
- Vierstra, R. D. (2009). The ubiquitin-26S proteasome system at the nexus of plant biology. *Nature Reviews*, 10, 385–397.
- Vijayan, P., Shockey, J., Lévesque, C. A., Cook, R. J., & Browse, J. (1998). A role for jasmonate in pathogen defense of *Arabidopsis*. *Proceedings of the National Academy of Sciences*, 95, 7209–7214.
- Wagner, G. M. (1997). *Azolla*: A review of its biology and utilization. *The Botanical Review*, 63, 1–26.
- Wang, C., Liu, Y., Li, S.-S., & Han, G. Z. (2015). Insights into the origin and evolution of the plant hormone signaling machinery. *Plant Physiology*, 167, 872–886.
- Wang, D., Amornsiripanitch, N., & Dong, X. (2006). A genomic approach to identify regulatory nodes in the transcriptional network of the systemic acquired resistance in plants. *PLoS Pathogens*, 2, e123.
- Wang, Q., Wang, M., Zhang, X., Hao, B., Kaushik, S. K., & Pan, Y. (2011). WRKY gene family evolution in *Arabidopsis thaliana*. *Genetica*, 139, 973–983.
- Wasternack, C., & Hause, B. (2013). Jasmonates: Biosynthesis, perception, signal transduction and action in plant stress response, growth and development. An update to the 2007 review in *Annals in Botany*. *Annals in Botany*, 111, 1021–1058.
- Wasternack, C., & Parthier, B. (1997). Jasmonate-signalled plant gene expression. *Trends in Plant Science*, 2, 302–307.
- Watanabe, I., Roger, P. A., Ladha, J. K., & Van Hove, C. (1992). *Azolla*. In I. Watanabe, P. A. Roger, J. K. Ladha, & C. Van Hove (Eds.), *Biofertilizer germplasm collections at IRRRI* (pp. 5–15). Manila: International Rice Research Institute.
- Westfall, C. S., Sherp, A. M., Zubieta, C., Alvarez, S., Schraft, E., Marcellin, R., ... Jez, J. M. (2016). *Arabidopsis thaliana* GH3.5 acyl amido synthetase mediates metabolic crosstalk in auxin and salicylic acid homeostasis. *Proceedings of the National Academy of Sciences USA*, 113, 13917–13922.
- Westfall, C. S., Zubieta, C., Herrmann, J., Kapp, U., Nanao, M. H., & Jez, J. M. (2012). Structural basis for preceptor modulation of plant hormones by GH3 proteins. *Science*, 336, 1708–1711.
- Wildermuth, M. C., Dewdney, J., Wu, G., & Ausubel, F. M. (2001). Isochorismate synthase is required to synthesize salicylic acid for plant defence. *Nature*, 414, 562–571.
- Wu, J., Wang, L., & Baldwin, I. T. (2008). Methyl jasmonate-elicited herbivore resistance: Does MeJA function as a signal without being hydrolyzed to JA. *Planta*, 227, 1161–1168.
- Wu, Y., Zhang, D., Chu, J. Y., Boyle, P., Wang, Y., Brindle, I. D., ... Després, C. (2012). The *Arabidopsis* NPR1 protein is a receptor for the plant defense hormone salicylic acid. *Cell Reports*, 1, 639–647.
- Xie, D.-X., Feys, B. F., James, S., Nieto-Rostro, M., & Turner, J. G. (1998). COI1: An *Arabidopsis* gene required for jasmonate-regulated defense and fertility. *Science*, 280, 1091–1094.
- Xu, M., Dong, J., Wang, H., & Huang, L. (2009). Complementary action of jasmonic acid on salicylic acid in mediating fungal elicitor-induced flavonol glycoside accumulation of *Ginkgo biloba* cells. *Plant, Cell and Environment*, 32, 960–967.
- Yamamoto, Y., Ohshika, J., Takahashi, T., Ishizaki, K., Kohchi, T., Matsuura, H., & Takahashi, K. (2015). Functional analysis of allene

- oxide cyclase, MpAOC, in the liverwort *Marchantia polymorpha*. *Phytochemistry*, 116, 48–56.
- Zander, M., La Camera, S., Lamotte, O., Métraux, J.-P., & Gatz, C. (2010). *Arabidopsis thaliana* class-II TGA transcription factors are essential activators of jasmonic acid/ethylene-induced defense responses. *The Plant Journal*, 61, 200–210.
- Záveská Drábková, L., Dobrev, P. I., & Motyka, V. (2015). Phytohormone profiling across the bryophytes. *PLoS One*, 10, e0125411.
- Zhang, J., Du, X., Wang, Q., Chen, X., Lv, D., Xu, K., ... Zhang, Z. (2010). Expression of pathogenesis related genes in response to salicylic acid methyl jasmonate and 1-aminocyclopropane-1-carboxylic acid in *Malus hupehensis* (Pamp.) Rehd. *BMC Research Notes*, 3, 208.
- Zhang, Y., Fan, W., Kinkema, M., Li, X., & Dong, X. (1999). Interaction of NPR1 with basic leucine zipper protein transcription factors that bind sequences required for salicylic acid induction of the PR-1 gene. *Proceedings of the National Academy of Sciences USA*, 96, 6523–6528.
- Zhang, Y., Tessaro, M. J., Lassner, M., & Li, X. (2003). Knockout analysis of *Arabidopsis* transcription factors TGA2, TGA5, and TGA6 reveals their redundant and essential roles in systemic acquired resistance. *The Plant Cell*, 15, 2647–2653.
- Zheng, W., Bergman, B., Chen, B., Zheng, S., Guan, X., & Rasmussen, U. (2009). Cellular responses in the cyanobacterial symbiont during its vertical transfer between plant generations in the *Azolla microphylla* symbiosis. *New Phytologist*, 181, 53–61.
- Zheng, Z., Qualley, A., Fan, B., Dudareva, N., & Chen, Z. (2009). An important role of a BAHD acyl transferase-like protein in plant innate immunity. *The Plant Journal*, 57, 1040–1053.
- Zhou, J.-M., Trifa, Y., Silva, H., Pontier, D., Lam, E., Shah, J., & Klessig, D. F. (2000). NPR1 differentially interacts with members of the TGA/OBF family of transcription factors that bind an element of the PR-1 gene required for induction by salicylic acid. *Molecular Plant-Microbe Interaction*, 13, 191–202.
- Zhu, Z., An, F., Feng, Y., Li, P., Xue, L., Mu, A., ... Guo, H. (2011). Depression of ethylene-stabilized transcription factors (EIN3/EIL1) mediates jasmonates and ethylene signaling synergy in *Arabidopsis*. *Proceedings of the National Academy of Sciences USA*, 108, 12539–12544.
- Ziegler, J., Hamberg, M., Miersch, O., & Parthier, B. (1997). Purification and characterization of allene oxide cyclase from dry corn seeds. *Plant Physiology*, 114, 565–573.
- Ziegler, J., Stenzel, I., Hause, B., Maucher, H., Hamberg, M., Grimm, R., ... Wasternack, C. (2000). Molecular cloning of Allene Oxide Cyclase. *Journal of Biological Chemistry*, 275, 19132–19138.
- Zimmerli, L., Stein, M., Lipka, V., Schulze-Lefert, P., & Somerville, S. (2004). Host and non-host pathogens elicit different jasmonate/ethylene responses in *Arabidopsis*. *The Plant Journal*, 40, 633–646.
- Zimmerman, D. C., & Feng, P. (1978). Characterization of a prostaglandin-like metabolite of linolenic acid produced by a flaxseed extract. *Lipids*, 13, 313–316.
- Zipfel, C., & Oldroyd, G. E. D. (2017). Plant signalling in symbiosis and immunity. *Nature*, 543, 328–336.

SUPPORTING INFORMATION

Additional Supporting Information may be found online in the supporting information tab for this article.

How to cite this article: de Vries S, de Vries J, Teschke H, von Dahlen JK, Rose LE, Gould SB. Jasmonic and salicylic acid response in the fern *Azolla filiculoides* and its cyanobiont. *Plant Cell Environ*. 2018;41:2530–2548. <https://doi.org/10.1111/pce.13131>

Broad-spectrum inhibition of *Phytophthora infestans* by fungal endophytes

Status **Published**

Journal FEMS Microbiology Ecology

Citation de Vries, S., **von Dahlen, J. K.**, Schnake, A., Ginschel, S., Schulz, B., & Rose, L. E. (2018). Broad-spectrum inhibition of *Phytophthora infestans* by fungal endophytes. *FEMS Microbiology Ecology*, 94(4), fiy037.

Own contribution Contributed to co-inoculation assays in planta and in vitro; contributed to data analyses of infection progress; performed microscopy of endophytes; evaluated the anthocyanin content; contributed in writing of the manuscript

RESEARCH ARTICLE

Broad-spectrum inhibition of *Phytophthora infestans* by fungal endophytes

Sophie de Vries^{1,2,3,†}, Janina K. von Dahlen¹, Anika Schnake¹,
Sarah Ginschel¹, Barbara Schulz⁴ and Laura E. Rose^{1,2,5,*}

¹Institute of Population Genetics, Heinrich-Heine University Duesseldorf, Universitaetsstr. 1, 40225 Duesseldorf, Germany, ²iGRAD-Plant Graduate School, Heinrich-Heine University Duesseldorf, Universitaetsstr. 1, 40225 Duesseldorf, Germany, ³Department of Biochemistry and Molecular Biology, Dalhousie University, Halifax, NS B3H 4R2, Canada, ⁴Institute of Microbiology, Technische Universitaet Braunschweig, Spielmannstr. 7, 38106 Braunschweig, Germany and ⁵Ceplas, Cluster of Excellence in Plant Sciences, Heinrich-Heine University Duesseldorf, Universitaetsstr. 1, 40225 Duesseldorf, Germany

*Corresponding author: Institute of Population Genetics, Heinrich-Heine University, Universitaetsstr. 1, 26.03.00.25, 40225 Duesseldorf, Germany. Tel: +49-211-81-13406; Fax: +49-211-81-12817; E-mail: laura.rose@hhu.de

One sentence summary: Abundance of and symptoms caused by *Phytophthora infestans*, one of the most devastating crop pathogens, can be highly reduced by the fungal endophyte *Phoma eupatorii*.

Editor: Angela Sessitsch

†Sophie de Vries, <http://orcid.org/0000-0002-5267-8935>

ABSTRACT

Phytophthora infestans is a devastating pathogen of tomato and potato. It readily overcomes resistance genes and applied agrochemicals and hence even today causes large yield losses. Fungal endophytes provide a largely unexplored avenue of control of *Phy. infestans*. Not only do endophytes produce a wide array of bioactive metabolites, they may also directly compete with and defeat pathogens *in planta*. Here, we tested 12 fungal endophytes isolated from different plant species *in vitro* for their production of metabolites with anti-*Phytophthora* activity. Four well-performing isolates were evaluated for their ability to suppress nine isolates of *Phy. infestans* on agar medium and *in planta*. Two endophytes reliably inhibited all *Phy. infestans* isolates on agar medium, of which *Phoma eupatorii* isolate 8082 was the most promising. It nearly abolished infection by *Phy. infestans in planta*. Our data indicate a role for the production of anti-*Phytophthora* compounds by the fungus and/or an enhanced plant defense response, as evident by an enhanced anthocyanin production. Here, we present a potential biocontrol agent, which can inhibit a broad-spectrum of *Phy. infestans* isolates. Such broadly acting inhibition is ideal, because it allows for effective control of genetically diverse isolates and may slow the adaptation of *Phy. infestans*.

Keywords: *Phytophthora infestans*; fungal endophytes; *Phoma eupatorii*; plant-microbe interaction; antimicrobial metabolites; biocontrol

INTRODUCTION

Phytophthora infestans is a major pathogen of cultivated tomato (*Solanum lycopersicum*) and cultivated potato (*Solanum tuberosum*).

Even today its impact cannot be ignored as it is still capable of destroying entire fields of its hosts, leading to up to 100% yield losses (Nowicki et al. 2012). The two major control measures for *Phy. infestans* are resistance breeding and agrochemical

Received: 1 November 2017; Accepted: 5 March 2018

© FEMS 2018. This is an Open Access article distributed under the terms of the Creative Commons Attribution Non-Commercial License (<http://creativecommons.org/licenses/by-nc/4.0/>), which permits non-commercial re-use, distribution, and reproduction in any medium, provided the original work is properly cited. For commercial re-use, please contact journals.permissions@oup.com

applications. While several resistance genes have been identified in screens of wild relatives of *S. lycopersicum* and *S. tuberosum* (Song et al. 2003; Van der Vossen et al. 2003; Pel et al. 2009; Zhang et al. 2013), many of them are readily overcome by isolates of *Phy. infestans* (Vleeshouwers et al. 2011). Similarly, agrochemicals can have a low durability in their protective function against *Phy. infestans* (Grünwald et al. 2006; Childers et al. 2015). Hence, continual scientific effort in terms of breeding, development of agrochemicals and other approaches, such as biological control, is needed for effective crop protection against this pathogen.

One approach that is gaining more and more attention is the use of endophytes for crop protection (Le Cocq et al. 2016). Endophytes are microorganisms that grow within plants, and at the time of sampling, do not cause obvious symptoms on their host (Schulz and Boyle 2005; Le Cocq et al. 2016). Many studies have explored the bacterial, fungal and protist endophytic communities associated with different plants (e.g. Bulgarelli et al. 2012; Lundberg et al. 2012; Bodenhausen, Horton and Bergelson 2013; Schlaeppli et al. 2013; Bulgarelli et al. 2015; Edwards et al. 2015; Busby, Peay and Newcombe 2016; Coleman-Derr et al. 2016; Ploch et al. 2016; U'Ren and Arnold 2016; Sapp et al. 2018). These studies indicate that the diversity of microbes living inside of plants is largely underestimated and that the distribution of some microorganisms is host and/or environment specific.

Furthermore, in some cases such endophytic microorganisms have been evaluated for their potential benefit to their hosts (Busby, Ridout and Newcombe 2016; Fesel and Zuccaro 2016). Such benefits include growth promotion and protection against parasites and pathogens (e.g. Arnold et al. 2003; Schulz 2006; Lahlali and Hijri 2010; Tellenbach and Sieber 2012; Panke-Buisse et al. 2015; Rolli et al. 2015; Busby, Peay and Newcombe 2016; Hiruma et al. 2016; Martínez-Medina et al. 2017). Often these functions are linked to metabolites produced and secreted by the endophytes (Son et al. 2008; Dubey et al. 2013; Puopolo et al. 2014; Mousa et al. 2016; Suryanarayanan, Govinda Rajulu and Vidal 2016), highlighting the endophyte's metabolic versatility (Schulz et al. 2002; Strobel and Strobel 2007; Verma, Kharwar and Strobel 2009; Mousa and Raizada 2013; Brader et al. 2014). In addition to secreted compounds, microorganisms produce a spectrum of volatile compounds (Piechulla, Lemfack and Kai 2017), some of which are effective in reducing pathogen growth (Kottb et al. 2015). Endophytes may also directly compete with potential pathogens of their host plants (Alabouvette et al. 2009), induce plant defense responses (Shoresh, Harman and Mastouri 2010) and/or produce bioactive anti-microbial metabolites (Brader et al. 2014). Fluorescent *Pseudomonas* spp. are examples of endophytes able to colonize roots and outcompete other pathogens (O'Sullivan and O'Gara 1992). An example of the induction of defense responses by an endophyte is the root endophyte *Serendipita indica* (formerly *Piriformospora indica*). In association with *Arabidopsis thaliana*, *Se. indica* induces a jasmonic acid-dependent defense response upon co-inoculation with a pathogen (Stein et al. 2008). Furthermore, a recent study by Mousa et al. (2016) describes an *Enterobacter* sp. strain isolated from an ancient African crop (*Eleusine coracana* [finger millet]) with the ability to suppress the grass pathogen *Fusarium graminearum*. *Enterobacter* sp. traps *F. graminearum* in the root system of its host and simultaneously produces several antifungal compounds that kill the fungus.

Several bacterial and fungal endophytes with the potential to inhibit *Phy. infestans*' growth have been described (Sturz et al. 1999; Kim et al. 2007; Miles et al. 2012; Puopolo et al. 2014). However, these endophytes have only been tested against single isolates of *Phy. infestans*, but alternative approaches, such as biocontrol, can show different outcomes depending on the pathogen

isolate (Bahramisharif et al. 2013). Therefore, the identification of endophytic species with a broad inhibition spectrum is of critical importance.

In this study, we analyzed the metabolite extracts of 12 fungal endophytes isolated from different plant hosts for their ability to inhibit growth of *Phy. infestans*. Using a plate assay with the four most successful fungal endophytes, we show that they inhibit the growth of a broad spectrum of European *Phy. infestans* isolates in co-culture. According to our phylogenetic analyses, these four endophytes are members of the Ascomycota. The endophyte with the strongest inhibition potential both on plates and *in planta* was *Phoma eupatorii*, isolate 8082. This endophyte prohibited proliferation of *Phy. infestans* and in some cases abolished its infection completely. Since we selected *Pho. eupatorii* based on the inhibition potential of its metabolite extract, the active component may be a secreted metabolite or a cocktail of metabolites. A broad-spectrum activity as observed for *Pho. eupatorii* suggests either a conserved target for such secreted metabolite(s) or several targets that are specific for the pathogen isolate and that are covered by the complexity of the metabolite cocktail. Both can result in slower counter-adaptation of *Phy. infestans* to either the direct application of the endophyte or to the application of its metabolites.

MATERIAL AND METHODS

Isolation of endophytes

To isolate the endophytes, plant tissues of the respective hosts (Table S1, Supporting Information) were first thoroughly washed under running water, and then immersed for 1 min in 70% ethanol, followed by 1–3 min in 3% NaOCl and subsequently rinsed three times in sterile water. Sterilized tissues were imprinted on potato–carrot medium (Höller et al. 2000) to test for effectiveness of sterilization and to optimize the sterilization procedure. The tissues were then cut with a sterile scalpel into 2 mm slices, plated on potato–carrot agar medium with antibiotics (Höller et al. 2000) and incubated for 3 weeks at 20°C. The emerging mycelia were taken into culture on potato–carrot agar medium and were initially identified according to morphology (Table S1, Supporting Information).

Analysis of crude metabolite extracts for anti-*Phytophthora infestans* activity

To test the growth inhibition potential of the 12 fungal endophytes, the endophytes were first grown on barley-spelt medium and/or biomalt agar medium (Schulz et al. 2011) at room temperature for 21 days. To isolate the secondary metabolites, the cultures were extracted with ethyl acetate (Schulz et al. 2011). 25 µl of culture extracts (40 mg/ml) were then applied to a filter disc and placed onto rye agar medium that had been inoculated with *Phy. infestans* isolate D2; subsequent incubation was at 20°C in the dark for 2–3 days (Schulz et al. 2011). Only fungal endophytes whose culture extracts resulted in a zone of inhibition ≥ 20 mm were used for further analyses.

Co-culture on plates

The fungal endophytic isolates 8082 (DSMZ accession: 106 583), 9907 (DSMZ accession: 106 584) and 9913 (DSMZ accession: 106 585), whose culture extracts had inhibited *Phy. infestans* in the agar diffusion assays and *Phialocephala fortinii* isolate 4197 (Schulz 2006; DSMZ accession: 106 586) were tested for their

bioactivity against nine isolates of the late blight pathogen *Phy. infestans* (NL10001, NL88069, NL90128, IPO-C, IPO428-2, 3928A, D12-2, T15-2 and T20-2). The *Phialocephala fortinii* isolate was included based on previous experiments (Schulz et al. 2002; Schulz 2006). The co-culture experiments were performed and evaluated according to Peters et al. (1998). In brief, we estimated the difference in radial growth of *Phy. infestans* and endophytes when grown in co-culture or alone. Fungal endophytes and *Phy. infestans* isolates were grown on rye-sucrose agar (RSA, Caten and Jinks 1968) at room temperature. The duration of the experiments depended on the endophytes' growth rates: eight days for all co-cultures that included 9913 and 14–16 days for the remaining co-cultures. A minimum of 10 plates was analyzed per treatment. The Mann-Whitney U test (Mann and Whitney 1947) was used to determine if differences between co-culture and control plates were significant. Average growth inhibition was estimated as follows: 1-(average radius in co-culture/average radius in control conditions). All experiments were evaluated again after eight weeks of incubation to assess long-term effects. Pictures were taken with an EOS 70D camera (Canon).

Co-inoculation in planta

The surfaces of the *S. lycopersicum* cv. M82 seeds were sterilized using 70% ethanol for 3 s, followed by ~5% NaOCl for 30 s. The sterilized seeds were washed three times with sterile water for 3 min. Seeds were incubated in the dark on 1.2% H₂O-agar with a day-night temperature cycle of 18°C/15°C (16 h/8 h). After three days, the seeds were transferred to a day-night cycle with 16 h light ($166 \pm 17 \mu\text{mol quanta}\cdot\text{m}^{-2}\cdot\text{s}^{-1}$). Temperature conditions were the same as before. 9 to 11 days post-sterilization (dps), the germinated seedlings were transferred to 9 mm Petri dishes containing 0.5% MS-medium (Murashige and Skoog 1962) with 1% sucrose, poured as a slope.

Preliminary experiments with isolate 8082 inoculated on different plant tissues showed that root inoculations with a mycelial suspension resulted in consistent colonization. Hence, we used this strategy for further co-cultivations with all endophytes. An endophyte mycelial suspension was prepared from a two- to four-day old liquid culture for each endophyte (potato-carrot liquid medium; 100 g potato-carrot mash [prepared according to Höller et al. 2000] in 1 l medium). Mycelium was equally dispersed in 25 ml potato-carrot liquid medium using Tissuelyser II (Qiagen, Hilden, Germany) for a few seconds.

Preliminary inoculations of *S. lycopersicum* roots with 25–50 μl of mycelial suspensions of all four endophytes were prepared to assess the effect of the endophytes on the plant. Isolate 9907 and *Phi. fortinii* killed the seedlings. Hence, only endophyte isolates 8082 and 9913 were used for further inoculation studies. For inoculations with endophyte isolate 8082, 5 or 10 μl of the mycelial suspension or H₂O (mock control) was applied to each root at 16 dps. After 27 dps seedlings were transferred to vessels (10 cm x 6.5 cm x 6.5 cm) with MS agar medium. For inoculations with endophyte isolate 9913, 10 μl of dispersed mycelium or H₂O was applied to the roots of axenic seedlings at 18 dps. However, the endophyte isolate 9913 did not grow sufficiently, so we performed a second inoculation with undispersed mycelium from the liquid culture at 22 dps. These seedlings were transferred to vessels at 28 dps. At 34–36 dps, each leaflet of endophyte and mock inoculated plants was inoculated with 10 μl of *Phy. infestans* zoospore suspension (4°C cold) or with 10 μl H₂O (4°C cold). The zoospore suspension ($5 \cdot 10^4$ spores/ml) was harvested from a 25 day old culture of *Phy. infestans* isolate D12-2 and was kept on ice during the entire procedure. For the isolation of zoospores

from *Phy. infestans*, see de Vries et al. (2017). Plants were sampled for microscopic evaluation, to evaluate anthocyanin content and pathogen abundance at three days post-inoculation with *Phy. infestans*.

To confirm the endophytic fungal colonization of roots, three different sterilization procedures were conducted: (i) 70% EtOH for 3 s (isolate 8082) or 30 s (isolate 9913), ~5% NaOCl for 30 s, followed by washing three times with sterile H₂O for 3 min each (treatment 1), (ii) 70% EtOH for 5 min, 0.9% NaOCl for 20 min, followed by washing three times with H₂O (treatment 2, Cao et al. 2004) and (iii) 97% EtOH for 30 s, 10% NaOCl for 2 min, followed by rinsing four times with H₂O (treatment 3, Terhonen, Sipari and Asiegbu 2016). These sterilization procedures were applied to the roots of the mock controls, as well as the endophyte inoculated and co-inoculated samples. Roots were imprinted on RSA plates to test for the efficacy of sterilization and then placed on new RSA plates. The plates were evaluated at 8 dps (isolate 8082) and 6 dps (isolate 9913).

Microscopy

Two aspects of host physiology were evaluated microscopically following the co-inoculation: chlorophyll intensity and relative necrotic area. Pictures to evaluate chlorophyll intensity were taken with the SMZ18 dissection microscope and a DS-Ri1 camera (Nikon, Japan) using a 600 LP filter (Transmission Filterset F26-010, AHF Analysetechnik, Germany), with an exposure time of 200 ms and 100% gain. Intensity was measured using ImageJ2 (Schindelin et al. 2015). Pictures for necrosis measurements were taken with a SteREO Discovery V8 binocular and an AxioCam ICc5 camera (Zeiss, Germany). The relative necrotic area was calculated as the necrotic area of a leaflet over the total area of the leaflet. The necrotic and total leaflet area were estimated using the ZEN Blue edition (Zeiss, Germany). Differences in relative necrotic area and chlorophyll content in the treatments were calculated using a Kruskal-Wallis test (Kruskal and Wallis 1952) combined with a Tukey and Kramer test for pairwise comparisons using a Tukey-distance approximation (Sachs 1997). Furthermore, a Benjamini-Hochberg method was used to correct for multiple testing (Benjamini and Hochberg 1995).

Photographs of mycelial growth on RSA plates were taken with the SteREO Discovery V8 binocular and an AxioCam ICc5 camera (Zeiss, Germany). Additionally, root tissue from co-inoculations with the endophytes and *Phy. infestans* as well as mycelium from RSA plates or potato-carrot liquid medium was stained with trypan blue (de Vries et al. 2017). The root tissue was sectioned and the endophytic growth in the root tissue, as well as trypan blue stained and unstained hyphae from culture-grown endophytes were visualized using an AxioPhot microscope with an AxioCam ICc5 camera with the ZEN blue software (Zeiss, Germany) and a Zeiss AxioStar Plus and an AxioCam ICc1 with the Axio Vision Release 4.8 (Zeiss, Germany).

Anthocyanin content evaluation

The anthocyanin content was measured and calculated according to Lindoo and Caldwell (1978). We analyzed three to six biological replicates per treatment. Samples were tested for normality using a Shapiro-Wilk test (Shapiro and Wilk 1965) and for equal variance. Accordingly, significant differences were calculated using a two-sided t-test with the assumption of equal or unequal variances depending on the sample combination tested. All statistical analyses were done in R v3.2.1.

DNA and RNA extraction and cDNA synthesis

DNA was extracted from the mycelium of the fungal endophytes and *Phy. infestans* isolates grown on RSA medium using the DNeasy® Plant Mini Kit (Qiagen, Germany). RNA was extracted from infected and mock control leaflets of seedlings of *S. lycopersicum* using the Universal RNA/miRNA Purification Kit (Roboklon, Germany). Three to four leaflets were pooled per replicate. To evaluate RNA quality, 5 µl of RNA were treated with 6 µl deionized formamide, incubated at 65°C for 5 min, followed by 5 min incubation on ice. This mixture was then visualized on a 2% agarose gel.

All RNA extractions were treated with DNaseI (Thermo Fisher Scientific, Lithuania). For subsequent cDNA synthesis of the DNaseI-treated samples, the reactions were adjusted for 200 ng of total RNA and the cDNA was synthesized with the RevertAid First Strand cDNA Synthesis Kit (Thermo Fisher Scientific, Lithuania).

To test whether the RNA samples contained residual DNA even after the DNaseI treatment, control reactions were performed. For this, 200 ng of total RNA of each sample was treated with RNaseA (Macherey-Nagel, Germany) and incubated at 37°C for 30 min. These RNaseA treated samples were then used in a RT reaction using the RevertAid First Strand cDNA Synthesis Kit without the reverse transcriptase and RiboLock.

For the experiments with isolate 9913, we performed a PCR with *SlElf1α* as described in de Vries et al. 2017. For the samples from the experiments with isolate 8082, we used the *ITS1* and *ITS4* primers (White et al. 1990). These primers amplify the internal transcribed spacer (*ITS*) and 5.8S region in *S. lycopersicum*, the endophytes and *Phy. infestans*.

For our control experiment to determine if residual DNA was present in the samples, only the positive controls (cDNA from mycelium and untreated leaflets from *S. lycopersicum*) had an amplicon, showing that there was no remaining DNA contamination in the DNaseI-treated samples.

Molecular identification of endophytes

To determine the phylogenetic placement of the fungal endophytes, we sequenced their *ITS* and 5.8S regions. *ITS1* and *ITS4* primers were used. The 20 µl PCR-reaction contained 1x Green GoTaq® Flexi Buffer, 0.1 mM dNTPs, 2 mM MgCl₂, 1U GoTaq® Flexi DNA Polymerase (Promega, WI, USA), 0.2 µM of each primer and 40–95 ng of template DNA. The PCR protocol included an initial denaturation step of 95°C for 3 min, followed by 35 cycles of a denaturation step at 95°C for 30 s, an annealing step at 60°C for 30 s and an elongation step at 72°C for 90 s, followed by a final elongation step of 72°C for 7 min. All PCR products were purified with the peqGOLD Cycle-Pure Kit (Peqlab, Germany). The products were cloned into the pCR 4-TOPO® vector of the TOPO® TA Cloning® Kit for Sequencing (Invitrogen, CA, USA) and the plasmid DNA was extracted with the QIAprep Spin Miniprep Kit (Qiagen, Germany). Sequencing was performed at Eurofins MWG Operon (Germany). Sequences were blasted using BLASTn (Altschul et al. 1990) and the best hits were retrieved. To assemble a dataset of closely related organisms from which to infer the phylogenetic placement of the unknown endophytes, the sequences of species with high similarity to our initial query sequences were downloaded. Taxonomic classification of these sequences was done using mycobank.org (provided by the CBS-KNAW Fungal Biodiversity Center, The Netherlands). Additional

sequences were retrieved from GenBank (Table S2, Supporting Information). Taxonomically distant outgroups were chosen based on the systematic classifications in MycoBank (Crous et al. 2004). The sequences were aligned using CLUSTAL-W and a Neighbor-Joining phylogeny was inferred using the Kimura-2 model with five gamma categories and pairwise deletion of gaps. One hundred bootstrap replicates were evaluated. All analyses were done using MEGA 5.2.2 (Tamura et al. 2011).

Assessment of endophyte and *Phytophthora infestans* growth after eight weeks of co-culture

To determine whether either the endophyte had overgrown *Phy. infestans* or *Phy. infestans* had overgrown the endophyte on the co-culture plates, we performed PCR reactions on DNA extracted from both sides of eight-week old co-cultures of five to nine *Phy. infestans* isolates with *Phi. fortinii*, isolate 8082 and isolate 9913 as well as their respective controls. We amplified the *ITS* loci (for primers see White et al. 1990) and the cytochrome oxidase subunit2 (*COX2*) using *Phytophthora*-specific primers from Hudspeth, Nadler and Hudspeth (2000) with the protocol described above. Between 50 and 100 ng of template DNA was used.

Spread of endophyte isolate 8082 in plant tissue

To evaluate the spread of isolate 8082 in *planta* over the course of infection, we used molecular analyses (*ITS*, 28S and *beta tubulin* sequences) for determining the presence of root-inoculated isolate 8082 (i) in the leaflets from the co-inoculations experiments (*ITS* and 28S) and (ii) in roots, stems (i.e. between the cotyledons and the first true leaves) following mono-inoculation with 8082 as well as in mock controls (*ITS*, 28S and *beta tubulin*). The seedlings were grown and treated as described above, harvested at 34 dps (the time point when *Phy. infestans* would otherwise be inoculated in a co-inoculation experiment), and RNA was extracted and processed as described above. We amplified the *ITS* locus to confirm that cDNA synthesis was successful. To determine whether the endophyte was present in the seedling tissues, we used *Pe28S* primers (forward primer: 5'TCGGGGAGAACTTATAGGGGA3', reverse primer: 5'TGGCTTCACCTATTCAAGCA3') designed using NCBI primer BLAST to bind specifically to isolate 8082. Therefore, we first cloned a partial 28S sequence (Accession: MG973066) of isolate 8082 using primers LR0R (Cubeta et al. 1991) and LR5 (Vilgalys and Hester 1990) as described above. We also used the *beta tubulin* (*PeTub*) gene (Accession: GU237608.1) of this fungus as a marker (forward primer: 5'TCGACGGCTCTGGTGTCTAC3', reverse primer: 5'CGCAGTCCGTCTAAGGAAAGT3'). The PCR reaction was set up as described above using the GoTaq® Flexi DNA Polymerase (Promega, Madison, WI, USA). For the amplification of the *ITS1*, 5.8S and *ITS2* locus in the leaflet samples from the co-inoculation experiment, the protocol included an initial denaturation at 95°C for 3 min, 38 cycles of denaturation at 95°C for 30 s, annealing at 60°C for 30 s and elongation at 72°C for 1.30 min, followed by a final elongation step at 72°C for 5 min. For the root, stem and leaflet samples from seedlings that were root-inoculated with isolate 8082 the number of cycles was reduced to 35. Amplification of the *Pe28S* and the *PeTub* genes followed a similar protocol with minor modifications: *Pe28S* was run with 33 cycles and an annealing temperature of 65°C and *PeTub* was run with 40 cycles.

Presence and abundance of *Phytophthora infestans*

To quantify the abundance of *Phy. infestans* in the seedlings pre-inoculated with the two endophytes (isolate 8082 and 9913) and the seedlings only inoculated with *Phy. infestans*, we performed a quantitative RT-PCR (qRT-PCR). The two markers, *PiH2a* and *PiElf1 α* , were used for the pathogen and the three markers, *SAND*, *TIP* and *TIF3H*, were used as tomato (host) reference genes (de Vries, Kloesges and Rose 2015; de Vries et al. 2017). Two independent qRT-PCR runs were used for the pathogen genes. All qRT-PCRs were performed in a CFX Connect Real-Time System (Bio-Rad, Hercules, CA, USA) and included an initial denaturation at 95°C for 3 min, followed by 40 cycles of a denaturation step at 95°C for 10 s and an annealing and elongation step of 60°C for 45 s. For *PiH2a* the annealing temperature was lower: 59°C in the first run and 55°C in the second run. In general, three biological replicates per treatment were used: (i) isolate 8082 (5 μ l mycelial suspension) with *Phy. infestans*, (ii) isolate 9913 with *Phy. infestans* and (iii) *Phy. infestans* without endophyte. The only exception is the treatment with isolate 8082 (10 μ l mycelial suspension) with *Phy. infestans*. In this case, two instead of three biological replicates were used. In each run, we analyzed three technical replicates for each biological replicate, resulting in six technical replicates for each biological replicate for both marker genes. To calculate the relative abundance of *Phy. infestans* in these samples, we set the C_q-values of those biological replicates that gave no biomass marker amplicon to 41. As the two independent runs gave the same results, they were combined. *PiH2a* and *PiElf1 α* expression was then calculated according to Pfaffl (2001). Data were tested for normal distribution using a Shapiro–Wilk test and the appropriate statistical tests were then applied. For co-inoculations with isolate 8082, significant differences were calculated using a Mann–Whitney U-test. For co-inoculations with isolate 9913, significant differences were calculated using a two-tailed t-test. The statistical analyses were done using R v3.2.1.

RESULTS

Metabolite assay identifies three endophytes with biocontrol potential

In this study, we analyzed the potential of several endophytes to inhibit the growth of and infection by the plant pathogen *Phy. infestans*. The endophytes were isolated from eight different plant species from three different European countries (Table S1, Supporting Information) from surfaced sterilized leaves, shoots and roots. Twelve fungal endophytes were selected for further testing of their metabolites for an inhibition potential against *Phy. infestans*.

To identify fungal endophytes that, on the basis of their secreted metabolites, could be used as biocontrol agents against *Phy. infestans*, we evaluated culture extracts of the 12 fungal endophytes for growth inhibition of *Phy. infestans* isolate D2 using an agar diffusion assay. Inhibition of *Phy. infestans* varied considerably, depending both on the endophyte isolate and on the culture medium. The average growth inhibition was 12.4 \pm 8.7 mm ranging from 0 to 35 mm from the point of extract application (Table S3, Supporting Information). Culture extracts of 3 of the 12 isolates inhibited growth of *Phy. infestans* with a radius \geq 20 mm. These three fungal endophytes (isolates 8082, 9907 and 9913) with the greatest *Phy. infestans* growth inhibition

were chosen for further studies. An additional fungal strain, *Phi. fortinii* (isolate 4197) was included due to its beneficial interaction with another host, *Larix decidua* (Schulz et al. 2002; Schulz 2006).

Phylogenetic placement of fungal endophytes

To determine the taxonomic identity and phylogenetic placement of the four selected fungal endophytes, we sequenced their *ITS1*, 5.8S and *ITS2* regions. To support their phylogenetic placement, we further used morphological and ecological information on the endophytes (Table S1, Supporting Information). First, we used the cloned sequences in a BLASTn search to identify the closest relatives of the fungal endophytes (Table S4, Supporting Information). All four endophytes belong to the ascomycetes. Our analyses further supported the previous characterization of isolate 4197 as *Phi. fortinii* (99% identity, Grünig et al. 2008). For isolate 8082, the best BLAST hit with 100% identity was *Pho. eupatorii*. This is in agreement with its morphological description as *Phoma* sp. (Table S1, Supporting Information). Additionally, it was supported by the fact that isolate 8082 was isolated from *Eupatorium cannabinum* (Table S1, Supporting Information). The placement of isolates 4197 and 8082 in our phylogenetic analyses together with the extremely short branch lengths to their best BLAST hits further support these phylogenetic assignments (Fig. 1a and b). The best hit for isolate 9907 was *Pyrenochaeta cava* (95% identity) and for isolate 9913 it was *Monosporascus ibericus* (97% identity). This suggests that no completely identical sequence/taxa are currently represented in the database. *Pyrenochaeta* does not form a monophyletic group within the order of Pleosporales (Zhang et al. 2009; Aveskamp et al. 2010; Fig. 1c), thus based on the phylogenetic analysis, isolate 9907 can only be placed within the order Pleosporales. Isolate 9913 was isolated from the roots of *Aster tripolium*, a plant that was growing in the salt marshes of the Mediterranean Sea (Table S1, Supporting Information). Of note is that *Monosporascus ibericus*, the fungal endophyte clustering most closely with isolate 9913 in the phylogenetic analysis, has been described as an endophyte of plants growing in environments with high salinity (Colrado et al. 2002). Furthermore, the genus *Monosporascus* is monophyletic; isolate 9913 has been placed within this monophyletic group and herewith termed *Monosporascus* sp. (Fig. 1d).

Fungal endophytes show broad-spectrum inhibition of *Phytophthora infestans* growth

Our initial analysis of the culture extracts identified endophytes with the potential to inhibit the growth of a single *Phy. infestans* isolate. We therefore wondered whether the inhibition could be effective against a wider range of isolates of *Phy. infestans*. To test this, we conducted a co-culture assay on RSA medium with the four fungal endophytes against nine European *Phy. infestans* isolates (Fig. 2). For this analysis, the fungal isolates were co-cultured with *Phy. infestans* isolates for 14–16 days, with the exception of the co-cultivations with *Monosporascus* sp., which were evaluated after eight days of co-culture due to its fast growth rate. We then compared the radial growth of the *Phy. infestans* isolates and the endophytes with their respective controls. In the plate assay, all four endophytes were capable of significantly restricting growth of *Phy. infestans* (Fig. 2m–p). *Phoma eupatorii* and isolate 9907 showed a global inhibition of all *Phy. infestans* isolates tested (Fig. 2n and o). We further noted that *Pho.*

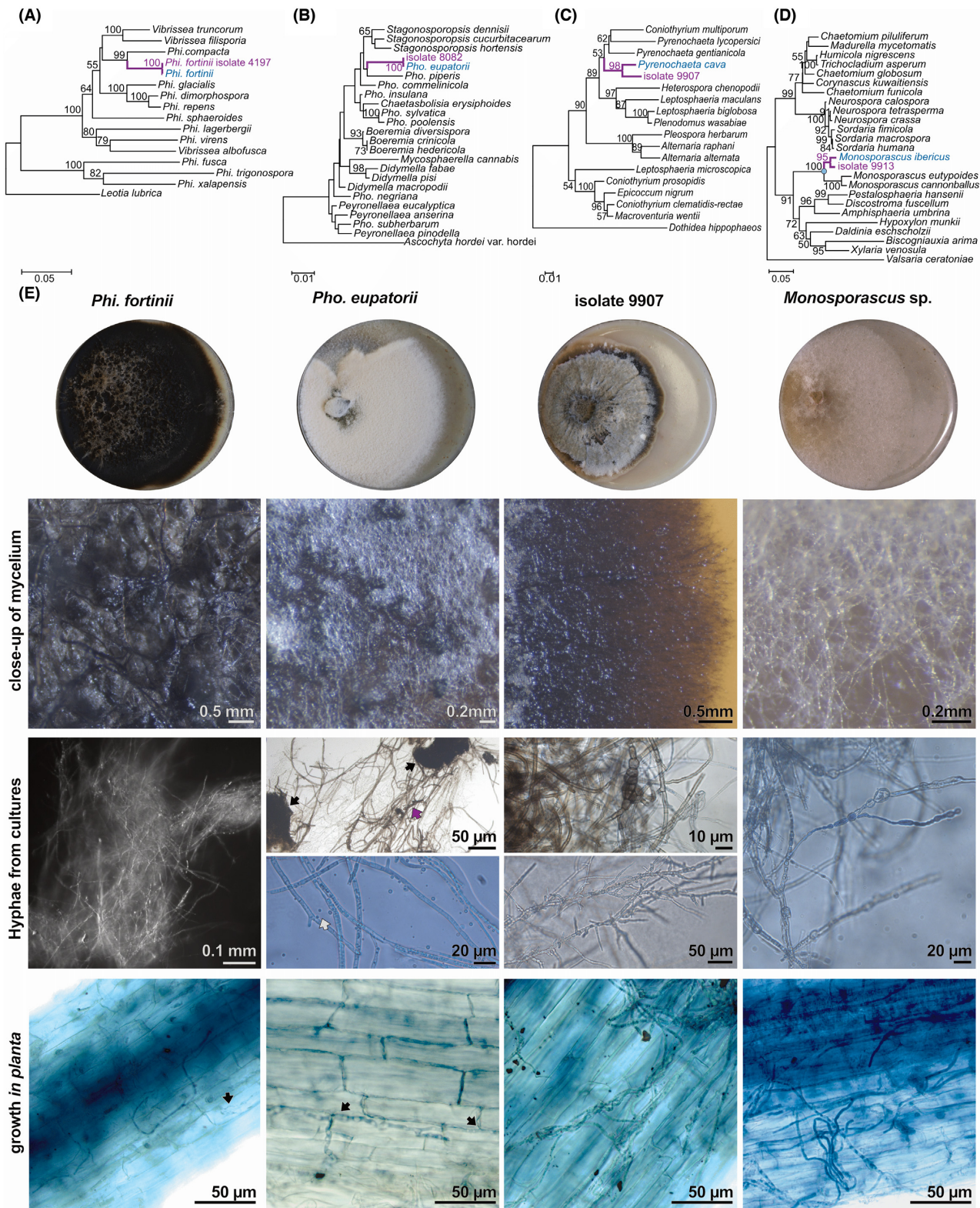


Figure 1. Phylogenetic placement of fungal endophytes. Neighbor-joining phylogeny of ascomycetes closely related to the four fungal endophytes (A-D). Cloned sequences are shown in purple and the best BLAST hit is shown in blue. The monophyletic clade of the genus *Monosporascus* is indicated by the blue dot (D). The trees are rooted with *Leotia lubrica* (A), *Ascochyta hordei* var. *hordei* (B), *Dothidea hippophaeos* (C) and *Valsaria ceratoniae* (D). Only bootstrap values >50 are shown. The bar below the phylogeny indicates the distance measure for the branches. (E) Pictures of the four fungal endophytes on plates, as well as close-ups of the mycelial growth on plates, microscopic pictures of hyphal growth in culture and in roots of *S. lycopersicum*. The cultures of *Pho. eupatorii* show pycnidia (black arrows) as well as chlamydospores (purple arrow) and pycnidiospores (grey arrow). Note the primarily intercellular growth of *Pho. eupatorii* in planta (black arrows), which may contribute to its asymptomatic root colonization of *S. lycopersicum*. *Phi. fortinii*, in contrast, colonized both inter- and intracellularly, as was observed for this isolate in other hosts (black arrow). Scale bars are given in the corner of each photograph.

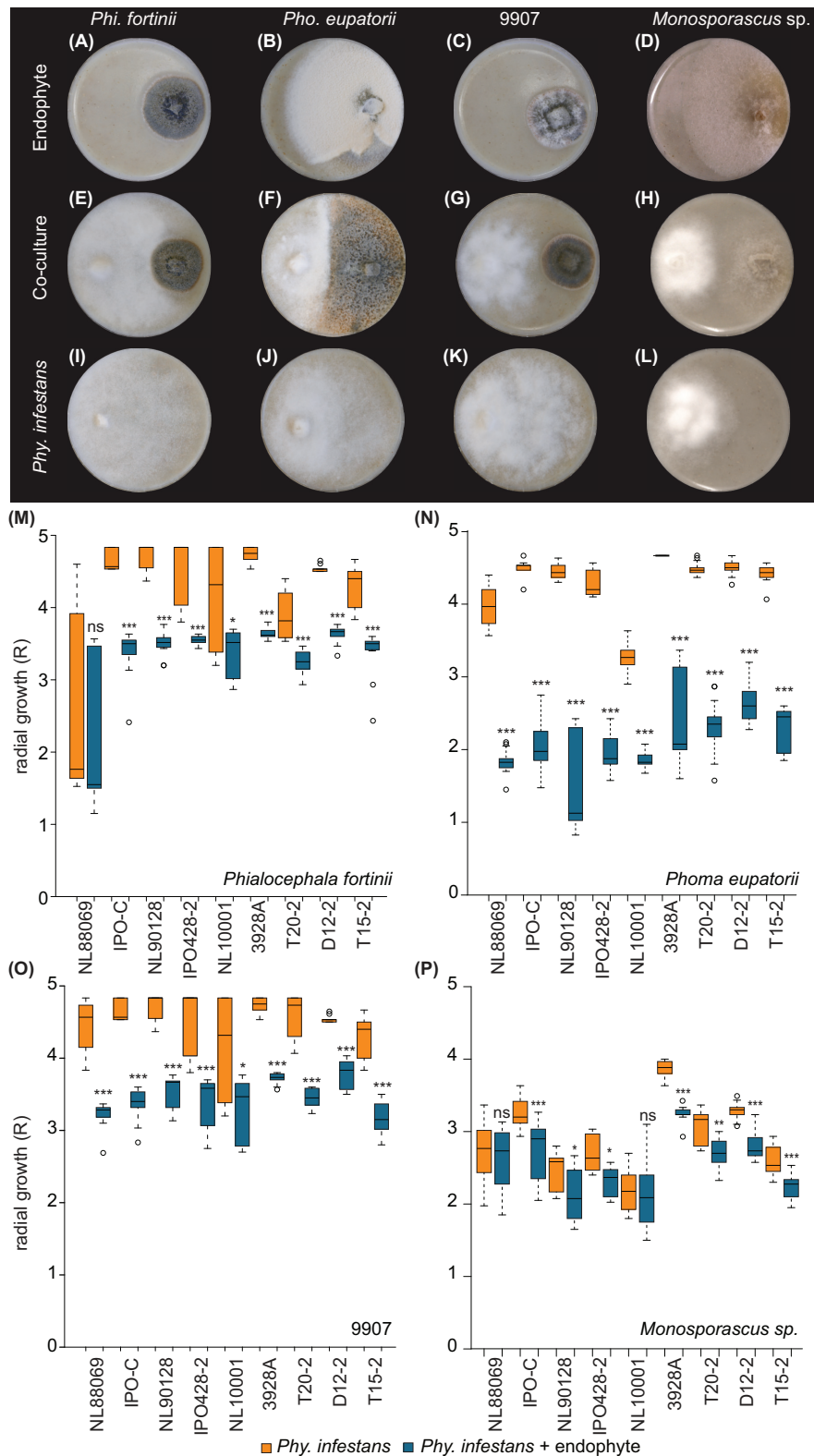


Figure 2. Co-cultivation of fungal endophytes with *Phytophthora infestans* on agar culture medium. Examples of two-week-old single and co-cultures of *Phialocephala fortinii* with *Phy. infestans* isolate 3928A (A,E,I), *Phoma eupatorii* with *Phy. infestans* isolate NL90128 (B,F,J) and 9907 with *Phy. infestans* isolate T15-2 (C,G,K) and eight-day old single and co-cultures of *Monosporascus* sp. with *Phy. infestans* isolate D12-2 (D,H,L). The diameter of each Petri dish is 9 cm. Radial growth inhibition of *Phy. infestans* isolates by fungal endophytes (M-P). Radial growth (R) of the different *Phy. infestans* isolates denoted on the x-axis when grown alone (orange) or in co-culture with the four fungal endophytes (blue): *Phi. fortinii* (M), *Pho. eupatorii* (N), isolate 9907 (O) and *Monosporascus* sp. (P). At least 10 biological replicates per control or co-cultivation were measured. The box indicates the upper and lower 50% quartile (interquartile range, IQR), the horizontal line in each box shows the median, the whiskers indicate the upper and lower bounds of the 1.5x IQR and the circles show data points, which are outliers. Significant differences are noted as * $P < 0.05$, ** $P < 0.01$, *** $P < 0.001$ and ns = not significant.

eupatorii showed a color change, which is due to enhanced spore production. Spore production occurred infrequently but did not alter the inhibition rate in co-culture. *Phialocephala fortinii* inhibited the growth of eight out of nine isolates and *Monosporascus* sp. inhibited the growth of seven of the nine isolates (Fig. 2m and p). *Phoma eupatorii* caused the greatest average relative growth inhibition of *Phy. infestans* with $50.6 \pm 2.2\%$, and *Monosporascus* sp. the lowest with $11.9 \pm 1.6\%$ (Table 1).

To exclude a mere reduction based on growth limitations we (i) measured the inhibition of the endophyte's growth by *Phy. infestans* after the initial co-cultivation phase (14–16 days, or eight days in case of co-cultures including *Monosporascus* sp.) and (ii) evaluated long-term co-cultures (i.e. eight weeks) to analyze the endophyte and pathogen growth progression. The growth of isolate 9907 was not inhibited by any of the *Phy. infestans* isolates (Fig. S1c, Supporting Information). However, some isolates of *Phy. infestans* were able to inhibit the growth of the other three fungal endophytes (Fig. S1a,b, and d, Supporting Information). In all cases, the average relative inhibition of an endophyte by *Phy. infestans* was, however, less than the average relative inhibition of *Phy. infestans* by an endophyte (Table 1, Table S5, Supporting Information). For example, whereas the average relative growth inhibition of *Phy. infestans* by *Pho. eupatorii* was $50.6 \pm 2.2\%$, the average relative inhibition of *Pho. eupatorii* by *Phy. infestans* was $4.7 \pm 0.9\%$.

After eight weeks, the endophytes (except for isolate 9907) visually overgrew the plates, including the regions colonized by *Phy. infestans* (Fig. 3). To substantiate this observation, we extracted DNA from some co-cultures with *Phi. fortinii* (12 co-cultures), *Pho. eupatorii* (18 co-cultures) and *Monosporascus* sp. (seven co-cultures) from both sides of the eight-week samples (Table S6, Supporting Information). In total, we analyzed 37 co-cultures and their respective controls for the presence of endophyte and *Phy. infestans*. We used the marker genes *COX* and *ITS*. Because our *ITS* primers were designed for fungi, we primarily observed amplicons from the fungal endophyte *ITS* loci when both organisms were present. However, presence of *Phy. infestans* could be determined by the presence of a *COX* amplicon. In general, we observed that the endophyte was present on both sides of the plates, whereas *Phy. infestans* was either not detected or only on the side of the plate on which it had been inoculated. Few exceptions occurred in which *Phy. infestans* was observed on the side of the original inoculation of the fungal endophyte (2/37 cases). Hence, *Phy. infestans* was usually not able to colonize the side of the plate where the endophyte was growing, while the endophyte was always able to colonize *Phy. infestans*' side of the plate. In addition, the endophytes showed a greater inhibition of *Phy. infestans* than *Phy. infestans* did of the endophytes. Therefore, resource limitation (due to the size of the plates) is unlikely to fully explain the unequal growth differential between *Phy. infestans* and the endophytes during co-cultivation. Instead, we hypothesize that factors actively secreted by the endophytes may also be involved in the growth inhibition of *Phy. infestans*.

Phoma eupatorii limits *Phytophthora infestans* infection success

We identified global, non-isolate-specific growth inhibition by all four endophytes in plate assays. To test whether the inhibitory potential of the endophytes holds true in planta, we inoculated the fungal endophytes in axenically grown *S. lycopersicum* cv. M82 seedlings. Our preliminary analysis showed that *Phi. fortinii* and isolate 9907 were too virulent and killed the *S. lycopersicum*

seedlings (Fig. S2 a, b, and d, Supporting Information). In contrast, *S. lycopersicum* seedlings inoculated with *Pho. eupatorii* or *Monosporascus* sp. survived (Fig. S2 a, c, and e, Supporting Information).

To confirm the endophytic colonization of the roots, we analyzed fungal outgrowth of surface sterilized roots and their imprints from inoculations with water, endophyte or endophyte and *Phy. infestans* (Table 2). Irrespective of the protocol, there was no fungal growth from the surface sterilized mock control roots or from their imprints. Generally, imprints of the surface sterilized endophyte inoculated roots did not show fungal growth, except for *Pho. eupatorii* inoculated roots after sterilization procedure 1 (1/16 imprints from the mono-inoculation and 5/12 imprints from the co-inoculations). This suggests that surface sterilization was successful in all other cases. *Phoma eupatorii* grew from several roots independently of the sterilization procedure, although the stronger treatments resulted in less outgrowth. Hence, these treatments may partially impact survival of endophytic mycelium. Nevertheless, these results show that *Pho. eupatorii* is capable of colonizing *S. lycopersicum* roots. *Monosporascus* sp. also showed outgrowth from several of the plated surface sterilized roots, suggesting that, like *Pho. eupatorii*, *Monosporascus* sp. also grows endophytically in the roots of *S. lycopersicum*. This was further confirmed by microcospy of the roots inoculated with the endophytes (Fig. 1e)

Solanum lycopersicum seedlings colonized by *Pho. eupatorii* are visually smaller than mock control seedlings and seedlings mono-inoculated with *Phy. infestans*. We also observed a reduction in leaflet number (Fig. S3 a and c, Supporting Information). Since the leaflets appeared sturdier and were darker green than the controls (Fig. 4a–f), we measured chlorophyll levels via chlorophyll fluorescence. However, chlorophyll abundance did not change following any of the treatments (Fig. 4g–m). We also observed that some of the stems and leaflets of the plants that had been inoculated with *Pho. eupatorii* developed a purple color (Fig. S3c, Supporting Information). Therefore, we reasoned that the darker leaflet color may have resulted from anthocyanin accumulation. Anthocyanin is a plant stress compound and hence we evaluated if *Pho. eupatorii* may stress the seedlings. In fact, we detected a significant increase in anthocyanin content in *Pho. eupatorii* inoculated versus mock control plants ($P = 0.001$ without *Phy. infestans*, $P = 0.04$ with *Phy. infestans*, Fig. 4n). In contrast to seedlings colonized by *Pho. eupatorii*, those inoculated with *Monosporascus* sp. did not visibly differ from the mock controls (Figs S3a and b, and S4a and c, Supporting Information). In agreement with this, anthocyanin content did not differ in *Monosporascus* sp. inoculated and mock control samples (relative anthocyanin content_{mock} = 0.5 ± 0.1 vs relative anthocyanin content_{9913/mock} = 2.3 ± 1.3 ; $P = 0.08$ without *Phy. infestans*). However, when both endophyte and pathogen were present, the anthocyanin content was elevated (relative anthocyanin content_{mock} = 0.5 ± 0.1 vs relative anthocyanin content_{9913/Phy} = 1.2 ± 0.1 ; $P = 0.007$), suggesting that the increase results from the presence of *Phy. infestans*.

Despite the visible effects of the colonization by *Pho. eupatorii* on the seedlings, we proceeded to investigate the effect of the endophyte on a subsequent infection with *Phy. infestans*. The relative necrotic area caused by the pathogen is significantly higher on plants inoculated only with *Phy. infestans* (in the absence of pre-inoculation by an endophyte) compared to the mock control (Fig. 4c; Fig. S4e, Supporting Information). To confirm the pathogen infection in the mock/*Phy. infestans* samples, we used the expression of the *Phy. infestans* biomass marker genes *PiH2a* and *PiElf1a*. In agreement with the increase

Table 1. Average relative growth inhibition of *Phy. infestans* (upper row) by endophytes (first column).

	NL88069	IPO-C	NL90128	IPO428-2	NL10001	3928A	T20-2	D12-2	T15-2	Average +/-SEM
<i>Phi. fortinii</i>	0.100	0.273	0.254	0.211	0.190	0.232	0.166	0.200	0.216	0.205 +/-0.016
<i>Pho. eupatorii</i>	0.537	0.546	0.661	0.539	0.429	0.471	0.480	0.411	0.482	0.506 +/-0.022
9907	0.276	0.276	0.251	0.250	0.210	0.215	0.244	0.166	0.262	0.239 +/-0.011
<i>Monosporascus</i> sp.	0.038	0.157	0.138	0.137	0.020	0.161	0.129	0.144	0.147	0.119 +/-0.016

The relative inhibition is calculated from the average radii estimated for co-cultivations and control plates. A minimum of ten biological replicates per control or co-cultivation were analyzed.

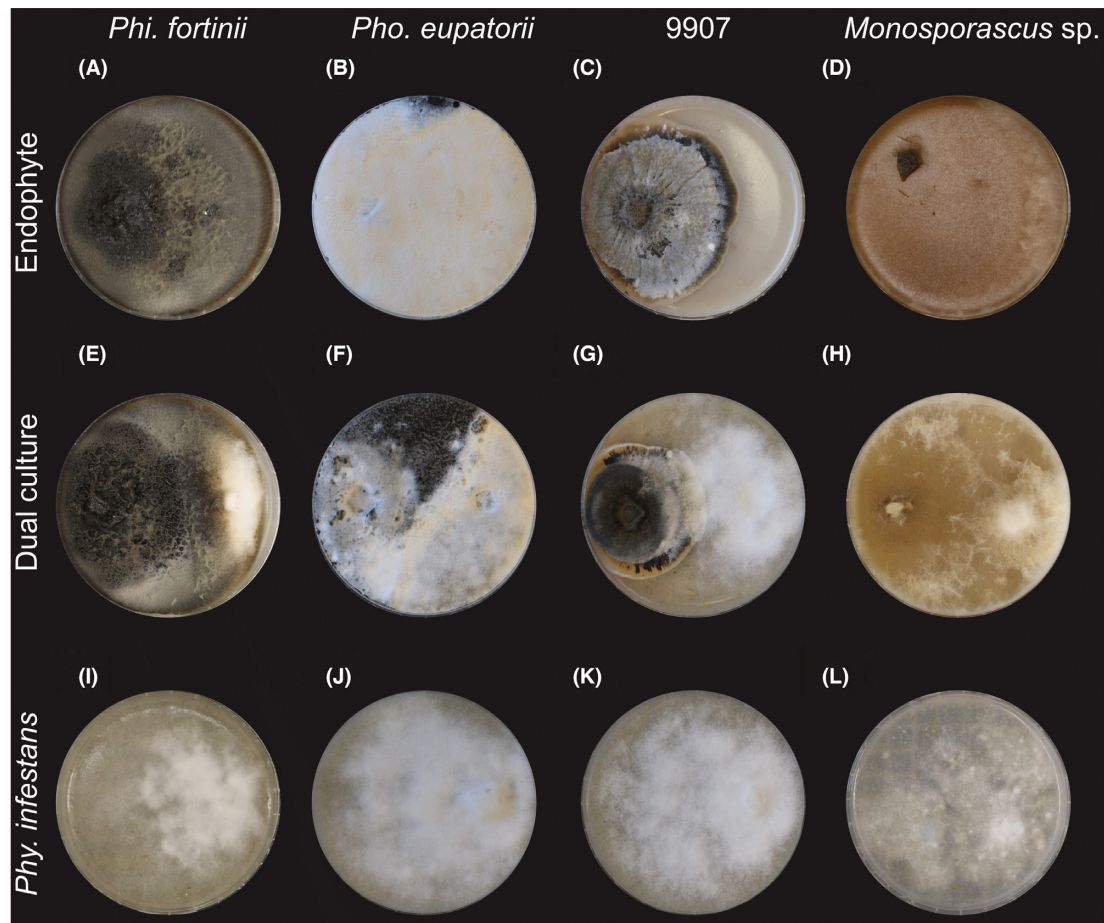


Figure 3. Long-term co-cultivation of fungal endophytes with *Phytophthora infestans* on agar growth medium. Examples of eight-week-old co-cultures and their respective controls. *Phi. fortinii* with *Phy. infestans* isolate NL88069 (A,E,I), *Pho. eupatorii* with *Phy. infestans* isolate NL88069 (B,F,J), isolate 9907 with *Phy. infestans* isolate T15-2 (C,G,K) and *Monosporascus* sp. with *Phy. infestans* isolate NL10001 (D,H,L). The diameter of each Petri dish is 9 cm.

in necrotic area, *Phy. infestans* was present in all biological replicates mono-inoculated with the pathogen, i.e. demonstrating a successful infection.

While the relative necrotic area in seedlings that were colonized only by *Pho. eupatorii* was 4.7-fold higher compared to the mock control, this was significantly less than the relative necrotic area of seedlings infected with only *Phy. infestans* (Fig. 4o). *Solanum lycopersicum* seedlings co-inoculated with *Pho. eupatorii* and *Phy. infestans* resulted in a significantly reduced relative necrotic area compared to seedlings mono-inoculated with

Phy. infestans (Fig. 4o). Importantly, the average relative necrotic area of leaflets colonized by both *Pho. eupatorii* and *Phy. infestans* did not differ from the mono-inoculations with the endophyte (Fig. 4o). Whether 5 or 10 μ l mycelial suspensions of *Pho. eupatorii* were used had no effect on the outcome of the experiments. The relative necrotic area between the treatment with *Monosporascus* sp. and the mock control did not differ (Fig. S4a, c and e, Supporting Information). This endophyte was neither able to inhibit *Phy. infestans* infection nor limit development of disease symptoms in planta (Fig. S4b, d, e and f, Supporting Information).

Table 2. Endophytic outgrowth from surface sterilized roots after inoculation with the endophyte.

	<i>Pho. eupatorii</i> imprint	8 dps roots	<i>Monosporascus</i> sp. imprint	6 dps roots
Procedure 1				
mock/mock	0/10	0/10	0/13	0/13
endophyte/mock	1/16	13/16	0/12	3/12
endophyte/ <i>Phy. infestans</i>	5/12	10/12	0/12	3/12
Procedure 2				
mock/mock	0/10	0/10	0/12	0/12
endophyte/mock	0/13	2/13	0/12	3/12
endophyte/ <i>Phy. infestans</i>	0/12	3/12	0/12	0/12
Procedure 3				
mock/mock	0/11	0/11	0/12	0/12
endophyte/mock	0/15	4/15	0/12	0/12
endophyte/ <i>Phy. infestans</i>	0/12	2/12	0/8	2/8

Roots were surfaces sterilized and an imprint of each root was prepared to test for efficiency of the treatment. The days after which the roots were surveyed is given as days post sterilization (dps). Procedure 1, 2 and 3 indicate the type of surface sterilization as described in the Material and Method section. The number of imprints and roots with fungal growth and the total number of analyzed roots is given for each sample type.

To quantify the biomass of *Phy. infestans* in planta after pre-inoculation with *Pho. eupatorii*, we performed a qRT-PCR with the two biomass marker genes *PiElf1 α* and *PiH2A* (Fig. 4p). In total, we tested the three biological replicates from the 5 μ l *Pho. eupatorii* inoculations and two from the 10 μ l *Pho. eupatorii* inoculations. In three of those five replicates, we did not detect an amplicon for either *PiH2a* or *PiElf1 α* . Yet, *PiH2a* and *PiElf1 α* were detected in every biological replicate of the mock/*Phy. infestans* infections. In addition, three plant-specific reference genes were tested; these showed no aberrant expression in any of the samples colonized by the endophyte in which *PiH2a* and *PiElf1 α* were not detected. Hence, the presence of the fungal endophyte did not affect the efficiency of the qRT-PCR. Also, those samples that were pre-inoculated with *Pho. eupatorii*, but gave an amplicon of the marker genes had reduced Cq-values for both marker genes compared to the mock/*Phy. infestans* samples. This suggests that *Pho. eupatorii* reduced the infection with *Phy. infestans* isolate D12-2 in the sampled leaflets. To estimate the reduction of *Phy. infestans* biomass, we assumed that the Cq-value of those replicates with no amplicon could theoretically have been amplified in later cycles. We therefore set the Cq-values in those samples to 41; i.e. one cycle more than the original runs included. Based on this assumption, we observed a significant reduction of gene expression in both biomass marker genes in the *Pho. eupatorii* pre-treated samples compared to mono-infections of *Phy. infestans* (Fig. 4p).

We further explored whether *Pho. eupatorii* inhibits *Phy. infestans* due to direct competition in the leaflets or indirectly via some form of long-distance signal. To do this, we analyzed (i) whether *Pho. eupatorii*, despite being root-inoculated, was able to colonize the leaflets in the co-inoculation experiment and (ii) how far *Pho. eupatorii* could spread from the time point of root inoculation with the endophyte to the day of leaflet-inoculation with *Phy. infestans*. Using two *Pho. eupatorii* marker genes (Fig. S5a, Supporting Information), we found that some of the co-inoculated leaflets, but not all, were colonized by the endophyte at the time of harvest. Additionally, in assays using the *Pe28S* marker, the endophyte was detected in all roots, many stems and some leaflets (Fig. S5b, Supporting Information). *PeTub* was detected in all root samples, but in contrast to *Pe28S*, only in two of the stems and none of the leaflet samples (Fig. S5b, Supporting Information). In agreement with *PeTub*, the *ITS1*, 5.8S

and *ITS2* band specific to *Pho. eupatorii* was also only found in two stem samples and no leaflet samples. Differences between endophyte detection across tissues by these three markers is likely related to differences in their sensitivity, with the greatest sensitivity provided by *Pe28S*, due to its high species specificity and substantial genomic copy number. All in all, these data show that in leaflet samples where we detected *Pho. eupatorii*, the endophyte was potentially in the leaflet tissue at the time of inoculation with *Phy. infestans*. However, since all co-inoculated samples showed a significant reduction in *Phy. infestans* infection, whether or not leaflet colonization with *Pho. eupatorii* was detected, it suggests that even the presence of *Pho. eupatorii* in the roots and stems brought about substantial pathogen suppression. In summary, despite—or perhaps because of—an increased stress response of the infected seedlings, *Pho. eupatorii* is capable of significantly inhibiting *Phy. infestans* infection of *S. lycopersicum* leaflets.

DISCUSSION

Fungal endophytes show a broad-spectrum growth inhibition of European *Phytophthora infestans* isolates

Of 12 fungi for which culture extracts were tested for inhibition of *Phy. infestans*, we identified three ascomycetes, *Pho. eupatorii*, isolate 9907 and *Monosporascus* sp., which effectively inhibited growth of the pathogen. While fungal endophytes produce a vast diversity of metabolites (Schulz et al. 2002; Strobel and Strobel 2007; Verma, Kharwar and Strobel 2009; Mousa and Raizada 2013; Brader et al. 2014) and numerous have antimicrobial activity (Son et al. 2008; Puopolo et al. 2014; Mousa et al. 2016), their metabolites may have a narrow spectrum of specificity. To avoid narrow spectrum of pathogen inhibition, we studied these three fungal endophytes and the endophyte *Phi. fortinii* for their capacity to inhibit the growth of nine European isolates of *Phy. infestans*. In our co-culture assays, *Pho. eupatorii* and isolate 9907 had a broad-spectrum inhibition against all tested isolates, whereas *Monosporascus* sp. and *Phi. fortinii* inhibited most of the isolates. Furthermore, after eight weeks of incubation, the pathogen was not able to grow on sections of the plates, in which the endophytes grew. The consistency of the results from the culture extract experiments and the plate assays of *Pho. eupatorii* and

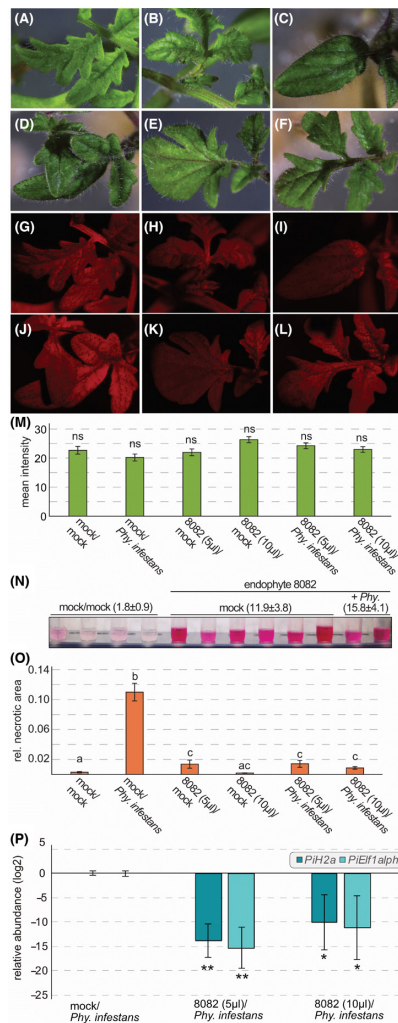


Figure 4. *In planta* co-inoculations of *Phoma eupatorii* isolate 8082 and *Phytophthora infestans*. *Solanum lycopersicum* cv. M82 seedlings were mock treated (A) or inoculated with *Phy. infestans* isolate D12-2 (B), 5 μ l of *Pho. eupatorii* mycelium suspension (C), 10 μ l of *Pho. eupatorii* mycelium suspension (D), 5 μ l of *Pho. eupatorii* mycelium suspension and *Phy. infestans* isolate D12-2 (E) and 10 μ l of *Pho. eupatorii* mycelium suspension and *Phy. infestans* isolate D12-2 (F). Chlorophyll fluorescence is depicted in red false coloring for all combinations (G–L) and was measured as mean fluorescence intensity using ImageJ2 (M). Bars give the average mean fluorescence ($n_{\text{leaflets}} = 17\text{--}37$). Error bars give the standard error of the mean (SEM); ns = not significant. Differences in anthocyanin content (N). A darker pink in the examples shown indicates a higher concentration of anthocyanins in the sample. Average relative anthocyanin content with standard deviation is given in brackets following each treatment. In total, three to six biological replicates per treatment were analyzed. The average relative necrotic area of the leaflets was calculated for each treatment ($n_{\text{leaflets}} = 38\text{--}156$). Bars give the average necrotic area per treatment and error bars indicate the SEM. Significant differences between the treatments are indicated by different letters above the bars with a cutoff of $P < 0.05$; same letter = not significant. The relative abundance of *Phy. infestans* isolate D12-2 was measured with a qRT-PCR of the two biomass marker genes *PIH2a* and *PIElf1 α* (P). Bars show average relative expression of the two biomass markers normalized against the three plant reference genes *SAND*, *TIP* and *TIF3H*. It compares relative abundance of *Phy. infestans* in *Pho. eupatorii*–*Phy. infestans* co-inoculations with that in control treatments (*Phy. infestans* only). Three biological replicates per treatment were used in all cases except for *Pho. eupatorii* (10 μ l mycelial suspension) with *Phy. infestans*, in which only two biological replicates were used. The error bars indicate the SEM. Significant differences between relative *Phy. infestans* abundance in samples pre-inoculated with the endophyte and the control are indicated by * $P < 0.05$ and ** $P < 0.01$. In all bar graphs, treatments with *Pho. eupatorii* are indicated by its isolate number 8082.

isolate 9907 shows that their inhibition is independent of the growth medium, suggesting an environmentally robust metabolite production of their anti-*Phytophthora* substances. A robust metabolite production would be of great advantage if these fungal endophytes are to be used as living biocontrol agents in the field.

As a first step towards identifying a potential biocontrol agent, we examined two essential questions: (i) Does infection by the endophyte damage the host in the absence of a pathogen? (ii) Does the endophyte successfully inhibit the pathogen in the host? In this study, the first question is especially relevant, because the fungal endophytes in question were not originally isolated from Solanaceae, to which tomato belongs. Furthermore, whether an endophyte remains benign and asymptomatic is likely to be affected by a number of different factors and in some cases the host endophyte relationship may shift to a pathogenic outcome from an initially protective interaction (Schulz and Boyle 2005; Junker, Draeger and Schulz 2012; Schulz et al. 2015; Busby, Ridout and Newcombe 2016). Along these lines, we excluded two isolates, *Phi. fortinii* and isolate 9907, for direct applications as biocontrol agents: seedlings of *S. lycopersicum* infected with either of these two isolates quickly died after inoculation. A third isolate, *Monosporascus* sp., neither inhibited *Phy. infestans* infection nor hindered its infection progress. This may not be surprising, because *Monosporascus* sp. had the lowest inhibition potential in our co-culture assays. It should, however, be noted that the metabolite composition of fungal endophytes varies depending on their environments, i.e. *in vitro* and *in planta* (Brader et al. 2014). It is therefore possible that the metabolite composition *Monosporascus* sp. produces *in planta* does not include the active anti-*Phytophthora* compound. Alternatively, the active compound may be only produced in specific stages of the infection. In the latter scenario, the infection of *Monosporascus* sp. may not have progressed far enough by the time we inoculated with *Phy. infestans*. Nevertheless, the outcome of the *in planta* co-inoculations does not exclude the possibility that the *in vitro* produced metabolites could be effective in field applications, especially since they showed a broad-spectrum reduction in *Phy. infestans* growth in our co-culture experiments. The broad-spectrum effectiveness of inhibition suggests that the metabolite composition either includes a metabolite with a conserved target in *Phy. infestans* or a mixture of anti-*Phytophthora* metabolites. Both would slow the counter-adaptation of the pathogen to the metabolites if used in field application. As a next step, the metabolite extracts with protective capabilities should be tested for their cytotoxicity *in planta*.

Phoma eupatorii isolate 8082 may inhibit *Phytophthora infestans* via secreted toxic metabolite(s)

Phoma eupatorii was the most effective fungal endophyte in our experiments, excelling both in co-culture as well as *in planta*. The presence of *Pho. eupatorii* not only reduced or inhibited the pathogen's growth, but perhaps entirely prevented infection. Here we used root inoculations of *Pho. eupatorii* combined with leaflet inoculations of *Phy. infestans* isolate D12-2. Because *Pho. eupatorii* was applied to roots and did not consistently spread to the leaflets by the time the plants were inoculated with *Phy. infestans*, niche competition is less likely to be the only mechanism by which *Pho. eupatorii* protects the seedlings of *S. lycopersicum*. Therefore, two other possible mechanisms by which the plant is defended against the pathogen include endophyte-dependent

induction of defense responses or the production of mobile anti-*Phytophthora* metabolites. The induction of plant defense responses by endophytes, such as *Se. indica* and non-pathogenic *Fusarium oxysporum*, has been previously shown (Stein et al. 2008; Aimé et al. 2013). Here, we observed an elevation of anthocyanin levels in leaf tissue of *S. lycopersicum* after root colonization of *Pho. eupatorii*. Accumulation of anthocyanins is a stress response and, among other factors, positively regulated by jasmonic acid (Franceschi and Grimes 1991; Feys et al. 1994; Li et al. 2006; Shan et al. 2009). Hence, it is possible that jasmonic acid dependent defense responses are induced upon colonization with *Pho. eupatorii* and may contribute to the inhibition of the *Phy. infestans* infection that we observed. Yet, the role of jasmonic acid in defense against *Phy. infestans* is not clear: The application of jasmonic acid to leaves of tomato and potato plants resulted in reduced infection of the pathogen (Cohen, Gisi and Niderman 1993). It is further reported that jasmonic acid is required for the initiation of defense responses triggered by a peptide secreted by *Phy. infestans* (Halim et al. 2009). Yet, potato RNA interference lines that downregulated jasmonic acid biosynthesis and signaling components showed no alterations in the infection rates of *Phy. infestans* (Halim et al. 2009). Hence, the production of anti-*Phytophthora* metabolites may be a more likely explanation for the observed reduction of *Phy. infestans* infection. A recently published example of a metabolite-based endophyte-mediated pathogen protection is that of *Enterobacter* sp. This endophyte produces many different antimicrobial compounds in its host plant and these are detrimental to the plant pathogen *F. graminearum* (Mousa et al. 2016). In our study, each of the four fungal endophytes undoubtedly produces anti-*Phytophthora* metabolites in the crude extract tests and in the co-cultures on agar media. This makes it likely that *Pho. eupatorii* also produces such metabolites during *in planta* co-inoculations with *Phy. infestans*. A combination of an elevated stress response (jasmonic acid mediated or not) and inhibition of *Phy. infestans* by antimicrobial compounds is, however, also possible.

Development of *Phoma eupatorii* as a biocontrol agent

Further questions should be addressed to determine if *Pho. eupatorii* is fit to become a biocontrol. For example: (i) How long do endophytes survive in the soil? (ii) Could the endophyte become an invasive species and/or pathogenic on other plants? (iii) Is a practical and efficient mode of application of the potential biocontrol available, i.e. could spores be used as a source of inoculum as shown for other biocontrol agents (Annesi et al. 2005)? We have shown that *Pho. eupatorii* is able to produce spores on plate. However, which plant organ would be suitable for reliable infection and how the potential biocontrol agent could be formulated would need to be determined and (iv) are the metabolites myco-toxins? If so registration would be problematic.

The longevity of the endophyte in soil is important, especially considering that the relationship between host and endophyte is environment dependent and that some endophytes may become pathogenic under certain conditions (Schulz and Boyle 2005). Moreover, *Pho. eupatorii* seems to have a broad host range, given that it was isolated from *E. cannabinum* and is also able to infect *S. lycopersicum*. A broad host range may become problematic for other plants in the environment, for example, if *Pho. eupatorii* is pathogenic on them. Hence, its ability to infect several common weeds, as well as other crop plants should be assessed.

Conclusion: *Phoma eupatorii* isolate 8082 is a potential novel *Phytophthora infestans* biocontrol agent

Out of an analysis of 12 fungal endophytes, we discovered four ascomycetes that inhibited the growth of *Phy. infestans* in co-culture, presumably through the secretion of secondary metabolites, particularly since their culture extracts were also active. Most importantly, two of the endophytes exhibited global inhibition of nine European *Phy. infestans* isolates, the other two showing a near-global inhibition. This indicates that a conserved target within *Phy. infestans* for a particular metabolite may be produced by these four endophytes. Alternatively, complex metabolite mixtures could be involved. In either case, the use of these fungi for biocontrol could slow the counter-adaptation of *Phy. infestans*. Hence, all four fungal endophytes can be considered good candidates for the production of such new and urgently needed compounds. Additionally, of the four fungal endophytes, *Pho. eupatorii* functioned as an effective biocontrol agent in *planta*. *Phoma eupatorii* may not only synthesize a reservoir of highly useful antimicrobial metabolites but may additionally induce resistance in the plant. *Phoma eupatorii* is hence a potential candidate to be tested as a novel biocontrol agent in the field providing an alternative to resistance gene breeding and application of agrochemicals.

SUPPLEMENTARY DATA

Supplementary data are available at FEMSEC online.

ACKNOWLEDGEMENTS

We thank Tuba Altinmakas, Klaudia Maas-Kantel, Melissa Mantz, Anja Melcher, Bianca Griebel and Corbinian Graf for technical support, Siegfried Draeger for isolation of the endophytes and initial identification based on morphology. We thank the TGRC Institute for providing the seeds of *S. lycopersicum* cv. M82 and Francine Govers (Wageningen University) for the *Phy. infestans* isolates NL10001, NL88069, NL90128, IPO-C, IPO428-2, 3928A, D12-2, T15-2 and T20-2. We thank Dr Bärbel Schöber-Butin for providing the German isolate *Phy. infestans* D2.

FUNDING

This work was supported by the Deutsche Forschungsgemeinschaft (Ro 2491/5-2, Ro 2491/6-1, Research Training Group GRK1525). SdV gratefully acknowledges funding through a Killam Postdoctoral Fellowship.

Conflict of interest. None declared.

REFERENCES

- Aimé S, Alabouvette C, Steiner C et al. The endophytic strain *Fusarium oxysporum* Fo47: a good candidate for priming the defense responses in tomato roots. *Mol Plant Microbe Interact* 2013;26:918–26.
- Alabouvette C, Olivain C, Migheli Q et al. Microbiological control of soil-borne phytopathogenic fungi with special emphasis on wilt-inducing *Fusarium oxysporum*. *New Phytol* 2009;184:529–44.
- Altschul SF, Gish W, Miller W et al. Basic local alignment search tool. *J Mol Biol* 1990;215:403–10.

- Annesi T, Curcio G, D'Amico L et al. Biological control of *Heterobasidium annosum* on *Pinus pinea* by *Phlebiopsis gigantea*. *Forest Pathol* 2005;**35**:127–34.
- Arnold AE, Mejía LC, Kylo D et al. Fungal endophytes limit pathogen damage in a tropical tree. *Proc Natl Acad Sci USA* 2003;**100**:15649–54.
- Aveskamp MM, de Gruyter J, Woudenberg JHC et al. Highlights of the Didymellaceae: a polyphasic approach to characterise *Phoma* and related pleosporalean genera. *Stud Mycol* 2010;**65**:1–60.
- Bahramisharif A, Lamprecht SC, Calitz F et al. Suppression of *Pythium* and *Phytophthora* damping-off of rooibos by compost and a combination of compost and non-pathogenic *Pythium*-taxa. *Plant Dis* 2013;**97**:1605–10.
- Benjamini Y, Hochberg Y. Controlling the false discovery rate: a practical and powerful approach to multiple testing. *J R Stat Soc B Met* 1995;**57**:289–300.
- Bodenhausen N, Horton MW, Bergelson J. Bacterial communities associated with leaves and the roots of *Arabidopsis thaliana*. *Plos One* 2013;**8**:e56329.
- Brader G, Compant S, Mitter B et al. Metabolic potential of endophytic bacteria. *Curr Opin Biotechnol* 2014;**27**:30–37.
- Bulgarelli D, Garrido-Oter R, Münch PC et al. Structure and function of the bacterial root microbiota in wild and domesticated barley. *Cell Host Microbe* 2015;**17**:392–403.
- Bulgarelli D, Rott M, Schlaeppli K et al. Revealing structure and assembly cues for *Arabidopsis* root-inhabiting bacterial microbiota. *Nature* 2012;**488**:91–5.
- Busby PE, Peay KG, Newcombe G. Common foliar fungi of *Populus trichocarpa* modify *Melampsora* rust disease severity. *New Phytol* 2016;**209**:1681–92.
- Busby PE, Ridout M, Newcombe G. Fungal endophytes: modifiers of plant disease. *Plant Mol Biol* 2016;**90**:645–55.
- Cao L, Qiu Z, You J et al. Isolation and characterization of endophytic *Streptomyces* strains from surface-sterilized tomato (*Lycopersicon esculentum*) roots. *Lett Appl Microbiol* 2004;**39**:425–30.
- Caten CE, Jinks JL. Spontaneous variability of single isolates of *Phytophthora infestans*. I. Culture variation. *Can J Bot* 1968;**46**:329–48.
- Childers R, Danies G, Myers K et al. Acquired resistance to mefenoxam in sensitive isolates of *Phytophthora infestans*. *Phytopathology* 2015;**105**:342–49.
- Cohen Y, Gisi U, Niderman T. Local and systemic protection against *Phytophthora infestans* induced in potato and tomato plants by jasmonic acid and jasmonic methyl ester. *Phytopathology* 1993;**83**:1054–62.
- Coleman-Derr D, Desgarenes D, Fonseca-Garcia C et al. Plant compartment and biogeography affect microbiome composition in cultivated and native *Agave* species. *New Phytol* 2016;**209**:798–811.
- Collado J, Gonzalez A, Platas G et al. *Monosporascus ibericus* sp. nov. an endophytic ascomycete from plants on saline soils, with observations on the position of the genus based on sequence analysis of the 18S rDNA. *Mycol Res* 2002;**106**:118–27.
- Crous PW, Gams W, Stalpers JA et al. MycoBank: an online initiative to launch mycology into the 21st century. *Stud Mycol* 2004;**50**:19–22.
- Cubeta MA, Echandi E, Abernethy T et al. Characterization of anastomosis groups of binucleate *Rhizoctonia* species using restriction analysis of an amplified ribosomal RNA gene. *Phytopathology* 1991;**81**:1395–400.
- de Vries S, Kloesges T, Rose LE. Evolutionarily dynamic, but robust, targeting of resistance genes by the miR482/2118 gene family in the Solanaceae. *Genome Biol Evol* 2015;**7**:3307–21.
- de Vries S, von Dahlen JK, Uhlmann C et al. Signatures of selection and host-adapted gene expression of the *Phytophthora infestans* RNA silencing suppressor PSR2. *Mol Plant Pathol* 2017;**18**:110–24.
- Dubey MK, Broberg A, Funck Jensen D et al. Role of the methylcitrate cycle in growth, antagonism and induction of systemic defence responses in the fungal biocontrol agent *Trichoderma atroviride*. *Microbiology* 2013;**159**:2492–500.
- Edwards J, Johnson C, Santos-Medellín C et al. Structure, variation, and assembly of the root-associated microbiomes of rice. *Proc Natl Acad Sci USA* 2015;**112**: E911–20.
- Fesel PH, Zuccaro A. Dissecting endophytic lifestyle along the parasitism/mutualism continuum in *Arabidopsis*. *Curr Opin Microbiol* 2016;**32**:103–12.
- Feys BJ, Benedetti CE, Penfold CN et al. *Arabidopsis* mutants selected for resistance to the phytotoxin coronatine are male sterile, insensitive to methyl jasmonate and resistant to a bacterial pathogen. *Plant Cell* 1994;**6**:751–9.
- Franceschi VR, Grimes HD. Induction of soybean vegetative storage proteins and anthocyanins by low-level atmospheric methyl jasmonate. *Proc Natl Acad Sci USA* 1991;**88**:6745–9.
- Grünig CR, Queloz V, Sieber TN et al. Dark septate endophytes (DSE) of the *Phialocephala fortinii* s.l.–*Acephala applanata* species complex in tree roots: classification, population biology, and ecology. *Botany* 2008;**86**:1355–69.
- Grünwald NJ, Sturbaum AK, Montes GR et al. Selection for fungicide resistance within a growing season in field populations of *Phytophthora infestans* at the center of origin. *Phytopathology* 2006;**96**:1397–403.
- Halim VA, Altmann S, Ellinger D et al. PAMP-induced defense responses in potato require both salicylic acid and jasmonic acid. *Plant J* 2009;**57**:230–42.
- Hiruma K, Gerlach N, Sacristán S et al. Root endophyte *Colletrichum tofieldiae* confers plant fitness benefits that are phosphate status dependent. *Cell* 2016;**165**:464–74.
- Höller U, Wright AD, Matthée GF et al. Fungi from marine sponges: diversity, biological activity and secondary metabolites. *Mycol Res* 2000;**104**:1354–65.
- Hudspeth DSS, Nadler SA, Hudspeth MES. A COX2 molecular phylogeny of the Peronosporomycetes. *Mycologia* 2000;**92**:674–84.
- Junker C, Draeger S, Schulz B. A fine line—endophytes or pathogens in *Arabidopsis thaliana*. *Fungal Ecol* 2012;**5**:657–62.
- Kim H-Y, Choi GJ, Lee HB et al. Some fungal endophytes from vegetable crops and their anti-oomycete activities against tomato late blight. *Lett Appl Microbiol* 2007;**44**:332–7.
- Kottb M, Gigolashvili T, Großkinsky DK et al. *Trichoderma* volatiles effecting *Arabidopsis*: from inhibition to protection against phytopathogenic fungi. *Front Microbiol* 2015;**6**:995.
- Kruskal WH, Wallis WA. Use of ranks in one-criterion variance analysis. *J Am Stat Assoc* 1952;**47**:583–621.
- Lahlali R, Hijri M. Screening, identification and evaluation of potential biocontrol fungal endophytes against *Rhizoctonia solani* AG3 on potato plants. *FEMS Microbiol Lett* 2010;**311**:152–9.
- Le Cocq K, Gurr SJ, Hirsch PR et al. Exploiting of endophytes for sustainable agriculture intensification. *Mol Plant Pathol* 2016;**18**:469–73.
- Li J, Brader G, Kariola T et al. WRKY70 modulates the selection of signaling pathways in plant defense. *Plant J* 2006;**46**:477–91.

- Lindoo SJ, Caldwell MM. Ultraviolet-B radiation-induced inhibition of leaf expansion and promotion of anthocyanin production. *Plant Physiol* 1978;**61**:178–282.
- Lundberg DS, Lebeis SL, Paredes SH et al. Defining the core *Arabidopsis thaliana* root microbiome. *Nature* 2012;**488**:86–90.
- Mann HB, Whitney DR. On a test of whether one of two random variables is stochastically larger than the other. *Ann Math Stat* 1947;**1**:50–60.
- Martínez-Medina A, Fernández I, Lok GB et al. Shifting from priming of salicylic acid- to jasmonate acid-regulated defences by *Trichoderma* protects tomato against the root knot nematode *Meloidogyne incognita*. *New Phytol* 2017;**213**:1363–77.
- Miles LA, Lopera CA, González S et al. Exploring the biocontrol potential of fungal endophytes from an Andean Colombian paramo ecosystem. *BioControl* 2012;**57**:697–710.
- Mousa WK, Raizada MN. The diversity of anti-microbial secondary metabolites produced by fungal endophytes: an interdisciplinary approach. *Front Microbiol* 2013;**4**:65.
- Mousa WK, Shearer C, Limay-Rios V et al. Root-hair endophyte stacking in finger millet creates a physiochemical barrier to trap the fungal pathogen *Fusarium graminearum*. *Nat Microbiol* 2016;**1**:16167.
- Murashige T, Skoog F. A revised medium for rapid growth and bio assays wity tobacco tissue cultures. *Physiol Plantarum* 1962;**15**:473–97.
- Nowicki M, Foolad MR, Nowakowska M et al. Potato and tomato late blight caused by *Phytophthora infestans*: an overview of pathology and resistance breeding. *Plant Dis* 2012;**96**:4–17.
- O'Sullivan DJ, O'Gara F. Traits of fluorescent *Pseudomonas* spp. involved in suppression of plant root pathogens. *Microbiol Rev* 1992;**56**:662–76.
- Panke-Buisse K, Poole AC, Goodrich JK et al. Selection on soil microbiomes reveals reproducible impacts on plant function. *ISME J* 2015;**9**:980–89.
- Pel MA, Foster SJ, Park T-H et al. Mapping and cloning of late blight resistance genes from *Solanum venturii* using an interspecific candidate gene approach. *Mol Plant Microbe Interact* 2009;**22**:601–15.
- Peters S, Aust H-J, Draeger S et al. Interactions in dual cultures of endophytic fungi with host and nonhost plant calli. *Mycologia* 1998;**90**:360–7.
- Pfaffl MW. A new mathematical model for relative quantification in real-time RT-PCR. *Nucleic Acids Res* 2001;**29**:e45.
- Piechulla B, Lemfack MC, Kai M. Effects of discrete bioactive microbial volatiles on plants and fungi. *Plant Cell Environ* 2017;**40**:2042–67.
- Ploch S, Rose LE, Bass D et al. High diversity revealed in leaf-associated protists (Rhizaria: Cercozoa) of Brassicaceae. *J Eukaryot Microbiol* 2016;**63**:635–41.
- Puopolo G, Cimmino A, Palmieri MC et al. *Lysobacter capsici* AZ78 produces cyclo(L-Pro-L-Tyr), a 2,5-diketopiperazine with toxic activity against sporangia of *Phytophthora infestans* and *Plasmopara viticola*. *J Appl Microbiol* 2014;**117**:1168–80.
- Rolli E, Marasco R, Vigani G et al. Improved plant resistance to drought is promoted by the root-associated microbiome as a water stress-dependent trait. *Environ Microbiol* 2015;**17**:316–31.
- Sachs L. *Angewandte Statistik*. Berlin: Springer, 1997, 395–7.
- Sapp M, Ploch S, Fiore-Donno AM et al. Protists are an integral part of the *Arabidopsis thaliana* microbiome. *Environ Microbiol* 2018;**20**:30–43.
- Schindelin J, Rueden CT, Hiner MC et al. The ImageJ ecosystem: an open platform for biomedical image analysis. *Mol Reprod Dev* 2015;**82**:518–29.
- Schlaeppli K, Dombrowski N, Oter RG et al. Quantitative divergence of the bacterial root microbiota in *Arabidopsis thaliana* relatives. *Proc Natl Acad Sci USA* 2013;**111**:585–92.
- Schulz B. Mutualistic interactions with fungal root endophytes. In: Schulz BJE, Boyle CJC, Sieber TN (eds). *Microbial Root Endophytes*. Berlin: Springer, 2006, 261–79.
- Schulz B, Boyle C, Draeger S et al. Endophytic fungi: a source of novel biologically active secondary metabolites. *Mycol Res* 2002;**106**:996–1004.
- Schulz B, Boyle C. The endophytic continuum. *Mycol Res* 2005;**109**:661–86.
- Schulz B, Krohn K, Meier K et al. Isolation of endophytic fungi for the production of biologically active secondary metabolites. In: Pirttilä AM, Sovari S (eds). *Prospects and Applications for Plant-Associated Microbes*. Turku: BioBien Innovations, 2011, 88–95.
- Schulz B, Haas S, Junker C et al. Fungal endophytes are involved in multiple balanced antagonisms. *Curr Sci* 2015;**109**:39–45.
- Shan X, Zhang Y, Peng W et al. Molecular mechanism for jasmonate-induction of anthocyanin accumulation in *Arabidopsis*. *J Exp Bot* 2009;**60**:3849–60.
- Shapiro SS, Wilk MB. An analysis of variance test for normality (complete samples). *Biometrika* 1965;**52**:591–611.
- Shoresh M, Harman GE, Mastouri F. Induced systemic resistance and plant responses to fungal biocontrol agents. *Ann Rev Phytopathol* 2010;**48**:21–43.
- Son SW, Kim HY, Choi GJ et al. Bikaverin and fusaric acid from *Fusarium oxysporum* show antioomycete activity against *Phytophthora infestans*. *J Appl Microbiol* 2008;**104**:692–8.
- Song J, Bardeen JM, Naess SK et al. Gene RB from *Solanum bulbocastanum* confers broad spectrum resistance to potato late blight. *Proc Natl Acad Sci USA* 2003;**100**:9128–33.
- Stein E, Molitor A, Kogel K-H et al. Systemic resistance in *Arabidopsis* conferred by the mycorrhizal fungus *Piriformospora indica* requires jasmonic acid signaling and the cytoplasmic function of NPR1. *Plant Cell Physiol* 2008;**49**:1747–51.
- Strobel SA, Strobel GA. Plant endophytes as a platform for discovery-based undergraduate science education. *Nat Chem Biol* 2007;**3**:356–9.
- Sturz AV, Christie BR, Matheson BG et al. Endophytic bacterial communities in the periderm of potato tubers and their potential to improve resistance to soil-borne plant pathogens. *Plant Pathol* 1999;**48**:360–9.
- Suryanarayanan TS, Govinda Rajulu MB, Vidal S. Biological control through fungal endophytes: gaps in knowledge hindering success. *Curr Biotechnol* 2016;**5**, DOI: 10.2174/2211550105666160504130322.
- Tamura K, Peterson D, Peterson N et al. MEGA5: molecular evolutionary genetics analysis using maximum likelihood, evolutionary distance and maximum parsimony methods. *Mol Biol Evol* 2011;**28**:2731–9.
- Tellenbach C, Sieber TN. Do colonization by dark septate endophytes and elevated temperature affect pathogenicity of oomycetes? *FEMS Microbiol Ecol* 2012;**82**:157–68.
- Terhonen E, Sipari N, Asiegbu FO. Inhibition of phytopathogens by fungal root endophytes of Norway spruce. *Biol Control* 2016;**99**:53–63.
- U'Ren JM, Arnold AE. Diversity, taxonomic composition, and functional aspects of fungal communities in living, senesced, and fallen leaves at five sites across North America. *PeerJ* 2016;**4**:e2768.
- van der Vossen E, Sikkema A, te Lintel Hekkert B et al. An ancient R gene from the wild potato species *Solanum bulbocastanum*

- confers broad-spectrum resistance to *Phytophthora infestans* in cultivated potato and tomato. *Plant J* 2003;**36**:867–82.
- Verma VC, Kharwar RN, Strobel GA. Chemical and functional diversity of natural products from plant associated endophytic fungi. *Nat Prod Commun* 2009;**4**:1511–32.
- Vilgalys R, Hester M. Rapid genetic identification and mapping of enzymatically amplified ribosomal DNA from several *Cryptococcus* species. *J Bacteriol* 1990;**172**:4238–46.
- Vleeshouwers VG, Raffaele S, Vossen JH et al. Understanding and exploiting late blight resistance in the age of effectors. *Ann Rev Phytopathol* 2011;**49**:507–31.
- White TJ, Bruns T, Lee S et al. Amplification and direct sequencing of fungal ribosomal RNA genes for phylogenetics. In: Innis MA, Gelfand DH, Sninsky JJ, White TJ (eds). *PCR Protocols: A Guide to Methods and Applications*. New York, NY: Academic Press, Inc., 1990, 315–22.
- Zhang C, Liu L, Zheng Z et al. Fine mapping of the *Ph-3* gene conferring resistance to late blight (*Phytophthora infestans*) in tomato. *Theor Appl Genet* 2013;**126**:2643–53.
- Zhang Y, Schoch CL, Fournier J et al. Multi-locus phylogeny of Pleosporales: a taxonomic, ecological and evolutionary re-evaluation. *Stud Mycol* 2009;**64**:85–102.

Publication VII

Rapid evolution in the tug-of-war between microbes and plants

Status	Published
Journal	The New phytologist
Citation	Frantzeskakis, L., von Dahlen, J. K. , Panstruga, R., & Rose, L. E. (2018). Rapid evolution in the tug-of-war between microbes and plants. <i>The New phytologist</i> , 219(1), 12-14.
Own contribution	Contributed to the writing of the manuscript (report meeting)

Meetings

Rapid evolution in the tug-of-war between microbes and plants

'Molecular mechanisms underlying the rapid evolution of plant–microbe interactions', New Phytologist/DFG SPP1819 Workshop, Vaals, the Netherlands, February 2018

Does the underlying co-evolutionary race between hosts and pathogens necessarily result in rapid evolution? Is the process of adaptation in these antagonistic interactions fundamentally different from other adaptive processes?

Members of the research priority programme SPP1819 (topic: 'Rapid evolutionary adaptation – potential and constraints') – funded by the German Science Foundation (DFG) – along with an international group of fellow scientists, met in February 2018 at the idyllic castle Bloemendal of Vaals in the Netherlands to discuss the latest advances on the emerging topic of evolutionary molecular plant–microbe interactions (EvoMPMI; for a recent review see Upson *et al.*, 2018). In the 20 talks delivered by both established and early career scientists in the field, the latest results covering a range of model systems were presented and discussed. While the limited space provided here does not allow for an extensive commentary on all of the talks, we present a few recurrent themes and highlights.

Can fungal pathogens shine light on the mechanisms of rapid evolution?

Much of the work presented at this workshop illustrated that plant-pathogenic fungi can be an invaluable tool for determining how pathogens adapt following the introduction of new host resistance specificities or during a shift to a new host. Their relatively small genomes (*c.* 20–200 Mb) can be easily (re-)sequenced, making them tractable for both comparative/population genomics and experimental evolution. A few laboratories have begun to incorporate genomic tracking with an experimental evolutionary approach involving serial passages of the pathogen through contrasting host species or genotypes, attempting to identify the mutations associated with host specialization. Since the price for short-read sequencing has decreased significantly in recent years, this genome 'monitoring' approach is also cost-efficient. In addition, advances in long-read sequencing can further aid in determining the contribution of structural changes such as chromosome length polymorphisms, large-scale deletions/duplications, and rearrangements in the process of adaptation. Considering the wide range of hosts, life-styles and propagation modes, fungi can deliver a cornucopia of insights for evolutionary biologists.

This notion was well reflected at the workshop. The laboratories of Antonio di Pietro (University of Córdoba, Spain), Jan Schirawski and Ralph Panstruga (both RWTH Aachen University, Germany) aim to understand the adaptive walk of three fungal pathogens (*Fusarium oxysporum*, *Sporisorium reilianum*, *Blumeria graminis*) to different host environments using experimental evolution. Using serial passaging of these pathogens through their respective hosts, they monitor the co-occurrence of genomic changes affecting virulence (Fig. 1). Preliminary results suggest that an increase in virulence on one host might come at a cost in other environments/hosts.

Utilizing a different approach, the laboratories of Bruce McDonald (ETH Zürich, Switzerland), Eva Stukenbrock (University of Kiel, Germany), Bart Thomma (Wageningen University & Research, the Netherlands) and Martijn Rep (University of Amsterdam, the Netherlands) are taking advantage of natural variation within and between species to home in on genetic factors that contribute qualitatively or quantitatively to the development of disease. The development of high-throughput imaging methods to collect data on the extent of infection including the number of pycnidia, the level of melanization or lesion area for the wheat pathogen, *Zymoseptoria tritici* (Karisto *et al.*, 2018) can provide major breakthroughs for the mapping of genetic factors associated with pathogenicity (Hartmann *et al.*, 2017). This approach has been extremely fruitful, providing not only insights on the

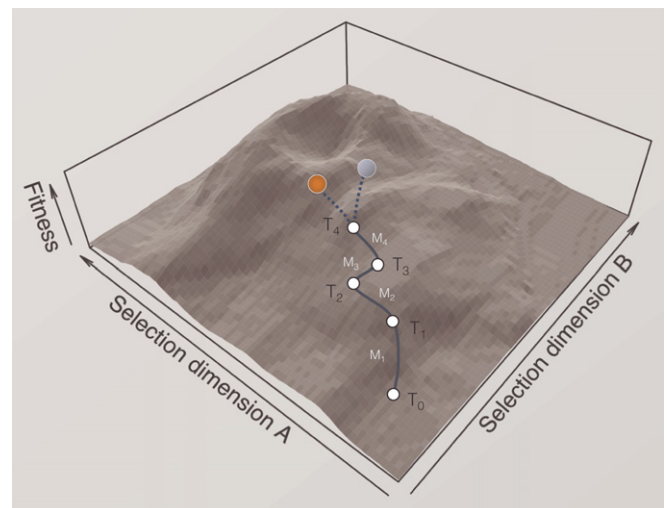


Fig. 1 Schematic representation of an adaptive walk a pathogen may take as it adapts to a new host species or to a new resistance specificity. Over time (T0–T4), adaptive mutations M1–M4 (e.g. gene duplications, deletions or nonsynonymous substitutions) will arise and be fixed in natural populations. The endpoint of an adaptive walk may be distinct fitness optima (represented here by red and blue dots) and these may correspond to different hosts or host genotypes.

quantitative effects of different pathogen effectors, but also offering a method to disentangle pathogen reproduction and virulence. Similar high-throughput experiments were presented by Dan Kliebenstein (University of California Davis, USA), in which *c.* 100 different *Botrytis cinerea* isolates were used to examine the polygenic basis of its virulence on tomato and other plant hosts (Soltis *et al.*, 2018). At the same time, comparative genomics between isolates of fungal species and their close relatives can reveal individual host-specific factors that are responsible for a large proportion of the colonization success and expose the role of lineage-specific, dispensable chromosomes or regions thereof in host shifts. This, for example, is nicely demonstrated by work on *Verticillium dahliae* and *F. oxysporum* (van Dam *et al.*, 2017; Shi-Kunne *et al.*, 2017).

Overall, it became evident that every research team is invigorated and blossoming in the new era of pathogenomics. Owing to the joint efforts of many laboratories around the world, resources have matured and now include multiple, curated and annotated datasets and nearly complete genomes, enabling the next generation of biologists to move forward and go beyond standard molecular genetics. Accumulating evidence, some of which was presented in this meeting, suggests that additional factors contribute to fungal virulence, and these might range from the life history of the isolates and their genetic backgrounds to the specific genome architecture (e.g. patterns of transposable element distribution, accessory chromosomes, etc.) and genome-wide epigenetic patterns (e.g. DNA methylation and histone marks).

The phyllosphere as a new frontier?

Embracing a taxonomically comprehensive approach, Eric Kemen (University of Tübingen, Germany) presented his work on the dynamics of the leaf microbe community. Following a series of combined experiments, the microbial community of the Arabidopsis phyllosphere could be reduced to a manageable number of culturable species to serve as synthetic microbial communities (SynComs). Alteration of the composition of these SynComs affected the infection success by the oomycete pathogen *Albugo laibachii*, suggesting that inter-microbe interactions may exert indirect effects on plant health. Joy Bergelson (University of Chicago, USA) pointed out that these plant microbial networks, despite being heritable across generations, are also vulnerable to disruptions originating from environmental change (Brachi *et al.*, 2017).

While binary host–pathogen interactions are still the standard model, the potential for a role of the associated microbial community to influence the outcome of host–pathogen interactions is widely acknowledged but rarely studied. Until now, the microbial community, as a third player in any host–pathogen interaction, has not been explicitly approached from the perspective of rapid evolution. However, it is likely that the process of adaptation of a pathogen to a new host also entails adapting to the associated indigenous microbial community. The associated microbial community may act in concert with the host immune system to negatively affect the pathogen or facilitate infection, depending on community structure. The experimental concepts that were presented in this workshop could be used to obtain a

deeper insight into how certain compositions of microbial communities can accelerate or hinder adaptation of phytopathogens to given plant species.

Rapid? Says who?

As new data accumulate, at what point can we generalize about specific scenarios conducive to rapid evolution? Is it as simple as characterizing the pathogen's own evolutionary potential (i.e. having a particular genome architecture, a given parasitic lifestyle, and a specific propagation mode; Dong *et al.*, 2015), or is it a sum of environmental factors (e.g. tighter co-association with certain other microbes)? Paraphrasing a quote from Oscar Wilde, factors associated with the rapid evolution of virulence and adaptation give an answer that at the moment is 'rarely pure and never simple'.

Depending on the pathogen species, different types of genetic variants were found to be associated with host specialization and adaptation (e.g. accessory chromosomes, copy number variation, the presence of active transposable elements, structural rearrangements and/or nucleotide polymorphisms). However, despite attempts to place these examples in a common framework, each pathogen still appears to represent a unique evolutionary trajectory and no single type of genetic variation serves as a predictor for a high rate of adaptive evolution.

Many factors, both intrinsic (such as genome flexibility, mating system, pathogen life style and/or mode of dispersal), and extrinsic (such as climatic variability, the structure of the host-associated microbial community and the spatial distribution/landscape coverage of the host relative to the mode of pathogen dispersal), influence the potential rate of adaptation. A new framework to study the presence of rapid evolution in plant–pathogen systems should not only address the all-important underlying genomic changes that lead to differences in host specificity or susceptibility, but also consider how these other factors have shaped the evolutionary trajectories.

Finally, an important first step to better understand the process of rapid adaptation is to characterize the underlying genetic changes associated with specialization and pathogenicity. Studying pathogens from many kingdoms, including bacteria, viruses, fungi and oomycetes, our field is making rapid progress to decipher these genetic changes associated with rapid evolution and can even deliver some new case studies (Inoue *et al.*, 2017). Looking into the future, our next challenge is to determine if there are any common, underlying patterns. Finding the answer to this question will likely require integration of many different research fields, including epidemiology, ecology, molecular biology, population genomics and computer science, to work on the common theme of rapid evolution.

Acknowledgements

The authors would like to thank the New Phytologist Trust and the DFG for providing financial support for the workshop. In addition, the authors are grateful to Sophien Kamoun (@Kamounlab) and Bart Thomma (@Team_Thomma) for sharing the content of the workshop in real time with the global research community through

Twitter (#NPW20). The authors are funded through the DFG priority programme SPP1819 (PA 861/14-1 and RO 2491/6-1).

ORCID

Lamprinos Frantzeskakis  <http://orcid.org/0000-0001-8947-6934>

Ralph Panstruga  <http://orcid.org/0000-0002-3756-8957>

Lamprinos Frantzeskakis¹ , Janina K. von Dahlen²,
Ralph Panstruga^{1*}  and Laura E. Rose²

¹Unit of Plant Molecular Cell Biology, Institute for Biology I, RWTH Aachen University, Worringerweg 1, Aachen 52056, Germany;

²Institute of Population Genetics, Heinrich-Heine University Düsseldorf, Universitätsstr. 1, Düsseldorf 40225, Germany
(*Author for correspondence: tel +49 241 80 26655; email panstruga@bio1.rwth-aachen.de)

References

- Brachi B, Filaault D, Darne P, Mentec M Le, Kerdaffrec E, Rabanal F, Anastasio A, Box M, Duncan S, Morton T *et al.* 2017. Plant genes influence microbial hubs that shape beneficial leaf communities. *bioRxiv*. doi: 10.1101/181198
- van Dam P, Fokkens L, Ayukawa Y, van der Gragt M, ter Horst A, Brankovics B, Houterman PM, Arie T, Rep M. 2017. A mobile pathogenicity chromosome in *Fusarium oxysporum* for infection of multiple cucurbit species. *Scientific Reports* 7: 9042.
- Dong S, Raffaele S, Kamoun S. 2015. The two-speed genomes of filamentous pathogens: waltz with plants. *Current Opinion in Genetics & Development* 35: 57–65.
- Hartmann FE, Sánchez-vallet A, McDonald BA, Croll D. 2017. A fungal wheat pathogen evolved host specialization by extensive chromosomal rearrangements. *The ISME Journal* 11: 1189–1204.
- Inoue Y, Vy TTP, Yoshida K, Asano H, Mitsuoka C, Asuke S, Anh VL, Cumagun CJR, Chuma I, Terauchi R *et al.* 2017. Evolution of the wheat blast fungus through functional losses in a host specificity determinant. *Science* 357: 80–83.
- Karisto P, Hund A, Yu K, Anderegg J, Walter A, Mascher F, McDonald BA, Mikaberidze A. 2018. Ranking quantitative resistance to *Septoria tritici* blotch in elite wheat cultivars using automated image analysis. *Phytopathology* 108: 568–581.
- Shi-Kunne X, Faino L, van den Berg GCM, Thomma BPHJ, Seidl MF. 2017. Evolution within the fungal genus *Verticillium* is characterized by chromosomal rearrangement and gene loss. *Environmental Microbiology* 20: 1362–1373.
- Soltis NE, Atwell S, Shi G, Fordyce R, Gwinner R, Gao D, Shafi A, Kliebenstein DJ. 2018. Crop domestication and pathogen virulence: interactions of tomato and *Botrytis* genetic diversity. *bioRxiv*. doi: 10.1101/255992
- Upson JL, Zess EK, Białas A, Wu C, Kamoun S. 2018. The coming of age of EvoMPMI: evolutionary molecular plant–microbe interactions across multiple timescales. *Current Opinion in Plant Biology* 44: 108–116.

Key words: co-evolution, pathogenomics, plant–microbe interactions, plant–microbial networks, plant–pathogenic fungi, rapid evolution.



About New Phytologist

- *New Phytologist* is an electronic (online-only) journal owned by the New Phytologist Trust, a **not-for-profit organization** dedicated to the promotion of plant science, facilitating projects from symposia to free access for our Tansley reviews and Tansley insights.
- Regular papers, Letters, Research reviews, Rapid reports and both Modelling/Theory and Methods papers are encouraged. We are committed to rapid processing, from online submission through to publication 'as ready' via *Early View* – our average time to decision is <26 days. There are **no page or colour charges** and a PDF version will be provided for each article.
- The journal is available online at Wiley Online Library. Visit **www.newphytologist.com** to search the articles and register for table of contents email alerts.
- If you have any questions, do get in touch with Central Office (np-centraloffice@lancaster.ac.uk) or, if it is more convenient, our USA Office (np-usaoffice@lancaster.ac.uk)
- For submission instructions, subscription and all the latest information visit **www.newphytologist.com**